Journal of

Tropical Biodiversity and Biotechnology

VOLUME 9 | ISSUE 1 | MARCH 2024

PUBLISHED BY

UNIVERSITAS GADJAH MADA
FAKULTAS BIOLOGI

IN COLLABORATION WITH

KOBI
Konsorsium Biologi

KBI
KONSORSIUM BIOTEKNOLOGI INDONESIA
INDONESIAN BIOTECHNOLOGY CONSORTIUM

Credits

Editor	Miftahul Ilmi Ardaning Nuriliani Furzani Binti Pa'ee Sri Nopitasari Liya Audinah Annisaa Widyasari Tanti Agustina
Copyeditor and Language Editor	Salwa Shabria Wafi Almaulidio Tazkia Dina Syarifah Rosana
Layout Editor	Salwa Shabria Wafi Muchamad Ulul Azmi
Cover Photo	Dewi Wahyuni K. Baderan
Editorial Board	Prof. Dr. Wibowo Mangunwardoyo Prof. Dr. Budi Setiadi Daryono, M.Agr.Sc. Prof. Dr. Jonathan A. Anticamara Prof. Jean W. H. Yong, Ph.D. Dr. Farid Asif Shaheen Ts. Dr. Kamarul Rahim bin Kamarudin Assoc. Prof. Dr. Wong Wey Lim Dr. Phoon Lee Quen Sukirno, M.Sc., Ph.D. Dr. rer. nat. Andhika Puspito Nugroho Assoc. Prof. Dr. Ruqiah Ganda Putri Panjaitan Dr. Abdul Razaq Chasani Dr. Ratna Stia Dewi Dr. Alona Cuevas Linatoc Prof. Madya Ts. Dr. Muhammad Abdul Latiff Bin Abu Bakar Ts. Dr. Siti Fatimah Binti Sabran

Table of Contents

Review Article

Journal of Tropical Biodiversity and Biotechnology
Volume 09, Issue 01 (2024): jtbb84523
DOI: 10.22146/jtbb.84523

Short Communications

Plukenetia volubilis L.: A New Record of a Cultivated Alien Species in Java

Alexander Tianara[1,2], Windri Handayani[2], Arifin Surya Dwipa Irsyam[3]*, Muhammad Rifqi Hariri[4], Asih Perwita Dewi[4], Peniwidiyanti Peniwidiyanti[5,6], Muhammad Hisyam Baidlowi[6], Dian Rosleine[7], Mega Atria[1,2]

1)Herbarium Depokensis (UIDEP), Department of Biology, Faculty of Mathematics and Natural Sciences, Universitas Indonesia, Pondok Cina, Beji, Depok City, West Java, 16424, Indonesia
2)Department of Biology, Faculty of Mathematics and Natural Sciences, Universitas Indonesia, Pondok Cina, Beji, Depok City, West Java, 16424, Indonesia
3)Herbarium Bandungense (FIPIA), School of Life Sciences and Technology (SITH), Institut Teknologi Bandung (ITB), Labtek VC Building, Jl. Let. Jen. Purn. Dr (HC) Mashudi No. 1 Jatinangor, West Java, 45363, Indonesia
4)Research Center for Biosystematics and Evolution, National Research and Innovation Agency (BRIN), Jl. Raya Jakarta-Bogor Km. 46, Cibinong, West Java, 16911, Indonesia
5)Research Center for Ecology and Ethnobiology, National Research and Innovation Agency (BRIN), Jl. Raya Jakarta-Bogor Km. 46, Cibinong, West Java, 16911, Indonesia
6)Botani Tropika Indonesia Foundation (BOTANIKA), Jl. Seruni No. 25, Loji, Bogor, West Java, 16117, Indonesia
7)Ecology Research Group, School of Life Sciences and Technology (SITH), Institut Teknologi Bandung (ITB), Labtek XI Building, Jl. Ganesha No. 10 Bandung, West Java, 40132, Indonesia
* Corresponding author, email: arifin@itb.ac.id

Keywords:
Alien
Cultivated
Euphorbiaceae
Java
kacang inka
Plukenetia volubilis
Submitted:
17 May 2023
Accepted:
31 August 2023
Published:
22 January 2024
Editor:
Ardaning Nuriliani

ABSTRACT
Plukenetia volubilis L. has been documented as a new record for the first time in Java, Indonesia. The species is easily distinguished from the native species, *P. corniculata* Sm., by its exstipellate basilaminar-glands, long cylindrical column, and wingless fruit-lobes. *Plukenetia volubilis* is cultivated mainly in South America for its beneficial values as food and medicine and was recently introduced to Asia. However, its occurrence in Java has not been reported. We collected specimens from West Java (Depok City, Bandung Barat and Sumedang Regency) and East Java (Malang Regency). Morphological description, identification key, and photographs of the species are provided.

Copyright: © 2024, J. Tropical Biodiversity Biotechnology (CC BY-SA 4.0)

The plant diversity in Java has been extensively studied, primarily since the Flora of Java was published in three volumes in 1963, 1965, and 1968. However, previous studies proved that the number of taxonomic studies has recently increased in Java. There have been numerous reports on the newly discovered native species in published works (Djarwaningsih 2010; Djarwaningsih 2012; Djarwaningsih 2013; Puspitaningrum et al. 2017; Metusala & Supriatna 2017; Rahayu & Rodda 2019). Furthermore, various authors have also recorded many additional alien species from the island (Hariri et al. 2019; Effendi & Mustaqim 2021; Mustaqim & Setiawan 2021; Irsyam et al. 2021; Peniwidiyanti et al. 2021; Al Anshori et al. 2022; Irsyam et al. 2022). It demonstrates that taxonomic studies on plant diversity in Java are still important.

Some additional alien species of the Euphorbiaceae *sensu lato* have been discovered on Java over the past five years, both naturalized and

cultivated, namely *Caperonia palustris* (L.) A.St.-Hil. (Al Anshori et al. 2020), *Cathetus myrtifolius* (Wight) R.W.Bouman (Hariri et al. 2020), *Cnidoscolus aconitifolius* (Mill.) I.M.Johnst. (Irsyam et al. 2020), *Croton bonplandianus* Baill. (Al Anshori et al. 2020), *Euphorbia graminea* Jacq. (Irsyam et al. 2019), *E. hyssopifolia* L. (Irsyam et al. 2019), and *Moeroris tenella* (Roxb.) R.W.Bouman (Hariri et al. 2020). Other undiscovered additional species may still occur on the island. Thus, this study aims to update the information on the Alien Flora of Java, particularly the Euphorbiaceae. The data will be used to prepare the database of alien plant species on the island.

Plukenetia L. is a tropical genus with 21 species distributed in tropical areas from Mexico, Africa, South Asia, to Southeast Asia and throughout Malesia (Cardinal-McTeague & Gillespie 2016; Cardinal-McTeague & Gillespie 2020). The genus is a monoecious or rarely dioecious vine. Its distinctive characteristics include papery leaves, a leaf base with two raised glands on the adaxial surface, 8–13 free stamens, and winged or horned capsules (van Welzen 2020). *Plukenetia corniculata* Sm., previously classified under *Pterococcus* Hassk., is the only species that naturally occurs in Asia, such as Thailand (Gillespie & Larsen 2023) and Singapore (Choo et al. 2022), including Java (Backer & Bakhuizen van den Brink 1963). In this study, we formally report the occurrence of *P. volubilis* L. for Java, a new cultivated alien species for Java. It is an introduced species from South America. Our discovery becomes the second species of *Plukenetia* found in Java.Botanical exploration was conducted in West Java (Depok City, Bandung Regency, and Sumedang Regency) and East Java (Malang Regency) from January to May 2023. Field exploration was carried out using a method based on Rugayah et al. (2004). Plant material collection and processing follows Bridson & Forman (1998). Plant materials were documented and observed at Herbarium Depokensis (UIDEP), Department of Biology, Faculty of Mathematics and Natural Sciences, Universitas Indonesia and Herbarium Bandungense (FIPIA), School of Life Sciences and Technology, Institut Teknologi Bandung. Specimen checking was conducted at Herbarium Bogoriense (BO), National Research and Innovation Agency (BRIN). Specimen identification was carried out using Backer & Bakhuizen van den Brink (1963), Gillespie (1993; 2007), and Cardinal-McTeague & Gillespie (2020). The description used terminologies from The Kew Plant Glossary (Beentje 2012), and the species name was validated at Plants of The World Online (2023). Collected specimens were deposited in UIDEP and FIPIA.

Key to the genus *Plukenetia* L. in Java

1. A. Basilaminar glands stipellate, styles connate into a depressed-globose column, the apex of fruit lobe have a central strap-shaped wing..... *P. corniculata* Sm.

   B. Basilaminar glands exstipellate, styles connate into a long cylindrical column, the apex of fruit lobe shortly horned and wingless.....*P. volubilis* L.

Plukenetia volubilis L., Sp. Pl.: 1192 (1753). *Sajorium volubile* (L.) Baill., Étude Euphorb.: 483 (1858). – TYPE: Plumier, Nov. Pl. Amer. t. 13, *Plukenetia* (1703); LT designated by Howard, Fl. Lessser Antilles 5: 82 (1989); cited by Gillespie, Syst. Bot. 18: 591 (1993). – Figure 1 & 2.
Fragariopsis paxii Pittier, J. Washington Acad. Sci. 19: 351 (1929). – TYPE: Venezuela, Federal District, Loma de En Medio, Valley of Puerto

la Cruz, 1000 m, *Pittier 8109* (iso GH, US).
Plukenetia macrostyla Ule, Verh. Bot. Vereins Prov. Brandenburg 50: 80 (1908 publ. 1909). – TYPE: Brazil, Amazonas, Rio Jurua, near Jaburiu, *Ule 5864* (iso G).
Plukenetia peruviana Müll.Arg., Linnaea 34: 157 (1865). – TYPE: Peru, *Herb. Pavon* (syn G-DC, photo F 7111, G).
Perennial vine, monoecious, up to 4 m long, without milky latex. *Stems* twining, becoming woody, pubescent, green. *Stipules* minute, triangular, 2.5–3 × 1 mm, caducous, green. *Leaves* simple, alternate; petiole 5–8 cm long, pubescent, green; lamina cordate to deltate-ovate or lanceolate, 3–12.8 × 0.7–10 cm, base cordate or truncate to subcordate, margin serrulate to denticulate, with hydathodes, apex caudate-acuminate, acumen 1–4 cm long, chartaceous, adaxial surface pubescent, shiny green, abaxial surface pubescent, pale green, trinerved, veins scalariform, veinlets reticulate; basilaminar glands elliptic, 1.2–3 × 1–1.8 mm, exstipellate, yellowish green. *Inflorescences* axillary, racemose thyrses, up to 8 cm long, pubescent, bisexual, pistillate flower(s) basal, 1–3; staminate bracts narrowly triangular, ca. 1 mm long, pistillate bracts ovate, ca. 0.7 mm long, green; bracteoles 2 per flower, minute; flowers unisexual, actinomorphic, pedicellate, petals absent. *Staminate flowers*: 4–9.5 mm in diameter when open; pedicels ca. 1 mm long; sepals 5, valvate, lobe elliptic, ca. 2.2–4.5 × 1–2.5 mm, yellow; stamens (18–)19–21, free, ca. 0.5 mm long; filaments short, green; anthers 4-locular, basifixed, yellow; pistillode absent. *Pistillate flowers*: pedicels ca. 4–5 mm long; sepals 4, triangular, 10 × 7 mm, green; disc absent; ovary 4–5-locular, 1 ovule per locule, 4–5-lobed, lobes 6 mm long, pubescent, green; styles connate into a cylindrical column, up to 2 cm long, green; stigmas 4–5, rounded, ca. 2 mm wide, yellow. *Fruits* capsule, star-shaped, up to 6 cm wide, 4–5-locular, horned at the apex of each lobe. *Seeds* flattened, lenticular, 1.6–1.8 × 1.9–2 cm, dark brown, ecarunculate.
Distribution: The Lesser Antilles, Suriname, and the northern and western edges of the Amazon basin in Venezuela, Colombia, Ecuador, Peru, Bolivia, and Brazil (Gillespie 1993). In this paper, *P. volubilis* was collected from the cultivation area in Western and Eastern parts of Java (Figure. 1).
Habitat: It grows in disturbed regions or along forest edges at elevations up to 900 meters above sea level (Gillespie 1993). *Plukenetia volubilis* was found cultivated in open areas at 79–786 m asl on Java.
Specimens examined: INDONESIA. JAVA – **West Java** • Depok City, Beji, Pondok Cina, Universitas Indonesia Campus, Parangtopo Laboratory, 16.I.2023, *A Tianara AT-P-021* (UIDEP, FIPIA); Bandung Barat Regency, Ngamprah Subdistrict, Pakuhaji, 30.IV.2023, *ASD Irsyam 807* (FIPIA); Sumedang Regency, Rancakalong Subdistrict, Sukahayu Village, Nagrak, 01.V.2023, *ASD Irsyam 808* (FIPIA). – **East Java** • Malang Regency, Poncokusumo Subdistrict, Karanganyar Village, Karanganyar Kidul, Jl. Pancuran, 30.IV.2023, *MH Badlowi 04* (FIPIA).
Vernacular names: *Kacang inka* (Indonesian); *sacha inchi* (Quechua); *inca nut*, *inca peanut*, *sacha peanut* (English).
Uses: The species is frequently used to produce pharmaceutical, cosmetic, and dietary products (Blancke 2016; Wang et al. 2018; Torres Sánchez et al. 2021).

Plukenetia volubilis is found in the Lesser Antilles, Brazil, Bolivia, Peru, Ecuador, Colombia, Venezuela, and the Western and Northern edges of the Amazon basin. It typically grows in moist or wet lowland forests below 900 meters, along forest borders, or in disturbed areas (Gillespie 1993; Kodahl 2020; POWO 2023). A previous study revealed

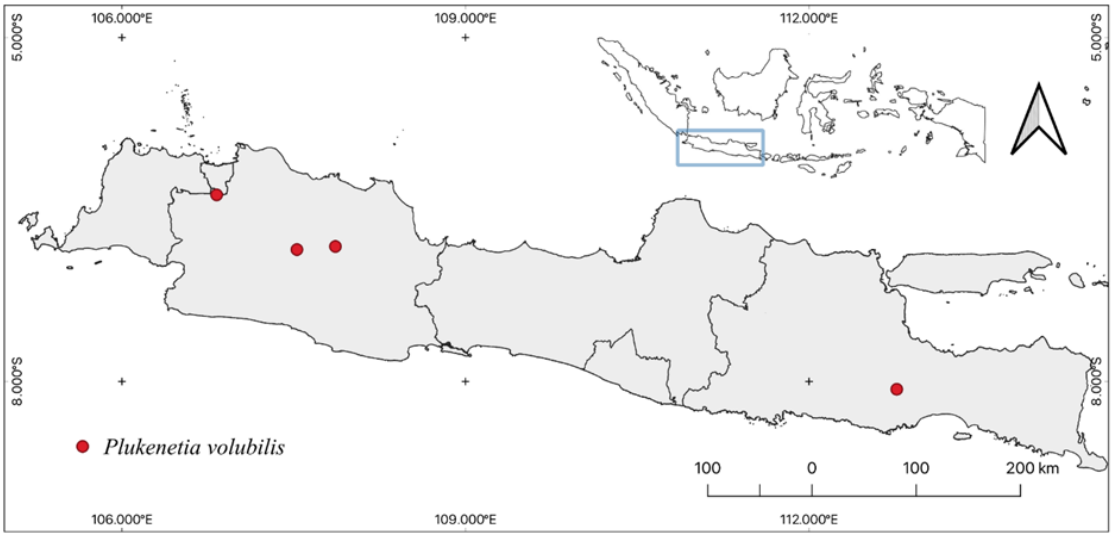

Figure 1. Distributions of *Plukenetia volubilis* in Java, Indonesia, collected from this study.

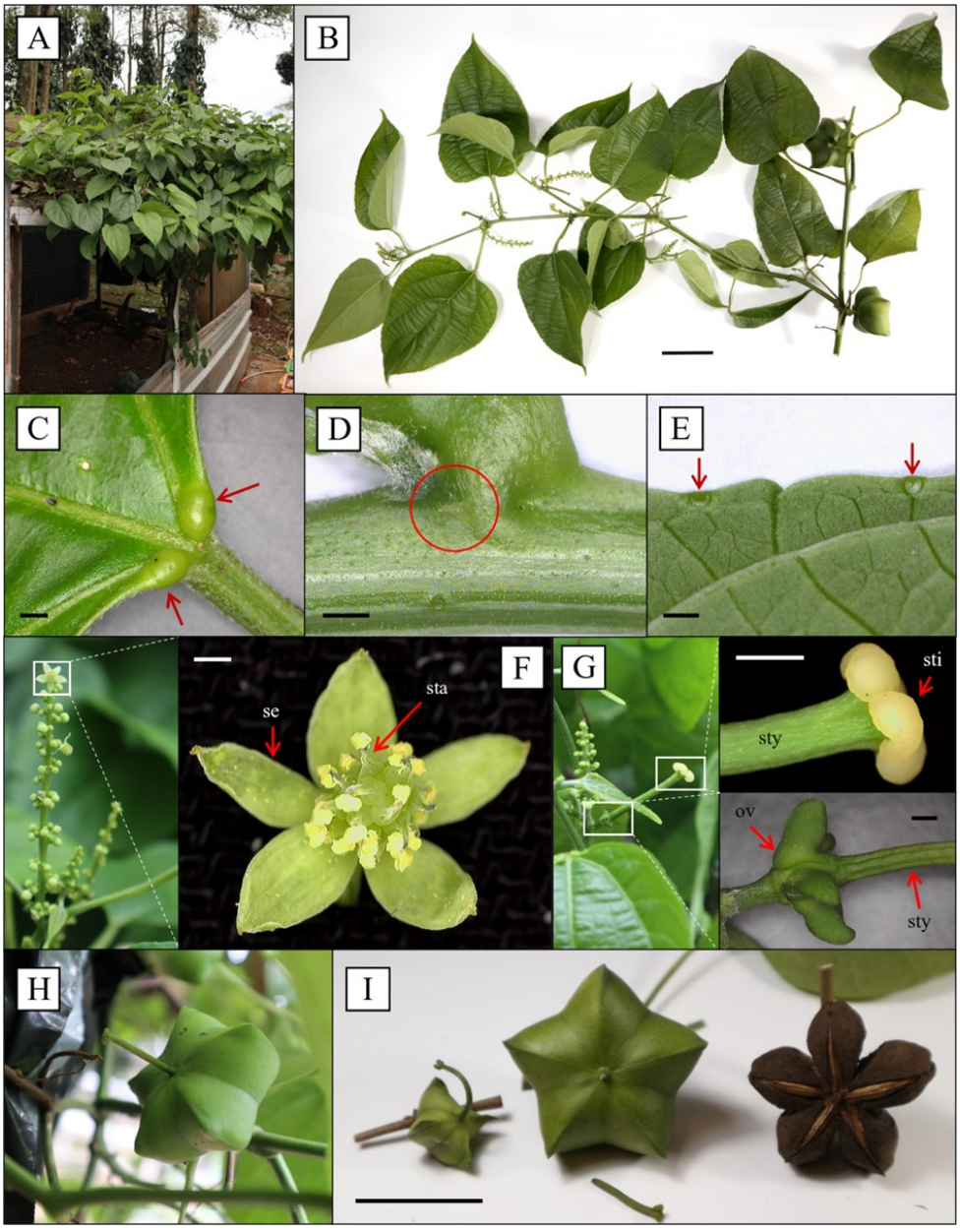

Figure 2. Morphological characters of *Plukenetia volubilis*. A-B. Habit; C. Adaxial basilaminar glands (arrows); D. Stipule (circled); E. Hydathodes (arrows); F. Staminate flower (se = sepal, sta = stamen); G. Parts of pistillate flower (sti = stigma, sty = style, ov = ovary, lobed); H. Fruit with pistil remnant; I. Development stages of fruit (young to old/dry; left to right). Scale bar = B. 5cm; C-F. 1mm; G. 2mm; I. 3cm.

that it had been recently introduced to Asia, such as China, Cambodia, Laos, and Thailand (Kodahl & Sørensen 2021). Previous botanists have not reported its occurrence in Java. *Plukenetia volubilis* is recorded for the first time for the Alien flora of Java in this paper. It was collected from West Java (Depok City, Bandung Barat Regency, and Sumedang Regency) and East Java (Malang Regency) at the cultivation area. Although, it is possible to find this species being cultivated elsewhere in Java. The history of its introduction to Java is not known. However, no specimens from Java were found during an examination at Herbarium Bogoriense (BO).

Our discovery increases the total number of *Plukenetia* in Java into two species, namely *P. corniculata* and *P. volubilis*. These two climbing species are quite similar to one another. *Plukenetia volubilis* differs from *P. corniculata*, a local species, based on the characteristics of the basilaminar glands, styles, fruit, and seeds. The morphological differences between those species are shown in Table 1.

Native South American communities have consumed seeds and leaves as a staple for at least three thousand years (Blancke 2016). Seeds of *P. volubilis* contain unsaturated fats, vitamins A, vitamins E, protein, essential amino acids, fiber, minerals, phenolic compounds, terpenoids, tocopherols, and phytosterols (Sathe et al. 2002; Blancke 2016; Kodahl 2020; Kodahl & Sørensen 2021; Torres Sánchez et al. 2021). The raw seeds are inedible and develop a nutty flavor after being roasted (Blancke 2016). The roasted seeds can be ground into flour, used to make butter, roasted and mixed with salt or sugar as a snack, or added to various traditional meals. In addition, many people blend salads or prepare tea with young leaves of *P. volubilis* (Flores 2010; Kodahl & Sørensen 2021).

Plukenetia volubilis has become more attention recently, especially because of the amount and composition of the seed oil. It is now possible to buy commercial items like oil and roasted seeds (Kodahl 2020). In Java, *P. volubilis* was known as *kacang inka* and has been cultivated for its leaves and seeds. In our study areas, the leaves are used for vegetables and tea, and the oil is extracted from the seeds. Moreover, previous studies showed that several ethnic groups in Peru have used seed oil of *P. volubilis* for centuries to rejuvenate and revitalize the skin, alleviate rheumatism, relieve muscle pain, and heal bug bites (Flores & Lock 2013; Gonzalez-Aspajo et al. 2015; Kodahl & Sørensen 2021). Pharmacological studies revealed that seed oil has potential in the cosmetics industry as an emollient (softening and smoothing skin), humectant, anti-aging, antioxidant, and penetration enhancer (Brinckmann 2013; Soimee et al. 2019;

Table 1. Morphological differences between *Plukenetia corniculata* and *P. volubilis*.

Morphological characters	*P. corniculata* (WFO 2023)	*P. volubilis*
Petiole	Moderately or sparsely pubescent	Pubescent
Lamina	Ovate, oblong-ovate, or sometimes elliptic	Cordate to deltate-ovate or lanceolate
Leaf margin	Serrulate or serrate	Serrulate to denticulate
Venation	Weakly palmate, nerves 2–4	Trinerved
Basillaminar glands	Stipellate	Exstipellate
Style	Connate into a depressed-globose column	Connate into a long cylindrical column
Apex of fruit lobe	Having a central strap-shaped wing	Shortly horned and wingless
Seed	Broadly lenticular and laterally compressed	Lenticular and flattened
Seed color	Cream, pale orangish-brown or brown	Dark brown

Poomanee et al. 2021; Maya & Sriwidodo 2022). The seed oil also has some biological activities, including antihypertensive, anticancer, anti-hypercholesterolemia, antimicrobial, and reduces the risk of stroke (Gonzalez-Aspajo et al. 2015; Wang et al. 2018; Silalahi 2022).

AUTHOR CONTRIBUTION

AT and ASDI designed the research. AT, WH, ASDI, MRH, MHB, P, and APD collected the plant materials, observed the specimen, and analyzed the data. AT, WH, ASDI, MRH, MHB, APD, P, DR, and MA wrote the original draft and agreed to the final manuscript.

ACKNOWLEDGMENTS

We are grateful to Bayuriana Arisko Apit and Asep Dudi for helping us collect plant material in the field.

CONFLICT OF INTEREST

All authors declare no conflict of interests.

REFERENCES

Al Anshori, Z. et al., 2020. The occurrence of *Croton bonplandianus* in Java and a new record of *Caperonia palustris* for Malesia Region. *Journal of Tropical Biology & Conservation*, 17, pp.273-283. doi: 10.51200/jtbc.v17i.2668.

Al Anshori, Z. et al., 2022. First Record of Naturalized *Acmella brachyglossa* and *Acmella radicans* (Asteraceae: Heliantheae) in Java, Indonesia. *Floribunda*, 7(1), pp.18-25. doi: 10.32556/floribunda.v7i1.2022.389.

Backer, C.A. & Bakhuizen van den Brink, R.C., 1963. *Flora of Java. Vol. I*, Groningen, The Netherlands: N.V.P. Noordhoff.

Blancke, R., 2016. *Tropical Fruits and Other Edible Plants of The World: An illustrated guide*, Ithaca, New York: Cornell University Press.

Beentje, H., 2012. *Kew plant glossary: An illustrated dictionary of plant terms (revised edition)*, London: Kew Royal Botanic Gardens.

Bridson, D.M. & Forman, L.L., 1998. *The Herbarium Handbook. 3rd ed.*, London: Kew Royal Botanic Gardens.

Brinckmann, J., 2013. *Market Analysis for Three Peruvian Natural Ingredients*, Geneva: International Trade Center.

Cardinal-McTeague, W.M. & Gillespie, L.J., 2016. Molecular phylogeny and pollen evolution of Euphorbiaceae tribe Plukenetieae. *Systematic Botany*, 41(2), pp.329-347. doi: 10.1600/036364416X691759.

Cardinal-McTeague, W.M. & Gillespie, L.J., 2020. A revised sectional classification of *Plukenetia* L. (Euphorbiaceae, Acalyphoideae) with four new species from South America. *Systematic Botany*, 45(3), pp.507-536. doi: 10.1600/036364420X15935294613572.

Choo, L.M., Ng, X.Y. & Lua, H.K., 2022. Rediscovery and lectotypification of a native vine, *Plukenetia corniculata* Sm. (Euphorbiaceae), in Singapore. *Nature in Singapore*, 15, doi: 10.26107/NIS-2022-0001.

Djarwaningsih, T., 2010. Rekaman baru beberapa jenis tumbuhan di Jawa. *Floribunda*, 4(1), pp.15-17. doi: 10.32556/floribunda.v4i1.2010.81.

Djarwaningsih, T. 2012. Species diversity of Euphorbiaceae in Karimunjawa Islands and new record for Java. *Jurnal Teknologi Lingkungan*, Edisi Khusus "Hari Bumi", pp.75-88.

Djarwaningsih, T., 2013. Koleksi lama herbarium tumbuhan Jawa yang luput dari pengamatan Backer. *Floribunda*, 4(6), pp.160. doi: 10.32556/floribunda.v4i6.2013.106.

Effendi, S. & Mustaqim, W.A., 2021. *Alstonia macrophylla* (Apocynaceae): A new record of naturalized species in Java, Indonesia. *Floribunda*, 6 (6), pp.207-212. doi: 10.32556/floribunda.v6i6.2021.321.

Flores, D., 2010. *Uso Histórico: Sacha Inchi Plukenetia volubilis* L., Peru: Proyecto Biocomercioperu.

Flores, D. & Lock, O., 2013. Revalorizando el uso milenario del sacha inchi (*Plukenetia volubilis* L.) para la nutrición, la salud y la cosmética. *Rev. Fitoter*, 13(1), pp.23-30.

Gillespie, L.J., 1993. A synopsis of neotropical *Plukenetia* (Euphorbiaceae) including two new species. *Systematic Botany*, 18(4), pp.575-592.

Gillespie, L.J., 2007. A revision of paleotropical *Plukenetia* (Euphorbiaceae) including two new species from Madagascar. *Systematic Botany*, 32(4), pp.780-802. doi: 10.1600/036364407783390782.

Gillespie, L.J. & Larsen S.S., 2020. 'Plukenetia' in *Flora of Thailand*, viewed 3 May 2023, from https://www.nationaalherbarium.nl/ThaiEuph/ThPspecies/Th*Plukenetia*T.htm.

Gonzalez-Aspajo, G. et al., 2015. Sacha Inchi Oil (*Plukenetia volubilis* L.), effect on adherence of *Staphylococcus aureus* to human skin explant and keratinocytes in vitro. *Journal of Ethnopharmacology*, 171, pp.330-334. doi: 10.1016/j.jep.2015.06.009.

Hariri, M.R., Irsyam, A.S.D. & Irwanto, R.R., 2019. *Plumeria pudica* Jacq.: Tambahan untuk Marga *Plumeria* (Apocynaceae) di Jawa. *Biotika Jurnal Ilmiah Biologi*, 17(2), pp.1-8. doi: 10.24198/biotika.v17i2.25454.

Hariri, M.R. et al., 2020. *Phyllanthus myrtifolius* (Moon ex Wight) Mull. Arg. and *Phyllanthus tenellus* Roxb. (Phyllanthaceae) in Java. *Floribunda*, 6(5), pp.188-194. doi: 10.32556/floribunda.v6i5.2020.308.

Irsyam, A.S.D. et al., 2019. Rekaman baru *Euphorbia graminea* Jacq. dan *E. hyssopifolia* L.(Euphorbiaceae) di Pulau Jawa. *Biotika Jurnal Ilmiah Biologi*, 17(1), pp.16-24. doi: 10.24198/bjib.v17i1.21902.

Irsyam, A.S.D. et al., 2020. The Genus *Cnidoscolus* Pohl (Euphorbiaceae) in Java. *Jurnal Al Kauniyah*, 13(1), pp.76-86. doi: 10.15408/kauniyah.v13i1.12704.

Irsyam, A.S.D. et al., 2021. Note on the genus *Dorstenia* Plum. ex L. (Moraceae) in Java (Indonesia) and noteworthy information on the identity of *D. bahiensis* through ITS sequence. *Biodiversitas*, 22(8), pp.3358-3363. doi: 10.13057/biodiv/d220832.

Irsyam, A.S.D. et al., 2022. Five newly recorded alien species of *Hydrocotyle* Tourn. ex L. (Araliaceae) in Java, Indonesia. *Check List*, 18(4), pp.763-772. doi: 10.15560/18.4.763.

Kodahl, N., 2020. Sacha inchi (*Plukenetia volubilis* L.)—from lost crop of the Incas to part of the solution to global challenges?. *Planta*, 251 (4), p.80. doi: 10.1007/s00425-020-03377-3.

Kodahl, N. & Sørensen, M., 2021. Sacha inchi (*Plukenetia volubilis* L.) is an underutilized crop with a great potential. *Agronomy*, 11(6), p.1066. doi: 10.20944/preprints202105.0090.v1.

Maya, I. & Sriwidodo, 2022. Potensi Minyak Biji Sacha Inchi Sebagai Anti-aging dalam Formula Kosmetik. *Majalah Farmasetika*, 7(5), pp.407-423. doi: 10.24198/mfarmasetika.v7i5.39510.

Metusala, D. & Supriatna, J., 2017. *Gastrodia bambu* (Orchidaceae: Epidendroi-deae), a new species from Java, Indonesia. *Phytotaxa*, 317 (3), pp.211-218. doi: 10.11646/phytotaxa.317.3.5.

Mustaqim, W.A. & Setiawan, E., 2021. An addition to the alien flora of Java: the first record of adventive *Costus dubius* (Costaceae). *Jurnal Biologi Tropis*, 21(2), pp.496-500. doi: 10.29303/jbt.v21i2.2514.

Peniwidiyanti, P. et al., 2021. Newly recorded alien species of *Ficus* L. (Moraceae) in Java, Indonesia. *Journal of Tropical Biodiversity and Biotechnology*, 6(2), p.65313. doi: 10.22146/jtbb.65313.

Plants of The World Online (POWO), 2023, '*Plukenetia volubilis* L.' in *Plants of The World Onlines*, viewed 01 February 2023, from https://powo.science.kew.org/taxon/urn:lsid:ipni.org:names:354970-1

Poomanee, W. et al., 2021. Application of factorial experimental design for optimization and development of color lipstick containing antioxidant-rich Sacha inchi oil. *Pakistan Journal of Pharmaceutical Sciences*, 34(4), pp.1437-1444. doi: 10.36721/PJPS.2021.34.4.REG.1437-1444.1.

Puspitaningrum, D., Mustaqim, W.A. & Ardiyani, M., 2017. A new record of *Etlingera pauciflora* (Zingiberaceae) in Java, Indonesia. *Reinwardtia*, 16(1), pp.1-4. doi: 10.14203/reinwardtia.v16i1.2825.

Rahayu, S. & Rodda, M., 2019. *Hoya amicabilis* sp. nov. (Apocynaceae, Asclepiadoideae), from Java discovered on Facebook. *Nordic Journal of Botany*, 37(12), pp.1-6. doi: 10.1111/njb.02563.

Rugayah, E.A., Widjaja & Praptiwi, 2004. *Pedoman Pengumpulan Data Keanekaragaman Flora*, Bogor: Pusat Penelitian Biologi-LIPI.

Sathe, S.K. et al., 2002. Isolation, purification, and biochemical characterization of a novel water-soluble protein from Inca peanut (*Plukenetia volubilis* L.). *Journal of Agricultural and Food Chemistry*, 50(17), pp.4906-4908. doi: 10.1021/jf020126a.

Silalahi, M., 2022. Sacha inchi (*Plukenetia volubilis* L.): Its potential as foodstuff and traditional medicine. *GSC Biological and Pharmaceutical Sciences*, 18(3), pp.213-218. doi: 10.30574/gscbps.2022.18.3.0117.

Soimee, W. et al., 2019. Evaluation of moisturizing and irritation potential of sacha inchi oil. *Journal of Cosmetic Dermatology*, 19(4), pp. 915-924. doi: 10.1111/jocd.13099.

Torres Sánchez, E.G., Hernández-Ledesma, B. & Gutiérrez, L.F., 2021. Sacha inchi oil press-cake: physicochemical characteristics, food-related applications, and biological activity. *Food Reviews International*, 39(1), pp.148-159. doi: /10.1080/87559129.2021.1900231.

van Welzen, P.C., 2020. Key to the families and genera of Malesian Euphorbiaceae in the wide sense. *Blumea*, 65(1), pp.53-60. doi: 10.3767/blumea.2020.65.01.05.

Wang, S., Zhu, F. & Kakuda, Y., 2018. Sacha inchi (*Plukenetia volubilis* L.): Nutritional composition, biological activity, and uses. *Food Chemistry*, 265, pp.316-328. doi: 10.1016/j.foodchem.2018.05.055.

WFO, 2023. '*Plukenetia corniculata* Sm.', in *WFO The World Flora Online*, viewed 4 May 2023, from http://www.worldfloraonline.org/taxon/wfo-0000279029.

Journal of Tropical Biodiversity and Biotechnology
Volume 09, Issue 01 (2024): jtbb76451
DOI: 10.22146/jtbb.76451

Short Communications

Scanning Electron Microscopy Analysis of Tea's Embryo Axis Explant Cultured on Murashige and Skoog Medium Containing 2,4-Dichlorophenoxyacetic acid

Ratna Dewi Eskundari[1,2], Taryono[1,3,5]*, Didik Indradewa[3], Yekti Asih Purwestri[1,4]
1)Department of Biotechnology, Graduate School of Universitas Gadjah Mada. Yogyakarta 55281, Indonesia.
2)Biology Education Study Program, Faculty of Teacher Training and Education, Universitas Veteran Bangun Nusantara, Sukoharjo, 57521, Central Java, Indonesia.
3)Department of Agriculture, Faculty of Agriculture, Universitas Gadjah Mada. Yogyakarta 55281, Indonesia.
4)Department of Tropical Biology, Faculty of Biology, Universitas Gadjah Mada. Yogyakarta 55281, Indonesia.
5)Agrotechnology Innovation Center, Universitas Gadjah Mada. Yogyakarta, Indonesia.
* Corresponding author, email: tariono60@ugm.ac.id

Keywords:
Camellia sinensis
somatic embryo
tea
ultrastructure
Submitted:
21 July 2022
Accepted:
07 September 2023
Published:
12 February 2024
Editor:
Furzani Binti Pa'ee

ABSTRACT
Camellia sinensis L. is an important crop in Indonesia as healthy beverage that contains several secondary metabolism compounds, such as polyphenols and catechins. Tissue culture including somatic embryogenesis and organogenesis has been used for propagating plant for various needs. In this present short-communication, scanning electron microscopic (SEM) analysis of tea was conducted and discussed. This study aimed to investigate surface ultrastructure of TRI2025 embryo axis tea clone cultured on Murashige and Skoog (MS) medium containing 2,4-Dichlorophenoxyacetic acid (2,4-D). The results revealed two different forms of explant's development, i.e. somatic embryo and transitional form between somatic embryogenesis and organogenesis; or called by "Globular-like Structure" (GLS). Surface ultrastructure analysis of somatic embryo and GLS revealed respectively many stages of somatic embryo development i.e. globular, torpedo, and cotyledon stage, and leaf development form GLS regeneration.

Copyright: © 2024, J. Tropical Biodiversity Biotechnology (CC BY-SA 4.0)

Tea is perennial and cross-pollinated plant (Mondal et al. 2004) with long life span and cultivated for its leaves. Tea's antioxidant contents such as polyphenols and catechins were reported as agent of anti-aging, anticancer, and antitumor (Lambert & Yang 2003; Zaveri 2006; Khan & Mukhtar 2019). According to the above studies, it is well known that tea's leaf can be formulated as healthy drink.

According to those facts, it is important to increase tea production for following the increasing of world population growth. For its propagation, it is well known that generative propagation of tea is by seed. However, in tea, seed propagation has disadvantages such as self-sterility (Chen et al. 2012) and adversity of manual pollination (Mondal et al. 2004) so that they made vegetative propagation became one of alternative choice for its clonal propagation. Furthermore, promising vegetative propagation methods such as cutting or grafting has many disadvantages such as limitation of source plant and lack of tap-root system (Mondal et al. 2004) so it brings up micropropagation or tissue culture being an al-

ternative choice for propagating tea within short-time with high yielding of propagated-plants.

Recently, micropropagation can be done by two common regeneration pathways, i.e. somatic embryogenesis and organogenesis. In somatic embryogenesis, totipotent ability of plant somatic cell is induced to develop a whole plant. During this process, biochemical changes occur resulting in growth and development of explant into a whole plant. In somatic embryogenesis, explant progresses through successive morphogenetic stages termed globular, heart-shaped, torpedo, and cotyledonary stage for dicots and conifers, or globular, scutellar, and coleoptilar stage for monocots. In tea, successful somatic embryogenesis regeneration has been reported with several types of clone and specific growth mediums (Akula & Dodd 1998; Tahardi et al. 2000; Seran et al. 2006; Kaviani 2013; Eskundari et al. 2018).

Another regeneration pathway in micropropagation is organogenesis. It also uses somatic cells as explants and goes through two stages of propagation, called by shoot and root induction (Duclercq et al. 2011). There are several successful reports of tea's organogenesis using specific mediums and plant growth regulations (PGRs) (Mondal et al. 1998; Gunasekare & Evans 2000; Gunasekare & Evans 2000; Gonbad et al. 2014).

Surface ultrastructure analysis gives detailed information about surface condition an object(s), and this analysis has been conducted for tissue culture of many commercial plants. Steinmacher et al. (2011) reported surface ultrastructure analysis of peach's globular stage with small groups of somatic embryos until its further development. Kumar et al. (2015) reported surface ultrastructure analysis of indirect somatic embryogenesis of *Pelargonium sidoides*. Mandal & Datta (2005) also reported asynchronous developmental stages of direct somatic embryogenesis from ray floret explant of *Chrysanthemum* using scanning electron microscopy.

Recently, surface ultrastructure analysis of tea's leaf powder showed the presence of many leaf's fragment and layer quiet lit of fine hairs (Ekayanti et al. 2017). Particularly, embryo axis of TRI2025 tea clone cultured on MS medium containing 2,4-D has not been observed yet by scanning electron microscopy to confirm and to reveal the detailed development of *in vitro* regeneration. The important significance of this study relies on the necessity of surface ultrastructure analysis for characterizing the process of tea's *in vitro* regeneration. The objective of the present study is to use scanning electron microscopy to obtain information regarding *in vitro* regeneration of TRI2025 tea clone cultured on MS medium containing 2,4-D.

Seed of TRI2025 tea clone were sterilized with antibacterial (Agrept 20 WP; Streptomicin sulphate 20%) and antifungal (Dithane M-45; Mankozeb 80%) then washed with running water. After that, those that were sterilized with 96% ethanol, burned, and cut their shell off to get uncovered seed aseptically. The embryonic axes then were taken, removed their growth points and then cultured on MS medium containing 2,4-D with concentration 0; 1; 2; and 5 mg. L^{-1}. Induction of somatic embryogenesis and GLS regeneration were conducted following Eskundari et al. (2018).

Somatic embryos and GLS with many stages were vacuumed for several minutes then were coated with platinum particles JEC-3000FC (JEOL, Tokyo, Japan). After that, somatic embryos and GLS were analysed to get surface ultrastructure information using scanning electron microscopy JSM-6510LA (JEOL, Tokyo, Japan).

Surface ultrastructure analysis revealed smooth surface at former incision of shoot apical meristem (SAM) at 0-DAC (Figure 1A). These explants then cultured on MS medium containing 2,4-D 2 mg.L^{-1} for inducing somatic embryogenesis. The selection of 2,4-D as PGR for inducing somatic embryogenesis was based on consideration that 2,4-D is a powerful embryogenesis inducer and has succeeded in triggering explant response to embryogenesis (Caeiro et al. 2022; Gustian et al. 2022) although it was also reported can result in abnormalities related to epigenetic and genetic changes (Fraga et al. 2016; de Morais Oliveira et al. 2023). All of explants showed the mountain-like structure exactly at centre of former incision of SAM after 7-DAC (Figure 1B).

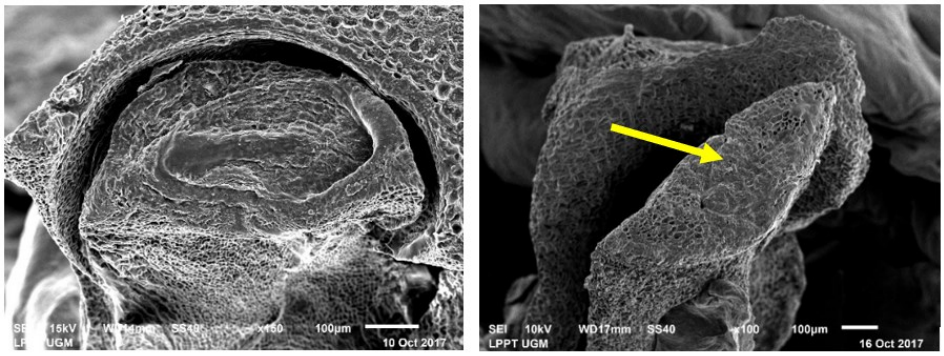

A B

Figure 1. Surface ultrastructure analysis of embryonic axis of TRI2025 tea clone. Removed growth point of embryonic axis at SAM at 0-DAC (A); Explant cultured on induction medium at 7-DAC (B). Yellow arrow showed mountain-like structure. Bars: 100 µm.

This mountain-like structure later called hereinafter referred to as GLS, viz., "transition" phenomenon between somatic embryogenesis and organogenesis; such as reported in *Camellia* genus (Lu et al. 2013). Seran et al. 2006 named this structure by nodular embryogenic structure or small succulent leaves. This structure can be induced by culturing explant on different medium either PGR(s) such as MS or Woody Plant Medium (WPM) using Kinetin, 6-Benzylaminopurine (BAP), and 1-Naphtaleneacetic Acid (NAA) as PGR(s) (Seran et al. 2006; Lu et al. 2013). In this study, this unique structure was almost similar to globular stage in somatic embryogenesis at its first occurrence, then it developed to be leaf with increasing culturing time.

This GLS formed in almost all of explants cultured on induction medium at 30-DAC. This GLS later developed to be leaf (Figure 2A) following its own mechanism that differ with common leaf development pathway. At first initial appearance, GLS structure was similar with early globular stage at somatic embryogenesis then it developed to be heart-like structure with indentation at its centre (Figure 2B). Later, this structure developed to "blooming-like" phenomenon with wider indentation (Figure 2C) compared to previous stage (see Figure 2B) and finally developed to be leaf.

In this study, a mountain-like structure at former incision of SAM was initial response of explant cultured on MS medium containing 2,4-D. This structure might be a response through reconstruction meristem by peripheral region cells, such as reported on tomato (Reinhardt et al. 2003). Auxin might be important for this process due to auxin's role at peripheral zone. Two most important genes related to auxin, PIN-FORMED1 (PIN1) (Reinhardt et al. 2000) and AUX1 (Reinhardt et al. 2003), were reported mainly worked at peripheral zone of SAM.

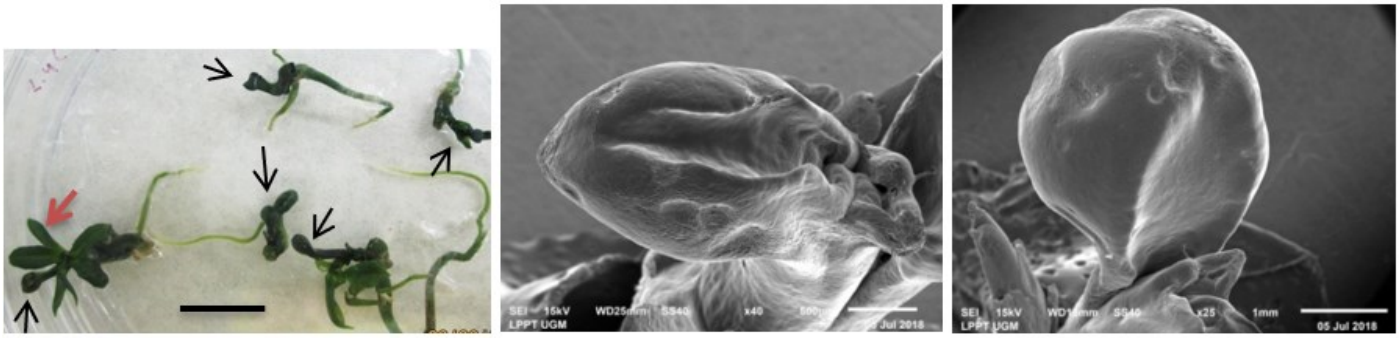

A B C

Figure 2. Morphological and surface ultrastructure analysis of GLS of TRI2025 tea clone. Morphological analysis of GLS-derived leaf (A); surface ultrastructure analysis at early stage of GLS (B); surface ultrastructure analysis at late stage of GLS (C). Black arrows indicated GLS, red arrows indicated GLS developing into leaves. Bars: 100 mm (A); 500 μm (B); 1 mm (C).

In this study, we proved that GLS was another pathway for leaf development. This unique structure was always seen at the initial stage of this process. Later, a heart-like structure with thick form confirmed to be further stage of this process and it might be a sponge-like structure inside. Eskundari et al. (2019) reported approximately 55,76 KDa of protein band found only at GLS and it might relate to stress-induced or storage protein.

Somatic embryogenesis was also occurred when explant cultured on induction medium, but occurrence of somatic embryo was fewer than that of GLS. Somatic embryos were unsynchronised form in morphology; one of them was at globular stage and the others were at further ones (Figure 3A). Surface ultrastructure analysis confirmed that unsynchronised form of somatic embryo i.e. the globular, heart, and torpedo stage occurred at an explant (Figure 3B).

Globular stage of somatic embryo was densely cytoplasmic structure and transparent in colour. Surface ultrastructure analysis revealed that globular embryo has globular shape and small in size, but surface ultrastructure of torpedo stage showed bigger size compared with globular, and has stem-like morphology with long pipe and pointed end. This globular embryo was similar with *Swertia chirayita* globular embryo from leaf explants cultured on MS medium containing 2,4-D and kinetin

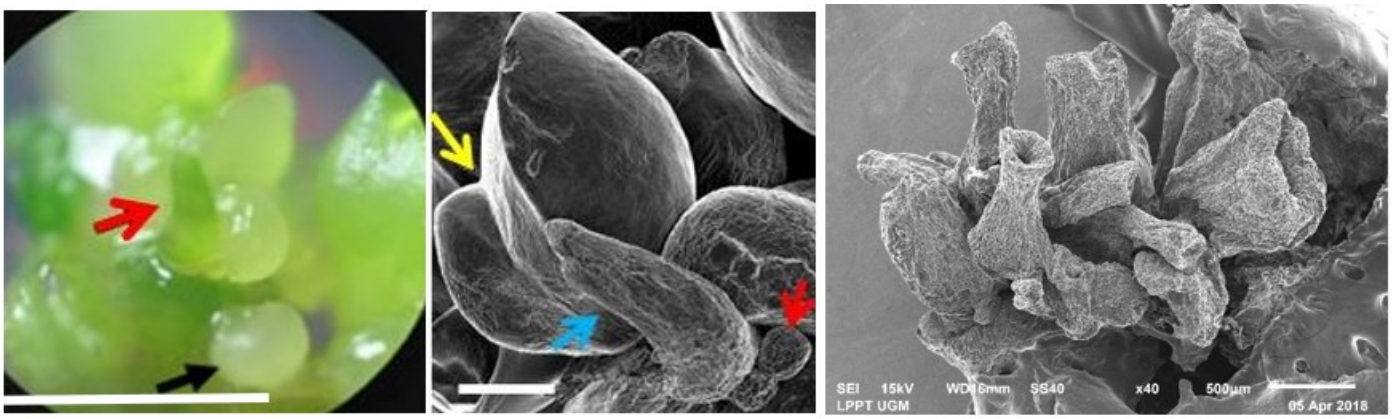

A B C

Figure 3. Morphological and surface ultrastructure analysis of somatic embryos of TRI2025 tea clone. Morphological analysis of somatic embryo at globular (black arrow) and torpedo stage (red arrow) (A); surface ultrastructure analysis of somatic embryo at globular (red arrow), heart (yellow arrow), and torpedo stage (blue arrows) (B); Abnormal of somatic embryo at cotyledon stage (C). Bars: 10mm (A); 500μm (B-C).

(Kumar & Chandra 2014) and in *Dendrobium* from leaf explants cultured on MS medium containing TDZ (Chung et al. 2007) .

Surface ultrastructure analysis revealed elongated structure at torpedo stage and this was distinctive shape with other stages. This morphology was similar with globular embryo of *Catharanthus roseus*, with specific elongated structure without any groove at apex region (Aslam et al. 2014). In this study, we also confirmed abnormality in somatic embryo at cotyledon stage marked by abnormal cup-shaped structure (Figure 3C). This abnormality was probably caused by usage of 2,4-D. Hadfi et al. (1998) reported many abnormalities in cotyledon stage of *Brassica juncea* and this abnormality might be caused by auxin and its inhibitors. In contrast with this study, Aslam et al. (2014) reported normal cotyledon stage of *Catharanthus roseus* characterized by the presence of two cotyledons that later developed to be leaf primordial from hypocotyl plant cultured on MS medium containing 2,4-D. Therefore, surface ultrastructure analysis using SEM along with others analysis such as morphology and histology are very useful for better understanding related to plant development.

Induction medium containing 2,4-D was powerful PGR for inducing GLS and somatic embryogenesis. This phenomenon could be associated with strong capability of 2,4-D for inducing somatic embryogenesis, as reported in many plant tissue culture (Raghavan 2004; Kaviani 2013; Aslam et al. 2014; Eskundari et al. 2018). Early response of explant cultured on growth medium containing 2,4-D in this study was relatively fast i.e. 7-DAC. This result was similar with inducing indirect somatic embryogenesis in *Arabidopsis* using 2,4-D that only needed 10-DAC for callusing (Raghavan 2004) and direct organogenesis in *Passiflora* that only needed few days (Fernando et al. 2007). In sugarcane, callus as first response of explants cultured on induction medium (containing 2,4-D, kinetin, and IAA) could be seen at 3-DAC (Rodríguez et al. 1996).

Surface ultrastructure analysis on tissue culture has been reported in many commercial plants. Surface ultrastructure analysis in maize revealed callus occurrence when shoot tips explant cultured on MS medium containing 2,4-D, benzyladenine, and adenin (Marín-Méndez et al. 2009). Rodríguez et al. (1996) revealed that sugarcane's callus was also as first response when spindle explants cultured on MS medium containing 2,4-D, kinetin, and IAA using SEM.

In this study, we did not prepare samples using a fixation solution. Dehydration step was done by vacuuming samples for a few moments. In our opinion, this unusual sample preparation technique still produced good SEM images because the vacuum technique was carried out only a few moments and the platinum are immediately coated. This is intended to reduce sample's damage due to fragility of the sample's structure and presence of a large number of air voids. It can be seen at SEM image that the sample remained in good condition, no imbalance of light-dark distribution was detected on sample surface. Simplification of sample preparation process for SEM analysis has been widely reported, such as in blood samples using tetramethylsilane (TMS) (Ting-Beall et al. 1995) and in cell culture using carbon tape continued air-drying (Ali et al. 2021).

This study showed the stages of somatic embryogenesis and GLS regeneration of tea using SEM so that might be useful for increasing the knowledge on tea's tissue culture. Globular, heart, and torpedo stages could be seen clearly but cotyledonary stage was in abnormality. GLS regeneration might be the other pathway of leaf development on tissue culture-derived plant.

AUTHOR CONTRIBUTION

R.D.E, T.T., D.I., and Y.A.P. designed the research. R.D.E. collected and analysed data and wrote the manuscript. T.T., D.I., and Y.A.P. supervised all the processes.

ACKNOWLEDGMENTS

The authors would like to thank to the Indonesian Ministry of Research and Technology-Higher Education (Kemristek-DIKTI) for the scholarship of BPPDN-DIKTI. The Authors also said thank you for PT. Pagilaran for supplying TRI2025 tea's fruit for explant.

CONFLICT OF INTEREST

The authors declare that there is no conflict of interest in preparing this research article.

REFERENCES

Akula, A. & Dodd, W.A., 1998. Direct somatic embryogenesis in a selected tea clone, "TRI-2025" (Camellia sinensis (L.) O. Kuntze) from nodal explants. *Plant Cell Reports*, 17(10), pp.804–809. doi: 10.1007/s002990050487.

Ali, R., El-Boubbou, K. & Boudjelal, M., 2021. An easy, fast and inexpensive method of preparing a biological specimen for scanning electron microscopy (SEM). *MethodsX*, 8, 101521. doi: 10.1016/j.mex.2021.101521.

Aslam, J., Mujib, A. & Sharma, M.P., 2014. Somatic Embryos in Catharanthus roseus: A Scanning Electron Microscopic Study. *Notulae Scientia Biologicae*, 6(2), pp.167–172. doi: 10.15835/nsb629337.

Caeiro, A. et al., 2022. Induction of Somatic Embryogenesis in Tamarillo (Solanum betaceum Cav.) Involves Increases the Endogenous Auxin Indole-3-Acetic Acid. *Plants*, 11(10), 1347. doi: 10.3390/plants11101347.

Chen, X. et al., 2012. Late-acting self-incompatibility in tea plant (Camellia sinensis). *Biologia*, 67(2), pp.347–351. doi: 10.2478/s11756-012-0018-9.

Chung, H.H., Chen, J.T. & Chang, W.C., 2007. Plant regeneration through direct somatic embryogenesis from leaf explants of Dendrobium. *Biologia Plantarum*, 51(2), pp.346–350. doi: 10.1007/s10535-007-0069-x.

Duclercq, J. et al., 2011. De novo shoot organogenesis: From art to science. *Trends in Plant Science*, 16(11), pp.597–606. doi: 10.1016/j.tplants.2011.08.004.

Ekayanti, M. et al., 2017. Pharmacognostic and phytochemical standardization of white tea leaf (Camellia sinensis L. Kuntze) ethanolic extracts. *Pharmacognosy Journal*, 9(2), pp.221–226. doi: 10.5530/pj.2017.2.37.

Eskundari, R.D. et al., 2018. Induction of Indirect Somatic Embryogenesis on Embryonic Axis of TRI2025 Tea Clone. *Journal of Agricultural Science*, 10(10), 224. doi: 10.5539/jas.v10n10p224.

Eskundari, R.D. et al., 2019. Protein Profile of Tissue Culture of TRI2025 Tea Clone. *Biosaintifika: Journal of Biology & Biology Education*, 11(1), pp.8–14. doi: 10.15294/biosaintifika.v11i1.17522.

Fernando, J.A. et al., 2007. New insights into the in vitro organogenesis process: The case of Passiflora. *Plant Cell, Tissue and Organ Culture*, 91(1), pp.37–44. doi: 10.1007/s11240-007-9275-7.

Fraga, H.P.F. et al., 2016. DNA methylation and proteome profiles of Araucaria angustifolia (Bertol.) Kuntze embryogenic cultures as affected by plant growth regulators supplementation. *Plant Cell, Tissue and Organ Culture*, 125(2), pp.353–374. doi: 10.1007/s11240-016-0956-y.

Gonbad, R.A. et al., 2014. Influence of cytokinins in combination with GAon shoot multiplication and elongation of tea clone iran 100 (camellia sinensis (L.) O. kuntze). *The Scientific World Journal*, 2014, 943054. doi: 10.1155/2014/943054.

Gunasekare, M. & Evans, P., 2000. In Vitro Shoot Organogenesis in Callus Derived from Stem Tissue of Tea (Camellia sinensis L.). *S.L.J. Tea Sci*, 66(1/2), pp.16–26.

Gustian et al., 2022. Somatic Embryogenesis of Soybean Glycine Max (L.) Merr. *IOP Conference Series: Earth and Environmental Science*, 1097, 012012. doi: 10.1088/1755-1315/1097/1/012012.

Hadfi, K., Speth, V. & Gunther, N., 1998. Auxin-induced developmental patterns in Brassica juncea embryos. *Development*, 125(5), pp.879–887. doi: 10.1086/327427.

Kaviani, B., 2013. Somatic Embryogenesis and Plant Regeneration from Embryonic Axes and Cotyledons Explants of Tea (Camellia sinenesis L.). *Journal of Ornamental and Horticultural Plants*, 3(1), pp.33–38.

Khan, N. & Mukhtar, H., 2019. Tea polyphenols in promotion of human health. *Nutrients*, 11(1), 39. doi: 10.3390/nu11010039.

Kumar, V. & Chandra, S., 2014. High frequency somatic embryogenesis and synthetic seed production of the endangered species Swertia chirayita. *Biologia (Poland)*, 69(2), pp.186–192. doi: 10.2478/s11756-013-0305-0.

Kumar, V., Moyo, M. & Van Staden, J., 2015. Somatic embryogenesis of Pelargonium sidoides DC. *Plant Cell, Tissue and Organ Culture*, 121(3), pp.571–577. doi: 10.1007/s11240-015-0726-2.

Lambert, J.D. & Yang, C.S., 2003. Mechanisms of Cancer Prevention by Tea Constituents. *The Journal of nutrition*, 133(27), pp.3255–3261. Available at: http://www.ncbi.nlm.nih.gov/pubmed/17073577.

Lu, J. et al., 2013. Plant regeneration via somatic embryogenesis and shoot organogenesis from immature cotyledons of Camellia nitidissima Chi. *Journal of Plant Physiology*, 170(13), pp.1202–1211. doi: 10.1016/j.jplph.2013.03.019.

Mandal, A.K.A. & Datta, S.K., 2005. Direct somatic embryogenesis and plant regeneration from ray florets of chrysanthemum. *Biologia Plantarum*, 49(1), pp.29–33. doi: 10.1007/s10535-005-0033-6.

Marín-Méndez, W. et al., 2009. Ultrastructure and histology of organogenesis induced from shoot tips of maize (Zea mays, Poaceae). *Revista de Biologia Tropical*, 57(SUPPL. 1), pp.129–139.

Mondal, T., Bhattacharya, Amita Laxmikumaran, M. & Ahuja, P.S., 2004. Recent Advances of Tea (Camellia Sinensis) Biotechnology. *Plant Cell, Tissuea nd Organ Culrure*, 76(3), pp.195–254. doi: 10.1023/B.

Mondal, T.K. et al., 1998. Micropropagation of tea (Camellia sinensis (L.) O. Kuntze) using thidiazuron. *Plant Growth Regulation*, 26(1), pp.57–61. doi: 10.1023/A:1006019206264.

de Morais Oliveira, J.P. et al., 2023. Embryonic abnormalities and genotoxicity induced by 2,4-dichlorophenoxyacetic acid during indirect somatic embryogenesis in Coffea. *Scientific Reports*, 13(1), pp.1–14. doi: 10.1038/s41598-023-36879-7.

Raghavan, V., 2004. Role of 2 4-dichlorophenoxyacetic acid 2 4-D in somatic embryogenesis on. *American J of Botany*, pp.1743–1756. doi: 10.3732/ajb.91.11.1743.

Reinhardt, D. et al., 2003. Regulation of phyllotaxis by polar auxin transport. *Nature*, 426(6964), pp.255–260. doi: 10.1038/nature02081.

Reinhardt, D., Mandel, T. & Kuhlemeier, C., 2000. Auxin regulates the initiation and radial position of plant lateral organs. *Plant Cell*, 12 (4), pp.507–518. doi: 10.1105/tpc.12.4.507.

Rodríguez, S. et al., 1996. Sugarcane somatic embryogenesis: A scanning electron microscopy study. *Tissue and Cell*, 28(2), pp.149–154. doi: 10.1016/S0040-8166(96)80003-6.

Seran, T.H., Hirimburegama, K. & Gunasekare, M.T.K., 2006. Somatic Embryogenesis from Embryogenic Leaf Callus of Tea (*Camellia sinensis* (L .) Kuntze). *Tropical Agricultural Research*, 18.

Steinmacher, D.A. et al., 2011. A temporary immersion system improves in vitro regeneration of peach palm through secondary somatic embryogenesis. *Annals of Botany*, 108(8), pp.1463–1475. doi: 10.1093/aob/mcr033.

Tahardi, J. et al., 2000. Direct somatic embryogenesis and plant regeneration in tea by temporary liquid immersion. *Menara Perkebunan*, 68 (1), pp.1–9.

Ting-Beall, H.P., Zhelev, D. V. & Hochmuth, R.M., 1995. Comparison of different drying procedures for scanning electron microscopy using human leukocytes. *Microscopy Research and Technique*, 32(4), pp.357–361. doi: 10.1002/jemt.1070320409.

Zaveri, N.T., 2006. Green tea and its polyphenolic catechins: Medicinal uses in cancer and noncancer applications. *Life Sciences*, 78(18), pp.2073–2080. doi: 10.1016/j.lfs.2005.12.006.

Journal of Tropical Biodiversity and Biotechnology
Volume 09, Issue 01 (2024): jtbb87438
DOI: 10.22146/jtbb.87438

Short Communications

Occurrence of Cassava Lace Bug *Vatiga illudens* (Drake, 1922) (Hemiptera: Heteroptera: Tingidae) in Bali, Indonesia

I Putu Sudiarta[1]*, Shah Mahapati Dinarkaya[1], Komang Saraswati Devi[1], I Putu Bawa Ariyanta[1,2], Gusti Ngurah Alit Susanta Wirya[1], Dwi Sugiarta[1], Dewa Gede Wiryangga Selangga[1], I Wayan Diksa Gargita[1], Putu Perdana Kusuma Wiguna[1], Ketut Ayu Yuliadhi[1], Putu Shinta Devi[3]

1)Faculty of Agriculture Udayana University. Panglima Sudirman Street, Dangin Puri, Denpasar, Bali, Indonesia, 80232
2)Karangasem Department of Agriculture, Ngurah Rai Street no. 61 Amlapura, Karangasem, Bali, Indonesia, 80811
3)Denpasar Agriculture Quarantine Station, Sesetan Street No.312, Pedungan, South Denpasar, Denpasar, Bali, Indonesia, 80222
* Corresponding author, email: putusudiarta@unud.ac.id

Keywords:
Alien species
Cassava
Damage symptom
Distribution
Morphology identification
Submitted:
28 July 2023
Accepted:
25 September 2023
Published:
23 February 2024
Editor:
Miftahul Ilmi

ABSTRACT
Cassava Lace Bugs (*CLB*) are native pest of cassava (*Manihot esculenta* Crantz, Euphorbiaceae) to the Neotropical Region, mainly in Brazil. On the other hand, East Java was the first region in Indonesia to record the presence of *CLB* in 2021, however, it has not been reported in other regions in Indonesia. Therefore, the very importance to recognise the occurrence of *CLB* in other regions in Indonesia. Based on this, the research has been carried out starting with a field survey, observing behaviour of insect in the field and identify morphologically in the laboratory. The survey results show that the infestation of *CLB* has been found in lowland, medium, and highland areas in Bali. Symptoms of infestation on the upper leaf surface are small yellow spots with brownish variations. Based on the identification key, *CLB* from Bali Indonesia, shows a characteristic of a head with a pair of frontal spines. Based on this evidence, the *CLB* insect can be identified as *Vatiga illudens* (Hemiptera: Heteroptera: Tingidae). It is the first report of novel distribution areas for *V. illudens* in Bali, Indonesia. The results of this research are important because *V. illudens* is one of the main pests of cassava.

Copyright: © 2024, J. Tropical Biodiversity Biotechnology (CC BY-SA 4.0)

Cassava Lace Bug (*CLB*) is a significant pest of cassava plants (*Manihot esculenta* Crantz, Euphorbiaceae) that are profuse on the undersides of the leaf (Fialho et al. 2009; Bellotti et al. 2012). When exposed to light, the nymphs and adults are extremely active beneath the leaf's surface. This insect damages plant leaf by sucking the liquid from cassava leaf. There are five species of *CLB* (Froeschner 1993), but only two have an economic impact on cassava, *Vatiga illudens* and *V. manihotae* (Bellon et al. 2012; dos Santos et al. 2019). Both species are indigenous to the Neotropical Region (Central America, the Caribbean, and South America), primarily Brazil (Froeschner 1993; Bellon et al. 2017). According to the report by Puspitarini et al. (2021), *CLB* was discovered for the first time in Indonesia, in the East Java region, but has not been reported in any other regions of Indonesia including Bali. Before report by Puspitarini et

al. (2021), the occurrence of the *CLB* in Indonesia has not been documented, including in "The Pests of Crops in Indonesia" (Kalshoven 1981). As well as according to the Indonesian Agency for Agricultural Research and Development, *CLB* has not been distributed in Indonesia (Saleh et al. 2013). If we look at the occurrence of *V. illudens* in Indonesia, it is very similar to *Phenacoccus manihoti*, an invasive pest from South America. *P. manihoti* first entered Africa in 1973 (Schulthess et al. 1991). Then in 2008, the pest was reported to have entered Thailand (Parsa et al. 2012). In 2010, *P. manihoti* entered Indonesia for the first time in Bogor (Muniappan et al. 2011; Muhammad et al. 2019). Likewise, *P. manihoti* entered Bali Province in 2010 (Supartha et al. 2020), and now is it the main pest in Indonesia as well Bali.

Given that *CLB* is native to the Neotropics, like the Neotropical cassava pest *P. manihoti* which entered Indonesia in 2010, the presence of *CLB* must be monitored, as a basis of future control. *Vatiga* spp. infestations was reported as main pest of cassava indicating a yield loss of 39% (Bellotti et al. 1999), and 48–55% (Fialho et al. 2009). Based on this, it is necessary to conduct research in regions other than East Java, including Bali. The research about identifying and mapping these pests is necessary to facilitate further control measures, such as policy-based controls like quarantine.

During the field survey of Cassava mosaic virus vector in January-February 2023 in low (0-400 asl), medium (400-800 asl), and high land (>800 asl) areas in Bali, we found lace bugs in cassava. Sample collection was based on the presence of cassava plants in low, medium and high land area in Bali. Mapping the distribution of the *CLB* pest in the Province of Bali, Indonesia, began with the collection of secondary data to analyse the potential locations of the *CLB* pest. Field surveys were conducted to record the coordinated location of the *CLB* pest. The coordinate point data was then converted into spatial data in a shapefile (shp) format. The spatial data were then arranged to produce a map of the *CLB* distribution in the Province of Bali. When an insect was found in the field, the insect's behaviour was observed and documented, the photo of living individuals of *CLB* in the host plant was taken with Olympus OM-D camera, E-M 1, 50 mm Macro lens. The *CLB* was transported to the laboratory by placing it in 70% alcohol (Bellon et al. 2012). At the Laboratory of Plant Pests and Diseases, Faculty of Agriculture, Udayana University, insect samples were prepared for morphological identification under the microscope Nikon smz25. The characterisation of insect morphology was matched with a key determination from a previous publication by Puspitarini et al. (2021), and validation of the identification process was conducted by Puspitarini.

Based on the survey of the distribution of *CLB* in Bali, it is discovered that *CLB* was found in the lowlands, including the Sesetan (Denpasar), Peguyangan (Denpasar), Munduk Pakel Gadungan (Tabanan), Margarana (Tabanan) areas; medium, including Sidemen (Karangasem), Baturiti (Tabanan); and highland in the Pancasari area (Buleleng). Complete location data and altitude are presented in Table 1, and the distribution map is presented in Figure 1.

CLB is a pest originating in the Neotropics (Froeschner 1993). Currently, *CLB* is already in Indonesia (East Java). In East Java *CLB* was discovered in Malang, Pasuruan, Blitar, Mojokerto, and Probolinggo, according to the findings of Puspitarini et al. (2021). In addition, the distribution of *CLB* Bali has not been reported. As with the invasive parasite *Phenacoccus manihoti* Matile-Ferrero (Hemiptera: Pseudococcidae) on cassava crops in Bali and Indonesia (Muniappan et al. 2011; Supartha et al.

Table 1. The areas of distribution of cassava lace bugs in Bali.

No.	Location	Regency	Altitude (masl)	Coordinate
1	Sesetan	Denpasar	10	8°41'42"S,115°12'50"E
2	Peguyangan	Denpasar	62	8°37'20"S, 115°13'20"E
3	Munduk Pakel Gadungan	Tabanan	264	8°27'39"S, 115°05'15"E
4	Margarana	Tabanan	289	8°27'49"S, 115°09'53"E
5	Sidemen	Karangasem	445	8°27'09"S, 115°27'45"E
6	Baturiti	Tabanan	806	8°20'23"S, 115°11'16"E
7	Pancasari	Buleleng	1200	8°15'04"S, 115°09'05"E

Figure 1. Distribution map of cassava lace bugs (*CLB*) in Bali.

2020), *CLB* must be monitored seriously, to provide the future control.

The symptoms that observed in the field, it is possible to use as a reference to determine the infestation of *CLB*. Symptoms of attack on the upper leaves surface are small yellow spots with brownish variations (Figure 2A). If the attack is heavy, the spots spread across the plant leaves (Figure 2B). Severe attack on young shoots of cassava plants is indicated by symptoms of curling with a brownish yellow colour (Figure 2C). *V. illudens* is a *CLB* species that is very detrimental to cassava plants (Bellotti et al. 1999). According to Bellotti et al. (2012), yellow spots due to *CLB* feed the cassava leaf by sucking the parenchyma cell's protoplasm. It is also reported that heavy damage could reduce cassava production. This is due to leaf damage, characterized by early leaf loss and complete defoliation in cases of severe infestation (Fialho et al. 2009; Bellotti et al. 2012). The symptoms that are caused by *CLB* have almost the same symptoms as other insect attacks such as curled leaves caused by *Phenacoccus manihoti* (Supartha et al. 2020). Therefore, attack symptoms are not an absolute measure to determine the presence of *CLB*. Further research is related to measuring the severity of pest attacks in detail to confirm the effect of *CLB* attacks on reducing yield.

Figure 2. Variation of attack symptoms from the cassava lace bugs (*CLB*) in the form of necrotic spots symptom on its leaves, **A.** Symptoms of attack on the upper leaves surface are small yellow spots with brownish variations, **B.** If the attack is heavy, the spots spread across the plant leaves, **C.** Severe attack on young shoots of cassava plants is indicated by symptoms of curling with a brownish yellow colour.

Lace bugs are generally identified by the lace-like appearance of the dorsum (Figure 3B, 4B, 5B). This is in line with the research by Cho et al. (2020). Morphological identification was carried out following the results of previous publications (Froeschner 1993; Bellon et al. 2012; Puspitarini et al. 2021). Referring to these morphological characters, the key to identification is the head with a pair of frontal spines (median spine), antennal segment I, and the costal area of the hemelytron. According to Bellon et al. (2012), *Vatiga illudens* has small thorns at the anterior angle of the head near the antennae, while *V. manihotae* has a solitary central thorn. Based on this key, the sample from Bali, Indonesia, exhibits the following characteristics: a head with a pair of frontal spines (sometimes lacking one of the pairs, but the position is not in the centre) (Figure 4E, 5E). According to Froeschner (1993) the *V. illudens* has antennal segment I (scape) not longer than head (Figure 4F, 5F). According to Puspitarini et al. (2021) costal area of hemelytron with two rows of areolae without apex throughout its length (Figure 4D, 5D). Those keys show that this species is clearly compatible with *V. illudens* (Figures 3, 4 and 5). *V. illudens* underwent several instars marked by molting (Figure 3AC). Nymphs measure ± 1.5 mm (Figure 3A), adult males measure ± 2.5 mm, and adult females measure ± 2.8 mm (Figures 4A,B,C, and Figures 3B, 5A,B,C, respectively). *V. illudens* lives in groups the lower surface of cassava leaf (Figure 3E,F), and when exposed to sunlight, it moves very quickly.

Male insects (Figure 4) and female insects (Figure 5) are difficult to distinguish based solely on their morphological characteristics. Adult male and female insects have a brownish yellow colour. The difference between the two can be seen in the ventral abdomen (Figure 6). The adult female has a single groove along the midline of the ventral side of the apical part of the abdomen. The adult male has no groove at the apical part of the abdomen (Figure 6), the morphological character was compared with previously report by Puspitarini et al. (2021). Male insects have a distinctive part like nails (claws) at the end of their abdomen (Figure 6B), while females do not have them (Figure 6A). Finally, we conclude the cassava lace bugs (*CLB*) from Bali Indonesia was identified as *Vatiga illudens* (Hemiptera: Heteroptera: Tingidae). The first report of novel distribution areas for *V. illudens* in Bali Indonesia. Information about the presence of this pest is important as an effort to prevent the spread of *CLB*. This is because *CLB* is not a native pest in Indonesia, it is feared that it will become an invasive species such as *Phenacoccus manihoti*.

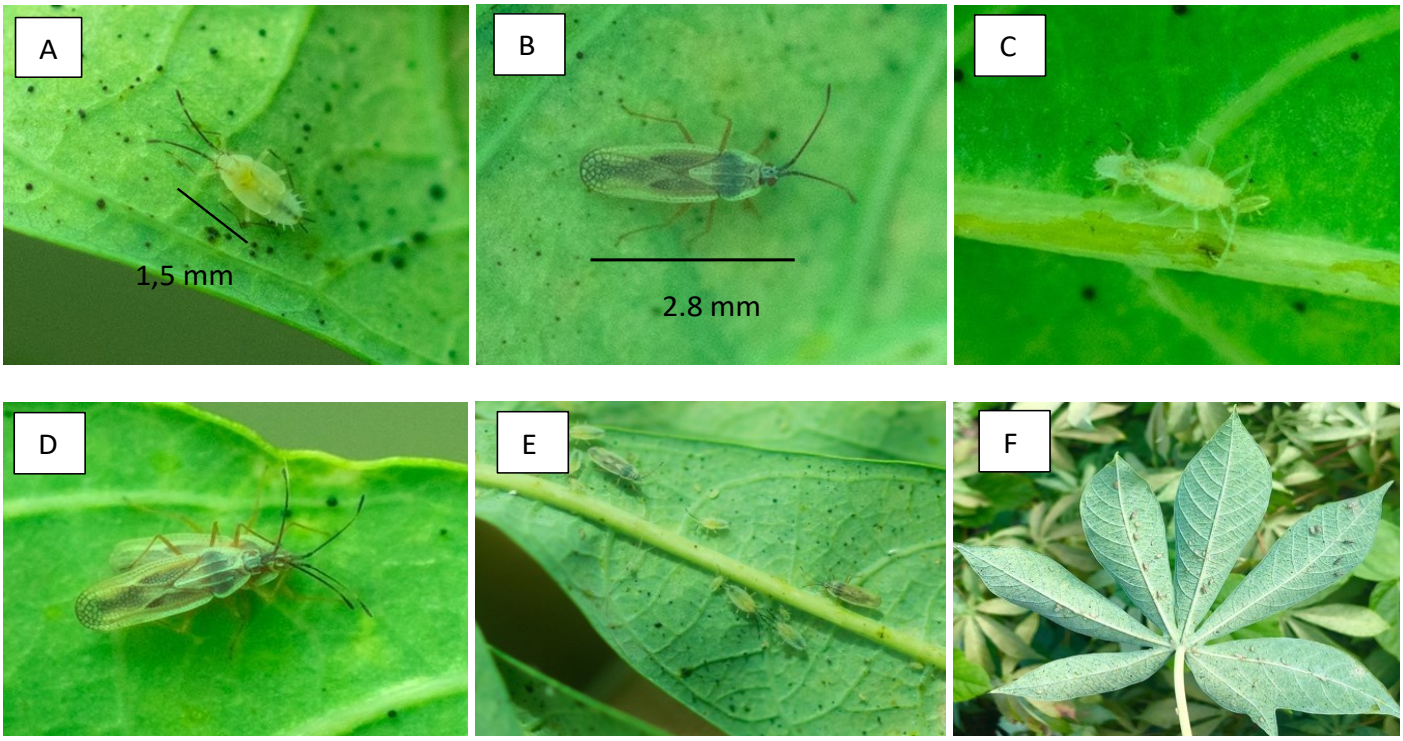

Figure 3. Living individuals of cassava lace bugs in the field, **A.** Nymph, **B.** Imago, **C.** Molting nymph, **D.** Mating pair of adults, **E-F.** a Colony of cassava lace bugs on the lower surface of cassava leaf. Photos were taken with an Olympus OM-D camera, E-M 1, 50mm Macro lens.

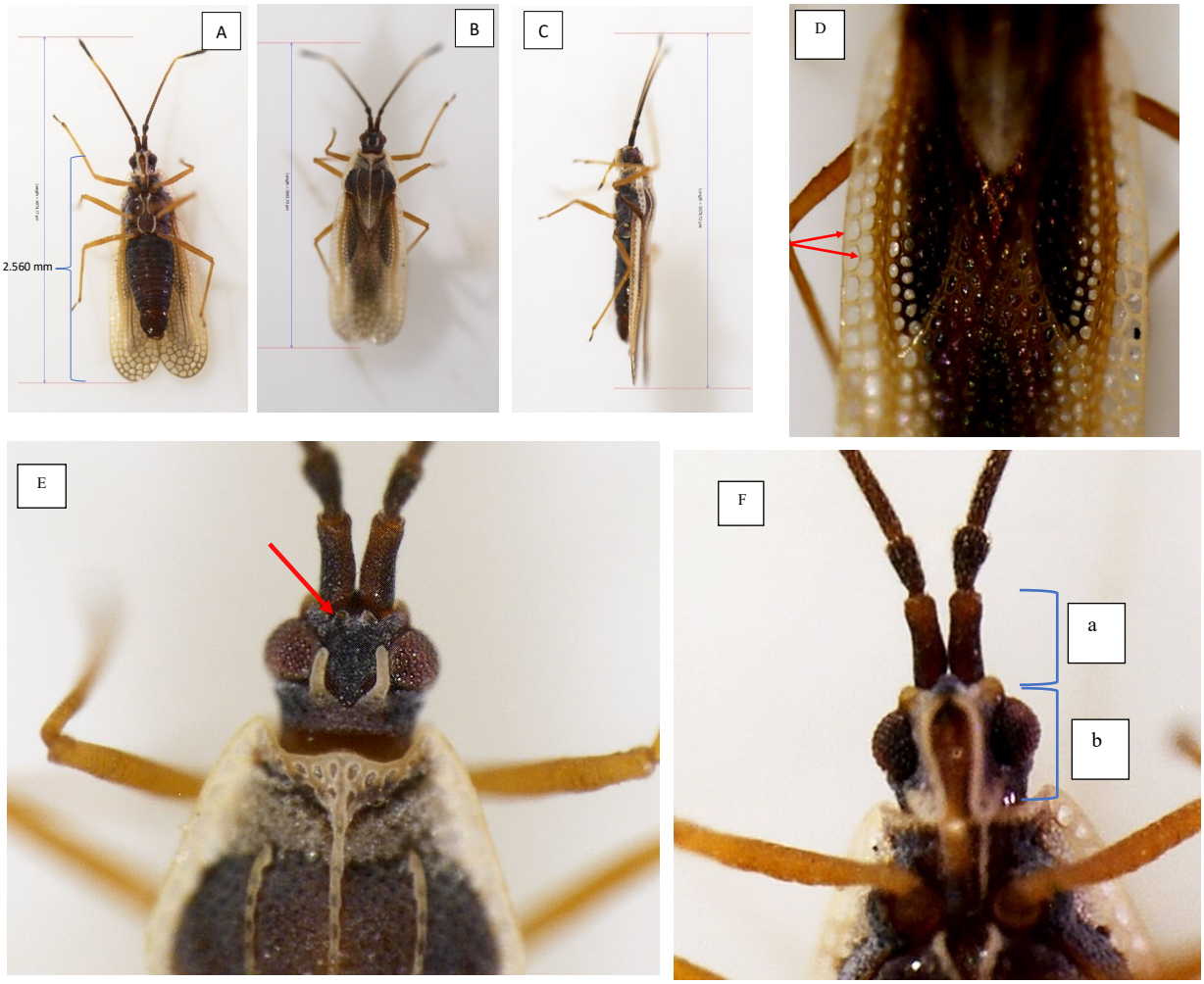

Figure 4. The male morphological characters of *Vatiga illudens* ventral, dorsal, and lateral view, head and antenna character, **A.** Ventral view, **B.** Dorsal view, **C.** Lateral view, **D.** Dorsal view of hemelytra showing the costal area, **E.** Head with a pair of frontal spines, and **F.** Antennal segment I (scape) not longer than head, a. The scape (first segment), b. head.

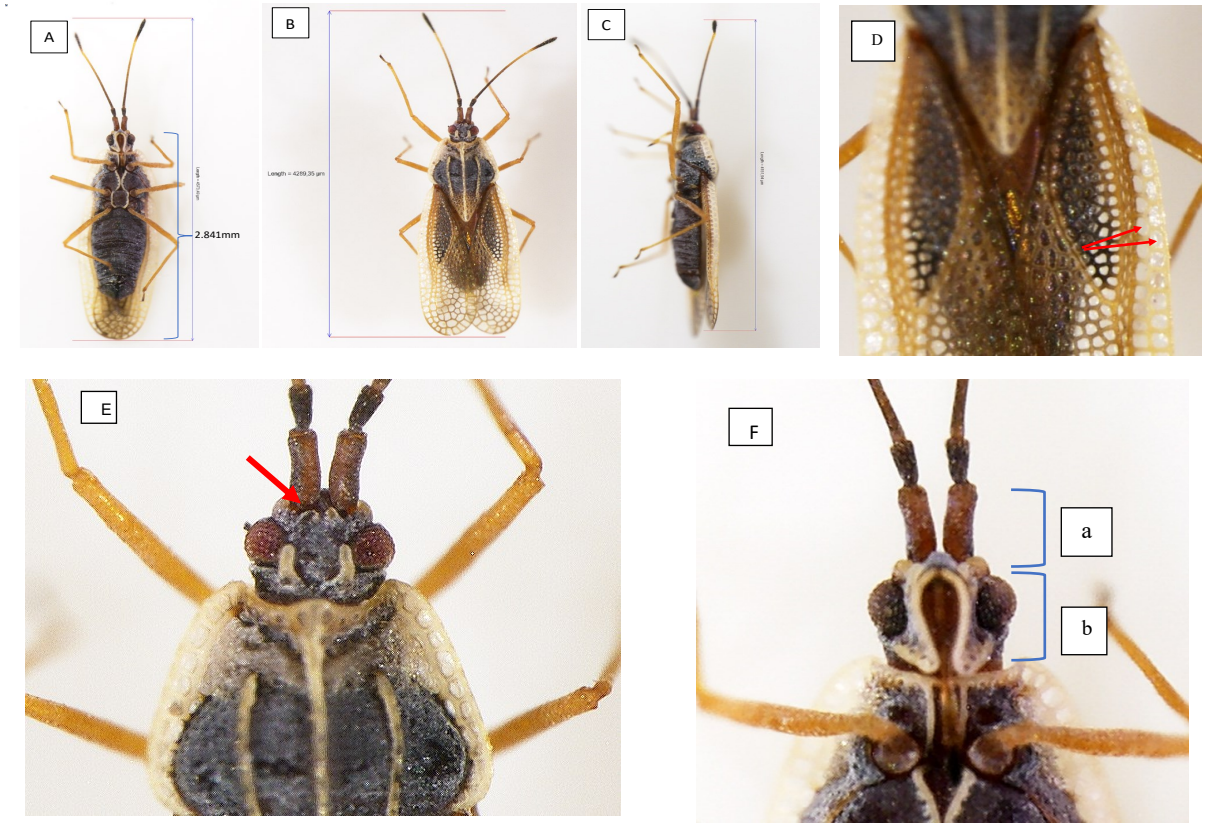

Figure 5. The female morphological characters of *Vatiga illudens* ventral, dorsal, and lateral view, head and antenna character, **A.** Ventral view, **B.** Dorsal view, **C.** Lateral view, **D.** Dorsal view of hemelytra showing the costal area, **E.** Head with a pair of frontal spines, and **F.** Antennal segment I (scape) not longer than head, a. The scape (first segment), b. head.

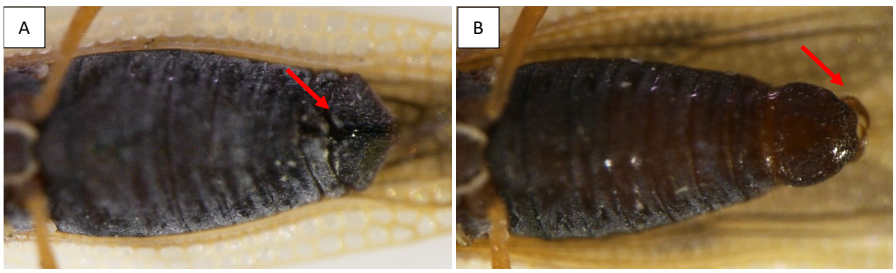

Figure 6. The differentiations of adult males and females of *Vatiga illudens* (Body ventral side), **A.** Female, **B.** Male.

AUTHORS CONTRIBUTION

IP.S., I S.M.D., K.S.D, D.S., and IP.B.A contributed to the article equally. I S.M.D., K.S.D, D.S., IP.B.A. collected the samples from the field and P.P.K.W provide the map and spatial data analysis. IP.S. and P.S.D. carried out the morphological identification. G.N.A.S.W and D.G.W.S. prepared the manuscript and final editing by IW.D.G. and K.A.Y.

ACKNOWLEDGMENTS

The authors would like to acknowledge Dr. Retno Dyah Puspitarini (Department of Plant Pests and Diseases, Faculty of Agriculture, Universitas Brawijaya) for validating the species identity and Denpasar Agriculture Quarantine Station, Bali, Indonesia for equipment support.

CONFLICT OF INTEREST

Authors declare that there is no competing interest regarding the publication of manuscripts.

REFERENCES

Bellon, P.P. et al., 2012. Occurrence of lace bug *Vatiga illudens* and *Vatiga manihotae* (Hemiptera: Tingidae) in Mato Grosso do Sul, midwestern Brazil. *An Acad. Bras. Cienc.*, 84(3), pp.703-705.

Bellon, P.P. et al., 2017. Populational fluctuation of lace bug in cassava. *Arq. Inst. Biol.*, 84, pp.1-6. doi: 10.1590/1808-1657000602015.

Bellotti, A.C., Smith, L. & Lapointe, S.L., 1999. Recent advances in cassava pest management. *Ann. Rev. Entomol.*, 44, pp.343-370. doi: 10.1146/annurev.ento.44.1.343.

Bellotti, A., Campo, B.V.H. & Hyman, G., 2012. Cassava production and pest management: Present and potential threats in a changing environment. *Trop. Plant. Biol.*, 5, pp.39-72. doi:10.1007/s12042-011-9091-4.

Cho, G. et al., 2020. Checklist of the lace bugs (Hemiptera: Tingidae) of Korea. *J. Asia-Pac. Entomol.*, 23, pp.736-745. doi: 10.1016/j.aspen.2020.04.005.

dos Santos, J.K.B. et al., 2019. Correlation of climatic elements with phases of the lace bug *Vatiga illudens* (Hemiptera: Tingidae) in two cassava cultivars (*Manihot esculenta* Crantz, Euphorbiaceae). *Afr. J. Agric. Res.*, 14(9), pp.559-564. doi: 10.5897/AJAR2018.13780.

Fialho, J. et al., 2009. Danos causados por percevejo-de-renda na produção de parte aérea e raízes de mandioca. *Sci Agr*, 2, pp.151-155. doi: 10.5380/rsa.v10i2.13587

Froeschner, R.C., 1993. The neotropical lace bugs of the genus Vatiga (Heteroptera: Tingidae), pests of cassava: New synonymies and key to species. *Proc. Biol. Soc. Wash.*, 95, pp.457-462.

Kalshoven, L.G.E., 1981. The Pests of Crops in Indonesia. Revised by Van der Laan PA. P.T. Ichitar Baru – Van Hoeve, Jakarta.

Muhammad, Z.F. et al., 2019. Geographic distribution of the invasive mealybug *Phenacoccus manihoti* and its introduced parasitoid *Anagyrus lopezi* in parts of Indonesia. *Biodiversitas*, 20(12), pp.3751-3757.

Muniappan, R. et al., 2011. New records of invasive insects (Hemiptera: Sternorrhyncha) in Southern Asia and West Africa. *J. Agric. Urban Entomol.*, 26(4), pp.167-174.

Parsa, S., Kondo, T. & Winotai, A., 2012. The cassava mealybug (*Phenacoccus manihoti*) in Asia: First records, potential distribution, and an identification key. *PLoS One*, 7(10), e0047675. doi: 10.1371/journal.pone.0047675.

Puspitarini, R.D. et al., 2021. First record of the cassava lace bug *Vatiga illudens* (Drake, 1922) (Hemiptera: Heteroptera: Tingidae) from East Java, Indonesia. *Biodiversitas*, 22(7), pp.2870-2876. doi: 10.13057/biodiv/d220738.

Saleh, N. et al., 2013. *Pests, Diseases, and Weeds on Cassava Plants*, Jakarta, Indonesia: IAARD Press.

Schulthess, F. et al., 1991. The influence of the cassava mealybug, *Phenacoccus manihoti* Mat-Ferr (Homoptera: Pseudococcidae) on yield formation of cassava, *Manihot esculenta* Crantz. *J. Appl. Entomol.*, 111, pp.155-165.

Supartha, I.W. et al., 2020. Response of parasitoids to invasive pest *Phenacoccus manihoti* Matile-Ferrero (Hemiptera: Pseudococcidae) on cassava crop in Bali, Indonesia. *Biodiversitas*, 21, pp.4543-4549. doi: 10.13057/biodiv/d211011.

Journal of Tropical Biodiversity and Biotechnology
Volume 09, Issue 01 (2024): jtbb86477
DOI: 10.22146/jtbb.86477

Short Communications

Intraspecific Variability and Phenetic Relationships of *Centella asiatica* (L.) Urb. Accessions from Central Java Based on Morphological Characters

Anshary Maruzy[1,2,3]*, Ratna Susandarini[3]

1)Bureau for Organization and Human Resources, National Research and Innovation Agency. Gedung B.J. Habibie Jalan M.H. Thamrin Nomor 8, Jakarta Pusat 10340, Indonesia.
2)Research Center for Pharmaceutical Ingredients and Traditional Medicine, National Research and Innovation Agency, Kawasan Sains dan Teknologi Dr. (H.C.) Ir. H. Soekarno Jl. Raya Jakarta-Bogor Km. 46, Cibinong, Kabupaten Bogor 16911, Indonesia.
3)Faculty of Biology, Universitas Gadjah Mada, Jl. Teknika Selatan, Sekip Utara, Sleman 55281, Yogyakarta, Indonesia.
* Corresponding author, email: anshary.maruzy@brin.go.id

Keywords:
asiatic pennywort
morphology
numerical taxonomy
phenotype
Submitted:
03 July 2023
Accepted:
12 October 2023
Published:
01 March 2024
Editor:
Miftahul Ilmi

ABSTRACT

Centella asiatica (L.) Urb. is a plant species native to Java and one of the main basic materials in traditional and modern medicine. This study is the first to report the intraspecific variation and taxonomic relationships of *C. asiatica* accession from natural populations in Central Java. The purpose of this study was to reveal phenotypic variations of *C. asiatica* populations and to asses phenetic relationships based on morphological characters. Thirty-two accessions of *C. asiatica* were collected from natural populations from eight mountains in Central Java. Observation on vegetative organs resulted in 25 morphological characters as a basis for assessing phenetic relationships using cluster analysis and principal component analysis. Result of cluster analysis showed that the grouping of accessions was not correlated to the localities from where the samples were collected, although there was a tendency that accessions from the same localities grouped in one cluster. The results of this study confirmed the existence of intraspecies morphological variability in *C. asiatica* which was not affected by geographical aspects. Results of principal component analysis indicated that the grouping of accessions was mainly determined by similarities in petiole color, stolon color, leaf margin, petiole length, stolon length, and leaf color. Given that the characters contributing to the grouping of accessions were mainly qualitative characters, the results indicated a genetic basis underlying phenotypic variations of *C. asiatica* accession.

Copyright: © 2024, J. Tropical Biodiversity Biotechnology (CC BY-SA 4.0)

Centella asiatica (L.) Urb. or Asiatic pennywort is a member of Apiaceae family which has a wide range of local distribution in Indonesia. This species has the ability to grow in various habitats and is well adapted to wide range of altitudes. Global distribution of *C. asiatica* covers tropical Asia, Australia, Africa, South America and the Pacific islands (Parker 2014). *C. asiatica* is well-known as medicinal plant having various medicinal properties such as antioxidant, antigastritic, antitumor, wound healing, immuno-modulatory, and antiproliferative effect (Mariska et al. 2015; Gray et al. 2016). Moreover, Arribas-López et al. (2022) mentioned that the use of *C. asiatica* for wound healing was due to

its anti-inflammatory effect, so this species also has the potential for the treatment of rheumatoid arthritis. In a review of the pharmacology of the two major secondary metabolites found in *C. asiatica*, Bandopadhyay et al. (2023) noted that in traditional and modern medicine it is especially targeted on neurological problems and dermatitis. This species has even been used as herbal materials for modern medicine and cosmetic products.

The need for *C. asiatica* for the traditional medicine industry nationally reaches 100 tons per year, with an average local factory needing 25 tons per year, of which only 4 tons can be supplied (Vinolina 2018). At present, fresh materials of Asiatic pennywort are still harvested from nature, and considering the high demand for this species, the uncontrolled harvest from wild natural populations might have negative impact on the scarcity of this plant in nature (Vinolina 2018; Vinolina & Sigalingging 2021).

Although *C. asitica* is widely known as a medicinal plant, until now there has been no cultivation of this species in Indonesia as indicated by data from the Agriculture and Plantation Office of Central Java Province (eData 2019) and the Central Bureau of Statistics (BPS 2023) regarding the production of biopharmaceutical plants. Data from these two government agencies showed that *C. asiatica* is not included as species for biopharmaceutical cultivation. Given that *C. asiatica* has wide distribution and ability to grow in a variety of habitats, there is a potential risk of erroneous sampling of this species used as material for medicinal products. The reason behind this risk is mainly because *C. asiatica* is morphologically similar to other species in the same genus or even those from different genera within the family of Apiaceae as mentioned by Maruzy et al. (2020). Two species from two different genera that have morphological similarities with *C. asiatica* are *Hydrocotyle verticillata* and *Merremia emarginata*, as mentioned by Daminar & Bajo (2013) and Subramanian & Subramanian (2013). Concerning its function as a medicinal ingredient, the risk of erroneous sampling become a serious problem. In an effort to overcome this problem, a study on morphological characterization to reveal intraspecific variations of *C. asiatica* is very important. Such study will provide scientific information as a basis for the authentication of this species.

Previous studies on morphological variations of *C. asiatica* were carried out on samples grown in experimental gardens with various treatments, and observations were made on the effects of those treatments on growth and morphology as reported by Bermawie & Purwiyanti (2008) and Mumtazah et al. (2020). Research on morphology, anatomy, phytochemistry, and molecular analysis for the characterization of *C. asiatica* from natural populations has been reported by Subositi et al. (2016) and Maruzy et al. (2020). These two studies aimed to develop an authentication method for *C. asiatica* as raw material for medicinal products, and were not focused on assessing phenotypic variation. Meanwhile, a study on variations in the morphological characters of *C. asiatica* originating from natural populations has been reported by Vinolina (2019) with samples originating from North Sumatra.

Research on the intraspecific variation of *C. asiatica* from various mountains in Central Java is still lacking. This study aimed to reveal the phenotypic variations of *C. asiatica* based on morphological characterization of natural populations originating from eight mountains in Central Java. Determination of sampling sites is made by considering that C. asiatica is a herb that can grow in a variety of habitats and soil types with an altitude range of up to 2,300 meters above sea level (Parker 2014;

Devkota & Jha 2019). Based on this fact, the selected areas for collecting plant materials in this study are the localities that have geographical characteristics of *C. asiatica* habitat, especially in terms of altitude range, which in this case are represented by eight mountains in Central Java. The results of this study will produce a mapping of morphological diversity and scientific evidence on the phenotypic variations of *C. asiatica* which can be used as a basis for formulating recommendations for cultivation programs of this species to meet the needs of materials for herbal-based medicine. The mapping of morphological characteristics was carried out by conducting comprehensive characterization of *C. asiatica* accessions collected from various geographic locations so as to reflect intraspecific variations. Information regarding the intraspecific variations will be the basis for recommending accessions that are suitable for cultivation of this species as herbal ingredients, since differences in accessions characterized by morphotypes have an impact on the content of secondary metabolites (Rahajanirina et al. 2012; Prasad et al. 2014).

Plant specimens were collected from natural populations in eight mountains in Central Java, namely Mount Lawu, Mount Merapi, Mount Merbabu, Mount Sindoro, Mount Sumbing, Mount Slamet, Mount Prau and Mount Ungaran (Figure 1). The fieldwork was carried out from June 2022 to February 2023. Sampling locations were determined based on data and information on the presence of *C. asiatica* which covers the areas of altitude ranges of this species, namely from 400 - more than 2,000 m asl. Four accessions representing populations of *C. asiatica* from different altitudes were collected, resulting in a total of 32 accessions used in this study (Table 1). Living specimens of *C. asiatica* collected as materials for morphological characterization were those that met the criteria of healthy adult individuals representing the general features of the population. From each population, 2-3 duplicate samples were taken for the purposes of characterization and preparing herbarium specimens. Observation of morphological characters was carried out in the field and at the Plant Systematics Laboratory, Faculty of Biology Universitas Gadjah Mada, and Plant Systematics Laboratory, Laboratory of Traditional Pharmaceutical Ingredients (*Laboratorium Bahan Baku Obat Tradisional*),

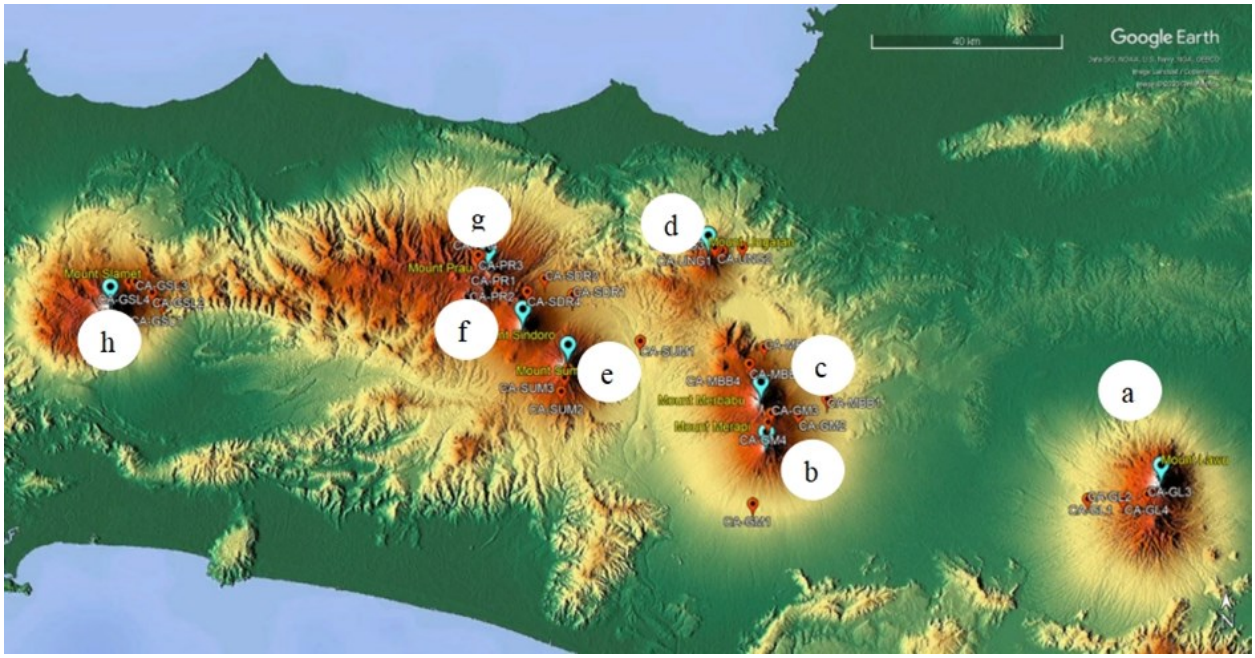

Figure 1. Location of eight mountains in Central Java as sampling sites of C. asiatica accessions. a. Mt. Lawu, b. Mt. Merapi,c. Mt. Merbabu, d. Mt. Ungaran, e. Mt. Sumbing, f. Mt. Sindoro, g. Mt. Prau, h. Mt. Slamet (Google Earth Pro 2023).

Soetarman Co-working Space of National Research and Innovation Agency in Tawangmangu.

Morphological data were obtained by observing characters characterizing the species in Flora of Java (Backer & Brink 1963), The Plant Systematics literature (Simpson 2010), and other characters found in the specimens. Observation of morphological characters was carried out on stolons, petioles, and leaf blades. In this study, no observations were made on flower characters because not all samples were found in flowering phase, but the inflorescence characters can be observed from the remaining parts. All measurements were made based on observation of 10 replicates. Determination of color was carried out referring to RHS Colour Chart 6th version (Royal Horticultural Society 2019).

Table 1. Accessions of *C. asiatica* used in this study.

Accession code	Location	Elevation (m asl)
LWU1	Mount Lawu - Karanganyar Regency	896
LWU2	Mount Lawu - Karanganyar Regency	501
LWU3	Mount Lawu - Karanganyar Regency	1564
LWU4	Mount Lawu - Karanganyar Regency	1759
MRP1	Mount Merapi - Sleman Regency	431
MRP2	Mount Merapi - Boyolali Regency	977
MRP3	Mount Merapi - Boyolali Regency	1585
MRP4	Mount Merapi - Boyolali Regency	1901
MBB1	Mount Merbabu - Boyolali Regency	621
MBB2	Mount Merbabu - Semarang Regency	1075
MBB3	Mount Merbabu - Semarang Regency	1560
MBB4	Mount Merbabu - Semarang Regency	1913
UNG1	Mount Ungaran - Semarang Regency	1064
UNG2	Mount Ungaran - Semarang Regency	1277
UNG3	Mount Ungaran - Semarang Regency	1406
UNG4	Mount Ungaran - Semarang Regency	554
SMB1	Mount Sumbing - Temanggung Regency	493
SMB2	Mount Sumbing - Magelang Regency	1134
SMB3	Mount Sumbing - Magelang Regency	1516
SMB4	Mount Sumbing - Magelang Regency	2080
SDR1	Mount Sindoro - Temanggung Regency	801
SDR2	Mount Sindoro - Temanggung Regency	1027
SDR3	Mount Sindoro - Temanggung Regency	1608
SDR4	Mount Sindoro - Wonosobo Regency	1961
PRU1	Mount Prau - Wonosobo Regency	1345
PRU2	Mount Prau - Wonosobo Regency	1547
PRU3	Mount Prau - Wonosobo Regency	2215
PRU4	Mount Prau - Wonosobo Regency	2280
SLM1	Mount Slamet - Purbalingga Regency	708
SLM2	Mount Slamet - Purbalingga Regency	1055
SLM3	Mount Slamet - Purbalingga Regency	1511
SLM4	Mount Slamet - Purbalingga Regency	1829

Morphological data of *C. asiatica* consisting of qualitative and quantitative characters were analyzed to determine grouping patterns and establish phenetic relationships between accessions using numerical taxonomy methods namely cluster analysis and principal component analysis. The degree of similarity between accessions was determined using the Euclidean distance, followed by clustering using the Unweighted Pair Group Method with Arithmetic Average (UPGMA) method to produce a dendrogram. Assessment of characters contributing to the formation of clusters was done using principal component analysis.

Cluster analysis and principal component analysis were performed using PAST software version 4.13.

Observations on the morphology of 32 accessions of *C.asiatica* resulted in 25 characters used in determination of taxonomic relationships between accessions. Among the 25 characters, 13 were obtained from leaves, 6 from petioles, 4 from stolons, and 2 from inflorescences. Considering that the leaves are the part used as a medicinal ingredient, characterization of this organ is very important and need to be carried out in detail. Leaf shape in all accessions was reniform although there was slight variation when calculating the ratio of the width to the length of the leaf blade. In the four organs observed, the highest variation was found in color, including leaf color, petiole color, and stolon color. The color of the leaf upper surface varied from medium green to light green, while the color on the lower surface varied from medium green to medium yellow-green. Characters that also showed prominent variations in leaves were the leaf margin, namely crenate and dentate. Higher color variations were found in petioles and stolons, ranging from light green, medium green, medium yellow-green, light brown, medium brown to red-brown. The morphology of accessions representing each location, namely from eight mountains in Central Java, is shown in Figure 2. Detail

Figure 2. Morphology of *C. asiatica* representing eight locations of sample origin: (A) Mount Lawu; (B) Mount Merapi; (C) Mount Merbabu; (D) Mount Ungaran; (E) Mount Sumbing; (F) Mount Sindoro; (G) Mount Prau; (H) Mount Slamet.

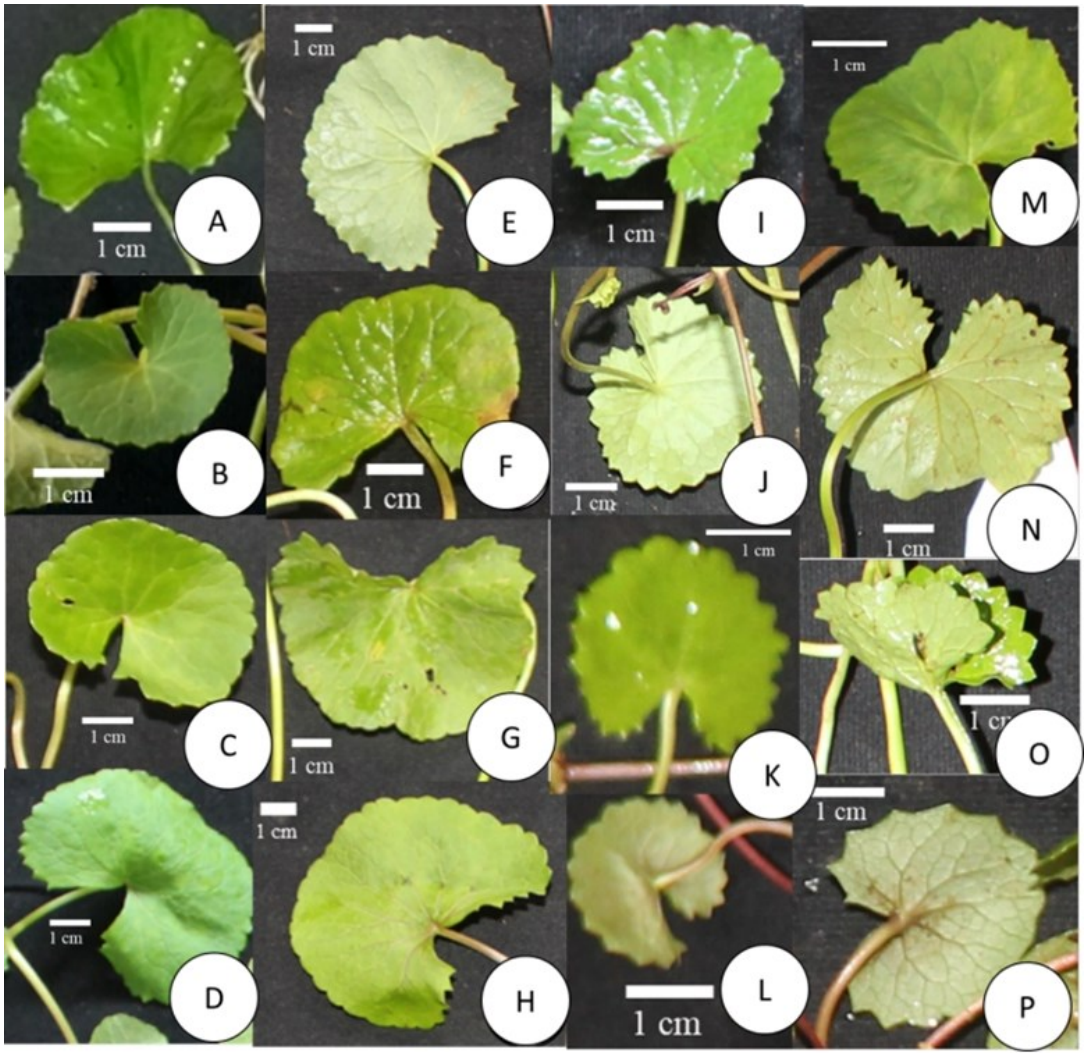

Figure 3. Variations in the shape of the leaf margins of *C. asiatica* representing the several accessions used in this study (Remarks: Leaf margins edged = (A) LWU1; (B) LWU2; (C) LWU3; (D) LWU4; (E) SLM1 ; (F) SLM2; (G) SLM3; (H) SLM4. Leaf margin toothed = (I) MRP4; (J) MBB3; (K) UNG1; (L) UNG2; (M) UNG3; (N) PRU1; (O) PRU2; (P) PRU4).

photographs of *C. asiatica* leaves showing variations on leaf shape and leaf margins of representative accessions are displayed in Figure 3.

Result of cluster analysis based on 25 morphological characters showed the grouping of 32 accessions into three clusters (Figure 4). Cluster I consisted of three accessions, namely one from Mount Sumbing and two from Mount Lawu. Cluster I was formed at a branching point which was clearly separated from clusters II and III. The members of this cluster were characterized by crenate leaf margin as a morphological feature that clearly distinguished it from members of clusters II and III. Apart from the leaf margin, members of cluster I generally had leaves with medium to dark green color on their lower surface, while members of clusters II and III generally had light green in color. In terms of color, the stolons also showed notable differences, in which members of cluster I had stolon with light to medium green in color, while the accessions in clusters II and III showed a more varied range of stolon colors from green, orange, brown to red.

In the dendrogram, 29 of the 32 accessions in this study formed clusters II and III, with relatively closer relationship between the two compared to cluster I. Observations of leaves, petioles, and stolons showed that members of cluster II could be distinguished from members of cluster III especially on the color of the petioles and stolons. The petiole and stolons of accessions in cluster II had a wide range of colors from

light green, medium green, medium yellow-green, to medium orange. Meanwhile, the petioles and stolons belonging to cluster III showed color variations from light brown, medium brown, orange-brown, brown-red, and dark purple red to dark purple.

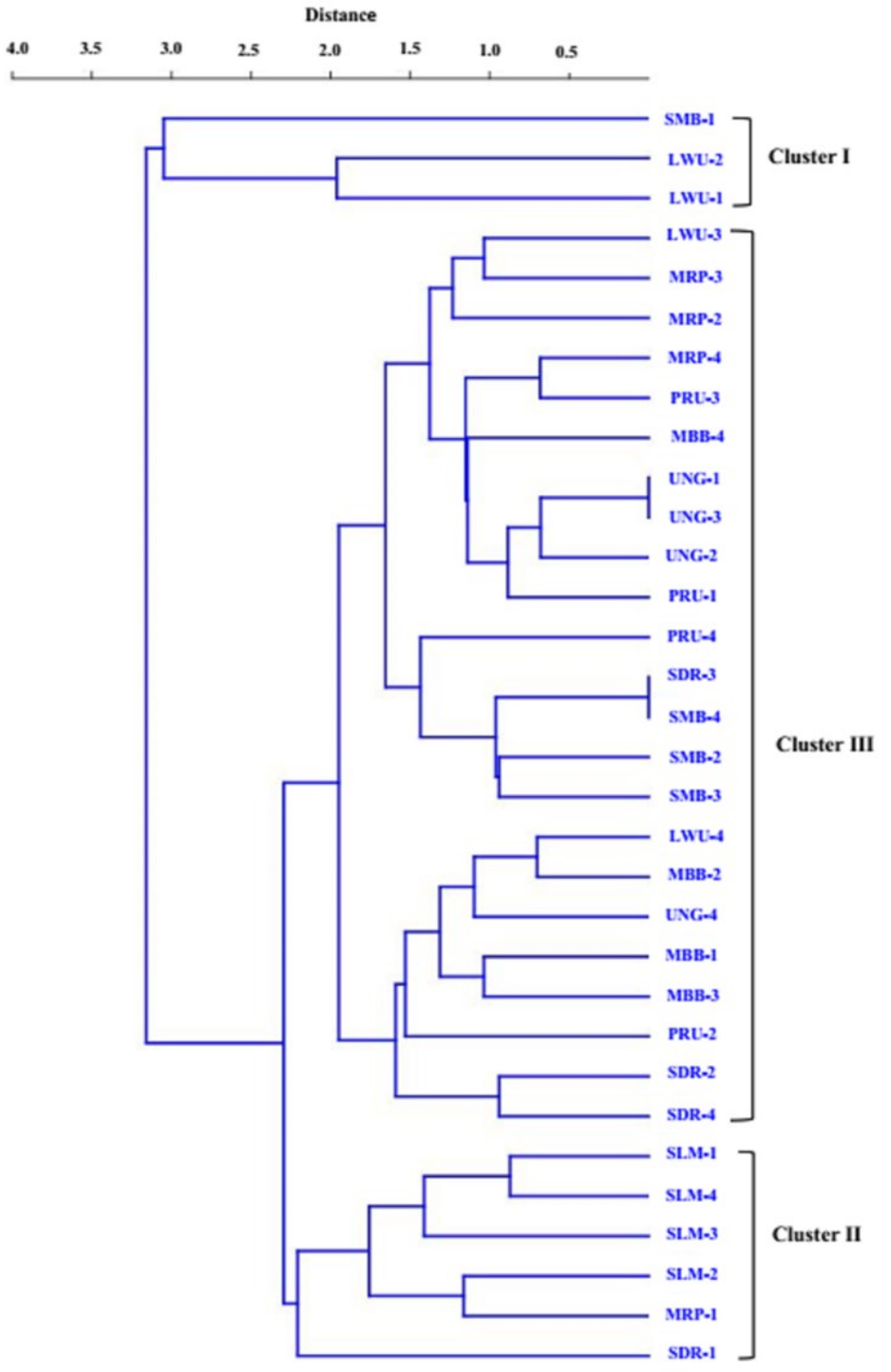

Figure 4. Dendrogram of *C. asiatica* accessions based on morphological characters.

The leaf length varied from 1.5 to 4.1 cm, and most of the accessions have leaves with a length of 1.5-2.3 cm, while nine accessions have 2.4-3.2 cm leaf length, and the longest leaf is found in SMB1 accession with a leaf length of 4.1 cm. Leaf width characters showed variations from 2.8 to 6.3 cm. Most of the accessions have leaf width of 2.8-3.9 cm, ten accessions with leaf width of 4.0-5.1 cm, and the widest leaves are found in accessions SMB1, MBB2 and UNG4. The size of the leaf width

in these three accessions is probably caused by exposure to fertilizers or nutrients from the environment, because the three accessions were found in areas close to rice fields. The variation in the length of the petiole was from 5.1 to 18.8 cm, while the variation in the length of the stolon was 7.5 to 23.0 cm.

Based on the observations of morphological variations, and to confirm the contribution of characters in the grouping of accessions, a principal component analysis (PCA) was carried out. In plant taxonomy studies PCA was generally used to provide a basis for recognizing distinguishing characters between groups. The results of principal component analysis were presented as character loadings (Table 2) indicated the contribution of the characters in forming the grouping of accessions. In this study character's loadings that showed an absolute value of > 0.2 were considered as characters that had important roles in grouping *C. asiatica* accessions. In Table 2 there were nine characters that have a relatively large contribution in the grouping of accessions into three clusters as shown in the dendrogram. These characters were leaf width, color of the leaf upper surface, petiole color, petiole length, and stolon length. The role of these characters was indicated by the loadings values of > 0.2 on the first and second axes in Table 2 This result indicated that these five characters were those differentiated cluster I from clusters II and III collectively. The characters that both showed high loadings on both axis 1 and axis 2 were not only considered as having direct contribution to distinguishing cluster I from clusters II and III, but also differentiating between cluster II and cluster III.

The morphological variability found in this study was in line with those reported in several studies from other regions. Research on *C. asiatica* by Sudhakaran (2017) for the purpose of identifying diagnostic characters showed that leaf shape, leaf margin, enlargement at the base of petiole, stolon length, and stolon color were characters to recognize this species. The characterization study of *C.asiatica* for determining potential accessions for cultivation as a medicinal plant material was reported by Chachai et al. (2021) on 30 accessions from Thailand based on 11 morphological and agronomic characters, which showed that variation between accessions was mainly found in leaf number, leaf length, leaf width, shoot number and stolon number. Variation on leaf margin found in this study as a distinguishing character between clusters align with the report of Chua et al. (2022) on characterization of *C. asiatica* based on a computational analysis on leaf morphology which noted that leaf margin were found to be an easily recognizable character for identification. The research was used as a basis for differentiating *C. asiatica* from *Hydrocotyle verticillata*, a species that is often mistakenly recognized as *C. asiatica* because of the similarities between the two species.

In general, the result of cluster analysis showed that accessions originating from the same location, in this case represented by a mountain, were not always placed in the same cluster. In the dendrogram, it can be seen that there were only few accessions that formed groups based on their geographical origin. The accession from the same origin which formed notable groups were three accessions from Mount Ungaran, (UNG-1, UNG-3, UNG-2), and three accessions from Mount Sumbing (SUM-3, SUM-2, SUM-4) which become the members of cluster III. The same phenomenon was found in four accessions from Mount Slamet, all of which were in cluster II. The three accessions from Mount Ungaran were similar to one another, indicated by their position in one branch of the dendrogram. The level of similarity of these three accessions was higher than those of Mount Sumbing and Mount Slamet, which, alt-

hough they were grouped in the same cluster, they were not in the same branches of the dendrogram. In other words, the grouping of *C. asiatica* accession in this study was influenced more by their morphological similarity, and not by geographical origin. The grouping pattern of accessions that did not match the geographical origin indicated that there was a genetic basis underlying the morphological variability found in *C. asiatica*. Patterns of population grouping that showed no relation to geographical area were also reported in other species, including *Musa* sp. cv. Rastali from Peninsular Malaysia based on cluster analysis and principal component analysis (Putra et al. 2010). The same result was reported in *Cyamopsis tetragonoloba* in which the grouping of samples based on cluster analysis and principal component analysis on morphological characteristics was not related to their geographical origin (Manivannan et al. 2015).

The results of this study indicated that there was notable infraspecies variation in *C. astiatica*, and most of the variability encountered was in qualitative characters. Variations in qualitative characters found in this study, especially leaf margin, petiole color, and stolon color, were morphological characters that were determined by genetic factors. This indication was supported by the results of cluster analysis which showed the grouping of accession which were in general not influenced by the geographic origin of accessions. The results of this study not only confirmed that *C. asiatica* is a species with high morphological variability, but also

Table 2. Character loadings, eigenvalues, and percentage of variance resulted from PCA.

No	Code	Character	PC 1	PC 2
1	LSH	Leaf shape	0.006	-0.069
2	LAP	Leaf apex	0.006	-0.069
3	LMG	leaf margin	**-0.209**	-0.161
4	LBS	Leaf base	0.006	-0.069
5	LLG	Leaf length	0.174	**0.302**
6	LWD	Leaf width	**0.228**	**0.342**
7	LVE	Leaf venation	0.006	-0.069
8	LUC	Color of upper leaf surface	**0.391**	**-0.462**
9	LLC	Color of lower leaf surface	**-0.287**	-0.083
10	LUT	Trichomes on upper leaf surface	-0.015	-0.156
11	LLT	Trichomes on lower leaf surface	0.006	-0.069
12	LWT	Types of trichomes on lower leaf surface	0.006	-0.069
13	LGF	Leaf growth form	0.045	-0.084
14	PBE	Petiole base enlargement	0.006	-0.069
15	PSH	Petiole shape	0.006	-0.069
16	PCL	Petiole color	**-0.486**	**0.332**
17	PLG	Petiole length	**0.299**	**0.493**
18	PGF	Petiole growth form	0.006	-0.069
19	PTR	Trichomes of petiole	-0.032	-0.079
20	SSH	Stolon shape	0.006	-0.069
21	SLG	Stolon length	**0.345**	**0.246**
22	SCL	Stolon color	**-0.424**	0.187
23	STR	Trichomes on stolon	-0.108	-0.048
24	IFT	Inflorescence type	0.006	-0.069
25	IFP	Inflorescence position	0.006	-0.069
Eigenvalues			1.053	0.509
Variance explained (%)			42.284	20.413
Cumulative variance (%)			42.284	62.697

provide a basis for further research to examine whether the variations found can be recognized as indicators of the existence of morphotypes or ecotypes in *C. asiatica*, as reported from previous studies in other regions. Rahajanirina et al. (2012) documented two morphotypes of *C. asiatica* that grew sympatrically in Madagascar, namely the morphotype with small renifrom leaves and the morphotype characterized by large rounded leaves. Similar results were reported by Prasad et al. (2014) in a characterization study of *C. asiatica* collected from various populations growing in the altitudes range of 116 to 2,050 m asl from India, which showed that there were two morphotypes recognized based on the leaves qualitative characters. Ravi et al. (2019) in a study of 39 accessions of *C. asiatica* from eight locations with different altitudes reported that there were variations in all organs examined, and that differences in the color of the petioles and stolons was claimed as genetic expression of the accessions. In this study it was also known that the color variation of the petiole was the same as that of the stolons, which was also found in the study reported here. Meanwhile, the results of Nav et al. (2021) who also used cluster analysis and principal component analysis found that morphological characters that had considerable role in the classification of three *C. asiatica* ecotypes originating from different geographical areas were leaf length, leaf width, petiole diameter, petiole length, and root per node. It could be concluded here that results of this study clearly showed the intraspecific morphological variations of *C. asiatica* which was not influenced by differences in the habitat and geographical origin.

AUTHORS CONTRIBUTION

A.M. designed the research, collected and analyzed the data, and wrote the manuscript; R.S. designed the research, analyzed the data, wrote the manuscript, and supervised all the process.

ACKNOWLEDGMENTS

The author would like to thank for research funding support from the Ministry of Health of the Republic of Indonesia (HK.01.07/III/3038/2002). Thanks were extended to Muhammad Irfan Makruf for his technical assistance in sample collection. Also thank you for the support from researchers at the Soetarman Co-working Space and Laboratory of Traditional Pharmaceutical Ingredients (*Laboratorium Bahan Baku Obat Tradisional*) in Tawangmangu. This research was part of the first author's master thesis under the supervision of the second author.

CONFLICT OF INTEREST

There is no conflict of interest regarding the research or the research funding.

REFERENCES

Arribas-López, E. et al., 2022. A Systematic Review of the Effect of Centella asiatica on Wound Healing. *International Journal of Environmental Research and Public Health*, 19(6), 3266. doi: 10.3390/IJERPH19063266.

Backer, C.A. & Brink, B. van den, 1963. *Flora of Java (Spermatophyte Only): vol.II. angiopermae, families*, Groningen: N.V.P. Noordhoff.

Bandopadhyay, S. et al., 2023. Therapeutic properties and pharmacological activities of asiaticoside and madecassoside: A review. *Journal of Cellular and Molecular Medicine*, 27(5), pp.593–608. doi: 10.1111/jcmm.17635.

Bermawie, N. & Purwiyanti, S., 2008. KERAGAAN SIFAT MORFOLOGI , HASIL DAN MUTU PLASMA NUTFAH PEGAGAN (Centella asiatica (L .) Urban .) Variation in Morphological Characteristics , Yield and Quality of Asiatic Pennywort (Centella mengatasi berbagai masalah kesehatan . nutrisi dan komponen. *Bul. littro*, XIX (1), pp.1–17.

BPS, 2023, 'Produksi Tanaman Biofarmaka (Obat) 2020-2022' in *Badan Pusat Statistik*, viewed 12 August 2023, from https://www.bps.go.id/indicator/55/63/1/produksi-tanaman-biofarmaka-obat-.html

Chachai, N. et al., 2021. Variability of morphological and agronomical characteristics of centella asiatica in Thailand. *Trends in Sciences*, 18 (23), pp.1–10. doi: 10.48048/tis.2021.502.

Chua, L.S., Abdullah, F.I. & Sari, E., 2022. Comparing herbal phytochemicals in different Pegaga: Centella asiatica and Hydrocotyle verticillata. *Future of Food: Journal on Food, Agriculture and Society*, 10(4). doi: 10.17170/kobra-202204136015.

Daminar, N.L. & Bajo, L.M., 2013. Isolation and partial characterization of the most bioactive metabolite from the hexane extract of the aerial part of Hydrocotyle verticillata (whorled marsh pennyworth). *Global Journal of Science Frontier Research Chemistry*, 13(2).

Devkota, A. & Jha, P.K., 2019. Phenotypic plasticity of Centella asiatica (L.) Urb. growing in different habitats of Nepal. *Tropical Plant Research*, 6(1), pp.01–07. doi: 10.22271/tpr.2019.v6.i1.001

eData, 2019, 'Report 2020 Produksi Tanaman Hortikultura' in *Dinas Pertanian & Perkebunan Jawa Tengah*, viewed 12 August 2023, from https://edata.distanbun.jatengprov.go.id/index.php/data/atap_horti_tbf_tahun

Google Earth Pro, 2023, 'Earth Versions – Google Earth' in *Google Earth Pro Ver. 7.3.6.*, viewed 24 May 2023, from https://www.google.com/earth/versions/

Gray, N.E. et al., 2016. Centella asiatica modulates antioxidant and mitochondrial pathways and improves cognitive function in mice. *Journal of Ethnopharmacology*, 180, pp.78–86. doi: 10.1016/j.jep.2016.01.013.

Manivannan, A. et al., 2015. Genetic diversity of Guar genotypes (Cyamopsis tetragonoloba (L.) Taub.) based on Agro-Morphological traits. *Bangladesh Journal of Botany*, 44(1), pp.59–65. doi: 10.3329/BJB.V44I1.22724.

Mariska, E., Sitorus, T.D. & Rachman, J.A., 2015. Effect of Centella asiatica Leaves on Gastric Ulcer in Rats. *Althea Medica Journal*, 2(1), pp.114–118.

Maruzy, A., Budiarti, M. & Subositi, D., 2020. Autentikasi Centella asiatica (L.) Urb. (Pegagan) dan Adulterannya Berdasarkan Karakter Makroskopis, Mikroskopis, dan Profil Kimia. *Jurnal Kefarmasian Indonesia*, 10(1), pp.19–30. doi: 10.22435/jki.v10i1.1830.

Mumtazah, H.M. et al., 2020. The diversity of leaves and asiaticoside content on three accessions of Centella asiatica with the addition of chicken manure fertilizer. *Biodiversitas*, 21(3), pp.1035–1040. doi: 10.13057/biodiv/d210325.

Nav, S.N. et al., 2021. Variability, association and path analysis of centellosides and agro-morphological characteristics in Iranian Centella asiatica (L.) Urban ecotypes. *South African Journal of Botany*, 139, pp.254–266. doi: 10.1016/j.sajb.2021.03.006.

Parker, C., 2014. *Centella asiatica* (Asiatic pennywort). *CABI Compendium*, CABI Compend. doi: 10.1079/CABICOMPENDIUM.12048.

Prasad, A. et al., 2014. Morphological, chemical and molecular characterization of Centella asiatica germplasms for commercial cultivation in the Indo-Gangetic plains. *Natural Product Communications*, 9(6), pp.779–784. doi: 10.1177/1934578x1400900612.

Putra, E.T.S. et al., 2010. Morphological Variation and Geographical Distribution of Musa sp. cv. Rastali in Peninsular Malaysia. *J Cell & Plant Sci*, 1(1), pp.23–32.

Rahajanirina, V. et al., 2012. The influence of certain taxonomic and environmental parameters on biomass production and triterpenoid content in the leaves of Centella asiatica (L.) Urb. from Madagascar. *Chemistry and Biodiversity*, 9(2), pp.298–308. doi: 10.1002/cbdv.201100073.

Ravi, C.S. et al., 2019. Collection and Morphological Variability in Ecotypes of Indian Pennywort (Centella asiatica L.) of Hill Zone of Karnataka, India. *International Journal of Current Microbiology and Applied Sciences*, 8(09), pp.994–1008. doi: 10.20546/ijcmas.2019.809.117.

Royal Horticultural Society, 2019. *RHS Colour Chart*, London: Royal Horticultural Society (Great Britain) & Bloemenbureau Holland.

Simpson, M.G., 2010. *Plant Systematics* 2nd ed., AMSTERDAM: Academic Press.

Subositi, D., Harto, W. & Nita, S., 2016. Skrining Marka ISSR untuk Autentikasi Pegagan (Centella asiatica (L.) Urb.). *Bul. Plasma Nutfah*, 22(1), pp.49–54.

Subramanian, S. & Subramanian, M.P., 2013. Merremia emarginata (Burm. F.) Hall. F.: A substituted market source for Centella asiatica (L.) Urban: An observation from Salem district, Tamil Nadu Ancient Science of Life, 33(2), pp.139-140.

Sudhakaran, M.V., 2017. Botanical pharmacognosy of centella Asiatica (Linn.)Urban. *Pharmacognosy Journal*, 9(4), pp.546–558. doi: 10.5530/pj.2017.4.88.

Vinolina, N.S., 2018. Centelloside content of cultivated pegagan (Centella asiatica) with application of phosporus fertilizer. *Journal of Physics: Conference Series*, 1116(5). doi: 10.1088/1742-6596/1116/5/052072.

Vinolina, N.S., 2019. Secondary Metabolite Content in Pegagan(Centella asiatica) from North Sumatera. *Journal of Physics: Conference Series*, 1175(1), pp.3–8. doi: 10.1088/1742-6596/1175/1/012003.

Vinolina, N.S. & Sigalingging, R., 2021. Centella asiatica tendril growth of Samosir – Indonesia accession. *IOP Conference Series: Earth and Environmental Science*, 883(1), 012057. doi: 10.1088/1755-1315/883/1/012057.

Journal of Tropical Biodiversity and Biotechnology
Volume 09, Issue 01 (2024): jtbb87309
DOI: 10.22146/jtbb.87309

Short Communications

Basidiomycota Macrofungal Communities Across Four Altitudinal Ranges in Bukit Baka Bukit Raya National Park, Indonesia

Natasya Adelia Harun[1], Irwan Lovadi[1]*, Rahmawati Rahmawati[1], Didin Joharudin[2]
1)Department of Biology, Faculty of Mathematics and Natural Sciences, Universitas Tanjungpura, Jl. Prof. Dr. Hadari Nawawi, Pontianak, Indonesia, 78124.
2)Bukit Baka Bukit Raya National Park Office, Jl. Dr. Wahidin Sudirohusodo No. 75, Sintang, Indonesia, 78612
* Corresponding author, email: irwan.lovadi@fmipa.untan.ac.id

Keywords:
Basidiomycota
Community structure
Elevation
Macrofungi
Submitted:
25 July 2023
Accepted:
04 December 2023
Published:
18 March 2024
Editor:
Miftahul Ilmi

ABSTRACT
The influence of elevation gradient has been investigated across different taxa. However, such studies are scarce for macrofungal communities. This study examined the community structure of Basidiomycota macrofungi across four elevations in Bukit Baka Bukit Raya National Park, Indonesia. Macrofungi were collected from randomly placed five 10 x 10 m plots at each altitude and identified at the genus level. The results showed that there were 32 genera belonging to 20 families. The NMDS ordination and ANOSIM confirmed that macrofungal composition and abundance do not differ between the studied altitudinal ranges.

Copyright: © 2024, J. Tropical Biodiversity Biotechnology (CC BY-SA 4.0)

Ecological and evolutionary responses to elevational gradients have been investigated across different biota around the globe. Such studies are useful for understanding the responses of biota toward changes in environmental conditions along elevational gradients, particularly temperature, atmospheric pressure, and clear-sky turbidity (Korner 2007). However, there is little published data on patterns in macrofungal communities along elevational gradients. Published works on this subject include Mt. Korbu (Malaysia), central Veracruz (Mexico), the Moldavian Plateau, Sub-Carpathians Hills, and the Eastern part of Eastern Carpathians (Romania) (Gómez-Hernández et al. 2012; Copot & Tanase 2019; Nur 'Aqilah et al. 2020). These studies suggest that macrofungal communities differ depending on elevation, and environmental factors along elevational gradients, such as vegetation structure and temperature, may be attributed to the ecological responses of macrofungal communities. However, these previous works employed different approaches and were conducted in different vegetation types and elevation ranges. For example, Nur 'Aqilah et al. (2020) investigated macrofungal communities in Mt. Korbu, Malaysia, using convenience sampling along different trails up to 1,000 masl with dipterocarp forests as the dominant vegetation type. The other two published data used plot-based sampling to study the influence of elevation on macrofungal communities. Convenience sampling may lead to collector bias and has no standardization of sampling efforts, while plot-based sampling provides standardization of sampling efforts

(O'Dell et al. 2004).

This study used quantitative data on macrofungi from four elevational ranges of Bukit Baka Bukit Raya National Park, Indonesia, to investigate macrofungal communities along four elevational gradients. We are particularly interested in confirming elevation's effects on macrofungal communities in the area having similar vegetation types to a study by Nur 'Aqilah et al. (2020) using plot-based sampling. We use Basidiomycota as a model system because it is a major phylum of Fungi with more than 40,000 fungal species (He et al. 2022), and contains several well-known macrofungal species (Tang et al. 2015). Macrofungi produce visible structures (fruiting bodies) and have parasitic, saprophytic, or symbiotic lifestyles. Macrofungi play essential roles in the ecosystem as food sources and decomposers for faunas (Tang et al. 2015).

This study was conducted in the tropical rainforest of Bukit Baka Bukit Raya National Park (Figure 1). The national park lies between 112°12' and 112°56' east longitude and 0°28' and 0°56' south latitude and consists of four ecosystems dominated by lowland and highland Dipterocarps and mossy forests at high altitudes. The elevation of the national park ranges from 150 to 2,278 m above sea level (masl) and has a type A climate with an average air temperature of 18°C and rainfall exceeding 60 mm (Abduh et al. 2018).

The macrofungal community was examined at four sites with different altitudes: 250, 500, 750, and 1000 meters above sea level (asl). We did not locate any sampling sites at higher altitudes due to high slopes and safety reasons. Five 10 x 10 m plots were randomly established at each site, with a minimum distance between plots of 10 m. Plot sizes and spacing between plots follow (Gómez-Hernández et al. 2012). Macrofungi found in each plot were collected and then identified in the field at the

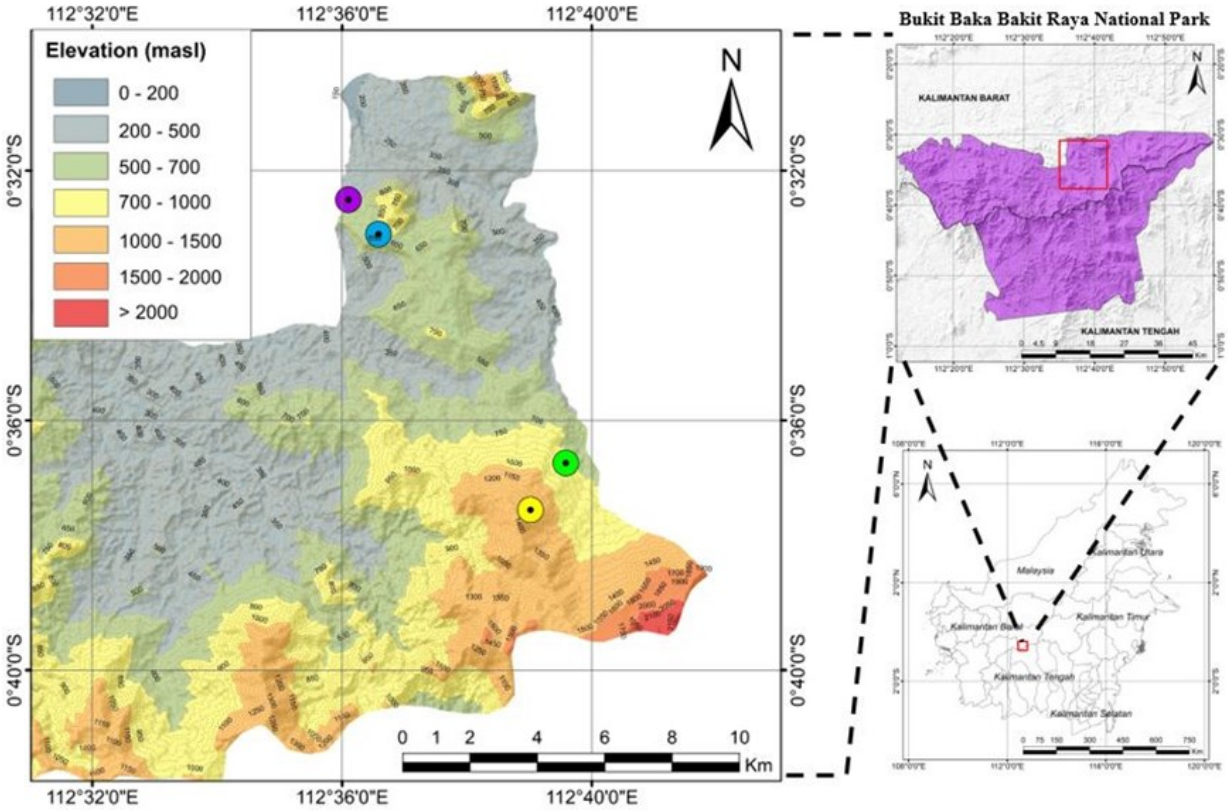

Figure 1. Sampling sites in the study area within Bukit Baka Bukit Raya National Park, Indonesia. Colored dots on the large map represent sampling sites at four altitudinal ranges (250 masl, 500 masl, 750 masl, and 1000 m).

genus level (if possible). Any unidentified samples were photographed, preserved, and transported to the Laboratory of Ecology, Department of Biology, Faculty of Mathematics and Natural Sciences, Universitas Tanjungpura, for further identification. Macrofungal identification was based on macroscopic characteristics, such as cap shape, cap margin, gills, stalks, and ring, using existing literature, such as Tjiu et al. (2022) and McKnight &McKnight (1987). Macrofungal nomenclature follows the Index Fungorum (http://www.indexfungorum.org/names/Names.asp).

For each elevation, we also calculated the Shannon-Wiener index (H'), Evenness index (E'), and Simpson index (D'). We used Non-metric Multidimensional Scaling (NMDS) analysis and Analysis of Similarities (ANOSIM) to examine macrofungal compositional and abundance differences. NMDS ordination was chosen because it is suitable for ecological datasets which contain a mixture of continuous metrics with varying degrees of homogeneity and normality (Walker et al. 2011), and graphically demonstrates the relationships among communities based on a distance matrix (Clarke 1993). We used ANOSIM because it is a formal hypothesis test to confirm whether the differences seen among communities in the NMDS plot were significant or not (Laaker 2018). ANOSIM is similar to one-factor analysis of variance, but it uses the Bray-Curtis dissimilarity to provide a test statistic (Clarke 1993).

Jaccard and Bray-Curtis matrices were used in the NMDS analyses for compositional and abundance data, respectively. The flexibility of dissimilarity matrices used in this study reflects one of advantages of NMDS ordination to meet a specific goal of the research. The use of Jaccard matrix, for example, is intended to analyze compositional data by transforming abundance input into binary data. However, the NMDS ordination also has disadvantages, such as failing to reach the best solution with low stress values and slow computation due to large datasets (McCune et al. 2002). In this research, the NMDS computation succeeded in reaching the best solution at low stress values (<0.2) for both compositional and abundance data (see Figure 3 & 4). The NMDS analysis and ANOSIM were done using the vegan package in R (Oksanen et al. 2022), and NMDS results were visualized using the ggplot2 package in R (Wickham 2016). Before the analysis, any rare genera (less than 1% of total macrofungal abundance) were excluded.

A total of 2344 individual macrofungi were encountered across four altitudes. All sampled macrofungi comprise 32 genera belonging to 20 families (Table 1). *Marasmius* was the most abundant macrofungal genus across four altitudes, and its highest abundance was documented at 750 masl (1.042 individual fungi/m^2). This finding can be attributed to the fact that *Marasmius* has a wide distribution in temperate and tropical areas, including tropical mountain forests (Singer 1976). Moreover, Polyporaceae is the largest family reported in this study. It contains eight genera, namely *Amauroderma*, *Favolus*, *Fomes*, *Ganoderma*, *Microporellus*, *Microporus*, *Polyporus* and *Trametes* (Table 1). Two out of the eight genera (i.e. *Ganoderma* and *Microporus*) had a high abundance level and were found at four different elevations. The taxonomic status of Polyporaceae as one of major families in Basidiomycota may explain this finding (Cui et al. 2019).

There are eight major genera based on abundance across four altitudinal ranges. These genera are *Campanella*, *Exidia*, *Ganoderma*, *Gymnopus*, *Hemimycena*, *Marasmius*, *Microporus* and *Mycena*. Figure 2 shows the eight largest macrofungal genera found at different elevations in the Bukit Baka Raya National Park.

In this research, some genera were reportedly only observed at re-

Table 1. Diversity and abundance of macrofungal taxa (no of individuals per square meter) found at four altitudes in Bukit Baka Bukit Raya, Kalimantan Barat, Indonesia. The top eight genera, printed in bold, are included in the NMDS ordination.

Taxa	Abundance (individual fungi/m²) at four elevations (masl)			
	250	500	750	1000
Agaricaceae				
Agaricus	0.024	0	0	0
Leucocoprinus	0	0	0	0.002
Amanitaceae				
Amanita	0	0.018	0	0
Auriculariaceae				
Exidia	0	0	0	0.128
Boletaceae				
Boletus	0	0	0.002	0
Clavariaceae				
Clavaria	0	0.004	0	0
Cortinariaceae				
Cortinarius	0	0.002	0	0
Entolomataceae				
Leptonia	0	0.006	0	0
Hydnaceae				
Clavulina	0	0	0.006	0
Craterellus	0.024	0	0	0
Hyemenochaetaceae				
Phellinus	0	0	0	0.016
Hygrophoraceae				
Hygrocybe	0	0.006	0	0
Irpicaceae				
Byssomerulius	0	0	0.012	0
Marasiaceae				
Campanella	0	0	0.050	0
Marasmius	0.460	0.932	1.042	0.716
Mycenaceae				
Hemimycena	0	0.120	0	0
Mycena	0.094	0.034	0.016	0.008
Omphalotaceae				
Gymnopus	0.026	0.096	0	0
Panaceae				
Cymatoderma	0	0	0.032	0.012
Phanerochaetaceae				
Inflastostereum	0	0	0.004	0
Physalacriaceae				
Flammulina	0.032	0	0	0
Polyporaceae				
Amauroderma	0.008	0.002	0.014	0
Favolus	0	0	0	0.018
Fomes	0	0.016	0.008	0
Ganoderma	0.030	0.020	0.082	0.124
Microporellus	0.012	0	0	0.004
Microporus	0.088	0.070	0.068	0.122
Polyporus	0	0.022	0.008	0
Trametes	0.008	0	0.010	0
Russulaceae				
Lactarius	0.002	0	0	0
Russula	0	0.002	0	0
Stereaceae				
Stereum	0	0	0	0.026

Figure 2. Eight major genera of macrofungi found in the study area within the montane tropical rainforest of Bukit Baka Bukit Raya National Park, Indonesia (A. *Campanella*, B. *Exidia*, C. *Ganoderma*, D. *Gymnopus*, E. *Hemimycena*, F. *Marasmius*, G. *Microporus*, H. *Mycenae*).

stricted altitudes. For example, *Agaricus*, *Craterellus*, and *Lactarius* were exclusive to 250 masl, while *Amanita*, *Clavaria*, *Cortinarius*, and *Leptonia* only occurred at 500 masl. Higher altitudes demonstrate a similar pattern. *Boletus*, *Byssomerulius*, *Clavulina*, *and Inflatostereum* only occur at 750 masl; *Exidia*, *Favolus*, and *Leucocoprinus* were only observed at 1000 masl (Table 1). Similar patterns were also demonstrated in a study by Nur 'Aqilah et al. (2020) on Mount Korbu, Malaysia. They reported that *Cymatoderma* and *Stereum* occur at 800 and 1030 masl, respectively. These patterns reflect different macrofungal growth requirements linked to altitudinal ranges, such as relative humidity, soil temperature, soil moisture, light intensity, slope, and litter depth (Gómez-Hernández et al. 2012).

Macrofungal diversity varied between elevations. This study demonstrated that the highest species richness was recorded at 500 masl (15 genera), and the lowest was observed at 750 masl (Table 2). The Shannon-Wiener (H') and Evenness Indices have the same pattern. The highest Shannon-Wiener Index was documented at 250 masl (1.55), and the lowest was observed at 750 masl (1.02). Surprisingly, the Shannon-Wiener Index increased to 1000 masl (1.33). (Table 2). This observed pattern is consistent with a study by Ping et al. (2017), which shows soil fungal diversity decreases at 699-937masl but increases at 937-1044 masl in the Pine Forest, Changbai Mountain, Korea.

To evaluate differences in macrofungal communities along studied elevational gradients, we used the Non-metric Multidimensional scaling (NMDS) technique and Analysis of Similarities (ANOSIM). Based on the NMDS plot, the composition of macrofungal genera does not differ among four altitudinal ranges. There is no clear distinction among macrofungal communities at four altitudes as shown by overlapping col-

Table 2. Genera richness, Shannon-Wiener Index (H'), Evenness (E), and Simpson Index (D) at different elevations in Bukit Baka Bukit Raya National Park, West Kalimantan.

Elevation (m asl)	Genera richness	Index		
		H	E	D
250	12	1,55	0,62	0,36
500	15	1,24	0,46	0,49
750	14	1,02	0,39	0,60
1000	11	1,33	0,56	0,41

ored dots in NMDS plot (Figure 3). The result of ANOSIM confirmed the pattern shown in NMDS ordination (p-value = 0.19, ANOSIM R = 0.06). This phenomenon has never been recorded for macrofungi. Research by Nur 'Aqilah et al. (2020) displayed contradicting patterns; macrofungal composition differed depending on altitudinal ranges. Nur 'Aqilah et al. (2020) investigated macrofungal composition along elevational ranges from 350 to 1040 masl. Using NMDS ordination, they detected changes in macrofungal composition along elevational gradients. The contradicting results may be due to differences in sampling methods. In this study, we employed plot-based sampling across four altitudinal ranges from 250 to 1000 masl, while Nur 'Aqilah et al. (2020) collected macrofungal samples along three trails at the elevation ranging from 350 to 1040 masl during a four-day expedition.

The abundance of macrofungal genera displays the same pattern as the compositional data. Overlapping macrofungal communities at each altitude were observed on NMDS plot (Figure 4), suggesting macrofungal abundance at each altitude was similar. ANOSIM analysis confirmed such pattern; there were no significant differences in macrofungal abundance among different elevations (p-value = 0.17 ANOSIM R = 0.06). Some abundance data, particularly at the elevation below 1000 masl from the present study, are consistent with Gómez-Hernández et al. (2012).

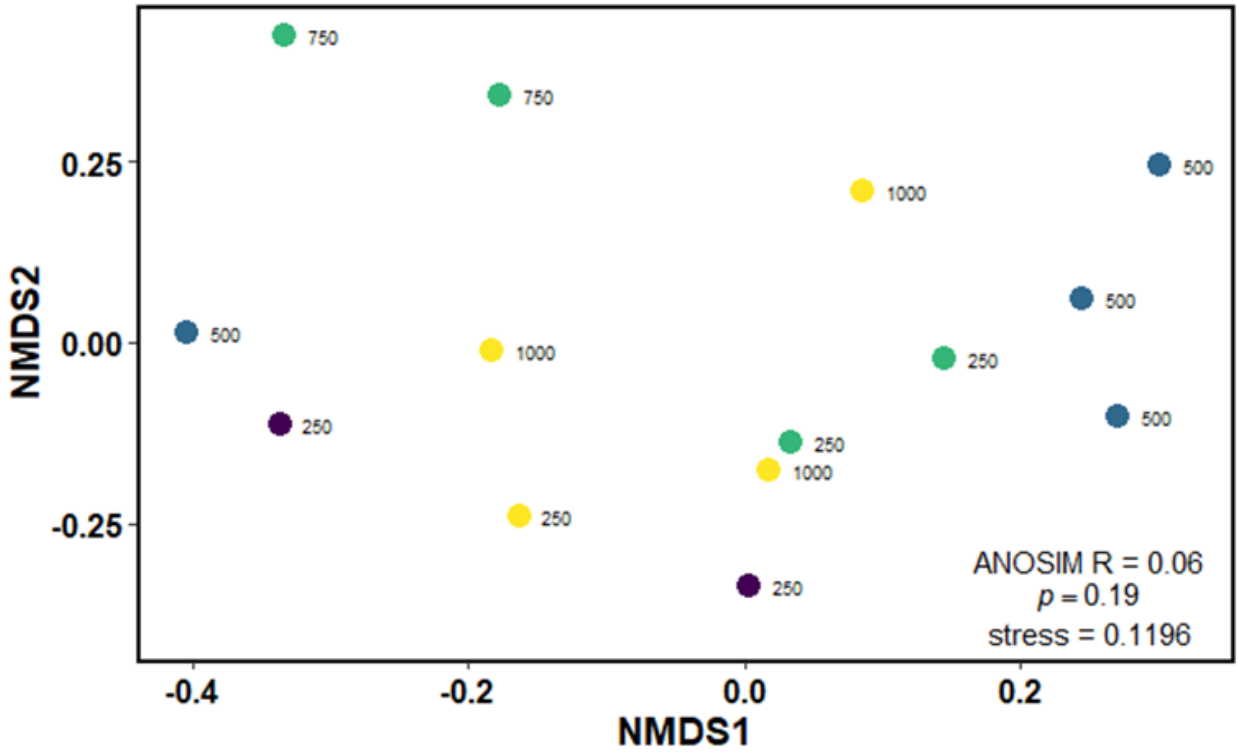

Figure 3. Non-metric multidimensional scaling (NMDS) ordination of macrofungal composition at four altitudinal ranges in the montane tropical rainforest of Bukit Baka Bukit Raya National Park, Indonesia. Colored dots indicate four altitudinal ranges, i.e. ● 250 masl, ● 500 masl, ● 750 masl, dan ● 1000 masl.

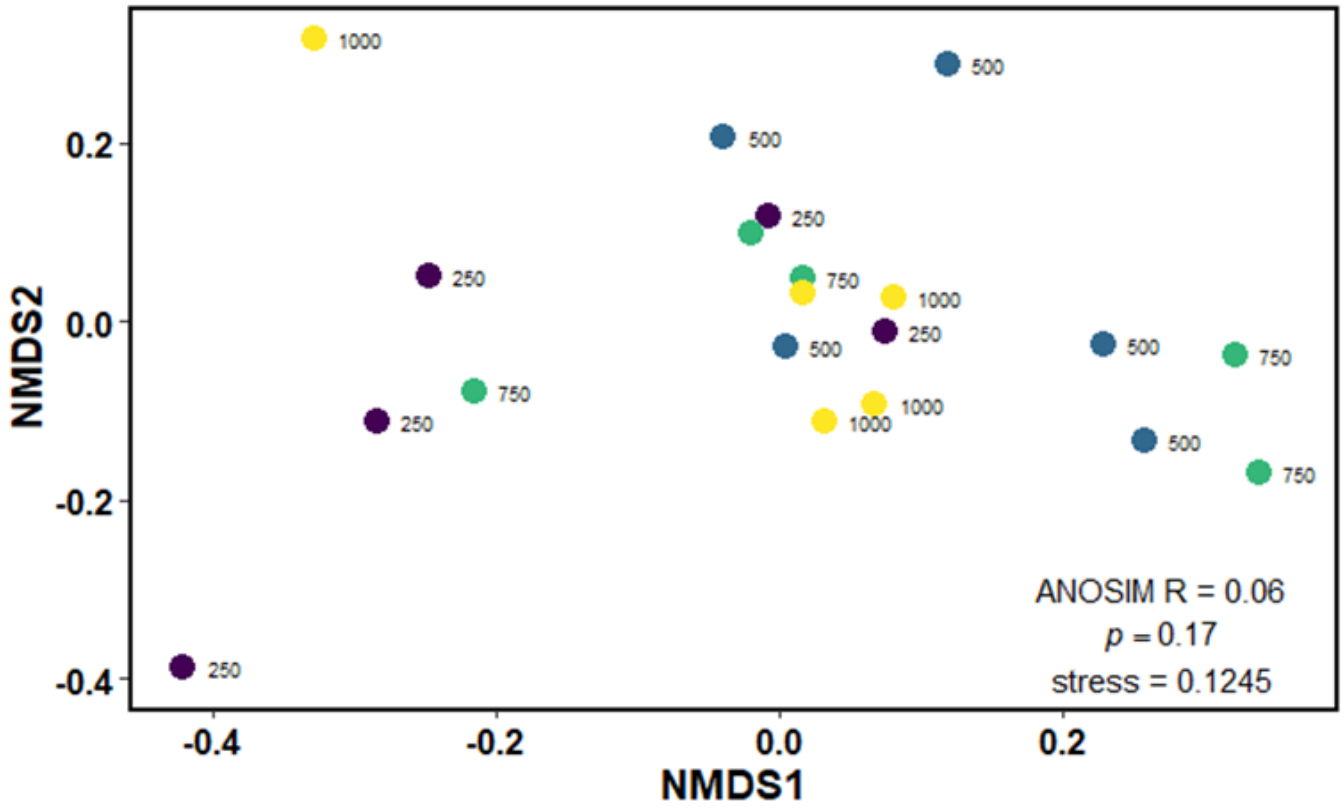

Figure 4. Non-metric multidimensional scaling (NMDS) ordination of macrofungal abundance at four altitudinal ranges in the montane tropical rainforest of Bukit Baka Bukit Raya National Park, Indonesia. Colored dots indicate four altitudinal ranges, i.e. ● 250 masl, ● 500 masl, ● 750 masl dan ● 1000 masl.

Their study demonstrated no clear grouping of macrofungal abundance between 100 and 500 masl using canonical correspondence analysis (CCA). However, abundance data on 1,000 masl in this study differed from Gómez-Hernández et al. (2012). This research found no significant differences in macrofungal abundance along four elevational gradients based on ANOSIM. On the contrary, Gómez-Hernández et al. (2012) suggest that macrofungal abundance differed between the altitudes below 1,000 and 1,000 masl. This contradictory pattern is probably due to differences in vegetation. Gómez-Hernández et al. (2012) conducted their study in various forest types along elevational gradients, i.e., seasonally dry tropical forest, tropical montane cloud forest, and conifer forest. In contrast, this research was conducted in a montane tropical rainforest dominated by dipterocarp forests (Abduh et al. 2018).

Our study clearly shows that elevation has no effects on macrofungal composition and abundance at low (below 1,000 masl) and mid altitudes (1,000 masl) of Bukit Baka Bukit Raya National Park, Indonesia. Our research in a mountainous area of Borneo tropical rainforests confirms that the diversity of macrofungi varied across altitudinal ranges based on diversity index. Further research is required to explain the causes of no elevation effects on macrofungal communities at low and mid altitudes.

AUTHOR CONTRIBUTION

N.A.H. collected and analyzed data and wrote the manuscript, I.L. designed the research, analyzed data, supervised all the processes and wrote the manuscript, R.R. supervised macrofungal identification and wrote the manuscript, D.J. collected data

ACKNOWLEDGEMENTS

The authors thank Bukit Baka Bukit Raya National Park for granting a research grant and permitting macrofungal collection. Mikael Reporman-to dan Agnes Megawati Gultom are thanked for helping in macrofungal sampling. We acknowledge the Nature Conservation Agency of West Kalimantan (BKSDA) for granting a macrofungal sample transportation permit (SATS-DN) from the field to our laboratory at Universitas Tan-jungpura. The authors also thank Dr Rafdinal and Mr Riyandi for their comments on the first draft of the manuscript.

CONFLICT OF INTEREST

The authors have no conflicts of interest to declare.

REFERENCES

Abduh, M., Hendro, P. & Adi, S., 2018. *Database keanekaragaman hayati Balai Taman Nasional Bukit Baka Bukit Raya*, Sintang, Indonesia: Balai Taman Nasional Bukit Baka Bukit Raya.

Clarke, K.R., 1993. Non-parametric multivariate analyses of changes in community structure. *Australian Journal of Ecology*, 18(1), pp.117-143. doi: 10.1111/j.1442-9993.1993.tb00438.x.

Copot, O. & Tanase, C., 2019. Dead wood, forest fragmentation and elevation influences macrofungal diversity on downed coarse woody debris in beech and oak old forest ecosystems from northeastern Romania. *Journal of Plant Development*, 26, pp.161-172. doi: 10.33628/jpd.2019.26.1.161.

Cui, B-K. et al., 2019. Species diversity, taxonomy and phylogeny of Polyporaceae (Basidiomycota) in China. *Fungal diversity*, 97(1), pp.137-392. doi: 10.1007/s13225-019-00427-4.

Gómez-Hernández, M. et al., 2012. Patterns of macromycete community assemblage along an elevation gradient: options for fungal gradient and metacommunity analyse. *Biodiversity and conservation*, 21(9), pp.2247-2268. doi: 10.1007/s10531-011-0180-3.

He, M-Q. et al., 2022. Species diversity of Basidiomycota. *Fungal diversity*, 114(1), pp.281-325. doi: 10.1007/s13225-021-00497-3.

Korner, C., 2007. The use of 'altitude' in ecological research. *Trends in ecology & evolution*, 22(11), pp.569-574. doi: 10.1016/j.tree.2007.09.006.

Laaker, D.J. 2018. *Avian Use of Floodplain Forest Communities along the Upper Mississippi River*. ProQuest Dissertations Publishing.

Mccune, B., Grace, J.B. & Urban, D.L., 2002. *Analysis of ecological communities*, Gleneden Beach, Oregon: MjM Software Design.

Mcknight, K. & Mcknight, V., 1987. *A Field Guide to Mushrooms*, Boston, New York: Houghton Mifflin Company

Nur 'Aqilah, M.B. et al., 2020. Elevation influence the macrofungi diversity and composition of Gunung Korbu, Perak, Malaysia. *Biodiversitas*, 21(4), pp.1707-1713. doi: 10.13057/biodiv/d210453.

O'dell, T., Lodge, D. & Mueller, G.M., 2004. Approaches to sampling macrofungi, In *Biodiversity of Fungi: Inventory and Monitoring Methods*. California, USA: Elsevier Academic Press, pp.163-168.

Oksanen, J. et al., 2022. _vegan: Community Ecology Package_. R package version 2.6-4.

Ping, Y., et al., 2017. Vertical zonation of soil fungal community structure in a Korean pine forest on Changbai Mountain, China. *World Journal of Microbiology and Biotechnology*, 33(1), pp.1-10. doi: 10.1007/s11274-016-2133-1.

Singer, R.S., 1976. *Marasmieae (Basidiomycetes-Tricholomataceae)*, Bronx, N.Y: New York Botanical Garden.

Tang, X., et al., 2015. Diversity, population genetics, and evolution of macrofungi associated with animals. *Mycology*, 6(2), pp.94-109. doi:10.1080/21501203.2015.1043968.

Tjiu, A. et al., 2022. *A Photographic Guide to The Wild Mushrooms of Borneo: 1*, Kuching: Print Lab Enterprise.

Walker, D.A. et al., 2011. Vegetation of zonal patterned-ground ecosystems along the North America Arctic bioclimate gradient. *Applied vegetation science*, 14(4), pp.440-463. doi: 10.1111/j.1654-109X.2011.01149.x.

Wickham, H., 2016. *ggplot2: Elegant Graphics for Data Analysis*, New York: Springer-Verlag.

Journal of Tropical Biodiversity and Biotechnology
Volume 09, Issue 01 (2024): jtbb84500
DOI: 10.22146/jtbb.84500

Research Article

Isolation and Characterization of Phosphate Solubilizing Bacteria from Upland Rice Cultivation Areas in Bangka Regency

Kartika Kartika[1,2], Abdul Munif[3], Endah Retno Palupi[4], Satriyas Ilyas[4], Mohamad Rahmad Suhartanto[4]*

1)Postgraduate doctoral student of Seed science and Technology Study Program, Department of Agronomy and Horticulture, IPB University IPB University, Jl. Meranti, Babakan, Kec. Dramaga, Kabupaten Bogor, Jawa Barat 16680
2)Bangka Belitung University Kampus Terpadu Universitas Bangka Belitung Desa Balunijuk, Kecamatan Merawang, 33172
3)Phytopathology Study Program, Department of Plant Protection, IPB University, Jl. Meranti, Babakan, Kec. Dramaga, Kabupaten Bogor, Jawa Barat 16680
4)Seed science and Technology Study Program, Department of Agronomy and Horticulture, IPB University, Jl. Meranti, Babakan, Kec. Dramaga, Kabupaten Bogor, Jawa Barat 16680
* Corresponding author, email: m.r.suhartanto@apps.ipb.ac.id

Keywords:
Upland rice
Ultisol
P solubilizing bacteria
Phosphatase
organic acids
Submitted:
17 May 2023
Accepted:
22 August 2023
Published:
05 January 2024
Editor:
Miftahul Ilmi

ABSTRACT

The availability of phosphorus (P) in ultisol acid soils presents a significant challenge due to its attachment to aluminum (Al) or iron (Fe) compounds. A potential solution to address this issue is the utilization of phosphate solubilizing bacteria (PSB). Therefore, this study aimed to analyze the potential of PSB originating from upland rice cultivation on ultisol soils. The bacterial isolates were obtained from soil samples taken from the rhizosphere area and root tissue of upland rice plants cultivated in Payabenua and Saing Villages, Bangka Regency. The pathogenicity testing encompassed hypersensitivity and hemolysis tests, while the P solubilization included the evaluation of the phosphate solubilizing index (PSI) and P dissolution. Subsequently, the selected isolates were subjected to phosphatase enzyme and organic acid content assessment. The results showed a total of 120 isolates, predominantly distributed in the Payabenua area and primarily consisting of endophytic bacteria. Among the six selected isolates, genus *Burkholderia* dominated four isolates, while the remaining isolates belonged to genus *Serratia*. Furthermore, in *Burkholderia vietnamiensis*, the solubility value of P in $AlPO_4$ and $Ca_3(PO_4)_2$ liquid media exhibited a range of 0.0013 to 0.0344% and 0.0008 to 0.1842%, respectively.

Copyright: © 2024, J. Tropical Biodiversity Biotechnology (CC BY-SA 4.0)

INTRODUCTION

Farmers in Bangka Belitung Province have a tradition of cultivating padi gogo, which is locally known as "berhume". This cultivation activity is typically conducted in upland areas that are newly opened or in between black pepper and rubber plantations. Among the districts in the province, Bangka Regency serves as a central location for padi gogo cultivation. However, the soil has a pH below 5 and is classified as an ultisol soil type. Wahyudin et al. (2017) and Asril and Lisafitri (2020) highlighted that ultisol soils typically exhibited low nutrient content. The essential nutrient phosphorus (P) is bound to aluminum (Al) and iron (Fe), rendering it in an insoluble phosphate form. Consequently, a significant

portion of the P is not readily available for plant absorption and utilization.

Phosphate solubilizing bacteria (PSB) offers a viable approach for releasing P element form of Al and Fe bonds within ultisol soil. By harnessing the metabolic abilities, the bonds between Al and Fe in the ultisol soil can be effectively released, thereby facilitating the availability of phosphates for plant uptake (Sugianto et al. 2019; Sonia & Setiawati 2022). Numerous studies have been undertaken to investigate the efficacy of bacterial inoculation in enhancing P availability. Setiawati and Pranoto (2015) highlighted that the capacity of these bacteria to solubilize phosphate faced limitations when introduced into different environments. Furthermore, Awais et al. (2017) emphasized the variability in population sizes of PSB across different soil types.

PSB is able to convert insoluble phosphates into forms available to plants through the secretion of organic acids (Pande et al. 2020) and the production is one of the indicators of the activity of PSB (Fitriatin et al. 2020). The organic acids produced by PSB are chelating agents for calcium (Ca), magnesium (Mg), Fe, and Al to form stable complexes (Yadav et al. 2015). Meanwhile, the amount and type of organic acids vary between microorganisms (Krishnaraj & Dahale 2014).

Isolation of PSB from rice crops has been carried out by (Putriani et al. 2019; Hartanti 2020; Wiraswati et al. 2020; Damo et al. 2022). *Enterobacter asburiae* is PSB isolated from the planting of paddy in the Aceh region (Putriani et al. 2019). Genus *Pseudomona*s, genus *Bacillus*, genus *Enterobacte*r, and genus *Azotobacte*r are PSB that are isolated from the paddy plant Situbagendit (Hartanti 2020). *Basil* sp., *Enterobacter* sp., and *Brachybacterium* sp. bacteria are also isolated from the paddy plant philosopher originating in West Java (Wiraswati et al. 2020). Furthermore, *Acidovorax* sp., *Pseudomonas* sp., *Burkholderia* sp., *Sphingomonas* sp., *Mycolicibacterium* sp., and *Variovorax* sp. are PSB isolated from paddy field soils in Japan (Damo et al. 2022).

PSB isolated from the cultivated land of paddy has several capabilities as *Indole Acetic Acid* (IAA) producers, inhibitors of pathogens, and biological control agents. *Enterobacter asburiae* is also a PSB isolated from the Aceh region with the ability to produce IAA hormones (Putriani et al. 2019). According to Parida et al. (2017), *Bacillus subtilis* shows promising potential as an inducer of resistance against HDB (Hawar Daun Bakteri/Bacterial Leaf Blight) disease in paddy plants. Furthermore, Wiraswati et al. (2020) highlighted its effectiveness as a biological control agent, owing to the production of an anti-fungal compound that aids in combatting Blast disease. Munif and Nurjayadi (2021) also identified several endophytic bacteria isolates, namely GH1, Si2, Si33, Sp24, and G053, which possess the capability to control *Meloidogyne graminicola* in rice crops. In another study conducted by Prihatiningsih et al. (2021), three endophytic bacteria strains are identified as potential agents for promoting plant growth and controlling bacterial leaf blight on rice.

Klebsiella and Acinetobacter are two isolates of PSB isolated from Pekanbaru's ultisol soil (Oksana et al. 2020). There is a scarcity of study focused on microbes, particularly PSB, originating from the ultisol soil of Bangka Island. According to Prihastuti (2012), several isolates isolated from ultisols are useful isolates. In addition, the original isolate originating from an area has adaptability to the local environment so that it is easier to apply it again to that area. Therefore, this study conducts an inventory and assessment of the potential PSB derived from paddy gogo cultivation in Bangka's ultisol.

MATERIALS AND METHODS

Materials

Soil samples were collected from upland rice cultivation areas located in Payabenua and Saing regions of Mendo Barat District, Bangka Regency. The samples were processed using pikovskaya medium (5 g of $AlPO_4$; 0.5 g $(NH_4)_2SO_4$, 0.1 g $MgSO_4.2H_2O$, 0.001 g $MnSO_4$, 0.001 g $FeSO_4$, 0.5 g yeast extract, and 15 g agar), 2% NaOCl, 70% alcohol, the tobacco leaf, sterile aquadest, Tryptone Soya Agar (TSA) media, Blood Agar media, 1% glucose, 0.05% yeast extract, and 0.5% phosphate, boric acid 0.5%, ammonium molybdate 0.38%, HCl 7.5%, KH_2PO_4, universal primers (Primer F: 16F27 and Primer R: 16R 1492).

Methods

The followings are four steps in this study.

Isolation of Rhizosphere and Endophytic Bacteria

Soil sampling was conducted during both the vegetative and generative phases of the study. The bacteria isolated were identified as rhizospheric and endophytic bacteria. The rhizospheric bacteria were derived from the soil surrounding the roots of the upland rice plant. To begin the process, 10 g soil samples were collected and subsequently dissolved in 90 ml of sterile aquadest. The resulting solution was then shaken vigorously for 2 minutes, resulting in a dilution of 10^{-1}. Subsequently, 1 ml of the soil solution was transferred to a test tube containing 9 ml of sterile aquadest, and the mixture was agitated using a vortex to achieve a dilution of 10^{-2}. This process was repeated until a dilution of 10^{-7} was obtained. From each series, 1 ml was aseptically transferred to a petri dish containing Pikovskaya agar medium. Petri dishes containing bacterial inoculations were incubated at room temperature for 3-6 days till a clear zone appeared. Isolates with clear zones were taken aseptically with a sterile needle and scratched on the agar medium as selected isolates.

Endophytic bacteria were isolated from the roots of the upland rice plant and carefully washed under a continuous stream of running water. The washed roots were then cut into 1-2 cm fragments and soaked in running water for 1-2 hours. Subsequently, the roots were dried on sterile tissue and to ensure the sterility of the surface, a sterilization procedure was conducted. The surface of the roots was treated with 2% NaOCl for 2-3 minutes, followed by a 70% alcohol treatment for 1-2 minutes. To eliminate any residual contaminants, the roots were then rinsed with sterile aquadest, repeating the rinsing process up to three times for 1 minute each time. Finally, they were dried again on sterile tissue and the browning areas were carefully removed, ensuring the integrity of the samples. The roots were then weighed 1 g and crushed using a sterile mortar. To obtain a root extract suitable for further analysis, the crushed roots were mixed with 9 mL of sterile aquadest and diluted accordingly to achieve a ratio of 10^{-4}. For the cultivation of the bacterial suspensions, 100 µL of the diluted root extract was inoculated onto Tryptone Soya Agar (TSA) media using surface plating method. The inoculated media plates were then incubated at room temperature for 48 hours, allowing the growth and development of the bacterial colonies.

Pathogenicity Testing

This study conducted pathogenicity testing, which comprised hypersensitivity and hemolysis tests. The hypersensitivity test method employed in this study was developed by Ropalia (2015). Bacterial colonies approximately 5 mm in diameter were collected using a loop and subsequently

suspended in 2.5 mL sterile water. The amount of 0.5 mL suspension was then injected onto the lower surface of the leaf, without penetrating the upper layer. After inoculation, the leaves were incubated for 24-48 hours, during which observations were made to detect any symptoms on the tobacco leaves. A positive hypersensitive reaction was identified by the presence of necrotic symptoms on the injected tobacco leaves. However, isolates that exhibited negative reactions were classified as non-pathogenic. The hemolysis test involved growing bacteria selected during the hypersensitivity test on Blood Agar medium, followed by an incubation period of 24 hours at room temperature. The presence of a clear zone surrounding the perimeter of the isolate indicated pathogenicity to both humans and animals.

Testing of the isolates in phosphate solubilization

The test of PSB ability to dissolve phosphates consisted of the phosphate solubilizing index (PSI) and the P dissolution test. P nutrient solubilizing index test was carried out by streaking the PSB isolates on tricalcium phosphate agar medium, which was a modification of Pikovskaya media consisting of 10 g glucose, 5 g $Ca_3(PO_4)_2$, 0.5 g $(NH_4)2SO_4$, 0.2 g KCL, 0.1 g $MgSO_4.7H_2O$, 0.5 g yeast extract, 25 mg $MnSO_4$, and 25 mg $FeSO_4$ as well as 20 g agar in 1 L aquadest. Furthermore, isolates of bacteria aged 48 hours were taken using sterile oasis needles and grown on Pikovskaya medium. The clear zone around isolates was observed 7 days after incubation and the PSI was measured using the following formula:

$$\text{PSI} = \frac{\text{clear zone diameter - isolate diameter}}{\text{isolate diameter}}$$

The P dissolution test was carried out by isolating bacteria on 25 ml of the growing medium for 7 days. The growing medium used consists of 1% glucose, 0.05% yeast extract, and 0.5% phosphate binding sources (Al and Ca). After incubation, the suspension of isolates was subjected to centrifugation at 4000 rpm for 25 minutes. This process aimed to separate the supernatant from microbial cells and insoluble phosphates. Following centrifugation, the supernatant was carefully collected and subsequently filtered. The measurement of dissolved phosphate was carried out by using modified method of Susilowati and Syekhfani (2014), in which 1 ml of the supernatant is mixed with reagent solution (boric acid 0.5%, ammonium molybdate 0.38%, HCl 7.5%) with 5 drops of reducing solution. The reaction solution was measured using a spectrophotometer with a wavelength of 880 nM and a standard solution using KH_2PO_4. Based on the results of phosphate measurements in liquid media, the percentage of phosphate solubility was calculated to determine the amount of PSB dissolving in phosphates. The percentage of phosphate solubility is calculated by the formula:

$$\text{Solubility Percentage (\%)} = \frac{\text{available P level (ppm)}}{\text{Total P level at source (ppm)}} \text{ x } 100\%$$

Testing of Organic Acids Content, Enzyme Phosphatase and Molecular Identification of Selected Bacteria Isolates

Selected PSB isolates were sent to the test laboratory to determine the content of organic acids, phosphatase enzymes, and molecular identification. Extraction of organic acids was carried out in Bogor Agrochemical Residue Laboratory using the HPLC analysis method. Measurement of phosphatase enzyme activity was conducted in the Soil Biology Laboratory, Faculty of Agriculture, Padjajaran University, using a spectropho-

tometer at a wavelength of 400 nm. Furthermore, the molecular identification of bacterial isolates was conducted in Bogor Environmental Biotechnology Laboratory for sequencing 16 Sr DNA gene with universal primers (Primer F: 16F27 and Primer R: 16R 1492).

RESULTS AND DISCUSSION

Result

Isolate of Rhizospheric and Endophytic Bacteria

The number of PSB isolates from the rhizosphere and endophytes of field rice cultivation during the vegetative and generative phases at different locations is shown in Table 1. The total isolates of PSB isolated from rice field cultivation areas at all locations in Bangka Regency were 120 isolates with the most distribution in the Payabenua area with 76 isolates. The 120 bacterial isolates were dominated by endophytic bacteria, namely 109 isolates, and 68 were found in the vegetative phase.

Pathogenicity Testing

About 120 isolates were successfully isolated and subjected to hypersensitivity testing. According to the results detected, 64 bacterial isolates caused chlorosis in tobacco leaves (Table 2) that caused chlorosis in tabacco leaves (Figure 1).

Figure 1. Tobacco leaves showing chlorosis after being tested for hypersensitivity.

Furthermore, 29 out of the 40 PSB isolates tested for hemolysis passed. Bacterial isolates that cause hemolysis on blood agar media are shown in Figure 2.

Figure 2. Clear zones (indicated by arrows) formed in hemolysis test.

Table 1. PSB isolates from rhizosphere and endosphere of gogo rice cultivation areas in Bangka Regency.

Location	Sample	Growth phase	Rhizospheric bacteria	Endophytes bacteria
			----------isolate------	
Payabenua	1	Vegetative	0	14
		Generative	4	1
	2	Vegetative	5	15
		Generative	0	37
Total			9	67
Saing	1	Vegetative	0	37
		Generative	1	2
	2	Vegetative	1	2
		Generative	0	1
Total			2	42
Totally			11	109

Table 2. Recapitulation of Hypersensitive Test of isolates of PSB from isolation in upland rice cultivation areas in Bangka Regency.

Location	Bacteria	Hypersensitive test	
		Vegetative phase	Generative phase
Payabenua	Rhizosphere	9	19
	Endophytes	4	4
Total		13	23
Saing	Rhizosphere	27	0
	Endophytes	1	0
Total		28	0
Totaly		41	23

Ability of isolates in dissolving phosphate

Testing the capacity to dissolve P was conducted on 23 bacterial isolates. The ability to dissolve P was examined in a total of 23 PSB isolates, as presented in Table 3. The dissolved P values varied among the 23 isolates, ranging from 9 to 200 mg L^{-1} in $AlPO_4$ liquid media and 3.8 to 843 mg L^{-1} in $Ca_3(PO_4)_2$ liquid media. The solubility value of P in $AlPO_4$ and $Ca_3(PO_4)_2$ liquid media exhibited a range of 0.0013 to 0.0344% and 0.0008 to 0.1842%, respectively.

Testing of Organic Acids Content, Enzyme Phosphatase and Molecular Identification of Selected Bacteria Isolates

Phosphatase enzymes and organic acids were measured in the 6 selected bacterial isolates that exhibited significantly dissolved P value and particularly high solubility in AlPO4 medium. These selected isolates were identified as BEP1V4, BEP1V7, BEP2G15, BEP2G18, BEP2V11, and BRP2V6 (Table 4), originating from Payabenua Village. BEP1V4 and BEP1V7 came from location 1, namely the upland rice cultivation area on new openings, while BEP2G15, BEP2G18, BEP2V11, and BRP2V6 were derived from the rice field cultivation area superimposed with pepper plants. BEP2G15 and BEP2G18 isolates were in the generative growth phase, while the others were in the vegetative phase.

Molecular identification results showed that BEP1V4, BEP1V7, BEP2G15, and BEP2G18 were the genus *Burkholderia*, while BEP2V11 and BRP2V6 were the genus *Serratia* as shown in Table 5 and Figure 3.

Discussion

The dominant bacteria obtained from isolation are endophytic PSB isolates derived from the root of the upland rice plant. Hartanti (2020) also succeeded in isolating four types of endophytic bacteria from the roots of the Situbagendit variety rice plant, while Putriani et al. (2019) isolated

Table 3. The ability of selected isolates to dissolve phosphates from upland rice cultivation in Bangka Regency.

No	Isolate Code	PSI_{Ca}	Dissolved P		Solubility P	
			$AlPO_4$	$(Ca_3PO_4)_2$	$AlPO_4$	$(Ca_3PO_4)_2$
			---------mg L^{-1}----------		----------%	----------
1	BEP_1V_3	0.24	12.5	5.8	0.0021	0.0013
2	BEP_1V_4	0.25	17.3	48	0.0030	0.0105
3	BEP_1V_7	0.27	17.8	54	0.0031	0.0118
4	BEP_1V_9	0.27	7.8	4.3	0.0013	0.0009
5	BEP_1V_{10}	0.40	13	6.3	0.0022	0.0014
6	BEP_1V_{12}	0.34	11.5	811	0.0020	0.1772
7	BEP_1V_{13}	0.45	14.8	18.3	0.0025	0.0040
8	BEP_1V_{14}	0.68	14.8	19.8	0.0025	0.0043
9	BEP_1V_{16}	0.24	14	39	0.0024	0.0085
10	BEP_2G_1	0.26	15.5	9	0.0027	0.0020
11	BEP_2G_2	0.15	16.3	9.3	0.0028	0.0020
12	BEP_2G_3	0.27	9	8.5	0.0015	0.0019
13	BEP_2G_4	0.18	13.3	5.8	0.0023	0.0013
14	BEP_2G_5	0.25	17.8	9.3	0.0031	0.0020
15	BEP_2G_6	0.42	17.8	11.5	0.0031	0.0025
16	BEP_2G_{15}	0.14	200	843	0.0344	0.1842
17	BEP_2G_{18}	0.22	26.3	11	0.0045	0.0024
18	BEP_2V_1	0.52	16.3	13.3	0.0028	0.0029
19	BEP_2V_4	0.30	16	6.3	0.0027	0.0014
20	BEP_2V_9	0.32	14.5	14.5	0.0025	0.0032
21	BEP_2V_{11}	0.15	47	378	0.0081	0.0826
22	BEP_2V_{15}	0.45	26.3	3.8	0.0045	0.0008
23	BRP_2V_6	-	22	367	0.0038	0.0802

Table 4. The content of phosphatase enzymes and organic acids of PSB from upland rice cultivation in Bangka Regency.

No	Isolate code	Phosphatase Enzyme (ppm)	Organic acids				
			Acetic acid	*Lactic acid*	Malic acid	Citric acid	Oxalic acid
		---ppm---	---------mg L^{-1}----------				
1	BEP_1V_4	1.36	3.98	nm	nm	0.251	0.373
2	BEP_1V_7	2.63	2.026	1.058	nm	0.063	0.139
3	BEP_2G_{15}	2.43	3.292	nm	nm	0.173	0.343
4	BEP_2G_{18}	2.69	4.35	0.655	1.456	0.211	0.335
5	BEP_2V_{11}	2.04	2.372	1.00	0.455	0.078	0.202
6	BRP_2V_6	0.90	0.493	0.907	0.921	0.088	nm

ppm=part per million, nm= not measured

six endophytic isolates from rice roots in the Aceh area. According to Ji et al. (2014), endophytic bacteria in rice plants had a fairly important role in spurring plant growth. Marwan et al. (2021) reported that the isolates from local Jambi rice varieties had the potential to be developed as biological control agents against blast disease caused by *P. oryzae*. Meanwhile, Prihatiningsih et al. (2021) concluded that three endophytic bacteria (SM1, SB 1, and SB 3) associated with rice roots could be categorized as potential plant growth promoters.

The population of endophytic bacteria was found in Payabenua when compared to the Saing area. In the Payabenua area, bacteria were isolated from rice fields cultivated in dry areas. In Saing area, the rice field area is pure upland area since the land become flooded when rainy season. Therefore, the conditions of the different planting areas caused the variety of isolates found. Bacterial isolates from the Payabenua area

Table 5. Molecular identification of selected isolates based on 16 Sr DNA sequence similarity.

No	Isolate code	Bacterial name	Similarity index
1	BEP_1V_4	*Bukholderia sp*	Homology 99,92% with *Burkholderia* sp. strain RB141 16S ribosomal RNA gene, partial sequence.
2	BEP_1V_7	*Bukholderia cenocepcia*	Homology 99,93% with *Burkholderia cenocepacia* strain PC184 Mulks chromosome 3, complete sequence.
3	BEP_2G_{15}	*Bukholderia latens*	Homology 99,78% with *Burkholderia latens* strain AU17928 chromosome 1, complete sequence.
4	BEP_2G_{18}	*Burkholderia vietnamiensis*	Homology 99,57% with *Burkholderia vietnamiensis strain TVV75*, partial sequence
5	BEP_2V_{11}	*Serratia marcescens*	Homology 99,86%, with *Serratia marcescens* strain CTC639-K12, partial sequence.
6	BRP_2V_6	*Serratia surfactantfaciens*	Homology 99,81% with *Serratia surfactantfaciens* strain YD25.

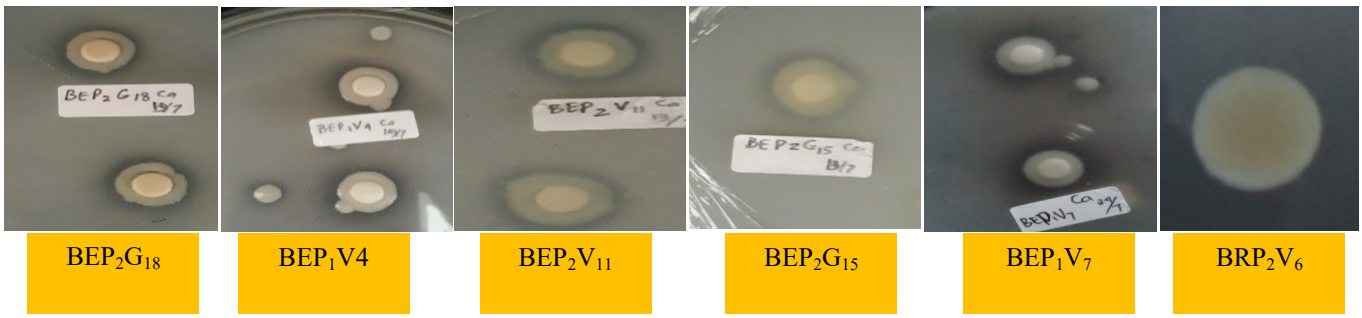

Figure 3. The six selected isolated from Upland Rice Cultivation Areas in Bangka Regency.

were predominantly reported in the vegetative growth phase and came from rice field cultivation areas superimposed with pepper plants. Pande et al. (2020) stated that physical and chemical characteristics of the soil, organic matter, phosphorus concentration, and cultural activities had an impact on the PSB population.

Despite the HDB prevalence in the vegetative growth phase, dominant selected isolates originated from the generative growth phase. However, the measurement of the phosphatase enzyme as well as the levels of organic acids obtained from the generative phase were relatively higher than the vegetative phase. According to Setiawati et al. (2014), the ability to produce enzyme phosphatase and the production of organic acids is a characteristic of the ability of PSB isolates. According to Ranjan et al. (2013), a phosphatase is a group of enzymes that catalyzes an enzymatically hydrolytic mineralization reaction with the release of undissolved phosphates into dissolved. Situmorang et al. (2015) explained that the higher the enzyme activity produced by PSB, the greater clear zone. Fitriatin et al. (2020) stated that the important role of the phosphatase enzyme was in the hydrolysis process of organic phosphate into inorganic phosphate.

In addition to the production of phosphatase enzymes, PSB also generated organic acids, which played a crucial role in the P solubilization. These organic acids contributed to the process through several mechanisms by acidifying the rhizosphere, aiding in the chelation of cations responsible for phosphate precipitation, facilitating the availability of metal ions associated with insoluble Ca, Al, and Fe phosphate compounds, and competing with P for adsorption sites on the soil. (Kishore et al. 2015). Organic acids in PSB include citric, gultamic, succinic, oxalic,

malic, fumaric,and tartaric acids (Seshachala & Tallapragada 2012; Asrul & Aryantha 2020). Malic, citric and oxalic acids have low molecular weight and are effective in alkalizing Al (Hafif et al. 2010). Bacterial isolates of the *Burkholderia* sp group also produced low molecular weight organic acids compared to *Serratia* sp. Therefore, the solubilization ability of *Burkholderia* sp. group is more effective in Al medium compared to the *Serratia* sp. Fitriatin et al. (2021) reported that organic acids (lactate, citrate, oxalate, and tartrate) in *Burkholderia* sp. bacteria (WK strain 11 and MQ-14W strain) were produced more at pH 4.5 than at pH 7 or 10.5.

Genus of endophytic bacteria that dominate the internal tissues of rice plants are *Pseudomonas*, *Bacillus*, *Streptomyces*, *Azospirillum*, and *Azotobacter* (Kumar et al. 2020). Furthermore, *Burkholderia* is a common bacterial family involved in the solubilization of phosphate (Kishore et al. 2015). Raweekul et al. (2016) isolated endophytic bacteria from rice and reported that the genus *Burkholderia* was dominant on the stalks. However, Aroumougame's (2020) study found that *Burkholderia* was dominant in the roots of rice plants. Several studies related to the genus in food crops have been reported, such as *Burkholderia caribensis* of rice agroecosystems of South Assam, India (Roy et al. 2013) and *Burkholderia cepacia* in maize (Zhao et al. 2014). The genus consists of more than 40 bacteria that cluster to form a species complex known as *B. cepacia* (Bcc) (Arriel-Elias et al. 2019) *Burkholderia* is a bifunctional genus because some of its species establish symbiotic-mutualistic relationships with plants, and symbiotic-pathogenic associations with plants, animals, and humans (Espinosa-Victoria et al. 2020).

The phosphate-solubilizing bacteria obtained in this study are local bacterial isolates, so they have prospects for development in the Bangka region in particular. In addition, generally, the bacteria obtained are endophytic bacteria, so it is possible to use them on other crops besides rice. Allegedly, besides having a mechanism as a phosphate solubilizer, the bacterial isolates obtained have other functions as biocontrol as well as the ability to PGPR. Therefore, there is a need for further research to find out some information related to the bacteria obtained in this study.

CONCLUSIONS

In conclusion, a total of 6 isolates of potential PSB were obtained from the ultisol land of upland rice cultivation in Payabenua Village, Bangka Regency. Among these isolates, *Bukholderia* sp., *Bukholderia cenocepcia*, *Bukholderia latens*, and *Burkholderia vietnamiensis* belonged to the genus *Burkholderia*. Furthermore, the remaining two were identified as *Serratia marcescens*, belonging to the genus *Serratia*. The levels of both phosphatase enzymes and organic acids produced by the genus *Burkholderia* were found to be higher than those produced by *Serratia*. The solubility value of P in $AlPO_4$ and $Ca_3(PO_4)_2$ liquid media exhibited a range of 0.0013 to 0.0344% and 0.0008 to 0.1842%, respectively.

AUTHOR CONTRIBUTION

KK designed the study process, collected and analyzed the data, as well as wrote the manuscript. MRS designed, supervised the study, and wrote the manuscript. AB, ERP, and SI supervised the study and edited the manuscript.

ACKNOWLEDGMENTS

The authors are grateful to Lembaga Pangkal Data Pendidikan (LPDP) Republic of Indonesia for funding this study through the 2017 Indonesian Lecturer Excellence Scholarship (BUDI DN 2017).

CONFLICT OF INTEREST

The authors declare no conflict of Interest

REFERENCES

Aroumougame, S., Mannan Geetha, T. & Thangaraju, M., 2020. Exploitation of PGPR endophytic *Burkholderia* isolates to enhance organic agriculture. *American Journal of BioScience*, 8(3), 57. doi: 10.11648/j.ajbio.20200803.12.

Arriel-Elias, M.T. et al., 2019. Induction of resistance in rice plants using bioproducts produced from *Burkholderia pyrrocinia* BRM 32113. *Environmental Science and Pollution Research*, 26(19), pp.19705–19718. doi: 10.1007/s11356-019-05238-3.

Asril, M. & Lisafitri, Y., 2020. Isolasi bakteri pelarut fosfat genus *Pseudomonas* dari tanah masam bekas areal perkebunan karet di kawasan Institut Teknologi Sumatera. *Jurnal Teknologi Lingkungan*, 21(1), pp.40–48. doi: 10.29122/jtl.v21i1.3743.

Asrul, A. & Aryantha, I.N.P., 2020. Isolasi dan Identifikasi Bakteri Pelarut Fosfat dari Tanah Rhizofer Kelapa Sawit (*Eleis guineensis*). *Lumbung*, 19(1), pp.30–39. doi: 10.32530/lumbung.v19i1.204.

Awais, M. et al., 2017. Isolation, characterization and inter-relationship of phosphate solubilizing bacteria from the rhizosphere of sugarcane and rice. *Biocatalysis and Agricultural Biotechnology*, 11, pp.312–321. doi: 10.1016/j.bcab.2017.07.018.

Damo, J.L.C. et al., 2022. Isolation and characterization of phosphate solubilizing bacteria from paddy field soils in Japan. *Microbes and Environments*, 37(2), ME21085. doi: 10.1264/jsme2.ME21085.

Espinosa-Victoria, D. et al., 2020. The Burkholderia genus: between mutualism and pathogenicity. *Revista Mexicana de Fitopatología, Mexican Journal of Phytopathology*, 38(3), pp.1–23. doi: 10.18781/r.mex.fit.2004-5.

Fitriatin, B.N., Dewi, V.F. & Yuniarti, A., 2021. The impact of biofertilizers and NPK fertilizers application on soil phosphorus availability and yield of upland rice in tropic dry land. *E3S Web of Conferences*, 232, 03012. doi: 10.1051/e3sconf/202123203012.

Fitriatin, N.B. et al., 2020. Compatibility, phosphate solubility and phosphatase activity by phosphate solubilizing bacteria. *Haya: The Saudi Journal of Life Sciences*, 5(12), pp.281–284. doi: 10.36348/sjls.2020.v05i12.003.

Hafif, B. et al., 2010. Khelatisasi ion aluminium oleh asam organik eksudat akar *Brachiaria*. *Biota : Jurnal Ilmiah Ilmu-Ilmu Hayati*, 15(3), pp.316–324. doi: 10.24002/biota.v15i3.2585.

Hartanti, D.A.S., 2020. Isolasi bakteri endofit pelarut fosfat pada tanaman padi (Oryza sativa) var.situbagendit. *STIGMA: Jurnal Matematika dan Ilmu Pengetahuan Alam Unipa*, 13(1), pp.8-14. doi: 10.36456/stigma.13.1.2417.8-14.

Ji, S.H., Gururani, M.A. & Chun, S.C., 2014. Isolation and characterization of plant growth promoting endophytic diazotrophic bacteria from Korean rice cultivars. *Microbiological Research*, 169(1), pp.83–98. doi: 10.1016/j.micres.2013.06.003.

Kishore, N; Pindi, Pavan K; Reddy, S.R., 2015. Phosphate-solubilizing microorganisms: A Critictial Review. *Plant Biology and Biotechnology: Plant Diversity, Organization, Function and Improvement*, 1, pp.1–827. doi: 10.1007/978-81-322-2286-6.

Krishnaraj, P.U. & Dahale, S., 2014. Mineral phosphate solubilization: Concepts and prospects in sustainable agriculture. *Proceedings of the Indian National Science Academy*, 80(2), pp.389–405. doi: 10.16943/ptinsa/2014/v80i2/55116.

Kumar, J.K. et al., 2020. Rice endophytes and their potential applications. *Journal of Scientific Agriculture*, 4, pp.64–65. doi: 10.25081/jsa.2020.v4.6315.

Marwan, H., Nusifera, S. & Mulyati, S., 2021. Potensi bakteri endofit sebagai agens hayati untuk mengendalikan penyakit blas pada tanaman padi. *Jurnal Ilmu Pertanian Indonesia*, 26(3), pp.328–333. doi: 10.18343/jipi.26.3.328.

Munif, A. & Nurjayadi, M.Y., 2021. Potensi beberapa isolat bakteri endofit untuk pengendalian biologi *Meloidogyne graminicola* pada tanaman padi. *Jurnal Fitopatologi Indonesia*, 17(1), pp.28–34. doi: 10.14692/jfi.17.1.28-34.

Oksana, O. et al., 2020. Isolasi dan identifikasi bakteri pelarut fosfat pada tanah Ultisol di Kecamatan Rumbai, Pekanbaru. *Agrotechnology Research Journal*, 4(1), pp.22–25. doi: 10.20961/agrotechresj.v4i1.36063.

Pande, A. et al., 2020. Isolation, characterization, and identification of phosphate-solubilizing *Burkholderia cepacia* from the sweet corn cv. Golden Bantam rhizosphere soil and effect on growth-promoting activities. *International Journal of Vegetable Science*, 26(6), pp.591–607. doi: 10.1080/19315260.2019.1692121.

Parida, I., Damayanti, T.A. & Giyanto, G., 2017. Isolasi, seleksi, dan identifikasi bakteri endofit sebagai agens penginduksi ketahanan padi terhadap hawar daun bakteri. *Jurnal Fitopatologi Indonesia*, 12(6), 199. doi: 10.14692/jfi.12.6.199.

Prihastuti, 2012. Upaya pengelolaan biologis lahan kering masam Ultisol. *Balai Penelitian Tanaman Kacang-Kacangan dan Umbi-Umbian*, 2 (2), pp.104–111.

Prihatiningsih, N., Djatmiko, H.A. & Lestari, P., 2021. Endophytic bacteria associated with rice roots from suboptimal land as plant growth promoters. *Biodiversitas*, 22(1), pp.432–437. doi: 10.13057/biodiv/d220153.

Putriani, Fitri, L. & Ismail, Y.S., 2019. The potensial endophytic bacteria isolated from rice (*Oryza sativa*) as biofertilizer. *Biosaintifika: Journal of Biology & Biology Education*, 11(3), pp.178–185.

Ranjan, A., Mahalakshmi, M.R. & Sridevi, M., 2013. Isolation and characterization of phosphate-solubilizing bacterial species from different crop fields of Salem, Tamil Nadu, India. *International Journal of Nutrition, Pharmacology, Neurological Diseases*, 3(1), 29. doi: 10.4103/2231-0738.106982.

Raweekul, W. et al., 2016. Plant growth promotion by endophytic bacteria isolated from rice (*Oryza sativa*). *Science & Technology Asia*, pp.6–17. doi: 10.14456/tijsat.2016.2.

Ropalia, 2015. *Potensi mikrob endofit dan aplikasinya dengan kompos tandan kosong kelapa sawit untuk pengendalian penyakit kuning pada lada*. Bogor: IPB.

Roy, B.D., Deb, B. & Sharma, G.D., 2013. Isolation , characterization and screening of Burkholderia caribensis of rice agro-ecosystems of. *African Journal of Agricultural Research*, 8(4), pp.349–357. doi: 10.5897/AJAR11.825.

Seshachala, U. & Tallapragada, P., 2012. Phosphate Solubilizers from the Rhizospher of *Piper nigrum* L. in Karnataka, India. *Chilean journal of agricultural research*, 72(3), pp.397–403. doi: 10.4067/s0718-58392012000300014.

Setiawati, M.R. et al., 2014. Karakterisasi isolat bakteri pelarut fosfat untuk meningkatkan ketersediaan P pada media kultur cair tanaman jagung (*Zea mays* L.). *Bionatura-Jurnal Ilmu-ilmu Hayati dan Fisik*, 16(1), pp.30–34.

Setiawati, M.R. & Pranoto, E., 2015. Perbandingan beberapa bakteri pelarut fosfat eksogen pada tanah Andisol sebagai areal pertanaman teh dominan di Indonesia. *Jurnal Penelitian The dan Klna*, 18(2), pp.159–164.

Situmorang, E.C. et al., 2015. Indigenous phosphate solubilizing bacteria from peat soil for an eco-friendly biofertilizer in oil palm plantation. *KnE Energy*, 1(1), p.65. doi: 10.18502/ken.v1i1.324.

Sonia, A.V. & Setiawati, T.C., 2022. Aktivitas bakteri pelarut fosfat terhadap peningkatan ketersediaan fosfat pada tanah masam. *Agrovigor: Jurnal Agroekoteknologi*, 15(1), pp.44–53. doi: 10.21107/agrovigor.v15i1.13449.

Sugianto, S.K., Shovitri, M. & Hidayat, H., 2019. Potensi Rhizobakteri Sebagai Pelarut Fosfat. *Jurnal Sains dan Seni ITS*, 7(2), pp.7–10. doi: 10.12962/j23373520.v7i2.37241.

Susilowati, L. & Syekhfani, 2014. Characterization of phosphate solubilizing bacteria isolated from Pb contaminated soils and their potential for dissolving tricalcium phosphate. *Journal of Degraded and Mining Land Management*, 1(2), pp.57–62.

Wahyudin, A. et al., 2017. Respons tanaman jagung (*Zea mays* L.) akibat pemberian pupuk fosfat dan waktu aplikasi pupuk hayati mikroba pelarut fosfat pada Ultisols Jatinangor. *Kultivasi*, 16(1), pp.246–254. doi: 10.24198/kultivasi.v16i1.11559.

Wiraswati, S.M. et al., 2020. Rice phyllosphere bacteria producing antifungal compounds as biological control agents of blast disease. *Biodiversitas*, 21(4), pp.1273–1278. doi: 10.13057/biodiv/d210401.

Yadav, A. et al., 2015. Rhizospheric microbes are excellent plant growth promoters. *Indian Journal of Natural Sciences*, 5(30), pp.6584-6595.

Zhao, K. et al., 2014. Maize rhizosphere in Sichuan, China, hosts plant growth promoting *Burkholderia cepacia* with phosphate solubilizing and antifungal abilities. *Microbiological Research*, 169(1), pp.76–82. doi: 10.1016/j.micres.2013.07.003.

Journal of Tropical Biodiversity and Biotechnology
Volume 09, Issue 01 (2024): jtbb83140
DOI: 10.22146/jtbb.83140

Research Article

Chrysin Inhibits Indonesian Serotype Foot-and-Mouth-Disease Virus Replication: Insights from DFT, Molecular Docking, and Molecular Dynamics Analyses

Agus Susilo[1]*, Miftakhul Cahyati[2], Nurjannah[3], Dodyk Pranowo[4], Feri Eko Hermanto[5], Elma Putri Primandasari[6]

1)Department of Animal Products Technology, Faculty of Animal Science, Universitas Brawijaya, Malang 65145, Indonesia
2)Department of Oral Medicine, Faculty of Dentistry, Universitas Brawijaya, Malang 65145, Indonesia
3)Department of Statistics, Faculty of Mathematics and Natural Sciences, Universitas Brawijaya, Malang 65145, Indonesia
4)Department of Agro-industrial Technology, Faculty of Agricultural Technology, Universitas Brawijaya, Malang 65145, Indonesia
5)Faculty of Animal Sciences, Universitas Brawijaya, Malang 65145, Indonesia
6)Department of Business and Hospitality, Faculty of Vocational, Universitas Brawijaya, Malang 65145, Indonesia
* Corresponding author, email: agussusilo@ub.ac.id

Keywords:
3C Protease
antivirus
Chrysin
Foot-and-Mouth-Disease Virus
Propolis.
Submitted:
15 March 2023
Accepted:
23 August 2023
Published:
08 January 2024
Editor:
Furzani Binti Pa'ee

ABSTRACT

Chrysin, a predominant compound in Propolis, possesses diverse bioactivities, including antiviral properties. However, its antiviral efficacy against the Indonesian Foot-and-Mouth Disease Virus (FMDV) serotype remains unexplored. This study investigates Chrysin's inhibitory potential against FMDV Indonesian serotype by targeting the 3C Protease (3CP), a vital enzyme for viral replication. Multiple sequence alignment was used to reveal unique characteristics of the Indonesian serotype's 3CP compared to global serotypes. Density Functional Theory (DFT) calculations assessed Chrysin's interaction with 3CP based on electronegativity features. Molecular docking and molecular dynamics analyses evaluated Chrysin's inhibitory activity against 3CP, using homology modeling for the Indonesian serotype's 3CP structure. Luteolin, a known FMDV 3CP inhibitor with a similar structure to Chrysin, served as a reference. Results showed distinct 3CP sequences in the Indonesian serotype compared to O serotypes and others. Chrysin exhibited potential electron-donor activity with lower HOMO and LUMO values than Luteolin, but they had similar energy gaps, i.e., 4.016 and 4.044 eV, respectively. Molecular docking indicated similar binding affinities, with Chrysin (-6.365 kcal/mol) and Luteolin (-6.864 kcal/mol) bound to active site residues. Molecular dynamics analysis demonstrated stable 3CP-Chrysin and 3CP-Luteolin complexes, with minor differences in Radius of gyration (Rg) and Root-Mean-Square Fluctuation (RMSF) below 1 Å. From the ligand stability point of view, Chrysin had comparable stability with Luteolin. However, Chrysin formed fewer hydrogen bonds and displayed greater free-binding energy than Luteolin during simulation periods. These findings suggest that Chrysin holds promise as an inhibitor of the Indonesian serotype's FMDV 3C Protease.

Copyright: © 2024, J. Tropical Biodiversity Biotechnology (CC BY-SA 4.0)

INTRODUCTION

The recent Foot-Mouth-Disease (FMD) outbreak in Indonesia has struck cattle farming in Indonesia. The outbreak affected 20 provinces, which

was first reported in East Java province before it had widespread across the Indonesian archipelago. Although no zoonotic case was reported, the outbreak has affected human welfare by attacking economic values since livestock is categorized as a valuable asset in the community (IFRC 2022). As acute and systemic domestic animal diseases, FMD was caused by FMD Virus (FMDV) infection. Seven serotypes have been identified: A, O, C, Asia1, and South African Territories (SAT) serotypes SAT1, SAT2, and SAT3 (Grubman & Baxt 2004), and Indonesian serotype is classified as serotype O (Carrillo et al. 2005). The genetic diversity of FMDV, as represented by various serotypes, impacts both its antigenicity and viral structure, thereby hindering effective control through cross-protection measures, including vaccination (Li et al. 2021; Tesfaye et al. 2022). Hence, a promising approach to control FMDV involves targeting the non-structural proteins of the virus (Curry et al. 2007), as most vaccines primarily target structural proteins (typically inactivated or live-attenuated forms) (Kamel et al. 2019).

Non-structural proteins are typically enzymes that play a role in the assembly of viral structures (Han et al. 2015). Upon infection, FMDV will quickly transcribe and translate its genome to construct both structural and non-structural proteins, then produces a new virus particle (Wang et al. 2015). Those processes are mainly orchestrated by 3 Cysteine Protease (3CP), a non-structural protein and also an enzyme that catalyzes the cleaving of immature proteins into mature viral particles (Wang et al. 2015). Most drugs have been developed targeting this enzyme due to its essential activity in increasing viral load (Curry et al. 2007; Roqué Rosell et al. 2014). Besides, some natural products like Luteolin, Isoginkgetin, Andrographolide, and Deoxyandrographolide have also been evaluated to have antiviral activity through inhibition of 3CP of FMDV serotype A (Theerawatanasirikul et al. 2021; Theerawatanasirikul et al. 2022). Nevertheless, there is no information on the inhibitory activity against 3CP from the Indonesian serotype, since Indonesian serotype was classified into serotype O (Carrillo et al. 2005). Still, there is an opportunity for natural products to be involved in the development of controlling FMDV infection.

Propolis, also known as bee glue, is one of the products from bee farms. It is collected by bee workers from various plants' resinous secretion and mixed with a salivary and enzymatic substance to produce a wax-like substance (Anjum et al. 2019). Beyond the plant resins and essential oils, propolis also contains several bioactive molecules ranging from polyphenols to several minerals (Trusheva et al. 2011; Anjum et al. 2019). Due to its rich active compound, propolis has been widely used as an active pharmaceutical ingredient with countless biological activities (Rosyidi et al. 2018; Šuran et al. 2021; Zulhendri et al. 2021; Hidayat et al. 2022) Among several bioactive molecules in propolis, Chrysin constitutes the largest compounds (Wang et al. 2015). A previous study reported that Chrysin could inhibit the activity of 3CP of Enterovirus 71 and Coxsackievirus B3 as the primary infectious agent in Hand-Foot-and-Mouth Disease (HFMD)(Wang et al. 2014; Song et al. 2015). However, there is no information regarding the activity of Chrysin against the 3CP of FMDV.

Density functional theory (DFT) is a widely used computational method in chemistry and materials science to calculate the electronic structure of molecules and solids. One of the applications of DFT is in mapping the electronegativity of ligands prior to the molecular docking process (Yele et al. 2021). Electronegativity quantifies an atom's ability to attract electrons to itself in a chemical bond. The objective of molecu-

lar docking is to predict the binding affinity between a ligand and a protein. As it influences the distribution of electrons in the ligand and the protein, the electronegativity of a ligand may influence its binding affinity to a protein (Palko et al. 2021). Employing quantum mechanical method to predict the electronegativity, as DFT does, would be useful in improving binding affinity estimations (Ryde & Söderhjelm 2016). Moreover, the DFT technique also produced a geometry- optimized and energy -minimized structure (Bálint & Jäntschi 2021), which helps to reach the optimum molecular docking analysis (Ramírez-Velásquez et al. 2022). Therefore, by combining the DFT technique, molecular docking, and molecular dynamics approach, this study will explore the potential activity of Chrysin as the inhibitor of 3CP of FMDV, particularly for Indonesian serotype.

MATERIALS AND METHODS

Alignment of 3CP of FMDV serotypes

Amino acid sequences of several 3CPs from available FMDV serotypes were retrieved from GenBank database. The detailed identities of selected sequences as mentioned in the supplementary file table S1. Sequence alignment was performed in BioEdit software (Hall 1999) with the default parameters.

Protein Modeling and Binding Site Determination

The 3D structure of 3CP was homology-modeled by SwissModel (Waterhouse et al. 2018) according to the sequence obtained from the GenBank protein database with accession number AAT01756.1 (Carrillo et al. 2005). The structure of 3CP from FMDV serotype A10 (Protein Data Bank Identity, PDB ID: 2WV5) was used as the template. The active site residues were selected according to the previous elucidated structure, i.e., 2WV5 (Zunszain et al. 2010). Those active site then selected to guide the molecular docking step.

Ligand Structure Retrieval

Chrysin' and Luteolin's Three-dimensional (3D) structure was retrieved from the PubChem database (Kim et al. 2023) with compound identity (CID) 5281607 and 5280445, respectively. The isomeric Simplified Molecular-Input Line-Entry System (SMILES) was used for geometry optimization in the subsequent analysis.

Geometry Optimization and Density-Functional Theory Calculation

The 3D of Chrysin and Luteolin was built by Avogadro 1.2.0 software (Hanwell et al. 2012) according to the SMILES code. The geometry optimization was performed by ORCA 5.0.3 (Neese et al. 2020). The input for ORCA software was generated by Avogadro extension with B3LYP hybrid functional and def2-SVP basis set (Weigend & Ahlrichs 2005; Siiskonen & Priimagi 2017) settings. The Density Functional Theory (DFT) calculation output was analyzed and visualized using Avogadro to study the electronegativity properties of Chrysin and Luteolin. This involved representing the Highest Occupied Molecular Orbital (HOMO) and Lowest Unoccupied Molecular Orbital (LUMO) as blue for atoms with positive energy and red for atoms with negative energy. In addition, the value of the energy gap (ΔE) was calculated by the following equation (Rammohan et al. 2020; Maqsood et al. 2022):

$$\Delta E = E_{LUMO} - E_{HOMO} \quad (1)$$

Also, ionization potential (IP) and electron affinity (EA) were also determined according to the Hartree–Fock (HF) model with the following

equations (Rammohan et al. 2020; Hossen et al. 2021):

$$IP = -E_{HOMO} \quad (2)$$

$$EA = -E_{LUMO} \quad (3)$$

Molecular Docking

AutoDock Vina version 1.2.3 was employed to do molecular docking in a PyRx packages (Trott & Olson 2010; Dallakyan & Olson 2015; Eberhardt et al. 2021) according to the previous workflow (Hermanto et al. 2019). The 3D structure of Chrysin was inserted into PyRx software by OpenBable software (O'Boyle et al. 2011). The structure was energy-minimized using a universal force-field (uff) before the docking process. The docking was performed by setting 3CP and Chrysin as macromolecule and ligand, respectively. The docking will provide the ligand's binding energy and the binding pose. The structural interaction between 3CP and Chrysin was analyzed by Discovery Studio 2019 and visualized by PyMOL.

Molecular Dynamics and Free Binding Energy Calculation

YASARA 20.12.24 was employed to perform the molecular dynamics analysis (Krieger & Vriend 2015). The system was set as the previous study (Hermanto et al. 2022): pH 7.4; 0.9% NaCl concentration; 0.997 water density; 1 atm pressure, and 310°K temperature, cubic grid shape, 50 ns simulation time under AMBER14 forcefield (Maier et al. 2015). The structural dynamics were presented as the Root-Mean-Square Deviation (RMSD) of atom position or Root-Mean-Square Fluctuation (RMSF) of the residue's atoms. Furthermore, the free binding energy is also calculated according to the Molecular Mechanics – Poisson-Boltzmann Surface Area (MM-PBSA) (Homeyer & Gohlke 2012) equation in YASARA binding energy macros.

RESULTS AND DISCUSSION

Amino Acid Mutation of 3CP of Indonesian Serotypes Compared to Other Variants

The amino acid sequences alignment revealed slight variations in the arrangement of amino acids among Indonesian serotypes compared to other serotypes, excluding SAT serotypes. In particular, significant differences were observed at positions T104 and D177 among O serotypes, with most O serotypes having amino acids V and E. Notably, the sequences of the 3CP of Indonesian serotypes were distinct from other O serotypes, suggesting a unique structure for the 3CP of Indonesian serotypes. However, there were no mutations in the active site residues of Indonesian serotypes when compared to all the analysed serotypes (see supplementary file figure S1).

Structural Stability of 3CP of Indonesian Serotypes

Since the amino acid sequences of 3CP of Indonesian serotypes were different compared to the other O serotypes, the structural instability may happen. In addition, there is no available crystallographic structure of Indonesian serotypes in the database. Therefore, homology modelling was performed to obtain the 3D structure of 3CP of Indonesian serotypes. Upon modelling, the structure was then evaluated for its stability using molecular dynamics analysis compared to the available experimental structure of 3CP protein, i.e., 2WV5.

The modelling process resulted in a highly similar structure to the template, with both structures having a root mean square deviation (RMSD) of less than 1 Å (see figure 1A). The structural stability, as indi-

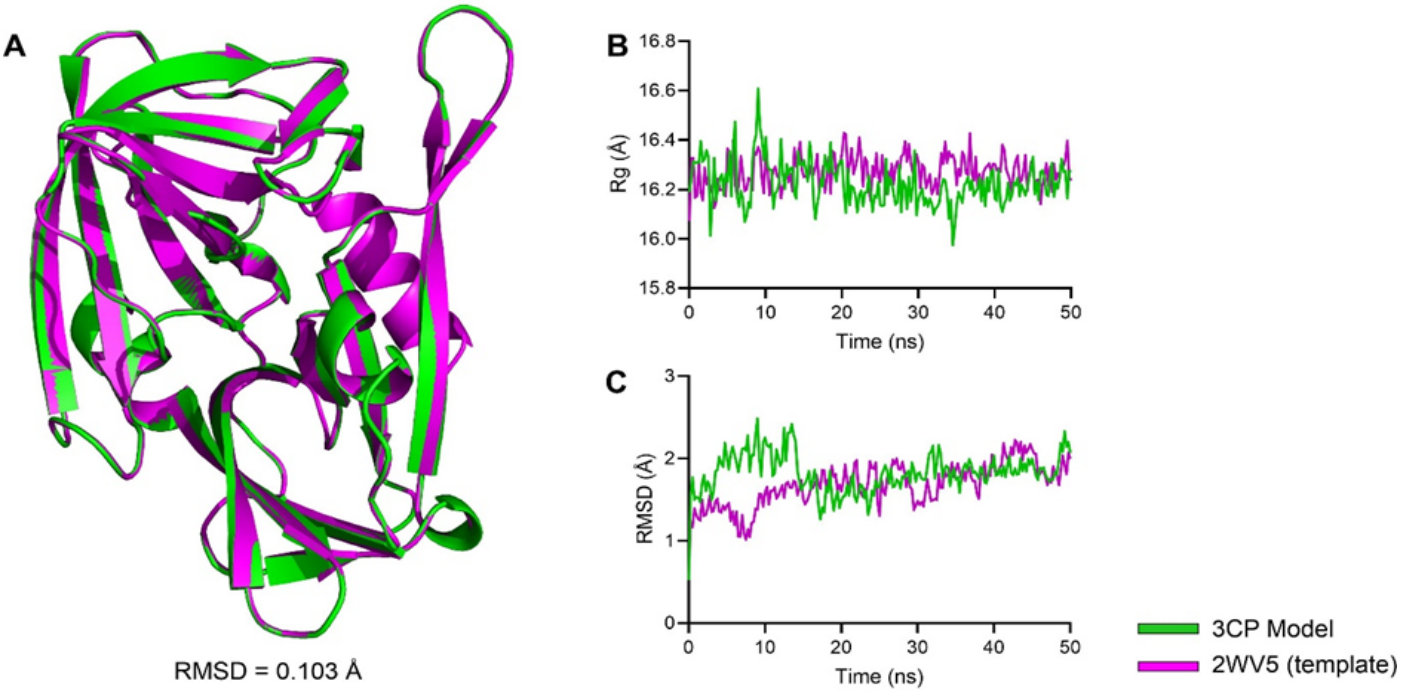

Figure 1. Structural differences and stability assessment of the 3CP of Indonesian serotypes with the template structure (PDB ID: 2WV5). Structural alignment of the model from 3CP of Indonesian serotypes (green ribbon) with the template (magenta ribbon) (A) along with the stability measures according to the Rg (B) and the RMSD of backbone atoms (C).

cated by the Radius of Gyration (Rg) and the RMSD of backbone atoms, also showed similarities between the model and the template. The Rg values revealed that both structures exhibited similar compactness, with minimal differences of less than 1 Å. Although minor fluctuations occurred during the initial 0-15 ns of the simulation, these differences were still within the range of less than 1 Å (figure 1B). The stability of the backbone atoms, as depicted in figure 1C, also demonstrated these small fluctuations. However, both structures experienced stabilization after the 15th ns of the simulation period, despite the presence of slight differences (figure 1C). Thus, small variations in the amino acid sequences of the 3CP of Indonesian serotypes have a small influence on the stability of its structure.

Electronegativity Properties

Chrysin, classified as a flavonoid based on its chemical structure, consists of two benzene rings and an additional oxygen-containing ring. It shares a similar structure with Luteolin, a compound known for its inhibitory activity against 3CP of FMDV as confirmed by Theerawatanasirikul et al. (2021). It is worth noting that Luteolin and Chrysin, two flavonoids, exhibit minor differences in their structures. These differences primarily occur in the hydroxylation patterns of the B-ring, where Luteolin possesses hydroxyl groups at positions 3' and 4', while chrysin lacks hydroxyl groups at these positions (figure 2A). Consequently, conducting a DFT analysis to evaluate their electronic properties and predict similar bioactivity against 3CP becomes an intriguing task.

The computational analysis using DFT reveals the favorable interaction potential between Chrysin and 3CP based on their respective electronegativity profiles, particularly considering the ΔE value. Notably, Chrysin exhibits a ΔE value similar to that of Luteolin, a known inhibitor of 3CP (see Figure 2B). ΔE, obtained by calculating the energy difference between the LUMO and the HOMO, reflects the molecules' capability in

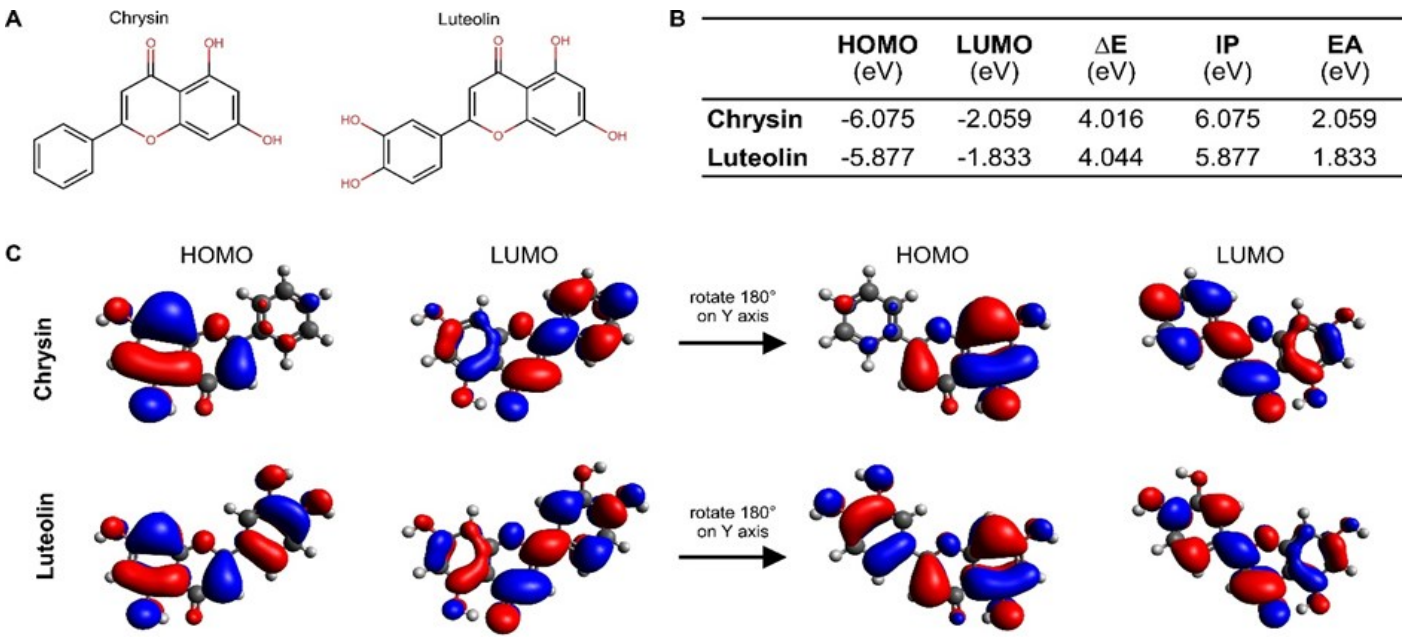

	HOMO (eV)	LUMO (eV)	ΔE (eV)	IP (eV)	EA (eV)
Chrysin	-6.075	-2.059	4.016	6.075	2.059
Luteolin	-5.877	-1.833	4.044	5.877	1.833

Figure 2. The structure and electronic properties of Chrysin and Luteolin. Both Chrysin and Luteolin have similar properties according to the chemical structure (A), electronegativity properties (B) and the HOMO and LUMO position (C) according to the DFT calculations.

electron transfer mechanisms (Rammohan et al. 2020). A smaller ΔE value indicates more efficient electron transfer (Islam 2015; Rammohan et al. 2020). Consequently, Chrysin is expected to have superior binding affinity towards the target protein compared to Luteolin. Furthermore, the IP and EA were determined using the Hartree-Fock (HF) model (Amati et al. 2020; Hossen et al. 2021). Molecules with lower ionization potentials and higher electron affinities possess increased reactivity and are more likely to engage in electron transfer or interaction (Rammohan et al. 2020). Hence, both Chrysin and Luteolin exhibit comparable interaction potential with Chrysin favoring an electron-donor role, while Luteolin acts as an electron acceptor during their interaction with 3CP (figure 2B).

The distribution map of HOMO and LUMO properties showed a similar pattern between Chrysin and Luteolin. Nonetheless, minor variations were observed, specifically in the B ring of both molecules (Figure 2C). Consistent with previous discussions on the impact of different functional groups on energy density (Xu et al. 2021), the presence of two hydroxyl groups appears to have an effect on the distribution of HOMO and LUMO for each molecule. Due to its hydroxyl groups, it is plausible that Luteolin possesses better activity compared to Chrysin. Despite this, based on their electronic properties, Chrysin and Luteolin are likely to interact similarly as inhibitors.

Binding of Chrysin to 3CP

As depicted in Figure 3A, the binding of Chrysin to the 3CP displayed a highly similar conformation to Luteolin. Both compounds demonstrated binding at comparable energies, although Chrysin displayed a higher binding energy than Luteolin. Notably, Chrysin and Luteolin shared a number of amino acid residues, and interactions occurred at the active site positions, specifically VAL 138, MET 141, TYR 152, and THR 156. Interestingly, Chrysin formed a greater number of hydrogen bonds during its binding to 3CP than Luteolin did. Chrysin formed hydrogen bonds with PHE 150, TYR 152, and GLY 185, whereas Luteolin bonded carbon to hydrogen with ALA 152. In addition, as shown in Figure 3B,

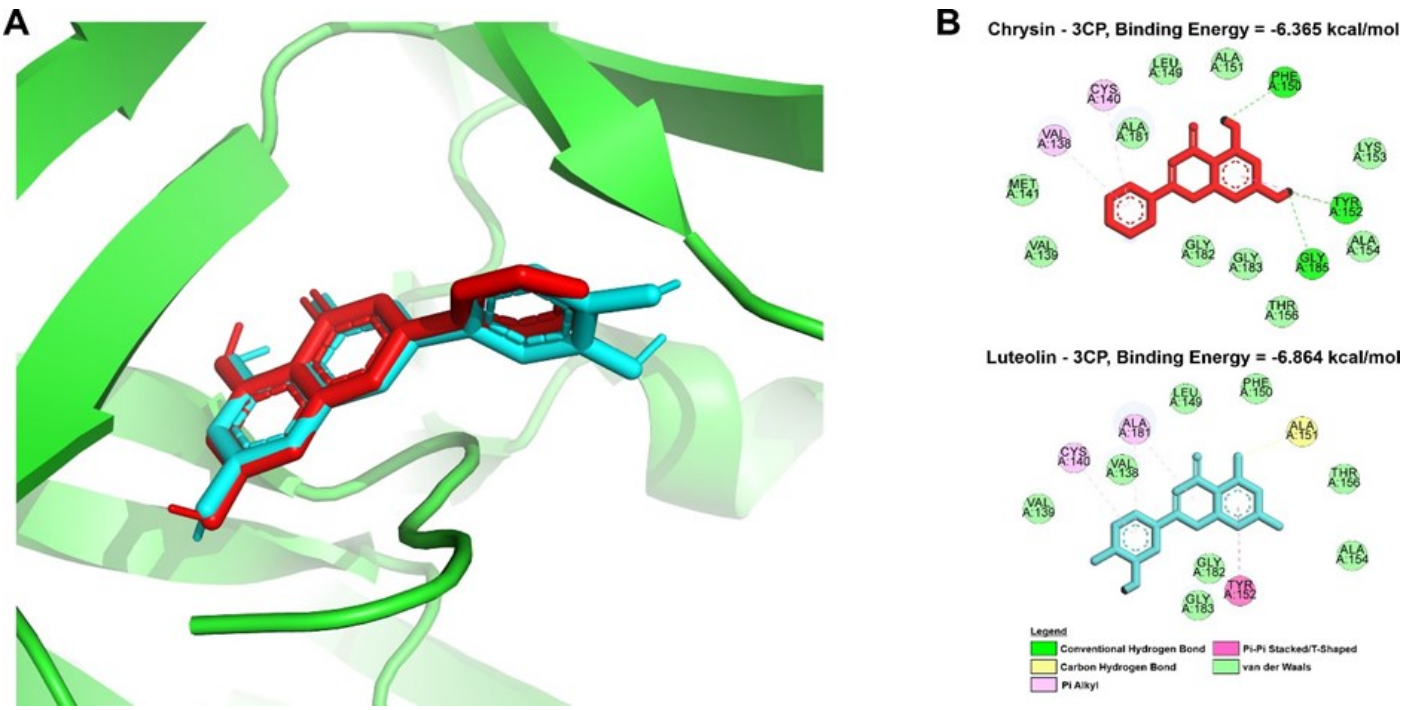

Figure 3. Structural conformation, binding energy and binding site of the Chrysin compared to the Luteolin to the 3CP. The 3D of the 3CP was visualized in green ribbon, while the Chrysin and the Luteolin were displayed in red and cyan sticks, respectively (A). Amino acids interaction was displayed in 2D map with amino acids visualized as a circular disc, and the color refers to each interaction chemistry (B).

both complexes were strengthened by hydrophobic bonds in their B- and A-rings as well as multiple Van der Waals interactions (Figure 3B). Chrysin is predicted to inhibit 3CP in a manner similar to that of Luteolin, based on the observed interaction patterns.

The 3CP enzyme plays a crucial role in the reproductive cycle of FMDV by processing the polyprotein precursor to form new viral particles (Wang et al. 2015). Previous studies have identified natural compounds capable of reducing viral load by inhibiting the 3CP, particularly for FMDV serotype A (Theerawatanasirikul et al. 2021; Theerawatanasirikul et al. 2022). One such compound is Luteolin (Theerawatanasirikul et al. 2021), which shares a similar chemical structure with Chrysin, the molecule of interest in this study. Both Chrysin and Luteolin interact effectively with key catalytic residues of the 3CP (figure 3). While Chrysin exhibits a higher binding energy than Luteolin, it forms a greater number of hydrogen bonds. As hydrogen bonds significantly contribute to the stability of protein-ligand interactions (Chen et al. 2016), Chrysin may serve as a more suitable candidate for comparison with Luteolin as an inhibitor of the 3CP. Furthermore, this study suggests that Luteolin may also exhibit similar inhibitory activity against the 3CP of FMDV serotype O, as previous investigations primarily focused on its inhibitory effects against serotype A.

Structural Dynamics of Chrysin-Bounded 3CP

The RMSD measures the deviation of an atom's position during simulations and indicates the instability of the structure (Sargsyan et al. 2017). Comparing the binding of Chrysin and Luteolin to 3CP, the RMSD of the atom backbone indicates that Chrysin-bounded 3CP is more stable (figure 4A). The Rg was also employed to evaluate the structural compactness of 3CP bound to Chrysin and Luteolin. A lower Rg value indicates greater density (Meylani et al. 2023). Until the end of the simulation, 3CP-Chrysin exhibited slightly fluctuating Rg values around 8 ns

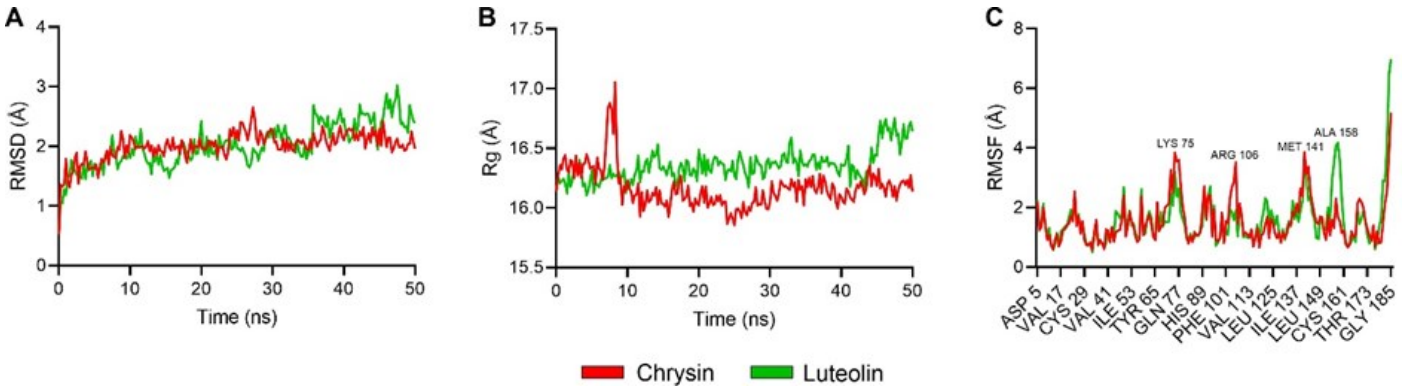

Figure 4. The structural stability of the 3CP upon binding with the Chrysin compared to the Luteolin. The structural stability was assessed through the value of the RMSD of backbone atoms (A), the radius of gyration (B), and the RMSF of each residue (C) of 3CP.

and lower Rg than 3CP-Luteolin (Figure 4B). Les disparities were negligible, less than 1 Å. The RMSF values, which indicate residual flexibility (Khan et al. 2021), differed lightly between 3CP-Chrysin and 3CP-Luteolin. Certain residues, including LYS 75, ARG 106, MET 141, ALA 158, and the C-terminal residues of 3CP, had higher RMSF values despite not being catalytic sites (Figure 4C). Only MET 141 interacted with Chrysin through Van der Waals forces. Terminal chain instability is a common characteristic of proteins (Iwakura & Honda 1996). Since ligand-induced protein conformation influences the affinity of the protein for the ligand (van den Noort et al. 2021), the degree of stabilization will minimize the dissociation of the protein-ligand complex to perform its bioactivity (Glas et al. 2017). The minimal effect of the compounds on the 3CP's structural stability, particularly Chrysin, suggests the possibility to inhibit the activity of 3CP in a stable complex formation.

From the compounds' structures and interactions point of view, Chrysin showed relatively stable conformation compared to the Luteolin. Although dramatic fluctuations appeared at around 20-30 ns, the value was less than 1 Å. A Similar event was also displayed by Luteolin, which showed some fluctuations during 7-10 ns of simulations (Figure 5A). However, Chrysin exhibited lower number of formed hydrogen bonds (Figure 5B) and described higher free-binding energy than Luteolin (Figure 5C). Previous study demonstrated that thermodynamic stability, which relates to binding affinity, does not require structural stability (Majewski et al. 2019). However, structural stability incurs an entropic penalty that hinders complex formation (Majewski et al. 2019). Hydrogen bonds contribute to this penalty, promoting a stable protein-ligand complex (Majewski et al. 2019). Hence, Chrysin may be less effective to

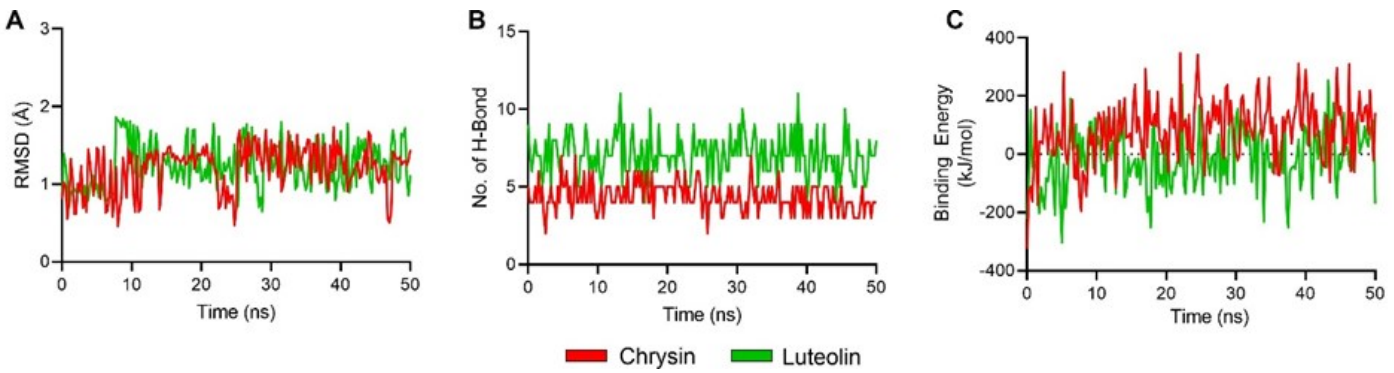

Figure 5. The stability of compounds and complexes interactions during molecular dynamics simulation. The stability of compounds as the ligands were displayed as the RMSD of ligand structure (A), while the interaction stability was assessed through the number of hydrogen bonds (B) and free-binding energy calculations (C).

interact with 3CP than Luteolin due to lower number of hydrogen bonds. Still, the differences of both compounds are plausible to perform a similar activity in inhibiting 3CP of FMDV. Nonetheless, experimental evidences are still required to validate the inhibitory properties of Chrysin against 3CP.

CONCLUSIONS

Indonesian serotype of FMDV had unique amino acid substitution at T104 and D177 compared to another O serotype. On the other hand, Chrysin has the potential as a 3CP inhibitor through its electronegativity properties, mainly at the benzene and carbonyl ring, as well as the hydroxyl group. Chrysin bound with several active sites, i.e., VAL 138, MET 141, TYR 152, and THR 156. The binding of Chrysin to 3CP remained stable without affecting the protein structure's integrity. Chrysin also showed stable structural conformation, although possessed fewer hydrogen bonds and higher free-binding energy than Luteolin. Still, Chrysin had promising potential to control FMDV infection by limiting viral replication through 3CP inhibition. Experimental validation is warranted to confirm these predictions and determine the therapeutic efficacy of Chrysin in combating FMDV infections.

AUTHOR CONTRIBUTION

AS acquired the funding and designed the experiment, MC analyzed and visualized the data, NN and DP wrote and revised the manuscript, FEH and EPP performed the experiments and calculations. All authors agreed to the final version of this manuscript.

ACKNOWLEDGMENTS

The authors thank Prof. Nashi Widodo, Ph.D.Med.Sc. for providing a license for YASARA Structure software. This research was funded by Internal Research Grant (Hibah Penelitian Unggulan) of Brawijaya University under funding scheme no. 975.37/UN10.C10/PN/2021.

CONFLICT OF INTEREST

The authors declare no conflict of interest raised in this study.

REFERENCES

Amati, M., Stoia, S. & Baerends, E.J., 2020. The Electron Affinity as the Highest Occupied Anion Orbital Energy with a Sufficiently Accurate Approximation of the Exact Kohn–Sham Potential. *Journal of Chemical Theory and Computation*, 16(1), pp.443–452. doi: 10.1021/acs.jctc.9b00981.

Anjum, S.I. et al., 2019. Composition and functional properties of propolis (bee glue): A review. *Saudi Journal of Biological Sciences*, 26(7), pp.1695–1703. doi: 10.1016/j.sjbs.2018.08.013.

Bálint, D. & Jäntschi, L., 2021. Comparison of Molecular Geometry Optimization Methods Based on Molecular Descriptors. *Mathematics*, 9 (22), p.2855. doi: 10.3390/math9222855.

Carrillo, C. et al., 2005. Comparative genomics of foot-and-mouth disease virus. *Journal of Virology*, 79(10), pp.6487–6504. doi: 10.1128/JVI.79.10.6487-6504.2005.

Chen, D. et al., 2016. Regulation of protein-ligand binding affinity by hydrogen bond pairing. *Science Advances*, 2(3), p.e1501240. doi: 10.1126/sciadv.1501240.

Curry, S. et al., 2007. Foot-and-mouth disease virus 3C protease: Recent structural and functional insights into an antiviral target. *The International Journal of Biochemistry & Cell Biology*, 39(1), pp.1–6. doi: 10.1016/j.biocel.2006.07.006.

Dallakyan, S. & Olson, A.J., 2015. Small-molecule library screening by docking with PyRx. *Methods in Molecular Biology (Clifton, N.J.)*, 1263, pp.243–250. doi: 10.1007/978-1-4939-2269-7_19.

Eberhardt, J. et al., 2021. AutoDock Vina 1.2.0: New Docking Methods, Expanded Force Field, and Python Bindings. *Journal of Chemical Information and Modeling*, 61(8), pp.3891–3898. doi: 10.1021/acs.jcim.1c00203.

Glas, A. et al., 2017. Increased Conformational Flexibility of a Macrocycle–Receptor Complex Contributes to Reduced Dissociation Rates. *Chemistry – A European Journal*, 23(64), pp.16157–16161. doi: 10.1002/chem.201702776.

Grubman, M.J. & Baxt, B., 2004. Foot-and-mouth disease. *Clinical Microbiology Reviews*, 17(2), pp.465–493. doi: 10.1128/CMR.17.2.465-493.2004.

Hall, T.A., 1999. BioEdit : a user-friendly biological sequence alignment editor and analysis program for Windows 95/98/NT. *Nucleic Acids Symp. Ser.*, 41, pp.95–98.

Han, S.-C., Guo, H.-C. & Sun, S.-Q., 2015. Three-dimensional structure of foot-and-mouth disease virus and its biological functions. *Archives of Virology*, 160(1), pp.1–16. doi: 10.1007/s00705-014-2278-x.

Hanwell, M.D. et al., 2012. Avogadro: an advanced semantic chemical editor, visualization, and analysis platform. *Journal of Cheminformatics*, 4, 17. doi: 10.1186/1758-2946-4-17.

Hermanto, F.E. et al., 2022. On The Hypolipidemic Activity of Elicited Soybeans: Evidences Based on Computational Analysis. *Indonesian Journal of Chemistry*, 22(6), pp.1626–1636. doi: 10.22146/ijc.75777.

Hermanto, F.E., Rifa'i, M. & Widodo, 2019. Potential role of glyceollin as anti-metastatic agent through transforming growth factor-β receptors inhibition signaling pathways: A computational study. *AIP Conference Proceedings*, 2155, 020035. doi: 10.1063/1.5125539.

Hidayat, S.A. et al., 2022. Optimization of East Java Propolis Extraction as Anti SARS-Cov-2 by Molecular Docking Study. *Jurnal Ilmu dan Teknologi Hasil Ternak (JITEK)*, 17(2), pp.123–134. doi: 10.21776/ub.jitek.2022.017.02.7.

Homeyer, N. & Gohlke, H., 2012. Free Energy Calculations by the Molecular Mechanics Poisson-Boltzmann Surface Area Method. *Molecular Informatics*, 31(2), pp.114–122. doi: 10.1002/minf.201100135.

Hossen, J., Ali, M.A. & Reza, S., 2021. Theoretical investigations on the antioxidant potential of a non-phenolic compound thymoquinone: a DFT approach. *Journal of Molecular Modeling*, 27(6), 173. doi: 10.1007/s00894-021-04795-0.

IFRC, 2022, 'Indonesia: Foot and Mouth Disease Outbreak - Emergency Plan of Action (EPoA), DREF Operation n° MDRID024 - Indonesia' in *ReliefWeb*, Indonesia viewed October 24 2022, from International Federation of Red Cross And Red Crescent Societies. Available at: https://reliefweb.int/report/indonesia/indonesia-foot-and-mouth-disease-outbreak-emergency-plan-action-epoa-dref-operation-ndeg-mdrid024

Islam, N., 2015. Investigation of comparative shielding of Morin against oxidative damage by radicals: A DFT study G. Weaver, ed. *Cogent Chemistry*, 1(1), 1078272. doi: 10.1080/23312009.2015.1078272.

Iwakura, M. & Honda, S., 1996. Stability and reversibility of thermal denaturation are greatly improved by limiting terminal flexibility of Escherichia coli dihydrofolate reductase. *Journal of Biochemistry*, 119 (3), pp.414–420. doi: 10.1093/oxfordjournals.jbchem.a021257.

Kamel, M., El-Sayed, A. & Castañeda Vazquez, H., 2019. Foot-and-mouth disease vaccines: recent updates and future perspectives. *Archives of Virology*, 164(6), pp.1501–1513. doi: 10.1007/s00705-019-04216-x.

Khan, Abbas et al., 2021. The SARS-CoV-2 B.1.618 variant slightly alters the spike RBD–ACE2 binding affinity and is an antibody escaping variant: a computational structural perspective. *RSC Advances*, 11(48), pp.30132–30147. doi: 10.1039/D1RA04694B.

Kim, S. et al., 2023. PubChem 2023 update. *Nucleic Acids Research*, 51(D1), pp.D1373–D1380. doi: 10.1093/nar/gkac956.

Krieger, E. & Vriend, G., 2015. New ways to boost molecular dynamics simulations. *Journal of Computational Chemistry*, 36(13), pp.996–1007. doi: 10.1002/jcc.23899.

Li, K. et al., 2021. Virus–Host Interactions in Foot-and-Mouth Disease Virus Infection. *Frontiers in Immunology*, 12, 571509. doi: 10.3389/fimmu.2021.571509

Maier, J.A. et al., 2015. ff14SB: Improving the Accuracy of Protein Side Chain and Backbone Parameters from ff99SB. *Journal of Chemical Theory and Computation*, 11(8), pp.3696–3713. doi: 10.1021/acs.jctc.5b00255.

Majewski, M., Ruiz-Carmona, S. & Barril, X., 2019. An investigation of structural stability in protein-ligand complexes reveals the balance between order and disorder. *Communications Chemistry*, 2, 110. doi: 10.1038/s42004-019-0205-5.

Maqsood, N. et al., 2022. DFT study of alkali and alkaline earth metal-doped benzocryptand with remarkable NLO properties. *RSC Advances*, 12(25), pp.16029–16045. doi: 10.1039/d2ra02209e.

Meylani, V. et al., 2023. Molecular Docking Analysis of Cinnamomum zeylanicum Phytochemicals against Secreted Aspartyl proteinase 4-6 of Candida albicans as Anti-Candidiasis Oral. *Results in Chemistry*, 5, 100721. doi: 10.1016/j.rechem.2022.100721.

Neese, F. et al., 2020. The ORCA quantum chemistry program package. *The Journal of Chemical Physics*, 152(22), 224108. doi: 10.1063/5.0004608.

van den Noort, M., de Boer, M. & Poolman, B., 2021. Stability of Ligand-induced Protein Conformation Influences Affinity in Maltose-binding Protein. *Journal of Molecular Biology*, 433(15), 167036. doi: 10.1016/j.jmb.2021.167036.

O'Boyle, N.M. et al., 2011. Open Babel: An open chemical toolbox. *Journal of Cheminformatics*, 3, 33. doi: 10.1186/1758-2946-3-33.

Palko, N., Grishina, M. & Potemkin, V., 2021. Electron Density Analysis of SARS-CoV-2 RNA-Dependent RNA Polymerase Complexes. *Molecules*, 26(13), 3960. doi: 10.3390/molecules26133960.

Ramírez-Velásquez, I. et al., 2022. Shape Theory Applied to Molecular Docking and Automatic Localization of Ligand Binding Pockets in Large Proteins. *ACS Omega*, 7(50), pp.45991–46002. doi: 10.1021/acsomega.2c02227.

Rammohan, A. et al., 2020. In silico, in vitro antioxidant and density functional theory based structure activity relationship studies of plant polyphenolics as prominent natural antioxidants. *Arabian Journal of Chemistry*, 13(2), pp.3690–3701. doi: 10.1016/j.arabjc.2019.12.017.

Roqué Rosell, N.R. et al., 2014. Design and synthesis of irreversible inhibitors of foot-and-mouth disease virus 3C protease. *Bioorganic & Medicinal Chemistry Letters*, 24(2), pp.490–494. doi: 10.1016/j.bmcl.2013.12.045.

Rosyidi, D. et al., 2018. Perbandingan Sifat Antioksidan Propolis pada Dua Jenis Lebah (Apis mellifera dan Trigona sp.) di Mojokerto dan Batu, Jawa Timur, Indonesia. *Jurnal Ilmu dan Teknologi Hasil Ternak (JITEK)*, 13(2), pp.108–117. doi: 10.21776/ub.jitek.2018.013.02.5.

Ryde, U. & Söderhjelm, P., 2016. Ligand-Binding Affinity Estimates Supported by Quantum-Mechanical Methods. *Chemical Reviews*, 116(9), pp.5520–5566. doi: 10.1021/acs.chemrev.5b00630.

Sargsyan, K., Grauffel, C. & Lim, C., 2017. How Molecular Size Impacts RMSD Applications in Molecular Dynamics Simulations. *Journal of Chemical Theory and Computation*, 13(4), pp.1518–1524. doi: 10.1021/acs.jctc.7b00028.

Siiskonen, A. & Priimagi, A., 2017. Benchmarking DFT methods with small basis sets for the calculation of halogen-bond strengths. *Journal of Molecular Modeling*, 23(2), 50. doi: 10.1007/s00894-017-3212-4.

Song, J.-H. et al., 2015. Antiviral Activity of Chrysin Derivatives against Coxsackievirus B3 in vitro and in vivo. *Biomolecules & Therapeutics*, 23(5), pp.465–470. doi: 10.4062/biomolther.2015.095.

Šuran, J. et al., 2021. Propolis Extract and Its Bioactive Compounds—From Traditional to Modern Extraction Technologies. *Molecules*, 26(10), 2930. doi: 10.3390/molecules26102930.

Tesfaye, Y., Khan, F. & Gelaye, E., 2022. Vaccine matching and antigenic variability of foot-and-mouth disease virus serotypes O and A from 2018 Ethiopian isolates. *International Microbiology*, 25(1), pp.47–59. doi: 10.1007/s10123-021-00178-w.

Theerawatanasirikul, S. et al., 2022. Andrographolide and Deoxyandrographolide Inhibit Protease and IFN-Antagonist Activities of Foot-and-Mouth Disease Virus 3Cpro. *Animals*, 12(15), 1995. doi: 10.3390/ani12151995.

Theerawatanasirikul, S. et al., 2021. Natural Phytochemicals, Luteolin and Isoginkgetin, Inhibit 3C Protease and Infection of FMDV, In Silico and In Vitro. *Viruses*, 13(11), 2118. doi: 10.3390/v13112118.

Trott, O. & Olson, A.J., 2010. AutoDock Vina: improving the speed and accuracy of docking with a new scoring function, efficient optimization and multithreading. *Journal of computational chemistry*, 31(2), pp.455–461. doi: 10.1002/jcc.21334.

Trusheva, B. et al., 2011. Indonesian propolis: chemical composition, biological activity and botanical origin. *Natural Product Research*, 25(6), pp.606–613. doi: 10.1080/14786419.2010.488235.

Wang, G. et al., 2015. How foot-and-mouth disease virus receptor mediates foot-and-mouth disease virus infection. *Virology Journal*, 12, 9. doi: 10.1186/s12985-015-0246-z.

Wang, J. et al., 2014. Anti-Enterovirus 71 Effects of Chrysin and Its Phosphate Ester. *PLOS ONE*, 9(3), e89668. doi: 10.1371/journal.pone.0089668.

Waterhouse, A. et al., 2018. SWISS-MODEL: homology modelling of protein structures and complexes. *Nucleic Acids Research*, 46(W1), pp.W296–W303. doi: 10.1093/nar/gky427.

Weigend, F. & Ahlrichs, R., 2005. Balanced basis sets of split valence, triple zeta valence and quadruple zeta valence quality for H to Rn: Design and assessment of accuracy. *Physical Chemistry Chemical Physics*, 7(18), pp.3297–3305. doi: 10.1039/B508541A.

Xu, Y. et al., 2021. HOMO–LUMO Gaps and Molecular Structures of Polycyclic Aromatic Hydrocarbons in Soot Formation. *Frontiers in Mechanical Engineering*, 7, 744001. doi: 10.3389/fmech.2021.744001

Yele, V. et al., 2021. DFT calculation, molecular docking, and molecular dynamics simulation study on substituted phenylacetamide and benzohydrazide derivatives. *Journal of Molecular Modeling*, 27(12), 359. doi: 10.1007/s00894-021-04987-8.

Zulhendri, F. et al., 2021. Antiviral, Antibacterial, Antifungal, and Antiparasitic Properties of Propolis: A Review. *Foods*, 10(6), 1360. doi: 10.3390/foods10061360.

Zunszain, P.A. et al., 2010. Insights into cleavage specificity from the crystal structure of foot-and-mouth disease virus 3C protease complexed with a peptide substrate. *Journal of Molecular Biology*, 395(2), pp.375–389. doi: 10.1016/j.jmb.2009.10.048.

SUPPLEMENTARY FILES

Table S1. The list of the amino acid sequences of 3CP from other serotype of FMDV along with the accession code in GenBank database.

No.	Locality	GenBank ID
1.	Indonesia	AAT01756.1
2.	United Kingdom	AAT01779.1
3.	Belgium	AAT01760.1
4.	Italy	AAT01773.1
5.	Poland	AAT01769.1
6.	Iran	AAT01777.1
7.	Turkey	AAT01766.1
8.	South Korea	AAT01767.1
9.	Philippines	AAT01754.1
10.	India	AAT01771.1
11.	Taiwan	AAT01778.1
12.	Japan	BAC06475.1
13.	China	AAM33345.1
14.	South Africa	AAK97007.1
15.	South Africa	AAK97010.1
16.	South Africa	AAK97009.1
17.	India	ACJ02480.1
18.	South Africa	AAM53441.1
19.	India	AAC36727.1
20.	Argentina	AAT01712.1
21.	Argentina	AAT01710.1
22.	Uruguay	AAT01744.1
23.	Uruguay	AAT01745.1
24.	Netherland	AAT01694.1
25.	Germany	AAT01702.1
26.	Great Britain	AAT01695.1
27.	France	AAT01723.1
28.	Italy	AAT01735.1
29.	Spain	AAT01721.1
30.	Philippines	AAT01736.1
31.	Thailand	AAT01698.1
32.	Turkey	AAT01708.1
33.	Iran	AAT01708.1
34.	Iran	AAT01734.1
35.	Iraq	AAT01705.1
36.	Iraq	AAT01706.1
37.	Kenya	AAT01704.1
38.	Kenya	AAT01709.1
39.	Lebanon	AAT01742.1
40.	Lebanon	AAT01743.1
41.	Pakistan	AAT01738.1
42.	Israel	AAT01739.1
43.	China	AAQ90285.1
44.	Great Britain	AAT01753.1
45.	Switzerland	AAT01747.1
46.	Germany	AAT01748.1
47.	Brazil	AAT01749.1
48.	Brazil	AAT01750.1
49.	Argentina	AAT01751.1
50.	Argentina	AAT01752.1
51.	Botswana	AAT01788.1
52.	Zimbabwe	AAT01789.1
53.	United Kingdom	AAT01782.1

Table S1. Contd.

No.	Locality	GenBank ID
54.	Israel	AAT01787.1
55.	South Africa	AAT01785.1
56.	Namibia	AAT01786.1
57.	Kenya	AT01792.1
58.	Botswana	AAT01794.1
59.	Zimbabwe	AAQ11227.1

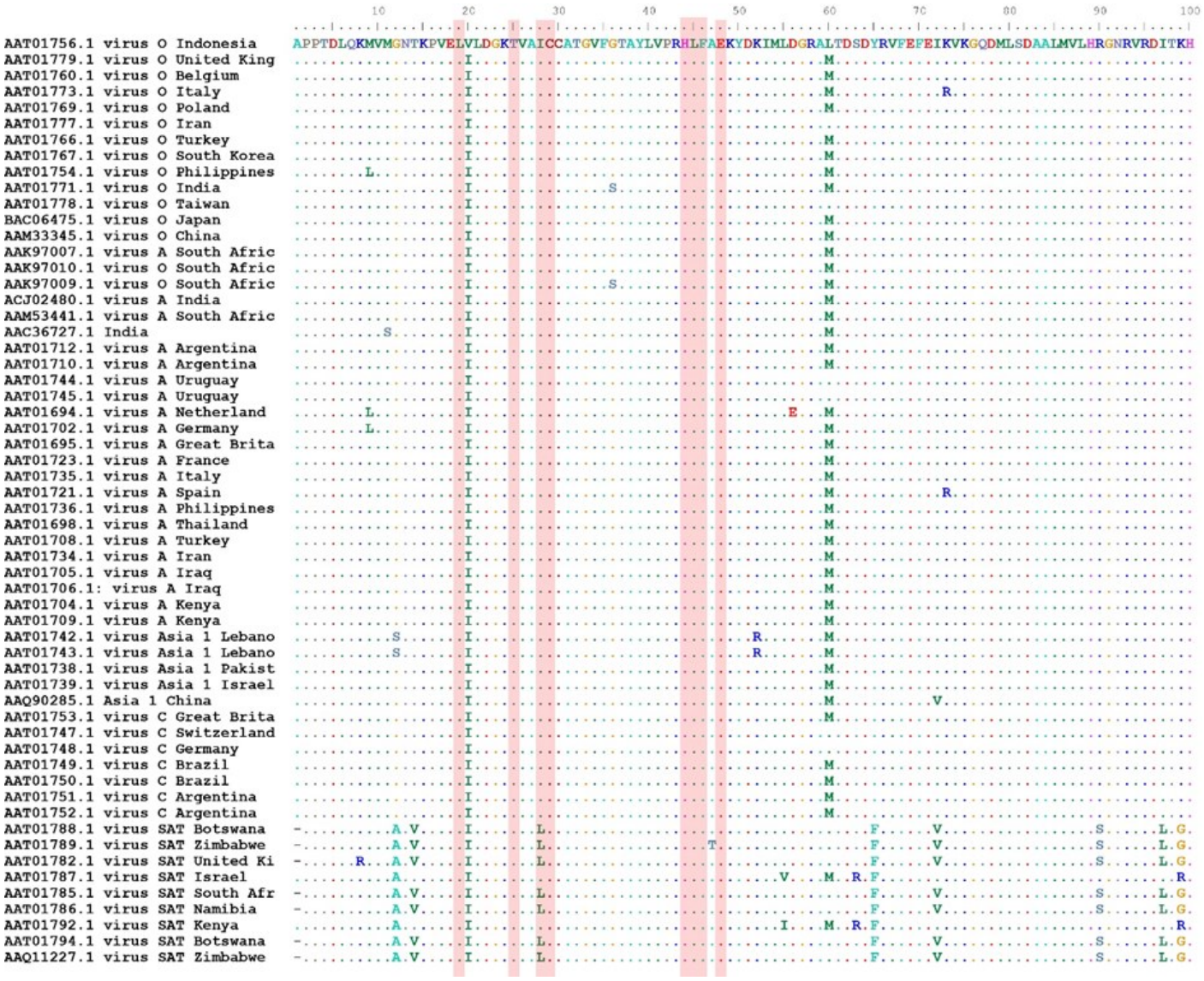

Figure S1. Multiple pairwise alignment of the 3CP sequences among several serotypes worlwide, including Indonesian serotype. The highlighted sequences indicated the active site residues.

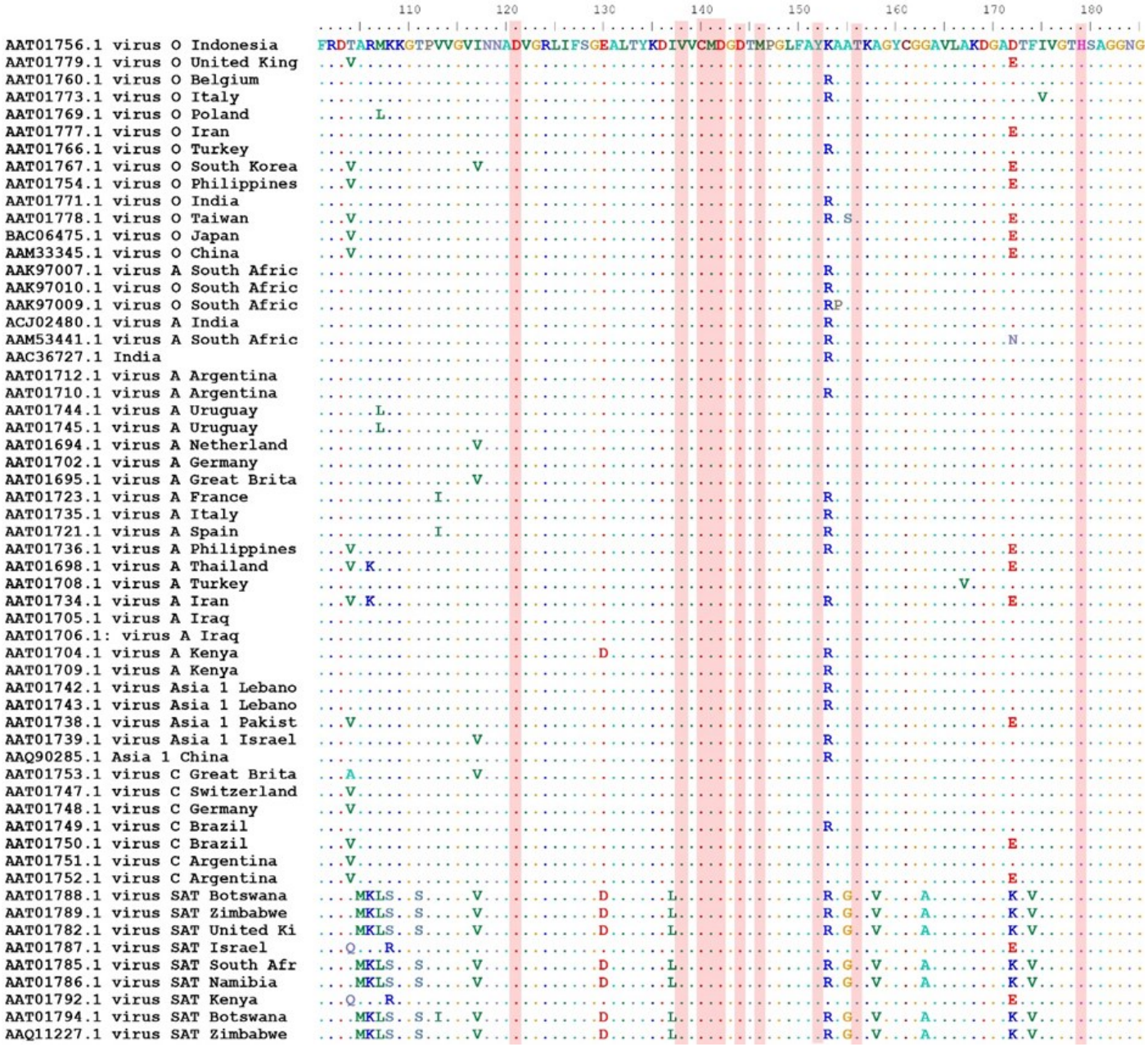

Figure S1. Contd.

Journal of Tropical Biodiversity and Biotechnology
Volume 09, Issue 01 (2024): jtbb85847
DOI: 10.22146/jtbb.85847

Research Article

Therapeutic Effects of BRC Functional Food from Indonesian Black Rice on Body Weight and Haematological Parameters in Obese Rats

Fajar Sofyantoro[1], Adi Mazdi Syam[1], Baik Aisyah Adania[1], Muhammad Fikri Almunawar[1], Nurlita Putri Bela Nasution[1], Rheina Faticha Asyamsa Hidayat[1], Made Bagus Auriva Mataram[2], Chesa Ekani Maharesi[1], Septika Nurhidayah[1], Yekti Asih Purwestri[1,3], Ardaning Nuriliani[1], Lisna Hidayati[1], Rarastoeti Pratiwi[1,3]*

1)Department of Tropical Biology, Faculty of Biology, Universitas Gadjah Mada, Yogyakarta, Indonesia 55281
2)Pre-clinical and Experimental Animal Unit (Unit IV), Integrated Research and Testing Laboratory, Universitas Gadjah Mada, Yogyakarta, Indonesia, 55281
3)Research Center for Biotechnology, Universitas Gadjah Mada, Yogyakarta, Indonesia 55281
* Corresponding author, email: rarastp@ugm.ac.id

Keywords:
Obesity
Black rice
Functional food
Body weight
Haematological profile
Submitted:
18 June 2023
Accepted:
30 August 2023
Published:
12 January 2024
Editor:
Miftahul Ilmi

ABSTRACT

Obesity increases the risk of various diseases. Black rice, renowned for its high anthocyanin content, is considered a potential functional food for preventing metabolic disorders. The current study investigated the effects of black rice crunch (BRC) on body weight and haematological profiles in obese rats. Rats were fed with high-fat diet to induce obesity and supplemented with different concentrations of BRC for 4 and 8 weeks. The results showed that high-fat diet effectively induced obesity, as evidenced by significant increase in body weight. Importantly, 75% BRC supplementation resulted in significant weight reduction in obese rats. Further analysis revealed an increase in erythrocyte numbers in obese groups supplemented with 75% BRC, but no significant changes in haemoglobin concentration or haematocrit percentage. Further investigation showed that 75% BRC led to a decrease in mean corpuscular haemoglobin (MCH), mean corpuscular haemoglobin concentration (MCHC), and mean corpuscular volume (MCV), potentially affecting the size and concentration of haemoglobin within erythrocytes. The total leucocytes count increased with the high-fat diet, while BRC supplementation alone did not have significant impact. Lymphocyte percentage remained stable across the groups, indicating minimal influence of the dietary interventions. Neutrophil percentage varied initially but was not specific to BRC or the high-fat diet. Platelet count and distribution width were not significantly influenced, but mean platelet volume (MPV) increased after 8 weeks of BRC treatment, suggesting larger platelet sizes associated with obesity. Overall, the study provides important insights into the effects of BRC supplementation on body weight and haematological parameters related to obesity.

Copyright: © 2024, J. Tropical Biodiversity Biotechnology (CC BY-SA 4.0)

INTRODUCTION

Overweight and obesity are triggered by accumulation of excess or abnormal fat (Lin & Li 2021). The accumulation of fat may heighten the chances of developing cardiovascular disease and lead to a range of metabolic disorders (Després & Lemieux 2006; Després 2012). Genetic and

non-genetic factors can lead to the accumulation of body fat that ultimately results in obesity. The monogenic disorders in the leptin and melanocortin signalling pathways have been reported to cause obesity (Brandl et al. 2012; Ren et al. 2019). Meanwhile, an imbalance in caloric intake and lack of physical activity are the main non-genetic factors that trigger obesity (Romieu et al. 2017).

The phenolic and anthocyanin contents of black rice are higher than white rice (Zhang et al. 2010). Phenolic compounds in black rice inhibit the activity of α-glucosidase and α-amylase in vitro, thus reducing the glycaemic index (An et al. 2016). In addition, anthocyanins significantly inhibit the pancreatic lipase activity and help to regulate lipid metabolism (Fabroni et al. 2016). Therefore, black rice contains various active compounds with health benefits and holds immense promise for becoming a functional food.

Indonesia boasts abundant biodiversity, encompassing a multitude of indigenous black rice cultivars (Kristamtini et al. 2012). Rukmana et al. (2017) demonstrated cytotoxic activity of black rice cultivars from Indonesia against cancer cells. A noteworthy variety hails from Yogyakarta, Indonesia, referred to as '*Cempo Ireng*' (Kristamtini et al. 2012). The anthocyanins, especially cyanidin 3-glucoside and peonidin 3-glucoside, in '*Cempo Ireng*' black rice is reported to activate the apoptosis pathways in human cervical cancer cells (Pratiwi et al. 2016). Similarly, extract from '*Cempo Ireng*' black rice bran also induces cell cycle arrest in breast cancer cells (Pratiwi et al. 2019). Sa'adah and Pratiwi (2016) reported that '*Cempo Ireng*' black rice and rice bran reduce cholesterol levels and atherogenic index in hyperlipidaemic rats. In addition, '*Cempo Ireng*' black rice effectively repairs liver function by reducing serum glutamic pyruvate transaminase (SGPT) levels in hyperlipidaemia rats (Chasanah & Pratiwi 2019).

In recent years, the development of black rice-containing functional food has been gaining significant attention. Black Rice Crunch (BRC), patent number IDP000081011, is a black rice-containing product which has been manufactured as functional food with various health benefits (Purwestri et al. 2022). The BRC products contain "*Sembada Hitam*" black rice cultivar from Sleman, Yogyakarta, Indonesia. In this study, BRC preclinical research was conducted using rats (*Rattus norvegicus*) as animal models. Obesity in rats can be induced by genetic modification or high-calorie feeding. High-calorie feeding is the simplest and most relevant method for obesity in humans (Von Diemen et al. 2006). Feeding with 30-85% of calories of lipids induce obesity and increase insulin resistance in animal models (Buettner et al. 2007; Hariri et al. 2010). The success of obesity induction in animal models can be determined by observing the increase in body weight and fat percentage (Hariri et al. 2010).

Feeding *R. norvegicus* a high-fat diet that induces obesity has been found to result in an elevation of white blood cell (WBC) levels (Shabbir et al. 2015; Monteomo et al. 2018). However, it has been observed that the administration of antioxidants can effectively reduce the WBC count in obese rats (Shabbir et al. 2015), bringing the levels closer to those observed in the control group comprising non-obese rats. Moreover, the administration of black rice extract has also been shown to have a reducing effect on WBC count (Park et al. 2020). In addition to leucocytes, platelet distribution width (PDW) and mean platelet volume (MPV) are commonly utilized as indicators of inflammation in obesity (Aktas et al. 2018). Furthermore, in a diet-induced obesity (DIO) rat model, increased platelet counts in obese rats was reported (Barrachina et al. 2020). These

findings highlight the association between obesity and alterations in immune cell and platelet parameters, suggesting a potential link between obesity-induced inflammation and haematological changes.

The evidence to support the benefits of black rice-containing products in promoting health and preventing metabolic diseases remains limited. Therefore, it is necessary to carry out preclinical studies to investigate the potential of black rice-containing products in preventing overweight and obesity by examining anthropometric, physiological, chemical, and biomolecular parameters. Body weight is one of the anthropometric parameters commonly used to identify obesity. In addition, haematological data is one of the basic parameters in preclinical tests, which might help to show the physiological response and changes in body metabolism. This research was conducted to determine the benefits of BRC, a black rice-containing product, in suppressing weight gain in obese rats and its safety by observing the haematological profiles. The use of animal models, such as *R. norvegicus*, may provide valuable insights into the potential benefits of BRC in mitigating obesity-associated diseases.

MATERIALS AND METHODS

Materials

The study design was approved by the Ethics Commission of the Integrated Research and Testing Laboratory, Universitas Gadjah Mada (UGM), Indonesia (Certificate No. 00023/04/LPPT/VIII/2022). A total of 25 male Wistar rats (*Rattus norvegicus* Berkenhout, 1769), 12 weeks of age, and weighing 130-170 g were used. The standard feed Rat Bio was purchased from PT. Citra Ina Freedmill, East Jakarta. The obesity and BRC feeds were manufactured as in Tsalissavrina et al. (2013) at the Centre for Food and Nutrition Studies, UGM, Indonesia.

The rats were divided into 5 groups, with each group consisting of 5 individuals. The control group (NO) and the placebo (BRC0) group were provided with standard feed and obesity feed, respectively. The treatment groups were fed with obesity feeds for 5 weeks (pre-BRC) followed by obesity and BRC feeds for 8 weeks (post-BRC), consisting of BRC 1 (25% BRC: 75% obesity feed), BRC2 (50% BRC: 50% obesity feed), and BRC3 (75% BRC: 25% obesity feed) (Nasution & Pratiwi 2023; Syam & Pratiwi 2023). The rats were weighed every two days.

Methods

Blood Sample Collection

Prior to blood sampling, the rats were anesthetized using a ketamine:xylazine cocktail (10:1 ratio) administered via the intramuscular route, with a dosage of 0.1 mL per 100 g of body weight. Blood collection was performed using the microhematocrit method through the retro-orbital plexus route, obtaining 2-5 drops of blood. The blood samples were then collected into a 1.5 mL microtube coated with EDTA.

Haematological Profile Analysis

Red Blood Cells (RBC) and White Blood Cells (WBC) analysis were performed using a haematology analyser (Sysmex KX-21). Parameters of RBC including RBC count, haemoglobin level, haematocrits percentage, and other erythrocyte indices such as mean corpuscular haemoglobin concentration (MCHC), mean corpuscular haemoglobin (MCH), and mean corpuscular volume (MCV). The parameters measured for WBC and platelets include WBC count, lymphocyte percentage, neutrophil percentage, mean platelet volume (MPV), platelet distribution width (PDW), and platelet count (PLT).

Data Analysis

The data were presented as mean ± SEM and tested using one-way ANOVA ($\alpha = 0.05$) followed by a Tukey test. Data analysis was performed using GraphPad Prism 8. The results were presented in a bar chart constructed in Microsoft Excel.

RESULTS AND DISCUSSION

BRC contributes to the suppression of weight gain in obese rats

At present, there is limited scientific evidence supporting the potential health advantages of incorporating black rice into food products to enhance overall well-being and prevent metabolic disorders. Hence, it is imperative to conduct preclinical studies to delve into the possibilities of these products in averting weight gain and obesity. These studies should encompass a range of parameters, including measurements of body size and shape, analysis of physiological responses, examination of chemical compositions, and evaluation of biomolecular profiles. Among the anthropometric parameters commonly used to assess obesity, body weight serves as a significant indicator.

Figure 1 shows that a significant increase in body weight was observed in obese-induced groups (BRC0, BRC1, BRC2, and BRC3). The results obtained provide clear evidence that the administration of an obesity-inducing diet over a period of 5 weeks effectively led to the development of obesity. Figure 1 also demonstrates that after 4 and 8 weeks of BRC treatment, there was a notable and statistically significant difference in body weight between the control group (NO) and the groups receiving BRC at various concentrations (BRC0, BRC1, BRC2, and BRC3). However, it is worth noting that the BRC0, BRC1, and BRC2 groups exhibited significant differences when compared to the BRC3 group. These findings suggest that 25% and 50% BRC were unable to effectively inhibit weight gain, as evidenced by the results observed in the BRC1 and BRC2 groups, respectively. Conversely, the obese rats receiving 75% BRC demonstrated a significant reduction in body weight, indicating its potential as an effective intervention in managing obesity.

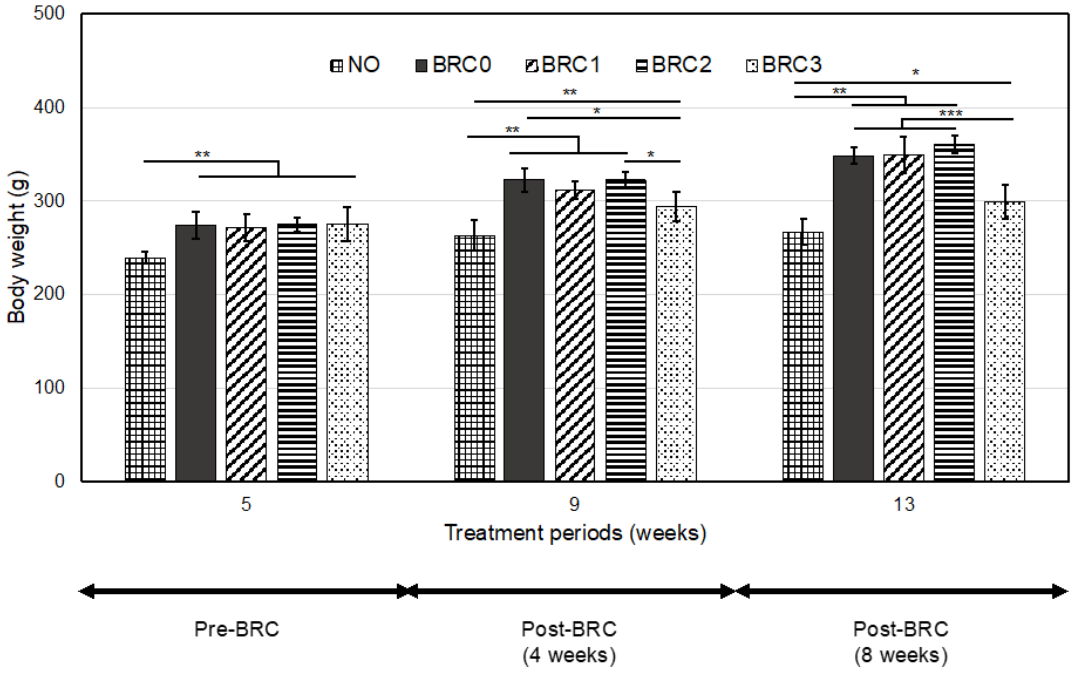

Figure 1. Body weight variations following the administration of high-fat diets and supplementation with Black Rice Crunch (BRC). The data is expressed as mean ± SD. Statistical significance between groups is denoted by asterisks (* for $P < 0.05$, ** for $P < 0.01$, and *** for $P < 0.001$).

The findings of this study highlight the potential benefits of incorporating BRC into the diet to combat weight gain associated with a high-fat diet. The presence of anthocyanins, which are natural pigments responsible for the dark colour of black rice, is believed to possess antioxidant and anti-inflammatory properties that can positively influence lipid metabolism and ultimately contribute to weight management. These results align with previous research that has demonstrated the potential health-promoting effects of anthocyanins in various metabolic disorders (Zhang et al. 2010; Fabroni et al. 2016; Lim et al. 2016). Further investigations are warranted to elucidate the specific mechanisms by which anthocyanins from black rice exert their effects on lipid metabolism and to explore their potential as therapeutic agents for the prevention and treatment of obesity-related conditions.

BRC supplementation modulates erythrocyte parameters

Figure 2A depicted the comparison of mean erythrocyte numbers among the groups at different time points. Initially, at the pre-BRC stage and after 4 weeks of BRC treatment, no significant differences were observed in the mean erythrocyte count between the groups. However, at the 8-weeks post-BRC, the BRC3 group exhibited a significantly higher mean erythrocyte count compared to both the NO and BRC1 groups. These findings suggest that supplementation of 75% BRC for 8 weeks led to an increase in erythrocyte numbers, indicating that BRC may have a positive impact on erythropoiesis, the process of erythrocyte production. Importantly, it is noteworthy that despite this increase, the erythrocyte counts for all groups remained within the normal range according to de Kort et al. (2020), indicating that the observed changes were not indicative of any pathological conditions.

As indicated in Figures 2B and C, no statistically significant differences were observed in the haemoglobin concentration and haematocrit percentage among the various groups at the pre-BRC stage, as well as after 4 and 8 weeks of BRC treatment. These findings suggest that both the obesity-inducing feeds and BRC consumption did not have a significant impact on the haemoglobin concentration or haematocrit percentage. Importantly, the haemoglobin concentration and haematocrit percentage values for all groups remained within the normal range as defined by de Kort et al. (2020), indicating that there were no abnormal deviations from the expected values. Thus, it can be concluded that the observed changes in the erythrocyte profile were not associated with alterations in the haemoglobin concentration or haematocrit percentage, highlighting the stability of these parameters during the study period.

To gain a comprehensive understanding of the erythrocyte profile, further investigation of mean corpuscular haemoglobin concentration (MCHC), mean corpuscular haemoglobin (MCH), and mean corpuscular volume (MCV) were performed. These additional measurements may provide valuable insights into the size, content, and concentration of haemoglobin within the erythrocytes, shedding light on potential variations that may contribute to the observed changes in the erythrocyte profile.

According to the findings presented in Figure 3A, it is evident that the MCV value of the BRC3 group at both 4 and 8 weeks post-BRC was significantly lower compared to the NO, BRC0, BRC1, and BRC2 groups. These MCV values fall below the range considered normal according to de Kort et al. (2020), suggesting that the administration of 75% BRC leads to a reduction in the MCV value. The MCV is a crucial parameter used to assess the size of erythrocytes and is an important indicator of red blood cell health and functionality. Values lower than the normal range may indicate the presence of underlying conditions such as micro-

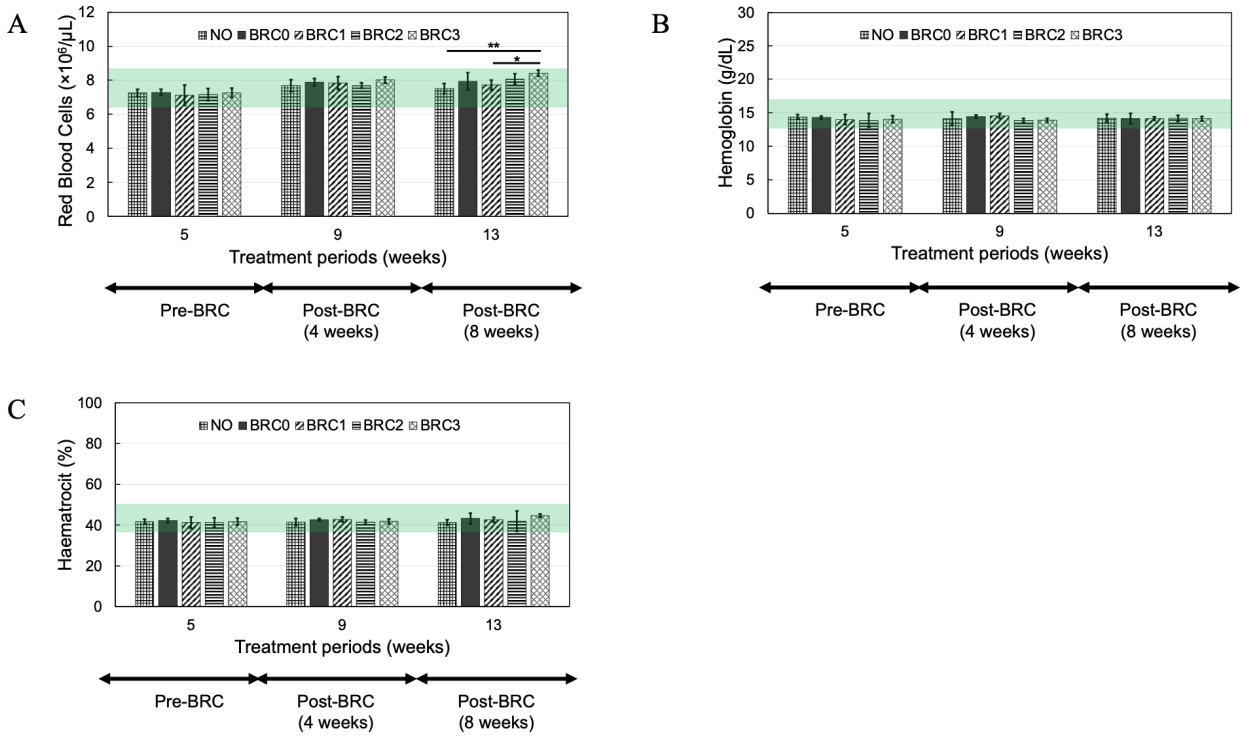

Figure 2. Mean values of erythrocyte numbers (A), haemoglobin concentration (B), and haematocrit values (C) following the administration of high-fat diets and supplementation with Black Rice Crunch (BRC). The data is presented as mean ± standard deviation (SD). Significant differences between groups are denoted by asterisks (* for $P < 0.05$, ** for $P < 0.01$, and *** for $P < 0.001$). The normal range of values, as defined by de Kort et al. (2020), is indicated by the green box.

cytosis, which is characterized by smaller-than-normal red blood cells. The observed decrease in MCV in the BRC3 group suggests that the consumption of 75% BRC has an impact on the size of erythrocytes, potentially influencing their physiological functions. This reduction in size could potentially be attributed to the bioactive components present in BRC, which may modulate erythrocyte maturation or turnover. Further investigations are necessary to explore the underlying mechanisms behind this decrease in MCV and to determine whether it is a direct consequence of BRC consumption or an indirect effect resulting from other factors.

The data presented in Figure 3B demonstrate notable observations regarding the average MCH values in response to BRC treatment. Specifically, it is evident that at 4 weeks post-BRC, the BRC3 group displayed a significantly lower average MCH value compared to the NO group, as well as the BRC0 and BRC1 groups. Likewise, after 8 weeks of BRC treatment, the average MCH value in the BRC3 group remained significantly lower than all other groups. These findings provide compelling evidence that the inclusion of 75% BRC in the diet leads to a decrease in MCH values. The MCH value serves as a key haematological parameter that reflects the average amount of haemoglobin contained within individual red blood cells. Thus, the significant decline in MCH observed in the BRC3 group after both 4 and 8 weeks of post-BRC treatment suggests that the consumption of BRC has an impact on the haemoglobin content within the red blood cells. Moreover, it is noteworthy that the MCH values of the BRC3 group at 4 and 8 weeks post-BRC were found to be lower than the reference values provided by de Kort et al. (2020). Further research efforts are needed to unravel the underlying mechanisms responsible for the decrease in MCH values following BRC consumption.

The results presented in Figure 3C provide insights into the mean MCHC values among the different groups at various time points. It is noteworthy that there were no significant differences in the mean MCHC values between the pre-BRC and the 4-week post-BRC phase across all groups. This suggests that the initial introduction of BRC did not have a substantial impact on the MCHC values. However, an interesting observation arises when examining the mean MCHC values at the 8-week post -BRC stage. Notably, the mean MCHC values of the BRC3 group were found to be significantly lower than those of the NO group, as well as the BRC0 and BRC1 groups. Thus, the lower mean MCHC values observed in the BRC3 group after 8 weeks of post-BRC treatment suggest a potential alteration in the haemoglobin concentration within the red blood cells due to the consumption of 75% BRC. However, it is important to note that despite the observed differences in the mean MCHC values, all groups throughout the course of the experiments maintained MCHC values within the acceptable range as established by de Kort et al. (2020). Hence, while there may be differences between groups, the MCHC values of all groups remained within the acceptable range, suggesting that the overall haemoglobin concentration within the red blood cells was still within normal limits.

Collectively, these results demonstrate that the lower concentration of haemoglobin within each erythrocyte observed in the BRC3 group is compensated by a higher number of erythrocyte counts, despite their smaller size. This phenomenon suggests a potential adaptation or response to BRC3 supplementation, where the body aims to maintain or optimize oxygen-carrying capacity. This observation highlights the complex interplay between erythrocyte count and haemoglobin concentration in the context of BRC3 supplementation. Further investigations are nec-

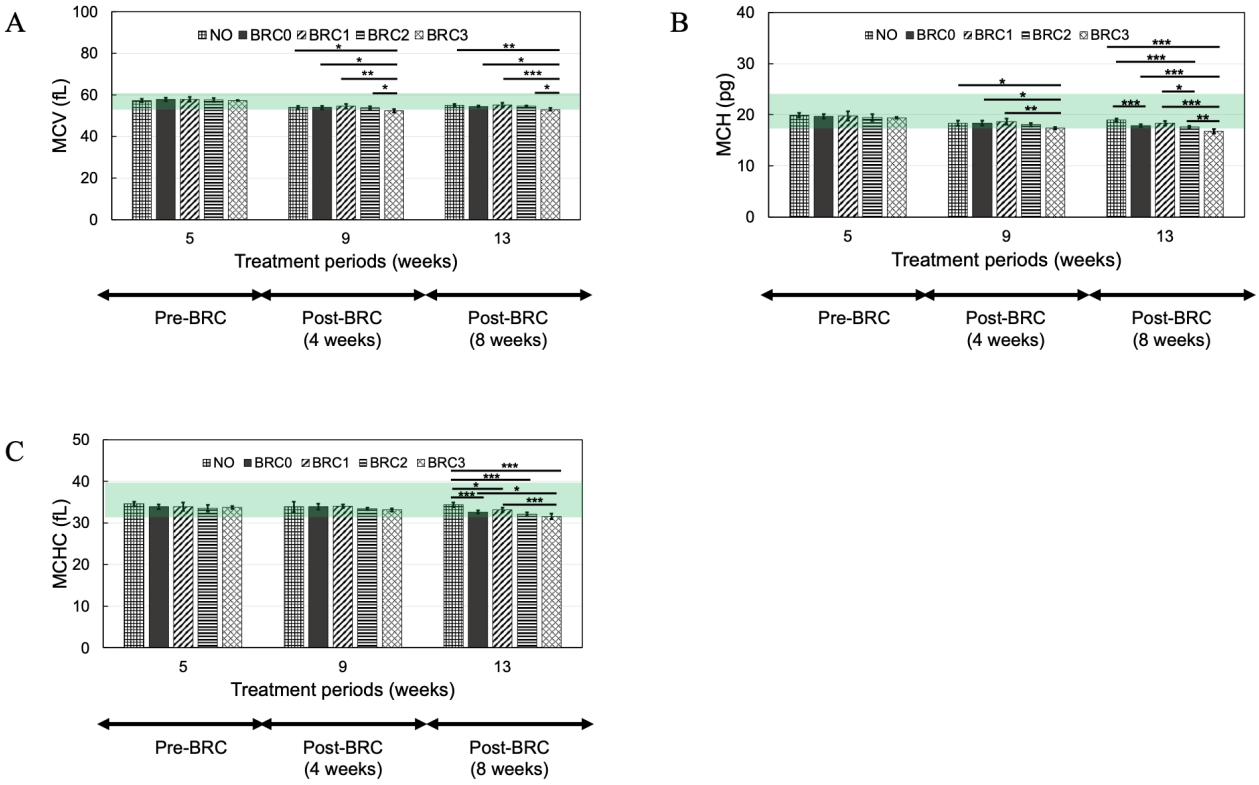

Figure 3. Mean Corpuscular Volume (MCV) (A), Mean Corpuscular Haemoglobin (MCH) (B), and Mean Corpuscular Haemoglobin Concentration (MCHC) (C) following the administration of high-fat diets and supplementation with Black Rice Crunch (BRC). The data is expressed as mean ± standard deviation (SD). Significant differences between groups are denoted by asterisks (* for $P < 0.05$, ** for $P < 0.01$, and *** for $P < 0.001$). The normal range of values, as defined by de Kort et al. (2020), is indicated by the green box.

essary to elucidate the underlying mechanisms that regulate these changes and to assess the physiological implications of this combined effect on erythrocyte parameters.

High-fat diet increases leucocyte counts

Figure 4A depicts the comparison of total leucocyte counts between the NO and BRC groups at different time points. Following a 4-week period of BRC treatment, no statistically significant differences were observed in the total leucocyte count between the BRC groups and the NO group. However, at the 8-week post-BRC supplementation stage, a significant increase in the total leucocyte count was observed in the BRC0 group compared to the NO group. These findings indicate that a significant increase in leucocytes was only evident after 13 weeks of high-fat diet administration. Additionally, following 8 weeks of BRC supplementation, there was no significant reduction in total leucocyte count observed in the BRC 1, 2, or 3 groups compared to the BRC0 group. This indicates that BRC supplementation alone is inadequate in decreasing leucocyte levels in obese rats.

To further elucidate the specific types of leucocytes that undergo changes in response to high-fat diets and BRC supplementation, a differential leucocyte count was performed. This analysis may provide valuable insights into the cellular components of the immune system that are influenced by BRC supplementation in the context of obesity. Analysis of the data presented in Figure 4B revealed that there were no statistically significant differences observed in the percentage of lymphocytes between the NO and BRC groups after 4 and 8 weeks of BRC treatment. Furthermore, even after a 13-week period of consuming a high-fat diet, there were no notable effects on the percentage of lymphocytes. These findings indicate that the dietary intervention of BRC supplementation and the duration of high-fat diet feeding did not result in significant alterations in the percentage of lymphocytes. It is important to note that lymphocytes play a critical role in the immune system and their levels are known to be influenced by various factors. However, in the context of the current study, the percentages of lymphocytes remained relatively stable across the different treatment groups, suggesting that these specific dietary conditions did not have a substantial impact on lymphocyte populations.

Meanwhile, as depicted in Figure 4C, notable differences in neutrophil percentage were observed in the pre-BRC phase, wherein the BRC3 group exhibited significant difference from the NO, BRC1, and BRC2 groups. However, no significant differences in neutrophil percentage were observed between the NO group and all BRC groups, suggesting that the increased neutrophil percentage may not be attributed to the consumption of a high-fat diet. The initial variation in neutrophil percentage observed in the pre-BRC phase, specifically with a higher percentage in the BRC3 group compared to other groups, suggests the possibility of underlying factors influencing neutrophil levels independent of the dietary interventions. These factors may include individual variations in immune response, genetic factors, or other environmental factors unrelated to the BRC or high-fat diet. Furthermore, during the 4-week post-BRC phase, all experimental groups displayed neutrophil percentages below the established reference range (Said & Abiola 2014). However, in the 8-week post-BRC phase, the neutrophil percentages of all groups returned to the normal range, indicating that this fluctuation is not specific to BRC supplementation or the high-fat diet. It is important to consider that neutrophils play a crucial role in the immune response and their lev-

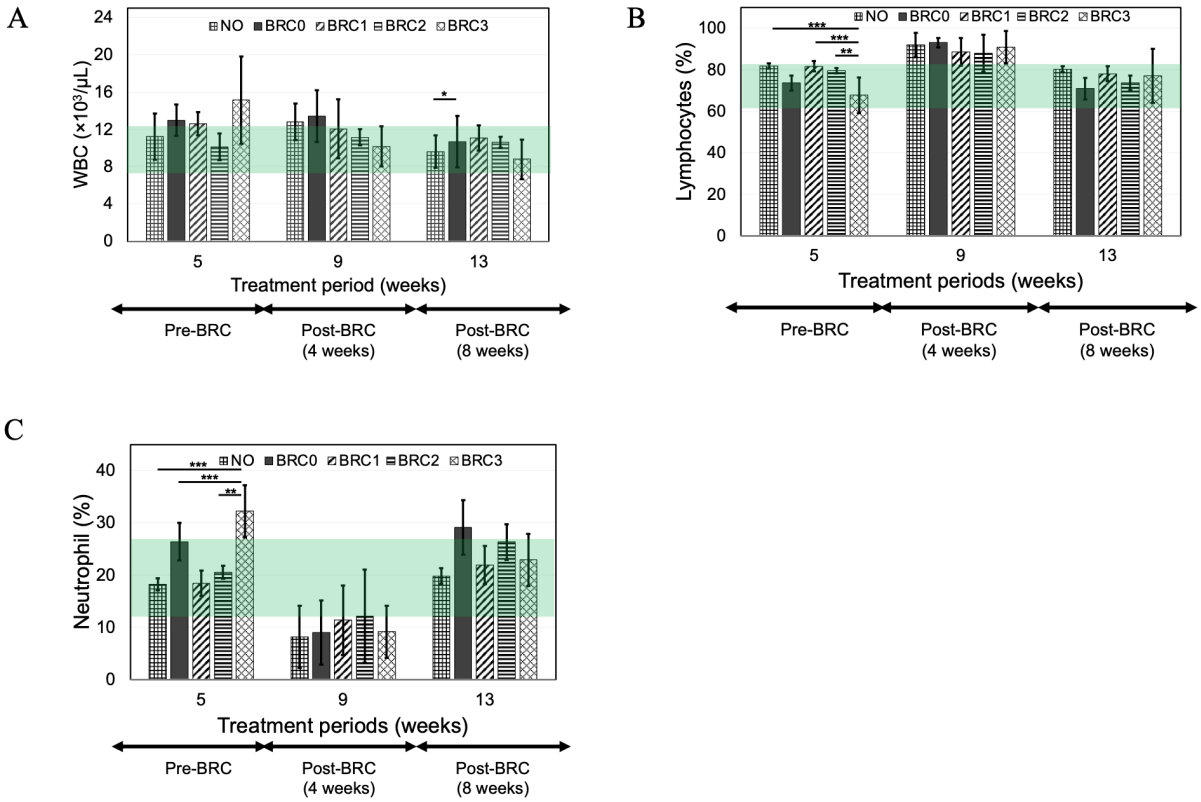

Figure 4. Mean values of White Blood Cells (WBC) numbers (A), percentage of lymphocytes (B), and percentage of neutrophils (C) following the administration of high-fat diets and supplementation with Black Rice Crunch (BRC). The data is expressed as mean ± standard deviation (SD). Significant differences between groups are denoted by asterisks (* for $P < 0.05$, ** for $P < 0.01$, and *** for $P < 0.001$). The normal range of leucocyte numbers (Said & Abiola 2014) and percentage of lymphocytes or neutrophils (Sharp & Villano 2012) are indicated by the green box.

els can be influenced by various physiological and external factors. Therefore, it is necessary to explore and understand the underlying mechanisms contributing to the observed fluctuations in neutrophil percentage. These findings underscore the importance of carefully interpreting and contextualizing neutrophil percentage changes in the context of BRC supplementation and high-fat diet studies. Further investigations are warranted to unravel the potential factors contributing to the initial variation and subsequent normalization of neutrophil percentages, as well as to elucidate the specific mechanisms through which BRC and high-fat diet might influence neutrophil function and overall immune response.

The mixed cell percentage (MXD) value, which encompasses the collective presence of monocytes, basophils, and eosinophils in a blood sample, serves as an indicator of their cumulative accumulation. In our current study, however, we observed a remarkably low MXD value implying that the organism under scrutiny is not undergoing an allergic reaction or being affected by pathogenic infections (data not shown).

High-fat diet affects the average size of platelets

As shown in Figure 5A, the platelet count (PLT) values at various time points do not exhibit any notable differences between the NO group and the BRC groups. Furthermore, it is worth noting that all groups, across all time points, fall within the range considered normal based on the reference values established by Cox et al. (2011), indicating that BRC supplementation and high-fat diet have minimal influence on platelet count. Figure 5B showed that the Platelet Distribution Width (PDW) values at

all time points also demonstrate no significant differences between the NO group and the BRC groups. However, after a 4-week period of BRC administration, the PDW values were observed to be higher than the normal range, as indicated by the reference values provided by (Mulyati et al. 2019). Elevated PDW values suggest an increased diversity in platelet size, potentially reflecting altered platelet activation or physiological conditions. Nonetheless, it is noteworthy that after an 8-week duration of BRC administration, the PDW values return to the normal range. This fluctuation in PDW values was observed across all groups, suggesting that it may occur independently of both the high fat diet and BRC supplementation. Taken together, these findings provide valuable insights into the platelet-related parameters in response to BRC supplementation and high-fat diet. The consistent platelet counts within the normal range suggest that BRC supplementation does not exert a significant impact on platelet number. Similarly, the lack of significant differences in PDW values between the NO and BRC groups indicates that platelet size heterogeneity remains unaffected by BRC supplementation.

According to the data presented in Figure 5C, the control group exhibits significant differences in mean platelet volume (MPV) when compared to both the BRC0 and BRC3 groups during the 8-week post-BRC treatment. These results suggest that a 13-week consumption of a high-fat diet leads to a notable increase in MPV among obese rats. Elevated MPV values are indicative of larger platelet sizes than those considered normal. This notable alteration in platelet morphology, as reflected by elevated MPV values, may have implications for platelet function and overall hemostatic processes. Larger platelet sizes, as indicated by high MPV values, can be associated with various pathological conditions, including cardiovascular diseases and inflammatory states. Such alterations in platelet size may affect platelet function, aggregation, and thrombotic events.

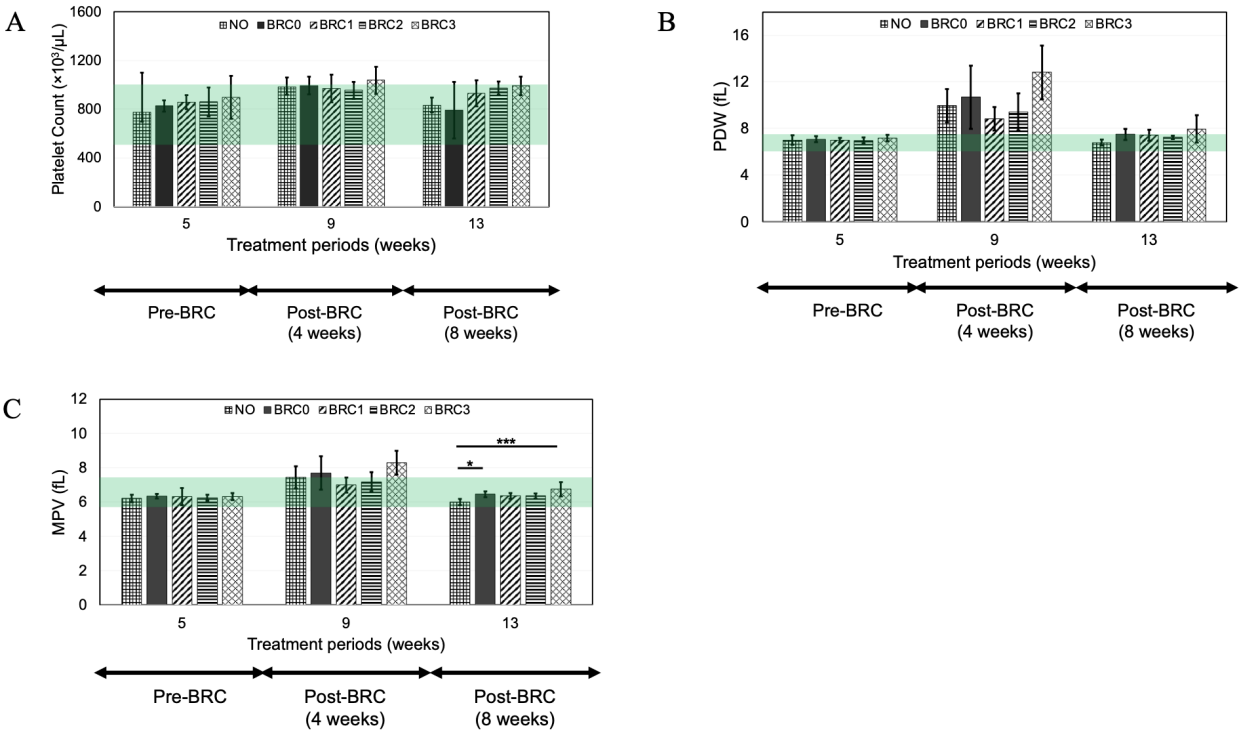

Figure 5. Platelet count (A), Platelet Distribution Width (PDW) (B), and Mean Platelet Volume (MPV) (C) following the administration of high-fat diets and supplementation with Black Rice Crunch (BRC). The data is expressed as mean ± standard deviation (SD). Significant differences between groups are denoted by asterisks (* for $P < 0.05$, ** for $P < 0.01$, and *** for $P < 0.001$). The normal range of platelet counts (Cox et al. 2011), PDW (Mulyati et al. 2019), and MPV (Said & Abiola 2014) are indicated by the green box.

CONCLUSION

In conclusion, this study demonstrates that administering an obesity-inducing diet for 5 weeks led to significant weight gain and obesity in rats. Importantly, supplementation with Black Rice Crunch (BRC) resulted in notable weight reduction in obese rats. Moreover, BRC consumption influenced erythrocyte numbers and mean corpuscular parameters. Interestingly, while the total leucocyte counts increased due to the high-fat diet, BRC had no significant impact on this parameter. Additionally, lymphocyte percentage remained stable across groups, indicating minimal influence of dietary interventions. Notably, mean platelet volume (MPV) increased after 8 weeks of BRC treatment, seemingly associated with obesity. Future research should investigate the molecular mechanisms behind BRC's effects on haematological parameters. Exploring the impact of BRC impact on inflammatory markers and adipose tissue could also provide further insights into its anti-obesity properties. Additionally, long-term studies on the safety and efficacy of BRC in human subjects are warranted to assess its potential as a functional food for obesity management.

AUTHORS CONTRIBUTION

R.P., Y.A.P, A.N., and F.S. designed the research and supervised all the processes; A.M.A., B.A.A., M.F.A., N.P.B.N., R.F.A.H., M.B.A.M., C.E.M., and S.N. collected and analysed the data, F.S., Y.A.P, A.N., and R.P. analysed the data and wrote the manuscript.

ACKNOWLEDGMENTS

The authors thank Universitas Gadjah Mada, Indonesia, for providing funding through the Rekognisi Tugas Akhir (RTA) Program with the reference number 633/UN1.P.III/SK/HUKOR/2022.

CONFLICT OF INTEREST

The authors declare that there is no conflict of interest.

REFERENCES

Aktas, G. et al., 2018. Mean Platelet Volume (MPV) as an inflammatory marker in type 2 diabetes mellitus and obesity. *Bali Medical Journal*, 7(3), pp.650-653. doi: 10.15562/bmj.v7i3.806.

An, J.S. et al., 2016. In vitro potential of phenolic phytochemicals from black rice on starch digestibility and rheological behaviors. *Journal of Cereal Science*, 70, pp.214–220. doi: 10.1016/j.jcs.2016.06.010.

Barrachina, M.N. et al., 2020. Analysis of platelets from a diet-induced obesity rat model: elucidating platelet dysfunction in obesity. *Scientific Reports*, 10(1), 13104. doi: 10.1038/s41598-020-70162-3.

Brandl, E.J. et al., 2012. Association study of polymorphisms in leptin and leptin receptor genes with antipsychotic-induced body weight gain. *Progress in Neuro-Psychopharmacology and Biological Psychiatry*, 38(2), pp.134–141. doi: 10.1016/j.pnpbp.2012.03.001.

Buettner, R., Schölmerich, J. & Bollheimer, L.C., 2007. High-fat Diets: Modeling the Metabolic Disorders of Human Obesity in Rodents. *Obesity*, 15(4), pp.798–808. doi: 10.1038/oby.2007.608.

Chasanah, S.N. & Pratiwi, R., 2019. Kadar Serum Glutamic Pyruvate Transaminase Darah Tikus (Rattus norvegicus Berkenhout, 1769) Hiperlipidemia dengan Asupan Pelet Nasi dan Bekatul Beras Hitam Padi (Oryza sativa L.) "Cempo Ireng." *Cendekia Eksakta*, 4(1), pp.33–38. doi: 10.3194/ce.v4i1.2672.

Cox, D., Kerrigan, S.W. & Watson, S.P., 2011. Platelets and the innate immune system: mechanisms of bacterial-induced platelet activation. *Journal of Thrombosis and Haemostasis*, 9(6), pp.1097–1107. doi: 10.1111/j.1538-7836.2011.04264.x.

Després, J.-P. & Lemieux, I., 2006. Abdominal obesity and metabolic syndrome. *Nature*, 444(7121), pp.881–887. doi: 10.1038/nature05488.

Després, J.-P., 2012. Body Fat Distribution and Risk of Cardiovascular Disease: An Update. *Circulation*, 126(10), pp.1301–1313. doi: 10.1161/CIRCULATIONAHA.111.067264.

de Kort, M. et al., 2020. Historical control data for hematology parameters obtained from toxicity studies performed on different Wistar rat strains: Acceptable value ranges, definition of severity degrees, and vehicle effects. *Toxicology Research and Application*, 4, 239784732093148. doi: 10.1177/2397847320931484.

Fabroni, S. et al., 2016. Screening of the anthocyanin profile and *in vitro* pancreatic lipase inhibition by anthocyanin-containing extracts of fruits, vegetables, legumes and cereals: Anthocyanin-containing extracts as inhibitors of pancreatic lipase. *Journal of the Science of Food and Agriculture*, 96(14), pp.4713–4723. doi: 10.1002/jsfa.7708.

Hariri, N., Gougeon, R. & Thibault, L., 2010. A highly saturated fat-rich diet is more obesogenic than diets with lower saturated fat content. *Nutrition Research*, 30(9), pp.632–643. doi: 10.1016/j.nutres.2010.09.003.

Kristamtini, T. et al., 2012. Morphological of genetic relationships among black rice landraces from Yogyakarta and surrounding areas.. *ARPN Journal of Agricultural and Biological Science*, 7(12), pp.982–989.

Lim, W.-C. et al., 2016. Germinated Waxy Black Rice Suppresses Weight Gain in High-Fat Diet-Induced Obese Mice. *Journal of Medicinal Food*, 19(4), pp.410–417. doi: 10.1089/jmf.2015.3590.

Lin, X. & Li, H., 2021. Obesity: Epidemiology, Pathophysiology, and Therapeutics. *Frontiers in Endocrinology*, 12, 706978. doi: 10.3389/fendo.2021.706978.

Monteomo, G., Kamagate, A. & Yapo, A., 2018. Effects of metabolic syndrome on blood cells to Wistar rats. *Journal of Diabetes, Metabolic Disorders & Control*, 5(6), pp.222-225. doi: 10.15406/jdmdc.2018.05.00170.

Mulyati et al., 2019. *Potensi Nutriulva sebagai Suplemen Hematologis (Laporan Penelitian Kolaborasi Dosen dan Mahasiswa)*, Universitas Gadjah Mada.

Nasution, N.P.B. & Pratiwi, R., 2023. *Effects of the Functional Food Product "Black Rice Crunch" on Leukocyte and Thrombocyte Profiles of Obese Rats (Rattus norvegicus Berkenhout, 1796)*. Universitas Gadjah Mada.

Park, Y.M. et al., 2020. Immunostimulatory Activity of Black Rice Bran in Cyclophosphamide-Induced Immunosuppressed Rats. *Natural Product Communications*, 15(7), p.1934578X2093491. doi: 10.1177/1934578X20934919.

Pratiwi, R. et al., 2016. Black Rice Bran Extracts and Fractions Containing Cyanidin 3-glucoside and Peonidin 3-glucoside Induce Apoptosis in Human Cervical Cancer Cells. *Indonesian Journal of Biotechnology*, 20(1), 69. doi: 10.22146/ijbiotech.15271.

Pratiwi, R. et al., 2019. Active Fractions of Black Rice Bran cv Cempo Ireng Inducing Apoptosis and S-phase Cell Cycle Arrest in T47D Breast Cancer Cells. *Journal of Mathematical and Fundamental Sciences*, 51(1), pp.47–59. doi: 10.5614/j.math.fund.sci.2019.51.1.4.

Purwestri, Y.A. et al., 2022. Makanan Fungsional Berbahan Dasar Beras Hitam dan Proses Pembuatannya.

Ren, D. et al., 2019. Hypolipidemic effects of fucoidan fractions from Saccharina sculpera (Laminariales, Phaeophyceae). *International Journal of Biological Macromolecules*, 140, pp.188–195. doi: 10.1016/j.ijbiomac.2019.08.002.

Romieu, I. et al., 2017. Energy balance and obesity: what are the main drivers? *Cancer Causes & Control*, 28(3), pp.247–258. doi: 10.1007/s10552-017-0869-z.

Rukmana, R.M. et al., 2017. The Effect of Ethanolic Extract of Black and White Rice Bran (Oryza sativa L.) on Cancer Cells. *Indonesian Journal of Biotechnology*, 21(1), 63. doi: 10.22146/ijbiotech.26814.

Sa'adah, N.N. & Pratiwi, R., 2016. Profil Lipid dan Indeks Aterogenik Tikus Putih (Rattus norvegicus Berkenhout, 1769) Hiperlipidemia dengan Asupan Pelet Nasi dan Bekatul Beras Hitam (Oryza sativa L.) "Cempo Ireng". *Seminar Nasional Biodiversitas VI*, pp.1–10.

Said, N. & Abiola, O., 2014. Haematological profile shows that Inbred Sprague Dawley rats have exceptional promise for use in biomedical and pharmacological studie. *Asian Journal of Biomedical and Pharmaceutical Sciences*, 4(37), pp.33–37. doi: 10.15272/ajbps.v4i37.597.

Shabbir, F., Hussain, M.M. & Rajput, T.A., 2015. Obesity: Effect of High Fat Diet Followed by Atorvastatin Administration on Serum Interleukin-6, White Blood Cell and Platelet Count in Male and Female Sprague Dawley Rats. *The Professional Medical Journal*, 22(06), pp.683–389. doi: 10.29309/TPMJ/2015.22.06.1231.

Sharp, P. & Villano, J.S., 2012. *The Laboratory Rat* 2nd Edition., Boca Raton: CRC Press. doi: 10.1201/b13862.

Syam, A.M. & Pratiwi, R., 2023. *Effects of Functional Food Product "Black Rice Crunch" on Body Weight and Red Blood Cell Profile of Obese Rats (Rattus norvegicus Berkenhout, 1769)*. Universitas Gadjah Mada.

Tsalissavrina, I., Wahono, D. & Handayani, D., 2013. Pengaruh Pemberian Diet Tinggi Karbohidrat dibandingkan Diet Tinggi Lemak terhadap Kadar Trigliserida dan HDL Darah pada Rattus novergicus galur wistar. *Jurnal Kedokteran Brawijaya*, 22(2), pp.80–89. doi: 10.21776/ub.jkb.2006.022.02.5.

Von Diemen, V., Trindade, E.N. & Trindade, M.R.M., 2006. Experimental model to induce obesity in rats. *Acta Cirurgica Brasileira*, 21 (6), pp.425–429. doi: 10.1590/S0102-86502006000600013.

Zhang, M.W. et al., 2010. Phenolic Profiles and Antioxidant Activity of Black Rice Bran of Different Commercially Available Varieties. *Journal of Agricultural and Food Chemistry*, 58(13), pp.7580–7587. doi: 10.1021/jf1007665.

Journal of Tropical Biodiversity and Biotechnology
Volume 09, Issue 01 (2024): jtbb84919
DOI: 10.22146/jtbb.84919

Research Article

Unravelling The Diversity of Cherry Tomato (*Solanum lycopersicum* var. *cerasiforme*) Seed Microbes and Their Effect on Seed Health

Herbert Dustin Aumentado[1,2], Jennelyn Bengoa[1], Mark Angelo Balendres[1,3,4]*

1)Institute of Plant Breeding, College of Agriculture and Food Science, University of the Philippines, Los Baños 4031, Laguna, Philippines
2)School of Science; Center of Excellence in Fungal Research, Mae Fah Luang University, Chiang Rai 57100, Thailand
3)Department of Biology, College of Science, De La Salle University 1004, Manila, Philippines
4)Plant and Soil Health Research Unit, Center for Natural Sciences and Environmental Research, De La Salle University 1004, Manila, Philippines
*)Corresponding author, email: mark.angelo.balendres@dlsu.edu.ph

Keywords:
Cherry tomato
Nigrospora
Curvularia
Stenotrophomonas
Citrobacter
Submitted:
29 May 2023
Accepted:
22 August 2023
Published:
15 January 2024
Editor:
Miftahul Ilmi

ABSTRACT

Healthy seeds are the foundation of healthy plants. Planting healthy seeds contributes to securing crop productivity and seed germplasm conservation. In this study, we have identified microbes associated with seeds of three cherry tomato genotypes and demonstrated their negative effect on general seed health. Through a combined morpho-cultural and molecular characterisation (using multi-loci analysis of the ITS, β-tubulin, tef1α, and gapdh gene regions for fungi and 16s rDNA for bacteria), we have identified three fungi (*Nigrospora sphaerica*, *N. lacticolonia*, and *Curvularia aeria*), and two bacteria (*Citrobacter freundii*, and *Stenotrophomonas maltophilia*) from healthy-looking tomato seeds. These fungi and bacteria, through seed-soaked-inoculation, caused seed discoloration, lesions, and low germination. To our knowledge, these are the first reports of *Nigrospora sphaerica*, *N. lacticolonia*, *Curvularia aeria*, *Citrobacter freundii*, and *Stenotrophomonas maltophilia* on tomato seeds and demonstrated their negative impact on seed health. Seed treatment and interventions are needed to negate the possible effect of these microbes. Future studies on possible seed transmission are warranted.

Copyright: © 2024, J. Tropical Biodiversity Biotechnology (CC BY-SA 4.0)

INTRODUCTION

The cherry tomato (*Solanum lycopersicum* var. *cerasiforme*) is a small round tomato genotype and a genetic mixture among wild currant-type tomatoes and domesticated garden tomatoes (Chanthini et al. 2019). In the Philippines, they have become cash crops or moneymakers for the farmers (Sarian 2018) compared to table tomatoes. It is used in many dishes, such as salads, garnishes, and toppings, e.g., pizza and pasta.

Quality seeds are indispensable in crop production and an essential farming input for smallholder farmers, including those that plant tomatoes. Healthy seeds are crucial to producing a yield that meets market demands. Quality seeds are also a prerequisite for successful seed germplasm conservation. Storing diseased and nonviable seeds can result in the loss of germplasm materials over time, and seeds contaminated with pathogenic microbes may contaminate the storage facilities, possibly

contaminating other healthy seeds.

Seeds harbour various fungi and bacteria that may be pathogenic or saprophytic (Utobo et al. 2011). Bacteria enter stomata and hydathodes, especially in wounds, which thrive in the apoplast (intercellular space). Fungi directly enter the plant's epidermal cells or spread hyphae on, between, or through plant cells (Nallathambi et al. 2020). These microbes can diminish seed quality and weaken germination, producing abnormal and diseased seedlings (Islam & Borthakur 2012). However, some of these microbes may be inactive or quiescent during a period. In such conditions, the seeds may not show any disease symptoms, or the pathogen does not show any sign of growth.

This study aimed to determine the diversity of microorganisms inhabiting cherry tomato seeds (*Solanum lycopersicum* var. *cerasiforme*). Specifically, this study aimed to identify and to characterise fungi and bacteria in healthy-looking cherry tomato seeds and determine the effect of these microbes on general seed health (cosmetic and germination).

MATERIALS AND METHODS

Microbial assay of cherry tomato seeds

Seeds of three open-pollinated cherry tomato genotypes 'Elmundo,' 'Betty,' and 'Cherrys' from the Institute of Plant Breeding, College of Agriculture and Food Science, University of the Philippines Los Baños) were placed equidistantly in Petri dishes containing potato dextrose agar (PDA) medium (Himedia Laboratories Ltd., India). Two experiments were performed simultaneously, one with surface-sterilised seeds and the other with non-surface-sterilised seeds. Both experiments were replicated three times and performed twice. Each replicate plate contained ten and six seeds in Trials 1 and 2. The surfaced-sterilised seeds were obtained as follows: first, seeds were immersed in 10% (v/v) commercial sodium hypochlorite (NaClO) bleach for 1 min, then seeds were rinsed thrice in sterile distilled water, and, finally, air-dried in sterile tissue paper before transferring onto PDA medium. Petri plates containing the seeds were incubated at room temperature (28.5 °C) for three days. Seeds were examined for growing microbes, which were isolated, purified, and maintained in PDA (for fungi) or Nutrient Agar (NA) medium (for bacteria).

Microbe Characterisation

Five mm of the fungal mycelial plug from each seven-day-old pure culture was transferred to a new PDA medium and incubated. Cultural characteristics, i.e., mycelial colour and form, were recorded seven days after incubation. Conidia length and width were measured from 30 randomly selected conidia of the seven-day-old fungal cultures under Olympus CX22 (Japan) microscopes. Photomicrographs were measured using the ImageJ software Version 1.51s (Wayne Rasband, National Institutes of Health, USA).

Bacterial isolates were streaked onto the NA medium to obtain a pure culture. The cultural characteristics were examined on their respective agar medium. Colony growth was examined, in terms of colour, shape, form, texture, size, and margin, after 48 hours of incubation.

Polymerase Chain Reaction (PCR) Assay

The bacterial genomic DNA of 2-day-old pure cultures of MBCTB01a and MBCTB01b isolates were extracted using Chen and Kuo's (1993) extraction method. The 16s rDNA gene region using the bacterial isolates was amplified by PCR using the 27F and 16s 1492R primers

(Suzuki & Giovannoni 1996). The fungal genomic DNA was extracted using CTAB (Cullings 1992; Doyle & Doyle 1987). The extracted genomic DNA of each isolate was used in subsequent PCR assays to amplify several fungal gene regions. The internal transcribed spacer (ITS), transcription elongation factor1-alpha (*tef1*), and partial β-tubulin (*tub2*) gene regions were amplified using primers ITS5/ITS4 (White et al. 1990), EF1-728F/EF1-986R (Carbone & Kohn 1999), and Bt2a/Bt2b (Glass & Donaldson 1995) and were used for isolates MBCTA01 and MBCTC02A. For isolate MMBCV02, ITS using primers ITS5/ITS4 (White et al. 1990) and glyceraldehyde 3-phosphate dehydrogenase (GAPDH) using primers GDF and GDR were used. Amplifications were performed in a MyCycler™ (Thermal Cycler System #1709703, Bio-Rad Laboratories, Inc., USA) using the different PCR conditions per gene loci (White et al. 1990; Carbone & Kohn 1999; Glass & Donaldson 1995). The PCR products were resolved by gel electrophoresis [1.5% Agarose (Vivantis) 0.5X TAE (Tris-Acetate-EDTA) buffer containing two µL GelRed solution (Biotium) (PowerPac™ and Sub-Cell GT, (Bio-Rad Laboratories)] and viewed using the GelDoc™ XR+ with Image Lab software (Bio-Rad Laboratories Inc., USA). PCR products were purified and sequenced with the primers specified above at Apical Scientific Sdn. Bhd. (Malaysia).

Phylogenetic Analysis

The consensus sequences were assembled from the forward and reverse sequences using the Geneious sequence editing software. The BLASTN search program (Zhang & Madden 1997; Zhang 2000) was carried out to determine the isolates' closest fungal and bacterial genera based on the highest percent similarity e-value and highest query cover. Then, phylogenetic analyses were performed using the Maximum likelihood (ML) method in MEGA-X software (Kumar et al. 2018). Sequences were aligned using CLUSTALW. The concatenated sequences of the MBCTA01 and MBCTC02A isolates' ITS, tef1α, and *tub2* genes were assembled and compared with the sequences of other *Nigrospora* species (Table 1; Wang et al. 2017). *Arthrinium kogelbergense* (CBS 113333) (Crous & Groenewald 2013) was used as an outgroup. The ML tree was generated using the HKY (Hasegawa-Kishino-Yano) model (Hasegawa et al. 1985) with gamma-distributed and invariants sites (G+I). The concatenated ITS and GAPDH genes of isolate MBCV02 were compared with the sequences of *Curvularia* species (Table 2) and other members of Pleosporaceae, *i.e.*, *Bipolaris maydis* (CBS 136.29) and *B. panici-miliacei* (CBS 199.29) were used as outgroup. The ML tree was generated using the Kimura-2 parameter model (Kimura 1980) with gamma-distributed and invariants sites (G+I).

Bacterial isolates MBCTB01A and MBCTB01B were aligned with the species 16s rRNA sequences of their genera. MBCTB01a isolate was compared and aligned with sequences of *Citrobacter* species and other Enterobacteriaceae, *i.e.*, *Klebsiella pneumonia* (DSM 30104), *Proteus vulgaris* (ATCC 29905), and *Serratia marcescens* subsp. *marcescens* (ATCC 13880) (Table 3). MBCTB01b was compared with sequences of *Stenotrophomonas* species and other Xanthomonadaceae, *i.e.*, *Pseudoxanthomonas taiwanensis* (CB-2660), *Xanthomonas campestris* (ATCC 33913), *Xylella fastidiosa*. (PCE-FF) (Table 4). The ML tree was generated using the Kimura-2 parameter model (Kimura 1980) with gamma-distributed and invariants sites (G+I). Support values of all trees were evaluated with 1000 bootstrap replicates.

Table 1. *Nigrospora* species used in phylogenetic analysis and their corresponding accession numbers.

Species	Isolate*	Host	Country	ITS	β-tubulin	*tef1*
Nigrospora aurantiaca	CGMCC 3.18130*=LC 7302	*Nelumbo* sp. (leaf)	China	KX986064	KY019465	KY019295
N. bambusae	CGMCC 3.18327*=LC 7114	Bamboo (leaf)	China	KY385307	KY385319	KY385313
N. camelliae-sinensis	LC 3287	*Camellia sinensis*	China	KX985975	KY019502	KY019323
N. chinensis	CGMCC 3.18127*=LC 457	*Machilus breviflora*	China	KX986023	KY019462	KY019422
N. gorlenkoana	CBS 480.73	*Vitis vinifera*	Kazakhstan	KX986048	KY019456	KY019420
N. guilinensis	CGMCC 3.18124*=LC 3481	*Camellia sinensis*	China	KX985983	KY019459	KY019292
N. hainanensis	CGMCC 3.18129*=LC 7030	*Musa paradisiaca* (leaf)	China	KX986091	KY019464	KY019415
N. lacticolonia	LC 7009	*Musa paradisiaca* (leaf)	China	KX986087	KY019594	KY019454
N. musae	CBS 319.34*	*Musa paradisiaca* (fruit)	Australia	KX986076	KY019455	KY019419
N. sphaerica	LC 4303	*Rhododendron arboreum*	China	KX986004	KY019528	KY019345
N. oryzae	LC 6759	*Oryza sativa*	China	KX986054	KY019572	KY019374
N. osmanthi	CGMCC 3.18126*=LC 4350	*Osmanthus* sp.	China	KX986010	KY019461	KY019421
N. pyriformis	CGMCC 3.18122*=LC 2045	*Citrus sinensis*	China	KX985940	KY019457	KY019290
N. rubi	CGMCC 3.18326*=LC 2698	*Rubus* sp.	China	KX985948	KY019475	KY019302
N. vesicularis	CGMCC 3.18128*=LC 7010	*Musa paradisiaca* (leaf)	China	KX985948	KY019463	KY019294
N. zimmermanii	CBS 290.62*	*Saccharum officinarum* (leaf)	Ecuador	KY385309	KY385317	KY385311
Arthrinium kogelbergense	CBS 113333	*Restionaceae*	South Africa	KF144892	KF144984	KF145026

*CGMCC= China General Microbiological Culture Collection, Institute of Microbiology, Chinese Academy of Sciences, Beijing, China; CBS= Culture Collection of the Westerdijk Fungal Biodiversity Institute, Utrecht, The Netherlands; LC= working collection of Lei Cai, housed at the Institute of Microbiology, Chinese Academy of Sciences, Beijing, China. Reference: Wang et al. (2017), Crous et al. (2013).

Table 2. *Curvularia* species used in phylogenetic analysis and their corresponding accession numbers.

Species	Isolate*	Host	Country	ITS	GAPDH	References
Bipolaris maydis	CBS 136.29	*Zea mays*	Japan	KJ909769	KM034845	Manamgoda et al. 2014
B. panici-miliacei	CBS 199.29	*Panicum miliaceum*	Japan	KJ909773	KM042896	Manamgoda et al. 2014
Curvularia aeria	BRIP:61232b	*Oryza sativa*	Australia	KU552200	KU552162	Khemmuk et al. 2016
C. affinis	CBS 154.34	Unknown	Indonesia	KJ909780	KM083608	Manamgoda et al. 2015
C. akaii	CBS 317.86	*Themada triandra*	Japan	KJ909782	KM230402	Manamgoda et al. 2015
C. alcornii	BRIP:61672a	*Oryza* sp.	Queensland	KU552202	KU552157	Khemmuk et al. 2016
C. arcana	CBS 127224	-	-	MN688801	MN688828	Marin-Felix et al. 2020
C. asianensis	MFLUCC 10-0711	*Panicum* sp.	Thailand	JX256424	JX276436	Manamgoda et al. 2012b
C. australiensis	IMI 53994	*Oryza sativa*	Australia	JN601026	KC747744	Manamgoda et al. 2012a
C. australis	BRIP 12521	*Sporobolus carolii*	Australia	KJ415541	KJ415405	Tan et al. 2014
C. austriaca	CBS 102694	Nasal cavity of patient with sinusitis	Austria	MN688802	MN688829	Marin-Felix et al. 2020
C. bannonii	BRIP 16732	*Jacquemontia tamnifolia*	USA	KJ415542	KJ415404	Tan et al. 2014
C. borreriae	AR5176r	*Sorghum bicolor*	South Africa	KP400637	KP419986	Manamgoda et al. 2015

Table 2. Contd.

Species	Isolate*	Host	Country	ITS	GAPDH	References
C. bothriochloae	BRIP 12522	*Bothriochloa bladhii*	Australia	KJ415543	KJ415403	Tan et al. 2014
C. buchloës	CBS 246.49	*Buchloë dactyloides*	USA	KJ909765	KM061789	Manamgoda et al. 2014
C. cactivora	CBS 580.74	Cactaceae	Suriname	MN688803	MN688830	Marin-Felix et al. 2020
C. canadiensis	CBS 109239	Overwintered grass	Canada	MN688804	MN688831	Marin-Felix et al. 2020
C. clavata	BRIP 61680	*Oryza rufipogon*	Australia	KU552205	KU552167	Khemmuk et al. 2016
C. coicis	CBS 192.29	*Coix lacryma*	Japan	JN192373	JN600962	Manamgoda et al. 2015
C. crustacea	BRIP 13524	*Sporobolus* sp.	Indonesia	KJ415544	KJ415402	Tan et al. 2014
C. dactyloctenii	BRIP 12846	*Dactyloctenium radulans*	Australia	KJ415545	KJ415401	Tan et al. 2014
C. ellisii	CBS 193.62	Air	Pakistan	JN192375	JN600963	Manamgoda et al. 2011
C. gladioli	ICMP 6160	*Gladiolus* sp.	New Zealand	JX256426	JX276438	Manamgoda et al. 2012a
C. geniculata	CBS 187.50	Unknown seed	Indonesia	KJ909781	KM083609	Manamgoda et al. 2015
C. graminicola	BRIP 23186a	-	Australia	JN192376	JN600964	Manamgoda et al. 2012a
C. harveyi	BRIP 57412	*Triticum aestivum*	Australia	KJ415546	KJ415400	Tan et al. 2014
C. hawaiiensis	BRIP 11987	*Oryza sativa*	USA	KJ415547	KJ415399	Tan et al. 2014
C. heteropogonicola	BRIP 14579	*Heteropogon contortus*	India	KJ415548	KJ415398	Tan et al. 2014
C. heteropogonis	CBS 284.91	*Heteropogon contortus*	Australia	JN192379	JN600969	Manamgoda et al. 2012
C. hominis	Cu_RgMdu	*Luffa acutangula*	India	MK737953	MK737951	Balamurugan et al., 2020
C. inaequalis	CBS 102.42	Sand dune soil	France	KJ922375	KM061787	Manamgoda et al. 2014
C. lunata	DMCC2087	*Zea mays*	USA	MG971304	MG979801	Garcia-Aroca et al., 2018
C. miyakei	CBS 197.29	*Eragrostis pilosa*	Japan	KJ909770	KM083611	Manamgoda et al. 2014
C. muehlenbeckiae	BRIP:61671	*Oryza* sp.	Australia	KU552201	KU552163	Khemmuk et al., 2016
C. neergaardii	BRIP 12919	*Oryza sativa*	Ghana	KJ415550	KJ415397	Tan et al. 2014
C. neoindica	IMI129790	*Brassica nigra*	India	MH414910	MH433649	Tan et al. 2018
C. nicotiae	BRIP 11983	Soil		KJ415551	KJ415396	Tan et al. 2014
C. nodulosa	CBS 160.58	*Eleusine indica*	USA	JN601033	JN600975	Manamgoda et al. 2015
C. oryzae	CBS 169.53	*Oryza sativa*	Vietnam	KP400650	KP645344	Manamgoda et al. 2015
C. ovariicola	BRIP 15882	*Eragrostis interrupta*	Australia	JN192384	JN600976	Manamgoda et al. 2012a
C. papendorfii	CBS 308.67	*Acacia karroo*	South Africa	KJ909774	KM083617	Manamgoda et al. 2014
C. pallescens	CBS 156.35	Air	Indonesia	KJ922380	KM083606	Manamgoda et al. 2015
C. perotidis	CBS 350.90	*Perotis rara*	Cape York	JN192385	HG779138	Manamgoda et al. 2011; Madrid et al. 2014; Manamgoda et al. 2015;
C. protuberata	CBS 376.65	*Deschampsia flexuosa*	UK	KJ922376	KM083605	Manamgoda et al. 2014
C. ravenelii	BRIP 13165	*Sporobolus fertilis*	Australia	JN192386	JN600978	Manamgoda et al. 2012a
C. richardiae	BRIP 4371	*Richardia brasiliensis*	Australia	KJ415555	KJ415391	Tan et al. 2014
C. robusta	CBS 624.68	*Dichanthium annulatum*	USA	KJ909783	KM083613	Manamgoda et al. 2014
C. ryleyi	BRIP 12554	*Sporobolus creber*	Yetman	KJ415556	KJ415390	Tan et al. 2014
C. sorghina	BRIP 15900	*Sorghum bicolor*	Australia	KJ415558	KJ415388	Tan et al. 2014
C. spicifera	CBS 274.52	-	-	JN192387	JN600979	Manamgoda et al. 2011
C. subpapendorfi	CBS 656.74	Desert soil	Egypt	KJ909777	KM061791	Manamgoda et al. 2015

Table 2. Contd.

Species	Isolate*	Host	Country	ITS	GAPDH	References
C. tsudae	ATCC 44764	*Chloris gayana*	Japan	KC424596	KC747745	Deng et al. 2014
C. trifolii	ICMP 6149	*Setaria glauca*	New Zealand	KM230395	JX276457	Manamgoda et al. 2015
C. tripogonis	BRIP 12375	-	Australia	JN192388	JN600980	Manamgoda et al. 2011
C. tropicalis	BRIP 14834	*Coffea arabica*	India	KJ415559	KJ415387	Tan et al. 2014
C. verruculosa	CPC 28792	-	Thailand	MF490825	MF490847	Marin-Felix et al. 2017

*ATCC- American Type Culture Collection, University Boulevard, Manassas; BRIP- The Plant Pathology Herbarium, Department of Agriculture, Fisheries and Forestry Indooroopilly, Queensland; CBS: Culture collection of the Centraalbureau voor Schimmelcultures, Fungal Biodiversity Centre, Utrecht, The Netherlands; CPC- Culture collection of Pedro Crous; ICMP- International Collection of Microorganisms from Plants Landcare Research, Auckland Mail Centre, Auckland; IMI= Culture Collection of CABI Europe UK Centre, Egham, UK.

Table 3. *Stenotrophomonas* species used in phylogenetic analysis and their corresponding accession numbers.

Species	Isolate*	Host	Country	*16s*	References
Pseudoxanthomonas taiwanensis	CB-226	hot spring	Taiwan	NR_025198	Chen et al. 2002
Stenotrophomonas acidaminiphila	AMX 19 16S	anaerobic sludge blanket	Mexico	NR_025104	Assih et al. 2002
Stenotrophomonas bentonitica	BII-R7	clay	Spain	NR_157765	Sánchez-Castro et al. 2017
Stenotrophomonas chelatiphaga	LPM-5	sewage sludge	Russia	NR_116366	Kaparullina et al. 2009
Stenotrophomonas daejeonensis	MJ03	sewage	South Korea	NR_117259	Lee et al. 2011
Stenotrophomonas ginsengisoli	DCY01	ginseng field	South Korea	NR_115687	Kim et al. 2010
Stenotrophomonas humi	R-32729	soil	Belgium	NR_042568	Heylen et al. 2007
Stenotrophomonas koreensis	TR6-01	compost	South Korea	NR_041019	Yang et al. 2006
Stenotrophomonas maltophilia	K13M1Y001	coastal dune	India	MK106330	Shet & Garg 2021
Stenotrophomonas maltophilia	OsEnb_HZB_H21	*Oryza sativa*	India	MN889407	Sahu et al. 2021
Stenotrophomonas maltophilia	ATCC 13637T	polluted urban soil	Japan	NR_040804	Iizuka et al. 1998
Stenotrophomonas maltophilia	IAM 12423	plastic industry soil	Pakistan	MN240936	Javaid et al. 2020
Stenotrophomonas maltophilia	S11-5	soil	USA	MN733007	Lopez et al. 2020
Stenotrophomonas nitritireducens	L2	biofilters	-	NR_025305	Finkmann et al. 2000
Stenotrophomonas panacihumi	MK06	soil	South Korea	NR_117406	Yi et al. 2010
Stenotrophomonas pavanii	ICB 89	*Saccharum officinarum* stalk	Brazil	NR_116793	Ramos et al. 2011
Stenotrophomonas pictorum	LMG 981	-	-	NR_041957	Hauben et al.1999
Stenotrophomonas rhizophila	e-p10	-	Germany	NR_028930	Minkwitz & Berg 2001
Stenotrophomonas terrae	R-32768	soil	Belgium	NR_042569	Heylen et al. 2007
Stenotrophomonas tumulicola	T5916-2-1b	yellow-cream viscous gel biofilm	Japan	NR_148818	Handa et al. 2016
Xanthomonas campestris	ATCC 33913	-	-	NR_074936	da Silva et al. 2002
Xylella fastidiosa	PCE-FF	-	-	NR_041779	Chen et al. 2000

*ATCC- American Type Culture Collection, University Boulevard, Manassas; LMG- LMG Bacteria Collection BCCM/LMG, Ghent University, Laboratory for Microbiology, Gent; ICB- Departamento de Patologia/ICB Campus Universitario, Estrada do Contorno, Manaus, Amazonas.

Table 4. *Citrobacter* species used in phylogenetic analysis and their corresponding accession numbers.

Species	Isolate	16s	References
Citrobacter amalonaticus	CECT 863	NR_104823	Yarza et al. 2013
Citrobacter cronae	XY1017	MW793480	Cui 2021
Citrobacter europaeus	CIP:106467	NR_156052	Ribeiro et al. 2017
Citrobacter farmeri	DP4R2A60	MH972183	Nimonkar et al. 2019
Citrobacter freundii	ATCC 8090 = MTCC 1658	NR_028894	Spröer et al. 1999
Citrobacter freundii	JCM 1657	NR_113340	Yarza et al. 2013
Citrobacter freundii	BAB-173	KF535108	Joshi et al. 2013
Citrobacter freundii	SS1KSU	MH973163	Tankrathok & Karnmongkol 2018
Citrobacter freundii	BAB-161	KF535107	Joshi et al. 2013
Citrobacter freundii	MD2	MZ047972	Joy et al. 2021
Citrobacter gillenii	CIP 106783	KM515970	Clermont et al. 2015
Citrobacter koseri	CDC-8132-86	NR_104890	Yarza et al. 2013
Citrobacter murliniae	HOP4	MT664058	Yang et al. 2020
Citrobacter rodentium	ATCC 51459	AB045737	Okutani et al. 2001
Citrobacter sedlakii	YL090822	GU726186	Wei et al. 2010
Citrobacter werkmanii	CIP 104555	KM515974	Clermont et al. 2015
Citrobacter youngae	GTC 1314	NR_041527	Nhung et al. 2007
Klebsiella pneumoniae	DSM 30104	NR_036794	Ludwig et al. 1995
Proteus vulgaris	ATCC 29905	NR_115878	Pignato et al. 1999
Serratia marcescens subsp. *marcescens*	ATCC 13880	NR_041980	Spröer et al. 1999

*ATCC- American Type Culture Collection, University Boulevard, Manassas; BAB- Instituto Nacional de Tecnologia Agropecuaria, Instituto de Recursos Biologicos, Castelar, Buenos Aires; CECT- Coleccion Espanola de Cultivos Tipo Edificio de Investigacion, Campus de Burjasot, Burjasot; DSM- Deutsche Sammlung von Mikroorganismen und Zellkulturen GmbH, Inhoffenstraße 7 B, 38124 Braunschweig; GTC- Gifu Type Culture Collection, Department of Microbiology, Gifu University School of Medicine, Gifu; JCM- Japan Collection of Microorganisms, Hirosawa, Wako, Saitama

Seed Germination assay

Two independent seed germination assays of the three cherry tomato genotypes ('Elmundo,' 'Betty,' and 'Cherrys') were performed to evaluate the effect of the isolated bacteria and fungi on percent seed germination. Fifteen seeds of each genotype, replicated three times, were soaked for 24 hours with a 3 mL suspension of the two identified bacteria. The turbidity and optical density of the suspension of both bacterial isolates were adjusted to OD_{600}= 0.3 in a spectrophotometer (SPECTRO 23 RS, LaboMed, Inc.), bringing a concentration of 10^8 CFU/mL. The three fungal isolates were scraped and strained in Muslin cloth. Seeds were soaked in 3 mL spore suspension (10^8 spores mL^{-1}). After 24 hours of seed soaking in the bacterial and fungal spore suspension, seeds were plotted equidistantly in Petri dishes and incubated (Memmert Incubator IN750, Memmert GmbH + Co. KG) (28.5 °C) for seven days. Germination percentages (%) were recorded seven days after incubation, and the appearance of the seeds was examined.

Statistical analysis

All statistical analyses were performed in SPSS statistical software (ver. 26, IBM, Armonk, NY). Data were analysed using one-way analysis of variance (ANOVA). Post hoc analyses of means were evaluated using Tukey's Honest Significant Difference (HSD) test (Tukey 1951) with a 95% significance level.

RESULTS AND DISCUSSION

Seed-borne microbes in cherry tomato seeds

A higher incidence of bacteria was observed and recorded compared to fungi (Table 1). All fungal isolates were obtained from non-surface-sterilised seeds of all three genotypes (Table 1). Both bacterial isolates MBCTB01A and MBCTB01b were found in non-surfaced-sterilised seeds of three tomato genotypes (Table 5). Only the bacterial isolate MBCTB01A was consistently found in all three tomato genotypes in surfaced-sterilized seeds. Bacterial isolate MBCTB01b was found in surfaced -sterilised seeds of genotype 'Cherrys' but not in 'Elmundo' and 'Betty.' A significant percent reduction in the incidence of fungi and bacteria ($p= 0.002$) was recorded in surface-sterilised seeds.

Table 5. Percent (%) incidence of seed-borne microbes found in three cherry tomato seed cultivars.

Cultivar	Isolate	Identity	Non-surfaced-sterilised (%)	Surfaced-sterilised (%)
'Elmundo'	MBCTB 01A	*Citrobacter freundii*	45.83	10.42
	MBCTB 01b	*Stenotrophomonas maltophilia*	18.75	0.00
	MBCT A01	*Nigrospora lacticolonia*	8.33	0.00
'Betty'	MBCTB 01A	*Citrobacter freundii*	95.83	18.75
	MBCTB 01b	*Stenotrophomonas maltophilia*	8.33	0.00
	MBCV0 2	*Curvularia aeria*	4.17	0.00
'Cherrys'	MBCTB 01A	*Citrobacter freundii*	60.42	2.08
	MBCTB 01b	*Stenotrophomonas maltophilia*	22.92	8.33
	MBCT C02A	*Nigrospora sphaerica*	8.33	0.00

Morphological and cultural characteristics

Fungal isolate MBCTA01 (Figure 1A) is floccose, creamy-white with a dark greenish-brown patch on the obversed centre and reversed. Conidia are smooth, dark brown to black, solitary, aseptate, globose to ellipsoidal-shaped, measuring an average of 134.21 µm² (30 conidia, ranging from 93.51 to 176.81 µm²), observed from the seven-day-old culture. Fungal isolate MBCTC02A (Figure 1B) is a floccose, grayish white colony. Conidia are smooth, dark brown to black, solitary, aseptate, globose to ellipsoidal-shaped (identical to conidia of MBCTA01 isolate), measuring an average of 140.85 µm² (n=30 conidia, ranging from 107.32 to 179.71 µm²), observed from the seven-day-old culture. Based on previous reports, the morpho-cultural characteristics resemble *Nigrospora* sp. (Wang et al. 2017; Taguiam et al. 2020). Whereas, fungal isolate MBCV02 is black with a velvety texture and smooth margins, and grew rapidly on PDA, reaching the edge of the Petri plate on the seventh-day post-incubation. Conidia are straight to pyriform-shaped, smooth-walled, four-celled, and obliquely septate with mainly three septa, and pale brown to dark brown-coloured with the middle two cells being darker than the end cells, measuring an average of 6.30 µm × 2.52 µm (n=30 conidia, ranging

from 4.64 to 8.32 µm × 1.93 to 3.06 µm). Based on these morphological features and previous reports (Khemmuk et al. 2016), MBCV02 is identified as *Curvularia* sp.

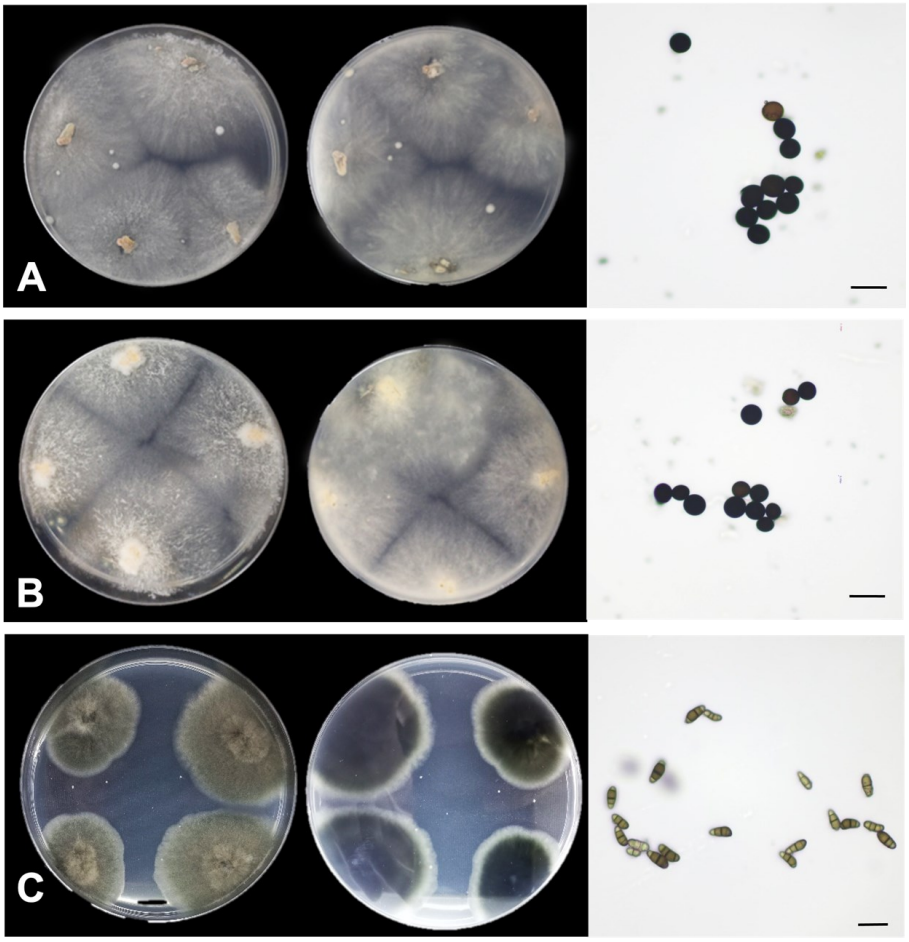

Figure 1. Cultural and conidial morphology of fungal isolates from cherry tomato seeds at 7 days after incubation (DAI). a. MBCTA01, b. MBCTC02, c. MBCV02. Scale bar = 20µm.

Bacterial isolate MBCTB01A produced bacterial colonies that are small, mucoid, and round-shaped with an entire (smooth) margin and convex elevation. Bacterial isolate MBCTB01B produced bacterial colonies that are dry, small, flat, round-shaped, and off-white-coloured with undulated to lobate margins (Figure 2).

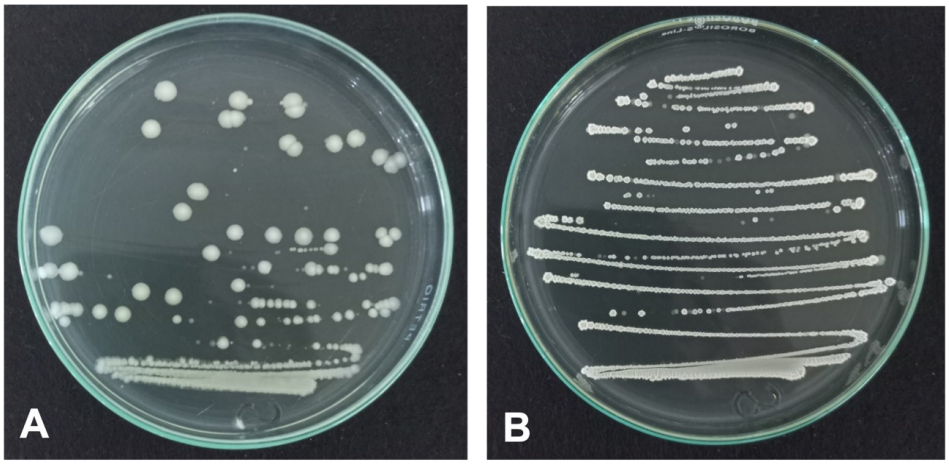

Figure 2. Cultural characteristics of bacteria found in cherry tomato seeds at 2 days after incubation (DAI). a. MBCTB01A, b. MBCTB01B.

Molecular identity

In the initial BLASTN analysis of the fungal isolates, the ITS gene sequences of MBCTA01, MBCTC02A, and MBCV02 isolates showed a 100% similarity to *Nigrospora lacticolonia* isolate KoRLI047323 (MN341462) and 14 *N. lacticolonia* strains, 100% similarity to *Nigrospora sphaerica* strain SX 4-1 (MH393359) (and 95 other *N. sphaerica* strains), and *Curvularia aeria* isolates B3153 (MT043775), and other 47 *C. aeria* isolate, respectively. The *tef1* gene of MBCTA01 and MBCTC02A isolates showed 99.55% similarity to *Nigrospora lacticolonia* strain LC12061 (MN264024) and 13 other *N. lacticolonia* strains, 99.54% similarity to *Nigrospora sphaerica* culture MFLUCC:18-0895 (MN995332), and other 105 *N. sphaerica* strains, respectively. The *tub2* gene of MBCTA01 and MBCTC02A isolates showed 100% *Nigrospora lacticolonia* strain LC12059 (MN329947) and 13 other *N. lacticolonia* 100% similarity to *Nigrospora sphaerica* isolate PC KS4A1 C R2 (MK408565) and 105 other *N. sphaerica* strains, respectively. The GAPDH gene of the MBCV02 isolate showed 98.31% similarity to *Curvularia* sp. isolate USJCC-0002 (MN053011). All isolates' sequences (Table 6) were deposited in NCBI GenBank.

Using the concatenated sequences of the ITS, *tef1*, and *tub2* gene regions, the phylogenetic analysis of fungal isolate MBCTA01 showed the isolate was grouped with *N. lacticolonia* LC7009 clade with 100 % ML support (Figure 3) and MBCTC02A grouped with the *N. sphaerica* LC4303 clade with 100% ML support (Figure 3). The fungal isolate MBCV02 grouped with the *C. aeria* BRIP:61232b clade (Figure 4) with 85% ML support.

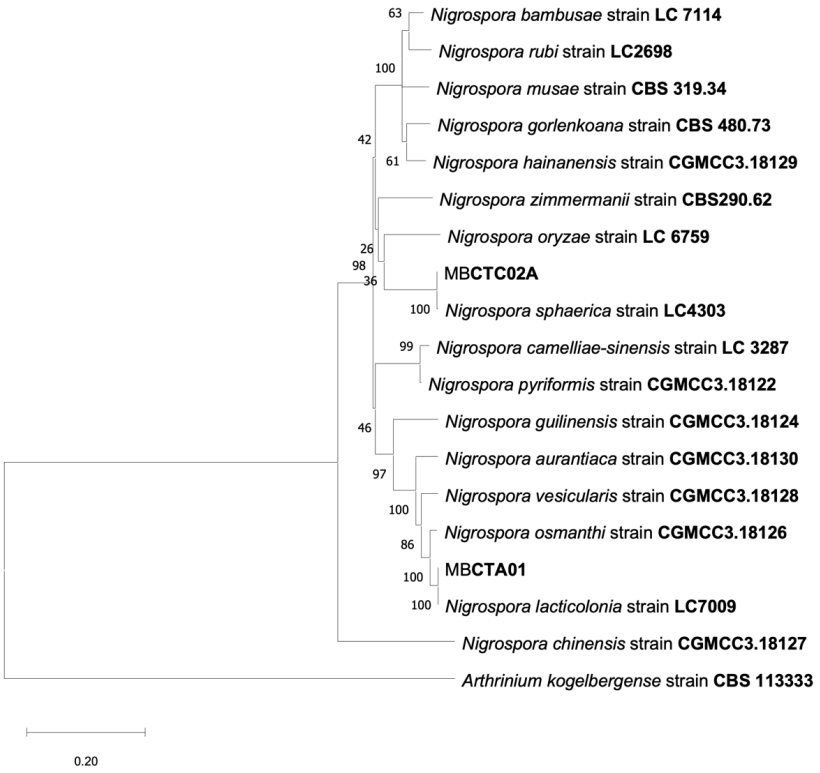

Figure 3. Phylogenetic tree generated by maximum likelihood analysis of the concatenated sequences of ITS, tef1α, and tub2 genes of *Nigrospora* species. ML (%) bootstrap support values are indicated near the nodes. Isolates MBCTA01 and MBCTC02A used in this study are in black arrowheads. The tree is rooted with *Arthrinium kogelbergense* CBS 113333. Bar = 0.20 indicates substitutions per nucleotide position.

Table 6. GenBank accession numbers of microbes isolated from tomato seeds.

Isolate	Identity	ITS	TUB	TEF	GAPDH	16sRNA
MBCTA01	*N. lacticolonia*	OR256266	OR271208	OR271206	-	-
MBCTA02A	*N. sphaerica*	OR256267	OR271209	OR271207	-	-
MBCV02	*C. aeria*	OR256268	-	-	OR271210	-
MBCTB01A	*C. freundii*	-	-	-	-	OR256216
MBCTB01B	*S. maltophilia*	-	-	-	-	OR256217

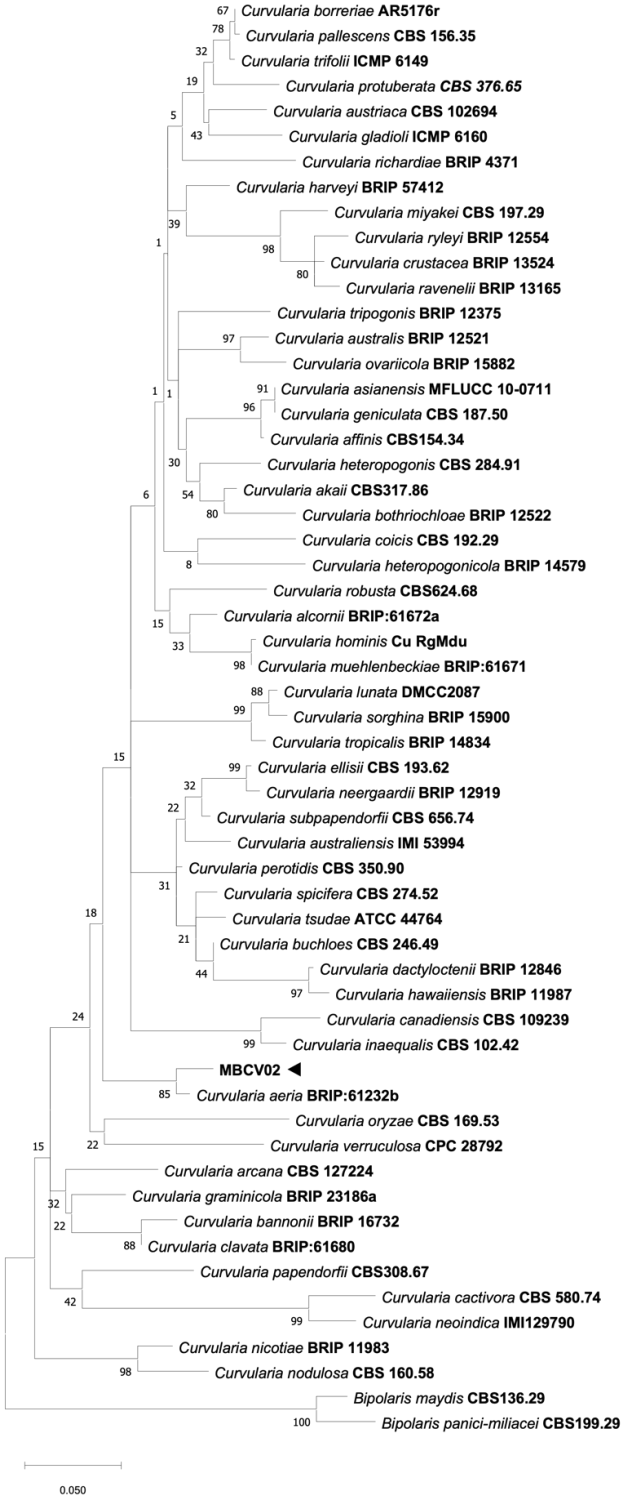

Figure 4. Phylogenetic tree generated by maximum likelihood analysis of the ITS and GAPDH gene of *Curvularia* species. ML (%) bootstrap support values are indicated near the nodes. Isolate MBCV02 used in this study is in black arrowhead. The tree is rooted with *Bipolaris maydis* CBS 136.29 and *Bipolaris panici-miliacei* CBS 199.29. Bar = 0.050 indicates substitutions per nucleotide position.

The initial BLASTN analysis of the bacterial isolates, using the 16s gene region, revealed that MBCTB01A was 99.44% similar to *Citrobacter freundii* strain BAB-173 (KF535108) and further supported with high similarity to 20 other *C. freundii* strains. The MBCTB01b isolate was 99.64% similar to *Stenotrophomonas maltophilia* strain K13M1Y001 (MK106330) and 33 other *S. maltophilia* isolates deposited in GenBank. The phylogenetic analyses confirmed this with isolate MBCTB01a grouped with the *Citrobacter freundii* clade (Figure 5) and the MBCTB01B isolate grouped with the *Stenotrophomonas maltophilia* clade (Figure 6).

Seed germination assay

Seeds soaked in fungal and bacterial suspension had significantly lower germination ($p < 0.001$) as compared to the controls (Figure 7). However, no significant variation in germination rate within inoculated seeds was observed among cherry tomato genotypes ($p = 0.673$). Rotting, discoloration, and lesions on the testa, cotyledons, and radicle of the roots and shoots were observed in the cherry tomato seeds that sprouted and germinated compared to controls (Figure 8). Similar symptoms were observed in both fungi and bacteria-treated seeds.

DISCUSSION

This study isolated and identified three fungi (*Nigrospora sphaerica*, *N. lacticolonia*, and *Curvularia aeria*) and two bacteria species (*Citrobacter freundii* and *Stenotrophomonas maltophilia*) from seeds of three cherry tomato genotypes ('Elmundo,' 'Betty,' and 'Cherrys'). These microbes are

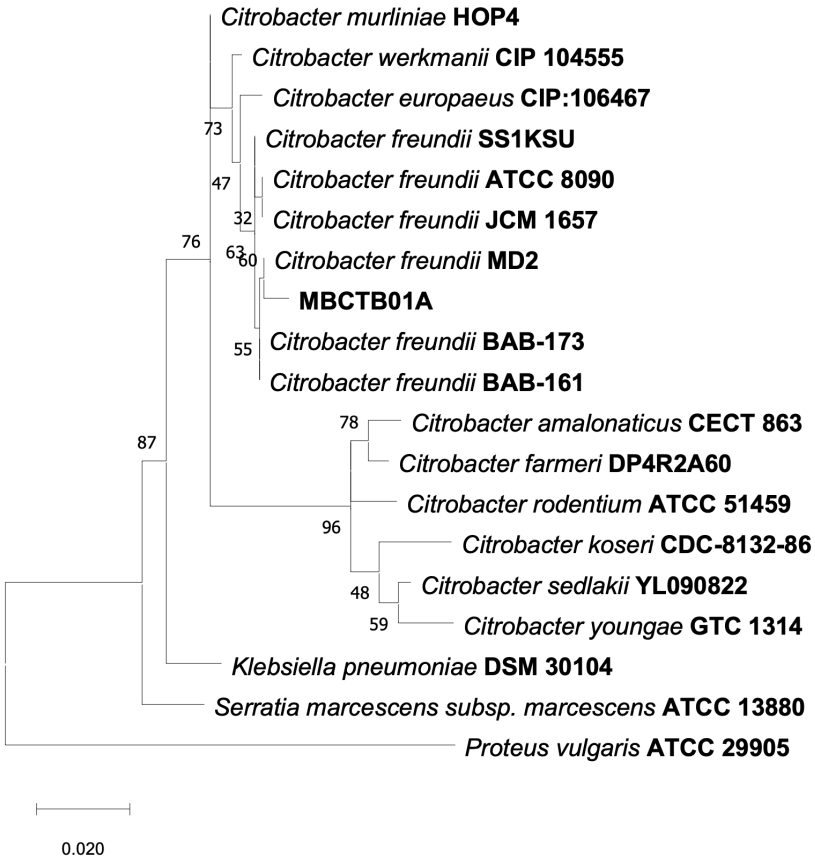

Figure 5. Phylogenetic tree generated by maximum likelihood analysis of the 16s RNA gene of *Citrobacter* species. ML (%) bootstrap support values are indicated near the nodes. Isolate MBCTB01A used in this study is in black arrowhead. *Klebsiella pneumoniae* DSM 30104, *Serratia marcescens* subsp. *marcescens* ATCC 13880, and *Proteus vulgaris* ATCC 29905 were used as an outgroup. Bar = 0.020 indicates substitutions per nucleotide position.

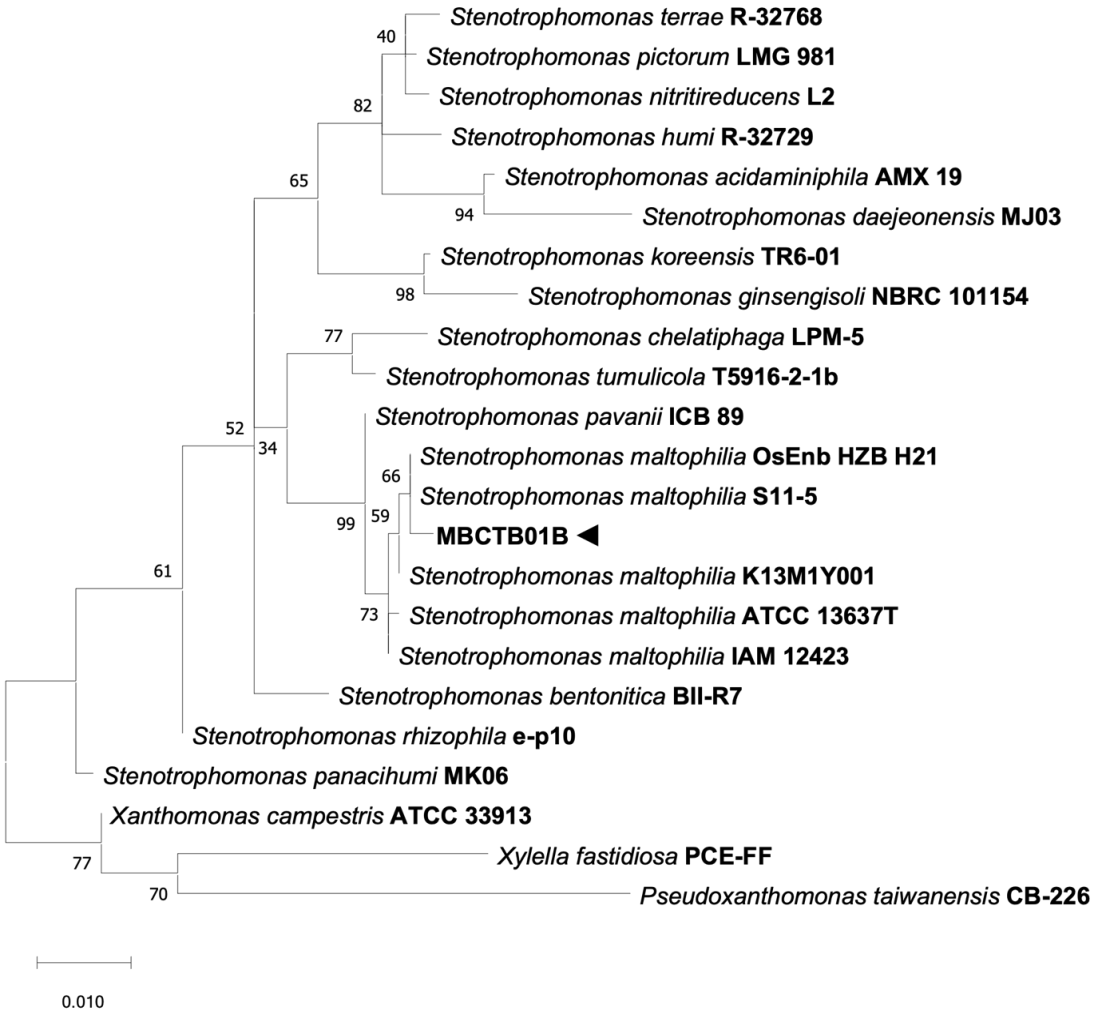

Figure 6. Phylogenetic tree generated by maximum likelihood analysis of the 16s rRNA gene of *Stenotrophomonas* species. ML (%) bootstrap support values are indicated near the nodes. Isolate MBCTB01B used in this study is in black arrowhead. *Xylella fastidiosa* PCE-FF and *Pseudoxanthomonas taiwanensis* CB-266 strains were used as an outgroup. Bar = 0.010 indicates substitutions per nucleotide position.

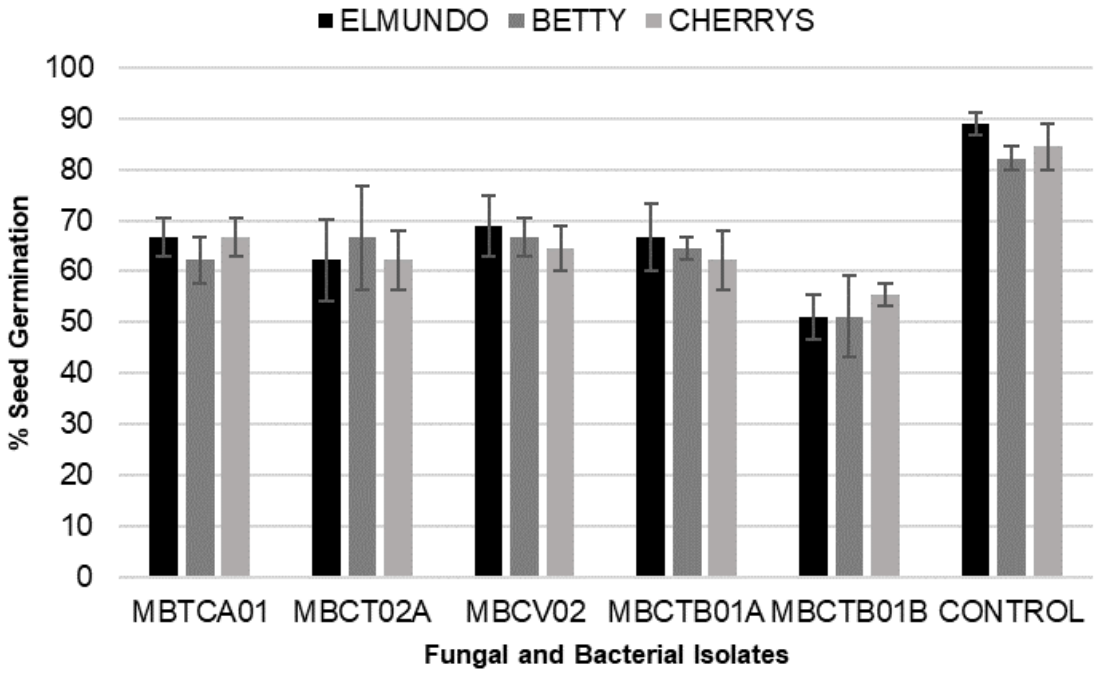

Figure 7. Mean percent (%) seed germination of cherry tomato genotypes at 7 days after sowing, soaked-inoculated with fungal and bacterial isolates.

Figure 8. Germinated seedlings of cherry tomatoes soaked-inoculated by seed-borne fungi and bacteria at 7dpi; a. control, b. MBCTA01, c. MBCTC02A, d. MBCV02, e. MBCTB01A, f. MBCTB01B.

reported for the first time in association with tomato seeds. These microbes reduce the number of healthy seeds (low germination) and have a noticeable negative effect on root and shoot growth. The results demonstrate that pathogens lurking in apparently-healthy seeds, initially as endophytes, could become pathogenic when introduced to its host externally and at high inoculum pressure.

Curvularia aeria (Bat., J.A. Lima & C.T. Vasconc.) Tsuda 1994 (Nakada et al. 1994), being a plurivorous species, has been reported recently on *Etlingera linguiformis* in India (Kithan & Daiho 2014), *Ficus religiosa* in Pakistan (Nayab & Akhtar 2016), *Helianthus annuus* in Mexico (Valázquez-del Valle et al. 2017), *Lactuca sativa* in Thailand (Pornsuriya et al. 2018), *Oryza sativa* in Queensland (Khemmuk et al. 2016), and *Cyperus rotundus* (Ferreira & Barreto 2020) among others. *Curvularia species* such as *C. lunata* had been previously reported in seeds of *Coix lacryma-jobi* (Kim & Lee 1998), *Andropogon* sp. (Santos et al. 2018), *Dalbergia sissoo* (Gupta et al. 2017), and *Solanum lycopersicum* in Pakistan (Iftikhar et al. 2016). This study first reported *C. aeria* associated from seeds of cherry tomatoes (*Solanum lycopersicum* var. *cerasiforme*).

Nigrospora lacticolonia Wang et al. (2017) is a filamentous fungus from the ascomycetes. It has been reported in *Hylocereus polyrhizus* in Malaysia (Kee et al. 2019; Hao et al. 2020), *Phoenix dactylifera* in Oman (Al-Nadabi et al. 2020), *Bougainvillea spectabilis* (Li et al. 2022), *Camellia sinensis*, *Saccharum officinarum*, and *Musa* × *paradisiaca* in China (Wang et al. 2017; Raza et al. 2019). *Nigrospora sphaerica* (Sacc.) E.W. Mason 1927, an endophyte, saprobe, and plant pathogen with a relatively larger number of reported hosts than *N. lacticolonia*, has been reported in about 386 plant species (Farr & Rossman 2022). Among these are *Actinidia deliciosa* (Chen et al. 2016), *Hylocereus undatus* in China (Liu et al. 2016), *Solanum tuberosum* in Brunei Darussalam (Peregrine & Ahmad 1982), *H. megalanthus*, *H. undatus*, and *H. polyrhizus* (Taguiam et al. 2020), and *Saccharum officinarum* (Teodoro 1937) in the Philippines. This species has been reported and transmitted in seeds of *Heliocarpus americanus* in Brazil (Bernardi et al. 2022). Other *Nigrospora* species, e.g., *N. oryzae*, have been confirmed to be transmitted in rice, maize, and soybean seeds (Vasantha et al. 1987; Soesanto et al. 2020). Our work adds cherry tomatoes as a host of *N. sphaerica* and *N. lacticolonia*.

Stenotrophomonas maltophilia (Hugh) Palleroni & Bradbury (1993) is a bacterial pathogen that has been lately increasingly associated with tomatoes in various studies, viz., tomato seeds in Zimbabwe along with

Xanthomonas species (Sibiya et al. 2003), tomato roots and rhizosphere (Marquez-Santacruz et al. 2010), bald seeds of tomato (Stoyanova et al. 2018), tomato fruits (Stoyanova & Bogatzevska 2012). It has been isolated from the soil, rhizosphere, and waters and reported as an endophyte in plants (Ryan et al. 2009). *Citrobacter freundii* (Braak 1928) Werkman & Gillen, 1932, a bacterium of the Enterobacteriaceae and an opportunistic food-borne pathogen (Liu et al. 2020) has been recently reported from *Zingiber officinale* in China (Zhao et al. 2021) and *Morus alba* in Iran (Allahverdi et al. 2020). Our study reports *S. maltophilia* and *C. freundii* from cherry tomato seeds in the Philippines. Nonetheless, only *C. fruendii* was consistently isolated from surfaced sterilized seeds. This bacterium could pose more problems if contaminated seeds are sown without intervention, e.g., seed treatment.

Several studies have reported on microbial diversity in seeds of different plants, e.g., maize (Brito et al. 2022), orchid (Gao et al. 2019), cauliflower (Dhekle et al. 2013), cacao (de Araujo et al. 2019) lima bean (Mota et al. 2017), common bean (Parsa et al. 2016), and rice (Fisher & Petrini 1992). Our study looked into the microbes associated with cherry tomato seeds. Here, we provide baseline knowledge on the diversity of seed pathogens that impacted tomato seed health. The fungi and bacteria isolated from this study resulted in a reduced seed germination rate. They also caused discoloration and lesions on the germinated seeds' testa, cotyledons, and radicle. Seed-borne pathogens may cause the weakening or death of embryos and gradually kill the embryos of the seeds they invade (Christensen 1962; Bewley & Black 2012). Moreover, seed-borne pathogens are also accountable for plant morphology variation and yield loss in the field. The bacteria and fungi isolated from non-surfaced sterilised seeds may be considered epiphytic or surface contaminants (Vishnuvat & Shukla 1979; Khare 1996) as most were isolated frequently in the non-surfaced-sterilised seeds. Their incidence was significantly reduced when seeds were chemically surfaced-sterilised, leaving *C. freundii* as the only microbe isolated from the three tomato seeds. Hence, it demonstrates that intervention, e.g., surface sterilisation, can reduce pathogenic seed microbes' inoculum (and even eliminate it). Nonetheless, the chemical seed treatment choice must not affect seed germination or subsequent plant development. Moreover, the choice of farming practice, e.g., organic or inorganic, should be considered when identifying chemical seed treatments or any intervention.

Proper seed sterilisation methods before sowing and planting are recommended. They should be communicated to tomato growers and vegetable farmers, especially in small farming communities, to ensure pathogen-free and healthier plants that will contribute to a better yield. Management of these pathogens while still in seeds is an early and practical disease control approach. Healthy seeds are the foundation of healthy plants, contributing to better and higher plant yields. Moreover, seeds used for germplasm conservation should be free of any microbes that may negatively impact seed germination in the future. Seed treatment and interventions are needed to negate the possible impact of these microbes.

CONCLUSIONS

This study isolated and identified *N. sphaerica*, *N. lacticolonia*, *C. aeria*, *S. maltophilia*, and *C. freundii* from cherry tomato seeds 'Elmundo,' 'Betty,' and 'Cherry.' These microbes were frequent in non-surfaced-sterilised seeds. However, their presence was significantly reduced (or eliminated) in surface-sterilized seeds. At high inoculum pressure, these microbes

caused discoloration and lesions on the testa, cotyledons, and radicle and have proved to diminish the cherry tomato seeds' germination. Future studies to determine if these microbes affect other plant organs (leaves, stems, and fruits) are warranted to quantify the scale of the impact of these microbes on tomato health and yield. Furthermore, future studies on possible seed transmission are warranted.

AUTHOR CONTRIBUTION

H.D.A. conceived the work, conducted the experiments, collected and analysed he data, and drafted the manuscript. J.B. edited the manuscript. M.A.B. conceived the work, contributed to the experimental design, and edited the manuscript.

ACKNOWLEDGMENTS

This study was supported by the Institute of Plant Breeding, College of Agriculture and Food Science, University of the Philippines, Los Baños, with partial support from the Department of Science and Technology-Philippine Council for Agriculture, Aquatic and Natural Resources Research and Development (DOST-PCAARRD). We thank Maria Cielo Paola Rodriguez, Loida Pascual, Pamela Quintos, Rosana Matienzo, Christine Joy Corpuz, Ryan Tiongco, Richard Sanchez, Joseph Lagman, Alben Manilay, and Fe Dela Cueva for their technical assistance.

CONFLICT OF INTEREST

The authors declare that they have no conflict of interest.

REFERENCES

Allahverdi, T., Rahimian, H. & Ravanlou, A., 2016. First report of bacterial canker in mulberry caused by *Citrobacter freundii* in Iran. *Plant Disease*, 100(8), pp.1774. doi: 10.1094/PDIS-01-16-0020-PDN

Al-Nadabi, H. et al., 2020. Molecular identification of fungal pathogens associated with leaf spot disease of date palms (*Phoenix dactylifera*). *All Life*, 13(1), pp.587–597. doi: 10.1080/26895293.2020.1835740

Assih, E.A. et al., 2002. *Stenotrophomonas acidaminiphila* sp. nov., a strictly aerobic bacterium isolated from an upflow anaerobic sludge blanket (UASB) reactor. *International journal of systematic and evolutionary microbiology*, 52(2), pp.559–568. doi: 10.1099/00207713-52-2-559

Balamurugan, A. et al., 2020. First report of *Curvularia hominis* inciting fruit rot of ridge gourd (*Luffa acutangula*) in Tamil Nadu, India. *Journal of Plant Pathology*, 102(2), pp.529–529. doi: 10.1007/s42161-019-00417-0

Bernardi, C. et al., 2020. The first report of *Nigrospora sphaerica* associated with *Heliocarpus americanus* seeds in Brazil. *Floresta e Ambiente*, pp. 28. doi: 10.1590/2179-8087-FLORAM-2019-0103

Bewley, J.D. & Black, M., 2012. Physiology and biochemistry of seeds in relation to germination, 2, *Viability, dormancy, and environmental control*. Springer Science & Business Media. doi: 10.1007/978-3-642-68643-6

Braak, H.R., 1928. Onderzoekingen over vergisting van glycerine.

Brito, V.D. et al., 2022. Fungal diversity and mycotoxins detected in maize stored in silo-bags: a review. *Journal of the Science of Food and Agriculture*, 102(7), pp.2640–2650. doi: 10.1002/jsfa.11756

Carbone, I. & Kohn L.M., 1999. A method for designing primer sets for speciation studies in filamentous ascomycetes. *Mycologia*, 91, pp.553–556. doi: 10.1080/00275514.1999.12061051

Chanthini, K.M.P. et al., 2019. Sustainable agronomic strategies for enhancing the yield and nutritional quality of wild tomato, *Solanum lycopersicum* (l) var *cerasiforme* Mill. *Agronomy*, 9(6), pp.311. doi: 10.3390/agronomy9060311

Chen, W.P. & Kuo, T.T., 1993. A simple and rapid method for the preparation of gram-negative bacterial genomic DNA. *Nucleic acids research*, 21(9), pp.2260. doi: 10.1093/nar/21.9.2260

Chen, J. et al., 2000. 16S rDNA sequence analysis of *Xylella fastidiosa* strains. *Systematic and applied microbiology*, 23(3), pp.349–354. doi.org: 10.1016/S0723-2020(00)80064-8

Chen, M.Y., et al., 2002. *Pseudoxanthomonas taiwanensis* sp. nov., a novel thermophilic, N2O-producing species isolated from hot springs. *International journal of systematic and evolutionary microbiology*, 52(6), pp.2155–2161. doi: 10.1099/00207713-52-6-2155

Chen, Y. et al., 2016. First report of leaf spot caused by *Nigrospora sphaerica* on kiwifruit in China. *Plant Disease*, 100(11), pp.2326. doi: 10.1094/PDIS-04-16-0486-PDN

Christensen, C.M., 1972. Microflora and seed deterioration. In *Viability of seeds*. Springer, Dordrecht. pp.59–93. doi: 10.1007/978-94-009-5685-8_3

Clermont, D. et al., 2015. Multilocus sequence analysis of the genus Citrobacter and description of *Citrobacter pasteurii* sp. nov. *International journal of systematic and evolutionary microbiology*, 65(5), pp.1486–1490. doi: 10.1099/ijs.0.000122

Crous, P.W. & Groenewald, J.Z., 2013. A phylogenetic re-evaluation of Arthrinium. *IMA fungus*, 4(1), pp.133–154. doi: 10.5598/imafungus.2013.04.01.13

Crous, P.W., Verkley, G.J., & Groenewald, J.Z., 2013. *Phytopathogenic Dothideomycetes*. CBS-KNAW Fungal Biodiversity Centre.

Cui, X.Y., et al., 2021. Isolation, identification of lactic acid degrading bacteria in alfalfa silage and their degradation characterization. *Biotechnology Bulletin*, 37(9), pp.58. doi: 10.13560/j.cnki.biotech.bull.1985.2021-0813

Cullings, K.W., 1992. Design and testing of a plant-specific PCR primer for ecological and evolutionary studies. *Molecular Ecology*, 1, pp.233–234

da Silva, A.R. et al., 2002. Comparison of the genomes of two *Xanthomonas* pathogens with differing host specificities. *Nature*, 417(6887), pp.459–463. doi: 10.1111/j.1365-294X.1992.tb00182.x

De Araújo, J.A. et al., 2019. Filamentous fungi diversity in the natural fermentation of Amazonian cocoa beans and the microbial enzyme activities. *Annals of Microbiology*, 69(9), pp.975–987. doi: 10.1007/s13213-019-01488-1

Deng, H. et al., 2015. *Curvularia tsudae* comb. nov. et nom. nov., formerly *Pseudocochliobolus australiensis*, and a revised synonymy for *Curvularia australiensis*. *Mycoscience*, 56(1), pp.24–28. doi: 10.1016/j.myc.2014.02.002

Dhekle, N.M. & Bodke, S.S., 2013. Studies on fungal diversity associated with Cauliflower, Tomato and Bhendi. *Rev. Res. J.*, 2(6), pp.1-7.

Doyle, J.J. & Doyle J.L., 1987. A rapid DNA isolation procedure for small quantities of fresh leaf tissue. *Phytochemical Bulletin*, 19, pp.11–15.

Farr, D.F. & Rossman, A.Y., 2022. Fungal Databases, U.S. National Fungus Collections, ARS, USDA. Retrieved August 4, 2022, from https://nt.ars-grin.gov/fungaldatabases/

Ferreira, B.W. & Barreto, R.W., 2020. Debunking *Duosporium*. *Mycol. Progr.*, 19(7), pp.715–723.

Finkmann, W. et al., 2000. Characterization of N2O-producing Xanthomonas-like isolates from biofilters as *Stenotrophomonas nitritireducens* sp. nov., *Luteimonas mephitis* gen. nov., sp. nov. and *Pseudoxanthomonas broegbernensis* gen. nov., sp. nov. *International journal of systematic and evolutionary microbiology*, 50(1), pp.273–282. doi: 10.1099/00207713-50-1-273

Fisher, P.J. & Petrini, O., 1992. Fungal saprobes and pathogens as endophytes of rice (*Oryza sativa* L.). *New Phytologist*, 120(1), pp.137–143. doi: 10.1111/j.1469-8137.1992.tb01066.x

Garcia-Aroca, T. et al., 2018. First report of *Curvularia* leaf spot of corn, caused by *Curvularia lunata*, in the United States. *Plant Health Progress*, 19(2), pp.140–142. doi: 10.1094/PDIS-04-21-0742-PDN

Gao, Y., Guo, S. & Xing, X., 2019. Fungal diversity and mechanisms of symbiotic germination of orchid seeds: a review. *Mycosystema*, 38 (11), pp.1808–1825. doi: 10.13346/j.mycosystema.190163

Glass, N.L. & Donaldson, G.C., 1995. Development of primer sets designed for use with the PCR to amplify conserved genes from filamentous ascomycetes. *Applied and environmental microbiology*, 61(4), pp.1323–1330. doi: 10.1128/aem.61.4.1323-1330.1995

Gupta, S., Dubey, A. & Singh, T., 2017. *Curvularia lunata* as, a dominant seed-borne pathogen in Dalbergia sissoo Roxb: Its location in seed and its phytopathological effects. *African Journal of Plant Science*, 11 (6), pp.203–208.

Handa, Y. et al., 2016. *Stenotrophomonas tumulicola* sp. nov., a major contaminant of the stone chamber interior in the Takamatsuzuka Tumulus. *International journal of systematic and evolutionary microbiology*, 66(3), pp.1119–1124. doi: 10.1099/ijsem.0.000843

Hasegawa, M., Kishino H. & Yano T., 1985. Dating the human-ape split by a molecular clock of mitochondrial DNA. *Journal of Molecular Evolution*, 22, pp.160–174. doi: 10.1007/BF02101694

Hao, Y. et al., 2020. *Nigrospora* species associated with various hosts from Shandong Peninsula, China. *Mycobiology*, 48(3), pp.169–183. doi: 10.1080/12298093.2020.1761747

Hauben, L. et al., 1999. Genomic diversity of the genus Stenotrophomonas. *International Journal of Systematic and Evolutionary Microbiology*, 49(4), pp.1749–1760. doi: 10.1099/00207713-49-4-1749

Heylen, K. et al., 2007. *Stenotrophomonas terrae* sp. nov. and *Stenotrophomonas humi* sp. nov., two nitrate-reducing bacteria isolated from soil. *International Journal of Systematic and Evolutionary Microbiology*, 57(9), pp.2056–2061. doi: 10.1099/ijs.0.65044-0

Iftikhar, S., Shahid, A.A. & Ali, S., 2016. First report of *Curvularia lunata* var. *aeria* causing leaf blight on tomato in Pakistan. *Journal of Plant Pathology*, 98(1), pp.180. https://www.jstor.org/stable/24892659

Iizuka, T. et al., 1998. Isolation and phylogenetic analysis of aerobic copiotrophic ultramicrobacteria from urban soil. *The Journal of general and applied microbiology*, 44(1), pp.75–84. doi: 10.2323/jgam.44.75

Islam, N.F. & Borthakur, S.K., 2012. Screening of mycota associated with Aijung rice seed and their effects on seed germination and seedling vigour. *Plant Pathol Quar*, 2(1), pp.75–85.

Javaid, H. et al., 2020. Biosynthesis of polyhydroxyalkanoates (PHAs) by the valorization of biomass and synthetic waste. *Molecules*, 25(23), 5539. doi: 10.3390/molecules25235539

Joshi, M.N. et al., 2013. 16S ribosomal RNA full gene profiling of isolates from Microbial Repository of Biodiversity Gene Bank of Gujarat State Biotechnology Mission.

Joy, C., Sundar, G.N. & Narmadha, D., 2021, May. AI Driven Automatic Detection of Bacterial Contamination in Water: A Review. *5th International Conference on Intelligent Computing and Control Systems (ICICCS)*, pp.1281–1285

Kaparullina, E. et al., 2009. *Stenotrophomonas chelatiphaga* sp. nov., a new aerobic EDTA-degrading bacterium. *Systematic and applied microbiology*, 32(3), pp.157–162. doi: 10.1016/j.syapm.2008.12.003

Kee, Y.J. et al., 2019. First report of reddish-brown spot disease of red-fleshed dragon fruit (*Hylocereus polyrhizus*) caused by *Nigrospora lacticolonia* and *Nigrospora sphaerica* in Malaysia. *Crop Protection*, 122, pp.165–170. doi: 10.1016/j.cropro.2019.05.006

Khare, M.N., 1996. Methods to test seeds for associated fungi. *Indian Phytopathology*, 49, pp.319–328.

Khemmuk, W. et al., 2016. Fungi associated with foliar diseases of wild and cultivated rice (*Oryza* spp.) in northern Queensland. *Australasian Plant Pathology*, 45(3), pp.297–308. doi: 10.1007/s13313-016-0418-3

Kim, J.S. & Lee, D.H., 1998. Seed transmission of *Bipolaris coicis*, *B. cynodontis*, *B. maydis* and *Curvularia lunata* causing leaf blight of Job's tears. *Korean Journal Plant Pathology*, 14(4), pp.287-293

Kim, H.B. et al.., 2010. *Stenotrophomonas ginsengisoli* sp. nov., isolated from a ginseng field. *International journal of systematic and evolutionary microbiology*, 60(7), pp.1522–1526. doi: 10.1099/ijs.0.014662-0

Kimura, M., 1980. A simple method for estimating evolutionary rate of base substitutions through comparative studies of nucleotide sequences. *Journal of Molecular Evolution*, 16, 111–120. doi: 10.1007/BF01731581

Kimura, K. et al., 2013. Distribution of chitin/chitosan-like bioflocculant-producing potential in the genus Citrobacter. *Applied microbiology and biotechnology*, 97(21), pp.9569-9577. doi: 10.1007/s00253-012-4668-x

Kithan, C. & Daiho, L., 2014. First report of *Curvularia aeria* on *Etlingera linguiformis* from Nagaland, India. *Plant Dis*, 98, pp.1580. doi: 10.1094/PDIS-01-14-0060-PDN

Kumar S. et al., 2018. MEGA X: Molecular Evolutionary Genetics Analysis across computing platforms. *Molecular Biology and Evolution*, 35, pp.1547–1549. doi: 10.1093/molbev/msy096. doi: 10.1093/molbev/msy096

Lee, M. et al., 2011. *Stenotrophomonas daejeonensis* sp. nov., isolated from sewage. *International journal of systematic and evolutionary microbiology*, 61(3), pp.598–604.

Li, M. et al., 2022. First report of *Nigrospora lacticolonia* causing leaf spot of *Bougainvillea spectabilis* in China. *Canadian Journal of Plant Pathology*, 44(5), pp.695–701. doi: 10.1080/07060661.2022.2067245

Liu, F. et al., 2016. First report of reddish-brown spot disease on pitaya caused by *Nigrospora sphaerica* in China. *Pl. Dis.*, 100(8), pp.1792–1793. doi: 10.1094/PDIS-01-16-0063-PDN

Liu, L. et al., 2020. Lineage, antimicrobial resistance and virulence of *Citrobacter* spp. *Pathogens*, 9(3), pp.195. doi: 10.3390/pathogens9030195

Lopez, N.V. et al., 2020. Urban and agricultural soils in Southern California are a reservoir of carbapenem-resistant bacteria. *Microbiology Open*, 9(6), pp.1247–1263. doi: 10.1002/mbo3.1034

Ludwig, W. et al., 1995. Comparative sequence analysis of 23S rRNA from Proteobacteria. *Systematic and applied microbiology*, 18(2), pp.164–188. doi: 10.1016/S0723-2020(11)80388-7

Madrid, H. et al., 2014. Novel *Curvularia* species from clinical specimens. *Persoonia: Molecular Phylogeny and Evolution of Fungi*, 33, pp.48. doi: 10.3767/003158514X683538

Manamgoda, D.S. et al., 2011. *Cochliobolus*: an overview and current status of species. *Fungal diversity*, 51(1), pp.3–42. doi: 10.1007/s13225-011-0139-4

Manamgoda, D.S. et al., 2012. A phylogenetic and taxonomic re-evaluation of the Bipolaris-Cochliobolus-Curvularia complex. *Fungal diversity*, 56(1), pp.131-144.

Manamgoda, D.S., et al., 2012a. Two new *Curvularia* species from northern Thailand. *Sydowia*, 64(2), pp.255–266.

Manamgoda, D.S. et al., 2012b. A phylogenetic and taxonomic re-evaluation of the *Bipolaris-Cochliobolus-Curvularia* complex. *Fungal diversity*, 56(1), pp.131–144. doi: 10.1007/s13225-012-0189-2

Manamgoda, D.S. et al., 2014. The genus *Bipolaris*. *Studies in mycology*, 79 (1), pp.221–288. doi: https://doi.org/10.1016/j.simyco.2014.10.002

Manamgoda, D.S. et al., 2015. A taxonomic and phylogenetic re-appraisal of the genus *Curvularia* (Pleosporaceae): human and plant pathogens. *Phytotaxa*, 212(3), pp.175–198. doi: 10.11646/phytotaxa.212.3.1

Manamgoda, D.S. et al., 2015. *Phytotaxa*, 212(3), pp.175–198.

Marin-Felix, Y., et al., 2017. New species and records of *Bipolaris* and *Curvularia* from Thailand. *Mycosphere*, 8(9), pp.1556–1574

Marin-Felix, Y., Hernandez-Restrepo, M. & Crous, P.W., 2020. Multilocus phylogeny of the genus *Curvularia* and description of ten new species. *Mycological Progress*, 19, pp.559–588. doi: 10.1007/s11557-020-01576-6

Marquez-Santacruz, H. et al., 2010. Diversity of bacterial endophytes in roots of Mexican husk tomato plants (Physalisixocarpa) and their detection in the rhizosphere. *Gen. Mol. Res*, 9, pp.2372–2380. doi: 10.4238/vol9-4gmr921

Minkwitz, A. & Berg, G., 2001. Comparison of antifungal activities and 16S ribosomal DNA sequences of clinical and environmental isolates of *Stenotrophomonas maltophilia*. *Journal of Clinical Microbiology*, 39(1), pp.139–145. doi: 10.1128/JCM.39.1.139-145.2001

Mota, J.M. et al., 2017. Fungal diversity in lima bean seeds. *Revista Brasileira de Engenharia de Biossistemas*, 11(1), pp.79–87.

Nakada, M., et al., 1994. RFLP analysis for species separation in the genera *Bipolaris* and *Curvularia*. *Mycoscience*, *35*(3), pp.271–278. doi: 10.1007/BF02268449

Nallathambi, P. et al., 2020. Mechanism of Seed Transmission and Seed Infection in Major Agricultural Crops in India. *In Seed-Borne Diseases of Agricultural Crops: Detection, Diagnosis & Management*. Springer, Singapore, pp.749–791. doi: 10.1007/978-981-32-9046-4_26

Nayab, M. & Akhtar N., 2016. First report of *Curvularia aeria* causing leaf spot of *Ficus religiosa* in Pakistan. *Plant Dis*, 100, pp.2530. doi: 10.1094/PDIS-05-16-0650-PDN

Nhung, P.H. et al., 2007. Phylogeny and species identification of the family Enterobacteriaceae based on dnaJ sequences. *Diagnostic microbiology and infectious disease*, 58(2), pp.153–161. doi: 10.1016/j.diagmicrobio.2006.12.019

Nimonkar, Y.S. et al., 2019. Assessment of the role of wastewater treatment plant in spread of antibiotic resistance and bacterial pathogens. *Indian journal of microbiology*, 59(3), pp.261–265. doi: 10.1007/s12088-019-00793-2

Oberhettinger, P. et al., 2020. Description of *Citrobacter cronae* sp. nov., isolated from human rectal swabs and stool samples. *International journal of systematic and evolutionary microbiology*, 70(5), pp.2998. doi: 10.1099/ijsem.0.004100

Okutani, A. et al., 2001. Comparison of bacteriological, genetic and pathological characters between *Escherichia coli* O115a, c: K (B) and *Citrobacter rodentium*. *Experimental animals*, 50(2), pp.183–186. doi: 10.1538/expanim.50.183

Palleroni, N.J. & Bradbury, J.F., 1993. *Stenotrophomonas*, a new bacterial genus for *Xanthomonas maltophilia* (Hugh 1980) Swings et al. 1983. *Int. J. Syst. Bacteriol.*, 43, pp.606–609. doi: 10.1099/00207713-43-3-606

Peregrine, W.T.H. & Ahmad, K.B., 1982. Brunei: A first annotated list of plant diseases and associated organisms. *Phytopathol. Pap.*, 27, pp.1–87.

Parsa, S. et al., 2016. Fungal endophytes in germinated seeds of the common bean, *Phaseolus vulgaris*. *Fungal biology*, 120(5), pp.783–790. doi: 10.1016/j.funbio.2016.01.017

Pignato, S. et al., 1999. Molecular characterization of the genera Proteus, Morganella, and Providencia by ribotyping. *Journal of Clinical Microbiology*, 37(9), pp.2840–2847. doi: 10.1128/jcm.37.9.2840-2847.1999

Pornsuriya, C., Ito, S.I. & Sunpapao, A., 2018. First report of leaf spot on lettuce caused by *Curvularia aeria*. *Journal of general plant pathology*, 84(4), pp.296–299. doi: 10.1007/s10327-018-0782-7

Ramos, P.L. et al., 2011. Screening for endophytic nitrogen-fixing bacteria in Brazilian sugar cane varieties used in organic farming and description of *Stenotrophomonas pavanii* sp. nov. *International Journal of Systematic and Evolutionary Microbiology*, 61(4), pp.926–931. doi: 10.1099/ijs.0.019372-0

Raza, M. et al., 2019. Culturable plant pathogenic fungi associated with sugarcane in southern China. *Fung. Diversity*, 99, pp.1–104. doi: 10.1007/s13225-019-00434-5

Ribeiro, T.G. et al., 2017. *Citrobacter europaeus* sp. nov., isolated from water and human faecal samples. *International journal of systematic and evolutionary microbiology*, 67(1), pp.170–173. doi: 10.1099/ijsem.0.001606

Ryan R. et al., 2009. The versatility and adaptation of bacteria from the genus Stenotrophomonas. *Nat. Rev. Microbiol.*, 7, pp.514–525. doi: doi.org/10.1038/nrmicro2163

Sahu, K.P. et al., 2021. Rice Blast Lesions: An Unexplored Phyllosphere Microhabitat for Novel Antagonistic Bacterial Species Against Magnaporthe oryzae. *Microbial Ecology*, 81(3), pp.731–745. doi: 10.1007/s00248-020-01617-3

Sánchez-Castro, I. et al., 2017. *Stenotrophomonas bentonitica* sp. nov., isolated from bentonite formations. *International journal of systematic and evolutionary microbiology*, 67(8), pp.2779. doi: 10.1099/ijsem.0.002016

Santos, P.R.R.D. et al., 2018. Morphological and molecular characterization of *Curvularia lunata* pathogenic to Andropogon grass. *Bragantia*, 77, pp.326–332. doi: 10.1590/1678-4499.2017258

Sarian, Z., 2018. What's New In Cherry Tomatoes. Agriculture Magazine June 2018 issue. Retrieved August 4, 2022, from https://www.agriculture.com.ph/2018/02/01/whats-new-in-cherry-tomatoes/

Sibiya J. et al., 2003. Incidence and seed-borne status of bacterial pathogens of tomato and paprika in the smallholder-farming sector of Zimbabwe. *Afr. Crop Sci. Conf. Proc.*, 6, pp.299–302.

Shet, S.A. & Garg, S., 2021. Prokaryotic diversity of tropical coastal sand dunes ecosystem using metagenomics. *3 Biotech*, 11(5), pp.1–21. doi: 10.1007/s13205-021-02809-5

Soesanto, L. et al., 2020. Seed-borne pathogenic fungi on some soybean varieties. *Biodiversitas Journal of Biological Diversity*, 21(9). doi: 10.13057/biodiv/d210911

Spröer, C. et al., 1999. The phylogenetic position of *Serratia*, *Buttiauxella* and some other genera of the family Enterobacteriaceae. *International Journal of Systematic and Evolutionary Microbiology*, 49(4), pp.1433–1438. doi: 10.1099/00207713-49-4-1433

Stoyanova M.I. & Bogatzevska, N., 2012. *Stenotrophomonas maltophilia* in scabs of tomato fruits. *Science & Technologies*, 2, pp.35–38.

Stoyanova, M.I. et al., 2018. *Stenotrophomonas maltophilia*-an emerging pathogen of local varieties of tomatoes in Bulgaria. *Acta Microbiologica Bulgarica*, 34(3), pp.180–186.

Suzuki, M.T. & Giovannoni, S.J., 1996. Bias caused by template annealing in the amplification of mixtures of 16S rRNA genes by PCR. *Applied and environmental microbiology*, 62(2), pp.625–630. doi: 10.1128/aem.62.2.625-630.1996

Taguiam, J.D. et al., 2020. Detection of *Nigrospora sphaerica* in the Philippines and the susceptibility of three *Hylocereus* species to reddish-brown spot disease. *Journal of the Professional Association for Cactus Development*, 22. doi: 10.56890/jpacd.v22i.321

Tan, Y.P. et al., 2014. Johnalcornia gen. et. comb. nov., and nine new combinations in *Curvularia* based on molecular phylogenetic analysis. *Australasian Plant Pathology*, 43, pp.589–603. doi: 10.1007/s13313-014-0315-6

Tan, Y.P., Crous, P.W. & Shivas, R.G., 2018. Cryptic species of *Curvularia* in the culture collection of the Queensland Plant Pathology Herbarium. *MycoKeys*, 35, pp.1.

Tankrathok, A. et al., 2018. Identification of a Novel Bacterial Agent causing Early Mortality Syndrome (EMS) in *Penaeus monodon* in the 2018 outbreak of Bangladesh.

Tankrathok, A. & Karnmongkol, C., 2018. MH973163 Citrobacter freundii strain SS1KSU 16S ribosomal RNA gene, partial sequence, MH973163. GenBank NCBI, USA.

Teodoro, N.G., 1937. An Enumeration of Philippine Fungi. *Techn. Bull.* Dept. Agric. Comm. Manila, 4, pp.1–585.

Tukey, J.W., 1951. Components in regression. *Biometrics*, 7(1), pp.33–69.

Utobo, E.B., Ogbodo, E.N. & Nwogbaga, A.C., 2011. Seedborne mycoflora associated with rice and their influence on growth at Abakaliki, Southeast Agro-Ecology, Nigeria. *Libyan Agriculture Research Center Journal International*, 2(2), pp.79–84.

Valázquez-del Valle, M.G., Poudel, B. & Zhang, S., 2017. First report of *Curvularia* blight on sunflower caused by *Curvularia aeria* in Mexico. *Plant Dis*, 101, pp.1955. doi: 10.1094/PDIS-05-17-0704-PDN

Vasantha, K., Vasanthi, H.J. & Shetty, H.S., 1987. Detection, location and transmission of *Nigrospora oryzae* in maize. *International Journal of Tropical Plant Diseases*, 5(2), pp.153–163.

Vishnuvat, K. & Shukla P., 1979. Fungi associated with lentil seeds. *Indian Phytopathology*, 32, pp.279–280.

Wang, M. et al., 2017. Phylogenetic reassessment of Nigrospora: ubiquitous endophytes, plant and human pathogens. *Persoonia*, 39, pp.118–142. doi: 10.3767/persoonia.2017.39.06

Wei, X.X., et al., 2010. Isolation and identification of *Citrobacter sedlakii* from *Palea steindachneri* and its antibiotic sensitivity. *Freshwater Fisheries*, 2.

Werkman, C.H. & Gillen, G.F., 1932. Bacteria producing trimethylene glycol. *Journal of Bacteriology*, 23(2), pp.167–182. doi: 10.1128/jb.23.2.167-182.1932

White, T.J. et al., 1990. Amplification and direct sequencing of fungal ribosomal RNA genes for phylogenetics. *PCR protocols: a guide to methods and applications*, 18(1), pp.315–322.

Yang, H.C. et al., 2006. *Stenotrophomonas koreensis* sp. nov., isolated from compost in South Korea. *International journal of systematic and evolutionary microbiology*, 56(1), pp.81–84. doi: 10.1099/ijs.0.63826-0

Yang, Q., et al., 2020. Emerging pathogens caused disease and mortality in freshwater mussels, *Hyriopsis cumingii*, in China. *Aquaculture Research*, 51(12), pp.5096–5105. doi: 10.1111/are.14848

Yarza, P. et al., 2013. Sequencing orphan species initiative (SOS): Filling the gaps in the 16S rRNA gene sequence database for all species with validly published names. *Systematic and Applied Microbiology*, 36(1), pp.69–73. doi: 10.1016/j.syapm.2012.12.006

Yi, H., Srinivasan, S. & Kim, M.K., 2010. *Stenotrophomonas panacihumi* sp. nov., isolated from soil of a ginseng field. *The Journal of Microbiology*, 48(1), pp.30–35. doi: 10.1007/s12275-010-0006-0

Zhang, J. & Madden TL., 1997. PowerBLAST: a new network BLAST application for interactive or automated sequence analysis and annotation. *Genome Res.*, 7(6), pp.649–656. doi: 10.1101/gr.7.6.649

Zhang, J. et al., 2000. A greedy algorithm for aligning DNA sequences. *J. Comput. Biol.*, 7(1–2), pp.203–214. doi: 10.1089/10665270050081478

Zhao, N. et al., 2021. *Citrobacter freundii* causing ginger (*Zingiber officinale*) rot in Tangshan, China. *Plant Disease*, 105(11), pp.3737. doi: 10.1094/PDIS-11-20-2368-PDN

Journal of Tropical Biodiversity and Biotechnology
Volume 09, Issue 01 (2024): jtbb77078
DOI: 10.22146/jtbb.77078

Research Article

The Growth Response of Rendeu (*Staurogyne elongata* (Neese) Kuntze) to Shoot Pruning and Its Propagation by Shoot Cutting

Intani Quarta Lailaty[1]*, Sri Astutik[1], Muhammad Imam Surya[1]
1)Research Center for Plant Conservation, Botanic Gardens and Forestry, National Research and Innovation Agency, Indonesia (BRIN). Jl. Raya Jakarta-Bogor Km. 46 Cibinong. Bogor. West Java. 16911
* Corresponding author, email: intaniquarta@yahoo.com

Keywords:
Ex situ conservation
Gunung Halimun-Salak National Park
Indigenous vegetable
Medicinal plant
Rendeu
Staurogyne elongata
Submitted:
15 August 2022
Accepted:
16 August 2023
Published:
19 January 2024
Editor:
Furzani Binti Pa'ee

ABSTRACT
Rendeu (*Staurogyne elongata* (Neese) Kuntze) is a native Indonesian plant used as food and traditional medicine in the daily life of the people residing around Gunung Halimun-Salak National Park. Due to the potential source of herbal-based medicines and traditional food in the long-run purposes, the proper method of its propagation is required so that Rendeu can be conserved and utilised sustainably. This study employed two research designs. First, a completely randomized design with pruning and IAA (indole-3 acetic acid) treatment was used for seedling growth. Second, plant propagation applied a factorial randomized block design: planting media types and plant growth regulator (PGR) (rootone F) treatment. Observation included the number of buds, number of leaves, number of flowers, plant biomass, root length, and relative chlorophyll content using the SPAD tool. The data were analysed using ANOVA (SPSS ver. 17.0), followed by Pearson correlation analysis. The results showed that applying IAA and leaf pruning could increase the number of buds, the number of leaves and the fresh weight of *S. elongata* plants compared to the control plant. The addition of rootone increased the growth of Rendeu shoot cuttings, shown in all growth parameters and chlorophyll content. Humus was the best media for Rendeu's growth among all planting medium. Planting media affected the increase in the number of leaves and the number of buds of *S. elongata* significantly. The interaction of planting media and PGR somewhat influenced root length and total leaf chlorophyll. The growth and production of *S. elongata* increased with the time of planting.

Copyright: © 2024, J. Tropical Biodiversity Biotechnology (CC BY-SA 4.0)

INTRODUCTION
Indonesia possesses diverse ethnicities, and each uses various plants to meet its daily needs. Rendeu (*Staurogyne elongata* (Neese) Kuntze) is one of Indonesia's native plants that is widely utilized by people residing around Gunung Halimun-Salak National Park (TNGHS), West Java. The previous research (Dewi et al. 2023) reported that Rendeu is the most extensively used for traditional medicine by local people in the Cikaniki area, TNGHS. The Rendeu leaf boiled water is usually consumed to cure diseases such as; kidney problems, liver, and postpartum treatment. People located in five hamlets in the Cikaniki area, namely Garung, Cilanggar, Citalahap Kampung, Citalahab Sentral, and Citalahab

Bedeng, use Rendeu for food (*lalap* and vegetables). Local people believe that the consumption of Rendeu's fresh leaves has significant impacts on health. It is handed down from generation to generation. Sutandi et al. (2017), stated that indigenous vegetable plants have high levels of vitamins and minerals such as vitamin A, vitamin C, calcium, iron (Fe) and zinc (Zn).

Rendeu leaf extract is well-known to have antibacterial and antioxidant activity (Noverita & Sinaga 2021). Reundeu leaf surface is the favourable habitat for specific microflora such as phyllosphere bacteria. They actively inhibit gram-positive bacteria (e.g. *E. coli*) and gram-negative bacteria (e.g. *B. subtilis* and *S. aureus*) (Rizqoh 2009). The five isolates of phyllosphere bacteria had different inhibitory concentrations. Genetic identification showed that those were closely related to the species *Klebsiella pneumoniae*, *Bacillus subtilis*, *Pseudomonas stutzeri*, and *Bacillus sp.* (Rizqoh et al. 2016). The ethyl acetate fraction of Rendeu contains flavonoids, saponins, tannins, steroids and triterpenoids, as well as phenols (Maulani et al. 2017). Previous research highlighted that the ethanolic extract of *S. elongata* leaves has antioxidant and antibacterial activity, containing several compounds, including phytol, oleic acid, valeric acid and stearic acid (Dewi et al. 2023). It indicates that Rendeu has biological activities with health benefit.

The trend of nature-based materials or herbal medicine is growing remarkably. Many pharmaceutical companies compete to find plants raw materials that have medicinal properties (Superani et al. 2008). In general, many indigenous vegetable plants grow wild in open places, such as natural forests, yards, gardens and fields, and-along the river. Sutandi et al. (2017) pointed out that indigenous vegetable cultivation is generally less intensive, so their production level tends to be lower. In the case of Rendeu, they usually grow in shaded areas and are often found on the sidelines of other plants. Cuttings or seedlings can be the two promising propagation techniques for Rendeu. In this study, the cuttings method was selected due to some advantages. Kang et al. (2011) mentioned that the cuttings promoted adventitious buds' growth, and influences morphological and reproductive descriptors, also biomass yield (Sarwar et al. 2020). Some previous research also underlined that applying growth hormone treatment combined with various planting media types could significantly affect the growth of cuttings (Danu et al. 2017; Kumar et al. 2022; Manohar et al. 2022). Concerning the high potential advantages of Rendeu, conservation initiatives and sustainable use are urgently needed, one of which is through plant propagation. The study aims to disseminate and seek the appropriate propagation methods for Rendeu using a combination of pruning, growth hormone, and planting media types. Thus, observing the interaction of the three above factors might help find the best propagation method approach. It leads to assisting sustainable utilization of Rendeu in the context of ex-situ conservation.

MATERIALS AND METHODS

Materials

The study was conducted at the Nursery Unit of the Cibodas Botanic Gardens - Research Center for Plant Conservation, Botanic Gardens and Forestry, National Research and Innovation Agency of Republic Indonesia (BRIN). The plant material source was *Staurogyne elongata* seedlings taken from the mountain forest of Gunung Halimun Salak National Park, West Java (Figure 1). We used Rendeu seedlings with 5-10 cm height in vegetative phase.

Figure 1. *S. elongata* seedlings taken from the mountain forest of Gunung Halimun Salak National Park.

Methods

Shoot Pruning of Rendeu's Mother Plant

This study employed a randomized complete design (RCD), each treatment with 20 replications. The treatment consisted of seedlings with the application of the hormone IAA (indole-3 acetic acid) and the one without the hormone IAA. Pruning of shoots was carried out at the beginning of planting in polybags with a combination of humus-husk media. The addition of IAA was conducted two weeks after planting with a dose of 1 M.

Parameters investigated in this study included the number of shoots, number of leaves, number of flowers, and biomass per plant material. The observation process was carried out for 20 weeks after pruning. Measurement of the production amount of per plant material is conducted by harvesting plant shoots and young leaves. Then, they were calculated as the fresh weight of Rendeu. Furthermore, the dry weight of the yield per plant was obtained by drying the yield per plant at a temperature of 65 ^{o}C for three days.

Vegetative Propagation of Rendeu by Shoot Cutting

The plant material was *S. elongata* shoots taken from the Cibodas Botanical Gardens nursery. The leaves were trimmed from the shoots, then the base of the shoots was slashed. After that, the shoots were immersed in a solution of growth regulators (rootone-F) for 10 minutes. The shoots were planted in a box containing planting media. Rootone-F is primarily used to accelerate plant physiological processes, especially for root primordia formation.

The propagation of Rendeu used a Randomized Complete Block Design (RCBD) with grouping based on the provision of plant growth regulators (PGR). The treatment consisted of two factors arranged in a factorial (Table 1).

Table 1. Design of Rendeu propagation with a RCBD.

Plant growth regulators	Media				
	C	C-HS	H	H-HS	S
NR	NR + C	NR + C-HS	NR + H	NR + H-HS	NR + S
R	R + C	R + C-HS	R + H	R + H-HS	R + S

Notes: C = compost, C-HS = compost and husk (1:1), H = humus, H-HS = humus and husk (1:1), S = sand, NR = non rootone, R = rootone (2 mg/500 ml).

Each treatment combination was repeated nine times. Growth parameters observed included the number of shoots, number of leaves, number of flowers, root length, and relative leaf chlorophyll content. Leaf chlorophyll measurements were conducted using the SPAD-502 Plus tool. The observation process was carried out for 20 weeks after planting.

Data Analysis

The data were analysed using ANOVA (analysis of variance) with SPSS 17.0 software. Moreover, Pearson correlation analysis was carried out to determine the relationship between characters (Gomez & Gomez 1995).

RESULTS AND DISCUSSION

The Growth of *S. elongata* with Shoot Pruning Treatments

The results demonstrated that applying IAA and leaf pruning could increase the number of buds and the number of leaves and flowers of *S. elongata* in humus-husk media. The growth has developed alongside the increased time (weeks). However, bud growth stabilised and decreased between 18 and 20 weeks after pruning (Figure 2). Hence, the plant has entered the generative phase, which focuses on flowering.

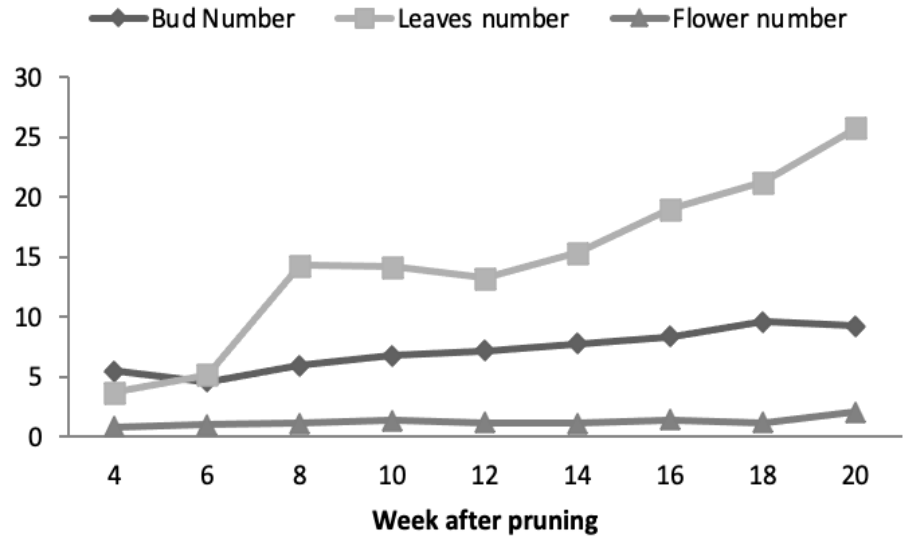

Figure 2. *Staurogyne elongata* growth rate for 20 weeks after pruning.

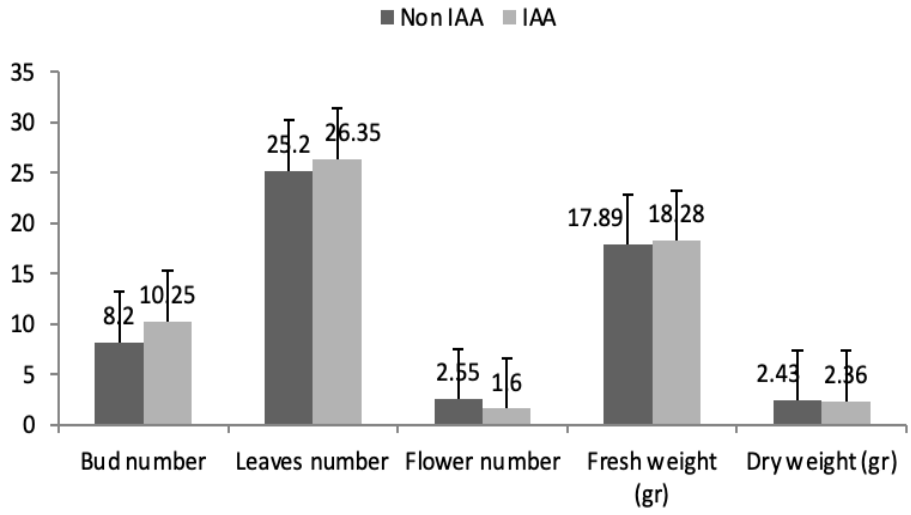

Figure 3. Growth and production of *Staurogyne elongata* by pruning and IAA treatment.

The addition of IAA can raise the number of buds and leaves also plant fresh weight of *S. elongata* compared to treatment without IAA in humus-husk media (Figure 3). Auxins play a vital role in the elongation of plant cells, root formation and root elongation, tropism, apical dominance, ripening fruits, also the promotion of ethylene production. Indole-3-acetic acid (IAA) is the common natural auxin that demonstrates all auxin-doing actions and extensively affects plants physiology (Narula et al. 2000). It is in line with Adinugraha et al. (2006), who underlined that treatment of exogenous growth regulators–containing synthetic auxin can support indigenous auxin to produce a higher percentage of bud than the control. Auxin accelerates the process of cell differentiation to form new cells, which in turn affect the formation of new buds. Those are in accordance with the study results which illustrated an increase in the number of shoots and leaves every week in the IAA treatment.

Based on statistical analysis, the IAA treatment did not exhibit a significant difference in the growth of *S. elongata* compared to the treatment without IAA (Table 2). Plant hormones and plant growth regulators (PGR) encourage plant growth and development. The effect of PGR depends on plant species, the PGR site of action on plants, plant growth stage and concentration of PGR. A PGR does not work alone in influencing the growth and development of plants. In general, some PGR concentrations' equilibrium will control plants growth and development (Fathonah & Sugiyarto 2019). In this study, the application of IAA with a dose of 1 M can increase the fresh weight of the plant, although it is not significant (Figure 3). It means the plant growth regulator provided at that concentration affects the plant growth optimally.

However, the application of IAA has not been able to increase the number of flowers and plant dry weight (Figure 3). On the other hand, auxins play an essential role in hormonal activity for plant flower production, especially for gibberellin formation. Auxin and gibberellin are synergists to flower induction (Hanaa & Safaa 2019). So, the IAA treatment can increase the number of flowers over time, although the yield is not higher than the control treatment.

Meanwhile, the dry weight of plants depends on the speed capability of cells to divide, enlarge, and elongate. The growth of hormones, such as endogenous auxin and cytokinin, can influence cell activity. The addition of some exogenous growth hormones is expected to accelerate the growth process. Auxin affects stem length increment, growth, differ-

Table 2. Effect of pruning and IAA treatment on the growth of *Staurogyne elongate*.

Plant age number	Parameter								
	Bud number			Leaves number			Flower		
	Non IAA	IAA	sig.	Non IAA	IAA	sig.	Non IAA	IAA	sig.
4 WAP	5,60	5,40	ns	3,75	3,70	ns	1,00	0,70	ns
6 WAP	4,15	5,00	ns	4,30	6,10	*	1,40	0,60	ns
8 WAP	5,20	6,70	*	13,85	14,80	ns	1,60	0,60	ns
10 WAP	6,95	6,55	ns	13,05	15,30	ns	1,90	0,80	ns
12 WAP	7,40	6,95	ns	12,00	14,50	ns	1,60	0,75	ns
14 WAP	7,25	8,25	ns	13,50	17,25	*	1,50	0,70	ns
16 WAP	9,10	7,60	ns	17,80	20,25	ns	1,65	1,20	ns
18 WAP	8,90	10,30	ns	19,60	22,85	ns	1,35	1,00	ns
20 WAP	8,20	10,25	ns	25,20	26,35	ns	2,55	1,60	ns

Notes: sig.= significance; ns = not significantly different; * = significantly different at the 5% alpha level; WAP = week after pruning

entiation and branching roots (Fathonah & Sugiyarto 2019). Based on plant biomass measurement, it indicated that the dry weight of plants with IAA treatment is no different from the control. It is because the dry weight of the plant is more related to the water content of the plant. In addition, the gibberellins hormone can also promote bud development, stem elongation and leaf growth, influencing growth and differentiation, which affects plant dry weight. Surya et al. (2020) reported that PGR's treatment such as NAA, GA_3, BA could be significantly affecting leaf area, SLA, water content, leaf weight, chlorophyll, stomata and transpiration rate in the seedling of loquat.

Vegetative Propagation of *S. elongata* by Shoot Cutting

The growth of *S. elongata* shoot cuttings has developed alongside the planting time stages. However, flower growth decreased at week 15 after planting (Figure 4). The growth regulator (rootone) treatment increased the growth of Rendeu shoot cuttings, as shown in all growth parameters and relative chlorophyll content (Table 3). The results illustrate that rootone treatment can increase the bud number and root length of *S. elongata*. It corresponds to Adinugraha et al. (2006), the use of growth regulators on breadfruit shoot cuttings significantly produced a higher number of bud and root lengths than that of the control treatment. The use of Rootone-F with a low concentration of 100 ppm resulted in a higher bud number and number of roots than that of the higher concentration. The proper concentration of auxin plays a significant role in cell differentiation. Still, it can be toxic at the above optimum concentration and reduce the yield.

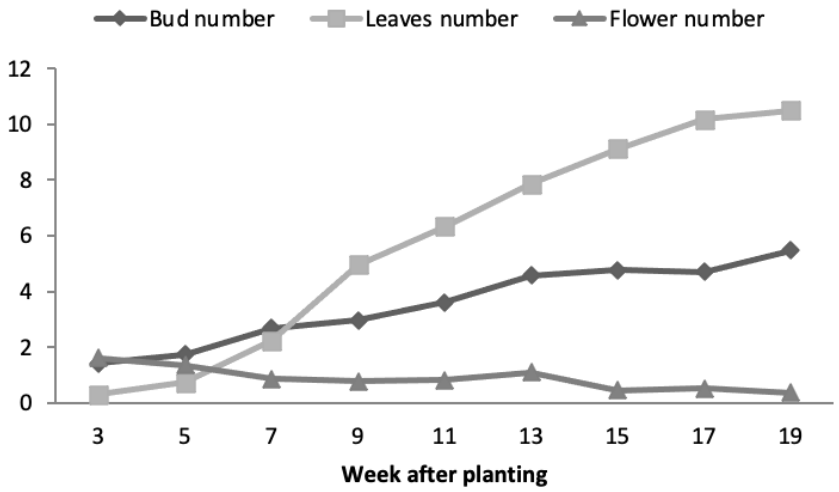

Figure 4. *Staurogyne elongata* shoot cutting growth rate for 19 weeks after planting.

Humus was the best planting media for shoot cuttings of *S. elongata*'s growth (Table 3). It is in line with the research of Normasiwi & Lailaty (2016) that humus media grants the best growth success rate for Violces leaf cuttings, herbs with beautifully coloured flowers. Leaf-based humus is the result of weathering of organic matter by microorganisms. Leaf-based humus has high ion exchange ability, so it can store nutrients. However, the weakness of humus media is that it induces fungus growth quickly once there is a change in temperature, humidity, or extreme aeration.

Planting media affected on the bud number and the number of leaves of *S. elongata* significantly (Table 4). According to Balitbanghut

(2007), planting media is one of the determinants of the success of the root formation process. Media selection must pay attention to several specific characteristics of the media. Good media must have minimal chemical content to interfere with the water absorption process by cuttings. Planting media should have appropriate physical properties, closely related to the ability to bind water and the porosity of the media. The ideal cutting media has sufficient aeration but can bind water. In addition, good media is a hygienic medium or has the low microbial population. The roots formation on cuttings is an initial and critical factor in shoot cuttings treatment. Roots absorb nutrients from the soil and are very influential for the growth of cuttings, especially buds and leaves on *S. elongata*.

This study also measured the relative chlorophyll content of *S. elongata* leaves. Chlorophyll is the most vital pigment in the process of photosynthesis. The amount of chlorophyll per unit leaf area is a crucial indicator of the overall condition of the plant. Healthy plants generally have more chlorophyll than unhealthy plants. This amount of chlorophyll can be used to identify the plants' growth rate and fertility, which can later be linked to predicting the production of these plants (Sukmono et al. 2012). Detection of this chlorophyll content conventionally takes a long time and adequate energy. At the same time, the chlorophyll data is needed quickly for fertility and production analysis. For that, we need a technology that can be used to detect leaf chlorophyll content promptly and efficiently. Then, we employed SPAD to measure the relative chlorophyll content of leaves.

Table 3 displayed that the application of rootone can increase the relative chlorophyll content of *S. elongata* leaves. The interaction of planting media and PGR were significantly different at the 1% alpha level (Table 4). The highest leaf chlorophyll content was produced from plants on humus media in SPAD units. Putri et al. (2016) explained that the SPAD value has a close relationship with plant health. A fertile and well-nourished plant will look green on its leaves and indicate sufficient nitrogen (N) content. Besides, plant productivity will also be higher if the nutrient content is adequate (Cen et al. 2006). Knowing the SPAD value contained in plants will also inform us about the N content of the leaves (Gholizadeh et al. 2009). The chlorophyll meter (SPAD meter) is a non-destructive alternative technology to effectively and efficiently determine the relative chlorophyll content in leaves.

The increase in bud number and the number of leaves were posi-

Table 3. Growth parameters and relative chlorophyll content of *S. elongata* with media and PGR treatments.

Media	Bud number		Leaves number		Flower number		Root length (cm)		Relative Chlorophyll Content (SPAD)	
	NR	R	NR	R	NR	R	NR	R	NR	R
C	11.44±1.02	13.56±3.15	5.11±0.51	8.56±2.27	0.11±0.19	0.11±0.19	4.89±1.73	5.11±2.57	18.57±2.05	21.63±2.05
H-HS	10.56±0.69	11.00±1.45	5.00±0.00	4.11±1.02	0.11±0.19	0.56±0.51	18.83±2.09	18.44±4.22	17.35±2.34	15.66±2.55
H	10.33±2.40	14.11±6.26	7.11±1.95	9.44±4.07	1.00±1.00	0.22±0.39	18.95±3.77	18.00±2.61	27.29±5.06	36.04±3.78
C-HS	8.00±3.61	8.67±3.22	3.33±1.00	2.11±0.19	0.56±0.39	0.44±0.77	7.17±3.46	14.06±3.74	10.05±3.64	14.73±8.14
S	7.78±0.69	9.44±0.69	4.89±1.02	5.00±1.53	0.00±0.00	0.56±0.51	14.78±4.69	14.39±5.06	20.10±3.36	14.57±3.25
Mean	9.62	11.36	5.09	5.84	0.36	0.38	12.92	14	18.67	20.53

Notes: C = compost, H-HS = humus and husk (1:1), H = humus, C-HS = compost and husk (1:1), S = sand, NR = non rootone, R = rootone.

Table 4. Significance of the effect of planting media, growth regulators and their interactions on the growth of *Staurogyne elongata* shoot cuttings.

No.	Parameters	Media	PGR	Interaction
1.	Number of leaves			
	3 WAP	**	ns	ns
	5 WAP	ns	ns	ns
	7 WAP	ns	ns	ns
	9 WAP	ns	**	ns
	11 WAP	ns	**	ns
	13 WAP	ns	*	ns
	15 WAP	ns	ns	ns
	17 WAP	*	*	ns
	19 WAP	**	*	ns
2.	Number of buds			
	3 WAP	ns	**	ns
	5 WAP	ns	*	ns
	7 WAP	**	ns	ns
	9 WAP	ns	ns	ns
	11 WAP	**	ns	ns
	13 WAP	**	ns	ns
	15 WAP	**	ns	ns
	17 WAP	**	ns	**
	19 WAP	**	ns	ns
3.	Number of flower (footstalk)			
	3 WAP	ns	ns	ns
	5 WAP	ns	ns	*
	7 WAP	ns	ns	ns
	9 WAP	ns	ns	ns
	11 WAP	ns	ns	ns
	13 WAP	*	ns	ns
	15 WAP	ns	ns	ns
	17 WAP	ns	ns	ns
	19 WAP	ns	ns	ns
4.	Relative chlorophyll content	**	*	**
5.	Root length (cm)	**	ns	**

Notes: ns = not significantly different; * = significantly different at the 5% alpha level; ** = significantly different at a 1% alpha level; PGR = plant growth regulator; WAP = week after planting

Table 5. Correlation value of three growth characters of *Staurogyne elongata* shoot cuttings.

		Leave number	Bud number	Flower number
Leaves number	Correlation coefficient	1	0.981**	- 0.843**
	Sig.		0.000	0.004
Bud number	Correlation coefficient	0.981**	1	- 0.838**
	Sig.	0.000		0.005
Flower number	Correlation coefficient	- 0.843**	- 0.838**	1
	Sig.	0.004	0.005	

tively correlated. The more of bud number, the more leaves are produced. On the other hand, the number of flowers negatively correlated with the bud number and the number of leaves (Table 5). These are because the formation of flowers is a part of the reproductive phase that focuses on assimilating results in leaves on flower growth and development. The results of Rendeu propagation with PGR treatment and variations of planting media are presented in Figure 5. This is in line with Surya et al. (2021) that the interaction of fertilization and plant growth regulators was significantly affecting the seedling growth such as plant height, number of leaves, bud, stem diameter, roots length, leaf surface area and total biomass. The study's results will be applicable for utilization by the

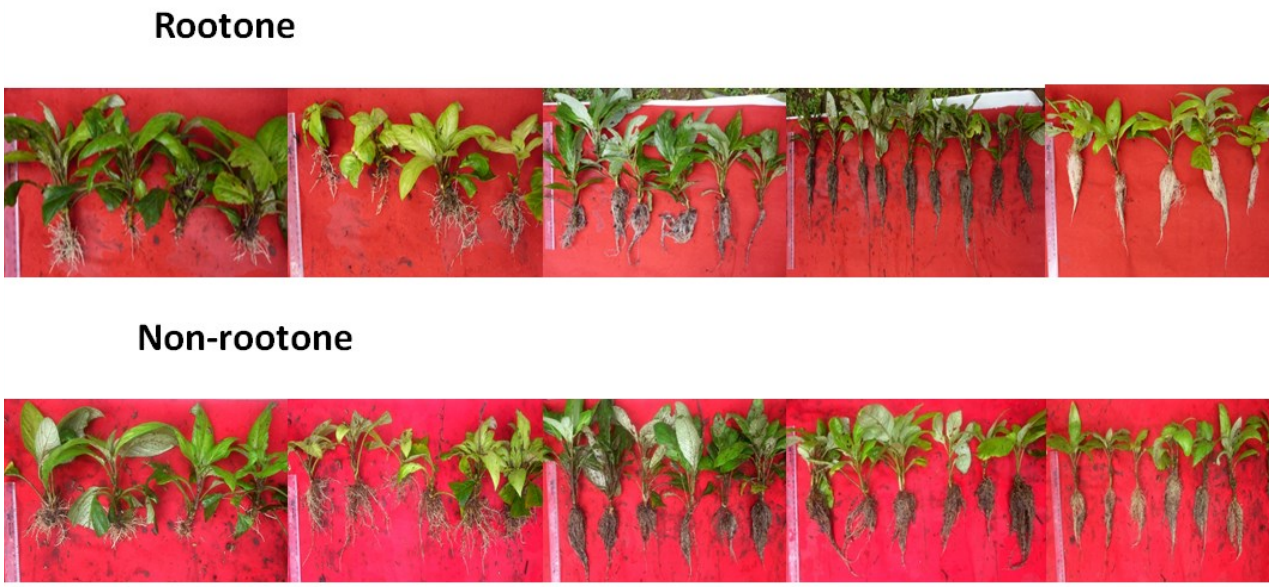

Figure 5. Growth of *S. elongata*'s shoot cuttings in various planting media. The picture from left to right: compost, compost-husk, humus, humus-husk, sand media.

community residing around Mount Halimun-Salak and serve as material sources for further research. Hopefully, this native Indonesian plant can continue to be conserved and more usable.

CONCLUSIONS

The combination of leaf pruning, the IAA hormone treatment, and planting media can promote *Staurogyne elongata's* growth development and production. In this study, the treatment of leaf pruning, IAA 1 M, and humus media indicates the best results on *S. elongata*'s growth parameters. The application of plant growth regulation (rootone-F) can increase the relative chlorophyll content of *S. elongata* leaves. Further research is required to increase the production of *S. elongata* using various combinations of growth regulators and planting media. Thus, the above propagation methods can assist the sustainable utilization of Rendeu.

AUTHOR CONTRIBUTION

M.I.S. designed the research, collected data, analysed data and wrote the manuscript, S.A. collected data and wrote the manuscript, I.Q.L. analysed the data, literature study, and wrote the manuscript.

ACKNOWLEDGMENTS

Authors thanked to Cibodas Botanic Gardens and Gunung Halimun-Salak National Park for supporting this research.

CONFLICT OF INTEREST

There is no conflict of interest regarding this research.

REFERENCES

Adinugraha, H.A., Moko, H. & Cepi, C., 2006. Pertumbuhan Stek Pucuk Sukun Asal dari Populasi Nusa Tenggara Barat dengan Aplikasi Zat Pengatur Tumbuh. *Jurnal Penelitian Hutan Tanaman*, pp.93–100. doi: 10.20886/jpht.2006.3.2.93-100.

Balitbanghut, 2007. *Pedoman Pembuatan Stek Jenis-Jenis Dipterokarpa Dengan KOFFCO System*. Bogor: Cooperation between Badan Litbang Kehutanan, KOMATSU and JICA.

Cen, H. et al. 2006. Non-destructive estimation of rape nitrogen status using SPAD chlorophyll meter. *International Conference on Signal Processing Proceedings, ICSP*, 1. doi: 10.1109/ICOSP.2006.344481.

Danu, Putri, K.P. & Sudrajat, D.J., 2017. Effect of media and growth regulators on the propagation of Nyawai (*Ficus variegata* Blume) shoot cutting. *Jurnal Pemuliaan Tanaman Hutan*, 11(1), pp.15–23

Dewi, A.P. et al. 2023. Ethnobotany of food, medicinal, construction and household utilities producing plants in Cikaniki, Gunung Halimun Salak National Park, Indonesia. *Journal of Mountain Science*, 20(1), pp.163-181 doi: 10.1007/s11629-021-7108-5.

Fathonah, D. & Sugiyarto, S., 2019. Effect of IAA and GA3 toward the growing and saponin content of purwaceng (*Pimpinella alpina*). *Nusantara Bioscience*, 1(1), pp.17–22. doi: 10.13057/nusbiosci/n010103.

Gholizadeth, A. et al. 2009. Evaluation of SPAD chlorophyll meter in two different rice growth stages and its temporal variability. *European Journal of Scientific Research*, 37, pp.591–598.

Gomez, K.A. & Gomez, A.A., 1995. *Statistical procedure for agriculture research*. Second eds. Universitas Indonesia Press.

Hanaa, H. & Safaa, A., 2019. Foliar application of IAA at different growth stages and their influenced on growth and productivity of bread wheat (*Triticum aestivum* L.). *Journal of Physics: Conference Series*, 1294(9). doi: 10.1088/1742-6596/1294/9/092029.

Kang, DJ., Ishii, Y. & Nishiwaki, A. 2011. Effects of the shoot-cutting method on field propagation in napiergrass (*Pennisetum purpureum* Schum.). *J. Crop Sci. Biotechnol.*, 14, pp.139–142. doi: 10.1007/s12892-010-0114-8

Kumar, P., Patel, P.K. & Sonkar, M.K., 2022. Propagation through juvenile shoot cuttings in difficult-to-root *Dalbergia latifolia* – examining role of endogenous IAA in adventitious rooting. *Plant Physiol. Rep.*, 27, pp.242–249. Doi: 10.1007/s40502-022-00664-x

Manohar, A.K. et al. 2022. Effects of plant growth regulators and growing media on propagation and field establishment of *Stevia rebaudiana*: a medicinal plant of commerce. *CABI Agric Biosci* 3, 4. doi: 10.1186/s43170-021-00072-5

Maulani, M. I., Purwanti, L. & Dasuki, U. A., 2017. Uji Aktivitas Antibakteri Ekstrak Daun Reundeu (*Staurogyne elongata* (Bl.) O.K) terhadap Staphylococcus aureus dan Eschericia coli. *Prosiding Farmasi*, 3(2), pp.565–569.

Narula, N. et al. 2000. Effect of P-solubilizing Azotobacter chroococcum on N, P, K uptake in p-responsive genotypes grown under greenhouse condition. *J. Plant Nutr. Soil Sci.*, 163, pp.393-398. doi: 10.1002/1522-2624(200008)163:4<393::AID-JPLN393>3.0.CO;2-W

Normasiwi, S. & Lailaty, I. Q., 2016. Inisiasi Perlakuan Media Tanam terhadap Pertumbuhan Stek Daun Violces (*Saintpaulia ionantha* H . Wendl.). *Seminar Nasional Biologi V*, UNNES, pp. 532–538.

Noverita & Sinaga, E., 2021. Antibacterial Bioactivity from Extract of Reundeu Caret (*Staurogyne longata*) and Honje (*Etlingera hemisphaerica*). *Journal of Tropical Biodiversity*, 2(1), pp. 21–32.

Putri, R. E. et al. 2016. Variability of Rice Yield With Respect To Crop Health. *Jurnal Teknologi*, 78(1–2), pp.79–85.

Rizqoh, D., 2009. *Bakteri filosfer daun Reundeu (Staurogyne elongata) penghasil senyawa antibakteri asal Wana Wisata Cangkuang*. Institut Pertanian Bogor.

Rizqoh, D. et al. 2016. Aktivitas Bakteri Filosfer Daun Reundeu (*Staurogyne longata*) Sebagai Penghasil Senyawa Antimikroba Potensial. *Jurnal Analis Laboratorium Medik*, 1(1), pp. 1–7.

Sarwar, A.K.M.G. et al. 2020. Influence of shoot cutting on growth descriptors and biomass yield of Dhaincha plant. *J Bangladesh Agril Univ.* 18(3), pp.585-592. doi: 10.5455/JBAU.116218

Sukmono, A., Handayani, H. H. & Wibowo, A., 2012. Algoritma Estimasi Kandungan Klorofil Tanaman Padi Dengan Data Airborne Hyperspectral. *Geoid*, 8(1), 47. doi: 10.12962/j24423998.v8i1.707.

Superani, R., Hubeis, M. & Purwanto, B., 2008. Prospek pengembangan obat tradisional perusahaan farmasi skala kecil menengah (Kasus PT Molex Ayus Pharmaceutical). *Jurnal MPI*, 3(2), pp.84-98

Surya, M.I. et al. 2020. Plant growth regulators affecting leaf traits of loquat seedling. *Annual Research & Review in Biology*, 35(11), pp.73-85.

Surya, M.I. et al. 2021. Response of loquat seedling growth to interaction between fertilizers and plant growth regulators. *Journal of Physics: Conference Series*, 1811, 012052. doi: 10.1088/1742-6596/1811/1/012052

Sutandi, I. A., Rahayu, A. & Rochman, N., 2017. Pertumbuhan dan Produksi Tanaman Pohpohan (*Pilea melastomoides* (Poir.) Wedd) dan Reundu (*Staurogyne elongate* Kuntze) Berbagai Taraf Naungan. *Jurnal Agronida*, 3(1), pp. 46–52.

Journal of Tropical Biodiversity and Biotechnology
Volume 09, Issue 01 (2024): jtbb73763
DOI: 10.22146/jtbb.73763

Research Article

Astaxanthin Production from Green Microalga *Haematococcus pluvialis* under Various Bean Sprout Media Concentrations and Duration of UV Radiations

Biaggi Rakhmat Rheinan Hary[1], Boy Rahardjo Sidharta[1]*, Ines Septi Arsiningtyas[2]
1)Biology Study Program, Faculty of Biotechnology, Universitas Atma Jaya Yogyakarta, Jalan Babarsari 44, Yogyakarta, Indonesia, 55281
2)Biotechno-Industry Research Group, Faculty of Biotechnology, Universitas Atma Jaya Yogyakarta, Jalan Babarsari 44, Yogyakarta, Indonesia, 55281
* Corresponding author, email: boy.sidharta@uajy.ac.id

Keywords:
Astaxanthin
Bean sprout media
Haematococcus pluvialis
UV radiation
Submitted:
25 March 2022
Accepted:
07 September 2023
Published:
26 January 2024
Editor:
Furzani Binti Pa'ee

ABSTRACT
Astaxanthin (AX) is known as a very strong antioxidant and has been utilised in many kinds of products such as foods, pharmaceutical, cosmetics, aquaculture, etc. One of the natural resources of AX is *Haematococcus pluvialis* which has been investigated by some researchers in order to enhance the AX production. However, the production of AX from the microalgae is still costly, hence, this present research is proposing low-cost methods namely bean sprout media (BSM) as an alternative growth media and UV radiation. The variations of BSM concentrations (2, 4, and 6 %) and times of UV radiation (1.5 and 3 hrs) were treated to *H. pluvialis* in laboratory conditions. BSM 4 % treatment showed an optimum growth of the microalga at 427 x 10^4 cell/ml (day 8) which also exhibited macrozooid, palmella, and aplanosore phases. UV radiation for 3 hr revealed that the concentration of AX production was as much as 17.37±0.04 mg/l. The research results were potential to be developed further in order to discover better and cheaper methods for scaling up AX production.

Copyright: © 2024, J. Tropical Biodiversity Biotechnology (CC BY-SA 4.0)

INTRODUCTION
Astaxanthin (AX) is a natural carotenoid which shows strong antioxidant, that is 500 times and 38 times higher than vitamin E and β-carotene, respectively (Han et al. 2013; Nurdianti et al. 2017; Han et al. 2019). It has a potency in health care products for skin, eyes, heart, liver, detoxification, photo protectant, immune response, and anticancer (Iwamoto 2000; Guerin et al. 2003). In addition, AX has also been utilized as natural pigment in food and aquaculture feed industries (Higuera-Ciapara et al. 2006). Therefore, demand for AX in some fields and industries are increasing worldwide and its market is estimated to gain 800 million USD in 2022 (Khazi et al. 2021).

AX belongs to a xanthophyll group, that dissolves in lipid and can be synthesised by some microalgae and marine animals (Ambati et al. 2014; Park et al. 2014; Hernayanti & Simanjuntak 2019). One of the microalgae that is rich in AX is *Haematococcus pluvialis* that can produce more than 30 g/kg dry weight (Butler et al. 2018). In order to fulfil the rising demand, researchers are trying to find best and low-cost methods

to increase AX production from *H. pluvialis* (Tocquin et al. 2011; Liu 2018).

There are some factors affecting AX production in microalgae such as light intensity, nutrition, salt content, pH, CO_2 concentration, and oxidative stress (Kavitha et al. 2015; Kwak et al. 2015; Huber & Blaha-Robinson 2016; dos Santos & Lombardi 2017). Nutrient contents in the growth media enhanced AX production in *H. pluvialis*, since nutrition compositions and nutrient concentrations determine biomass and metabolite productions (Prihantini et al. 2007; Putra et al. 2015; Trikuti et al. 2016). Natural medium such as bean sprout extract was common to be utilised for growing microalgae due to the nutrition compositions that compose of both macro and micro nutrients, such as protein, carbohydrate, lipid, P, K, Ca, Fe, Na, Cu, Zn, thiamine, riboflavin, nisin, and vitamin C (Ministry of Health of The Republic of Indonesia 2018).

Different light intensities and light qualities have been utilised in order to induce AX production (Kobayashi et al. 1992; Imamoglu et al. 2009; Saha et al. 2013). There were also some researches combining both light and nutrient factors to enhance AX production in *H. pluvialis* (Su et al. 2014; Ghosh et al. 2017; Zhang et al. 2018; Mehariya et al. 2020). Ultraviolet (UV) radiation and variation of growth media were reported to increase AX production (Muzaki 2008; Kavitha et al. 2015). However, there is no research report on the treatment of natural growth media (bean sprout media) and times of UV radiation to AX production of *H. pluvialis*.

Therefore, the objectives of this present research are to determine the optimum concentration of bean sprout medium (BSM) on the growth of *H. pluvialis* and to determine the time of UV radiation in order to enhance AX production.

MATERIALS AND METHODS

Materials

Stock culture of *H. pluvialis* was obtained from Estuarine Fishery Research Centre, Jepara, Central of Java. Acclimatization of *H. pluvialis* with initial culture at 100,000 cell/ml was done by providing Walne medium added with vitamin B12 and incubated at 25 °C with LED light 3200 lux illumination for 8 days (Putri & Alaa 2019; Khazi et al. 2021).

Methods

Bean sprout medium (BSM) preparation

As much as 750 g of bean sprouts were washed with tap water to cleanse the dirt. Clean bean sprouts were put into a bowl with 2000 ml distilled water and were boiled for 45 min. After getting warm, the bean sprouts were separated from the water by filtration. The filtered water was put into a flask and was utilized as BSM stock solution. Growth medium treatment for *H. pluvialis* were varied as follows BSM 2, 4, and 6 % respectively, with Walne as positive control medium and distilled water as negative control medium. All the growth media were sterilized at 121 °C for 20 min (Prihantini et al. 2007; Panis & Carreon 2016).

Inoculation of *H. pluvialis* in the growth media

Each medium was taken as much as 150 ml and put into 500 ml Erlenmeyer flasks and 150 ml of culture of *H. pluvialis* with density 100,000 cell/ml was added into every flask. Additional of 0.15 ml vitamin B12 was added into all the flasks. The cultures were incubated at 25 °C with aeration and were given LED 3200 lux light intensity with 10:14 dark:light cycle (Muzaki 2008; Kavitha et al. 2015).

Cell count and morphology of *H. pluvialis*

Cell count and morphology of the microalgae conducted before and during the treatments. Cell count was done utilising haemocytometer (Madigan et al. 2015; Liu 2018). The observation of cell morphology was done every two days throughout the research.

UV radiation treatment

As much as 150 ml media (BSM optimum treatment) and 150 ml *H. pluvialis* initial culture were mixed in a flask. Every flask was treated with UV lamp radiation for 1.5 and 3 hr. After irradiation, all the flasks were incubated for 18 days in order to achieve aplanospore phase (red phase) (Muzaki 2008; Han et al. 2013; Shang et al. 2016; Butler et al. 2018).

Astaxanthin (AX) extraction and analysis

Extraction of AX was done by taken as much as 5 ml *H. pluvialis* culture and was subsequently centrifuged for 15 min at 5900 rpm. KOH 5 % and methanol 30 % (v/v) solutions were prepared and then heated at 70 °C. The pellet was rinse three times with distilled water to discard alkali compound. Furthermore, the pellet was added with 5 ml DMSO (Wang et al. 2018). Extraction treatment was repeated until cell debris became colourless and the final volume reached 15 ml (Molino et al. 2018). The sample extract was diluted into 15 ml Dimethylsulfoxide (DMSO) and then was put into cuvettes. Every cuvette was placed into spectrophotometer and the absorbance was measured at 490 nm (Li et al. 2012). The concentration of AX (C_{AX}) was calculated utilizing the following formula (Liu 2018).

$$C_{AX}\ (mg/l) = 4.5 \times A_{490} \times (V_a/V_b)$$

where:
A_{490} = wavelength at 490 nm
V_a = extraction volume
V_b = sample volume

Data analysis

All treatments conducted in quintuplicates. Cell numbers of *H. pluvialis* data from different media treatments were analysed utilising Excel™ program. Anova with 95 % degree of confidence was applied for data of UV radiation treatments. Duncan Multiple Range Test (DMRT) was carried out whenever there were significant differences between the treatments.

RESULTS AND DISCUSSION

Cell morphology of *H. pluvialis*

Cell morphology of *H. pluvialis* was observed utilising trinocular microscope with 10 x 45 magnification (Figure 1). This present research found three different phases of cell morphology of *H. pluvialis*, namely macrozooid, palmella, and aplanospore. The round phase macrozooid was green in colour, but no flagellum visible.

According to Shah et al. (2016) macrozooid cells were round to ellipsoid or pear shape with 8-12 µm diameter. The disappearance of flagellum was due to the stress condition and cells were expanded in size and subsequently loss of their flagella (Figure 1A). Palmella phase was marked with reddish colour surrounding the nucleus which determines the accumulation of AX (Figure 1B). Wayama et al. (2013) reported that cell of *H. pluvialis* under stress condition will grow bigger with thicker

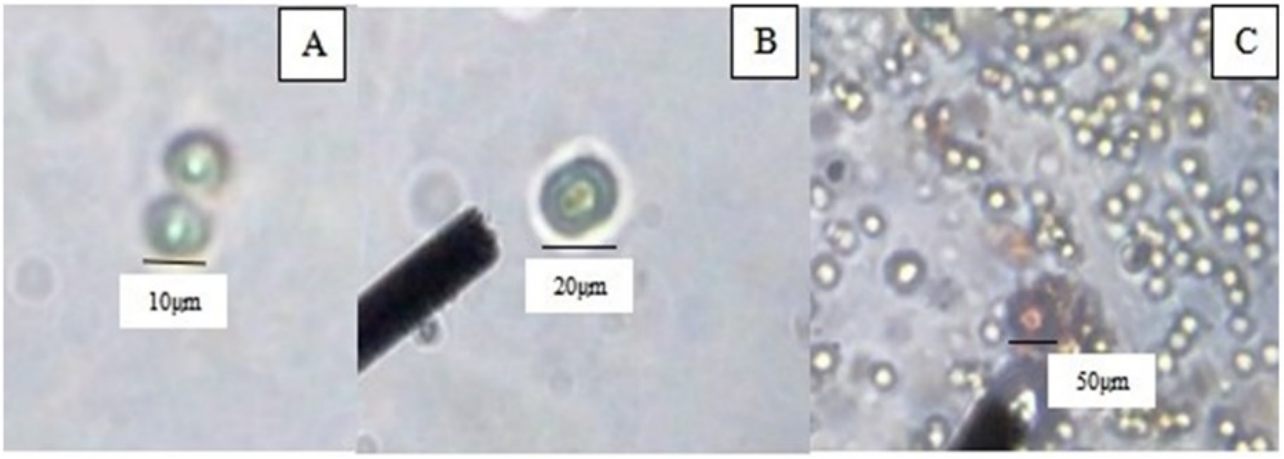

Figure 1. *Haematococcus pluvialis* cell's morphology. (A) round cell phase macrozooid, (B) early palmella phase, and (C) red phase aplanospore.

cell walls and reddish colour around the nucleus. If the stress condition continues the cell will transform into aplanospore phase with round shape, thick cell wall, and red colour in the cytoplasm (Figure 1C). Similar cell's morphological appearances in *H. pluvialis* were reported by Levin and Fleuerence (2018) and He et al. (2020).

Growth of *Haematococcus pluvialis* on various of media

The growth of *H. pluvialis* on various of media treatment was observed for 12 days. The growth was ended with death phase and followed by the decreasing of cell numbers in the media (Table 1, Figure 2).

In general, growth curve of *H. pluvialis* in different media reached stationary phase at day 8 and subsequently went into death phase at day 10. Negative control treatment showed no growth due to no additional nutrients for the cell. The highest cell number was obtained at BSM 4 % and considered as optimum concentration (Figure 2). Kavitha et al. (2015) observed *H. pluvialis* growth in Walne medium showed more turbid appearance in the flask. The media became more turbid and dark-green in colour due to the highest growth of the microalga at day 8 (Figure 3).

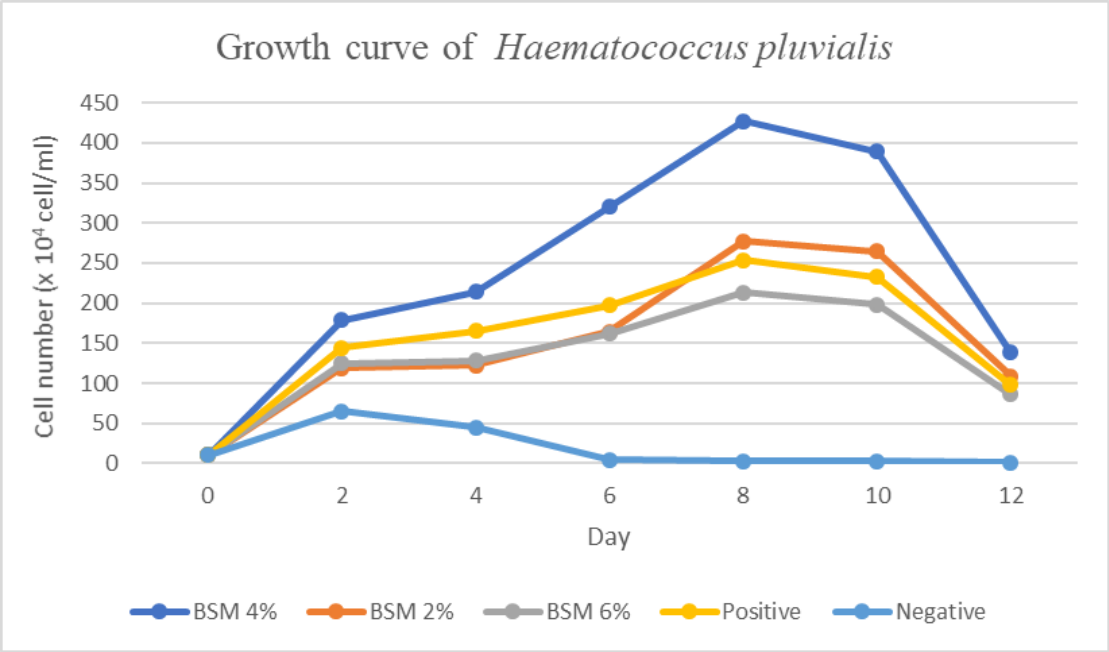

Figure 2. Growth curve of *H. pluvialis* in various BSM concentrations treated.

Table 1. Cell numbers of *H. pluvialis* (x 10^4 cell/ml) in various growth media.

Medium	Days of observation						
	0	2	4	6	8	10	12
BSM 2 %	10	119	122	164	277	265	109
BSM 4 %	10	179	214	320	427	389	138
BSM 6 %	10	125	128	162	213	198	8.6
Control +	10	144	165	197	254	233	9.8
Control -	10	65	45	40	30	30	1

Notes:
Control +: control positive (Walne medium)
Control -: control negative (distilled water)

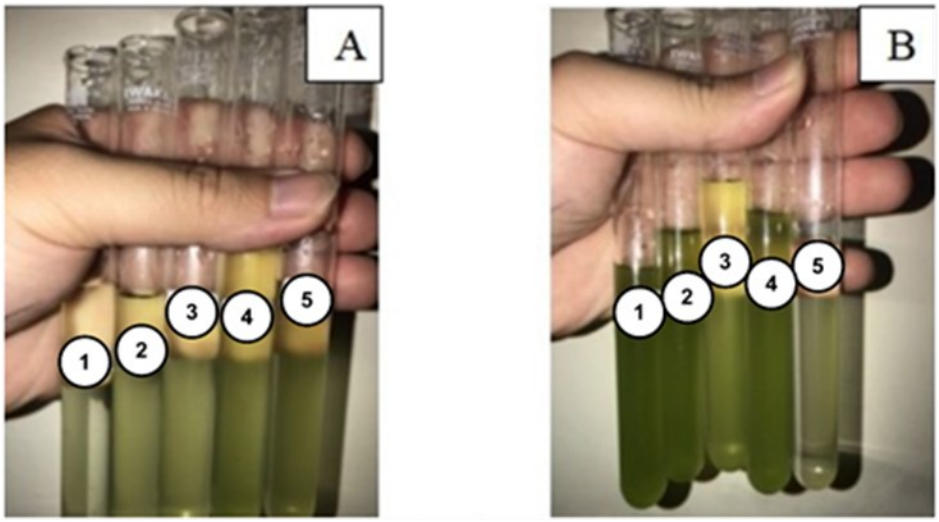

Figure 3. Visual observation of *H. pluvialis* growth in various media treated. (A) Day 0 and (B) Day 8. Notes: 1. BSM 4 %, 2. BSM 2 %, 3. BSM 6 %, 4. Control +, 5. Control –.

Astaxanthin (AX) production from *H. pluvialis*

The optimization of media variation revealed that BSM 4 % treatment showed the highest cell count of *H. pluvialis* and therefore BSM 4 % treatment was utilised in the subsequent step. *H. pluvialis* culture in the BSM 4 % medium was radiated with UV in order to put *H. pluvialis* in the stress condition and subsequently the cell will produce AX (Butler et al. 2018). UV radiations conducted within time variations 1.5 and 3 hr (Shang et al. 2016). The results were presented in Table 2.

No significant differences between treatments were shown from the growth of *H. pluvialis* cell cultures after UV radiation. The growth of the microalga cells was not affected by UV radiation variations for 1.5 and 3 hrs, although the cell numbers at UV radiation for 3 hr were higher than 1.5 hr treatment (Table 2). Previous researches reported that both light intensities and wave lengths affected the growth of *H. pluvialis* cultures (Evens et al. 2008). Logaritmic phase was ended at day 8 and the accumulation of AX required at least 10 days which were divided into three phases namely macrozooid phase (4 days), palmelloid phase (3 days) and aplanospore phase (3 days) (Butler et al. 2018).

Stress stimulation on the *H. pluvialis* cell cultures utilizing UV radiation can be observed in Figure 4. The figure revealed that *H. pluvialis* produces red colour in the cells which were expected coming from the AX. Therefore, the cell cultures were extracted utilising maceration method with DMSO as the solvent to reveal the AX contents in the cells (Wang et al. 2018). AX concentrations extracted from UV-stressed cell *H. pluvialis* were shown in Table 3.

Table 2. Growth of *H. pluvialis* cells (x 10^4 cell/ml) under UV radiation treatments.

Time of radiation (hr)	Medium	Day of observation									
		0	2	4	6	8	10	12	14	16	18
1.5	BSM 4%	10	144	183	217	348	204	128	111	99	91
	Ctrl +	10	82	165	175	266	158	103	68	42	35
	Ctrl -	10	37	12	5	3	0	0	0	0	0
3	BSM 4%	10	132	213	235	394	220	139	119	104	94
	Ctrl +	10	86	179	193	249	165	111	69	45	37
	Ctrl -	10	31	10	4	2	0	0	0	0	0

Notes:
Ctrl +: control positive (Walne medium)
Ctrl -: control negative (distilled water)

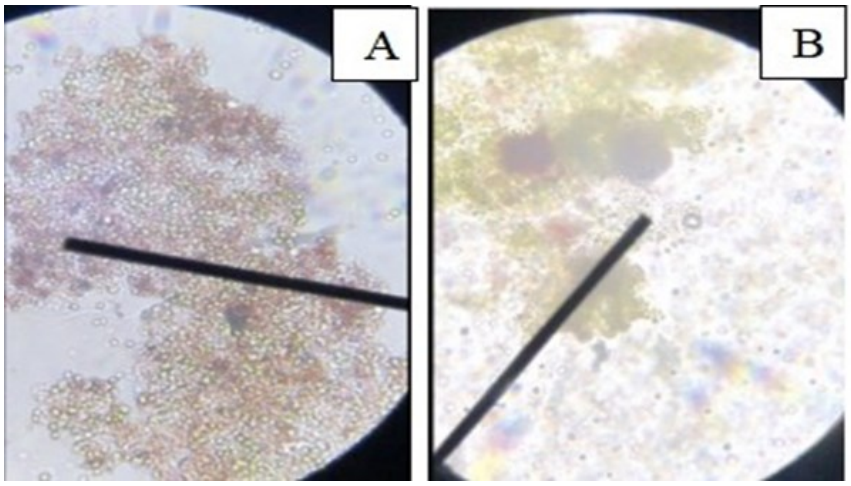

Figure 4. Red colour appearances were shown from *H. pluvialis* cell growth under UV radiation. (A) 3 hr radiation and (B) 1.5 hr radiation.

Table 3. Astaxanthin (AX) concentrations (mg/L) from *H. pluvialis* under UV radiation.

Medium	UV radiation (hr)	
	1.5	3
BSM 4 %	11.41 ± 0.03^a	17.37 ± 0.04^a
Control +	8.72 ± 0.02^a	12.36 ± 0.04^a
Control -	0.22 ± 0.01^b	0.24 ± 0.01^b

Notes: numbers with the same alphabet in the same row were no significant difference at $P<0.05$. Numbers were mean $\pm$ standard deviations (SD) from quintuplicates.

There was no significant difference between UV radiation variation treatments for 1.5 and 3 hrs, however AX concentrations at UV radiation for 3 hr were higher compare to 1.5 hr treatment (Table 3). This result was supported by the appearances of red cells after UV radiation for 3 hr (Figure 4). The length of radiation time was expected to stimulate the reactive oxygen species (ROS) and furthermore induced the AX production in the cell of *H. pluvialis* (Kavitha et al. 2015). This present research showed potential results and need to be explored further in order to discover better method with specific regard to scaling up the AX production. Therefore, some researchers have been proposing combination of growth media, radiation, and transgenic factors to enhance AX production from *H. pluvialis* (Gómez et al. 2013; Gao et al. 2015; Le-Feuvre et al. 2020).

CONCLUSION

Haematococcus pluvialis was able to grow optimally in bean sprout medium (BSM) 4 % with the highest cell number (427 x 10^4 cell/mL) achieved at day 8. Ultraviolet radiation for 3 hr enhanced astaxanthin production by the green microalga as much as 17.37±0.04 mg/L.

AUTHORS CONTRIBUTION

B.R.R.H. designed and conducted the research, B.R.S. supervised and wrote the manuscript, I.S.A. collected and analysed the data.

ACKNOWLEDGMENTS

The authors indebted to Head of Biotechno-Industry laboratory at Faculty of Biotechnology Universitas Atma Jaya Yogyakarta and their staffs for facilitating this research.

CONFLICT OF INTEREST

None of the authors declare conflict of interests in publishing the research data as well as the research funding.

REFERENCES

Ambati, R.R. et al., 2014. *Astaxanthin: Sources, extraction, stability, biological activities and its commercial applications - A review. Marine Drugs*, 12 (1), pp.128-152. doi: 10.3390/md12010128.

Butler, T.O. et al., 2018. Media screening for obtaining Haematococcus pluvialis red motile macrozooids rich in astaxanthin and fatty acids. *Biology*, 7(1), 2. doi: 10.3390/biology7010002.

dos Santos, A.C. & Lombardi, A.T., 2017. Growth, photosynthesis and biochemical composition of Haematococcus pluvialis at various pH Post-Graduate Program in Ecology and Natural Resources. *Journal of Algal Biomass Utilization*, 8(1), pp.1–15.

Evens, T.J., Niedz, R.P. & Kirkpatrick, G.J., 2008. Temperature and irradiance impacts on the growth, pigmentation and photosystem II quantum yields of Haematococcus pluvialis (Chlorophyceae). *Journal of Applied Phycology*, 20(4), pp.411–422. doi: 10.1007/s10811-007-9277-1.

Gao, Z. et al., 2015. Comparison of astaxanthin accumulation and biosynthesis gene expression of three Haematococcus pluvialis strains upon salinity stress. *Journal of Applied Phycology*, 27(5), pp.1853–1860. doi: 10.1007/s10811-014-0491-3.

Ghosh, S.A. et al., 2017. Nitrogen-doped carbon dots prepared from bovine serum albumin to enhance algal astaxanthin production. *Algal Research*, 23, pp.161–165. doi: 10.1016/j.algal.2017.01.011.

Gómez, P.I. et al., 2013. Fromgenetic improvementtocommercial-scalemassculture of a Chilean strain of the green microalga Haematococcus pluvialis with enhanced productivity of the red ketocarotenoid astaxanthin. *AoB PLANTS*, 5, plt026. doi: 10.1093/aobpla/plt026.

Guerin, M., Huntley, M.E. & Olaizola, M., 2003. *Haematococcus astaxanthin: Applications for human health and nutrition. Trends in Biotechnology*, 21(5), pp.210-216. doi: 10.1016/S0167-7799(03)00078-7.

Han, D., Li, Y. & Hu, Q., 2013. *Astaxanthin in microalgae: Pathways, functions and biotechnological implications. Algae*, 28(2), pp.131-147. doi: 10.4490/algae.2013.28.2.131.

Han, S. et al., 2019. A novel approach to enhance astaxanthin production in Haematococcus lacustris using a microstructure-based culture platform. *Algal Research*, 39, 101464. doi: 10.1016/j.algal.2019.101464.

He, B. et al., 2020. Ultrastructural changes of haematococcus pluvialis (Chlorophyta) in process of astaxanthin accumulation and cell damage under condition of high light with acetate. *Algae*, 35(3), pp.253–262. doi: 10.4490/algae.2020.35.5.22.

Hernayanti, H. & Simanjuntak, S.B.I., 2019. Antioxidant Effect of Chlorella vulgaris on Physiological Response of Rat Induced by Carbon Tetrachloride. *Biosaintifika: Journal of Biology & Biology Education*, 11(1), pp.84–90. doi: 10.15294/biosaintifika.v11i1.16393.

Higuera-Ciapara, I., Félix-Valenzuela, L. & Goycoolea, F.M., 2006. Astaxanthin: A review of its chemistry and applications. *Critical Reviews in Food Science and Nutrition*, 46(2), pp.185–196. doi: 10.1080/10408690590957188.

Huber, M. & Blaha-Robinson, K., 2016, 'Algae Culture and PH', in *Algae Research Supply*, viewed from https://algaeresearchsupply.com/pages/algae-culture-and-ph

Imamoglu, E., Dalay, M.C. & Sukan, F.V., 2009. Influences of different stress media and high light intensities on accumulation of astaxanthin in the green alga Haematococcus pluvialis. *New Biotechnology*, 26(3–4), pp.199–204. doi: 10.1016/j.nbt.2009.08.007.

Iwamoto, 2000. Inhibition of Low-Density Lipoprotein Oxidation by Astaxanthin. *J. Atheroscler. Thromb.*, 7(4), pp.216-222. doi: 10.5551/jat1994.7.216.

Kavitha, G. et al., 2015. Impact of UV-B Radiation on Haematococcus pluvialis Flotow Isolated from Himachal Pradesh under Laboratory Conditions. *Journal of Academia and Industrial Research (JAIR)*, 3 (11), pp.581-585.

Ministry of Health of the Republic Indonesia, 2018. *Tabel Komposisi Pangan Indonesia*. Direktorat Jendral Kesehatan Masyarakat.

Khazi, M.I. et al., 2021. Sequential Continuous Mixotrophic and Phototrophic Cultivation Might Be a Cost-Effective Strategy for Astaxanthin Production from the Microalga Haematococcus lacustris. *Frontiers in Bioengineering and Biotechnology*, 9, 740533. doi: 10.3389/fbioe.2021.740533.

Kobayashi, M. et al., 1992. Effects of light intensity, light quality, and illumination cycle on astaxanthin formation in a green alga, Haematococcus pluvialis. *Journal of Fermentation and Bioengineering*, 74 (1), pp.61–63.

Kwak, H.S., Kim, J.Y.H. & Sim, S.J., 2015. A microreactor system for cultivation of Haematococcus pluvialis and astaxanthin production. *Journal of Nanoscience and Nanotechnology*, 15(2), pp.1618–1623. doi: 10.1166/jnn.2015.9321.

Le-Feuvre, R. et al., 2020. *Biotechnology applied to Haematococcus pluvialis Fotow: challenges and prospects for the enhancement of astaxanthin accumulation. Journal of Applied Phycology*, 32, pp.3831-3852. doi: 10.1007/s10811-020-02231-z.

Levin, I.A. & Fleurence, J., 2018. *Microalgae in Health and Disease Prevention*, Academic Press.

Li, Y. et al., 2012. Accurate quantification of astaxanthin from Haematococcus crude extract spectrophotometrically. *Chinese Journal of Oceanology and Limnology*, 30(4), pp.627–637.

Liu, Y., 2018. *Optimization Study of Biomass and Astaxanthin Production by Haematococcus Pluvialis Under Minkery Wastewater Cultures*. Dalhousie University Halifax.

Madigan, M.T. et al., 2015. *Brock biology of microorganisms*. 14th ed. Pearson.

Mehariya, S. et al., 2020. An integrated strategy for nutraceuticals from haematoccus pluvialis: From cultivation to extraction. *Antioxidants*, 9(9), 825. doi: 10.3390/antiox9090825.

Molino, A. et al., 2018. Extraction of astaxanthin from microalga Haematococcus pluvialis in red phase by using generally recognized as safe solvents and accelerated extraction. *Journal of Biotechnology*, 283, pp.51–61. doi: 10.1016/j.jbiotec.2018.07.010.

Muzaki, 2008. Kultur mikroalga H pluvialis astaxantin. *J. Ris. Akuakultur*, 3(3), pp.351–361.

Nurdianti, L., Aryani, R. & Indra, I., 2017. Formulasi dan Karakterisasi SNE (Self Nanoemulsion) Astaxanthin dari Haematococcus pluvialis sebagai Super Antioksidan Alami. *Jurnal Sains Farmasi & Klinis*, 4(1), p.36. doi: 10.29208/jsfk.2017.4.1.168.

Panis, G. & Carreon, J.R., 2016. Commercial astaxanthin production derived by green alga Haematococcus pluvialis: A microalgae process model and a techno-economic assessment all through production line. *Algal Research*, 18, pp.175–190. doi: 10.1016/j.algal.2016.06.007.

Park, J.C. et al., 2014. Enhanced astaxanthin production from microalga, Haematococcus pluvialis by two-stage perfusion culture with stepwise light irradiation. *Bioprocess and Biosystems Engineering*, 37(10), pp.2039–2047. doi: 10.1007/s00449-014-1180-y.

Prihantini, B.N., Damayanti, D. & Yuniati, R., 2007. PENGARUH KONSENTRASI MEDIUM EKSTRAK TAUGE (MET) TERHADAP PERTUMBUHAN Scenedesmus ISOLAT SUBANG. *Makara Journal of Sains*, 11(1), pp.1–9.

Putra, I.K.R.W., Anggreni, A.A.M.D. & Arnata, I.W., 2015. Pengaruh Jenis Media Terhadap Konsentrasi Biomassa. *Rekayasa dan Manajemen Agroindustri*, 3(2), pp.40–46.

Putri, D.S. & Alaa, S., 2019. The Growth Comparison of Haematococcus Pluvialis in Two Different Medium. *Biota*, 12(2), pp.90-97. doi: 10.20414/jb.v12i2.202.

Saha, S.K. et al., 2013. Effect of various stress-regulatory factors on biomass and lipid production in microalga Haematococcus pluvialis. *Bioresource Technology*, 128, pp.118–124. doi: 10.1016/j.biortech.2012.10.049Get.

Shah, M.M.R. et al., 2016. *Astaxanthin-producing green microalga Haematococcus pluvialis: From single cell to high value commercial products*. *Frontiers in Plant Science*, 7, 531. doi: 10.3389/fpls.2016.00531.

Shang, M. et al., 2016. Enhanced astaxanthin production from Haematococcus pluvialis using butylated hydroxyanisole. *Journal of Biotechnology*, 236, pp.199–207. doi: 10.1016/j.jbiotec.2016.08.019.

Su, Y. et al., 2014. Metabolomic and network analysis of astaxanthin-producing Haematococcus pluvialis under various stress conditions. *Bioresource Technology*, 170, pp.522–529. doi: 10.1016/j.biortech.2014.08.018.

Tocquin, P., Fratamico, A. & Franck, F., 2011. Screening for a low-cost Haematococcus pluvialis medium reveals an unexpected impact of a low N:P ratio on vegetative growth. *Journal of Applied Phycology*, 24, pp.365-373.

Trikuti, I.K., Anggreni, A.A.M.D. & Gunam, I.B.W., 2016. Pengaruh Jenis Media Terhadap Konsentrasi Biomassa dan Kandungan Protein Mikroalga Chaetoceros Calcitrans. *Jurnal Rekayasa dan Manajemen Agroindustri*, 4(2), pp.13–22.

Wang, S. et al., 2018. Accurate quantification of astaxanthin from Haematococcus pluvialis using DMSO extraction and lipase-catalyzed hydrolysis pretreatment. *Algal Research*, 35, pp.427–431. doi: 10.1016/j.algal.2018.08.029Get.

Wayama, M. et al., 2013. Three-Dimensional Ultrastructural Study of Oil and Astaxanthin Accumulation during Encystment in the Green Alga Haematococcus pluvialis. *PLoS ONE*, 8(1), e53618. doi: 10.1371/journal.pone.0053618.

Zhang, W.W. et al., 2018. Enhancing astaxanthin accumulation in Haematococcus pluvialis by coupled light intensity and nitrogen starvation in column photobioreactors. *Journal of Microbiology and Biotechnology*, 28(12), pp.2019–2028. doi: 10.4014/jmb.1807.07008.

Journal of Tropical Biodiversity and Biotechnology
Volume 09, Issue 01 (2024): jtbb83889
DOI: 10.22146/jtbb.83889

Research Article

Diversity of Santigi (*Pemphis acidula* J.R.Forst. & G.Forst.), A Mangrove Association in Tomini Bay, Sulawesi, Indonesia

Dewi Wahyuni K. Baderan[1]*, Sukirman Rahim[2], Melisnawati H. Angio[3], Muh. Nur Akbar[1], Magfirahtul Jannah[1], Yuliana Retnowati[1], Ramli Utina[1,4]

1)Department of Biology, Faculty of Mathematics and Natural Sciences, Universitas Negeri Gorontalo, Jl. Prof. Dr. Ing. B.J. Habibie, Bone Bolango 96554, Gorontalo, Indonesia
2)Wallacea Research Center for Biodiversity Conservation and Climate Change, Universitas Negeri Gorontalo, Jl. Jend. Sudirman No.6, Gorontalo City 96128, Gorontalo, Indonesia
3)Research Center for Plant Conservation and Botanic Gardens and Forestry, National Research and Innovation Agency, Jl. Ir. H. Juanda 13, Bogor 16122, West Java, Indonesia
4)Research Center of Coastal Ecology Based on Local Wisdom (PKEPKL), Department of Biology, Universitas Negeri Gorontalo, Jl. Prof. Dr. Ing. B.J. Habibie, Bone Bolango 96554, Gorontalo, Indonesia
* Corresponding author, email: dewi.baderan@ung.ac.id

Keywords:
Pemphis acidula
environment
phenetic
genetic diversity
coastal area
Submitted:
14 April 2023
Accepted:
09 October 2023
Published:
29 January 2024
Editor:
Miftahul Ilmi

ABSTRACT

Pemphis acidula is a wild plant in rocky or sandy coastal areas and mangrove ecosystems. Different geographic characteristics may affect plant adaptability and have an impact on the emergence of various genotypes. This study was performed to reveal the phenetic relationship and genetic variation of *P. acidula* in 3 different areas in Tomini Bay, Gorontalo Province, Indonesia. We took 3 samples from each location and analysed them using 14 morphological characters and molecular approaches based on ISSR markers and ITS gene. The results showed that *P. acidula* on Olele had bigger sizes in some morphological features compared to the plants in other study areas. The phenetic analysis showed that *P. acidula* at Biluhu and Dulanga were more closely related, although *P. acidula* at the 3 locations had 100% similarity. Genetic variation analysis showed the highest genetic similarity based on ISSR markers was found in Dulanga and Biluhu samples (76.8%). Phylogenetic based on ITS gene revealed that Olele samples were in the same clade with *P. acidula* accession from GenBank (genetic distance 0-0.19%), while Biluhu samples were a sister group (genetic distance 24.97-25.03%) even though their percentage identity corresponds to *P. acidula* (81.34%). Plant adaptation to different habitat conditions may affect the genetic diversity of *P. acidula*.

Copyright: © 2024, J. Tropical Biodiversity Biotechnology (CC BY-SA 4.0)

INTRODUCTION

Gorontalo, one region of Sulawesi Island, is located in the northern part of Sulawesi and is geographically bordered by Tomini Bay, the largest bay in Indonesia. Tomini Bay is included in the coral triangle. The coastal area of Gorontalo has varied geographical conditions, contains a high level of endemic biodiversity, and one of which is sourced from mangrove ecosystem (Baderan et al. 2022).

Pemphis acidula J.R.Forst. & G.Forst. is one of the mangrove association plants. It is known as the only accepted member of Genus *Pemphis* in Family Lythraceae (POWO 2022). It is considered as a shrub or small

tree growing in coastal areas which are rocky, sandy, or at the edge of mangrove forests (Giesen et al. 2006; Utina et al. 2019). This coastal tree is typically 4-10 meters in height. It has a wavy stem with irregular branches (Irwansah et al. 2017; Manek & Puay 2020). Many people admire *P. acidula* and utilise it as an expensive ornamental plant in the form of *bonsai* (dwarf potted plant) (Cunningham et al. 2017). *Pemphis acidula* is naturally distributed in East Africa, India, Southeast Asia, and Australia. In Indonesia, this plant is mostly found in all main islands including Java, Moluccas, Kalimantan, and Sulawesi (George 1990; Rao & Ellis 1995; de Wilde & Duyfjes 2016; POWO 2022). The locals are known this plant by the name "Santigi" (Baderan et al. 2018).

Recent study in Gorontalo revealed that *P. acidula* is specifically found in three coastal areas of Tomini Bay, namely Biluhu, Dulanga and Olele Beaches (Baderan et al. 2022). Biluhu, Dulanga and Olele Beaches display various environmental conditions and plant species. Biluhu Beach exposes a dominantly sandy ground structure with 117 plant species distributed around the area (Baderan & Utina 2021). Dulanga Beach has a rocky characteristic and 56 plant species were found in the steep rocky hills. Meanwhile, Olele Beach has a partially sandy-rocky soil structure with 82 plant species on the rock hill (Baderan & Angio 2019). The distribution, richness, and diversity of plant species may affected by developmental stages of plant, geographical condition and environmental factors (Ibrahim 2021).

At present, research about the variety of *P. acidula* has not been massively conducted and the available information is too general while there are need for specific ones. However, information on plant morphological and genetic diversity on the individual, species, or population levels is essential to be used as basic consideration for conservation, breeding, management, and sustainable use of the species (Abdelhamid et al. 2014; Raji & Siril 2021). Hence, this study aims to reveal the morphological and genetic diversity of *P. acidula* in three different areas in Tomini Bay, Gorontalo Province, Indonesia based on the phenetic and DNA molecular marker.

MATERIALS AND METHODS

Fieldwork and Sample collection

This study was carried out from June 2021 to July 2022. Based on our previous findings, we chose three study areas of *P. acidula* as follows: Site 1 Biluhu Beach, Site 2 Dulanga Beach, and Site 3 Olele Beach. The three locations are located in the coastal area of Gorontalo's South Beach with coral limestone as the bedrock. Sampling sites were shown in Figure 1.

We found that there are only 12 mature individuals of *P. acidula* (tree or generative phase) spread in three different locations. There are also several seedling of *P. acidula* in the location, but we were used it as exclusion criteria. We did purposive sampling with only *P. acidula* in the generative stage and reachable as inclusion criteria. Morphological observations were conducted by describing the habit and the characteristics of the leaves, roots, stems, fruits and seeds. Measurement of plant height, stem diameter, length, width and weight of leaves, fruit and seeds, as well as the height of the buttress root were also carried out. Each character was documented and detailed the information in terms of collector's name, collection number, date, location, and habit which was noted on the prepared observation sheet. Several abiotic factors including altitude, light intensity, substrate pH, air humidity, air temperature and habitat were also measured over several days with a single measurement every day.

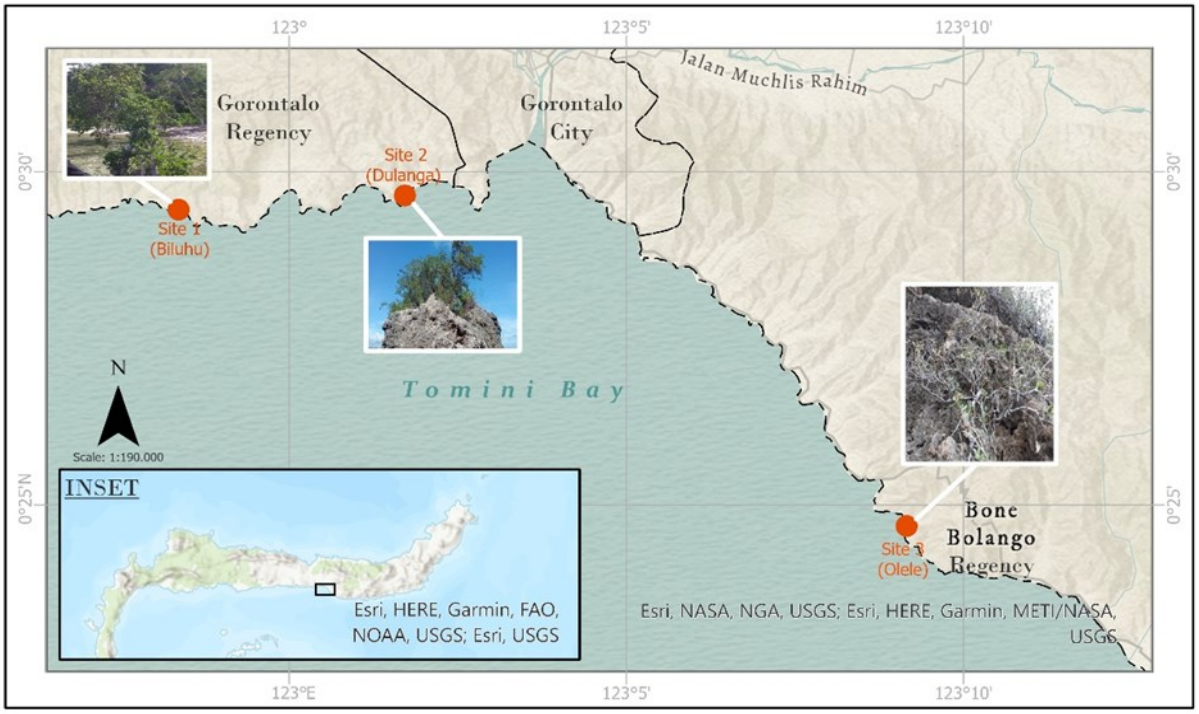

Figure 1. The study sites map of *P. acidula* at Tomini Bay of Gorontalo, Sulawesi: Site 1 Biluhu Beach, Site 2 Dulanga Beach, and Site 3 Olele Beach.

Leaf, root, stem, fruit and seed samples were collected from 3 *P. acidula* individuals in the generative stage from each provenance for further morphological analysis in laboratory. Leaves sample of *P. acidula* at each site were also taken for molecular analysis. Fresh young leaves sample from 3 individuals of *P. acidula* at each location were prepared by putting them into a separated plastic bags containing silica gel (Martida & Pharmawati 2019), then stored in cooler box for transportation. Leaf samples were sent to Integrated Research and Testing Laboratory of Universitas Gadjah Mada, Yogyakarta.

Species identification and Phenetic analysis

Identification of *P. acidula* was carried out by comparing the morphological features with the data in several references, namely Flora of Java Volume II (Backer & van den Brink 1965), Plant Identification Terminology (Harris & Harris 2001), Flora Malesiana Series 1 Moraceae: Ficeae (Berg & Corner 2005), as well as 4 herbarium specimens collection of Naturalis Biodiversity Center (Bijmoer et al. 2023). The speciment data were shown on Table 1.

Identification towards the validation of accepted names were conducted by using several sites i.e. https://www.gbif.org/ (GBIF Secretariat: GBIF Backbone Taxonomy), https://www.theplantlist.org/ (The Plant List 2022), and https://powo.science.kew.org/ (POWO 2022). Stipulated the conservation status of *P. acidula* were in reference to International Union of Conservation of Nature (IUCN) on Red List of Threatened Species (https://iucnredlist.org/) (IUCN 2022).

Phenetic analysis of *P. acidula* was carried out by comparing 14 qualitative morphological characters between samples from 3 locations with *Sonneratia alba* (Family Lythraceae) from Biluhu as outgroup considering *P. acidula* is the only member of Genus *Pemphis*. The qualitative morphological characters observed included habit; petiole, shape, tip, margin, surface, symmetry, colour, texture and section arrangement of leaves; petal colour; as well as texture, shape and colour of ripe fruit. The

morphological characters were converted into a binary matrix 0-1 based on the similarity and dissimilarity of each character with *S. alba* (Duncan & Baum 1981). Matrix data were analysed using MVSP 3.1 program and dendogram were constructed based on similarity index by using UPGMA with Jaccard's Coefficient.

Table 1. Herbarium specimen data of *Pemphis acidula* from Naturalis Biodiversity Center

Collection number	Collector	Location	Accessed URL
L.2487455	Turner, H.	Aru Islands, New Guinea	https://www.gbif.org/occurrence/2514336352
L.3923106	Afriastini, J.J.	Siberut Island, Sumatera	https://www.gbif.org/occurrence/2516885754
L.2487476	Snellius-II	Tiger Island, Sulawesi	https://www.gbif.org/occurrence/2514429373
L.2487469	Hidayat, A.	Pangkep Regency, Sulawesi	https://www.gbif.org/occurrence/2516308158

Molecular analysis

DNA Extraction and Amplification

Genomic DNA were extracted from 0.1g leaf sample according to Genomic DNA Mini Kit (Plant) (Geneaid) manufacturer's protocols, then were amplified using 10 ISSR primers (UBC-807, UBC-810, UBC-814, UBC-817, UBC-826, UBC-827, UBC-830, UBC-834, UBC-835, UBC-845) (Ibrahim 2021; Sevindik & Efe 2021). The PCR premix was contained 25 µL reaction volume consisting of 12.5 µL of 1x PCR-kit MyTaq™ HS Red Mix (Bioline), 20µM of each ISSR primer, 40 ng DNA template and nuclease free water. Thermal cycler was run at 35 cycles in condition of pre-denaturation at 94°C for 10 minutes, denaturation at 94°C for 1 minute, annealing at 45-55°C (according to the optimal annealing temperature of each ISSR primer) for 1 minute, extension at 72°C for 2 minutes, post extension at 72°C for 10 minutes, and hold at 12°C for infinity. The amplification products and 1 Kb DNA Ladder marker were electrophoresed using 2% agarose gel contained DNA staining in 1x TBE buffer at 100V for 1h (Seng et al. 2013), then were visualized on a UV transilluminator and documented using geldoc and optilab. All procedures were undertaken by Integrated Research and Testing Laboratory of Universitas Gadjah Mada, Yogyakarta (certificate number: 00875.01/IX/UN1/LPPT/2021).

Genetic variation analysis

Genetic variations of *P. acidula* were analysed by electrophoresis visualization of PCR products using ISSR primer. The DNA band patterns produced by ISSR markers were converted into a binary matrix 0-1 based on the absence or the presence of the DNA band (Ibrahim 2021). They were analysed using MVSP version 3.1 program with simple matching coefficient of UPGMA method to construct dendogram based on similarity index (Singh et al. 2014; Putri et al. 2023).

Phylogenetic analysis

Genetic relationship of *P. acidula* were analysed by Internal Transcribed Spacer (ITS) gene as the DNA barcode, using primer P674 (5′-CCTTATCATTTAGAGGAAGGAG-3′) and P675 (5′-TCCTCCGCTTATTGATATGC-3′) to amplify nuclear ITS region of 700-720 bp containing ITS1, 5.8S, and ITS2 (Nguyen et al. 2017). Ampli-

fication of the samples from Olele and Biluhu were undertaken by Integrated Research and Testing Laboratory of Universitas Gadjah Mada, Yogyakarta, according to a procedure by Nguyen et al. (2017) with some modifications. Sequencing of the amplification product were undertaken by Genetika Science Indonesia Ltd.

The ITS sequences data of samples Olele and Biluhu were BLAST with ITS gene sequences of *P. acidula* accession in GenBank (https://www.ncbi.nlm.nih.gov/genbank/) to determine the percentage of identity and query cover. The data of ITS gene sequences were also used to reconstruct a phylogenetic tree based on neighbor-joining (NJ) algorithm with Kimura 2 Parameter model using MEGA X software (Kumar et al. 2018), followed by the genetic distance analysis between samples and *P. acidula* accession in GenBank.

RESULTS AND DISCUSSION

Environmental condition

Pemphis acidula is a highly adaptive plant. Various geographical conditions, especially in the coastal area of Gorontalo may causing some morphological and genetic changes in the response of the plants toward the environmental condition. Based on our study, Biluhu and Dulanga Beaches (Site 1 and 2, respectively) have relatively similar physicochemical parameter values compared to Olele Beach (Site 3) which have slightly different altitude and habitat (Table 2). In Biluhu and Dulanga Beaches, *P. acidula* grows in coastal land with coral limestone at an altitude of 4 m asl. In contrast, *P. acidula* in Olele Beach grows in karst structural foothills at 11 m asl of altitude. *Pemphis acidula* in three locations were spread naturally and can only be found in certain points as it can only grow in an ideal location (Ellison et al. 2010).

Morphological description and Phenetic analysis

Comparison of morphological characters between samples from the three locations with a number of references and 4 herbarium specimens showed that all the samples studied were verified as *P. acidula* J.R.Forst. & G.Forst. The plant habit of *P. acidula* is perennial shrubs or small trees, with a height ranging from 1.78 to 3.8 meters (Figure 2 and Table 3). It is in contrast to *P. acidula* in East Africa, Australia and other Southeast Asian regions, which can reach 5-7 meters in height (George 1990; Rao & Ellis 1995; de Wilde & Duyfjes 2016). Even in the Andaman Islands, India, this plant can reach a height of 9.5 meters (Goutham-Bharathi et al. 2015). Plant growth can be affected by several factors, including developmental stage, age, nutrition and genetics. However, environmental condition also indirectly affects plant growth, thereby affecting plant height.

Differences in environmental conditions in Table 2, especially altitude and habitat, can affect the morphological characters at the three locations resulting in size variations (Table 3). *P. acidula* at Olele Beach

Table 2. The range measurements result of 6 physicochemical parameters in three research locations.

Physicochemical Parameter	Study Site		
	Site 1 Biluhu Beach	Site 2 Dulanga Beach	Site 3 Olele Beach
Altitude (m asl*)	4	4	11
Habitat	Coastal land	Coastal land	Structural foothills
Light intensity (mW/cm²)	0.428 – 0.485	0.493 – 0.552	0.516 – 0.523
pH	7.52 – 8.25	8.13 – 8.24	7.47 – 7.97
Humidity (%)	51 – 75	69 – 70	60 – 61
Temperature (°C)	23 – 28	24 – 25	26 – 26

*m asl = meters above sea level

Figure 2. Shrubs habit of *P. acidula* in three sites: (a) Biluhu Beach; (b) Dulanga Beach; and (c) Olele Beach.

performs a bigger size in plant height, diameter of stem, length and weight of leaf, length of petiole, fruit and peduncle, as well as the height of buttress roots than those observed in other study areas. At the Biluhu and Dulanga Beaches, these plants share relatively similar morphological character sizes, except that the seed weight of *P. acidula* at Dulanga Beach is twice as large as the other two locations. *P. acidula* which only grows on karst cliffs at an altitude of 11 m asl at Olele Beach has an advantage to their growth because it is not much affected by sea water. Meanwhile, *P. acidula* on Biluhu and Dulanga Beaches grows in rocky coastal areas at an altitude of 4 m asl which is still affected by tidal effects. Continuous exposure to salinity can be toxic and affect plant physiological processes, which in turn can suppress plant growth (Kodikara et al. 2018; Dittmann et al. 2022).

Pemphis acidula has such a knee root, where some parts of the root above the ground surface grow highly then bow and slip into the ground. It is bent, rounded, and slightly flat (Figure 3,4,5 A). The root surfaces are greyish-pale, rough, stiff enough, and are no spines. *Pemphis acidula* is growing in direction of perpendicular (*erectus*) with sympodial branching. It has a stiff and strong woody stem, grey-brownish, elongated round-like cylinder, rough surface and disclosed a cracked stem bark that looked like scales all over the stem surface (Figure 3,4,5 B). It has single leaves (*folium simplex*) which are arranged alternately, quite thick and stiff, succulent, ellipse (*elipticus*) to elongates (*oblongos*) in shape, and flat margin with no slices (*integer*) (Figure 3,4,5 D). The leaves are green with a hairy abaxial and adaxial surface and are not wrinkled. The petiole (*petiolus*) is cylindrical with a slightly flat upper side, green, thickened on the base

Table 3. The average measurement result of 15 morphological characters of *P. acidula* from 3 sites

Morphological Characters	Measurement result average at study area		
	Site 1 Biluhu Beach	Site 2 Dulanga Beach	Site 3 Olele Beach
Plant Height	1.787 m	2.157 m	3.831 m
Stem diameter	13 cm	14.8 cm	27 cm
Leaf length	19.11 mm	18.29 mm	27.34 mm
Leaf width	9.68 mm	9.03 mm	8.8 mm
Leaf weight	0.0963 g	0.073 g	0.917 g
Leaf thickness	0.68 mm	0.51 mm	0.44 mm
Petiole length	2.02 mm	2.05 mm	3.07 mm
Fruit length	7.09 mm	7.90 mm	9.1 mm
Fruit width	5.02 mm	5.55 mm	5.23 mm
Fruit weight	0.0958 g	0.1454 g	0.1336 g
Peduncle length	2.38 mm	4.83 mm	5.49 mm
Seed width	2.65 mm	3.32 mm	2.28 mm
Seed length	3.52 mm	4.09 mm	3.57 mm
Seed weight	0.0034 g	0.0072 g	0.0030 g
Buttress root height	13.5 cm	13.1 cm	50 cm

part, and a little hairy without a stipule. The leaves are pinnate (*penninervis*), attached laterally to the costa so that the leaves on both sides of the costa are not symmetrical. The vein does not always appear and stops before reaching the leaf margin. The vein has a smaller size, forms a net and do not stand out. The flowers are single or in pairs, axillary (*flos axillaris*) (Figure 3,4,5 C), with six white crumpled petals (Figure 3,4,5 F). The peduncle (*pedunculus*) is reddish-green, unbranched and a little hairy. The fruits are a true single, dry capsule, enclosed within hypanthium, containing about 2-10 tiny seeds with several pseudolayers and topped by style (Figure 3,4,5 E). The young fruit is green and turns brownish when it is ripe. These morphological features showed high similarities to *P. acidula* J.R.Forst. & G.Forst described elsewhere, such as in Andaman Island, India (Goutham-Bharathi et al. 2015) and in Somalia (POWO 2022).

Figure 3. *Pemphis acidula* J.R.Forst. & G.Forst. from Biluhu Beach: A - knee roots; B – Bark; C - Fruit in axilla; D – Leaves; E – Fruit with persistent style, side view; F – Flower with crumpled white petals.

A total of 14 qualitative morphological characters of *P. acidula* at three locations and *S. alba* from Biluhu were analysed in phenetics using the UPGMA method with Jaccard's Coefficient to determine the similarities between them. The similarity index may indicate their genetic relationship. If the similarity value is high, then the genetic relationship between them will also be close (Putri et al. 2023). The results shows that the analysis of phenetic relationship between *P. acidula* at the three locations and *S. alba* from Biluhu yielded in 3 clusters, namely A, B and C. Cluster A consist of *P. acidula* at Biluhu and Dulanga with similarity of 100%. Furthermore *P. acidula* at Biluhu and Dulanga fused with *P. acidu-*

Figure 4. *Pemphis acidula* J.R.Forst. & G.Forst. from Dulanga Beach: A - knee roots; B – Bark; C - Fruit in axilla; D – Leaves; E – Fruit with persistent style, side view; F – Flower with crumpled white petals.

Figure 5. *Pemphis acidula* J.R.Forst. & G.Forst. from Olele Beach: A - knee roots; B – Bark; C - Fruit in axilla; D – Leaves; E – Fruit with persistent style, side view; F – Flower with crumpled white petals.

la at Olele forming cluster B with similarity of 100%. Next, *S. alba* from Biluhu fused with *P. acidula* at 3 locations forming cluster C with similarity of 7.7% (Figure 6). It can be seen that *P. acidula* at 3 locations have a high level of similarity, so it can be said that the phenetic relationship between them is very close. However, *P. acidula* at Biluhu and Dulanga had the closest phenetic relationship.

Genetic diversity

The existence of associated mangroves particularly *P. acidula* species in three study areas with different habitats may show the possibility of plant to adapt towards the environmental condition which influenced by genet-

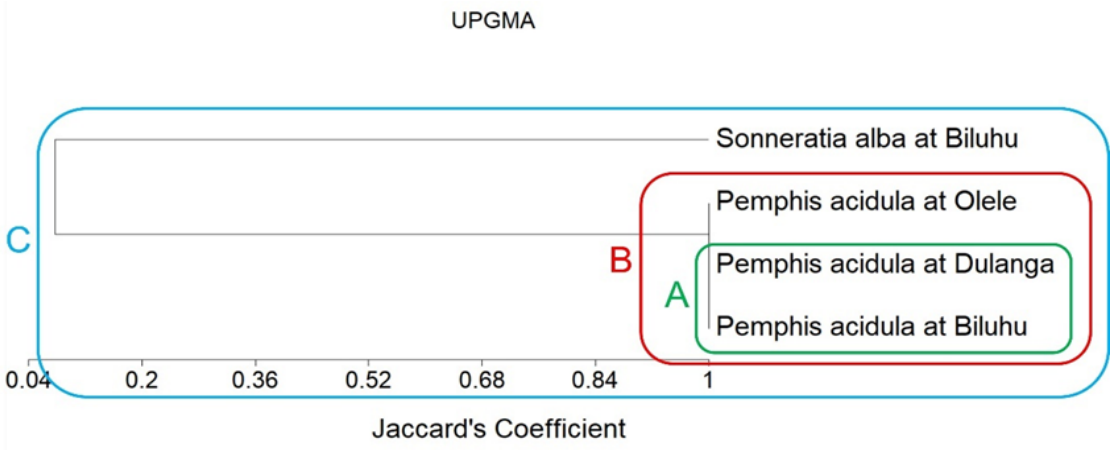

Figure 6. Dendogram showing the clustering of *P. acidula* at 3 locations and *S. alba* at Biluhu based on qualitative morphological characters using the UPGMA methods with Jaccard's Coefficient.

ic diversification of species level. Genetic diversity quantifies how big a genetic diversity is in or between populations. Genetic diversity can predict homogeneity or heterogeneity which makes the plants possibly adapt and survive in a dynamic environment (Ramzan et al. 2020).

Genetic variation analysis using ten primers ISSR showed that all primers are capable of detecting and amplifying the sequence of *P. acidula* and *S. alba* genome with 175 bp to 4400 bp in size (Figure 7). There were a total of 147 polymorphic bands from 156 DNA bands that appeared. This is in line with some previous studies which showed that ISSR primer had successfully detected the polymorphism between species (Wang et al. 2012; Hamza et al. 2013; Louati et al. 2019; Ramzan et al. 2020; Raji & Siril 2021; Sevindik & Efe 2021; Takele et al. 2021). The higher the level of polymorphism, the higher the genetic diversity in a species (Ezekiel et al. 2011). However, among the specimens, similarities were found mainly between *P. acidula* on the beaches of Biluhu and Dulanga compared to those in Biluhu and Olele or Dulanga and Olele.

Genetic variation similarities data based on ISSR marker (Figure 7) were supported by the analysis of similarities using UPGMA method with simple matching coefficient. A dendogram which revealed a genetic relationship resulted in a total of 3 clusters, namely I, II and III (Figure 8). Cluster I consist of *P. acidula* at Dulanga and Biluhu with similarity of 76.8%. Furthermore, *P. acidula* at Dulanga and Biluhu fused with *P. acidula* at Olele forming cluster II with similarity of 64.2% and 62.3%, respectively. Next, *S. alba* at Biluhu fused with *P. acidula* at Biluhu, Dulanga and Olele forming cluster III with similarity of 38.4%, 37.7% and 32.5%, respectively. This strengthens the results of the phenetic analysis (Figure 6) that *P. acidula* at Biluhu is more closely related genetically to *P. acidula* at Dulanga than to those in Olele.

Based on the results of genetic relationship analysis using ISSR marker (Figure 8) which showed high similarity between *P. acidula* at Biluhu and Dulanga (76.8%), we decided to only use *P. acidula* at Biluhu along with Olele sample for phylogenetic analysis based on ITS sequences. The ITS sequences of *P. acidula* at Biluhu and Olele were analysed using BLAST and obtained five *P. acidula* accession in GenBank (accession codes: MH768221.1, MH768222.1, MH768223.1, AY035762.1 and AF268394.1) with highest similar sequences to Biluhu and Olele sample, as well as *Sonneratia apetala*-MH244026.1, *Lafoensia pacari*-JN701292.1 and *Lafoensia acuminata*-AY905425.1 as outgroup. BLAST analysis of ITS sequences of *P. acidula* at Biluhu and Olele were shown in Table 4.

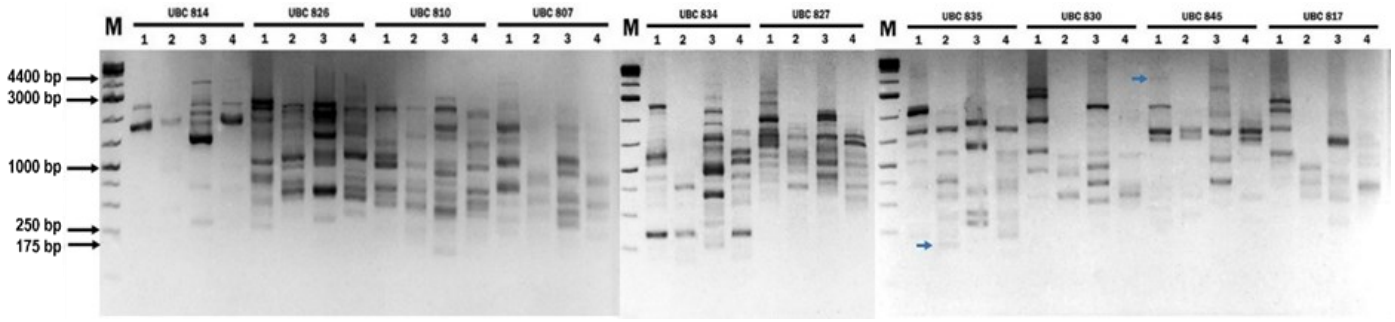

Figure 7. The pattern of ISSR bands of *P. acidula* and *S. alba* using 10 primers; M = 1 kb DNA Ladder Lane 1 = *P. acidula* from Olele; Lane 2 = *P. acidula* from Biluhu; Lane 3 = Sonneratia alba from Biluhu; Lane 4 = *P. acidula* from Dulanga; blue arrow = the longest and shortest band.

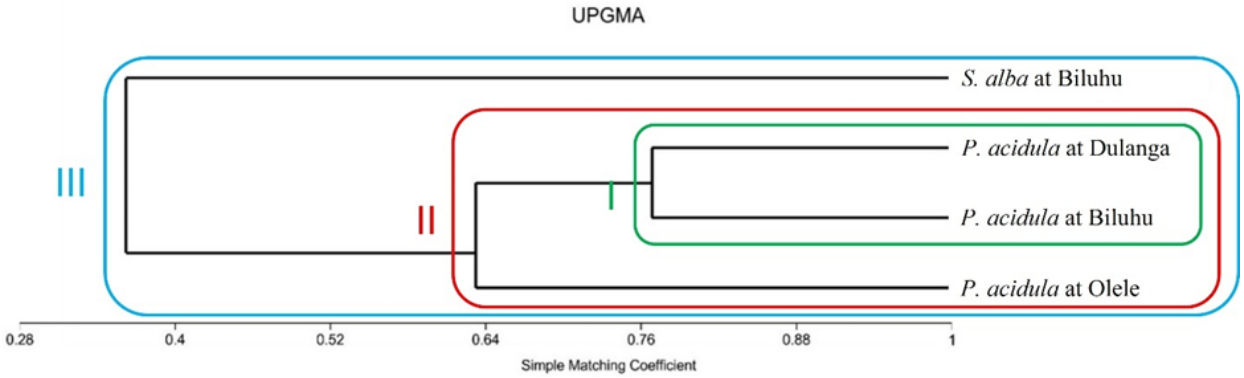

Figure 8. Dendogram showing the clustering of *P. acidula* at 3 locations and *S. alba* at Biluhu based on ISSR marker using the UPGMA methods with simple matching coefficient

Based on Table 4, the BLAST result of ITS gene sequences of Olele (Sample A1 R) was verified as *P. acidula* with the highest identity percentage of 100% and a query cover score of 98%. Meanwhile, ITS gene sequences of Biluhu (Sample B1 R) had acquired the highest identity percentage of 81.34% and a query cover score of 93%. It can be said that Biluhu sample has an ITS sequences with lower similarity to the ITS sequences of *P. acidula* accession in GenBank compared to the Olele sample.

Reconstruction of the phylogenetic tree with NJ method Kimura 2 Parameter model towards the samples from Olele and Biluhu, five accession samples of *P. acidula* from GenBank (accession codes: MH768221, MH768222, MH768223, AY035762 and AF268394), and 3 outgroup samples (*Sonneratia apetala*-MH244026, *Lafoensia pacari*-JN701292 and *Lafoensia acuminata*-AY905425) showed that *P. acidula* in Olele is located on the same clade with the accessions of *P. acidula* in GenBank with bootstrap score 97. Meanwhile, the sample located in Biluhu is considered as a sister group of *P. acidula* (Figure 9).

Cladogram and genetic distance data based on the ITS gene sequence among 5 accessions of *P. acidula* in GenBank with the Olele sample revealed an extremely low score (0 - 0.19%). Meanwhile, the samples located in Biluhu performed a high score (24.97 - 25.03%) (Table 5). This score implied a close phylogenetic relationship between Olele sample and five accessions of *P. acidula*, while the phylogenetic relationship between Biluhu sample and five *P. acidula* accessions is pretty far. According to Qin et al. (2017) and Ningrum et al. (2020), the genetic distance threshold for ITS2 in intraspecies of seed plants is 3.76%. Based on the value, it can be said that Olele sample and the fifth *P. acidula* accession were classified as intraspecies, while Biluhu sample was classified as different species. However, given the very high morphological similarity between the Biluhu and Olele samples, it is possible that the Biluhu sample is a species

complex of *P. acidula* in Olele.

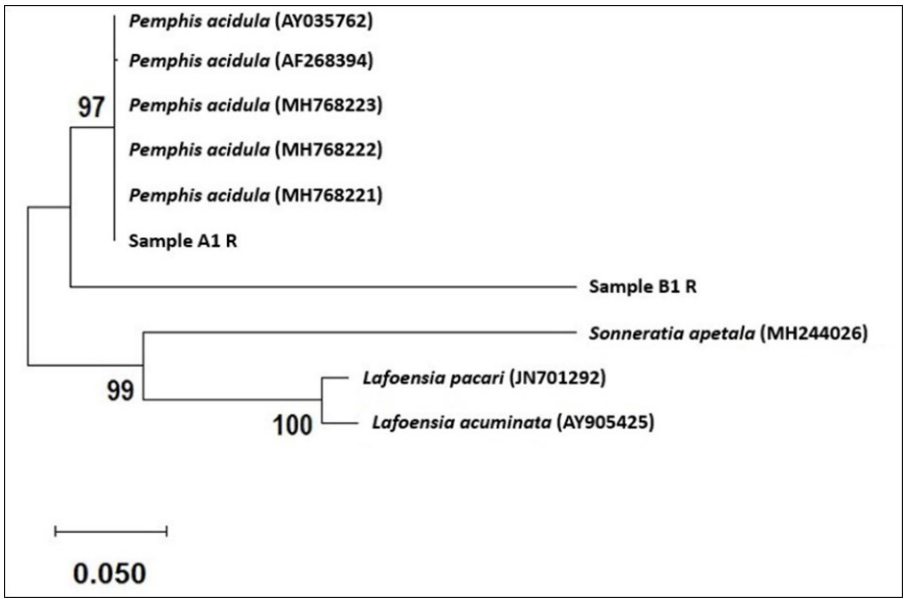

Figure 9. Reconstruction of phylogenetic tree using NJ method with Kimura 2 Parameter model (a bootstrap with 100 repetitions). Sample A1 R = Olele; Sample B1 R = Biluhu.

Implication for conservation

Our study underlined the influence of environmental variables on *P. acidula* diversities, with a focus on morphological and genetic variation. *Pemphis acidula* is the only member of Genus *Pemphis* in Family Lythraceae (Graham et al. 1987; POWO 2022). It is considered as the "least concern" plant by the International Union for Conservation of Nature (IUCN) since March 07, 2008 (Ellison et al. 2010). Due to its slow growth and limited availability in nature, *P. acidula* becomes one of the plants with extinction risks in wild nature.

Sulawesi Island, Indonesia, is known for its high level of endemicity of flora and fauna due to its isolation from the Asian and Australian continental shelves for a long period of time, thus allowing phenotypic and genotypic changes in individuals as an adaptation response to environ-

Table 4. BLAST analysis of ITS sequences of *P. acidula* at Olele and Biluhu showing the identity percentage and query cover.

Sample Code	Fragment Length (bp)	Accession number	Species	Identity (%)	Query Cover (%)
Sample A1 R (*P. Acidula* at Olele)	547	MH768222.1	*P. acidula*	100	98
		MH768221.1	*P. acidula*	100	98
		MH768223.1	*P. acidula*	100	97
		AY035762.1	*P. acidula*	99.43	95
		AF268394.1	*P. acidula*	99.23	94
		AY905425.1	*Lafoensia acuminata*	86.48	86
		JN701292.1	*Lafoensia pacari*	86.29	91
		MH244026.1	*Sonneratia apetala*	-	-
Sample B1 R (*P. Acidula* at Biluhu)	668	MH768221.1	*P. acidula*	81.34	93
		MH768223.1	*P. acidula*	81.06	92
		MH768222.1	*P. acidula*	81.18	90
		AY035762.1	*P. acidula*	79.93	85
		AF268394.1	*P. acidula*	79.62	84
		MH244026.1	*Sonneratia apetala*	78.01	27
		JN701292.1	*Lafoensia pacari*	-	-
		AY905425.1	*Lafoensia acuminata*	-	-

Table 5. Genetic distance between the studied samples with the accession of *P. acidula* in GenBank

	Olele R Sample	Biluhu R Sample	MH768221	MH768222	MH768223	AY035762	AF268394
Olele R Sample							
Biluhu R Sample	24.97						
MH768221*	0.00	24.97					
MH768222*	0.00	24.97	0.00				
MH768223*	0.00	24.97	0.00	0.00			
AY035762*	0.00	25.03	0.00	0.00	0.00		
AF268394*	0.19	25.30	0.19	0.19	0.19	0.19	

* *P. acidula* accession in GenBank

mental conditions. As one of the distribution areas of *P. acidula* in Indonesia, Gorontalo on Sulawesi Island provides a suitable habitat for the growth of this species, such as on Biluhu, Dulanga and Olele Beaches. The various environmental characteristics displayed by these three areas led to differences in the adaptive response of *P. acidula*. Our findings suggest that *P. acidula* at Biluhu and Dulanga Beaches developed distinct morphological and molecular characters, offering a rationale for conservation and management of *P. acidula* in Indonesia.

In addition, considering the low population of *P. acidula* in nature, especially in the three research locations, we hope that there will be an increase in public awareness to cultivate this plant as an effort to use it sustainably and prevent the destruction of coastal ecosystems. To date, *P. acidula* has been used as the ingredient of traditional medicine in various countries including Indonesia which perceives this plant as sacred. Local people also use it in traditional ceremonies and house construction (Baderan et al. 2022). This plant is also widely used as an expensive ornamental plant (one of the best bonsai species in the world) (Cunningham et al. 2017).

CONCLUSIONS

We demonstrated the importance of genetic analysis in biodiversity studies. We found that although samples from the three locations had the similarities in phenetics, they were genetically different. The differences in morphological and molecular characters between *P. acidula* at Biluhu and Dulanga Beaches and those at Olele Beach are thought to be the result of the adaptation of these plants over a long period of time to differences in environmental variables, especially the condition of limestone as a growth substrate. *Pemphis acidula* at Biluhu and Dulanga beaches evolved distinct morphological and molecular traits, providing a rationale for the conservation and management of *P. acidula* in Indonesia. Further studies are needed to study this species due to the possibility that the Biluhu and Dulanga samples are different species or even new species from the *Pemphis* genera.

AUTHORS CONTRIBUTION

D.W.K.B., S.R., Y.R. and R.U. designed the research; D.W.K.B., S.R., M.N.A., Y.R. and R.U. collected the data (field work); M.H.A. and D.W.K.B. analysed the morphological features; M.J. and M.N.A. analysed the genetic data; M.J. and D.W.K.B. wrote the manuscript, and all authors contributed to revisions. All the authors read and approved the final manuscript.

ACKNOWLEDGMENTS

The authors send their gratitude to the Research and Community Service Institution, Universitas Negeri Gorontalo, the Local Governments of

Gorontalo Regency (Chiefs of Bongo and Biluhu Villages) and Bone Bolango Regency (Chief of Olele Village) who had immensely given their helping hands upon the completion of this research.

CONFLICT OF INTEREST

The authors declare that they have no conflict of interest regarding the research or the research funding.

FUNDING

This research receives funding support from the 2021 Non-tax Revenue/ Public Service Agency (PNBP) Research Funding based on the Rector's Decree of Universitas Negeri Gorontalo No. 404/P/2021.

REFERENCES

Abdelhamid, K. et al., 2014. Determination of the Effect of the Environment on the Genetic Polymorphism in the Genus of Tamarix Using the Molecular Marker (Simple Sequence Repeats "PCR-SSR" (In Arid Areas of the Khenchela Region (Eastern of Algeria). *International Journal of Sciences: Basic and Applied Research (IJSBAR) International Journal of Sciences: Basic and Applied Research*, 16(2), pp.1–10.

Backer, C.A. & van den Brink, R.C.B., 1965. *Flora of Java (Spermatophytes only)*, Netherlands: N.V.P. Noordhoff-Groningen.

Baderan, D.W.K. & Angio, M., 2019. *Index Measurement of Biodiversity from a Geosite of Gorontalo Province (A Pioneer of Gorontalo Geopark). A Final Report of the Provincial Bappeda of Gorontalo*, Gorontalo, Indonesia: Development Planning Agency at Sub-National Level of Gorontalo Province.

Baderan, D.W.K., Retnowati, Y. & Utina, R., 2022. Conservation threats of Pemphis acidula in the Tomini Bay area, Gorontalo, Indonesia. *IOP Conference Series: Earth and Environmental Science. IOP Conf. Ser.: Earth Environ. Sci.*, 976, 012058. doi: 10.1088/1755-1315/976/1/012058.

Baderan, D.W.K. & Utina, R., 2021. *Biodiversity of Flora and Fauna of East Biluhu Beach (a review of coastal ecology-environment)*, Yogyakarta, Indonesia: Deepublish.

Baderan, D.W.K., Utina, R. & Lapolo, N., 2018. Vegetation structure, species diversity, and mangrove zonation patterns in the Tanjung Panjang Nature Reserve Area, Gorontalo, Indonesia. *Int. J. Appl. Biol.*, 2(2), pp.1–12. doi: 10.20956/ijab.v2i2.5752.

Berg, C.C. & Corner, E.J.H., 2005. Flora Malesiana Series I Moraceae: Ficeae. *Spermatophyta*, 17(2), pp.1–702.

Bijmoer, R, Scherrenberg, M, & Creuwels, J, 2023. *Naturalis Biodiversity Center (NL) - Botany*. Naturalis Biodiversity Center. doi: 10.15468/ib5ypt

Cunningham, A.B. et al., 2017. Opportunities, barriers and support needs: micro-enterprise and small enterprise development based on non-timber products in eastern Indonesia. *Australian Forestry*, 80(3), pp.161–177. doi: 10.1080/00049158.2017.1329614.

Dittmann, S. et al., 2022. Effects of Extreme Salinity Stress on a Temperate Mangrove Ecosystem. *Frontiers in Forests and Global Change*, 5, 859283. doi: 10.3389/ffgc.2022.859283.

Duncan, T. & Baum, B.R., 1981. Numerical Phenetics: Its Uses in Botanical Systematics. *Annual Review of Ecology and Systematics*, 12, pp.387–404. doi: https://doi.org/10.1146/annurev.es.12.110181.002131.

Ellison, J. et al., 2010, 'Pemphis acidula' in *The IUCN Red List of Threatened Species*, viewed 21 June 2022, from https://www.iucnredlist.org/species/178838/7622565

Ezekiel, C.N. et al., 2011. Genetic diversity in 14 tomato (Lycopersicon esculentum Mill.) varieties in Nigerian markets by RAPD-PCR technique. *Afr. J. Biotechnol.*, 10(25), pp.4961–4967.

GBIF Secretariat: GBIF Backbone Taxonomy, '*Pemphis acidula* J.R.Forst. & G.Forst.' in *Checklist dataset*, viewed 20 June 2022, from https://www.gbif.org/species/3188706

George, A.S., 1990. *Flora of Australia* George AS, ed., Canberra: Australian Government Publishing Service.

Giesen, W. et al., 2006. *Mangrove Guidebook for Southeast Asia*, Bangkok: FAO and Wetlands International.

Goutham-Bharathi, M.P. et al., 2015. Notes on Pemphis acidula J.R. Forst. & G. Forst. (Myrtales: Lythraceae) from Andaman Islands, India. *Journal of Threatened Taxa*, 7(8), pp.7471–7474. doi: 10.11609/JoTT.o4146.7471-4.

Graham, A. et al., 1987. Palynology and Systematics of The Lythraceae. II. Genera Haitia Through Peplis. *American Journal of Botany*, 74(6), pp.829–850. doi: 10.1002/j.1537-2197.1987.tb08687.x.

Hamza, H. et al., 2013. Comparison of the effectiveness of ISSR and SSR markers in determination of date palm (Phoenix dactylifera L.) agronomic traits. *Aust. J. Cr. Sci.*, 7(6), pp.763–769.

Harris, J.G. & Harris, M.W., 2001. *Plant Identification Terminology*, Utah: Spring Lake Publishing.

Ibrahim, E.A., 2021. Genetic diversity in Egyptian bottle gourd genotypes based on ISSR markers. *Ecological Genetics and Genomics*, 18, 100079. doi: 10.1016/j.egg.2021.100079.

Irwansah, Sugiyarto & Mahajoeno, E., 2017. Mangrove diversity in the Serewe Gulf of Lombok Island West Nusa Tenggara. *AIP Conference Proceedings.*, 1868, 090005. doi: 10.1063/1.4995197.

IUCN (International Union of Conservation of Nature), 2022, 'Red List of Threatened Species', in *IUCN Red List*, viewed 20 June 2022, from https://www.iucnredlist.org/

Kodikara, K.A.S. et al., 2018. The effects of salinity on growth and survival of mangrove seedlings changes with age. *Acta Botanica Brasilica*, 32(1), pp.37–46. doi: 10.1590/0102-33062017abb0100.

Kumar, S. et al., 2018. MEGA X: Molecular Evolutionary Genetics Analysis across Computing Platforms F. U. Battistuzzi, ed. *Molecular Biology and Evolution*, 35(6), pp.1547–1549. doi: 10.1093/molbev/msy096.

Louati et al., 2019. Genetic, Morphological, and Biochemical Diversity of Argan Tree (Argania spinosa L.) (Sapotaceae) in Tunisia. *Plants*, 8 (9), 319. doi: 10.3390/plants8090319.

Manek, L.M. & Puay, Y., 2020. Analysis of the pattern of spatial distribution of stigi (Pemphis acidula) species in the Meubesi Nature Reserve, Malaka Regency, East Nusa Tenggara. *Jurnal Biotropikal Sains*, 17(3), pp.24–32.

Martida, V. & Pharmawati, M., 2019. Comparison of DNA Yield from Different Plant Materials of Plumeria sp. (Apocynaceae). *Journal of Advances in Tropical Biodiversity and Environmental Sciences*, 3(1), pp.8–11. doi: 10.24843/ATBES.2019.v03.i01.p03.

Nguyen, X. et al., 2017. DNA BARCODING OF THE TRUE MANGROVE PLANTS, A SELECTION OF GENETIC MARKERS. *Journal of Marine Science and Technology*, 17(4A), pp.311–321. doi: 10.15625/1859-3097/17/4A/13230.

Ningrum, W.D.A. et al., 2020. Genetic variability of Begonia longifolia Blume from Indonesia based on Nuclear DNA internal transcribed spacer (ITS) sequence data. *Biodiversitas Journal of Biological Diversity*, 21(12), pp.5778–5785. doi: 10.13057/biodiv/d211239.

POWO (Plants of the World Online), 2022, 'Pemphis acidula J.R.Forst. & G.Forst' in *Plants of the World Online: Royal Botanic Garden Kew*, viewed 20 June 2022, from https://powo.science.kew.org/taxon/urn:lsid:ipni.org:names:554064-1

Putri, N.R.A. et al., 2023. Genetic Variation of Butternut Squash (*Cucurbita moschata* Duchesne) based on Inter-Simple Sequence Repeat. *Journal of Tropical Biodiversity and Biotechnology*, 8(1), jtbb77228. doi: 10.22146/jtbb.77228.

Qin, Y. et al., 2017. Molecular thresholds of ITS2 and their implications for molecular evolution and species identification in seed plants. *Scientific Reports*, 7(1), 17316. doi: 10.1038/s41598-017-17695-2.

Raji, R. & Siril, E.A., 2021. Genetic diversity analysis of promising Ceylon olive (Elaeocarpus serratus L.) genotypes using morphological traits and ISSR markers. *Current Plant Biology*, 26, 100201. doi: 10.1016/j.cpb.2021.100201.

Ramzan, M. et al., 2020. Assessment of Inter simple sequence repeat (ISSR) and simple sequence repeat (SSR) markers to reveal genetic diversity among Tamarix ecotypes. *Journal of King Saud University - Science*, 32(8), pp.3437–3446. doi: 10.1016/j.jksus.2020.10.003.

Rao, T. & Ellis, J.L., 1995. Flora of Lakshadweep islands off the Malabar coast, peninsular India, with emphasis on phytogeographical distribution of plants. *J. Econ. Taxon. Bot.*, 19, pp.235–250.

Seng, T.Y. et al., 2013. Recycling of superfine resolution agarose gel. *Genetics and Molecular Research*, 12(3), pp.2360–2367. doi: 10.4238/2013.March.11.1.

Sevindik, E. & Efe, F., 2021. Molecular Genetic Diversity and Phylogenetic Analyses of Punica granatum L. Populations Revealed by ISSR Markers and Chloroplast (cpDNA) trnL-F Region. *Erwerbs-Obstbau*, 63(3), pp.339–345. doi: 10.1007/s10341-021-00581-7.

Singh, A. et al., 2014. Efficiency of SSR, ISSR and RAPD markers in molecular characterization of mungbean and other Vigna species. *INDIAN J BIOTECHNOL*, 13, pp.81–88.

Takele, D., Tsegaw, M. & Indracanti, M., 2021. Genetic diversity assessment in some landraces and varieties of date palm (Phoenix dactylifera L.) from Afar Region, Ethiopia, using ISSR markers. *Ecological Genetics and Genomics*, 19, 100085. doi: 10.1016/j.egg.2021.100085.

The Plant List, 2022, '*Pemphis acidula* J.R. Forst. & G. Forst' in *The Plant List*, viewed 20 June 2022, from http://www.theplantlist.org/tpl1.1/record/tro-19200012

Utina, R. et al., 2019. The composition of mangrove species in coastal area of Banggai district, central Sulawesi, Indonesia. *Biodiversitas*, 20(3), pp.840–846. doi: 10.13057/biodiv/d200330.

Wang, H. et al., 2012. Genetic diversity and relationship of global faba bean (Vicia faba L.) germplasm revealed by ISSR markers. *Theoretical and Applied Genetics*, 124(5), pp.789–797. doi: 10.1007/s00122-011-1750-1.

de Wilde, W.J.J.O. & Duyfjes, B.E.E., 2016. *Flora Malesiana*, Djakarta: Noordhoff-Kolff N.V.

Journal of Tropical Biodiversity and Biotechnology
Volume 09, Issue 01 (2024): jtbb87079
DOI: 10.22146/jtbb.87079

Research Article

Safety Assessment of *Bacillus subtilis* G8 Isolated from Natto for Food Application

Nathania Calista Putri[1#], Hans Victor[1#], Vivian Litanto[1], Reinhard Pinontoan[1], Juandy Jo[1,2]*
1)Department of Biology, Faculty of Science and Technology, Universitas Pelita Harapan. Jl. M.H. Thamrin Boulevard 1100, Tangerang 15811, Banten, Indonesia.
2)Mochtar Riady Institute for Nanotechnology, Jl. Boulevard Jendral Sudirman No.1688, Tangerang 15811, Banten, Indonesia.
* Corresponding author, email: juandy.jo@uph.edu
# Co-first author

Keywords:
Bacillus subtilis G8
natto
antibiotic resistance,
disk diffusion method
whole-genome sequencing.
Submitted:
20 July 2023
Accepted:
09 October 2023
Published:
02 February 2024
Editor:
Miftahul Ilmi

ABSTRACT
Various bacteria are widely used as food-fermenting agents, including *Lactobacillus*, *Bifidobacterium*, and *Bacillus*. Despite they are generally recognized as safe to be consumed by humans, those bacteria could potentially cause antibiotic resistance as they could acquire and transfer antibiotic resistance genes from or to other microbes within the human gastrointestinal tract. Profiling antibiotic resistance pattern in those bacteria is therefore important to control the spread of antibiotic resistance. In this study, antibiotic resistance profile of *Bacillus subtilis* G8 was assessed. *B. subtilis* G8 had been isolated from commercialised Japanese natto in Indonesia and had been previously reported for its fibrinolytic characteristics. The antibiotic resistance phenotype and genotype of *B. subtilis* G8 were assessed through the Kirby-Bauer disk diffusion method and whole-genome analysis, respectively. *B. subtilis G8* exhibited resistance towards Oxacillin, Lincomycin and Tiamulin-Lefamulin. The bioinformatics analysis indicated several responsible genes mediating those resistance, i.e., *ybxI* (for Oxacillin), *lmrB* (for Lincomycin) and *vmlR* (for Lincomycin and Tiamulin-Lefamulin). All identified genes were found in the chromosomal DNA. Further analysis found no mobile genetic elements within the genome, therefore reducing a risk of resistance gene transfer via plasmid and subsequently supporting safety profile of *B. subtilis* G8 in food fermentation usage.

Copyright: © 2024, J. Tropical Biodiversity Biotechnology (CC BY-SA 4.0)

INTRODUCTION
Fermentation converts various food components through controlled microbial growth (Marco et al. 2017). Various bacterial strains have been used to ferment food with a particular criterion of selecting the fermentation agent is the safety concern of using a particular microbial strain. The safety concern could be assessed by detecting the presence of antibiotic resistance genes within the bacteria as well as the risk of resistance transfer (Gueimonde et al. 2013).

The human gastrointestinal tract is the place where daily interaction between environmental bacteria (e.g., from food) and gut-resident indigenous bacteria occurs. Food indeed could be a source of antibiotic-resistant bacteria. The foodborne transmission of antibiotic-resistant *Escherichia coli* as a cause of urinary tract infections among females lived in Montreal, Canada was an example of it (Vincent et al. 2010). The con-

stant interaction between environmental and indigenous bacteria could facilitate the horizontal transfer of antibiotic resistance genes (Penders et al. 2013). For example, various species of *Lactobacillus* and *Bifidobacterium*, the commensal bacteria in human gastrointestinal tract that commonly used as the starter cultures of fermented food, indeed harbour several antibiotic resistance genes (Ammor et al. 2007a, 2007b). Consequently, this potential reservoir of resistance genes among human gut microbiota might transfer those genes to pathogenic bacteria (Rolain 2013).

Among bacterial species used as starters in food fermentation process, *Bacillus subtilis* is commonly found in the soy-based food, including Korean cheonggukjang and Japanese natto (Kamada et al. 2015). Of note, *Bacillus subtilis* G8 had been isolated from a commercially available Japanese natto in Indonesia (Lucy et al. 2019), in which its whole genome and fibrinolytic characteristics had been recently published (Pinontoan et al. 2021; Dikson et al. 2022). Thus, it would be interesting to assess the genotype and phenotype of antibiotic resistance of *B. subtilis* G8 as well as the presence of any transferrable genetic element within its genome to investigate the safety profile of *B. subtilis* G8 as a fermentation agent. The antibiotic testing on *B. subtilis* G8 and the identification of resistance genes within its genome were therefore performed in this study.

MATERIALS AND METHODS

Bacterial Isolate

Bacillus subtilis G8 had been isolated by the Department of Biology of Universitas Pelita Harapan from Japanese fermented soybean natto commercially available in Indonesia (Lucy et al. 2019). *B. subtilis* G8 were cultured on the nutrient agar (Merck, Germany) until further testing.

Antibiotic Susceptibility Test

The Kirby-Bauer disk diffusion method was performed based on the Clinical and Laboratory Standards Institute reference method (Jorgensen & Turnidge 2015). *B. subtilis* G8 was inoculated in the nutrient broth (Merck, Germany) and incubated at 37°C to obtain a turbidity of 0.5 McFarland. The liquid culture was taken using a sterile cotton swab and pressed against the wall of the test tube to remove excess fluid, then streaked evenly on Mueller Hinton agar media (Himedia, India). Up to 15 minutes after bacterial streaking, twenty-four antibiotic discs, including inhibitors of cell wall synthesis (Amoxicillin (2 µg), Ampicillin (10 µg), Bacitracin (10 IU), Cefoxitin (30 µg), Methicillin (5 µg), Oxacillin (1 µg) and Vancomycin (30 µg)), inhibitors of protein synthesis (Chloramphenicol (30 µg), Clindamycin (2 µg), Erythromycin (15 µg), Gentamicin (10 µg), Kanamycin (30 µg), Lefamulin (20 µg), Lincomycin (2 µg), Neomycin (30 µg), Streptomycin (10 µg), Tetracycline (30 µg), Tiamulin (30 µg) and Tylosin (30 µg)), inhibitors of nucleic acid synthesis (Ciprofloxacin (5 µg), Nalidixic Acid (30 µg), Ofloxacin (5 µg)), inhibitor of DNA-dependent RNA Polymerase (Rifampicin (5 µg)) and inhibitor of folate synthesis (Sulfonamide (300 µg)) (Liofilchem, Italy) were aseptically pressed onto the agar surface. All plates were subsequently incubated at 37°C for 24 hours in an aerobic condition. Following the incubation, a ruler was utilized to measure the diameter of the clear zone, including the diameter of respective antibiotic disc (6 mm). All antibiotic discs were tested three times.

Bioinformatic Analysis

The whole genome of *B. subtilis* G8 had been sequenced by the Novogene

Company Limited (Hong Kong) using the Illumina technology platform (USA) and its data had been recently published (Dikson et al. 2022). Briefly, the whole-genome sequence of *B. subtilis* G8 was checked for its quality by FastQC (Andrews 2010). The contig assembly was subsequently performed using SPAdes (Bankevich et al. 2012). The contig coverage was checked using Qualimap 2 (Okonechnikov et al. 2016). Outliers are searched using the formula $z = (X - \mu) / \sigma$ where X is the mean coverage, μ is the mean, and σ is the standard deviation. The value of z above 3 or below -3 was considered as an outlier and removed. The remaining contigs were re-ordered using Mauve (Darling et al. 2004) with *Bacillus subtilis* subspecies *subtilis* strain 168 (RefSeq: NC_000964.3) as the reference genome. The re-ordered contigs were merged into one FASTA sequence using Artemis (Carver et al. 2012). The complete genome was finally submitted into dFAST for annotation (Tanizawa et al. 2016, 2018). The graphical map of *B. subtilis* G8 genome was created using Proksee (Grant et al. 2023).

Antibiotic resistance genes in the genome were examined using CARD and BacAnt (Alcock et al. 2020; Hua et al. 2021). The antibiotic resistance genes were identified using the Resistance Gene Identifier (RGI) application on CARD, in which the RGI could predict the antibiotic resistome, i.e., the collection of all antibiotic resistance genes in pathogenic and non-pathogenic bacteria (Wright 2007), by using a combination of open reading frame with Prodigal (Hyatt et al. 2010), sequence alignment with BLAST (Camacho et al. 2009) or DIAMOND (Buchfink et al. 2014), as well as curated resistance mutations included with the antimicrobial resistance detection model (Alcock et al. 2020). Similarly, the BacAnt was also used to annotate antibiotic resistance genes within the genome of *B. subtilis* G8 (Hua et al. 2021). If the CARD-RGI and BacAnt results were unavailable, a literature search would be performed to identify published antibiotic resistance genes. The identified resistance gene sequences were further examined using BLAST (Camacho et al. 2009). Results from CARD and BacAnt were subsequently cross-checked with results of dFAST. Outlier contigs were examined individually using BLAST, in which contigs known to be plasmids were examined for the presence of antibiotic resistance genes using CARD and BacAnt as well. The presence of mobile genetic elements within the genome was determined with BacAnt (Hua et al. 2021).

RESULTS AND DISCUSSION

Based on the genome assembly and subsequent bioinformatic analysis, total sequence length of *B. subtilis* G8 was 4,017,503 base pairs, which was comparable to other *Bacillus subtilis* strains (Dikson et al. 2022). *B. subtilis* G8 had GC content of 43.4% and predicted CDS of 4,279, suggesting that it was similar to other *B. subtilis* strains isolated from natto (Dikson et al. 2022). A visualization of its genomic map, along with five antibiotic resistance genes found in this study, were shown in Figure 1.

Susceptibility of *B. subtilis* G8 towards 24 types of antibiotics were assessed using the Kirby-Bauer disc diffusion method. The measurement of the clear zone diameters and their interpretation were depicted in Figure 2 and Table 1. The interpretation was based on the European Committee on Antimicrobial Susceptibility Testing (EUCAST) definition on susceptibility testing categories (susceptible, standard dosing regimen [S]; susceptible, increased exposure [I] and resistance [R]), in which while a microorganism was described as susceptible if its diameter was within the category of S or I, a microorganism was identified as resistant if its result was within the category of R (2022). Of note, the interpreta-

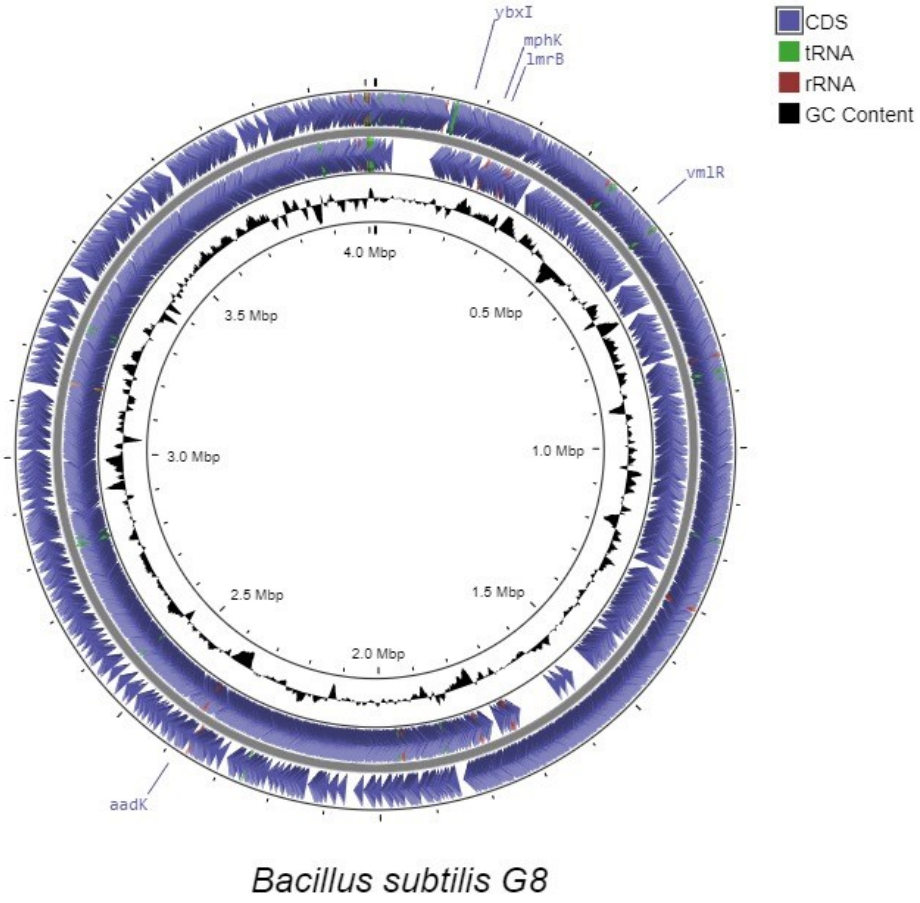

Figure 1. A visualisation of whole genome of *Bacillus subtilis* G8. The outer ring depicted location of predicted CDS and its strand, as well as the location of predicted tRNA and rRNA. The inner ring showed the GC content distribution plot. Genomic location of the identified antibiotic resistance genes was shown outside of the outer ring. The genomic map was constructed using Proksee (Grant et al. 2023).

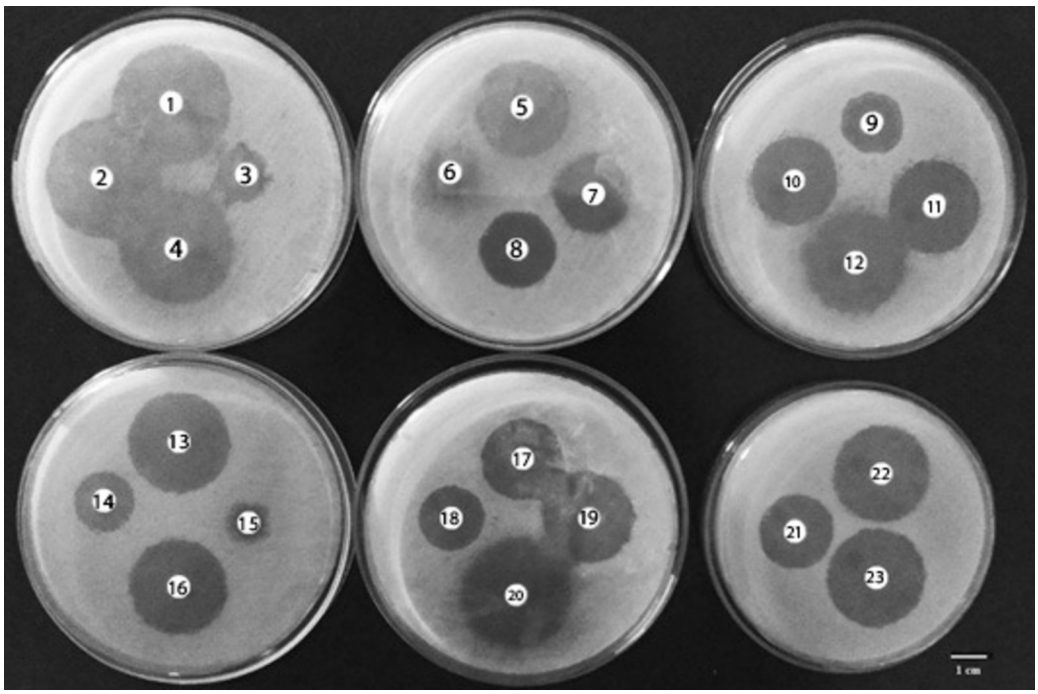

Figure 2. A representative result of the disc diffusion method on *Bacillus subtilis* G8. Each plate contained 3-4 antibiotic discs. The result was obtained after 24-hour incubation at 37°C. *(1)* Amoxicillin 2 µg; *(2)* Ampicillin 10 µg; *(3)* Bacitracin 10 IU; *(4)* Cefoxitin 30 µg; *(5)* Methicillin 5 µg; *(6)* Oxacillin 1 µg; *(7)* Vancomycin 30 µg; *(8)* Neomycin 30 µg; *(9)* Streptomycin 10 µg; *(10)* Gentamicin 10 µg; *(11)* Kanamycin 30 µg; *(12)* Tetracycline 30 µg; *(13)* Chloramphenicol 30 µg; *(14)* Clindamycin 2 µg; *(15)* Lincomycin 2 µg; *(16)* Erythromycin 15 µg; *(17)* Tylosin 30 µg; *(18)* Tiamulin 30 µg; *(19)* Sulfonamide 300 µg; *(20)* Ciprofloxacin 5 µg; *(21)* Nalidixic acid 30 µg; *(22)* Ofloxacin 5 µg; *(23)* Rifampicin 5 µg.

Table 1. Results of antibiotic disc diffusion assay on *Bacillus subtilis* G8.

Class	Antibiotic	Zone Diameter Interpretive Standard (mm)			Result (mm)
		S	I	R	*mean (min – max)*
Aminopenicillins	Amoxicillin 2 µg[B]	≥29	-	≤28	*36.0 (35-38)*
	Ampicillin 10 µg[A]	≥29	-	≤28	*34.7 (33-36)*
Polypeptide	Bacitracin 10 IU[A]	>13	-	-	*13.7 (13-15)*
Cephalosporins	Cefoxitin 30 µg[A]	≥25	-	≤24	*34.7 (32-38)*
Penicillinase-resistant penicillins	Methicillin 5 µg[C]	≥22	-	≤21	*29.3 (27-31)*
	Oxacillin 1 µg[A]	≥18	-	≤17	*12.0 (10-13)*
Glycopeptides	Vancomycin 30 µg[A]	≥17	15-16	≤14	*21.0 (20-22)*
Aminoglycosides	Neomycin 30 µg[A]	≥16	14-15	≤13	*21.3 (21-22)*
	Streptomycin 10 µg[A]	≥15	12-14	≤11	*15.0 (13-17)*
	Gentamicin 10 µg[A]	≥15	13-14	≤12	*24.7 (24-25)*
	Kanamycin 30 µg[A]	≥18	14-17	<13	*27.0 (26-28)*
Tetracyclines	Tetracycline 30 µg[A]	≥19	15-18	≤14	*28.0 (26-30)*
Phenicols	Chloramphenicol 30 µg[A]	≥18	13-17	≤12	*29.3 (26-31)*
Lincosamides	Clindamycin 2 µg[A]	≥21	15-20	≤14	*19.7 (16-22)*
	Lincomycin 2 µg[D]	≥21	-	≤14	*13.3 (8-17)*
Macrolides	Erythromycin 15 µg[A]	≥23	14-22	<13	*27.7 (27-28)*
	Tylosin 30 µg[E]	≥23	14-22	<13	*24.3 (24-25)*
Pleuromutilins	Tiamulin 30 µg[F]	≥23	-	-	*16.0 (15-17)*
	Lefamulin 20 µg[A]	≥23	-	-	*19.3 (19-20)*
Folate antagonists	Sulfonamide 300 µg[A]	≥17	13-16	≤12	*27.0 (26-28)*
Quinolones	Ciprofloxacin 5 µg[A]	≥21	16-20	≤15	*31.3 (31-32)*
	Nalidixic acid 30 µg[A]	≥19	14-18	≤13	*24.0 (21-26)*
	Ofloxacin 5 µg[A]	≥18	15-17	≤14	*29.7 (28-31)*
Ansamycins	Rifampicin 5 µg[A]	≥20	17-19	≤16	*30.3 (29-31)*

[A]The clear zone was primarily interpreted based on the CLSI (2021) standard against *Staphylococcus* spp.
[B]The standard for Amoxicillin 2 µg was unavailable, hence the standard for Ampicillin 10 µg was adopted.
[C]The standard for Methicillin 5 µg was unavailable, hence the standard for Oxacillin 1 µg was adopted.
[D]The standard for Lincomycin 2 µg was adopted from (Chukiatsiri et al. 2012).
[E]The standard for Tylosin 30 µg was unavailable, hence the standard for Erythromycin 15 µg was adopted.
[F]The standard for Tiamulin 30 µg was unavailable, hence the standard for Lefamulin 20 µg was adopted.
The measurement results included the diameter of the antibiotic disc (6 mm). *S*, susceptible, standard dosing regimen; *I*, susceptible, increased exposure; *R*, resistance; -. no available data. Results from triplicate experiments were presented as mean (minimum to maximum).

tive criteria was mainly adopted from those for *Staphylococcus* species (Clinical and Laboratory Standards Institute (CLSI) 2021).

Overall, *B. subtilis* G8 was described to be susceptible to most tested antibiotic discs (⌈S⌉=19 antibiotics and ⌈I⌉=1 antibiotic). These predominant phenotypes of antibiotic susceptibility were observed as well in *B. subtilis* HTI-23 isolated from stingless bees (Amin et al. 2020) and other strains of *B. subtilis* isolated from a hospital in Iraq (Yassin & Ahmad 2012). The isolate of *B. subtilis* G8 was observed to be resistant, however, towards Tiamulin (30 µg), Oxacillin (1 µg) and Lincomycin (2 µg) discs. The variation in clear zone diameters upon Tiamulin (30 µg) or Oxacillin (1 µg) treatment were very small, suggesting a clear resistance phenotype of *B. subtilis* G8 towards both antibiotics. First, the finding of Tiamulin resistance phenotype was in accordance with a published study, reporting that due to the presence of VmlR, an ATP-binding cassette protein of the F type, *B. subtilis* was resistant towards Tiamulin (Crowe-McAuliffe et al. 2018). Tiamulin belongs to the class of pleuromutilins, a natural antibiotic produced by *Pleurotus mutilus* (now known as *Clitopilus scyphoides*), which functions as the protein synthesis inhibitor through

rRNA binding in the ribosome (Islam et al. 2009). It is commonly used in veterinary medicine, hence prompting a question on why *B. subtilis* G8, obtained from human food, developed resistance towards Tiamulin. It is unknown on whether this resistance phenotype was recently acquired. However, it has been reported that the administration of antibiotics to animals could select the antibiotic resistance bacteria, which subsequently could transfer their antibiotic resistance genes to other bacteria (Rolain 2013). The resistance of *B. subtilis* G8 towards Lefamulin, the pleuromutilin used in humans (Paukner & Riedl 2017), was subsequently tested. Indeed, *B. subtilis* G8 was also resistant towards Lefamulin (Table 1), suggesting a similar resistance mechanism for various members of pleuromutilin existed in this bacterial strain.

Second, the finding of Oxacillin resistance phenotype in *B. subtilis* G8 was supported by another study, reporting that the tested strains of *B. subtilis* were highly resistant towards Oxacillin (Irkitova et al. 2019). Of note, Oxacillin and Cefoxitin are used to identify Methicillin-resistant *Staphylococcus aureus* (MRSA), one of the most common antibiotic-resistant pathogenic bacteria (Broekema et al. 2009; Larsen et al. 2022). Interestingly, *B. subtilis* G8 was observed to be sensitive towards Cefoxitin 30 µg and Methicillin 5 µg in this study, suggesting that *B. subtilis* G8 had a unique mechanism that mediated resistance only towards Oxacillin and were likely not having the *mecA* gene that conferred resistance to all beta-lactams in MRSA (Broekema et al. 2009; Ramandinianto et al. 2020).

Third, the variation in clear zone diameter upon Lincomycin (2 µg) treatment was relatively high, in which the individual clear zone diameter was 15 mm, 17 mm and 8 mm obtained from the first, second and third measurement, respectively (individual data not shown). Hence, the Lincomycin resistance phenotype of *B. subtilis* G8 should be interpreted cautiously. Lincomycin acts as a protein synthesis inhibitor that binds to the 50s ribosomal subunit, in which the presence of VmlR protein in *B. subtilis* could confer the resistance phenotype to Lincomycin (Crowe-McAuliffe et al. 2018). This finding was in contrast, however, to published results on *B. subtilis* isolated from food wastes (DET6) and from the soil (BYS2, BQ3, BD17, BG5 and BGY12), which reporting those strains were sensitive to Lincomycin (Patel et al. 2009; Guo et al. 2017). This discrepancy could be due to variation among *B. subtilis* strains as well as differences in the concentration of antibiotic disks and the reference standard used in those previous studies.

A subsequent bioinformatic analysis was performed to correlate the antibiotic resistance phenotypes of *B. subtilis* G8 with its putative genes that could mediate resistance to Oxacillin, Lincomycin and Tiamulin-Lefamulin. As shown in Table 2, three antimicrobial resistance genes of *B. subtilis* G8 were identified *in silico* to mediate resistance towards Oxacillin (*ybxI* gene), Lincomycin (*lmrB* and *vmlR* genes) and Tiamulin-Lefamulin (*vmlR* gene). Of note, all identified antibiotic resistance genes were found in the chromosomal DNA of *B. subtilis* G8. The *ybxI* gene encodes a class D β-lactamase, also known as oxacillinase or OXA-type β -lactamase (Antunes & Fisher 2014), with low activity (Colombo et al. 2004). The *ybxI* gene was suspected to mediate *B. subtilis* G8 resistance to Oxacillin. However, it had been reported that the *ybxI* gene did not encode true β-lactamases, as it did not hydrolyze D-alanyl-D-alanine peptidase (Colombo et al. 2004). Instead, the *ybxI* gene was assumed to encode Penicillin-binding protein (PBP) with low β-lactamase activity. The product of the *ybxI* gene were estimated belonging to the Penicillin-recognition enzyme family, but with an intermediate activity between

Table 2. Antimicrobial resistance genes of *Bacillus subtilis* G8 towards Oxacillin, Lincomycin and Tiamulin.

Gene	AMR gene family	Antibiotic class	Resistance mechanism
ybxI	*Class D β -lactamases*	Penicillinase-resistant penicillins	putative *β*-lactamase
lmrB	*ATP-binding cassette* (ABC) *antibiotic efflux pump*	Lincosamides	Antibiotic efflux
vmlR	*ABC-F ATP-binding cassette ribosomal protection protein*	Macrolides, Lincosamides, Streptogramin, Tetracyclines, Oxazolidinone, Phenicols, Pleuromutilins	Antibiotic target protection

AMR, antimicrobial resistance.

PBP and β-lactamase (Colombo et al. 2004). Thus, it was elusive yet whether the resistance to Oxacillin was mediated by the *ybxI* gene.

Next, the *lmrB* gene is a part of the *lmrAB* operon found in *B. subtilis* genome, in which the *lmrB* gene is a drug efflux transporter, while the *lmrA* gene is a suppressor of its own operon. As *lmrA* suppresses expression of *lmrB*. mutations within the *lmrA* gene causes the *lmrB* gene to be expressed, hence conferring a Lincomycin-resistant phenotype (Yoshida et al. 2004). It is unknown yet, however, whether *B. subtilis* G8 genome had a mutated *lmrA* gene or defect in its expression. Finally, the *vmlR* gene in *B. subtilis* genome had been described to encode a ribosomal protective protein that conferred resistance to Virginiamycin M, Lincomycin and Tiamulin, but not to Chloramphenicol, Linezolid and Erythromycin (Crowe-McAuliffe et al. 2018). The presence of *vmlR* gene in *B. subtilis* G8 genome could therefore mediate resistance towards Lincomycin and Tiamulin-Lefamulin.

Intriguingly, both BacAnt and CARD identified genes within genome of *B. subtilis* G8 that could induce resistance towards Macrolides (*mphK*) and Streptomycin (*aadK*) (Table 3), although *B. subtilis* G8 was observed to be sensitive against discs of Erythromycin, Tylosin and Streptomycin (Table 1). The *mphK* gene observed within *B. subtilis* G8 genome encodes macrolide phosphotransferase (mph). The enzyme mph inactivates macrolides by phosphorylating 2'-OH on essential dimethylamino sugars, thereby preventing macrolides from binding to bacterial ribosomes (Pawlowski et al. 2018). The mphK is a part of the mph enzyme family that targets Erythromycin, although the antibiotic disc diffusion assay in this study demonstrated that *B. subtilis* G8 was sensitive to Erythromycin. The mphK phosphorylated erythromycin poorly resulting in a sensitive phenotype (Pawlowski et al. 2018), which could explain the Erythromycin-sensitive phenotype in *B. subtilis* G8.

The *aadK* gene, originally found within *B. subtilis* 168 genome, contributes to a low-grade resistance to Streptomycin (Noguchi et al. 1993). The *aadK* gene encodes an aminoglycoside 6-adenylyltransferase or AAD (6), which is capable of inactivating Streptomycin through adenylation of the C-6 position on streptomycin (Noguchi et al. 1993). Based on the result of antibiotic disc diffusion assay, *B. subtilis* G8 was considered as sen-

Table 3. Putative antimicrobial resistance genes of *Bacillus subtilis* G8 detected by CARD and BacAnt.

Gene	AMR gene family	Antibiotic class	Resistance mechanism
mphK	*Macrolide phosphotransferase* (mph)	Macrolide	Antibiotic inactivation
aadK	*6-adenyltransferase* (AAD(6))	Aminoglycoside	Antibiotic inactivation

AMR, antimicrobial resistance.

sitive to Streptomycin (Table 1). However, this interpretation was based on the standard against *Staphylococcus* species (Clinical and Laboratory Standards Institute (CLSI) 2021), not against *Bacillus* species. It would be of interest to further investigate Streptomycin resistance phenotype and genotype of *B. subtilis* G8.

Considering the risk of antibiotic resistance gene transfer via mobile genetic elements, genome of *B. subtilis* G8 was also analysed using BacAnt to identify the presence of transposons and integrons. None of the transferrable genetic element was found with BacAnt in the genome of *B. subtilis* G8.

CONCLUSION

The isolate of *B. subtilis G8* exhibited resistance phenotype towards Oxacillin, Lincomycin and Tiamulin-Lefamulin. The antibiotic susceptibility's results were corroborated by the presence of respective antibiotic resistance genes within *B. subtilis* G8 genome, comprising *ybxI*, *lmrB* and *vmlR*. As those genes were present in its chromosomal genome and there were no transferrable genetic elements found, it is unlikely that *B. subtilis* G8 could disseminate those resistance genes via plasmid, supporting its safety to be used as the fermentation agent.

AUTHORS CONTRIBUTION

N.C.P. and H.V. contributed equally. N.C.P. and V.L. performed the experiments and collected the data. N.C.P., H.V. and J.V. analysed dan interpreted the data. N.C.P. and J.J. drafted the article. H.V., V.L., R.P. and J.J. critically reviewed the article. All authors approved the final version.

ACKNOWLEDGMENTS

This work was supported by the Directorate of Higher Education, Indonesian Ministry of Education, Culture, Research and Technology [No. 1218/LL3/PG/2021, 2021]. The authors thank Elvina, S.Si. and Dikson, S.Si., for their technical supports.

CONFLICT OF INTEREST

The authors declare no conflict of interest.

REFERENCES

Alcock, B.P. et al., 2020. CARD 2020: Antibiotic resistome surveillance with the comprehensive antibiotic resistance database. *Nucleic Acids Res*, 48, pp.D517–D525. doi: 10.1093/nar/gkz935.

Amin, F.A.Z. et al., 2020. Probiotic Properties of Bacillus Strains Isolated from Stingless Bee (Heterotrigona itama) Honey Collected across Malaysia. *Int J Environ Res Public Health*, 17, pp.1–15. doi: 10.3390/ijerph17010278

Ammor, M.S., Belén Flórez, A. & Mayo, B., 2007a. Antibiotic resistance in non-enterococcal lactic acid bacteria and bifidobacteria. *Food Microbiol*, 24, pp.559–70. doi: 10.1016/j.fm.2006.11.001.

Ammor, M.S. et al., 2007b. Molecular characterization of intrinsic and acquired antibiotic resistance in lactic acid bacteria and bifidobacteria. *J Mol Microbiol Biotechnol*, 14(1-3), pp.6–15. doi: 10.1159/000106077.

Andrews, S., 2010, 'FastQC: A Quality Control Tool for High Throughput Sequence Data', in *Babraham Bioinformatics*, viewed 16 July 2021, from https://www.bioinformatics.babraham.ac.uk/projects/fastqc/.

Antunes, N.T. & Fisher, J.F., 2014. Acquired class D β-Lactamases. *Antibiotics*, 3, pp.398–434. doi: 10.3390/antibiotics3030398.

Bankevich, A. et al., 2012. SPAdes: A new genome assembly algorithm and its applications to single-cell sequencing. *J Comput Biol*, 19, pp.455–77. doi: 10.1089/cmb.2012.0021.

Broekema, N.M. et al., 2009. Comparison of cefoxitin and oxacillin disk diffusion methods for detection of mecA-mediated resistance in staphylococcus aureus in a large-scale study. *J Clin Microbiol*, 47(1), pp.217–219. doi: 10.1128/JCM.01506-08.

Buchfink, B., Xie, C. & Huson, D.H., 2014. Fast and sensitive protein alignment using DIAMOND. *Nat Methods*, 12, pp.59–60. doi: 10.1038/nmeth.3176.

Camacho, C. et al., 2009. BLAST+: Architecture and applications. *BMC Bioinformatics*, 10, 421. doi: 10.1186/1471-2105-10-421.

Carver, T. et al., 2012. Artemis: An integrated platform for visualization and analysis of high-throughput sequence-based experimental data. *Bioinformatics*, 28(4), pp.464–469. doi: 10.1093/bioinformatics/btr703.

Chukiatsiri, K. et al., 2012. Serovar Identification, Antimicrobial Sensitivity, and Virulence of Avibacterium paragallinarum Isolated from Chickens in Thailand. *Avian Dis Dig*, 7(2). doi: 10.1637/10120-988112-digest.1.

Clinical and Laboratory Standards Institute (CLSI), 2021. *Performance Standards for Antimicrobial Susceptibility Testing: CSLI Supplement M100. 31st editi*. USA: Clinical and Laboratory Standards Institute.

Colombo, M.L. et al., 2004. The ybxI Gene of Bacillus subtilis 168 Encodes a Class D β-Lactamase of Low Activity. *Antimicrob Agents Chemother*, 48, pp.484–490. doi: 10.1128/AAC.48.2.484-490.2004.

Crowe-McAuliffe, C. et al., 2018. Structural basis for antibiotic resistance mediated by the Bacillus subtilis ABCF ATPase VmlR. *Proc Natl Acad Sci U S A*, 115(36), pp.8978–8983. doi: 10.1073/pnas.1808535115.

Darling, A.C.E. et al., 2004. Mauve: Multiple alignment of conserved genomic sequence with rearrangements. *Genome Res*, 14(7), pp.1394–1403. doi: 10.1101/gr.2289704.

Dikson, D. et al., 2022. Whole-genome analysis of Bacillus subtilis G8 isolated from natto. *Biodiversitas*, 23, pp.1293–1300. doi: 10.13057/biodiv/d230313.

Grant, J.R. et al., 2023. Proksee: in-depth characterization and visualization of bacterial genomes. *Nucleic Acids Res*, 51, pp.W484-W492. doi: 10.1093/nar/gkad326.

Gueimonde, M. et al., 2013. Antibiotic resistance in probiotic bacteria. *Front Microbiol*, 4, 202. doi: 10.3389/fmicb.2013.00202.

Guo, M. et al., 2017. Bacillus subtilis improves immunity and disease resistance in rabbits. *Front Immunol*, 8, 354. doi: 10.3389/fimmu.2017.00354.

Hua, X. et al., 2021. BacAnt: A Combination Annotation Server for Bacterial DNA Sequences to Identify Antibiotic Resistance Genes, Integrons, and Transposable Elements. *Front Microbiol*, 12, 649969. doi: 10.3389/fmicb.2021.649969.

Hyatt, D. et al., 2010. Prodigal: prokaryotic gene recognition and translation initiation site identification. *BMC Bioinformatics*, 11, 119. doi: 1471-2105/11/119.

Irkitova, A.N., Grebenshchikova, A.V. & Dudnik, D.E., 2019. Antibiotic susceptibilty of bacteria from the Bacillus subtilis group. *Ukr J Ecol*, 9, pp.363–366.

Islam, K.M.S., Klein, U. & Burch, D.G.S., 2009. The activity and compatibility of the antibiotic tiamulin with other drugs in poultry medicine - A review. *Poult Sci*, 88, pp.2353–2359. doi: 10.3382/ps.2009-00257.

Jorgensen, J.H. & Turnidge, J.D., 2015. Susceptibility Test Methods: Dilution and Disk Diffusion Methods. *Man. Clin. Microbiol, 11th edition*. Wiley, pp.1253–73. doi: 10.1128/9781555817381.

Kamada, M. et al., 2015. Whole-Genome Sequencing and Comparative Genome Analysis of Bacillus subtilis Strains Isolated from Non-Salted Fermented Soybean Foods. *PLoS One*, 10(10), e0141369. doi: 10.1371/journal.pone.0141369.

Larsen, J. et al., 2022. Emergence of methicillin resistance predates the clinical use of antibiotics. *Nature*, 602(7895), pp.135-141. doi: 10.1038/s41586-021-04265-w.

Lucy, J. et al., 2019. Clot Lysis Activity of Bacillus subtilis G8 Isolated from Japanese Fermented Natto Soybeans. *Appl Food Biotechnol*, 6 (2), pp.101–109. doi: 10.22037/afb.v6i2.22479.

Marco, M.L. et al., 2017. Health benefits of fermented foods: microbiota and beyond. *Curr Opin Biotechnol*, 44, pp.94–102. doi: 10.1016/j.copbio.2016.11.010.

Noguchi, N., Sasatsu, M. & Kono, M., 1993. Genetic mapping in Bacillus subtilis 168 of the aadK gene which encodes aminoglycoside 6-adenylyltransferase. *FEMS Microbiol Lett*, 114, pp.47–52. doi: 10.1016/0378-1097(93)90140-w.

Okonechnikov, K., Conesa, A. & García-Alcalde, F., 2016. Qualimap 2: Advanced multi-sample quality control for high-throughput sequencing data. *Bioinformatics*, 32, pp.292–4. doi:10.1093/bioinformatics/btv566.

Patel, A.K. et al., 2009. Comparative accounts of probiotic characteristics of Bacillus spp. isolated from food wastes. *Food Res Int*, 42(4), pp.505–510. doi: 10.1016/j.foodres.2009.01.013.

Paukner, S. & Riedl, R., 2017. Pleuromutilins: Potent drugs for resistant bugs-mode of action and resistance. *Cold Spring Harb Perspect Med*, 7, pp.1–16. doi: 10.1101/cshperspect.a027110.

Pawlowski, A.C. et al., 2018. The evolution of substrate discrimination in macrolide antibiotic resistance enzymes. *Nat Commun*, 9(1), 112. doi: 10.1038/s41467-017-02680-0.

Penders, J. et al., 2013. The human microbiome as a reservoir of antimicrobial resistance. *Front Microbiol*, 4, 87. doi: 10.3389/fmicb.2013.00087.

Pinontoan, R. et al., 2021. Fibrinolytic characteristics of Bacillus subtilis G8 isolated from natto. *Biosci Microbiota, Food Heal*, 40(3), pp.144–149. doi: 10.12938/bmfh.2020-071.

Ramandinianto, S.C., Khairullah, A.R. & Effendi, M.H., 2020. Meca gene and methicillin-resistant Staphylococcus aureus (MRSA) isolated from dairy farms in East Java, Indonesia. *Biodiversitas*, 21, pp.3562–8. doi: 10.13057/biodiv/d210819.

Rolain, J.M., 2013. Food and human gut as reservoirs of transferable antibiotic resistance encoding genes. *Front Microbiol*, 4. doi: 10.3389/fmicb.2013.00173.

Tanizawa, Y. et al., 2016. DFAST and DAGA: Web-based integrated genome annotation tools and resources. *Biosci Microbiota, Food Heal*, 35(4), pp.173–84. doi: 10.12938/bmfh.16-003.

Tanizawa, Y., Fujisawa, T. & Nakamura, Y., 2018. DFAST: A flexible prokaryotic genome annotation pipeline for faster genome publication. *Bioinformatics*, 34, pp.1037–9. doi: 10.1093/bioinformatics/btx713.

The European Committee on Antimicrobial Susceptibility Testing, 2022, 'New definitions of S, I and R from 2019 2022', in *EUCAST*, viewed 11 April 2022, from https://www.eucast.org/newsiandr/.

Vincent, C. et al., 2010. Food reservoir for Escherichia coli causing urinary tract infections. *Emerg Infect Dis*, 16(1), pp.88–95. doi: 10.3201/eid1601.091118.

Wright, G.D., 2007. The antibiotic resistome: The nexus of chemical and genetic diversity. *Nat Rev Microbiol*, 5, pp.175–86. doi: 10.1038/nrmicro1614.

Yassin, N.A. & Ahmad, A.M., 2012. Incidence and Resistotyping Profiles of Bacillus subtilis Isolated from Azadi Teaching Hospital in Duhok City, Iraq. *Mater Socio Medica*, 24, 194. doi: 10.5455/msm.2012.24.194-197.

Yoshida, K.I.l et al., 2004. Bacillus subtilis LmrA is a repressor of the lmrAB and yxaGH operons: Identification of its binding site and functional analysis of lmrB and yxaGH. *J Bacteriol*, 186(17), pp.5640–5648. doi: 10.1128/JB.186.17.5640-5648.2004.

Journal of Tropical Biodiversity and Biotechnology
Volume 09, Issue 01 (2024): jtbb86174
DOI: 10.22146/jtbb.86174

Research Article

Lead (Pb)-Resistant Bacteria Improve *Brassica chinensis* Biomass and Reduce Pb Concentration in Pb-Contaminated Soil

Beauty Laras Setia Pertiwi[1], Reni Ustiatik[2]*, Yulia Nuraini[2]
1)Master of Soil and Water Management, Faculty of Agriculture, Brawijaya University, Jl. Veteran, Malang 65145, East Java, Indonesia
2)Department of Soil Science, Faculty of Agriculture, Brawijaya University, Jl. Veteran, Malang 65145, East Java, Indonesia
* Corresponding author, email: reni.ustiatik@ub.ac.id

Keywords:
Pb-contaminated soil
Pb-resistant bacteria
Pb remediation
Submitted:
25 June 2023
Accepted:
09 October 2023
Published:
05 February 2023
Editor:
Miftahul Ilmi

ABSTRACT
Applications of inorganic fertilisers and pesticides frequently increase lead (Pb) content in the soil and food crops. This study aims to isolate Pb-resistant bacteria and test the isolated bacteria in reducing Pb concentration and increasing biomass production of *Brassica chinensis* on Pb-contaminated soil. Soil and plant samples were collected from agricultural land in Batu City, East Java, Indonesia. The isolated bacteria were tested for Pb resistance and then characterised according to 16S rRNA Sequence. A pot trial with a completely randomised block design consisting of 9 treatments and 3 replications was set to determine the effect of Pb-resistant bacteria inoculation on Pb residue, plant growth, and soil nutrients. The result showed that the isolated Pb-resistant bacteria were *Bacillus wiedmannii* and *Bacillus altitudinis*. The bacteria were resistant to Pb up to 10,000 mg/L $PbNO_3$. Inoculation of the bacteria increased *B. chinensis* growth and biomass production, namely increasing the number of leaves (12%) and dry weight (35%). Also, the bacteria reduced Pb residue in the soil by up to 88%. Moreover, soil essential nutrients such as total nitrogen, available phosphorus, and exchangeable potassium increased (12%, 73%, and 200%, respectively) after the application of Pb-resistant bacteria. The bacteria have the potential for bioremediation of Pb-contaminated soils on a large scale due to the bacteria prevent Pb uptake by food crops such as *B. chinensis* by reducing Pb content in the soil, which is good for food safety and environmental sustainability.

Copyright: © 2024, J. Tropical Biodiversity Biotechnology (CC BY-SA 4.0)

INTRODUCTION
Intensive farming is a type of agricultural system that usually uses large inputs of fertiliser and pesticides to increase plant production and prevent yield loss (Alexandratos & Bruinsma 2012; Scotti et al. 2015). Intensive farming is an agricultural system that farmers widely use, especially for horticultural crops (Mariyono 2019), such as in the highland of Batu City, East Java, Indonesia. Survey results showed that farmers in Sumberbrantas village, Batu City, apply ZA amount 300 kg/ha and NPK amount 200 kg/ha. While, application of various types of pesticides every two days. According to Statistics Indonesia (2018), the use of inorganic fertilisers and pesticides occupy almost 24.22% (potato) and 28.82% (cabbage) of total budget for these crops' cultivation. Using inorganic fer-

tilisers and pesticides continuously causes soil and water contamination (Sharma et al. 2019; Bisht & Chauhan 2020). Moreover, the residue remains in the crops and enters food chains, thus harmful to human health (Sharma et al. 2019). For ecosystem sustainability, pesticide use impacts biodiversity loss, e.g., loss of natural enemies and increased plant pests and disease resistance (Sánchez-Bayo 2021).

Intensive use of inorganic fertilisers and pesticides contributes to heavy metal contamination in agricultural land (Bisht & Chauhan 2020). Lead (Pb) is one of the heavy metals that contaminate agricultural soil, originally from agrochemical products such as fertilisers and pesticides containing Pb (Kumar et al. 2022). Pb content in fertiliser worldwide is around 1-300 mg/kg (phosphorus fertiliser), 1-15 mg/kg (nitrogen fertiliser), 2-125 mg/kg (lime fertiliser), 2-60 mg/kg (manure), respectively (Alengebawy et al. 2021). Several active ingredients of pesticides contain Pb above the permissible concentration (which is 10 ppb), such as glyphosate 58 ppb, isoproturon 30 ppb, and fluroxypyr 110 ppb, respectively (Defarge et al. 2018). The large amount of Pb content in fertilisers and pesticides applied during crop cultivation will increase Pb content in the soil and agricultural products (Kumar et al. 2022).

Pb contamination in soil is mainly from anthropogenic activities (Mallongi et al. 2022), such as agricultural activity. Pb concentration in agricultural soil ranges from 25.98 to 108.68 mg/kg (Astuti et al. 2021). The concentration exceeds the limit concentration of Pb in the soil for agricultural activities, which is less than 70 mg/kg (CCME - Canadian Council of Ministers of the Environment 1999). Moreover, Pb concentration in vegetable products, such as cabbage, is around 26.51 to 29.98 mg/kg. The concentration also exceeds the permissible level of Pb in vegetables according to the Regulation of Indonesia Food and Drug Agency Number 5 in 2018, which is less than 0.2 mg/kg. The results are alarming and remediation measures are crucially required to prevent further Pb contamination in the soil. The problem leads to disruption of soil function, affects plant growth, and is dangerous for human health as well as environmental sustainability (Bisht & Chauhan 2020).

There are many ways to remove Pb contamination in the soil. Yet, bioremediation is considered as cost-effective and environmentally friendly to remove metal contaminants from the soil (Dixit et al. 2015). Bioremediation uses microbes, either their biomass to absorb or their metabolism to detoxify contaminants in the soil (Ojuederie & Babalola 2017). Pb-resistant bacterium (e.g., *Rhodobacter sphaeroides*) is a promising alternative for Pb remediation in contaminated soil through the precipitation and formation of inert compounds such as Pb sulfate and Pb sulfide (Li et al. 2016). Also, phosphate (P) solubilising bacteria and biochar can immobilise Pb^{2+} and improve soil quality (Zhu et al. 2022). Compost and rhizobium addition are also a potential combination for removing Pb from contaminated soil (Rosariastuti et al. 2019). This study aims: 1) to isolate and to characterise Pb-resistant bacteria from Pb-contaminated soil due to intensive application of pesticides and fertilisers containing Pb; 2) to analyse the effect of Pb-resistant bacteria application in the soil and the growth of *Brassica chinensis* in Pb-contaminated soil. This study is crucial to support food safety and environmental sustainability.

MATERIALS AND METHODS

Soil and plants sampling site

Soil and plant samples were taken from agricultural land, specifically horticulture commodities such as Chinese Cabbage (*Brassica rapa* subsp. *pekinensis*) and potato (*Solanum tuberosum*), where farmers intensively ap-

plied pesticides and fertilisers containing Pb. The location lies on Sumber Brantas Village, Bumiaji Sub-Regency, Batu City, East Java, Indonesia (7°45'13" S and 112°31'04" E). The location is 953 m above sea level (m asl) with an average air temperature is 27 °C. Sampling points in a diagonal shape were determined using purposive random sampling (Figure 1). Soil samples were taken from rhizospheric areas and replicated three times at each sampling point. The samples (soil and plant) were kept in a polyethylene bag and stored in a cooling box. The samples were transported to the laboratory for further analysis.

Bacteria isolation and purification

Ten grams of Pb-contaminated soil were suspended in 90 mL of sodium chloride 0.85% in a 250 mL flask. Lead-resistant bacteria were isolated using a serial dilution method (10^{-1}-10^{-5}), 1 mL of aliquots were taken from serial dilutions 10^{-4} and 10^{-5} and then inoculated onto nutrient agar (NA) plates containing 50 mg/L $Pb(NO_3)_2$ according to a method proposed by Hafeez et al. (2018) with modification. To confirm that the isolated bacteria are Pb-resistant, the pure colonies were streaked three times onto NA agar plates containing 50 mg/kg $Pb(NO_3)_2$.

Lead minimum inhibitory concentration bioassay

Lead minimum inhibitory concentration test was done using paper discs 0.55 cm soaked with $Pb(NO_3)_2$ solution in different concentrations (0, 100, 1000, 5000, and 10000 mg/L). The tested bacteria were inoculated into Petri dishes containing NA medium using a pour plate method. The paper discs containing Pb were placed onto NA plates and then incubated at 28 °C for 48 h according to the method used by Ustiatik et al. (2022) with modification. The tested bacteria's ability in Pb detoxification was measured according to the inhibition zone on the medium (Equation 1).

$$LO = \pi r^2 \quad (1)$$

Where: LO = wide of inhibition zone

π = 3.14

r = inhibition zone (halo zone around the Paper Disc)

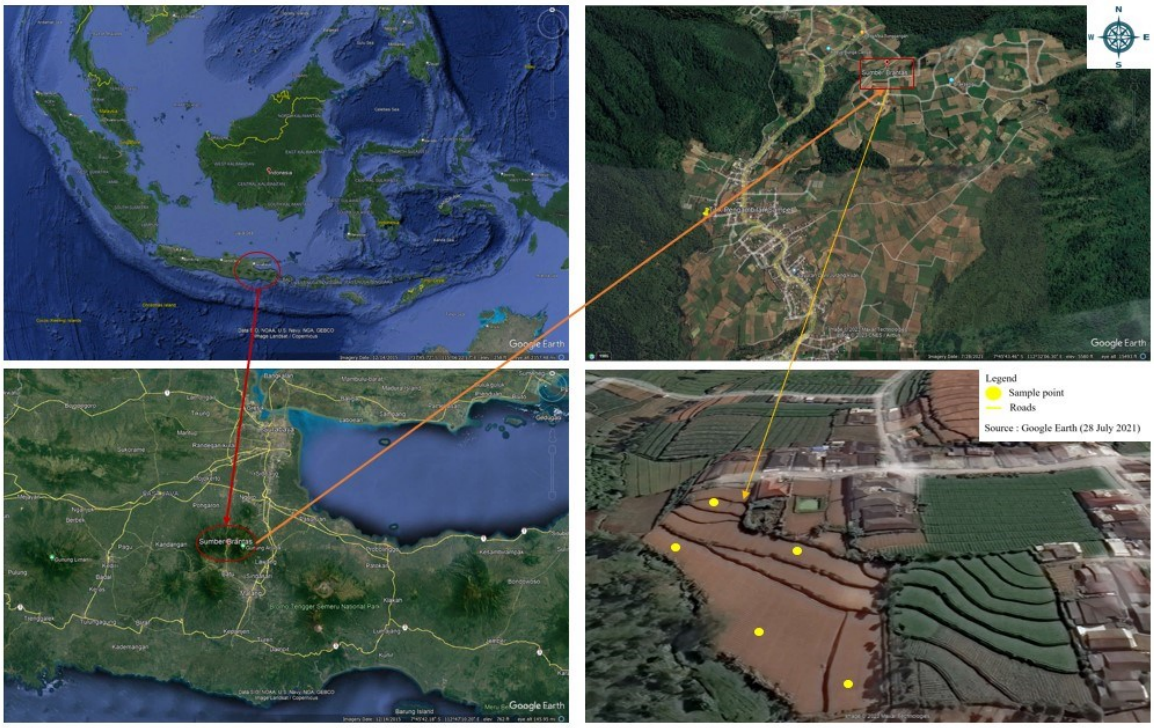

Figure 1. Soil and plant sampling site.

DNA isolation and 16S rRNA sequencing

Selected bacteria were chosen for genomic DNA extraction using Quick-DNA Fungal/Bacterial Miniprep Kit (Zymo Research, D6005). MyTaq Red Mix (Bioline, BIO-25048) was used for PCR amplification. For sample extraction, three loops of bacterial colonies (50-100 mg) were taken for bacterial lysis in ZR BashingBead™ Lysis Tubes (0.1 and 0.5 mm) containing BashingBead™ Buffer. Cell lysis was performed using mechanical lysis in a homogeniser with maximum speed for >5 min. After centrifugation, the supernatant was filtered and subsequently mixed with Genomic Lysis Buffer for DNA binding in a spin column. After DNA binding on the spin column, the column was then washed three times using DNA Pre-Wash Buffer and g-DNA Wash Buffer. The DNA was eluted using 35 µL DNA Elution Buffer. The DNA purity and concentration were measured using Nanodrop.

PCR master mix consisted of (1 x 25 µL) 9.5 dd H_2O, 12.5 MyTaq Red Mix (2x), 20 µM 27F Primer (AGAGTTTGATCMTGGCTCAG), 20 µM 1492R Primer (TACGGYTACCTTGTTACGACTT), and DNA Template, according to the product instruction (Ustiatik et al. 2022). For PCR condition, initial denaturation 95 °C (1 min), denaturation 96 °C (15 sec), annealing 52 °C (30 sec), extension 72 °C (45 sec). Subsequently, the PCR product was subjected to electrophoresis that was performed using 1% agarose gel run in 1x TBE Buffer. One microliter FloroSafe was added to 25 mL of 1% agarose for DNA staining, and then 2 µL PCR products of each sample were transferred to the well of agarose gel and run for 25 minutes at 135 V. For gel cutting, 10 µL FloroSafe was added to 25 mL of 1% agarose, and then the expected band was cut and proceed to gel purification before sequencing. Amplicons of 16S rRNA were purified and sequenced by Apical Scientific, Malaysia. The 16S rRNA sequences were compared with sequences in GenBank using BLAST program. The 16S rDNA sequences were aligned with reference sequences using MEGA V.6 program. Phylogeny trees were constructed and inferred with the neighbour-joining algorithm based on the Tamura-Nei model using 1000 replicates bootstraps.

Soil and plant analysis

Soil and plant samples were analysed for chemical properties that consisted of organic C (Walkey and Black), pH (Electrometry), available P (Bray I and HCl 25% extraction), total Pb of soil (acid mineralization) measured using Atomic Absorbance Spectrophotometry, Thermo-Fisher, USA.

Research design

Pot trial was designed as a completely randomised block design and consited of 9 treatments with 3 replications, i.e.: Pb-contaminated soil as control (KT); Pb-contaminated soil + fertiliser + pesticide application (TP); Pb-contaminated soil + fertiliser + pesticide application + *Bacillus altitudinis* (TA); Pb-contaminated soil + fertiliser + pesticide application + *B. wiedmannii* (TB); Pb-contaminated soil + fertiliser + pesticide application + *B. altitudinis* + *B. wiedmannii* (TAB); Pb-contaminated soil + fertiliser + pesticide application + *Brassica chinensis var. Parachinensis* (TS); Pb-contaminated soil + fertiliser + pesticide application + *B. chinensis* + *B. altitudinis* (TSA); Pb-contaminated soil + fertiliser + pesticide application + *B. chinensis* + *B. wiedmannii* (TSB); Pb-contaminated soil + fertiliser + pesticide application + *B. chinensis* + *B. altitudinis* + *B. wiedmannii* (TSAB). Polybags were filled with 3 kg of soil and base fertiliser was added (NPK 0.45 g/polybag). For pesticide and fertiliser application, ZA

0.3 g/polybag, pesticide abamectin 0.05 mL/polybag, sipermetrin 0.05 mL/polybag, and mancozeb 0.125 g/polybag. Bacteria starter in NB were prepared overnight and then applied 10 mL/polybag (1 x 10^8 CFU/mL).

Data analysis

Statistical analysis was conducted using GenStat 12th Edition. The obtained data were subjected to a data normality test using Shapiro Wilk's test. Abnormal distribution data were subsequently transformed using square root (Sqrt) or logarithm (Log10), and then statistically analysed using a one-way analysis of variance (ANOVA). The difference between treatment means was tested using Tukey Test at 5% significance level.

RESULTS AND DISCUSSION

Study site characteristics

Soil at the sampling site is fertile soil. According to Indonesia Soil Research Agency (2005) criteria soil organic C and available P were high, total N and exchangeable K were moderate. However, soil pH at the study site was acidic (Table 1). Intensive agriculture leads to soil acidification (decrease in pH) (Abure 2022) and is a sign of land degradation in a watershed (Felix et al. 2015). Total Pb in the soil was below the maximum Pb level, which is considered dangerous for agricultural activities (CCME - Canadian Council of Ministers of the Environment 1999). Pb content in the soil was below 140 mg/kg (111.81 mg/kg). However, Pb content in biomass exceeds the permissible level of Pb in vegetables according to Indonesia Food and Drug Agency Regulation Number 5 in 2018 (33.47 mg/kg). The concentration is harmful for human health as Pb is a non-bioessential and hazardous heavy metal (Naik & Dubey 2013).

Table 1. Soil and plant properties at the study site.

Parameter	Unit	Result
pH		5.01
Organic carbon	%	3.45
Total nitrogen	%	0.45
Available phosphorus	mg/kg	18.59
Exchangeable pottasium	me/100g	0.44
Lead content in Soil	mg/kg	111.81**
Lead content in biomass	mg/kg	33.47*
Total Pb-resistant bacteria	CFU/g	6.39 x 10^6

Remark: *Pb concentration exceeds Indonesia Food and Drug Agency Regulation Number 5 in 2018 (<0.2 mg/kg); **Pb concentration below the limit concentration of Pb in the soil for agricultural activities according to CCME - Canadian Council of Ministers of the Environment (1999).

Pb-resistant bacteria population

Pb-resistant indigenous bacteria have been successfully isolated from soil in a horticultural area that applies intensive farming and the total population was 6.39 x 10^6 CFU/g (Table 1). Previously Singh & Hiranmai (2021) reported that bacteria population in soil from different roadsides containing Pb >70 mg/kg is around 10^5-10^6 CFU/g. The isolated Pb-resistant are indigenous (local) bacteria that benefit the environment (Kumar & Gopal 2015). Indigenous bacteria have been reported to be beneficial for biodegradation, N fixation, P solubilisation, and other plant

growth-promoting (PGP) traits to increase soil fertility (Kumar & Gopal 2015; Bhat et al. 2022). However, this study did not test PGP traits of the isolated bacteria.

Pb minimum inhibitory concentration of the isolated Pb-resistant bacteria

Three potential Pb-resistant bacteria (isolate PT-3, PT-5, and PT-8) were tested for Pb resistant to reveal Pb minimum inhibitory concentration (MIC) of the tested bacteria. The result showed that MIC of the tested bacteria was 1000 mg/L. The concentration is higher compared to Manzoor et al. (2019) study, which is only 51 mg/L. The ability of the tested bacteria to survive under harsh environments (Pb presence in the medium) is significantly influenced by Pb concentration ($p<0.05$). High Pb concentrations inhibited bacteria growth, indicated by the width inhibition zone around paper discs containing Pb. There were significantly different among MIC of the tested bacteria ($p<0.05$). Two tested bacteria (isolate PT-3 and PT-5) survived up to 10,000 mg/L with an inhibition zone of less than 3 mm (Figure 2). Bacteria have several Pb-resistant mechanisms under high Pb concentration, i.e., bacterial cell wall adsorption, induction of Pb precipitation in the soil solution, and promoting bacterial community enrichment in producing plant growth-promoting substances (Qin et al. 2023).

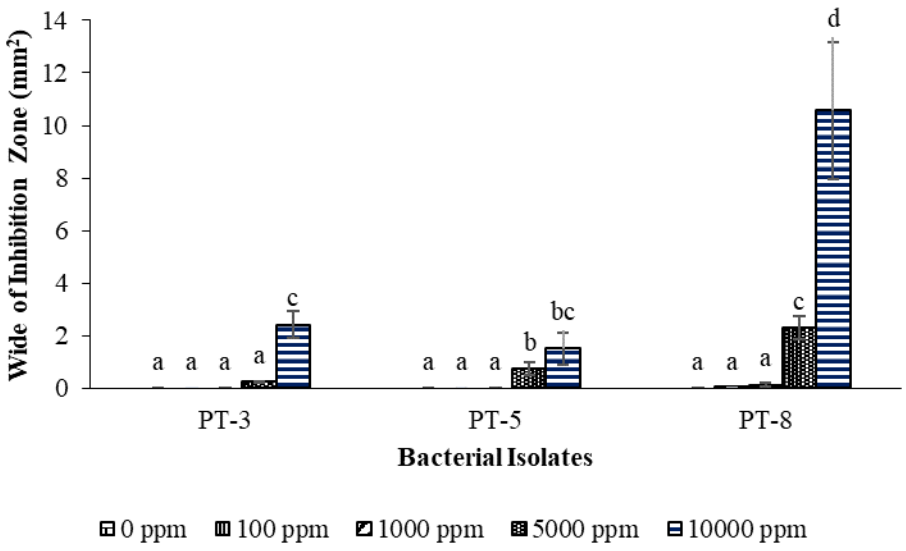

Figure 2. Pb minimum inhibitory concentration of the isolated Pb-resistant bacteria; Means with different letters are significantly different ($p<0.05$) as determined by Tukey's test.

Characteristics of the isolated Pb-resistant bacteria

16S rRNA sequencing result showed that isolate PT-3 is *Bacillus altitudinis* and PT-5 is *Bacillus wiedmannii* (Figure 3). *B. altitudinis* is a bacterium found in high-altitude places (Shivaji et al. 2006), such as the sampling site (intensive horticulture farming lands) at 953 m asl. The bacterium is also endophytic with plant growth-promoting traits (Zhang et al. 2021). The bacterium has also been reported to have the ability to lignocellulose degradation with many biotechnological applications, such as biofuels and biorefineries (Dar et al. 2021). Pb-resistance of *B. altitudinis* is related to the Stress-Alleviating Properties of the bacterium (Yue et al. 2019). The bacterium can detoxify Pb, or reduce the toxicity level of Pb by secreting enzymes or forming biofilms. A past study found that *B. altitudinis* can alleviate salinity and low phosphorus stress by producing en-

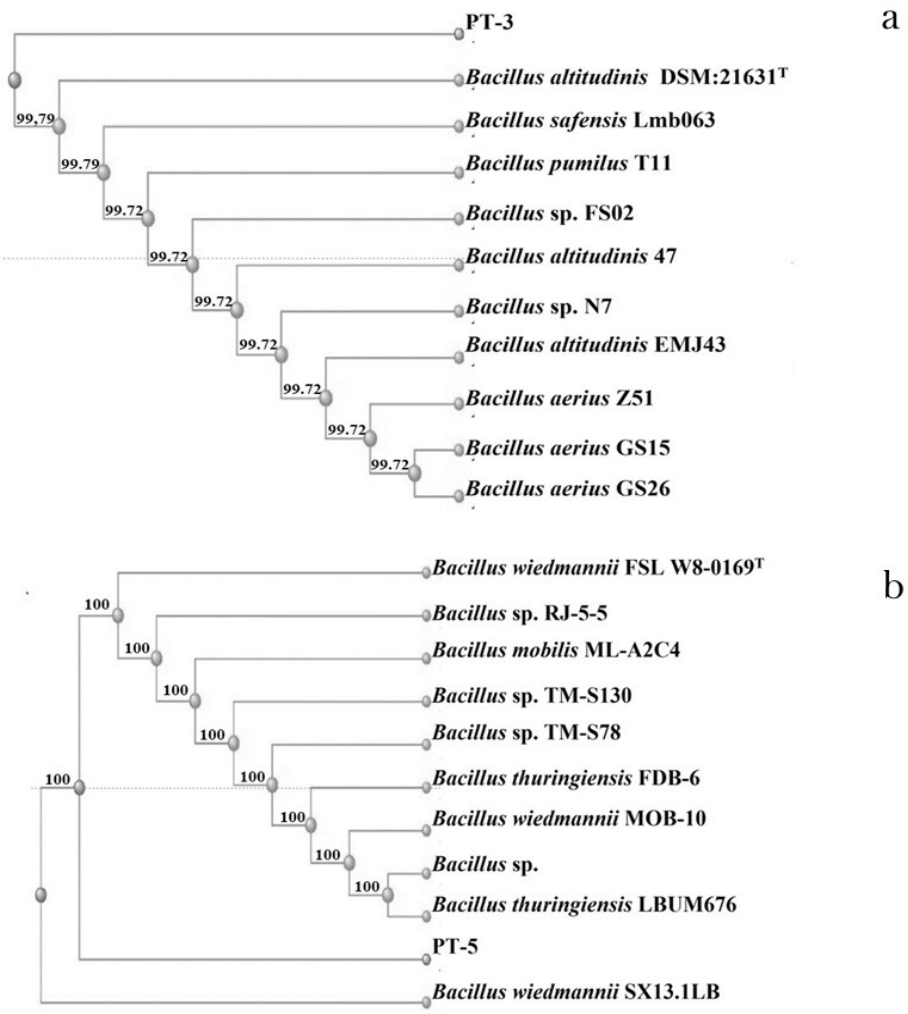

Figure 3. Phylogeny tree of the isolated Pb-resistant bacteria: a) *Bacillus altitudinis*, and; b) *Bacillus wiedmannii*.

zymes and biofilm (Yue et al. 2019). For isolate PT-5, *B. wiedmannii* is a psychrotolerant bacterium with a minimum growth temperature of up to 5 °C (Miller et al. 2016). The bacterium has agricultural importance as a biocontrol of root-knot nematode (Fallahzadeh-Mamaghani et al. 2023). Past studies revealed that the bacterium is tolerant to drought and heavy metals, also exhibits plant growth-promoting traits (Kalkan 2022; Fallahzadeh-Mamaghani et al. 2023). Plant growth-promoting traits are believed as tolerant mechanisms of bacteria under abiotic stress (Kumar et al. 2020), such as salinity, drought, and heavy metals. Pb resistance mechanism includes enhanced siderophore production, cell morphology alteration, extracellular sequestration, biosorption, precipitation, and intracellular bioaccumulation (Naik & Dubey 2013).

The effect of Pb-resistant bacteria inoculation on plant growth and Pb residue in the soil

The number of leaves

Pb-resistant bacteria consortium significantly increased the number of *B. chinensis* leaves ($p<0.05$; see Figure 4) by up to 12% compared to *B. chinensis* without Pb-resistant bacteria application. The increased number of leaves was found 3 and 4 weeks after planting. A similar result with the shoot length of *B. chinensis*, the highest number of leaves was recorded at TSAB treatment. A similar finding has been reported by Han et al. (2020) that Pb-resistant bacteria not only reduce Pb absorbed by plants but also increase plants' shoot length and the number of leaves.

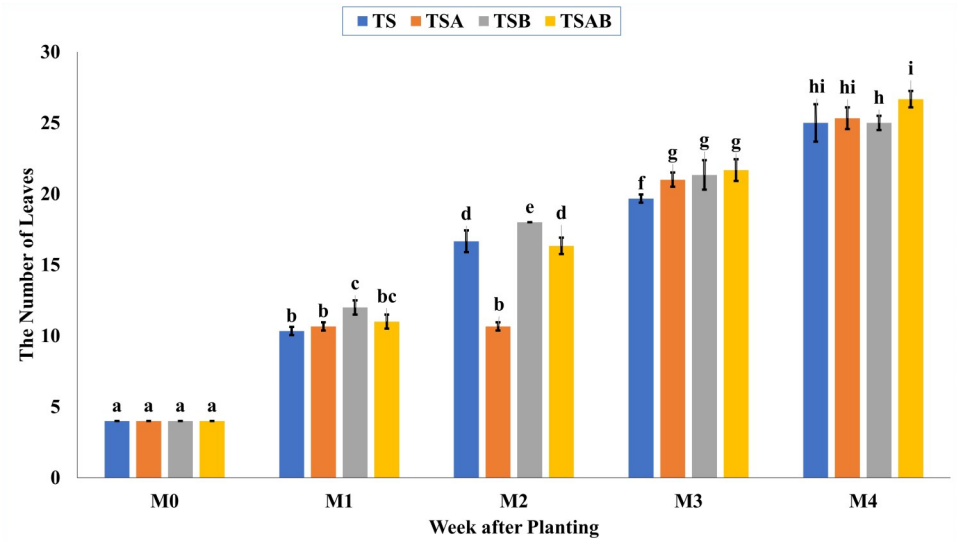

Figure 4. Effect of Pb-resistant bacteria inoculation on the number of *Brassica chinensis* leaves; Means with different letters are significantly different ($p<0.05$) as determined by Tukey's test.

Plant dry weight

Pb-resistant bacteria consortium significantly increased *B. chinensis* dry weight ($p<0.05$; see Figure 5) compared to *B. chinensis* without Pb-resistant bacteria application. *B. wiedmannii* had a similar effect as the Pb-resistant bacteria consortium (*B. altitudinis* + *B. wiedmannii)* on *B. chinensis* dry weight when applied as a single isolate ($p<0.05$). The highest *B. chinensis* dry weight was found at TSAB treatment. The dry weight increased by 30-35% after Pb-resistant bacteria inoculation. The results of this study agree with Najm-Ul-seher et al. (2021) that Pb-resistant bacteria can be used to improve the growth of *B. chinensis* where Pb pollution is a problem.

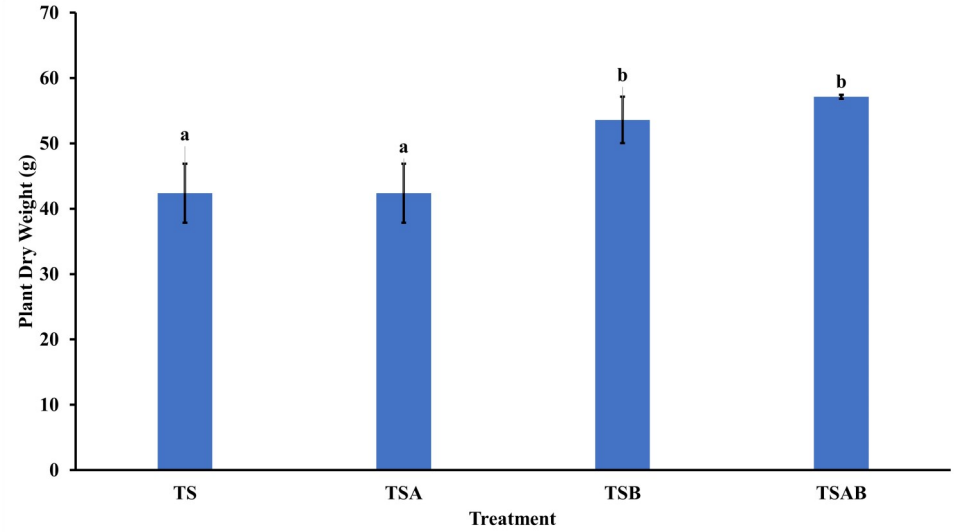

Figure 5. Effect of Pb-resistant bacteria inoculation on *Brassica chinensis* dry weight; Means with different letters are significantly different ($p<0.05$) as determined by Tukey's test.

Pb residue in the soil

This study revealed that intensive agriculture increases heavy metal concentrations in agricultural soil, especially from excessive fertiliser and pesticide application. Fertiliser and pesticide application on Pb-contaminated soil increase Pb residue in the soil by up to 0.9% (0.08 mg/kg) during the pot trial (Figure 6). Pb content will remain in the soil if

there are no further measures because Pb is an inert heavy metal (Alengebawy et al. 2021). Pb-resistant bacteria application significantly decreased Pb residue in the soil ($p<0.05$). The residues were 12 to 63% lower than untreated Pb-contaminated soil (control). Pb residues decreased around 55-88% in the treatment of Pb-resistant bacteria and *B. chinensis*, either applied as a single isolate or consortium. The lowest Pb residue was found on TSB (Pb-contaminated soil, *B. chinensis* and *B. wiedmannii*). The treatment reduced Pb residue by up to 88% compared to the control; the remaining Pb residue was only 10 mg/kg (Figure 6).

The low Pb residue in the soil on TSB treatment was due to *B. wiedmannii* adsorb Pb, as a previous study reported that *B. cereus*, which is closely related to *B. wiedmannii* can absorb Pb up to 96.58% through several mechanisms such as indole-3-acetic acid (IAA) secretion and inorganic phosphorus (P) dissolution (Miller et al. 2016; Li et al. 2023). Besides Pb adsorption ability, the bacterium is a biocontrol agent of the root-knot nematode (*Meloidogyne arenaria*) (Fallahzadeh-Mamaghani et al. 2023).

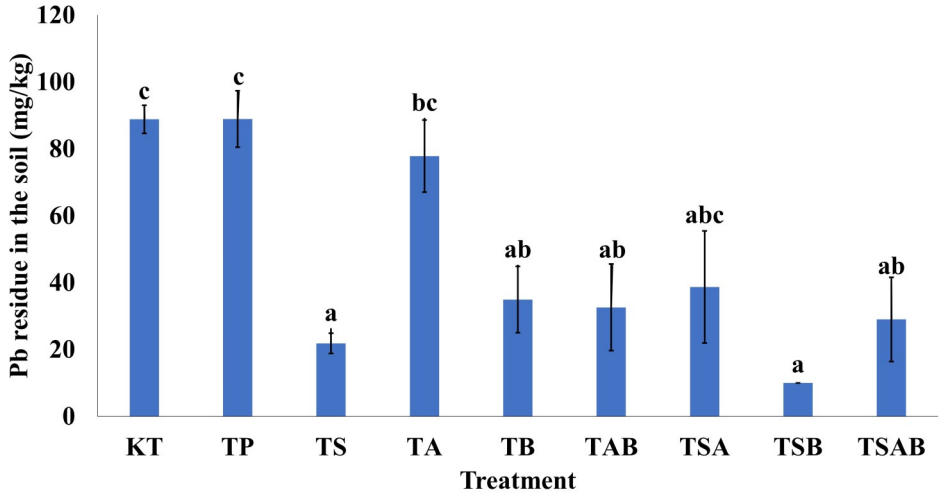

Figure 6. Effect of Pb-resistant bacteria inoculation on Pb residue in the soil; Means with different letters are significantly different ($p<0.05$) as determined by Tukey's test.

Effect of Pb-resistant bacteria inoculation on soil nutrients

Soil total-N

Pb-resistant bacteria inoculation significantly increased soil total N ($p<0.05$; Figure 7). Total N was significantly higher after inoculation of Pb-resistant bacteria consortium (TAB) compared to other treatments ($p<0.05$). This study noted that Pb-resistant bacteria inoculation increased total N from 4% to 36% compared to the control. Pb-resistant bacteria application on the soil without *B. chinensis* had significantly higher total N due to N in the soil absorbed by *B. chinensis*. The claim is proven by the low total N content on the soil planted with *B. chinensis*. Total N was 8-12% lower on the treatment with *B. chinensis* than control. The increase of total N content in the soil might be due to Pb-resistant bacteria consortium application leading to a symbiotic mutualism between these bacteria in fixing free N from the atmosphere. When these bacteria are applied to soil, they can form a symbiotic relationship with plants. The bacteria provide the plant with N, and the plant provides the bacteria with a safe place to live and nutrients. This can significantly improve crop yields (Kamaruzzaman et al. 2020; Roszak et al. 2021).

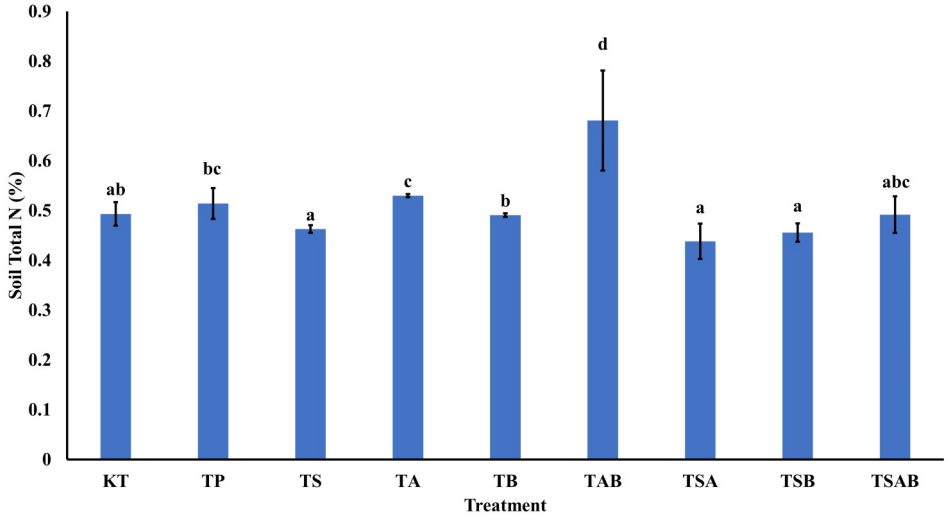

Figure 7. Effect of Pb-resistant bacteria inoculation on total N of Pb-contamiated soil; Means with different letters are significantly different ($p<0.05$) as determined by Tukey's test.

Soil available-P

The consortium of Pb-resistant bacteria application significantly increased available P on the Pb-contaminated soil ($p<0.05$; see Figure 8). The available P was increased up to 73% compared to the control. This finding indicates that Pb-resistant bacteria not only resistant to high concentrations of Pb in the soil but also exhibit P solubilising activity. A similar finding has been reported by Teng et al. (2019) that phosphate solubilising bacteria (PSB) were isolated from heavy metal-contaminated soils and had potentials for Pb immobilisation.

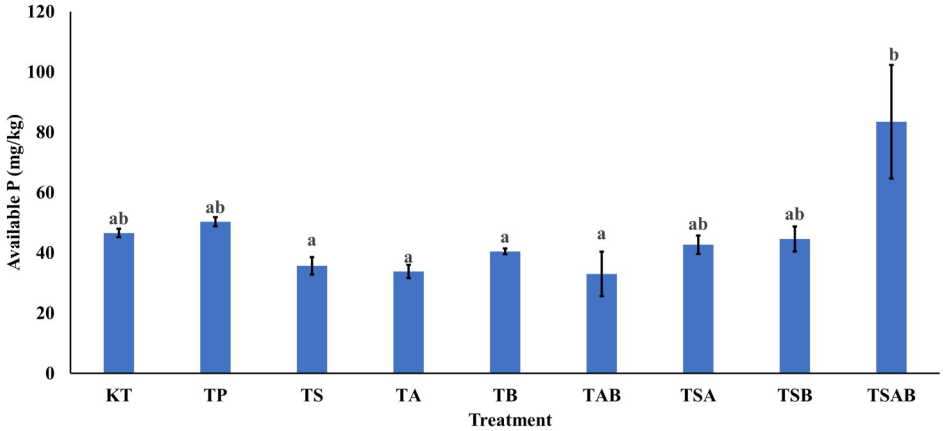

Figure 8. Effect of Pb-resistant bacteria inoculation on available P of Pb-contamiated soil; Means with different letters are significantly different ($p<0.05$) as determined by Tukey's test.

Soil exchangeable-K

Pb-resistant bacteria inoculation significantly influenced exchangeable K of Pb-contaminated soil ($p<0.05$, see Figure 9). Soil Exchangebale K increased from 85% to 200% after Pb-resistant bacteria inoculation, whether as a single isolate or consortium. However, on the treatment of Pb resistant bacteria and *B. chinensis* exchangeable K only increased 57% as K is an essential nutrient that is uptake by plants. This study agree with previous study that Pb-resistant bacteria change soluble-exchangeable fraction on soil nutrients in heavy metals-contaminated soil (Boechat et al. 2018).

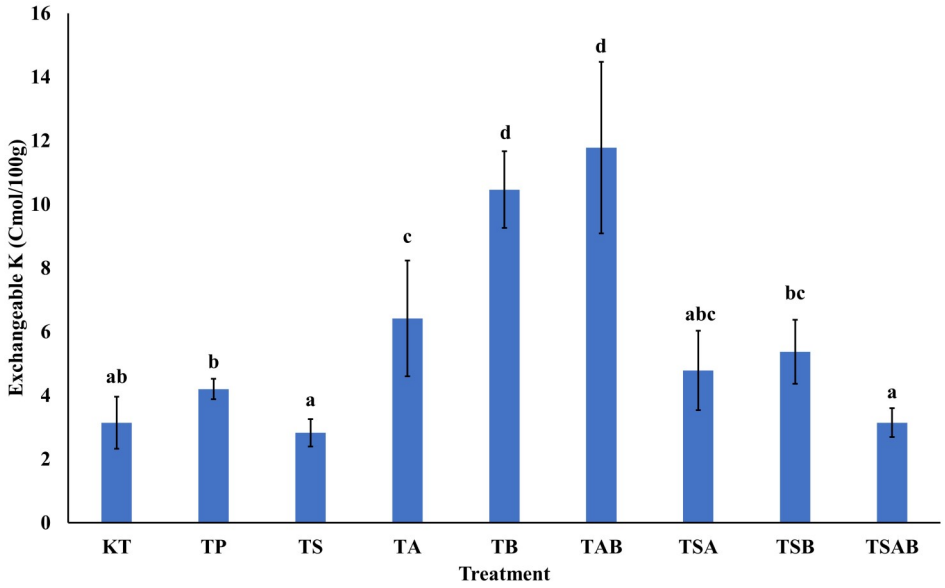

Figure 9. Effect of Pb-resistant bacteria inoculation on exchangeable K of Pb-contamiated soil; Means with different letters are significantly different ($p<0.05$) as determined by Tukey's test.

CONCLUSION

Intensive agriculture, frequent application of inorganic fertilisers and pesticides, lead to increase Pb content in the soil and food crops biomass. Bacteria isolated from Pb-contaminated soil exhibited Pb resistance (*Bacillus wiedmannii* and *Bacillus altitudinis*). The bacteria resistant to Pb up to 10,000 mg/L. Inoculation of the bacteria increased plant growth by increasing the number of leaves and dry weight of *Brassica chinensis* (12% and 35%, respectively). The bacteria reduced Pb residue in the soil by up to 88%. Moreover, the bacteria increased soil nutrients such as total N (12%), available P (73%), and exchangeable K (200%). The bacteria have the potential for bioremediation of Pb-contaminated soils in the field, as the bacteria can reduce Pb in the soil, thus preventing Pb uptake by food crops (such as *B. chinensis*), which is good for food safety and environmental sustainability.

AUTHORS CONTRIBUTION

B.L.S.P. designed the research, collected and analysed the data, wrote the initial draft of manuscript; R.U.: designed the research, analysed the data, project leader, supervised all the processes, wrote the manuscript; Y.N.: reviewed the manuscript;

ACKNOWLEDGMENTS

The study was funded by Faculty of Agriculture, Brawijaya University, through Hibah PNBP FP No 4108.10/UN10.F04/PN/2022.

CONFLICT OF INTEREST

There is no conflict of interest regarding the research or the research funding.

REFERENCES

Abure, T., 2022. Status of Soil Acidity under Different Land Use Types and Soil Depths: The Case of Hojje Watershed of Gomibora District, Hadiya Zone, Southern Ethiopia. *Applied and Environmental Soil Science*, 2022, 7060766. doi: 10.1155/2022/7060766.

Alengebawy, A. et al., 2021. Heavy metals and pesticides toxicity in agricultural soil and plants: Ecological risks and human health implications. *Toxics*, 9(3), pp.1–34. doi: 10.3390/toxics9030042.

Alexandratos, N. & Bruinsma, J., 2012. *WORLD AGRICULTURE TOWARDS 2030/2050*, Rome. doi: 10.1126/science.abo7429.

Astuti, R.D.P., Mallongi, A. & Rauf, A.U., 2021. Risk identification of Hg and Pb in soil: a case study from Pangkep Regency, Indonesia. *Soil Science Annual*, 72(1), 135394. doi: 10.37501/soilsa/135394.

Bhat, B.A. et al., 2022. The role of plant-associated rhizobacteria in plant growth, biocontrol and abiotic stress management. *Journal of Applied Microbiology*, 133(5), pp.2717–2741. doi: 10.1111/jam.15796.

Bisht, N. & Chauhan, P.S., 2020. Excessive and Disproportionate Use of Chemicals Cause Soil Contamination and Nutritional Stress. In *Soil Contamination-Threats and Sustainable Solutions*. InTech. doi: 10.5772/17205

Boechat, C.L. et al., 2018. Metal-resistant rhizobacteria change soluble-exchangeable fraction in multi-metal contaminated soil samples. *Revista Brasileira de Ciencia do Solo*, 42, e0170266. doi: 10.1590/18069657rbcs20170266.

CCME - Canadian Council of Ministers of the Environment, 1999. *Canadian Soil Quality Guidelines for the Protection of Environmental and Human Health*, Available at: http://energy.alberta.ca/BioEnergy/pdfs/HeavyMetalReport.pdf%5Cnhttp://ceqg-rcqe.ccme.ca/download/en/269.

Dar, M.A. et al., 2021. Valorization potential of a novel bacterial strain, *Bacillus altitudinis* RSP75, towards lignocellulose bioconversion: An assessment of symbiotic bacteria from the stored grain pest, *Tribolium castaneum*. *Microorganisms*, 9(9), 1952. doi: 10.3390/microorganisms9091952.

Defarge, N., Spiroux de Vendômois, J. & Séralini, G.E., 2018. Toxicity of formulants and heavy metals in glyphosate-based herbicides and other pesticides. *Toxicology Reports*, 5(December 2017), pp.156–163. doi: 10.1016/j.toxrep.2017.12.025.

Dixit, R. et al., 2015. Bioremediation of Heavy Metals from Soil and Aquatic Environment: An Overview of Principles and Criteria of Fundamental Processes. *Sustainability*, 7(2015), pp.2189–2212. doi: 10.3390/su7022189.

Fallahzadeh-Mamaghani, V. et al., 2023. Possible mechanisms of action of *Bacillus wiedmannii* AzBw1, a biocontrol agent of the root-knot nematode, *Meloidogyne arenaria*. *Egyptian Journal of Biological Pest Control*, 33, 28. doi: 10.1186/s41938-023-00668-1.

Felix, K.A. et al., 2015. Assessment of the level of soil degradation in three watersheds affected by intensive farming practices in Benin. *Journal of Experimental Biology and Agricultural Sciences*, 3(6), pp.529–540. doi: 10.18006/2015.3(6).529.540.

Hafeez, F. et al., 2018. Isolation and characterization of a lead (Pb) tolerant *Pseudomonas aeruginosa* strain HF5 for decolorization of reactive red-120 and other azo dyes. *Annals of Microbiology*, 68(12), pp.943–952. doi: 10.1007/s13213-018-1403-6.

Han, H. et al., 2020. Heavy metal-immobilizing bacteria increase the biomass and reduce the Cd and Pb uptake by pakchoi (*Brassica chinensis* L.) in heavy metal-contaminated soil. *Ecotoxicology and Environmental Safety*, 195, 110375. doi: 10.1016/j.ecoenv.2020.110375.

Indonesia Soil Research Agency, 2005. *Analisis Kimia Tanah, Tanaman, Air dan Pupuk*, Balai Penelitian Tanah, Departemen Pertanian.

Kalkan, S., 2022. Heavy metal resistance of marine bacteria on the sediments of the Black Sea. *Marine Pollution Bulletin*, 179, 113652. doi: 10.1016/j.marpolbul.2022.113652.

Kamaruzzaman, M.A. et al., 2020. Characterisation of Pb-resistant plant growth-promoting rhizobacteria (PGPR) from Scirpus grossus. *Biocatalysis and Agricultural Biotechnology*, 23, 101456. doi: 10.1016/j.bcab.2019.101456.

Kumar, A. et al., 2020. Plant Growth-Promoting Bacteria: Biological Tools for the Mitigation of Salinity Stress in Plants. *Frontiers in Microbiology*, 11, 1216. doi: 10.3389/fmicb.2020.01216.

Kumar, B.L. & Gopal, D.V.R.S., 2015. Effective role of indigenous microorganisms for sustainable environment. *3 Biotech*, 5(6), pp.867–876. doi: 10.1007/s13205-015-0293-6.

Kumar, S. et al., 2022. Lead (Pb) Contamination in Agricultural Products and Human Health Risk Assessment in Bangladesh. *Water, Air, & Soil Pollution*, 233, 257. doi: 10.1007/s11270-022-05711-9.

Li, Q. et al., 2023. Mechanism of lead adsorption by a *Bacillus cereus* strain with indole-3-acetic acid secretion and inorganic phosphorus dissolution functions. *BMC Microbiology*, 23(1), 57. doi: 10.1186/s12866-023-02795-z.

Li, X. et al., 2016. Bioremediation of lead contaminated soil with *Rhodobacter sphaeroides*. *Chemosphere*, 156, pp.228–235. doi: 10.1016/j.chemosphere.2016.04.098.

Mallongi, A. et al., 2022. Identification source and human health risk assessment of potentially toxic metal in soil samples around karst watershed of Pangkajene, Indonesia. *Environmental Nanotechnology, Monitoring and Management*, 17, 100634. doi: 10.1016/j.enmm.2021.100634.

Manzoor, M. et al., 2019. Metal tolerance of arsenic-resistant bacteria and their ability to promote plant growth of *Pteris vittata* in Pb-contaminated soil. *Science of the Total Environment*, 660, pp.18–24. doi: 10.1016/j.scitotenv.2019.01.013.

Mariyono, J., 2019. Stepping up from subsistence to commercial intensive farming to enhance welfare of farmer households in Indonesia. *Asia and the Pacific Policy Studies*, 6(2), pp.246–265. doi: 10.1002/app5.276.

Miller, R.A. et al., 2016. *Bacillus wiedmannii* sp. nov., a psychrotolerant and cytotoxic *Bacillus cereus* group species isolated from dairy foods and dairy environments. *International Journal of Systematic and Evolutionary Microbiology*, 66(11), pp.4744–4753. doi: 10.1099/ijsem.0.001421.

Naik, M.M. & Dubey, S.K., 2013. Lead resistant bacteria: Lead resistance mechanisms, their applications in lead bioremediation and biomonitoring. *Ecotoxicology and Environmental Safety*, 98, pp.1–7. doi: 10.1016/j.ecoenv.2013.09.039.

Najm-Ul-seher et al., 2021. Lead-tolerant Bacillus strains promote growth and antioxidant activities of spinach (*Spinacia oleracea*) treated with sewage water. *Agronomy*, 11(12), 2482. doi: 10.3390/agronomy11122482.

Ojuederie, O.B. & Babalola, O.O., 2017. Microbial and plant-assisted bioremediation of heavy metal polluted environments: A review. *International Journal of Environmental Research and Public Health*, 14(12), 1504. doi: 10.3390/ijerph14121504.

Qin, S. et al., 2023. Improving radish phosphorus utilization efficiency and inhibiting Cd and Pb uptake by using heavy metal-immobilizing and phosphate-solubilizing bacteria. *Science of the Total Environment*, 868, 161685. doi: 10.1016/j.scitotenv.2023.161685.

Rosariastuti, R. et al., 2019. Soil Bioremediation of lead (Pb) polluted paddy field using Mendong (*Fimbristylis globulosa*), *Rhizobium* sp. I3, compost, and inorganic fertilizer. *IOP Conference Series: Earth and Environmental Science*, 230, 012014. doi: 10.1088/1755-1315/230/1/012014.

Roszak, M. et al., 2021. Development of an autochthonous microbial consortium for enhanced bioremediation of PAH-contaminated soil. *International Journal of Molecular Sciences*, 22(24), 13469. doi: 10.3390/ijms222413469.

Sánchez-Bayo, F., 2021. Indirect effect of pesticides on insects and other arthropods. *Toxics*, 9(8), 177. doi: 10.3390/toxics9080177.

Scotti, R. et al., 2015. Organic Amendments as Sustainable Tool to Recovery Fertility in Intensive Agricultural Systems. *Journal of Soil Science and Plant Nutrition*, 15(2), pp.333–52. doi: 10.4067/s0718-95162015005000031.

Sharma, A. et al., 2019. Worldwide pesticide usage and its impacts on ecosystem. *SN Applied Sciences*, 1, 1446. doi: 10.1007/s42452-019-1485-1.

Shivaji, S. et al., 2006. *Bacillus aerius* sp. nov., *Bacillus aerophilus* sp. nov., *Bacillus stratosphericus* sp. nov. and *Bacillus altitudinis* sp. nov., isolated from cryogenic tubes used for collecting air samples from high altitudes. *International Journal of Systematic and Evolutionary Microbiology*, 56(7), pp.1465–1473. doi: 10.1099/ijs.0.64029-0.

Singh, S. & Hiranmai, R.Y., 2021. Monitoring and molecular characterization of bacterial species in heavy metals contaminated roadside soil of selected region along NH 8A, Gujarat. *Heliyon*, 7(11), e08284. doi: 10.1016/j.heliyon.2021.e08284.

Statistics Indonesia, 2018, 'Hasil survei pertanian antar sensus (SUTAS) 2018' in *Badan Pusat Statistik*, viewed from https://www.bps.go.id/publication/2019/01/02/c7cb1c0a1db444e2cc726708/ hasil-survei-pertanian-antar-sensus--sutas--2018.html

Teng, Z. et al., 2019. Characterization of phosphate solubilizing bacteria isolated from heavy metal contaminated soils and their potential for lead immobilization. *Journal of Environmental Management*, 231, pp.189–197. doi: 10.1016/j.jenvman.2018.10.012.

Ustiatik, R. et al., 2022. Mercury resistance and plant growth promoting traits of endophytic bacteria isolated from mercury-contaminated soil. *Bioremediation Journal*, 26(3), pp.208–227. doi: 10.1080/10889868.2021.1973950.

Yue, Z. et al., 2019. Microbiological insights into the stress-alleviating property of an endophytic *Bacillus altitudinis* WR10 in wheat under low-phosphorus and high-salinity stresses. *Microorganisms*, 7(11), 508. doi: 10.3390/microorganisms7110508.

Zhang, D. et al., 2021. Endophytic *Bacillus altitudinis* Strain Uses Different Novelty Molecular Pathways to Enhance Plant Growth. *Frontiers in Microbiology*, 12, 692313. doi: 10.3389/fmicb.2021.692313.

Zhu, X. et al., 2022. Bioremediation of lead-contaminated soil by inorganic phosphate-solubilizing bacteria immobilized on biochar. *Ecotoxicology and Environmental Safety*, 237, 113524. doi: 10.1016/j.ecoenv.2022.113524.

Journal of Tropical Biodiversity and Biotechnology
Volume 09, Issue 01 (2024): jtbb78019
DOI: 10.22146/jtbb.78019

Research Article

Identifying Single Nucleotide Polymorphisms (SNPs) in *OsFER1* and *OsFER2* Genes Linked to Iron Accumulation in Pigmented Indonesian Rice (*Oryza sativa* L.)

Apriliana Pratiwi[1#], Rizka Fahma Bassalamah[1#], I Sabila Elvani[1], Alfino Sebastian[2], Yekti Asih Purwestri[1,2*]

1)Department of Tropical Biology, Faculty of Biology, Universitas Gadjah Mada, Yogyakarta 55281, Indonesia
2)Research Center for Biotechnology, Universitas Gadjah Mada, Yogyakarta 55281, Indonesia
* Corresponding author, email: yekti@ugm.ac.id
# Co-first author

Keywords:
Ferritin
iron
OsFER
Oryza sativa
SNPs
Submitted:
26 September 2022
Accepted:
11 October 2023
Published:
19 February 2024
Editor:
Furzani Binti Pa'ee

ABSTRACT

Iron (Fe) is an essential micronutrient for the well-being of plants, animals, and bacteria. In plants, iron plays a pivotal role in a myriad of metabolic processes, encompassing redox reaction, photosynthesis, respiration, chlorophyll synthesis, and nitrogen fixation. For humans, iron is indespensable for several metabolic functions, particularly in the synthesis of haemoglobin. Iron deficiency can lead to health issues on a global scale, therefore identifying key crops, such as rice for providing sufficient iron in diet intake is very important. In rice, the maintenance of iron homeostasis is orchestrated by various genes, with *OsFER1* and *OsFER2* acting as iron accumulator genes in leaves, stems, flowers, and grains. The primary objective of this study was to ascertain the single nucleotide polymorphisms (SNP) in the *OsFER1* and *OsFER2* and to assess the iron content in Indonesian local rice cultivars. To achieve this, we examined partial sequences of *OsFER1* and *OsFER2* to identify SNPs in the Indonesian rice cultivars used (Cempo Ireng, Pari Ireng, Hitam Kalsel, Merah Pari Eja, and Ciherang). Concurrently, the iron content in the seeds was quantified using Atomic Absorption Spectrophotometry (AAS). The analysis revealed that the *OsFER1* gene sequence, specifically exon 5, exhibited a SNP in the form of a transition. In contrast, the *OsFER2* gene sequences, specifically in intron 2 displayed SNPs in the form of insertions. Notably, the iron content in the seeds was highest in Cempo Ireng (black rice), while it was lowest in Merah Pari Eja (red rice) and Ciherang (non-pigmented rice). Importantly, the identified SNPs in these partial gene sequences did not exert any discernible influence on iron levels or the formation of ferritin protein.

Copyright: © 2024, J. Tropical Biodiversity Biotechnology (CC BY-SA 4.0)

INTRODUCTION

Iron (Fe) plays a vital role for plants, animals, and bacteria. In plants, iron is involved in various metabolic reactions, including electron transport chain redox processes, photosynthesis, respiration reactions, chlorophyll synthesis, and nitrogen fixation (Stein et al. 2009; Briat et al. 2010). Iron deficiency in plants can lead to chlorosis in the leaves, disrupting biosynthetic and photosynthetic processes due to low iron concentration. This chlorosis is especially concerning in young leaves, which act as strong absorbers, and require more iron compared to older leaves

(Kobayashi et al. 2019). On the other hand, excess iron can be toxic to plant cells as it can generate reactive hydroxyl radicals through the Fenton reaction (Liang 2022). Consequently, maintaining iron homeostasis in plants, particularly in rice, is essential. Achieving iron homeostasis in plants involves a dynamic process that employs proteins and small organic molecules to extract metals from the soil, transport them within plant tissues, sequester them intracellularly, act as buffers, and store excess iron (Briat et al. 2010).

The genes responsible for regulating the transport and accumulation of iron play a pivotal role in internal iron regulation within plants. In terms of iron accumulation, particularly in grain storage, *OsFER1* and *OsFER2* genes are of utmost importance (Briat et al. 2010). Plant cells typically store ferritin protein, often referred to as phytoferritin, in plastids and mitochondria. Around 80% of the iron content in leaves is stored in chloroplasts, while in seeds it is stored in leucoplasts and amyloplasts (Mauseth 2021). Remarkably, ferritin protein in plants has the capacity to store up to 4,500 iron atoms (Helmyati et al. 2014). Ferritin protein enables rice plants to withstand iron stress, enabling them to accumulate more iron by tolerating high Fe concentrations in the leaves. Higher ferritin gene expression was found in rice that was resistant to iron (Silveira et al. 2009).

Genotypic diversity among rice cultivars can be genetically identified by comparing and analyzing partial ferritin gene nucleotide sequences, examining the expression of ferritin protein-coding genes, and detecting polymorphisms (Utami et al. 2009; Herlinda et al. 2013). The analysis of Single Nucleotide Polymorphisms (SNPs) aims to generate molecular markers capable of distinguishing between rice cultivar genotypes. SNPs within the nucleotide sequences of the rice ferritin genes provide valuable information of the iron (Fe) content of rice and is useful in plant breeding programs (Collard & Mackill 2008). Research by Stein et al. (2009) revealed differences in the expression of *OsFER1* and *OsFER2* genes, while the study by Paul et al. (2012) demonstrated that overexpression of *OsFER2* led to increased level of Fe and Zn in transgenic plants. This study aims to establish a correlation between iron levels in rice grains form Indonesian rice cultivars and the presence of SNPs the sequences of each *OsFER1* and *OsFER2* gene.

MATERIALS AND METHODS

Materials

The study utilized five local Indonesian rice cultivars: Ciherang, Merah Pari Eja, Hitam Kalsel, Cempo Ireng, and Pari Ireng (Table 1). The process sterilization and seed planting involved the use of various substances, including 5% sodium hypochlorite (NaClO), distilled water (aquadest), soil, goat manure, insecticide, fungicide, Nitrogen Phosphorus Potassium (NPK) fertilizer, Sulfur Phosphate (SP36) fertilizer, and Potassium Chloride (KCl) fertilizer. To prepare samples for iron content analysis through Atomic Absorption Spectrophotometry, we initially treated rice seeds with nitric acid (HNO_3), perchloric acid ($HClO_4$), and distilled water, following the metho described by Elango et al. (2021). Genomic DNA isolation was accomplished through a process that involved liquid nitrogen, Tris Boric EDTA (TBE) buffer, Na_2EDTA, 10% sodium dodecyl sulfate (SDS), sodium chloride (NaCl), isopropyl alcohol, ethanol (EtOH), and double-distilled water (ddH_2O). Subsequent to genomic DNA isolation, PCR amplification was carried out using GoTaq® Green Master Mix (Promega), along with forward and reverse primers (Table 2), Nuclease Free Water (NFW), and isolated genomic DNA sam-

ples.These primers were in silico designed via Primer3Plus, employing a DNA template sourced from the National Center for Biotechnology Information (NCBI) at https://www.ncbi.nlm.nih.gov/gene/9269178, with a target product size of 500 base pairs. The primer design was validated using Primer-BLAST, PCR Primer Stats, Oligo Calculator, and PrimerDimer software. Finally, the results of DNA genome isolation and amplification were evaluated using the electrophoresis method. The process involved materials such as a 1.2% agarose gel, 1x TBE buffer, a DNA ladder marker and ethidium bromide (EtBr).

Table 1. Rice sample cultivars used in this study.

No.	Cultivar	Origin	Pigment type
1.	Ciherang	Jawa Barat	White
2.	Merah Pari Eja	Gowa	Red
3.	Hitam Kalsel	Kalimantan Selatan	Black
4.	Cempo Ireng	Jawa Tengah	Black
5.	Pari Ireng	Sleman	Black

Table 2. Primers used for gene amplification in this study.

Gene	Primer	Sequence
OsFER1	Forward	TAGGAGAAAAGACACTGTGC
	Reverse	TAGCACACAGTAAGCAGAAG

Gene	*OsFER2*	
Product Size	582 bp	
Primer	**Forward**: 5'CCTTAGCTT-GTCATCCGTAG 3'	**Reverse**: 5'CAGACTAGCACACAG-TAAGG 3'
Start	1224	1805
Length	20 bp	20 bp
Tm	55.4 °C	55.2 °C
GC	50 %	50 %

Methods

Planting, cultivating and harvesting

The planting medium was prepared by homogenizing soil and goat manure in a 2:1 ratio. During the planting phase, rice pants were provided with nutrition through weekly fertilizer applications commencing at 30 days after planting (DAP). Harvesting was conducted at 78 DAP, where rice leaves were harvested by cutting and preserved at -20°C. For rice grains, they were harvested when they reached ripeness, characterized by their yellow-brown color and when approximately 50% of the flag leaves had turned yellow. The harvested grains were dried in an oven at a temperature of 30˚C to 40˚C for approximately three days and subsequently stored at 20˚C.

Iron concentration analysis

Samples of rice grains from each cultivar were weighed with a precision of ±3-5 grams. These samples were subsequently blended until achieving powder. Following this, the samples were homogenized and reweighed

with an accuracy of ±2 grams for each cultivar. They were then treated with a mixture of 15 mL of HNO_3 and $HClO_4$. The destruction was carried out on the heating plate until near to dryness, after which 10 mL of distilled water was added. The resulting solution was filtered into a 25 mL flask and topped up with distilled water to reach the mark. Finally, the prepared samples were subjected to iron (Fe) level anylysis using and Atom Absorption Spectrophotometer (AAS).

OsFER1 and *OsFER2* gene sequence analysis

The isolation of genomic DNA was carried out using an extraction buffer from 1.21 grams of Tris mixed with 5 mL of Na2EDTA (0.5M; pH 8) and 2.92 grams of NaCl. The pH of the mixture was adjusted to 8, followed by the addition of 100 mL of sterile distilled water. Next, 100 mg of leaf tissue was ground into a fine powder using liquid nitrogen. The leaf powder was subsequently transferred into a 1.5 mL microtube, and 500 µL of the extraction buffer was added to the tube. The sample was homogenized using a vortex. To this homogenized mixture, 66 µL of 10% SDS reagent was introduced, and the tube was then centrifuged at 13,000 rpm for 1 minute at 4 °C. Approximately 400 µL of the resulting supernatant was transferred to a new tube, and 400 µL of isopropyl alcohol was added. DNA precipitation was achieved by centrifugation at 13,000 rpm for 15 minutes at 4 °C, after which the supernatant was discarded, leaving the pellet DNA in the tube. To wash the pellets, 500 µL of 70% EtOH was added to the tube, which was then centrifuged again at 13,000 rpm for 1 minute at 4 °C. The pellet was dried by briefly inverting the tube, and 50 µL of ddH_2O was added. The rice DNA isolation was stored in a refrigerator at -20 °C. The DNA isolation results were quantified using a nanodrop spectrophotometer and visualized by electrophoresis.

Once the DNA genome was obtained, the results were amplified through PCR, with the *OsFER1* gene at an optimized annealing temperature of 58°C and the *OsFER2* gene at 59.2°C. The PCR product was then visualized by electrophoresis for further sequencing.

RESULTS AND DISCUSSION

Figure 1A depicts the growth status of five rice cultivars at 114 days after planting (DAP). Cempo Ireng and Merah Pari Eja cultivars exhibit the tallest plant heights among the cultivars, measuring over 230 cm, whereas Pari Ireng, Hitam Kalsel, and Ciherang reach a height of approximately 180 cm.

In Figure 1B, variations in seed morphology among the five rice cultivars are evident. Ciherang possesses the tallest seeds, while Merah Pari Eja shows the widest seed width. Cempo Ireng, Pari Ireng, and Hitam Kalsel display purplish-black seeds, Merah Pari Eja has reddish-brown seeds, and Ciherang features white seeds. This distinctive color result from varying concentrations of natural pigments in the seed coat called anthocyanins, which are water-soluble flavonoids (Devi & Badwaik 2022). Notably, white rice seeds (Ciherang) lack anthocyanins. Consequently, pigmented rice exhibits free radical scavenging activity, making it a potential source of antioxidants.

Figure 1C illustrates the average Fe content in different rice cultivars. Cempo Ireng black rice grains contain an average Fe content of 22.133 mg/kg ±10.87. Following closely is Pari Ireng with an average Fe content of 17.127 mg/kg ±2.95. Hitam Kalsel rank third, with an average Fe content of 16.815 mg/kg ±7.29. Merah Pari Eja red rice features an average Fe content of 13.913 mg/kg ± 1.35, and rice cultivars

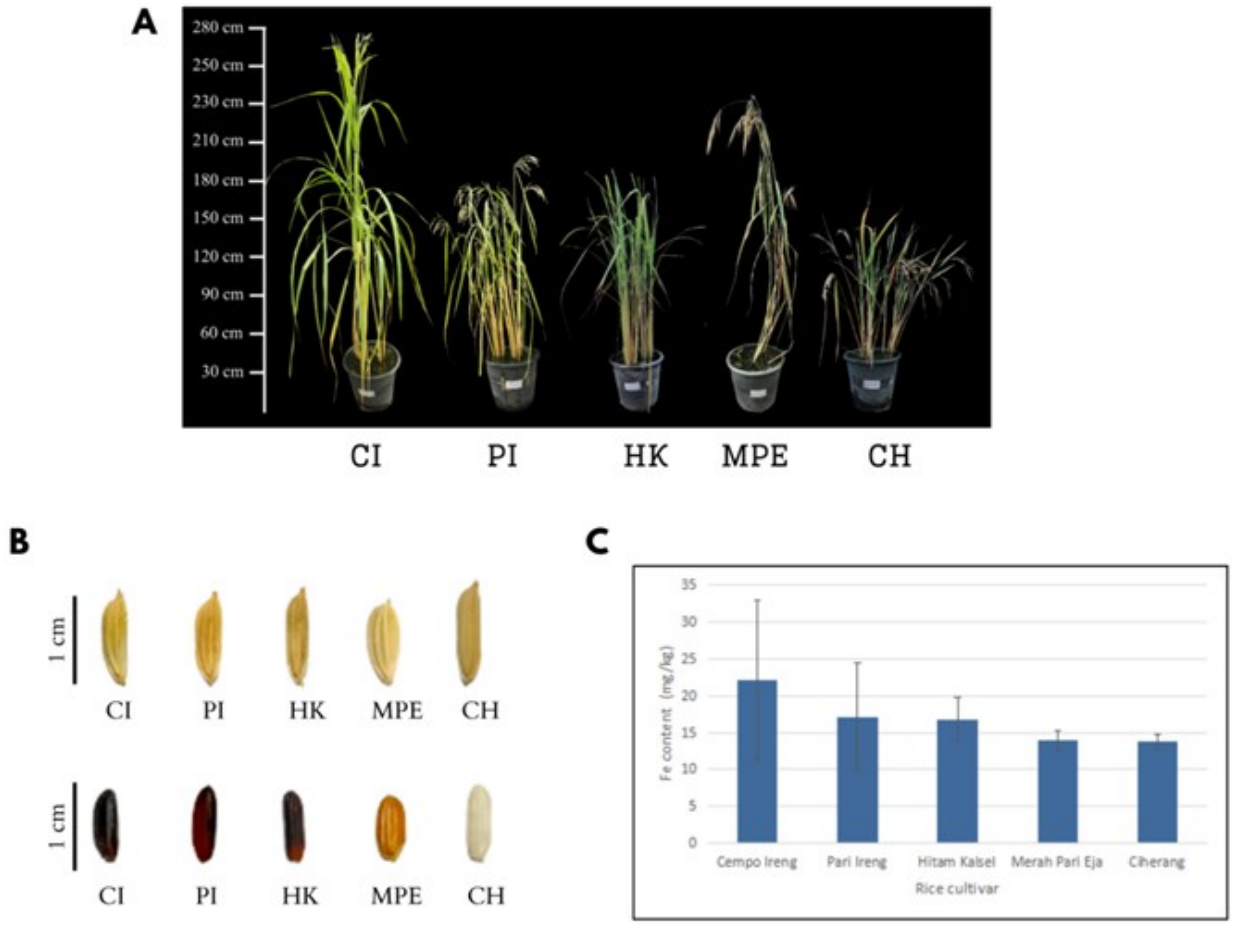

Figure 1. Rice plants morphology aged 114 DAP (A), undehulled (upper) and dehulled (lower) rice grains (B), iron content in rice grains from five cultivars used (C). (CI= Cempo Ireng, PI= Pari Ireng, HK=Hitam Kalsel, MPE= Merah Pari Eja, CH= Ciherang)

which has the lowest average Fe content is Ciherang white rice with an average of 13.756 mg/kg ± 1.06 (Figure 1C).

The isolated DNA sample from five cultivars exhibit a single band with a size of >10 kbp (Figure 2A). This result suggests a relatively high success rate for DNA isolation, affirming the suitability of the obtained genomic DNA as a template for amplifying the *OsFER1* and *OsFER2* genes.

Table 3. Quantification of genomic DNA from five rice cultivars used in this research.

Sample	Concentration (ng/µl)	A260/A230	A260/A280
Cempo Ireng	196.03	2.145	1.804
Pari Ireng	612.67	1.055	1.384
Hitam Kalsel	1190.72	1.095	1.206
Merah Pari Eja	293.25	2.050	1.848
Ciherang	518.86	0.917	1.166

The Table 3 reveals a wide range of DNA concentration, spanning from 196.03 ng/µl to 1190.72 ng/µl along with corresponding Optical Density (OD) values ranging from 0.917 to 2.145 (Table 3). The good ratio of OD A260/A280 and A260/A230 values ranging from 1.5 to 1.8 indicates that the level of DNA purity obtained is quite high (Ahmed et al. 2009). A low OD value at A260/A280 may suggest the presence of polyphenols contaminants, while a low OD at A260/A230 indicates the existence of salt residues (Aboul-Maaty & Oraby 2019).

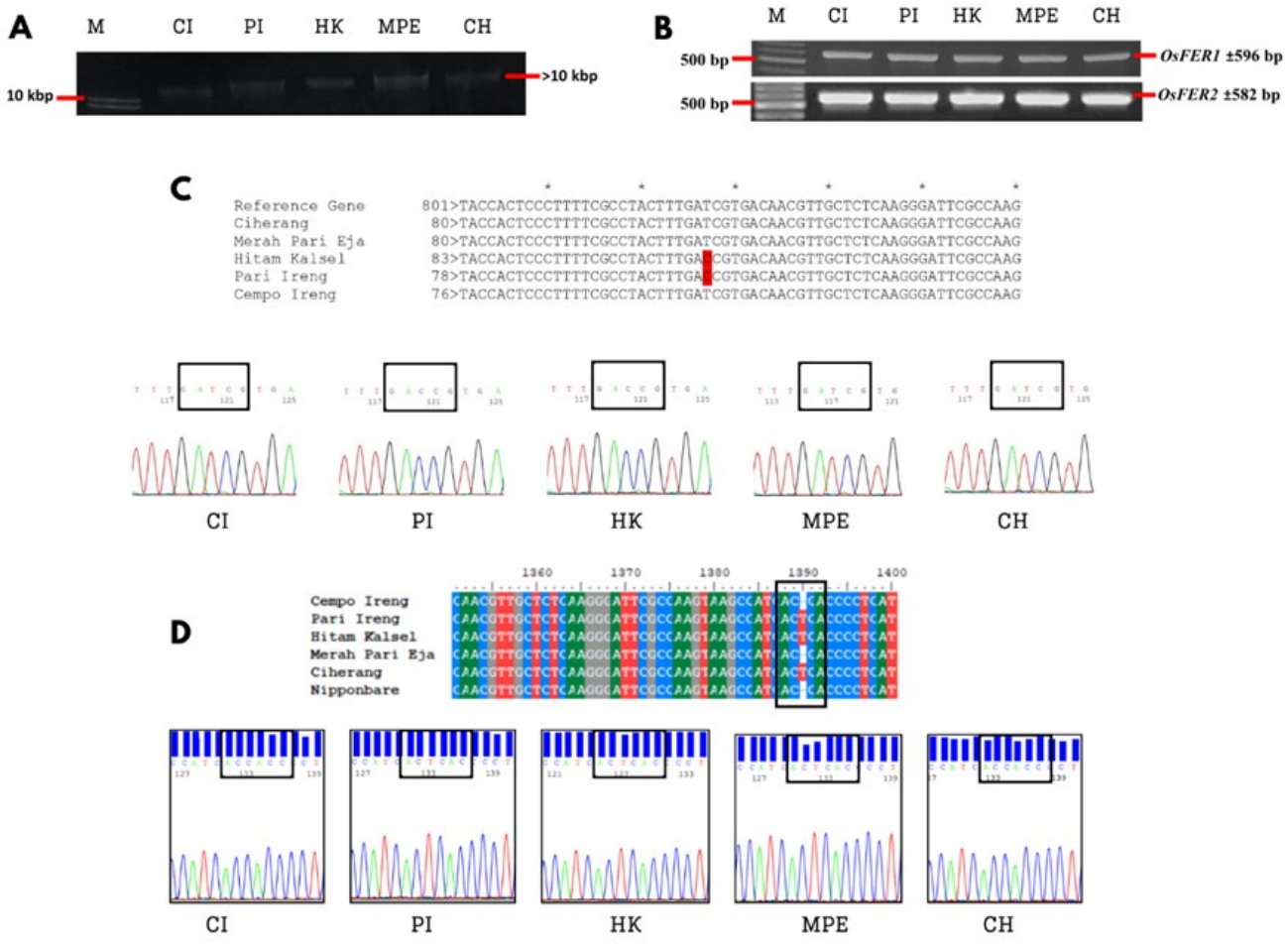

Figure 2. Visualization of genomic DNA isolation (A), Amplicon of *OsFER1* and *OsFER2* gene (B), Sanger sequencing and alignmnent result in partial *OsFER1* (C) and *OsFER2* (D) gene.
(M= Marker, CI= Cempo Ireng. PI= Pari Ireng, HK= Hitam Kalsel, MPE= Merah Pari Eja, CH= Ciherang)

Sanger sequenching was employed to decode the nucleotide sequences of partial *OsFER2* genes from the five rice cultivars. The sequencing results, represented in chromatograms, unveil the positions containing SNPs and are presented in Figure 2C and 2D. Alignment analysis using the BioEdit and MEGA11 software applications allowed a comparison of the nucleotide sequences of the five rice cultivars with the reference Nipponbare cultivar. High nucleotide sequence similarity indicates a close common ancestor (Kemena & Notredame 2009). The results of this analysis confirm the presence of 3 SNPs in the partial *OsFER2* gene sequence alignment confirms that there were 3 SNPs detected in the partial *OsFER2* gene sequence at the 1390 bp position.

In rice plants (*Oryza sativa, L.*), the ferritin gene consists of *OsFER1* on chromosome 11 and *OsFER2* on chromosome 12 (Herman et al. 2014). This study utilized the gene sequence of LOC4351264 *Fer2, chloroplastic Oryza sativa Japonica Group* from the Nipponbare cultivar (Gene ID: 4351264), located on chromosome 12, as the reference sequence. Chromosome 12 is linear DNA segment with a length of 27,531,856 bp (Nugraha et al. 2014).

The *OsFER2* gene is located at position 320,417 to 323,918 encompassing a length of 3,502 bp. Based on NCBI Refseq data NC_029267.1 with *accession* NC_029267 *REGION*: complement (320417..323918), the *OsFER2* gene (LOC4351264) is 3,502 bp long and consists of 8 exons and 7 introns (1..587, 588..1293, 1294..1377, 1378..1457, 1458..1518,

1519..1620, 1621. .1708, 1707..2460, 2461..2522, 2523..2655, 2656..2721, 2722..2834, 2835..2898, 2899..3004, 3005..3502).

The alignment analysis results reveal the presence of 3 SNPs in the sequence of *OsFER2* gene, specifically at the 1390 bp position. Pari Ireng, Hitam Kalsel, and Ciherang sequence exhibit a single thymine (T) insertion at 1390 bp. According to NCBI Refseq data NC_029267.1 from *Oryza sativa var. Nipponbare*, this 1390 bp region corresponds to intron 2 of the *OsFER2* gene, spanning from 1378 to 1457 bp. Importantly, intron regions are not part of the coding sequence (CDS) and are subsequently excised through mRNA splicing during post-translational modification. As a result, nucleotide changes within introns do not impact ferritin protein domain, amino acid composition, or variations in the Fe content of rice seeds.

Table 4. SNPs Positions in *OsFER1* and *OsFER2*.

Gene	Cultivar	SNP	Position (bp)	Nucleotide Base
OsFER1	Pari Ireng	Transition	104	T → C
	Hitam Kalsel	Transition	109	T → C
OsFER2	Pari Ireng	Insertion	1390	T
	Hitam Kalsel	Insertion	1390	T
	Ciherang	Insertion	1390	T

In contrast, the analysis also identifies 2 SNP in the sequence of the *OsFER1* gene, spesifically at the 104 bp and 109 bp positions. Pari Ireng and Hitam Kalsel both exhibit a single transition of thymine (T) to cytosine (C) at these locations. It's worth nothing that all of the identified SNPs in *OsFER2* are located in intron 2, while the SNPs in *OsFER1* are located in exon 5.

Previous studies (Nugraha et al. 2014; Roslim et al. 2016) have reported the presence of several SNPs in the *OsFER2* gene sequence from various local rice cultivars, including Siam Sintanur, Bakung, Mahsuri, Amat Candu, Sadani, and IR64, when compared with Nipponbare reference sequence. According to the findings of this study, there were at least 5 SNPs in intron 1 and 12 SNPs in intron 2. Furthermore, 2, 19, and 3 SNPs were detected in exon 2, exon 3, and exon 4, respectively. The increased number of SNPs reported in previous studies may be attributed to the greater diversity among the rice cultivars under investigation. This studies likely involved more contrasting traits, such as groups of rice cultivars with varying resistance or susceptibility to Fe stress, which could account for the heightened differences in nucleotide sequence observed.

Figure 3 presents a phylogenetic tree illustrating the evolutionary relationship among the plant organisms under investigation. This phylogenetic tree was constructed using the MegaX software with the Neighbor-joining statistical method. This statistical method used a distance-based algorithm to assess sequence similarity. Based on the dendogram, it become evident that the five studied cultivars (Pari Ireng, Hitam Kalsel, Ciherang, Cempo Ireng, and Merah Pari Eja) share a very close relationship by comparing the horizontal branch with the scale bar below. The distance between the nodes of each cultivar and the common ancestor node is shorter than the scale bar (0.20). More specifically, the distances are as follows: Merah Pari Eja 0.00; Cempo Ireng 0.05; Ciherang 0.08; Hitam Kalsel 0.09; and Pari Ireng 0.10. The phylogenetic tree construction employed a standard of 1000 bootstrap replications. A reliable interpretation for the percentage of confidence in the Bootstrap

Support (BS) value is typically set at 95% (Patrick et al. 2018). Nodes with a bootstrap value below 80% have been collapsed (Brandis 2021). Reviewing the dendogram's structure, it is evident that the BS value for each node exceeds 80%. This indicates that the constructed phylogenetic tree offers a high level of confidence in accurately depicting the relationships among the organisms under study.

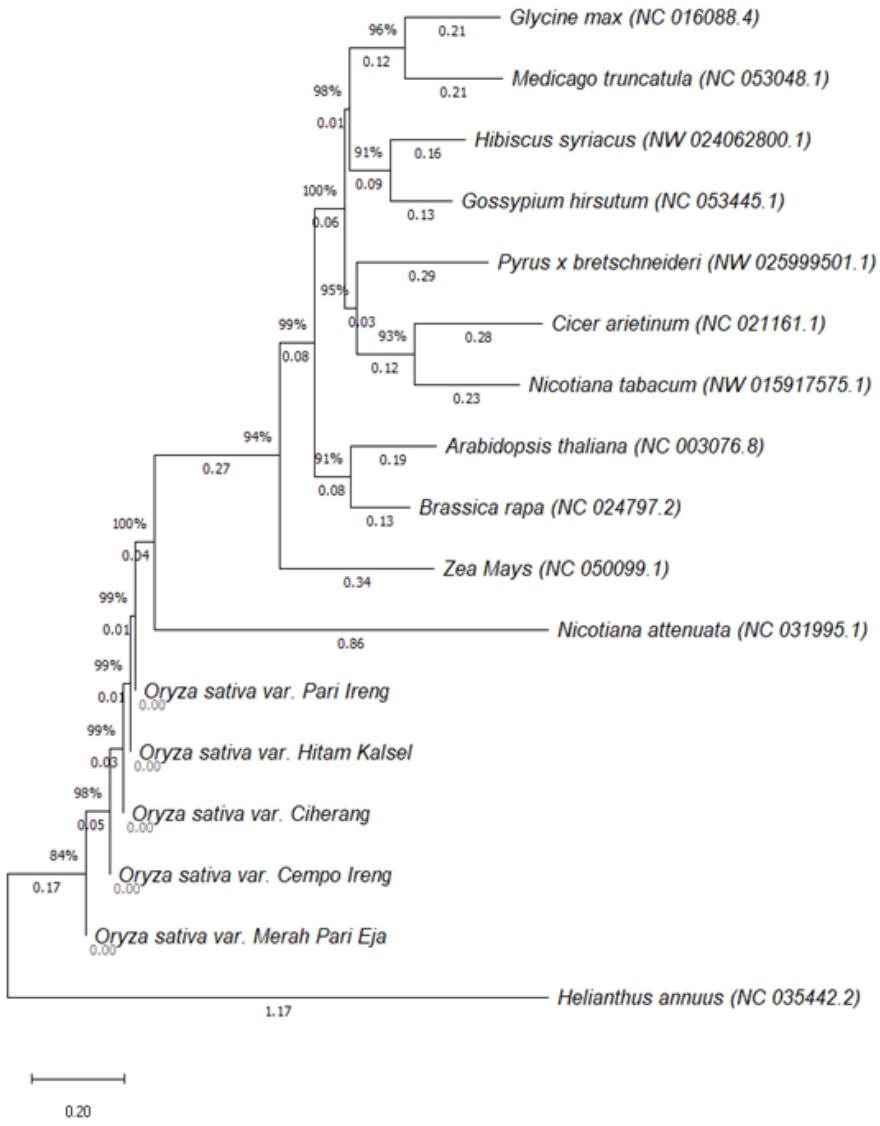

Figure 3. *OsFER1* phylogenetic tree of rice cultivars and out-group.

The dendrogram (Figure 4) constructed based on the *OsFER2* gene from various plants reveals that the five rice cultivars share the closest relationship with *O. sativa* var. *Nipponbare*. The distances between the nodes for each cultivar and the common ancestor node are remarkably close, measuring 0.00 for Ciherang, Hitam Kalsel, Pari Ireng, and Cempo Ireng, and 0,01 for Merah Pari Eja. In particular, the Ciherang cultivar is closely related to Nipponbare, forming the rice group. Pari Ireng, Hitam Kalsel, and Cempo Ireng cultivars exhibit a close relationship, constituting the black rice group. Meanwhile, Merah Pari Eja cultivar emerges as an outgroup in relation to the other rice cultivars. Furthermore, the *OsFER2* sequences of the five studied cultivars show a close relationship with the *OsFER1* sequence of *O. sativa var. Nipponbare*.

The dendogram also proves that organisms from the same genus have the closest relatives. It can be seen from *O. branchyantha* which is the

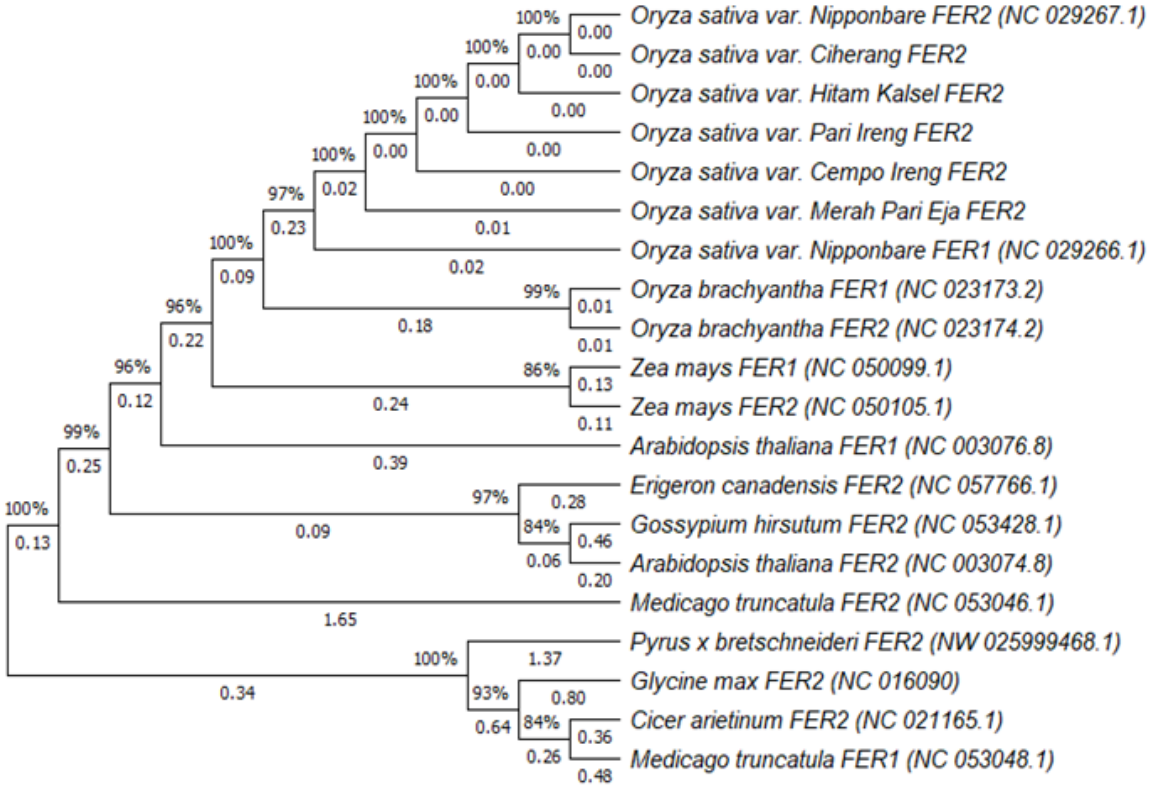

Figure 4. *OsFER2* phylogenetic tree of rice cultivars and out-group.

closest relative of *O. sativa*. Moreover, organisms within the same order also exhibit close relationships, as exemplified by the grouping of *O. sativa*, *O branchyantha*, and *Zea mays* which form a Poales group. Additionally, *FERI* and *FER2* gene sequences from the same organism demonstrate close relationships and form groups within the species, as observed in *O. branchyanta*, *O. sativa*, and *Z. mays*. The BS value for each node is >80% (Brandis 2021), confirming the phylogenetic tree's robust confidence in accurately depicting the relationship between organisms considered.

CONCLUSIONS

The target sequences in the *OsFER1* and *OsFER2* genes are known to have SNPs. However, the presence of SNPs in each of these gene sequences did not have a significant impact on the Fe concentration in the rice grains of each cultivar.

AUTHOR CONTRIBUTION

A.P. and R.F.B. contributed equally to this paper. Y.A.P supervised all the research process and writing the manuscript, A.P. designed the manuscript and analyzed the *OsFER1* gene data, R.F.B. analyzed the *OsFER2* gene data, reviewed, and edited the manuscript, I.S.E. assisted the isolation process, A.S. assisted the research process.

ACKNOWLEDGMENTS

The authors would like to thank the Pigmented Rice Research Group members who have helped in the research process. This research supported by Lecturer and Students Research Collaboration funding from the Faculty of Biology, Universitas Gadjah Mada under contract no. 1178/UN1/FBI.1/KSA/PT.01.03/2022.

CONFLICT OF INTEREST

The authors declare there is no conflict of interest in this research.

REFERENCES

Aboul-Maaty, N.A.F. & Oraby, H.A.S., 2019. Extraction of high-quality genomic DNA from different plant orders applying a modified CTAB-based method. *Bulletin of the National Research Centre*, 43(1), pp.1-10. doi: 10.1186/s42269-019-0066-1.

Ahmed, I. et al., 2009. High-quality plant DNA extraction for PCR: an easy approach. *J Appl Genet*, 50, pp.105-107. doi: 10.1007/BF03195661.

Brandis, G., 2021. Reconstructing the Evolutionary History of a Highly Conserved Operon Cluster in Gammaproteobacteria and Bacill. *Genome Biol Evol.*, 13(4), pp.1-14. doi: 10.1093/gbe/evab041.

Briat, J.F. et al., 2010. Ferritins and iron storage in plants. *Biochimica et Biophysica Acta (BBA)-General Subjects*, 1800(8), pp.806-814. doi: 10.1016/j.bbagen.2009.12.003.

Collard, B.C. & Mackill, D.J., 2008. Marker-assisted selection: an approach for precision plant breeding in the twenty-first century. *Philosophical Transactions of the Royal Society B: Biological Sciences*, 363(1491), pp.557-572. doi: 10.1098/rstb.2007.2170.

Elango, D. et al., 2021. Analytical Methods for Iron and Zinc Quantification in Plant Samples. *Communications in Soil Science and Plant Analysis*, 52(10), pp.1069-1075. doi: 10.1080/00103624.2021.1872608.

Helmyati, S. et al., 2014. *Fortifikasi Pangan Berbasis Sumber Daya Nusantara*, Yogyakarta: Gadjah Mada University Press. pp.140-144.

Herlinda, S. et al., 2013. Intensifikasi Pengelolaan Lahan Suboptimal dalam Rangka Mendukung Kemandirian Pangan Nasional. *Prosiding Seminar Nasional Lahan Suboptimal*. ISBN 979-587-501-9.

Herman et al., 2014. Analisis Sekuen Intron 1 sampai Sebagian Ekson 4 dari Gen Feritin2 pada Tiga Genotipe Padi (Oryza sativa L.) Lokal Indragiri Hilir, Riau. *Jurnal Dinamika Pertanian*, 29(1), pp.21–26.

Kemena, C. & Notredame, C., 2009. Upcoming challenges for multiple sequence alignment methods in the high-throughput era. *Bioinformatics.*, 25(19), pp.2455–2465. doi: 10.1093/bioinformatics/btp452.

Kobayashi, T., Nozoye, T. & Nishizawa, N.K., 2019. Iron transport and its regulation in plants. *Free Radical Biology and Medicine*, 133, pp.11-20. doi: 10.1016/j.freeradbiomed.2018.10.439.

Liang, G., 2022. Iron uptake, signaling, and sensing in plants. *Plant Communications*, 3(5), 100349. doi: 10.1016/j.xplc.2022.100349.

Mauseth, J.D., 2021. *Botany 7th Edition: An Introduction to Plant Biology*, USA: Jones and Bartlett Learning.

Nugraha, F. et al., 2014. Analysis of Partial Gene Sequence Ferritin2 on Rice Plants (Oryza sativa L.) Indragiri Hilir, Riau. *Biosaintifika*, 6 (2), pp.1-7. doi: 10.15294/biosaintifika.v6i2.3102.

Patrick, O. et al., 2018. Molecular Footprint of Kenya's Gene Bank Repositories Based on the cp-Genome Signatures. *American Journal of Molecular Biology*, 8, pp.215–244. doi: 10.4236/ajmb.2018.84019.

Paul, S. et al., 2012. Molecular breeding of Osfer2 gene to increase iron nutrition in rice grain. *GM crops & food*, 3(4), pp.310-316. doi: 10.4161/gmcr.22104.

Roslim, D.I., Deanesia, D., & Herman, H., 2016. Analisis Sekuen Ekson 6-8 dari Gen Ferritin pada Tiga Varietas Padi (Oryza sativa L.) Kecamatan Bantan, Bengkalis - Riau. *Jurnal Riau Biologia*, 1(1), pp.1-7. ISSN 2527-6409.

Silveira, V.C. et al., 2009. Role of ferritin in the rice tolerance to iron overload. *Scientia Agricola*, 66(4), pp.549-555. doi: 10.1590/S0103-90162009000400019.

Stein, R.J., Ricachenevsky, F.K. & Fett, J.P., 2009. Differential regulation of the two rice Ferritin genes (OsFER1 and OsFER2). *Plant Science*, 177(6), pp.563-569. doi: 10.1016/j.plantsci.2009.08.001.

Utami, Z.H., 2019. *Budidaya Padi Hitam dan Merah pada Lahan Marginal dengan Sistem SBSU*. Yogyakarta: Penerbit ANDI.

Journal of Tropical Biodiversity and Biotechnology
Volume 09, Issue 01 (2024): jtbb82196
DOI: 10.22146/jtbb.82196

Research Article

Growth Kinetic Modelling of Efficient *Anabaena* sp. Bioflocculation

Amalia Rahmawati[1], Irma Rohmawati[1], Istini Nurafifah[1], Brilian Ryan Sadewo[2], Eko Agus Suyono[1]*

1)Faculty of Biology, Universitas Gadjah Mada, Teknika Selatan, Yogyakarta, Indonesia 55281
2)Chemical Engineering Department, Faculty of Engineering, Universitas Gadjah Mada, Grafika No. 2, Yogyakarta, Indonesia 55281
* Corresponding author, email: eko_suyono@ugm.ac.id

Keywords:
Anabaena sp.,
Bioflocculation
Glagah consortium
Harvesting
Lipid
Submitted:
09 February 2023
Accepted:
25 June 2023
Published:
26 February 2023
Editor:
Miftahul Ilmi

ABSTRACT

Bioflocculation is a harvesting technique that employs flocculant agents such as bacteria and microalgae. The benefit is the absence of a chemical-added flocculant. Because bacteria need a particular medium, microalgae flocculant agents are more effective. This study used *Anabaena* sp. to collect fat, protein, and carbohydrates from the Glagah consortium. Three replications of those microalgae were grown in 300 ml of Bold Basal Medium culture for eight days. On the day of harvest, flocculant microalgae (*Anabaena* sp.) and non-flocculant microalgae (Glagah) were combined to accomplish flocculation. On the day of harvest, parameters were observed by combining *Anabaena* sp. with the Glagah consortium in the ratios 1: 1, 0.5: 1, and 0.25: 1. There were three times of each parameter test. Utilizing a wavelength of 750 nm, the proportion of precipitation was calculated spectrophotometrically. Bligh and Dyer were used to measure the lipids. The phenol sulfate technique was used to calculate the amount of carbohydrates. By employing the Bradford method, proteins were quantified. Biofocculation percentages and carbohydrate content were optimum on a ratio of 0.25:1. Lipid and protein content were optimum on a ratio of 1:1.

Copyright: © 2024, J. Tropical Biodiversity Biotechnology (CC BY-SA 4.0)

INTRODUCTION

The high-energy input for harvesting biomass makes current commercial microalgal biodiesel production economically unfeasible. In order to minimize energy consumption, it needed more efficient harvesting technique (Benemann 1997). Microalgae flocculation is a more effective technique than other microalgae harvesting techniques. They are considered safer and more environmentally friendly than synthetic flocculants. Furthermore, using microalgae as bioflocculants does not require special media, so they are more cost-effective than bacteria (Salim et al. 2011).

Global warming is driving the development of renewable energy. One of the renewable energy is from the Glagah consortium (Pradana et al. 2018). The Glagah consortium is a microalgae taken from the coast of Glagah Beach in Kulon Progo Regency, Yogyakarta. The Glagah consortium consists of 6 species, namely *Cyclotella polymorpha*, *Cylindrospermosis raciborskii*, *Golenkinia radiata*, *Corethron criophilum*, *Chlamydomonas* sp. and *Syracosphaera turquoise* (Suyono et al. 2016b). Glagah consortium is potential for biodiesel and lipid production (Suyono et al. 2016a). However, it

needs help in harvesting the Glagah consortium. To harvest the Glagah consortium using microalgae, *Anabaena* sp. is a potential bioflocculant. *Anabaena* sp. produces EPS that plays a role in bioflocculation. The increase in EPS production directly influences bioflocculant activity (Tiwari et al. 2015).

Bioflocculation is a spontaneous flocculation of microalgae cells due to the secretion of the EPS (Sathe 2010). This EPS causes the formation of clumps of cells, which will become biomass so that it is deposited. Stress conditions trigger EPS secretion in limited nutrients (Lee et al. 2009).

The harvesting Glagah consortium using *Anabaena* sp. has never been done before. Thus, it is important to study the harvesting Glagah consortium using *Anabaena* sp. to determine the percentage of flocculation, lipids, and protein of the Glagah consortium.

MATERIALS AND METHODS

Materials

The materials needed include Culture of *Anabaena* sp., medium cultivation, Glagah consortium, methanol, chloroform, phenol, sulfuric acid, Bradford solution, and Bovine Serum Albumin (BSA).

Methods

The culture of *Anabaena* sp. was harvested on the 4th day, while the Glagah consortium was on the 3rd day (based on preliminary tests). Samples were inserted in 15 ml conicles with a ratio of flocculant microalgae (*Anabaena* sp.), and non-flocculant (Glagah consortium) was 1: 1, 0.5: 1, and 0.25: 1. Treatment measurements were carried out three times with triplicate repetitions of control *Anabaena* sp. and the Glagah consortium. The samples parameters of lipids, carbohydrates, and proteins were left to stand for 24 h, aiming to mix the Glagah consortium and *Anabaena* sp. The parameter measurement method is as follows:

Growth Calculation of *Anabaena* sp. and Glagah consortium

Cell of *Anabaena* sp. and Glagah consortium density was counted every 24 h using hemocytometer (Neubauer, Germany). Cell density was determined on cells larger than 8 µ in size.

Bioflocculation Harvesting

Absorbance was measured at the wavelength of 750 nm, with t_0 0 hour and t_n 24 h. The percentage of precipitation was calculated using the following formula (Salim et al. 2011):

$$\% \text{ Flocculation} = \frac{OD_{750}(t_0) - OD_{750}(t_n)}{OD_{750}(t_0)} \times 100\%$$

Lipid content

The Bligh and Dyer (1959) method measured lipid content. The 15 ml sample was centrifuged at 4000 rpm for 15 minutes at 4° C. Supernatant was removed, and 2 ml of methanol and 1 ml of chloroform were added to pellets. Then the sample was vortexed for 1 minute. Next, 1 ml distilled water and 1 ml chloroform were added to the models. The sample was vortexed for 1 minute and centrifuged for 15 minutes at 1800 rpm at 4° C. The sample was divided into three layers. Lipids are at the bottom. Lipids were taken and placed on a petri dish; then the petri dish was put in the incubator. The chloroform evaporation process is carried out with an open petri in an incubator, for 12 h at 33° C. The empty weight of a petri dish, the weight of a petri dish with lipids, and the weight after the

oven is weighed, then calculated using the formula (Novaryatiin et al. 2015):

$$\text{Lipid content (mg/ ml)} = \frac{\text{filled weight} - \text{empty weight of petri dish}}{\text{dry weight x sample volume}}$$

Carbohydrate content

The method of Dubois et al. (1956) was used to measure carbohydrate content. A 15 ml was centrifuged at 3300 rpm for 10 minutes at room temperature. 0.5 ml of 5% phenol was added to the pellet. The sample was vortexed and allowed to stand for 10 minutes. 1 ml of sulfuric acid was added. The sample was vortexed and allowed to stand for 20 minutes. A spectrophotometer measured the absorbance of the sample at 490 nm. Carbohydrate concentration was measured using a glucose standard curve obtained from the FALITMA Laboratory, Faculty of Biology, Universitas Gadjah Mada. The glucose standard curve formula was:

$$Y = 0.0884x + 0.0095$$

Protein content

Protein was estimated by the (Bradford 1976) method. A total of 15 ml of the sample was centrifuged at 1800 rpm at room temperature for 10 minutes. The supernatant was removed. Pellets were added with 45 µl of 10% SDS to damage the cell wall. Samples were put on waterbath and heated at 95°C for 5 minutes. The sample was cooled for 5 minutes in an ice cupboard. An 8 µl of supernatant was taken and put into a microplate, and 200 µl of Bradford solution was added. Absorbance was measured using the ELX bioTek ELISA at 595 nm. Protein concentration was estimated based on the Bovine Serum Albumin standard curve obtained from the FALITMA Laboratory, Faculty of Biology, Universitas Gadjah Mada. The Bovine serum albumin standard curve formula was:

$$Y = 0{,}0005x + 0{,}011$$

RESULTS AND DISCUSSION

Microalgae have eight-day cycles. Increasing the number of cells showed that microalgae absorbed nutrients and used them for their metabolism. Based on Figure 1, the 4th day showed the highest number of *Anabaena* sp., indicating the harvest day. The death phase of *Anabaena* sp. occurred from the 5th day to the 8th day. The number of cells marked the occurrence significantly. The death phase of microalgae cells is caused by a decrease in nutrients directly proportional to the reduction in metabolic activity. Another possibility is the accumulation of organic substances (NO_2^- and NH_4^+) derived from dead microalgae cells. So, they can poison microalgae and can interfere with the absorption of dissolved oxygen and nutrients (Nugroho 2006; Suantika et al. 2009).

Glagah consortium occurred indicated that the lag phase is microalgae adaptation to the new environment (Figure 1). It was followed by an exponential phase and characterized by a high rate of cell division. The 3rd day was the harvest day of the Glagah consortium. The death phase of the Glagah consortium was from the 4th day to the 8th day and marked by a significant decrease in the number of cells.

Suitable kinetic modeling needs to be developed to learn the dynamics of biomass growth of microalgae; suitable kinetic modeling can be used for predicting the performance and optimization of photobioreactor operating conditions (Galvao et al. 2013).

The two non-linear models Logistic and Gompertz, were chosen for the *Anabaena* sp. and Glagah consortium. For rapid population

growth of organisms, Logistic and Gompertz models are commonly used (Lam et al. 2017). Logistic and Gompertz model was the simplest models in microbial growth because it is not limited by substrate type and consumption.

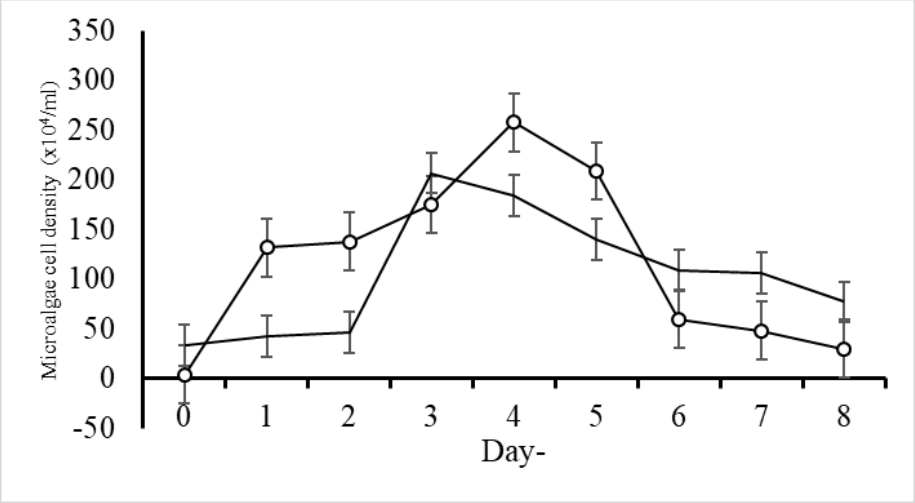

Figure 1. Microalgae growth curves *Anabaena* sp. and Glagah consortium with-BBM (Rahmawati 2020).

The Logistic model predicts the number of stable populations using the maximum growth rate per day as its parameter. The Logistic model was calculated using the following formula. X is cell density, X_0 is the initial cell density, X_{max} is the maximum cell density, and μ_{max} is the maximum specific growth rate (Phukoetphim et al. 2017; Hanief et al. 2020).

Based on logistic modeling (Figure 2), the maximum specific growth rate (μ_{max}) of *Anabaena* sp. and Glagah consortium were 1.6265/day and 0.8827/day, respectively. The R^2 error were 0.70 and 0.74 for the *Anabaena* sp. and Glagah consortium. For the Gompertz modeling, the maximum cell production rate (rm) of *Anabaena* sp. was 0.6370 x 10^6 cells/mL. The top cell production rate (rm) of the Glagah consortium was 1.6792 x 10^6 cells/mL.

Table 1 shows the results of the Logistic and Table 2 shows growth rate parameter of Gompertz Model of the *Anabaena* sp. and Glagah consortium experimental growth data. The Gompertz model (Table 2) fits the microalgae growth curves better than the Logistic model (Table 1) for two microalgae species. The coefficient of determination R^2 values established the goodness of fit of the Gompertz model over the Logistic model in the study.

Table 1. Growth Rate Parameter of Logistic Model.

Parameter	*Anabaena* sp.	Glagah consortium
μ_{max}	1.6265	0.8827
R^2	0.70	0.74

Table 2. Growth Rate Parameter of Gompertz Model.

Parameter	*Anabaena* sp.	Glagah consortium
rm	0.6370	1.6792
tl	-0. 3	1.9
R^2	0.88	0.90

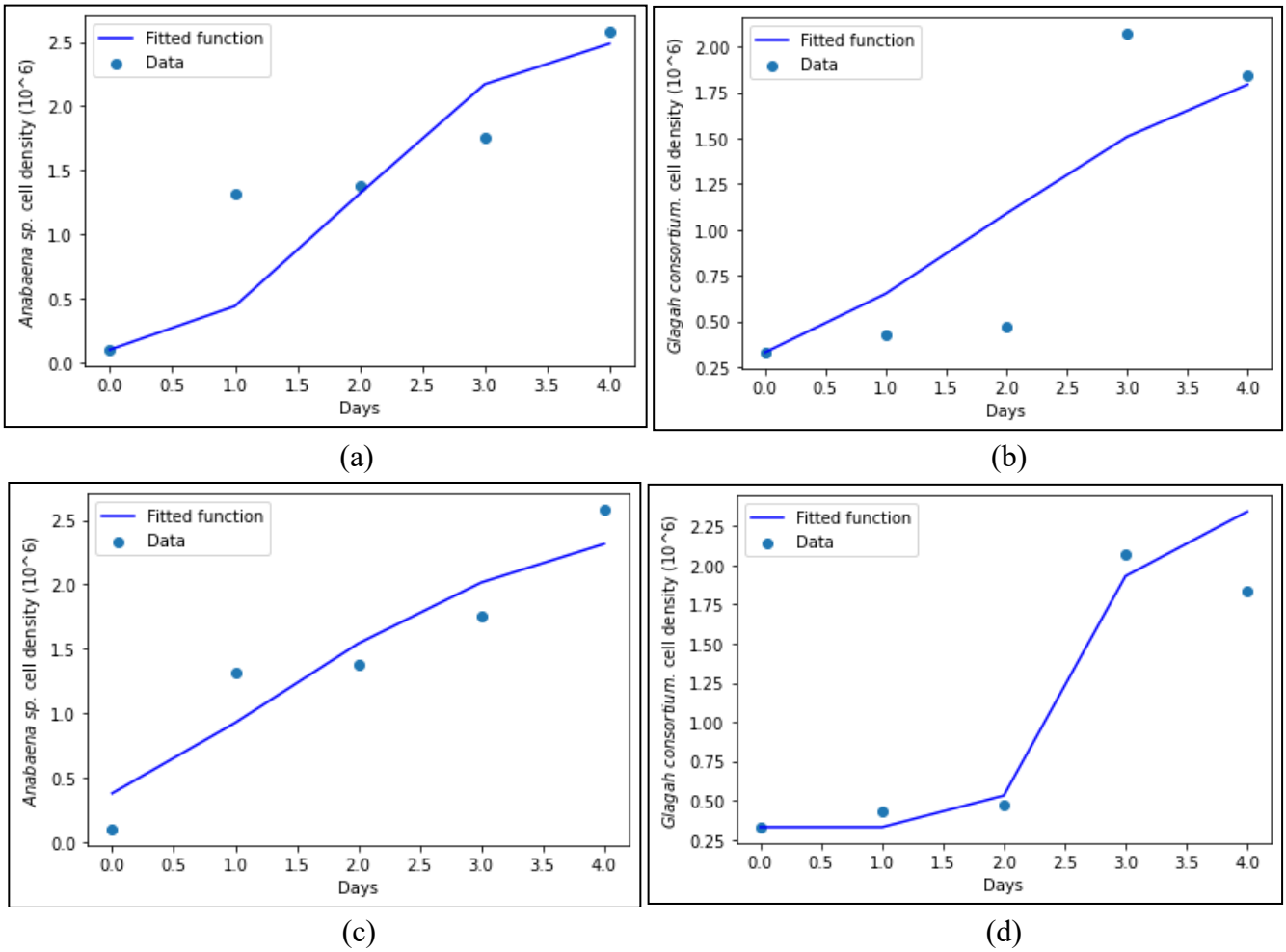

Figure 2. Modeling Growth Kinetic of *Anabaena* sp. and Glagah consortium (a)Logistic *Anabaena* sp. (b) Logistic Glagah consortium (c) Gompertz *Anabaena* sp. (d) Gompertz Glagah consortium.

Saputra (2013) recorded that the flocculation percentage of the Glagah consortium is relatively low. *Anabaena* sp. was used as a bioflocculant agent because it produced EPS. According to Pillai (1997), particle flocculation speed is influenced by particle size. The smaller particle size is more challenging to flocculate. Therefore, it was extended for the Glagah consortium to form floc and precipitate compared to *Anabaena* sp. Sathe (2010) declares that bioflocculation is a spontaneous flocculation of microalgae cells due to the secretion of the EPS when the microalgae are under stress. This EPS causes the formation of clumps of cells, which become biomass so that it precipitates. Limited nutrients are stress conditions that trigger EPS secretion (Lee et al. 2009).

The result indicated that the highest percentage of flocculation was obtained at a ratio of 1: 0.25, equal to 80.5%, while the lowest rate of flocculation was obtained at a ratio of 1: 1 equivalent to 49% (Figure 3). Salim et al. (2011) stated that adding flocculant species with high concentrations in harvesting could increase the percentage of precipitation. If referring to this journal, the highest rate of rainfall obtained should be at a ratio of 1: 1, but in this study the flocculation percentage was optimum at 1: 0.25. This is due to EPS, which is produced by *Anabaena* sp., some of the constituents are proteins (Tiwari et al. 2015). It is assumed that one of the proteins produced is anatoxin (Gangl et al. 2015).

According to Suyono et al. (2016b), The Glagah consortium is mixed culture. Mixed culture has rapid growth and high lipid level. According to Chisti (2007), Facilitation between species in diverse culture increase productivity. Thus, it causes the complex mechanism to produce

lipid (Behl et al. 2011). Suyono et al. (2016b) reported that the lipid percentage of the Glagah consortium was 1.25% and could be increased to 13.58% by stressing the treatment of environmental factors such as salinity. Based on Figure 4, it was found that the lipid concentration of *Anabaena* sp. was 0.007 mg/ml while the Glagah consortium was 0.009 mg/ml. The lowest lipid in treatment percentage was obtained at a ratio of 1: 0.25. This was assumed that microalgae were left alive without significant stress.

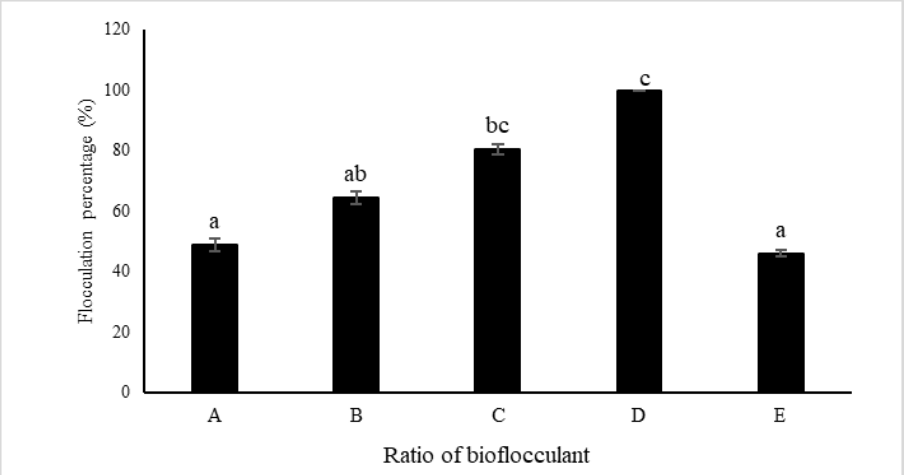

Figure 3. Bioflocculation percentages on harvest day using a medium of BBM with the ratio between non-flocculant and flocculant microalgae (A) 1:1, (B) 1:0.5, (C) 1: 0.25, (D) *Anabaena* sp., and (E) Glagah consortium (Rahmawati 2020). Data were means ±SD (n=5). Different bioflocculation percentages on harvest day using a medium of BBM with the ratio between non-flocculant and flocculant microalgae indicated significant differences between treatments and were calculated by one-way ANOVA followed by Duncan Multiple Range Test (DMRT) (p <0.05).

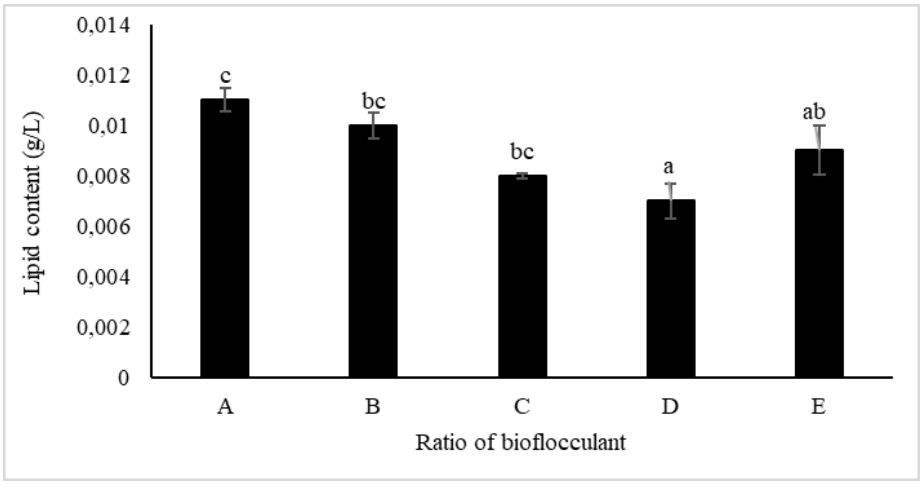

Figure 4. Lipid content harvest day using medium of BBM with the ratio between non-flocculant and flocculant microalgae (A) 1:1, (B) 1:0.5, (C) 1: 0.25, (D) *Anabaena* sp., and (E) Glagah consortium (Rahmawati 2020). Data were means ±SD (n=5). Different lipid content harvest days using a medium of BBM with the ratio between non-flocculant and flocculant microalgae indicated significant differences between treatments and were calculated by one-way ANOVA followed by Duncan Multiple Range Test (DMRT) (p <0.05).

Glagah consortium had a higher lipid percentage than *Anabaena*. It is caused by the symbiosis between species, especially with bacteria which helped absorb and supplied nutrients (Croft et al. 2005). The highest lipid concentration was at a ratio of 1: 1. This was caused by stress in the

treatment. Stress was possible because of limited nutrients and efficiency in using photosynthetic active radiation. This is a microalgae response to environmental changes that occur (Guschina & Harwood 2006; Ho et al. 2011).

Carbohydrate is a product of photosynthesis and component of cell walls, mainly in cellulose form. The carbohydrate content of the microalgae is used as an alternative fuel, for example for biofuels (Domozych et al. 2012; Yen et al. 2013). The carbohydrate content in the Glagah consortium is higher than *Anabaena* sp. (Figure 5). Mixing of Glagah and *Anabaena* sp. increased carbohydrate content. Because of the carbohydrate synergy that was contained in each species. The highest carbohydrate content was found at a ratio of 1: 0.25. The lowest carbohydrate concentration was found at a ratio of 1: 1. Addition of bioflocculant concentration decreases protein concentration. According to (Ritanti & Purwadi 2018), increasing the number of cells extends the time for hydrolysis of cell walls.

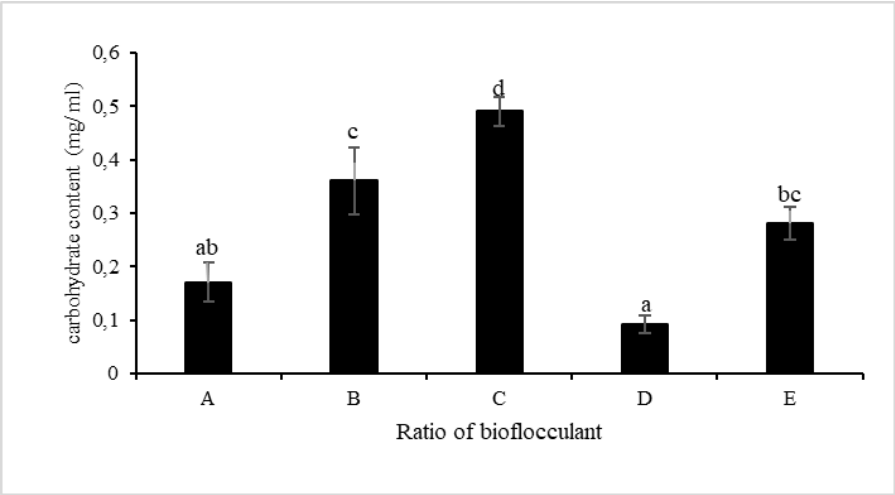

Figure 5. Carbohydrate content on harvest day using medium of BBM with the ratio between non-flocculant and flocculant microalgae (A) 1:1, (B) 1:0.5, (C) 1: 0.25, (D) *Anabaena* sp., and (E) Glagah consortium (Rahmawati 2020). Data were means ±SD (n=5). Different carbohydrate content on harvest day using a medium of BBM with the ratio between non-flocculant and flocculant microalgae indicated significant differences between treatments and were calculated by one-way ANOVA followed by Duncan Multiple Range Test (DMRT) (p <0.05).

The phenol-sulfate method was used for carbohydrate estimation. The reagent of the phenol-sulfate method is Phenol 5% and concentrated sulfuric acid (H_2SO_4). Phenol is used to detect simple sugars, while H_2SO_4 produces orange color (Agustini & Febrian 2019). Carbohydrate content in Glagah control was 0.28 mg/ml higher than *Anabaena* sp. 0.09 mg/ml. The highest carbohydrate content was obtained at a ratio of 1: 0.25, which is equal to 0.49 mg/ml, while the lowest carbohydrate concentration was obtained at a ratio of 1: 1, which is equal to 0.17 mg/ml. Their reverse trend of lipid and carbohydrate content casued by the metabolic pathways of high energy. This is due to harvesting microalgae carried out in the stationary phase, where microalgae change their metabolism by breaking down carbohydrates into energy reserves such as lipids, because the precursor of TAG is glyceraldehyde-3-phosphate (G3P). G3P is the result of carbohydrate catabolism (Sayanova 2017). Microalgae that produce high amounts of carbohydrates tend to have small amounts of lipids. Therefore, microalgae is identified as a reliable source of protein. The Bradford method was used for protein estimation. The Bradford is staining based on the measurement of absorbance (Yasmine 2011).

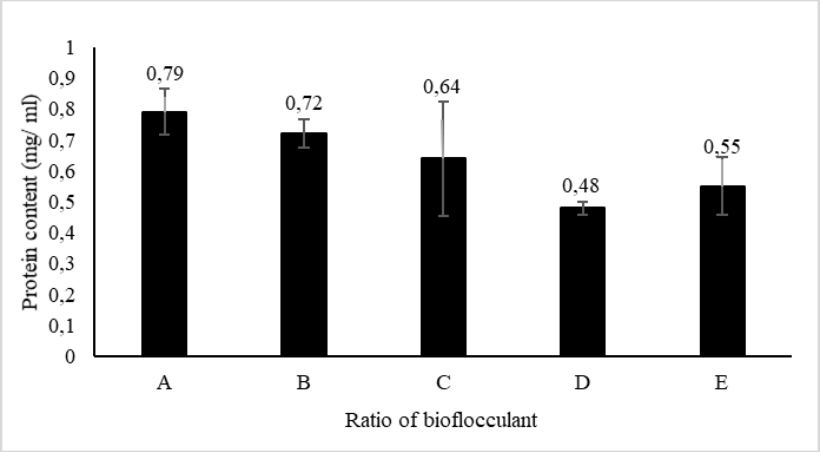

Figure 6. Protein content on harvest day using medium of BBM with the ratio between non-flocculant and flocculant microalgae (A) 1:1, (B) 1:0.5, (C) 1: 0.25, (D) *Anabaena* sp., and (E) Glagah consortium (Rahmawati 2020). Data were means ±SD (n=5). Different protein content on harvest day using a medium of BBM with the ratio between non-flocculant and flocculant microalgae indicated insignificant differences between treatments and were calculated by one-way ANOVA (p >0.05)

Based on Figure 6, the protein content in the Glagah consortium control was 0,55 mg/ml, while in *Anabaena* sp. was 0.48 mg/ml. The highest protein content was found at a ratio 1: 1. The lowest protein content was found at a ratio 1: 0.25. Glagah consortium protein content was higher when compared to *Anabaena* sp. This is due to the optimum utilization of nutrients in the Glagah consortium due to the effect of niche division in culture.

Anabaena sp. can produce EPS consisting of soluble protein and polysaccharides (Tiwari et al. 2015). The increased protein content along with the increased concentration of bioflocculants added. Increased bioflocculant concentrations cause an increased in EPS. EPS accumulation increased protein content, this is because protein is a constituent component of EPS.

CONCLUSION

Compared to *Anabaena* sp., the Glagah consortium took longer to precipitate and produce bioflocculation. The result indicated that the addition of bioflocculant *Anabaena* sp. increased the percentage of deposition of the Glagah consortium, with an optimum ratio of 0.25:1. The increased protein content, along with the increased concentration of bioflocculants added.

AUTHOR CONTRIBUTION

A.R. contributed to doing research, data interpretation, and editing. I.R. contributed to the interpretation of the data, review, and editing. I.N. contributed to the review and editing. B.R.S. contributed to data modeling, and E.A.S. contributed to designing the research, reviewing, editing, and supervising the process.

ACKNOWLEDGMENTS

This research was supported by The Ministry of Education, Culture, Research, and Technology. In addition, we thank our colleagues from the Chemical Engineering Department and Department of Food and Agricultural Product Technology Universitas Gadjah Mada, who provided insight and expertise that greatly assisted the research. This research was a part of the first author thesis.

CONFLICT OF INTEREST

The authors have declared that no conflict of interest exists.

REFERENCES

Agustini, N.W. & Febrian, N., 2019. Hidrolisis biomassa mikroalga Porphyridium cruentum menggunakan asam (H_2SO_4 dan HNO_3) dalam produksi bioetanol. *Jurnal Kimia dan Kemasan*, 41(1), pp.1-10. doi: 10.24817/jkk.v41i1.3962.

Behl, S., Donval, A. & Stibor, H., 2011. The relative importance of species diversity and functional group diversity on carbon uptake in phytoplankton communities. *Limnology and Oceanography*, 56(2), pp.683-694. doi: 10.4319/lo.2011.56.2.0683.

Benemann, J.R., 1997. Feasibility analysis of photobiological hydrogen production. *International journal of hydrogen energy*, 22(10-11), pp.979-987. doi: 10.1016/S0360-3199(96)00189-9.

Bligh, E.G. & Dyer, W.J., 1959. A rapid method of total lipid extraction and purification. *Canadian journal of biochemistry and physiology*, 37 (8), pp.911-917. doi: 10.1139/o59-099.

Bradford, M.M., 1976. A rapid and sensitive method for the quantitation of microgram quantities of protein utilizing the principle of protein-dye binding. *Analytical biochemistry*, 72(1-2), pp.248-254. doi: 10.1016/0003-2697(76)90527-3.

Chisti, Y., 2007. Biodiesel from microalgae. *Biotechnology advances*, 25(3), pp.294-306. doi: 10.1016/j.biotechadv.2007.02.001.

Croft, M.T. et al., 2005. Algae acquire vitamin B12 through a symbiotic relationship with bacteria. *Nature*, 438(7064), pp.90-93. doi: 10.1038/nature04056.

Domozych, D.S. et al., 2012. The cell walls of green algae: a journey through evolution and diversity. *Frontiers in plant science*, 3, 82. doi: 10.3389/fpls.2012.00082.

DuBois, M. et al., 1956. Colorimetric method for determination of sugars and related substances. *Analytical chemistry*, 28(3), pp.350-356. doi: 10.1021/ac60111a017.

Fachrullah, M.R., 2011. *Laju pertumbuhan mikroalga penghasil Biofuel jenis Chlorella sp. dan Nannochloropsis sp. yang dikultivasi menggunakan air limbah hasil penambangan timah di Pulau Bangka.* Institut Pertanian Bogor

Galvao, R.M. et al., 2013. Modeling of biomass production of *Haematococcus pluvialis*. *Applied Mathematics*, 4, pp.50–56, doi: 10.4236/am.2013.48A008.

Gangl, D. et al., 2015. Biotechnological exploitation of microalgae. *Journal of Experimental Botany*, 66(22), pp.6975- 6990.

Guschina, I.A. & Harwood, J.L., 2006. Lipids and lipid metabolism in eukaryotic algae. *Progress in lipid research*, 45(2), pp.160-186.doi: 10.1016/j.plipres.2006.01.001.

Hanief, S. et al., 2020. November. Growth kinetic of *Botryococcus braunii* microalgae using logistic and gompertz models. *AIP Conference Proceedings*, 2296(1), 02006. doi: 10.1063/5.0030459.

Hermiastuti, M., 2013. *Analisis kadar protein dan identifikasi asam amino pada ikan patin (Pangasius djambal).* University of Jember.

Ho, S.H. et al., 2011. Perspectives on microalgal CO_2-emission mitigation systems—a review. *Biotechnology advances*, 29(2), pp.189-198.doi: 10.1016/j.biotechadv.2010.11.001.

Lam, M.K. et al., 2017. Cultivation of *Chlorella vulgaris* using nutrients source from domestic wastewater for biodiesel production: Growth condition and kinetic studies. *Renewable Energy*, 103, pp.197-207, doi: 10.1016/j.renene.2016.11.032.

Lee, A.K., Lewis, D.M. & Ashman, P.J., 2009. Microbial flocculation, a potentially low-cost harvesting technique for marine microalgae for the production of biodiesel. *Journal of Applied Phycology*, 21, pp.559-567. doi: 10.1007/s10811-008-9391-8.

Levasseur, W. et al. 2020. A Review of High Value-Added Molecules Production by Microalgae in Light of the Classification. *Biotechnol.*, 41, 107545. doi: 10.1016/j.biotechadv.2020.107545.

Markou, G. et al. 2012. An Overview of the Factors Influencing Carbohydrates Production, and of Main Bioconversion Technologies for Production of Biofuels. *Appl. Microbiol. Biotechnol*, 96, pp.631–645. doi: 10.1007/s00253-012-4398-0.

Novaryatiin, S., Priyanto, B., Masduki, A., 2015. Isolasi dan karakterisasi potensi biodiesel mikroalga air tawar yang dikoleksi dari beberapa perairan umum sekitar Tangerang dan Bogor. *Jurnal Surya Medika*, 1(1), pp.23-30.

Nugroho, C., 2006. *Efek Pb terhadap laju pertumbuhan dan biomassa spirulina platensis*. Universitas Gadjah Mada.

Phukoetphim, N. et al., 2017. Kinetic models for batch ethanol production from sweet sorghum juice under normal and high gravity fermentations: Logistic and modified Gompertz models. *Journal of Biotechnology*, 243, pp.69-75, doi: 10.1016/j.jbiotec.2016.12.012.

Pillai, J., 1997. *Flocullants and Coagulants: The Keys to Water and Waste Management in Aggregate Production*, Illinois: Nalco Company.

Pradana, Y.S. et al., 2018. Extractive-transesterification of Microalgae *Arthrospira* sp. using Methanol-Hexane Mixture as Solvent. *International Journal of Renewable Energy Research*, 8(3), pp.1499-1507. doi: 10.20508/ijrer.v8i3.7817.g7448.

Rahmawati, A., 2020. *Bioflokulasi Konsorsium Glagah dengan Anabaena* sp. Universitas Gadjah Mada.

Rinanti, A. & Purwadi, R., 2018. May. Pemanfaatan Mikroalga Blooming dalam Produksi Bioethanol tanpa Proses Hidrolisis (Utilization of Blooming Microalgae in Bioethanol Production without Hydrolysis Process). *Seminar Nasional Kota Berkelanjutan*, 1(1), pp. 281-292.

Salim, S. et al., 2011. Harvesting of microalgae by bio-flocculation. *Journal of applied phycology*, 23, pp.849-855, doi: 10.1007/s10811-010-9591-x.

Saputra, D., 2013. *Pengembangan Bioflokulasi Sebagai Teknik Pemanenan Mikroalga Ramah Lingkungan*. Institut Pertanian Bogor.

Sathe, S., 2010. *Culturing and Harvesting Microalgae for the Large- scale Production of Biodiesel*. The University of Adelaide.

Huang, B. et al., 2017. Modulation of lipid biosynthesis by stress in diatoms. *Philosophical Transactions of the Royal Society B: Biological Sciences*, 372(1728), 20160407, doi: 10.1098/rstb.2016.0407.

Sayanova, O. et al., 2017. Modulation of lipid biosynthesis by stress in diatoms. *Philosophical Transactions*, 5(372), pp.1-14.

Suantika, G. & Pingkan, Y., 2009. *Pengaruh Kepadatan Awal Inokulum terhadap Kualitas Kultur Chaetoceros gracilis (Schuut) pada Sistem Batch*. Institut Teknologi Bandung.

Suyono, E.A., Nuhamunada, M. & Ramadhani, N., 2016a. Lipid content from monoculture of microalgae *Chlorella zofingiensis* Dönz and mixed culture of Glagah isolate in laboratory scale and raceway pond for biodiesel production. *Asian Journal of Microbiology, Biotechnology and Environmental Sciences*, 18(1), pp.101-106.

Suyono, E.A., Fahrunnida, N.S. & Utama, I.V., 2016b. Identification of microalgae species and lipid profiling of Glagah consortium for biodiesel development from local marine resource. *Journal of Engineering and Applied Sciences*, 11(16), pp.9970-9973.

Tiwari, O.N. et al., 2015. Characterization and optimization of bioflocculant exopolysaccharide production by cyanobacteria *Nostoc* sp. BTA97 and Anabaena sp. BTA990 in culture conditions. *Applied biochemistry and biotechnology*, 176, pp.1950-1963. doi: 10.1007/s12010-015-1691-2.

Yang, J.S. et al., 2011. Mathematical model of *Chlorella minutissima* UTEX2341 growth and lipid production under photoheterotrophic fermentation conditions. *Bioresource Technology*, 102(3), pp.3077-3082, doi: 10.1016/j.biortech.2010.10.049.

Yasmine, Q. 2011. *Pengaruh Metode freezing (-4 oC) terhadap kadar klorofil dan protein pada Train- stain Nostoc [Vaucher 1803) Bornett et Flauhalt.* Univeristas Indoneisa.

Yen, H.W. et al., 2013. Microalgae-based biorefinery–from biofuels to natural products. *Bioresource technology*, 135, pp.166-174, doi: https: 10.1016/j.biortech.2012.10.099.

Journal of Tropical Biodiversity and Biotechnology
Volume 09, Issue 01 (2024): jtbb88238
DOI: 10.22146/jtbb.88238

Research Article

Hesperitin Synergistically Promotes the Senescence Induction of Pentagamavunone-1 in Luminal Breast Cancer Cells, T47D

Fauziah Novita Putri Rifai[1,2], Mila Hanifa[2], Ummi Maryam Zulfin[2], Muthi Ikawati[2,3], Edy Meiyanto[2,3]*

1)Master of Biotechnology Study Program, Graduate School, Universitas Gadjah Mada, Yogyakarta 55281, Indonesia
2)Cancer Chemoprevention Research Center, Faculty of Pharmacy, Universitas Gadjah Mada, Yogyakarta 55281, Indonesia
3)Macromolecular Engineering Laboratory, Department of Pharmaceutical Chemistry, Faculty of Pharmacy, Universitas Gadjah Mada, Yogyakarta 55281, Indonesia
* Corresponding author, email: edy_meiyanto@ugm.ac.id

Keywords:
Curcumin analog
Hesperitin
Senescence
Synergistic effect
T47D cells
Submitted:
23 August 2023
Accepted:
03 November 2023
Published:
04 March 2024
Editor:
Ardaning Nuriliani

ABSTRACT

Pentagamavunone-1 (PGV-1), a curcumin analog, is a promising anticancer candidate for several cancers that have been proven *in vitro* and *in vivo*. However, the efficacy of PGV-1 against breast cancer is subject to improvement to achieve a more suitable application. Here we propose hesperitin, a citrus flavonoid, to increase the anticancer potency of PGV-1 in luminal breast cancer cells. We use the T47D cell as the model to investigate the effect of co-administration of PGV-1 and hesperitin on cell cycle block, apoptosis modulation, and senescence phenomena. PGV-1 and hesperitin showed strong and weak cytotoxicity with an IC_{50} value of 2 µM and 100 µM, respectively. The co-treatment of PGV-1 and hesperitin resulted in strong synergistic effects with combination index (CI) value of ≤ 0.2. This combination caused apoptosis in correlation with cell cycle disruption in G2/M phase at 48 h. In particular, PGV-1 and hesperitin combination increased the incidence of cellular senescence significantly higher than the single treatment. Despite its senescence potentiation, hesperitin did not induce senescence in normal cells. Taken together, hesperitin may increase the anticancer potency of PGV-1 by modulating cell cycle arrest and apoptosis via the senescence mechanism.

Copyright: © 2024, J. Tropical Biodiversity Biotechnology (CC BY-SA 4.0)

INTRODUCTION

Luminal breast cancer therapy remains a major challenge in oncology (Masoud & Pagès 2017). In addition to the complexity of the cellular physiology of cancer, there is also the emergence of resistance to specific targeted drugs (Baghban et al. 2020). Tamoxifen and its analogs are an example of a chemotherapeutic agent with a specific target, namely the estrogen receptor (ER) which is then referred to as an ER antagonist (Burstein 2020). Long-term use of ER antagonists can cause cancer cell resistance because cancer cells will divert their growth signal to the MAPK pathway (Clusan et al. 2023). In this case, the growth of cancer cells will not depend on ER signals anymore. Diversion of this pathway also occurs in the use of aromatase inhibitor drugs which causes a decrease in their effectiveness (Heery et al. 2020). Therefore, luminal breast

cancer therapy still requires other specific targeted agents. The application of agents that target DNA (e.g. doxorubicin) or microtubules (e.g. taxol) is an option, but there are still problems with side effects that make the patient's condition worse (Čermák et al. 2020). To overcome this problem, the finding of drugs that are safer but effective for luminal breast cancer is taken as a challenge.

Our group has developed a prospective anticancer agent, called Pentagamavunone-1 (PGV-1). This compound exhibits high cytotoxic activities against luminal breast cancer and triple negative breast cancer (TNBC) (Meiyanto & Larasati 2019; Utomo et al. 2022). In the xenograft model, PGV-1 also shows significant effect of tumor growth suppressor activity against several types of cancer, such as TNBC and leukemia (Lestari et al. 2019). Interestingly, the tumor growth inhibition ability of PGV-1 is comparable to that of standard drugs (Meiyanto et al. 2019). Moreover, PGV-1 did not show any significant side effects (Novitasari et al. 2021). Due to its potential anti-cancer characteristics, PGV-1 holds promise for future development as a chemotherapy treatment.

The distinctive ability of PGV-1 to impede the growth of cancer cells lies in its cleverness, specifically by hindering the process of mitosis during prometaphase (Lestari et al. 2019). However, the performance of PGV-1 as an anticancer still needs to be improved to gain more effectiveness to suppress tumor cell development. One strategy is to apply in combination with chemopreventive agents that can increase their cytotoxic effect on cancer cells synergistically (Hasbiyani et al. 2021; Musyayyadah et al. 2021; Endah et al. 2022). Chemopreventive agents are compounds that have weak tumor growth inhibiting properties through inhibition of growth signals, for example MAPK inhibitors (Haque et al. 2021). These compounds can be expected to support the cytotoxic properties of other anticancer compounds with different targets.

Those compounds that potentially act as MAPK inhibitors are mostly flavonoid substances, including ones that are largely found in citrus (Meiyanto et al. 2012). So far, there are several citrus flavonoid compounds that have been applied in combination with chemotherapeutics agents to suppress cancer growth, including the co-treatment with PGV-1 in some types of cancer cells. The results of all studies on the combination of flavonoids with chemotherapeutics agents synergistically increase their cytotoxic effects. For example, diosmin with PGV-1 synergistically enhances their cytotoxicity through modulation of senescence and mitotic catastrophe in TNBC 4T1 cells (Musyayyadah et al. 2021). Diosmin also enhances the cytotoxicity of PGV-1 in colon cancer cells (Ikawati et al. 2023). In accordance to those findings, the combination of a chemotherapy agent doxorubicin with hesperidin and its aglycone form, hesperitin, synergistically inhibits the migration of 4T1 and MCF7/HER2 cells (Nurhayati et al. 2020; Amalina et al. 2023). Both hesperidin and hesperitin have great potential to amplify the cancer-preventive efficacy of PGV-1 within breast cancer cells.

Hesperidin and hesperitin are two major methoxy flavonoids of *Citrus* sp. that are considerably safe to normal cells (Putri et al. 2022). They are selectively cytotoxic toward cancer cells but not toxic in normal cells (Filho et al. 2021; Choi et al. 2022). Even though showing similar bioactivities, the bioavailability of these two compounds remains critical in considering the best one as a co-chemotherapeutic agent. Hesperidin has lower bioavailability than hesperitin (Wdowiak et al. 2022). The low bioavailability of hesperidin in systemic circulation is due to the presence of the rutinoside sugar group attached to the flavonoid (Crescenti et al. 2022). Moreover, oral hesperidin undergoes first pass metabolism

(Corrêa et al. 2019). Hesperidin must be deglycosylated into hesperitin before it has the capability to be taken in by the intestine (Corrêa et al. 2019). Intestinal enterobacteria release α-rhamnosidase and β-rhamnosidase that will cleave the rutinoside sugar group in hesperidin into its aglycone (Mueller et al. 2018). Meanwhile, hesperitin can passively diffuse into the blood to obtain optimal bioavailability (Takumi et al. 2012; Wdowiak et al. 2022). Thus, the approach to exploring the potential of co-chemotherapeutic agents from the citrus flavonoid hesperitin has a more promising potential in the future.

We previously investigated hesperidin in combination with PGV-1. In this study, we focused on investigating the synergistic effect of applying combination treatment hesperitin and PGV-1 on luminal breast cancer cells. We used T47D as a model that represents ER expressing breast cancer cell lines. This cell line is also known to express PgP that facilitates efflux of some chemotherapeutic drugs resulting in resistance phenomenon (Lee & Choi 2022). Swiss Prediction analysis, fortunately shows that PGV-1 is not subjected to be the substrate of PgP. However, hesperitin shows inhibitory effects on the MAPK/Akt pathway to induce autophagy and apoptosis that might contribute to growth inhibitory effect of PGV-1 on T47D cells (Lin et al. 2023). Our primary aim is to assess the ability of hesperitin to augment the efficacy of PGV-1, particularly in luminal breast cancer. Additionally, we aim to explore the impact of combining these two compounds on the phenomenon of cell death.

MATERIALS AND METHODS

Ethical approval

Authorization for all research procedures was granted by the Medical and Health Ethical Committee of the Faculty of Medicine, Public Health and Nursing, Universitas Gadjah Mada (No. KE/FK1012/EC/2020).

Chemicals

Cancer Chemoprevention Research Center (CCRC), Faculty of Pharmacy, Universitas Gadjah Mada was provided PGV-1 with purity HPLC 95% (Utomo et al. 2022). Hesperitin (HST) was obtained from Sigma Aldrich (No. Cat. W431300-5G).

Cell culture

T47D cells, NIH-3T3 cells, and Vero cells were cultured in Dulbecco's Modified Eagle's Medium (DMEM) high glucose (Gibco), enriched with 10% fetal bovine serum (FBS) (Gibco), and 1% Penicillin-Streptomycin (Gibco). This cultivation was carried out in an incubator at 37°C with a 5% CO_2 atmosphere. The cells were collected using 0.25% Trypsin-EDTA (Gibco) when they reached approximately 80% confluence.

Trypan blue exclusion assay

Cultures of T47D cells (5×10^4 cells/well) were established in 24-well plates and allowed to incubate for one night. Cells were treated with 0.5-16 µM PGV-1, 15-1000 µM HST, or their combinations. After 24 h incubation, the cells were rinsed using 500 µL of phosphate buffer saline (PBS) 1×, followed by the addition of 100 µL of 0.25% trypsin-EDTA per well for a duration of 3 min. Cell suspension (10 µL) was treated with 10 µL of trypan blue 0.4%. Cells devoid of color were considered viable cells, while cells displaying a blue hue were regarded as dead cells. Viable and overall cell counts were performed within each well using an inverted microscope (Olympus). The percentage of cell viability was derived from the ratio of viable cells to total cells. This metric was utilized to compute

IC_{50} and CI values across three separate experiments, each conducted in triplicate (Musyayyadah et al. 2021).

MTT Assay

NIH-3T3 and Vero cells (1×10^4 cells/well) were introduced into 96-well plates and allowed to incubate overnight. Following this, the cells were exposed to varying concentrations of HST (ranging from 1 µM to 500 µM) for a duration of 24 h. Subsequently, the cells underwent a PBS wash, and a solution comprising 100 µL of 0.5% 3-(4,5-dimethylthiazol-2-yl)-2,5-diphenyltetrazolium bromide (MTT) (Sigma) in PBS 1× was added, followed by a 4 h incubation period. Once the conversion of tetrazolium salts to blue formazan crystals was complete, as denoted by their visible presence, 100 µL of 10% sodium dodecyl sulfate (SDS) stopper was introduced, and the cells were left to incubate overnight. The measurement of absorbance at 595 nm was performed using an ELISA reader (Bio-Rad) (Hanifa et al. 2022).

Measuring cell cycle profile

T47D cells (2×10^4 cells/well) were cultured in 6-well plates and left to incubate overnight. Following this, cells underwent treatment with PGV-1 at concentrations of 0.5 and 1 µM, HST at concentrations of 25 and 50 µM, as well as their combination, for a duration of 24 h. After treatment, the cells were subjected to a wash with 500 µL of PBS 1x, followed by detachment using 0.25% trypsin-EDTA for a 3 min interval. To deactivate the enzyme, 1 mL of culture medium was introduced, and the cells were gathered, subsequently undergoing a rinse with 500 µL of cold PBS 1x. Centrifugation at 600 rpm for 5 min facilitated the removal of the supernatant, after which the pellet cells were fixed using 500 µL of 70% alcohol, and this was done at room temperature for a span of 30 min, followed by another 5-min centrifugation. The pellet cells then underwent a wash with 500 µL of PBS 1x, once again followed by centrifugation. Subsequently, the resulting cells were stained with a solution composed of 1 mg/ml propidium iodide (Merck), 10 mg/mL RNAse (Merck), Triton-X 100 at a volume of 1 (Merck), and PBS 1x. Cell distribution across the SubG1, G0/G1, S, and G2/M phases, indicative of DNA content, was assessed utilizing Flow Cytometry (BD Biosciences Accuri C6) alongside BD Accuri C6 Software (Amalina et al. 2023).

Measuring apoptosis

T47D cells (2×10^4 cells/well) were cultivated within 6-well plates and left to incubate overnight. Subsequently, the cells were subjected to treatment with either PGV-1 or HST separately, as well as in combination, for durations of 24 and 48 h. Following treatment, the cells underwent a wash with 500 µL of PBS 1x, and then were detached utilizing 0.25% trypsin-EDTA for a span of 3 min. The enzyme reaction was deactivated through the introduction of 1 mL of culture medium, after which the cells were gathered. Centrifugation at 600 rpm for 5 min was performed, resulting in the removal of the supernatant. The pellet cells were subsequently exposed to 100 µL of binding buffer, 5 µL of FITC Annexin V, and 5 µL of propidium iodide (PI) (at a concentration of 50 µg/mL) for a 5 min interval. Analysis using Flow Cytometry (BD Biosciences Accuri C6) in conjunction with BD Accuri C6 Software was employed to discern between live, apoptotic, and necrotic cells (Amalina et al. 2023).

Measurement of senescent cells

All cell models (T47D, NIH-3T3, and Vero cells) were grown in the concentration of 1, 2, and 2, respectively 10^4 cells/well into 6-well plates and

allowed to incubate overnight. After incubation with the drugs for 24 h, the cells underwent a PBS 2× pH 6.0 rinse, followed by fixation using a 4% paraformaldehyde solution for 10 min. Subsequent washing was carried out twice with 1× PBS, followed by staining using a 1 mL X-gal solution. Following an incubation period of 72 hours, the cells were assessed under an inverted microscope at 200× magnification, and enumeration was conducted using ImageJ Software (Salsabila et al. 2023).

Data analysis

The gathered experimental data underwent analysis through SPSS 25 (SPSS Inc., Chicago, IL, USA, version 25). One-way ANOVA was implemented to assess distinctions between groups and an independent sample *t*-test was used to ascertain differences between individual samples. Following that, the Bonferroni test was employed in conjunction with one-way ANOVA, with considering significance at a level of $p < 0.05$.

RESULTS

Growth inhibitory effects of PGV-1 and HST on T47D cells

We assessed the cytotoxic characteristics of PGV-1, HST, and their combined effect on T47D luminal breast cancer cells through the trypan blue exclusion assay. First, we performed a single cytotoxic assay using PGV-1 and HST in T47D cells for 24 h. We found that both PGV-1 and HST exhibited cytotoxic properties, with IC_{50} values of 2 µM and 100 µM, respectively (Figure 1a and 1b). These results indicate that PGV-1 shows strong cytotoxic activity, whereas HST has a weak cytotoxic effect on T47D cells. Thus, PGV-1 has a stronger inhibitory effect on cell growth than HST does ($p < 0.001$).

Next, we combined the growth suppression properties of PGV-1 and HST against T47D at different concentrations of PGV-1 0.25 µM, 0.5 µM, 1µM and HST 12.5 µM, 25 µM, 50 µM. Interestingly, HST in-

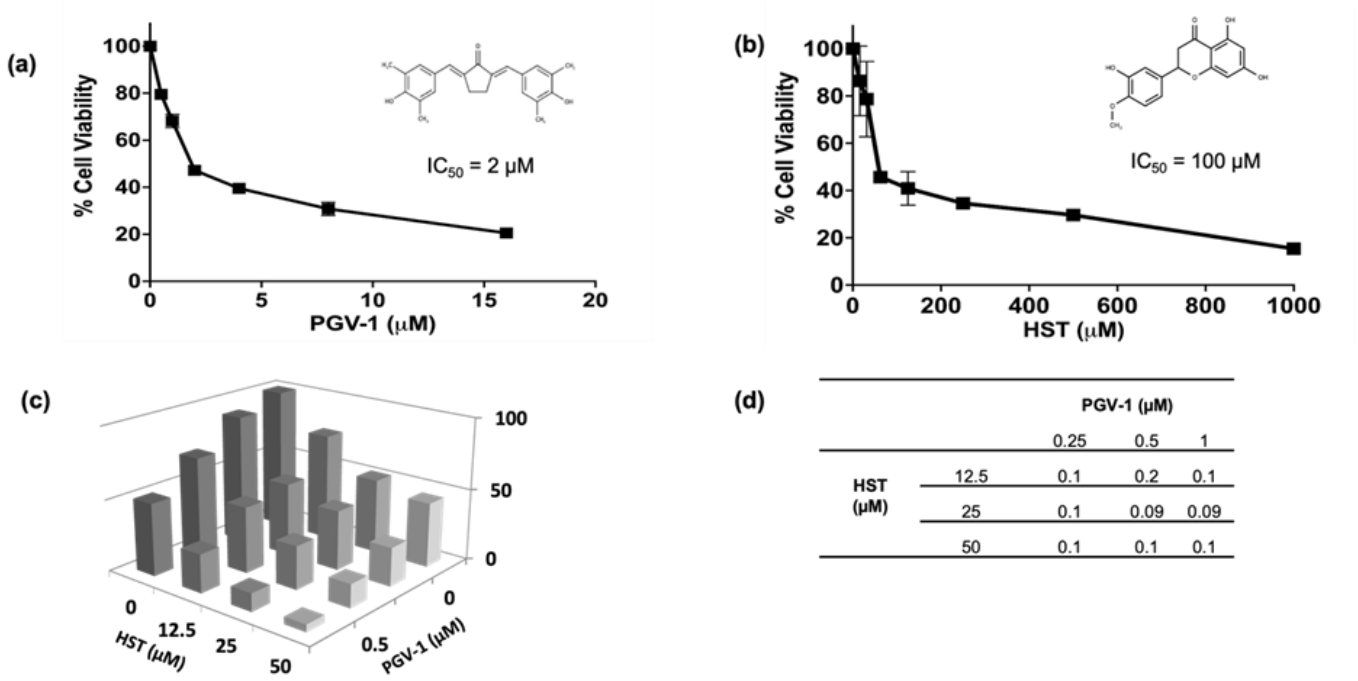

Figure 1. Growth suppression properties of PGV-1, HST, and their co-administration in T47D cells. Cells were subjected with PGV-1 (a), HST (b), or their co-administration (c). The concentrations of PGV-1 and HST used in the combination were based on IC_{50} value, which are PGV-1 0.25 µM, 0.5 µM, 1 µM and HST 12.5 µM, 25 µM, 50 µM, respectively. Cell viability and CI value (d) are expressed as the mean ± standard error (SE) for a total of three replicates.

creased the efficacy of PGV-1 synergistically with CI values ≤ 0.2 (Figure 1c and 1d). The combination of PGV-1 and HST is believed to have good prospects as a chemotherapeutic agent. Thus, we used the combined cytotoxic assay concentrations of PGV-1 and HST for further testing on cell cycle, apoptosis, and cellular senescence effects.

Effect of PGV-1 and HST on cell cycle profile

To investigate the impact of combining HST and PGV-1 in restraining cancer cell growth, we examined the influence of HST and PGV-1 individually and in co-administration on hindering the progression of cell cycle. HST and PGV-1 showed cell cycle arrest phenomenon in 24 h incubation time. In this case, PGV-1 0.5 and 1 µM exert cell cycle inhibition especially at G2/M phase by 33% and 34% (Figure 2, $p < 0.05$). A comparable outcome was likewise witnessed in the examinations involving HST concentrations of 25 and 50 µM, resulting in a 31% adjustment in cell cycle inhibition at the G2/M phase (Figure 2). Additionally, the co-administration application of all doses of HST and PGV-1 led to cell cycle inhibition within the G2/M phase (Figure 2). Notably, the co-administration of HST at 50 µM and PGV-1 at 0.5 µM exhibited the most substantial cell cycle inhibition in the G2/M phase among the various concentrations, particularly within T47D. Halting the cell cycle progression at the G2/M phase prompts cancer cells to cease their proliferation and eventually undergo cell death. Nevertheless, additional verification is necessary to substantiate the collaborative impact of the two compounds on inducing cancer cell demise.

Effect of PGV-1 and HST on apoptosis induction

To validate the impact of HST, PGV-1, and their co-administration ap-

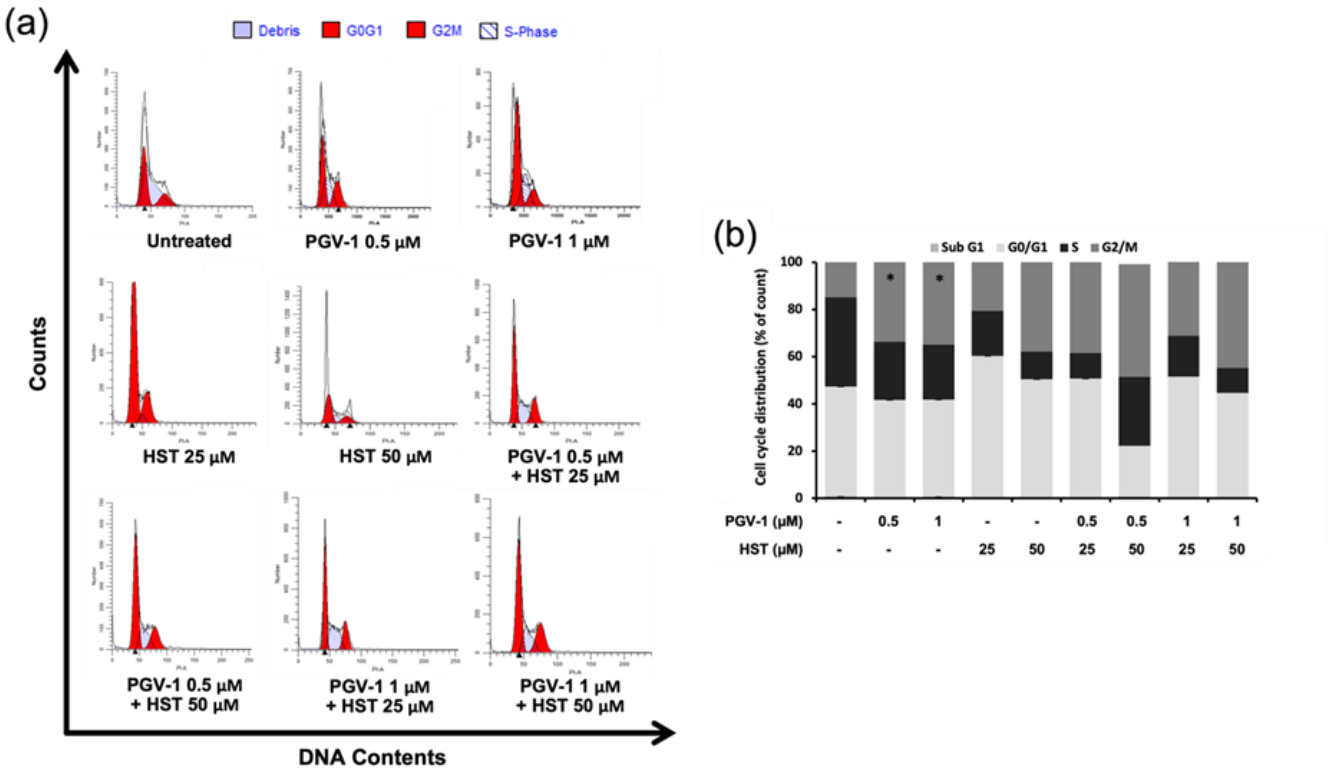

Figure 2. Cell cycle profile after treatment with PGV-1, HST, and their co-administration on T47D. Cells were subjected with PGV-1, HST, or both co-administration in various concentrations as indicated followed by 24 h incubation. After washing with PBS, the cells were stained with propidium iodide and then subjected to flow cytometry. Cell cycle profile were generated from flow cytogram (a) into quantitative diagram (b) to obtained the significance differences (*$p < 0.05$) of the data within three replicated measurement ($n = 3$).

plication on inducing cancer cell death, we performed apoptosis analysis through flow cytometry. HST and PGV-1 alone and its combination manifest apoptosis phenomenon under 10% for 24 h. The percentage of cells undergoing apoptosis is low due to the short incubation period. Therefore, we extended the incubation time of the apoptosis assay to 48 h. After 48 h, their combination exerted apoptotic cells in 21% (Figure 3b). The number of apoptotic cells was two times greater than that of the control. Furthermore, the combination of HST and PGV-1 increased cell death by modulating apoptosis at 48 h. The mechanism of apoptosis induction is associated with DNA damage. Damaged cells undergo senescence before regeneration. We conducted senescence tests to determine morphological cell changes due to the aging of cancer cells, especially luminal breast cancer.

Cellular Senescence Effect

We explored the influence of HST and PGV-1 on inducing senescence in T47D using an assay involving associated *β-galactosidase*. Senescent cells were distinguished by the emergence of a green hue within the cells, indicating the presence of *β-galactosidase* expression (Figure 4a).

PGV-1 and HST alone increased *β-galactosidase* positive cells significantly by two up to three fold compared to the control. Interestingly, their combination showed two-fold induction of green cells than the single treatment (Figure 4b). These results indicate that combining PGV-1 and HST can increase cell senescence in T47D cells, where this pro-senescence effect is highly desirable in cancer. Pro-senescence activity

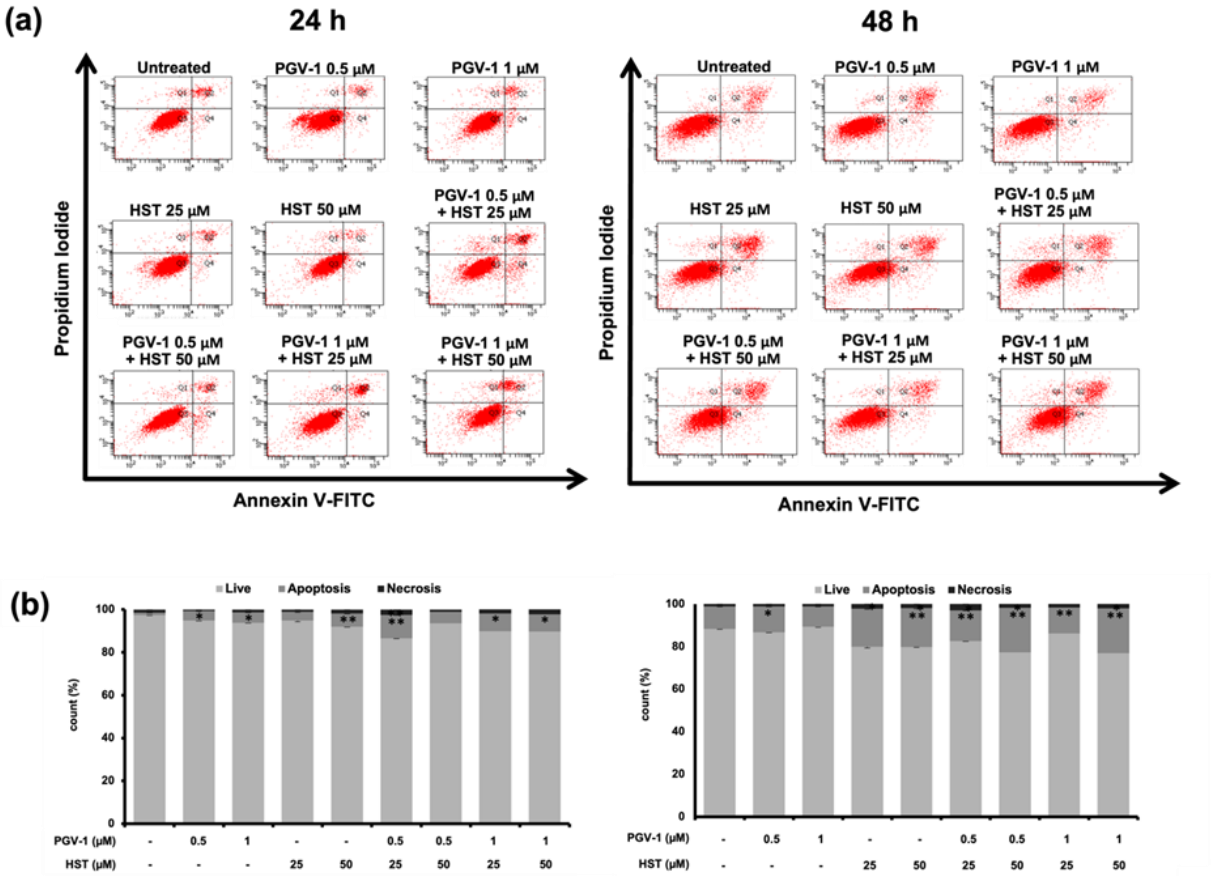

Figure 3. Apoptosis effects after treatment with PGV-1, HST, and their co-administration on T47D. Cells were subjected to PGV-1, HST, or both co-administration in various concentrations as indicated followed by 24 h incubation. After washing with cold PBS, the cells were stained with FITC Annexin V and Propidium Iodide, then subjected to flow cytometry. Apoptosis effects were generated from flow cytogram (a) into quantitative diagram (b) to obtain the significance differences (*p <0.05; **p <0.001) of the data within three replicated measurements (n = 3).

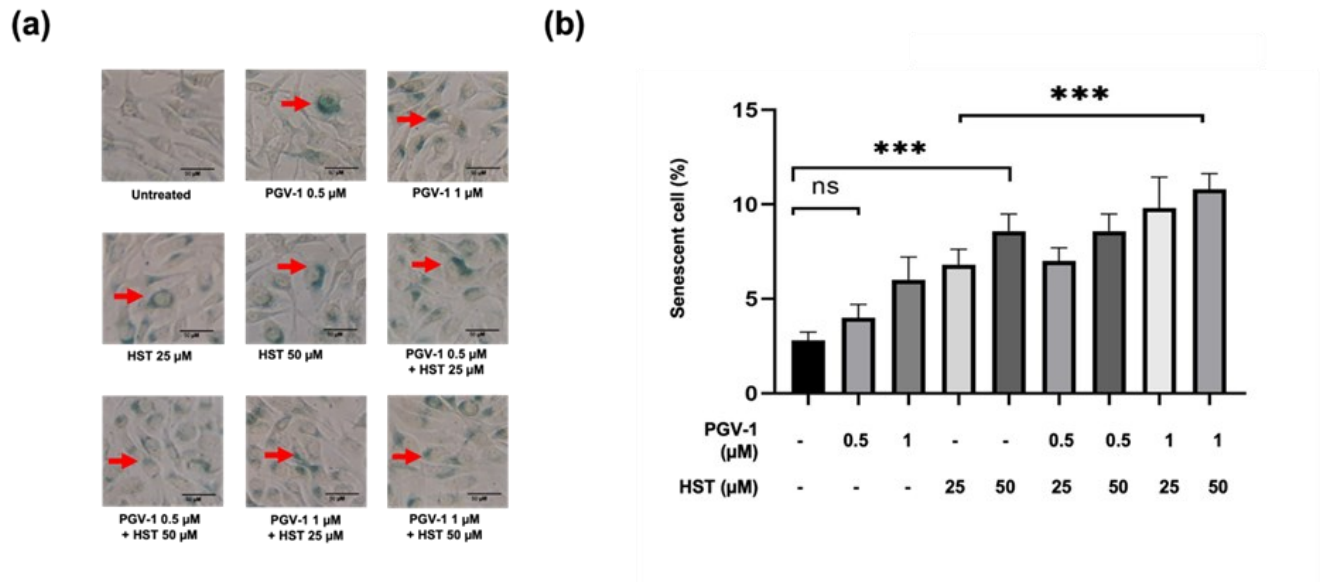

Figure 4. Senescent effects after treatment with PGV-1, HST, and their co-administration on T47D. Cells were subjected to PGV-1, HST, or both co-administration in various concentrations as indicated followed by 24 h incubation. They were stained using X-Gal. (a) Green color (red arrows) indicated cells stained with X-Gal hydrolyzed by β-galactosidase, expressed when cells were senescent. (b) The quantification of cellular senescence. The data are presented as average ($n = 3$). ns, not significant; ***$p \leq 0.001$.

demonstrated as a result of this treatment has a beneficial impact on inhibiting cancer cell development. However, further knowledge of its selectivity in normal cells is still needed to ensure its safety.

HST attenuates DOX induced-normal cells senescence

We evaluated the cytotoxicity and senescent cell effects in NIH-3T3 normal fibroblasts and Vero normal kidney cells. We explored the cytotoxic effects of HST through the MTT assay. HST performs IC_{50} values of 700 µM and 314 µM in NIH-3T3 and Vero cells, respectively (Figure 5a). Consequently, HST was found to be non-toxic to Vero and NIH-3T3 cells.

Additionally, we evaluated the senescence effect of HST on both normal cells by using doxorubicin (DOX) as a cell senescence-inducing agent. DOX produced five times more green cells than green cells in control. Hence, DOX can serve as a positive reference for the senescence assessment (Figure 5b). The combination of DOX with HST of 50 and 100 µM reduced the number of green cells significantly with p value < 0.001 compared to DOX alone. This response suggests that HST reduces intracellular senescent cells in NIH-3T3 and Vero cells.

DISCUSSION

Hesperitin (HST) has long been used as a human health supplement to promote immunity, hormone balance, and inflammatory responses. Knowing the health response to HST, this study challenges its potential as a co-chemotherapeutic agent with PGV-1. The data showed that HST weakly suppressed the growth of T47D cells; however, when combined with PGV-1, HST escalated its cytotoxic effect synergistically. These results indicate that HST potentially enhances PGV-1 efficacy in luminal breast cancer cells by modulating its cytotoxic activity. This effect is probably triggered by differences in the molecular mechanisms of the two compounds.

In order to gain deeper insights into the impact of HST on cellular physiology, we examined the influence of HST alone and in co-

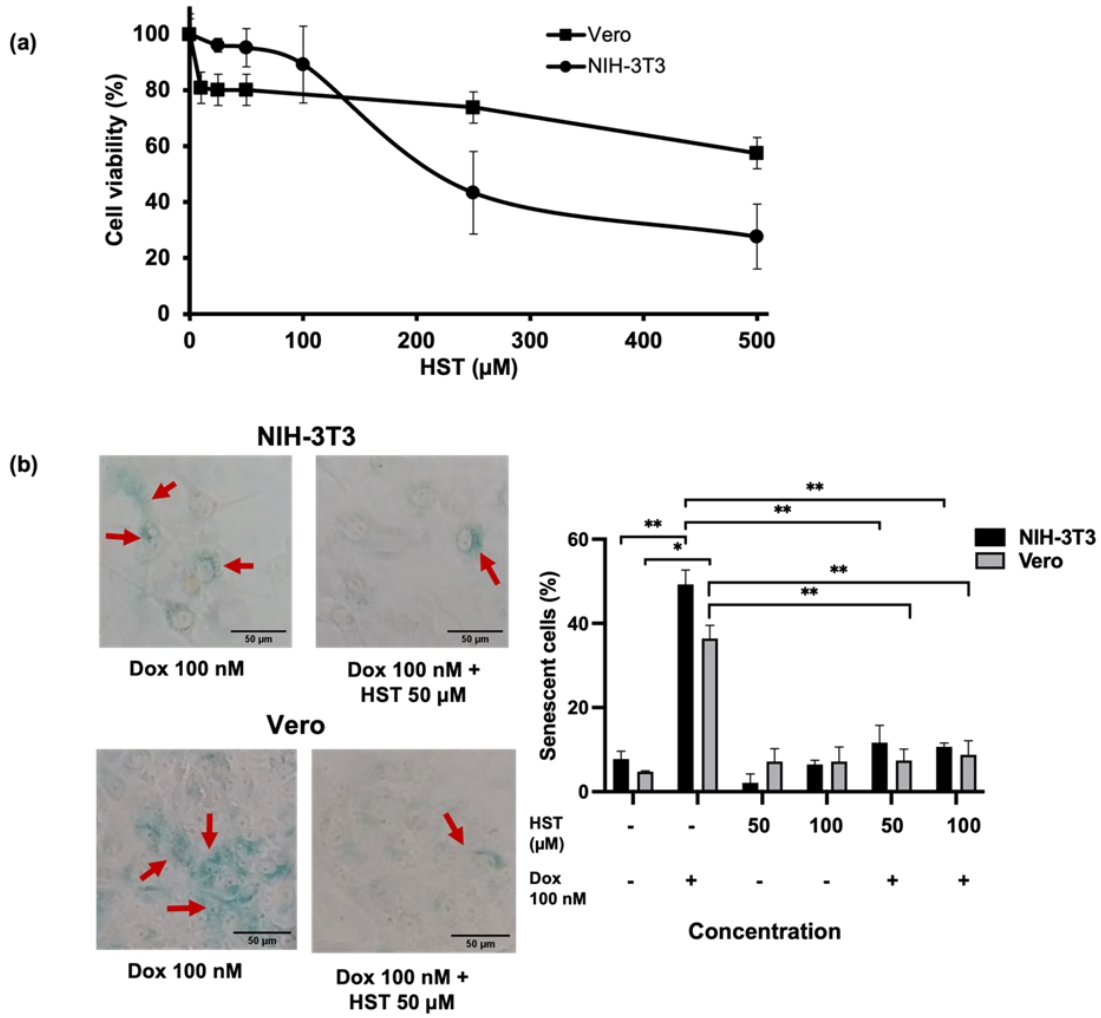

Figure 5. The effect of HST on NIH-3T3 and Vero. (a) Cell viability profile after treatment with drug followed by 24 h incubation. (b) Observation of senescence and its quantification in NIH-3T3 and Vero after being given HST. The results are shown as the mean ± SE for a total of three replicates. Dox: doxorubicin. *p <0.05; **p <0.001.

administration with PGV-1 on the progression of the cell cycle. Remarkably, these combinations exhibited distinct targets for inhibiting the cell cycle. A concentration of 50 μM HST led to the arrest of the cell cycle at the G2/M phase within T47D. Notably, the co-administration of HST and PGV-1 triggered a more pronounced cell cycle helt at the G2/M phase, surpassing the effect of HST treatment alone. A similar effect was observed with a single HST administration in U937 cells (Lin et al. 2023). On the other hand, PGV-1 targets the M phase, specifically the prometaphase (Lestari et al. 2019; Meiyanto et al. 2022). The different target of cell cycle inhibition could result in strong cell growth inhibition and lead to apoptosis (Suski et al. 2021; Hanifa et al. 2022). In this regard, we found that HST elicited modulation of apoptosis of T47D cells at 48 h. Uniquely, HST also causes cell autophagy (Lin et al. 2023). Autophagy triggers the apoptotic response by activating caspase-8 and reducing anti-apoptotic proteins (Fan & Zong 2012). The simultaneous presence of apoptosis and autophagy can strengthen the effect of cancer cell death. We traced the events of cell death further by observing the morphology associated with the process of senescent cells.

Senescent cells become one of the strategic cancer inhibition targets because some cancer cells adapt by deactivating senescence signals (Hanahan & Weinberg 2011). Cell senescence is affected by the presence of cellular stress signals, such as DNA damage and under cellular abrogation (Huang et al. 2022). The concurrent application of HST and PGV-

1 led to a higher count of cells exhibiting senescence. In line with the results of this assay, we know that HST with PGV-1 modulates senescent cells, and this effect is positively correlated with increased inhibition of mitotic cells and cell death. Although the co-administration of these two compounds shows good molecular death effects on luminal breast cancer cells, tracing their cytotoxic activity on normal cells is necessary to ensure their efficacy and safety.

HST possesses strong antioxidant and immunomodulatory properties that hopefully can play a role as the normal cell protection from oxidative stress (Parhiz et al. 2015). For this purpose, we used NIH-3T3 cell line and vero cell line as the representative of skin and kidney tissues respectively, which are usually to be the riskiest tissue against cellular damaging agents (Endah et al. 2022). Our data reveal that individual HST application did not result in toxicity for either NIH-3T3 or Vero cells. Aligned with the outcomes of the cytotoxicity assessment, HST exhibited a reduction in the count of senescent cells induced by doxorubicin (DOX) in both normal cell types. We used DOX as the representative of strong senescent inducing-agents that have been known to cause cellular damage via Reactive Oxygen Species (ROS) generation (Salsabila et al. 2023). These results indicated that HST potentially protects against premature aging and damage to skin and kidney tissues. In this study, HST demonstrated its ability to increase the efficacy of PGV-1 and could help to protect surrounding cells from damage. In general, cell damage can be induced by oxidative agents including drugs, cellular stress, and poisons (Madkour 2020; Zulfin et al. 2021). These findings provide backing for the prospective development of HST as a co-chemotherapeutic agent, capable of enhancing the cytotoxic impact of chemotherapy agents and to reduce the cellular damages caused by toxic agents, including oxidative stress.

CONCLUSION

In conclusion, HST synergistically enhanced PGV-1 efficacy by increasing its growth suppression effect against T47D as representative of luminal breast cancer. This phenomenon correlates to their inhibition of cell cycle machinery especially at mitosis, which leads to senescence and apoptosis. Treatment of HST in combination with PGV-1 may also protect cells from premature aging and prevent damage to kidney tissue. These results suggest the possibility of utilizing HST as a co-chemotherapeutic agent targeting luminal breast cancer, eliciting cell death.

AUTHORS CONTRIBUTION

FNPR and UMZ conducted laboratory experiments and analyzed data; MH analyzed statistical data and prepared the manuscript; MI proofed outline and revised the manuscript; EM constructed the idea, organized and validated all data projects, and finalized the manuscript.

ACKNOWLEDGMENTS

We thank the Cancer Chemoprevention Research Center (CCRC) for assisting in running the research and completing this manuscript. This publication is supported by the Rekognisi Tugas Akhir (RTA) program of UGM 2022. All these experiments are partially supported by the LPDP project 2021.

CONFLICT OF INTEREST

The authors declare no conflicts of interest.

REFERENCES

Amalina, N.D. et al., 2023. In vitro synergistic effect of hesperidin and doxorubicin downregulates epithelial-mesenchymal transition in highly metastatic breast cancer cells. *Journal of the Egyptian National Cancer Institute*, 35(1), 6. doi: 10.1186/s43046-023-00166-3.

Baghban, R. et al., 2020. Tumor microenvironment complexity and therapeutic implications at a glance. *Cell Communication and Signaling*, 18(1), 59. doi: 10.1186/s12964-020-0530-4.

Burstein, H.J., 2020. Systemic Therapy for Estrogen Receptor–Positive, HER2-Negative Breast Cancer. *New England Journal of Medicine*, 383(26), pp.2557–2570. doi: 10.1056/NEJMra1307118.

Čermák, V. et al., 2020. Microtubule-targeting agents and their impact on cancer treatment. *European Journal of Cell Biology*, 99(4), 151075. doi: 10.1016/j.ejcb.2020.151075.

Choi, S.S., Lee, S.H. & Lee, K.A., 2022. A Comparative Study of Hesperitin, Hesperidin and Hesperidin Glucoside: Antioxidant, Anti-Inflammatory, and Antibacterial Activities In Vitro. *Antioxidants*, 11(8), 1618. doi: 10.3390/antiox11081618.

Clusan, L. et al., 2023. A Basic Review on Estrogen Receptor Signaling Pathways in Breast Cancer. *International Journal of Molecular Sciences*, 24(7), 6834. doi: 10.3390/ijms24076834.

Corrêa, T.A.F. et al., 2019. The Two-Way Polyphenols-Microbiota Interactions and Their Effects on Obesity and Related Metabolic Diseases. *Frontiers in Nutrition*, 6, 188. doi: 10.3389/fnut.2019.00188.

Crescenti, A. et al., 2022. Hesperidin Bioavailability Is Increased by the Presence of 2S-Diastereoisomer and Micronization—A Randomized, Crossover and Double-Blind Clinical Trial. *Nutrients*, 14(12), 2481. doi: 10.3390/nu14122481.

Endah, E. et al., 2022. Piperine Increases Pentagamavunon-1 Anti-cancer Activity on 4T1 Breast Cancer Through Mitotic Catastrophe Mechanism and Senescence with Sharing Targeting on Mitotic Regulatory Proteins. *Iranian Journal of Pharmaceutical Research*, 21 (1), e123820. doi: 10.5812/ijpr.123820.

Fan, Y.J. & Zong, W.X., 2012. The cellular decision between apoptosis and autophagy. *Chinese Journal of Cancer*, 32(3), pp.121-129. doi: 10.5732/cjc.012.10106.

Filho, I.K. et al., 2021. Optimized Chitosan-Coated Gliadin Nanoparticles Improved the Hesperidin Cytotoxicity over Tumor Cells. *Brazilian Archives of Biology and Technology*, 64(spe), e21200795. doi: 10.1590/1678-4324-75years-2021200795

Hanahan, D. & Weinberg, R.A., 2011. Hallmarks of Cancer: The Next Generation. *Cell*, 144(5), pp.646–674. doi: 10.1016/j.cell.2011.02.013.

Hanifa, M. et al., 2022. Different Cytotoxic Effects of Vetiver Oil on Three Types of Cancer Cells, Mainly Targeting CNR2 on TNBC. *Asian Pacific Journal of Cancer Prevention*, 23(1), pp.241–251. doi: 10.31557/APJCP.2022.23.1.241.

Haque, A., Brazeau, D. & Amin, A.R., 2021. Perspectives on natural compounds in chemoprevention and treatment of cancer: An update with new promising compounds. *European Journal of Cancer*, 149, pp.165–183. doi: 10.1016/j.ejca.2021.03.009.

Hasbiyani, N.A.F. et al., 2021. Bioinformatics Analysis Confirms the Target Protein Underlying Mitotic Catastrophe of 4T1 Cells under Combinatorial Treatment of PGV-1 and Galangin. *Scientia Pharmaceutica*, 89(3), 38. doi: 10.3390/scipharm89030038.

Heery, A. et al., 2020. Precautions for Patients Taking Aromatase Inhibitors. *Journal of the Advanced Practitioner in Oncology*, 11(2), pp.184-189. doi: 10.6004/jadpro.2020.11.2.6.

Huang, W. et al., 2022. Cellular senescence: The good, the bad and the unknown. *Nature Reviews Nephrology*, 18(10), pp.611–627. doi: 10.1038/s41581-022-00601-z.

Ikawati, M. et al., 2023. The Synergistic Effect of Combination of Pentagamavunone-1 with Diosmin, Galangin, and Piperine in WiDr Colon Cancer Cells: *In vitro* and Target Protein Prediction. *Journal of Tropical Biodiversity and Biotechnology*, 8(2), 80975. doi: 10.22146/jtbb.80975.

Lee, H.J & Choi, C.H., 2022. Characterization of SN38-resistant T47D breast cancer cell sublines overexpressing BCRP, MRP1, MRP2, MRP3, and MRP4. *BMC Cancer*, 22(1), 446. doi: 10.1186/s12885-022-09446-y.

Lestari, B. et al., 2019. Pentagamavunon-1 (PGV-1) inhibits ROS metabolic enzymes and suppresses tumor cell growth by inducing M phase (prometaphase) arrest and cell senescence. *Scientific Reports*, 9 (1), Article 1. doi: 10.1038/s41598-019-51244-3.

Lin, C.Y, Chen, Y.H. & Huang, Y.C., 2023. Hesperitin Induces Autophagy and Delayed Apoptosis by Modulating the AMPK/Akt/mTOR Pathway in Human Leukemia Cells In Vitro. *Current Issues in Molecular Biology*, 45(2), pp.1587–1600. doi: 10.3390/cimb45020102.

Madkour, L.H., 2020. Oxidative stress and oxidative damage-induced cell death. In *Reactive Oxygen Species (ROS), Nanoparticles, and Endoplasmic Reticulum (ER) Stress-Induced Cell Death Mechanisms*, pp.175–197. doi: 10.1016/B978-0-12-822481-6.00008-6.

Masoud, V. & Pagès, G., 2017. Targeted therapies in breast cancer: New challenges to fight against resistance. *World Journal of Clinical Oncology*, 8(2), 120. doi: 10.5306/wjco.v8.i2.120.

Meiyanto, E., Hermawan, A. & Anindyajati, A., 2012. Natural Products for Cancer-Targeted Therapy: Citrus Flavonoids as Potent Chemopreventive Agents. *Asian Pacific Journal of Cancer Prevention*, 13(2), pp.427–436. doi: 10.7314/APJCP.2012.13.2.427.

Meiyanto, E. & Larasati, Y.A., 2019. The Chemopreventive Activity of Indonesia Medicinal Plants Targeting on Hallmarks of Cancer. *Advanced Pharmaceutical Bulletin*, 9(2), pp.219–230. doi: 10.15171/apb.2019.025.

Meiyanto, E. et al., 2019. Anti-proliferative and Anti-metastatic Potential of Curcumin Analogue, Pentagamavunon-1 (PGV-1), Toward Highly Metastatic Breast Cancer Cells in Correlation with ROS Generation. *Advanced Pharmaceutical Bulletin*, 9(3), pp.445–452. doi: 10.15171/apb.2019.053.

Meiyanto, E. et al., 2022. Bioinformatic and Molecular Interaction Studies Uncover That CCA-1.1 and PGV-1 Differentially Target Mitotic Regulatory Protein and Have a Synergistic Effect against Leukemia Cells. *Indonesian Journal of Pharmacy*, 33(2), pp.225-233. doi: 10.22146/ijp.3382.

Mueller, M. et al., 2018. Rhamnosidase activity of selected probiotics and their ability to hydrolyse flavonoid rhamnoglucosides. *Bioprocess and Biosystems Engineering*, 41(2), pp.221–228. doi: 10.1007/s00449-017-1860-5.

Musyayyadah, H. et al., 2021. The Growth Suppression Activity of Diosmin and PGV-1 Co-Treatment on 4T1 Breast Cancer Targets Mitotic Regulatory Proteins. *Asian Pacific Journal of Cancer Prevention*, 22(9), pp.2929–2938. doi: 10.31557/APJCP.2021.22.9.2929.

Novitasari, D. et al., 2021. CCA-1.1, a Novel Curcumin Analog, Exerts Cytotoxic anti- Migratory Activity toward TNBC and HER2-Enriched Breast Cancer Cells. *Asian Pacific Journal of Cancer Prevention*, 22(6), pp.1827–1836. doi: 10.31557/APJCP.2021.22.6.1827.

Nurhayati, A.P.D. et al., 2019. The phagocytosis activity of isoeugenol-ester compound on Mus musculus macrophage cell. *Nusantara Bioscience*, 11(2), Article 2. doi: 10.13057/nusbiosci/n110201.

Parhiz, H. et al., 2015. Antioxidant and Anti-Inflammatory Properties of the Citrus Flavonoids Hesperidin and Hesperetin: An Updated Review of their Molecular Mechanisms and Experimental Models. *Phytotherapy Research*, 29(3), pp.323–331. doi: 10.1002/ptr.5256.

Putri, D.D.P. et al., 2022. Acute toxicity evaluation and immunomodulatory potential of hydrodynamic cavitation extract of citrus peels. *Journal of Applied Pharmaceutical Science*, 12(4), pp.136–145. doi: 10.7324/JAPS.2022.120415.

Salsabila, D. et al., 2023. Cytoprotective Properties of Citronella Oil (Cymbopogon nardus (L.) Rendl.) and Lemongrass Oil (Cymbopogon citratus (DC.) Stapf) through Attenuation of Senescent-Induced Chemotherapeutic Agent Doxorubicin on Vero and NIH-3T3 Cells. *Asian Pacific Journal of Cancer Prevention*, 24(5), pp.1667–1675. doi: https://doi.org/10.31557/APJCP.2023.24.5.1667.

Suski, J.M. et al., 2021. Targeting cell-cycle machinery in cancer. *Cancer Cell*, 39(6), pp.759–778. doi: 10.1016/j.ccell.2021.03.010.

Takumi, H. et al., 2012. Bioavailability of orally administered water-dispersible hesperitin and its effect on peripheral vasodilatation in human subjects: Implication of endothelial functions of plasma conjugated metabolites. *Food & Function*, 3(4), 389. doi: 10.1039/c2fo10224b.

Utomo, R.Y. et al., 2022. Preparation and Cytotoxic Evaluation of PGV-1 Derivative, CCA-1.1, as a New Curcumin Analog with Improved-Physicochemical and Pharmacological Properties. *Advanced Pharmaceutical Bulletin*, 12(3), pp.603–612. doi: 10.34172/apb.2022.063.

Wdowiak, K. et al., 2022. Bioavailability of Hesperidin and Its Aglycone Hesperitin—Compounds Found in Citrus Fruits as a Parameter Conditioning the Pro-Health Potential (Neuroprotective and Antidiabetic Activity)—Mini-Review. *Nutrients*, 14(13), 2647. doi: 10.3390/nu14132647.

Zulfin, U. et al., 2021. Reactive oxygen species and senescence modulatory effects of rice bran extract on 4T1 and NIH-3T3 cells co-treatment with doxorubicin. *Asian Pacific Journal of Tropical Biomedicine*, 11(4), 174. doi: 10.4103/2221-1691.310204.

Journal of Tropical Biodiversity and Biotechnology
Volume 09, Issue 01 (2024): jtbb86455
DOI: 10.22146/jtbb.86455

Research Article

First Report on Wild Occurrences of Phoenix Mushroom (*Pleurotus pulmonarius* Fr. Quél.) in Indonesia

Ivan Permana Putra[1]*, Oktan Dwi Nurhayat[2], Mada Triandala Sibero[3], Rudy Hermawan[4]
1)Department of Biology, Faculty of Mathematics and Natural Sciences, IPB University. Gedung Biologi, Jalan Agatis Kampus IPB Dramaga, Bogor 16680, Indonesia
2)Research Center for Applied Microbiology, National Research and Innovation Agency (BRIN), Bogor, West Java, 16914, Indonesia
3)BETA Research, Perum Bintang Regency, Jabungan 50266, Semarang City, Central Java, Indonesia
4)Alumni of Microbiology Program, Department of Biology, Faculty of Mathematics and Natural Sciences, IPB University. Gedung Biologi, Jalan Agatis Kampus IPB Dramaga, Bogor 16680, Indonesia.
* Corresponding author, email: ivanpermanaputra@apps.ipb.ac.id

Keywords:
Basidiomycota
Edible
Morphology
Phylogeny
Pleurotus
Submitted:
03 July 2023
Accepted:
12 October 2023
Published:
08 March 2024
Editor:
Miftahul Ilmi

ABSTRACT
The genus *Pleurotus* is known as a commercially important mushroom and one of the most well-known cultivated mushrooms worldwide. Of many species of *Pleurotus*, the phoenix mushroom (*P. pulmonarius*) is cultivated in many countries, including Indonesia. In Indonesia, the farmers and larger companies usually use commercial strains of phoenix mushroom which they purchased from other countries. To date, there was no prior information regarding wild occurrences of *P. pulmonarius* in Indonesia. During our regular mushroom hunting in Sukabumi, West Java, Indonesia, some edible wild fruiting bodies of light brown *Pleurotus* were collected. The current study aimed to determine the taxonomical position of our specimens based on morphological and molecular evidence. The combination of morphological and molecular analysis confirmed our specimens as *P. pulnonarius.* Morphologically, our specimens were distinguished by the small to medium sized fruiting bodies, pileus light brown, pinkish brown, to pale brown, flabelliform in the beginning to expanding broadly ovoid in maturity, lamellae shortly to deeply decurrent, stipe fleshy, eccentric to lateral, concolorous with lamellae, Basidiospores cylindrical to ellipsoid, basidia clavate to club shaped, basidioles are abundant, oleiferous hyphae common. The BLAST result revealed that our specimens posed a high similarity to *P. pulnonarius* from several countries as the top hits. The ITS phylogenetic tree placed *Pleurotus* FIPIA-DEP51 in the same clade of *P. pulnonarius* with 100% BS value. This study reports for the first time the wild occurences of *P. pulmonarius* in Indonesia. Future study should be done to characterize the cultures of reported mushroom which can potentially be the local strain for cultivation of *P. pulmonarius* industry in Indonesia.

Copyright: © 2024, J. Tropical Biodiversity Biotechnology (CC BY-SA 4.0)

INTRODUCTION
Pleurotus (Fr.) P. Kumm. (Fries 1821: 178) Kummer (1871: 24) is a complex genus of Pleurotaceae with more than 700 recorded taxa worldwide (IndexFungorum 2023). Kirk et al. (2008) noted that there are 20 species of *Pleurotus*, but other authors have recognized 30 to 40 species (Hilber 1982; Singer 1986). This is due to the multiple names and species delimitation problems which occurred in this genus (Menolli Jr. et al. 2010).

Pleurotus is lignicolous fungi belongs to the order Agaricales, characterized by flabelliform carpophores, decurrent lamellae, short lateral stipe, presence of versiform shaped cheilocystidia, monomitic hyphal tissue and inamyloid ellipsoidal to cylindrical spores (Kirk et al. 2008). The genus *Pleurotus* is one of the most cultivated edible mushrooms globally (Cohen et al. 2002) due to its great economic, dietary, and ecological importance. Of many species of *Pleurotus*, the phoenix mushroom (*P. plumonarius*) is known as an important cultivated edible mushroom in many countries (Pham et al. 2023).

Currently, Index Fungorum (2023) records 8 species variation of phoenix mushroom including: *Pleurotus pulmonarius* sensu auct., *P. pulmonarius* (Fr.) Quél. 1872, *P. pulmonarius* * juglandis (Fr.) P. Karst. 1879, *P. pulmonarius* var. indicus Sapan, Atri & Gulati 2014, *P. pulmonarius* var. juglandis (Fr.) Sacc. 1887, *P. pulmonarius* var. lapponicus E. Ludw. 2001, *P. pulmonarius* var. pulmonarius (Fr.) Quél. 1872, and *P. pulmonarius* var. stechangii Wasser & Zmitr. 2016. Phoenix mushroom is considered as important cultivated mushroom in many Africa, Asia, and Latin American countries (Zmitrovich & Wasser 2016; Raman et al. 2021). This is due to the ability of this mushroom to be cultivated in a broad range of temperatures, which can optimize the potential requirements for commercial production in tropical and subtropical regions (Chang & Miles 2004; Zmitrovich & Wasser 2016). In Southeast Asia, this mushroom is commonly grown at the southern region of Vietnam (Pham et al. 2023) and Malaysia (Samsudin & Abdullah 2019).

The *Pleurotus* species are primarily distributed in tropical forests and usually colonize the fallen branches, dead, decaying tree stumps, and wet logs (Bao et al. 2004; Raman et al. 2021). However, the knowledge of phoenix mushroom both in wild occurrence and cultivation in Indonesia remains poor. Till time, only few reports have been found regarding the wild distribution of *P. pulmonarius* in Indonesia. Khayati and Warsito (2018) reported the consumption of *P. pulmonarius* in Papua, Indonesia. In addition, Putra et al. (2022) recorded the phoenix mushroom as *jamur gromo* (local name) in Sumatra, Indonesia. However, no further information data was provided regarding those edible macro-fungi. During our fungus foray in a collaboration with the Indonesian mushroom hunter community (KPJI) in Sukabumi (West Java, Indonesia), some pinkish brown pileus of *Pleurotus* were collected. At glance, the fruiting bodies resembled the phoenix mushroom. However, the taxonomical and phylogenic identification of *Pleurotus* species is quite complex and can potentially lead to its misidentification. Therefore, the goal of our work was aimed to ensure the taxonomical position of our *Pleurotus* specimens based on morphological and molecular evidence in Indonesia.

MATERIALS AND METHODS

Specimen collection

The specimens were obtained at Goalpara Forest, Sukabumi, West Java, Indonesia (6°50'24.185" S 106°59'03.350" E), in November 2022, May 2023, and July 2023 during the mushroom hunting of the Indonesian mushroom hunter community (KPJI). The exploration was done using opportunistic sampling method following O'Dell et al. (2004). The fruiting bodies were photographed *in situ* and ecological information (coordinate, substrate, vegetations) was recorded. Some of the specimens were deposited to Herbarium Bandungense Indonesia with the collection number FIPIA-DEP51.

Morphological examination

The macromorphological features were observed from the fresh materials in the research location and in the Mycology Laboratory, Department of Biology, Faculty of Mathematics and Natural Sciences, IPB University, Indonesia and in the Integrated Laboratory of Bioproducts (iLaB), BRIN, Bogor, Indonesia. The macromorphological characters observed including color, size, pileus surface, pileus margin, wetness level, lamella, stipe dimension, and stipe ornamentation. The micromorphological parameters including pileipellis, basidium, cystidia, spores (shape, size, colour, ornamentation), trama, stipe, and clamp connection were observed using light microscope. The hymenium was also subjected to electron microscopy (SEM) observation, which was prepared following the methods of Goldstein et al. (1992) at iLaB, BRIN, Bogor, Indonesia. The hymenium layers were cut into small pieces (5 × 5 mm), pre-fixed in 2.5% glutaraldehyde of a cacodylate buffer with a pH of 8.4 at 27°C for two days. Next, they were pre-fixed in 2% tannic acid for six hours and washed with four different cacodylate buffers. The samples were dehydrated in 50%–100% ethanol series, infiltrated with t-butanol twice for 10 minutes, and freeze-dried. Freeze-dried samples were mounted on an aluminium stub with double-sided carbon tape and coated with gold. Samples were observed using the JSM IT 200 SEM system (JEOL, Tokyo, Japan). The specimens were identified using related identification references (Singer 1986; Lechner et al. 2004; Venturella et al. 2015).

Molecular analyses

The fresh specimen (stipe) was used for DNA isolation materials. DNA extraction followed by PCR from fresh specimens was done in (iLaB), BRIN, Bogor, Indonesia. Fresh specimens were extracted using hexadecyltrimethylammonium bromide following Hermawan et al. (2020). The amplification was performed to Internal Transcribed Spacer (ITS) region of ITS 5 (5'-GGA AGT AAA AGT CGT AAC AAG G-3') and ITS 4 (5'-TCC TCC GCT TAT TGA TAT GC-3') primers (White et al. 1990). The PCR amplification was performed in 40 µL total reaction containing 12 µL ddH2O, 2 µL of 10 pmol of each primer, 20 µL PCR mix from 2× Kappa Fast 2G, and 6 µL 100 ng template DNA. The PCR condition was set as follows: initial denaturation at 94 °C for 2 minutes, followed by 30 cycles of denaturation at 94 °C for 30 seconds, annealing at 56 °C for 45 seconds, and extension at 72 °C for 1 minute. The final extension was set at 72 °C for 10 minutes. The amplicons were checked on 1 % agarose gels and visualized by the Gel DocTM XR system. PCR products were sent to the 1st Base Malaysia for sequencing.

The sequences were assembled using ChromasPro software. The alignment of sequences used Clustal X Ver. 2.0 (Larkin et al. 2007). The final aligned sequence was deposited in GenBank (https://www.ncbi.nlm.nih.gov/) to obtain the accession number. The sequence then was subjected to Basic Local Alignment Search Tool (BLAST) in NCBI to compare homology with prior database. Selected published sequences based on BLAST results were used for phylogenetic tree analyses with *Lentinus squarrosulus* as an outgroup (Table 1). The phylogenetic tree of Randomized Axelerated Maximum Likelihood (RAxML) Black Box was generated on CIPRES (Stamatakis 2014). All trees were then edited using TreeGraph Software version 2.9.2-622 beta. The Bootstrap value (BS)≥70 % was shown on the branch on the phylogenetic trees.

Table 1. *Pleurotus* species and outgroup used in this study with collection code and GenBank accession numbers.

Species	Collection Code	ITS Accession Number
Lentinus squarrosulus	Voucher BO 24427	MT815466
Pleurotus calyptratus	Strain C-1	JQ837485
Pleurotus calyptratus	Strain 1935	KF932720
Pleurotus citrinopileatus	Strain 691 AG-30015	KF932725
Pleurotus citrinopileatus	Strain ACCC51261	UE424285
Pleurotus cornucopiae	Strain 88	KF932717
Pleurotus cornucopiae	Isolate 8763	AY450341
Pleurotus cornucopiae	Strain 82	KF932716
Pleurotus cystidiosus	AG-55-466	FJ608592
Pleurotus cystidiosus	Strain CBS 297.35	AY315766
Pleurotus djamor	Strain 1526	KF932719
Pleurotus djamor	Strain H-10	JQ837488
Pleurotus dryinus	Strain 468 AG-II	KF932723
Pleurotus dryinus	Strain 467 AG-I	KF932722
Pleurotus eryngii	Strain 1504	KF932718
Pleurotus eryngii	Strain H-6	JQ837481
Pleurotus eryngii	Strain Somycel 3065 H-7	KF932727
Pleurotus euosmus	Strain CBS 307.29	EU424298
Pleurotus ostreatus	Strain M-8	JQ837476
Pleurotus ostreatus	Strain 38d	JQ837475
Pleurotus ostreatus	Strain M-9	JQ837474
Pleurotus pulmonarius	Strain ZBS2012	KF932728
Pleurotus pulmonarius	Isolate 4203	AY450349
Pleurotus pulmonarius	**Voucher FIPIA-DEP51**	**OP861541**
Pleurotus sajor-caju	Strain H-1	JQ837470

RESULTS AND DISCUSSION

Taxonomy (Figure 1-4)

Pleurotus pulmonarius (Fr.) Quél., Mém. Soc. Émul. Montbéliard, Sér. 2 5: 11 (1872)

Basionym:

Agaricus pulmonarius Fr., Systema Mycologicum 1: 187 (1821)

Synonyms:

Pleurotus ostreatus f. *pulmonarius* (Fr.) Pilát, Bulletin Trimestriel de la Société Mycologique de France 49: 281 (1934)

Pleurotus ostreatus var. *pulmonarius* (Fr.) Iordanov{?}, Vanev & Fakirova (1979)

Dendrosarcus pulmonarius (Fr.) Kuntze: 464 (1898)

Pleurotus araucariicola Singer, Lilloa 26: 141 (1953)

Pileus 30–32 × 23–24 mm, light brown to pinkish brown, pale brown in some basidiomata, flabelliform in a young stage, expanding to broadly ovoid in maturity, surface smooth, wet to gelatinous, margin entire to somewhat wavy, slightly unrolled, occasionally hygrophanous. Lamellae shortly to deeply decurrent, up to 20 mm length, 2-2.5 mm broad, wavy, margin mostly entire, sometimes almost serrulate, crowded, cream to pale cream, with series of lamellulae. Stipe fleshy, varies from eccentric to lateral, concolorous with lamellae, discoloring at the base with shade of yellow on edge, without ornamentation, 10–11 mm × 6–7 mm, sometimes two stipes emerge from the same base. Odor indistinct. Spores 6–8 µm × 2.5–3.5 µm, thin-walled, smooth, cylindrical to ellipsoid, hyaline, apex with knob. Basidia hyaline, thin-walled, 10–18 µm × 2–6 µm, clavate to club shaped, four sterigmata. Hymenial cystidia rare, pleurocystidia sublageniform. Basidioles are abundant. Hymenium trama composed by intermingling hyphae, 6–11 µm diam, thin-walled, with clamp connection. Oleiferous hyphae can be observed from pileipellis and

hymenial trama, 2–3 µm diam, thick-walled, with prominent cytological content. Pileipellis a cutis, intertwined to parallel arranged.

Habitat: Solitary or scattered on board log of *Cinnamomum camphora*, Goalpara Forest, Sukabumi, West Java, Indonesia, 6°50'24.185" S 106°59'03.350" E, May 2023, collected by Putra IP, FIPIA-DEP51.

Figure 1. Macroscopic morphology of *Pleurotus pulmonarius* FIPIA-DEP51. A: Basidiomata habitus growth on decaying wood. B: Underside view of pileus C: Upperside view of pileus features. D: Lamella characters.

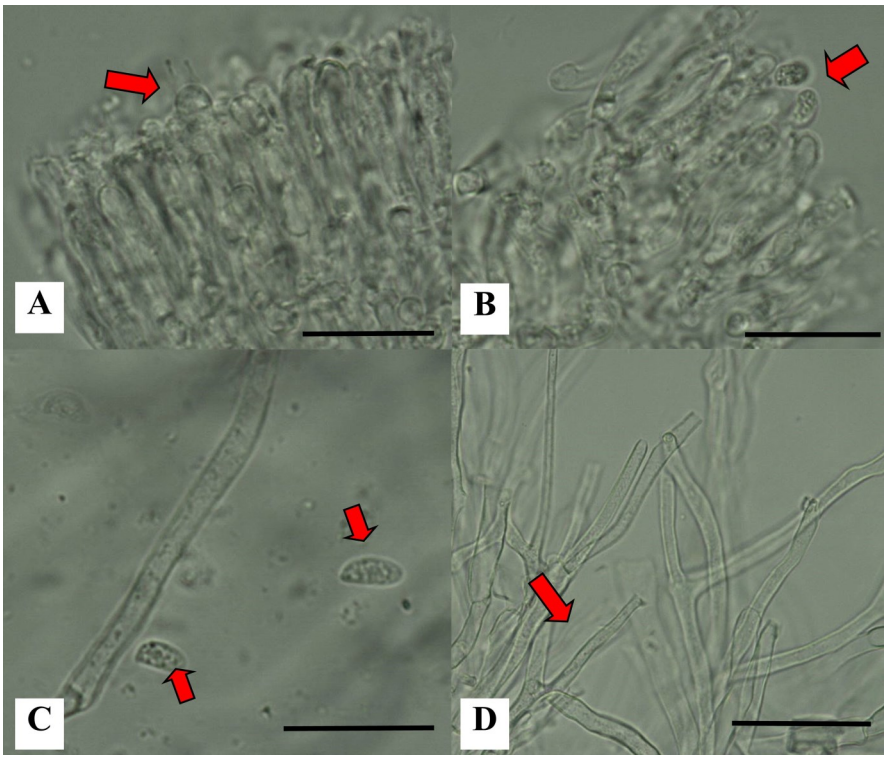

Figure 2. The microscopic characters of *Pleurotus pulmonarius* FIPIA-DEP51. A: Basidium with sterigma (arrow). B: Basidium with sterigma and basidiospores (arrow). C: Cylindrical to ellipsoid basidiospores (arrow). D: Hymenium trama (arrow). Bars= A-C: 20 µm, D: 50 µm.

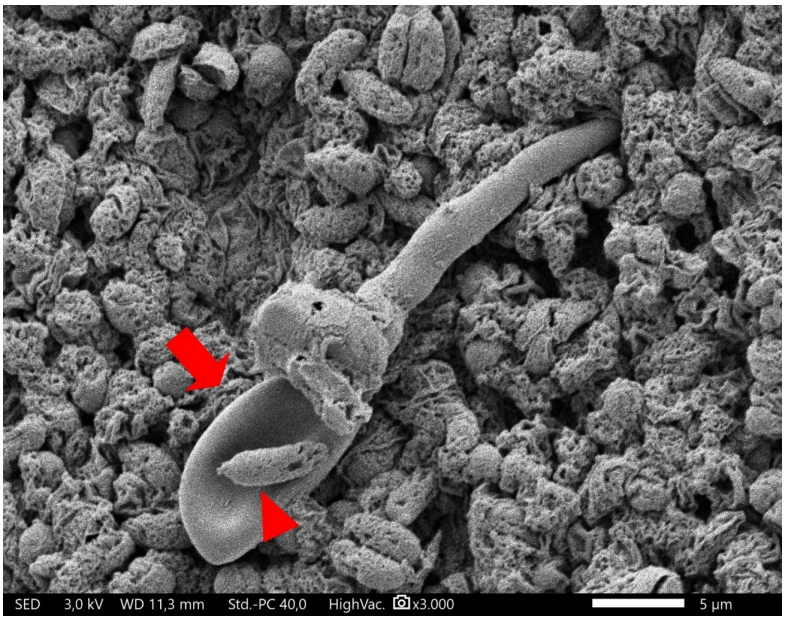

Figure 3. The SEM image of *Pleurotus pulmonarius* FIPIA-DEP51. Pleurocystidia (arrow). Basidiospore (arrow head).

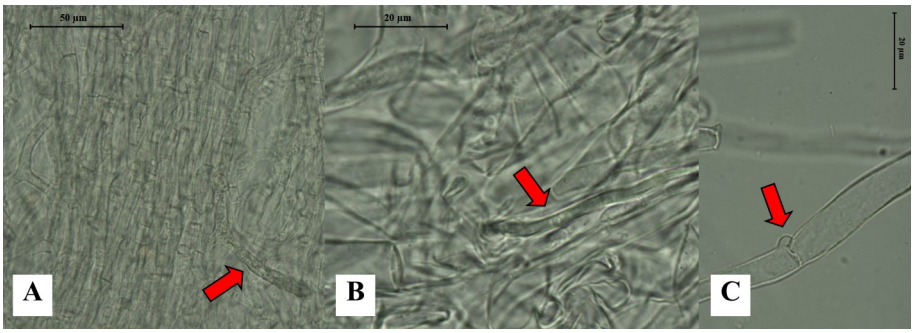

Figure 4. The micromorphological characters of *Pleurotus pulmonarius* FIPIA-DEP51. A: Pileipellis with oleiforous hyphae (arrow). B: Oleiferous hyphae of trama (arrow). C: Clamp connection (arrow).

Molecular Analyses

Our specimens' ITS nucleotide sequence was deposited to the GenBank with the accession number ITSOP861541. The homology comparison in GenBank library via BLAST revealed that our specimens posed high similarity to *Pleurotus pulmonarius* from India and China (100%) as the 10 top hits. The ITS phylogenetic tree revealed our specimens in the same clade as *P. pulmonarius* with 100% BS value. The phylogenetic tree resolved our sample as *P. pulmonarius* FIPIA-DEP51 (Figure 5).

The species of *Pleurotus* species are considered edible mushrooms and used by many local tribals due to their unique texture and flavor (Bastos et al. 2023). The current study report for the first time the wild occurrence of *P. pulmonarius* in Indonesia. Currently, the GBIF (2023) records 10.554 occurrences of *P. pulmonarius* worldwide, mostly from Europe and America, with one report from Borneo (Indonesia). *P. pulmonarius* or known as the phoenix mushroom, is one of the important edible mushrooms for cultivation worldwide (Pham et al. 2023). In Indonesia, this mushroom is popularly known as a commercial mushroom for cultivation. However, no comprehensive prior information regarding the distribution and consumption of this species in Indonesia. Khayati and Warsito (2018) recorded *P. pulmonarius* in Arboretum Inamberi Papua, Indonesia. However, the information cannot be validated as no documentation, description, herbarium, or any other data were provided regarding the species.

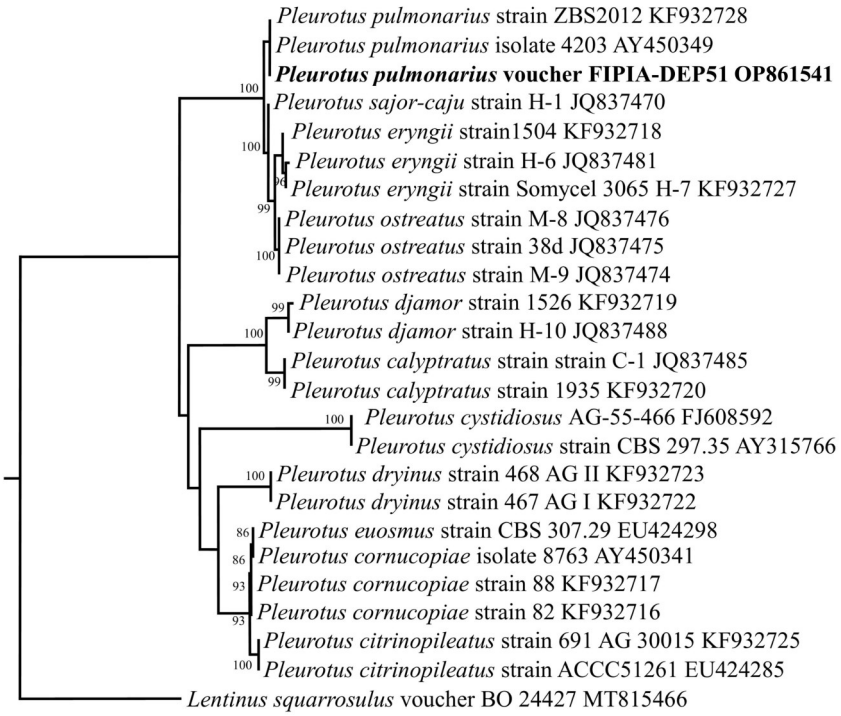

Figure 5. *Pleurotus pulmonarius* FIPIA-DEP51 phylogenetic tree based on ITS 1/2 region using Randomized Axelerated Maximum Likelihood method and 1000 Bootstrap Analysis. Our specimen is bold on the phylogenetic tree.

The pileus color of our specimens was different from those reported by Lechner et al. (2004). Petersen and Hughes (1993) reported the variation of features of *P. pulmonarius* was common, especially the pileus color. Recently, Wang et al. (2019) suggested the morphological plasticity of macro-fungi species can be impacted by environmental factors. The spore's length of *P. pulmonarius* FIPIA-DEP51 was slightly shorter compared to the same species reported from Argentina by Lechner et al. (2004). In line with Lechner et al. (2004), we found prominent pleurocystidia as the morphological characters and provide the SEM image for future references. Unlike the prior reports, we observed the prominent oleiferous hyphae both in pileipellis and hymenial trama. Morphologically, *P. pulmonarius* FIPIA-DEP51 posed a similarity to *P. ostreatus* by the basidiomata appearance. The plasticity of fruiting bodies morphology of mushroom species, especially those distributed in separate areas of the world sometimes has led to multiple names for the same species of *Pleurotus* (Menoli Jr. et al. 2010). Therefore, we agreed that distinguishing between *P. pulmonarius* and *P. ostreatus* is difficult, which led us to combine morphological evidence with molecular analysis.

It is noted that the delimitation of *Pleurotus* species is difficult due to their morphological similarity (Avin et al. 2014). Previously, Shnyreva and Shnyreva (2015) confirmed a close relationship between *P. pulmonarius* and *P. sajor-caju*. However, our specimens did not pose the typical ring of *P. sajor-caju* and were more similar to *P. ostreatus*. The *P. pulmonarius* FIPIA-DEP51 is morphologically similar to *P. ostreatus* (Petersen & Hughes 1993), and the BLAST result showed that the homology between them was 100%. However, the ITS phylogenetic tree displayed that they were in a different clade. Schoch et al. (2012) reported that ITS can be used as universal DNA barcode marker for fungal identification. In relation to the Indonesian fungi, Putra et al. (2023) proved that ITS sequence revealed new record of *Omphalotus nidiformis* in particular country. In the last two decades, phylogenetic analysis has been employed in understanding the delimitation and relationships of the species

in *Pleurotus* (Avin et al. 2014; Li et al. 2020). Yet, the selection of DNA sequences from GenBank reference strains for phylogenetic analysis should be with careful consideration (Shnyreva & Shnyreva 2015). In the phylogenetic tree, *P. pulmonarius* FIPIA-DEP51 was in the same clade with specimens reported from Rusia (KF932728) and USA (AY450349). The ITS sequence of current works is the only available sequence of *P. pulmonarius* from Indonesia and can be used for future studies of taxonomy of *Pleurotus*.

Some of the indigenous people (*Sunda* tribe) of Sukabumi (West Java, Indonesia) and the mushroom foragers in the research site usually collected this species throughout the year, especially in the rainy season. To date, they only collect and consume this mushroom for themselves. No information regarding the trading of this wild edible mushroom species in the sampling site or any other place in Indonesia. In the current studies, this mushroom was found to grow on *C. camphora* wood. Previous study report stated that *P. pulmonarius* usually colonised *Populus nigra*, *Salix humboldtiana*, *Araucaria angustifolia*, and *Fraxinus*, as both pathogen and saprobic fungi (Petersen & Hughes 1993; Lechner et al. 2004). Considering the nutritional composition and pharmacological properties of this species, such as, antitumor, antioxidants, immunomodulating, antibacterial (Wahab et al. 2014; Nguyen et al. 2016; Ni 2016; Zhang et al. 2016), the cultivation efforts of *P. pulmonarius* FIPIA-DEP51 need a warrant, which can probably be the indigenous strain for *P. pulmonarius* cultivation and production in Indonesia.

CONCLUSIONS

The current work unravels the comprehensive taxonomical information of *Pleurotus pulmonarius* for Indonesia. Morphologically, *P. pulmonarius* FIPIA-DEP51 was distinguished by the light brown to pinkish brown pileus, flabelliform in the beginning to expanding broadly ovoid in maturity, cylindrical to ellipsoid basidiospores, clavate to club shaped basidia, and abundant oleiferous hyphae. The BLAST result and phylogenetic tree confirmed our specimen as *P. pulmonarius* with 100% homology and Bootstraps value. Future study should be focused on the cultivation which can potentially be the local strain for cultivation of *P. pulmonarius* industry in Indonesia.

AUTHOR CONTRIBUTION

I.P.P. and O.D.N. contributed to the study conception, designed, and obtained data. I.P.P. and O.D.N. were responsible for morphological characterisation. M.T.S. and R.H. provided the molecular and phylogenetic analysis. All authors wrote the manuscript. All authors read, critically revised, and approved the final manuscript.

ACKNOWLEDGMENTS

This study was supported by the grant of "Dana Masyarakat IPB 2023 - Penelitian Dosen Muda" with reference number 11401/IT3/PT.01.03/P/B/2023 to Dr. Ivan Permana Putra. We would like to thank Mr. Yos Husni Alfian for the field assistance. We thank the Resort PTN Goalpara for the field support. We are grateful to Department of Biology, Faculty of Mathematics and Natural Sciences, IPB University, Indonesia, The Research Center for Applied Microbiology, National Research and Innovation Agency (BRIN), Bogor, West Java, Indonesia, BETA Research, Perum Bintang Regency, Jabungan 50266, Semarang City, Central Java, Indonesia. We thank the Herbarium Bandungense, Indonesia for the herbarium support.

CONFLICT OF INTEREST

The authors declare no competing interests.

REFERENCES

Avin, F.A. et al., 2014. Molecular divergence and species delimitation of the cultivated oyster mushrooms: integration of IGS1 and ITS. *The Scientific World Journal*, 2014, 793414. doi: 10.1155/2014/793414

Bao, D., Kinugasa, S. & Kitamoto, Y., 2004. The biological species of oyster mushrooms (Pleurotus spp.) from Asia based on mating compatibility tests. *Journal of Wood Science*, 50(2), pp.162-168. doi: 10.1007/s10086-003-0540-z

Bastos, C. et al., 2023. Ethnomycological prospect of wild edible and medicinal mushrooms from Central and Southern Africa—A review. *Food Frontiers*, 4(2), pp.549–575. doi: 10.1002/fft2.215

Chang S.T. & Miles P.G., 2004. *Mushrooms: cultivation, nutritional value, medicinal effect and environmental impact - second Ed*, Florida, USA: CRC Press.

Cohen, R. Persky, L. & Hadar, Y., 2002. Biotechnological applications and potential of wood-degrading mushrooms of the genus *Pleurotus*. *Appl. Microbiol. Biotechnol.*, 58(5), pp.582-594. doi: 10.1007/s00253-002-0930-y

GBIF Secretariat., 2023, '*Pleurotus pulmonarius* (Fr.) Quél, in *GBIF Backbone Taxonomy*, Checklist dataset, viewed 29 June 2023, from doi: 10.15468/39omei accessed via GBIF.org

Goldstein, J.I. et al., 1992. *Scanning electron microscopy and X-ray microanalysis, 2nd ed*, New York: Plenum Press.

Hermawan, R., Amelya, M.P. & Julia, Z.R., 2020. *Trichaleurina javanica* from West Java. *Jurnal Mikologi Indonesia*. 4,(2), pp.175-181. doi: 10.46638/jmi.v4i2.85.

Hilber, O., 1982. Die Gattung Pleurotus. *Bibl. Mycol.*, 87, pp.1-448.

Index Fungorum., 2023. Index Fungorum. http://www.indexfungorum.org/names/Names.asp

Khayati, L. & Warsito, H., 2018. Keanekaragaman Makrofungi di Arboretum Inamberi. *Jurnal Mikologi Indonesia*, 2(1), pp.30-38. doi: 10.46638/jmi.v2i1.30

Kirk, P.M. et al., 2008. *Dictionary of the Fungi, 10th ed*, Wallingford, UK: CAB International.

Larkin, M.A. et al., 2007. Clustal W and Clustal X version 2.0. *Bioinformatics*, 23(21), pp.2947–2948. doi: 10.1093/bioinformatics/btm404

Lechner, B.E., Wright, J.E., & Alberto, E., 2004. The Genus *Pleurotus* in Argentina. *Mycologia*, 96(4), 845. doi: 10.2307/3762117

Li, J. et al., 2020. The saprotrophic *Pleurotus ostreatus* species complex: late Eocene origin in East Asia, multiple dispersal, and complex speciation. *IMA Fungus*, 11, 10. doi: 10.1186/s43008-020-00031-1

Menolli Jr., N. et al., 2010. Morphological and molecular identification of four Brazilian commercial isolates of *Pleurotus* spp. and cultivation on corncob. *Brazilian Archives of Biology and Technology*, 53(2), pp.397–408. doi: 10.1590/s1516-89132010000200019

Nguyen, T.K. et al., 2016. Evaluation of antioxidant, anti-cholinesterase, and anti-infammatory efects of culinary mushroom *Pleurotus pulmonarius*. *Mycobiology*, 44(4), pp.291–301. doi: 10.5941/MYCO.2016.44.4.291

Ni, D., 2016. The biological characteristics and cultivation techniques of *Pleurotus pulmonarius*. *J Changjiang Vegetables*, 22,70–72.

O'Dell, T.E., Lodge, D.J. & Mueller, G.M., 2004. Approaches to sampling macrofungi. In *biodiversity of fungi: inventory and monotoring methods*, San Diego: Elsevier Academic Press.

Petersen, R.H., & Hughes, K.W., 1993. Intercontinental interbreeding collections of *Pleurotus pulmonarius* , with notes on *P . ostreatus* and other species. *Sydowia*, 45 (1), 139-152.

Pham, V.L. et al., 2023. Monokaryotic characteristics and mating types of phoenix mushroom (*Pleurotus pulmonarius*) cultivars in the South Vietnam. *International Journal of Agricultural Technology*, 19(1), pp.189-202.

Putra, I.P. et al., 2022. Review: Current Checklist of Local Names and Utilization Information of Indonesian Wild Mushrooms. Journal of Tropical Biodiversity and Biotechnology, 7(3), 71407. doi: 10.22146/jtbb.71407

Putra, I.P. et al., 2023. The ghost fungus *Omphalotus nidiformis* (Berk.), new to Indonesia, poisoned foragers. *Kuwait Journal of Science*, 50 (3), pp.326–332. doi: 10.1016/j.kjs.2023.01.002

Raman, J. et al., 2021. Cultivation and nutritional value of prominent *Pleurotus* spp.: An Overview. *Mycobiology*, 49(1), pp.1-14. doi: 10.1080/12298093.2020.1835142

Samsudin, N.I. & Abdullah, N., 2019. Edible mushrooms from Malaysia; a literature review on their nutritional and medicinal properties. *International Food Research Journal*, 26(1), pp.11–31.

Schoch, C.L. et al., 2012. Nuclear ribosomal internal transcribed spacer (ITS) region as a universal DNA barcode marker for Fungi. *Proc. Natl. Acad. Sci. USA.*, 109(16), pp.6241–6246. doi: 10.1073/pnas.1117018109

Shnyreva, A.A. & Shnyreva, A.V., 2015. Phylogenetic analysis of *Pleurotus* species. *Russian Journal of Genetics*, 51(2), pp.148–157. doi: 10.1134/s1022795415020131

Singer, R., 1986. The Agaricales in Modern Taxonomy. Koeltz Scientific Books, Königstein

Stamatakis, A., 2014. RAxML version 8: a tool for phylogenetic analysis and post-analysis of large phylogenies. B*ioinformatics*, 30(9), pp.1312–1313. doi: 10.1093/bioinformatics/btu033

Venturella, G., Gargano, M.L. & Compagno, R., 2015. The genus *Pleurotus* in Italy. *Flora Mediterranea*, 25(Special Issue), pp.143-156. doi: 10.7320/flmedit25si.143

Wahab, N.A.A., Abdullah, N. & Aminudin, N., 2014. Characterisation of potential antidiabetic-related proteins from *Pleurotus pulmonarius* (Fr.) Quél. (grey oyster mushroom) by MALDI-TOF/TOF mass spectrometry. *Biomed Res Int*, 2014, 131607. doi: 10.1155/2014/131607

Wang, S. et al., 2019. Evaluation of five regions as DNA barcodes for identification of *Lepista species* (Tricholomataceae, Basidiomycota) from China. *PeerJ*, 7, e7307. doi: 10.7717/peerj.7307

White, T.J. et al., 1990. Amplification and Direct Sequencing of Fungal Ribosomal RNA Genes for Phylogenetics. In *PCR Protocols: A Guaide to Methods and Applications*. pp.315–322.

Zhang, S. et al., 2016. Cultivation technology improvement of *Pleurotus geesteranus*. *J Anhui Agric*, 44(36), pp.63–64

Zmitrovich, I.V. & Wasser, S.P., 2016. Is widely cultivated "*Pleurotus sajor-caju*", especially in Asia, indeed an independent species?. *International Journal of Medicinal Mushrooms*, 18, pp.583-588. doi: 10.1615/intjmedmushrooms.v18.i7.30

Journal of Tropical Biodiversity and Biotechnology
Volume 09, Issue 01 (2024): jtbb85308
DOI: 10.22146/jtbb.85308

Research Article

Nannoplankton Biostratigraphy from Banggai-Sula Basin, Central Sulawesi

Efrilia Mahdilah Nurhidayah[1], Akmaluddin[1]*, Didit Hadi Barianto[1], Salahuddin Husein[1], Asep Saripudin[2]

1)Geological Engineering Department, Faculty of Engineering, Universitas Gadjah Mada, Jl. Grafika No. 2, Yogyakarta, 55281, Indonesia.
2)JOB Pertamina-Medco E&P Tomori Sulawesi, Jl. Jend. Gatot Subroto Kav 71-73. Jakarta, 12870, Indonesia.
* Corresponding author, email: akmaluddin@ugm.ac.id

Keywords:
Biostratigraphy
Banggai-Sula Basin
Miocene
Nannoplankton
Unconformity
Submitted:
06 June 2023
Accepted:
06 October 2023
Published:
11 March 2024
Editor:
Ardaning Nuriliani

ABSTRACT

The nannoplankton research was conducted in the MH-2 well, Banggai-Sula Basin, Central Sulawesi. Thirty-four ditch-cutting samples were utilized to observe the Minahaki, Kintom, and Biak Formations. Age determination was carried out using biostratigraphy method and standard procedure for first and last occurrence of nannoplankton biodatum and had an absolute age, widely known as a zone indicator. This study aims to determine the age and nannoplankton biozonation of each geological formation in Banggai-Sula Basin. Based on the biostratigraphic analysis, 39 species from 14 genera with abundance frequencies ranging from rare to abundant were found in the MH-2 well. In this study, new results of the age of Banggai-Sula Basin areMiddle Miocene – Early Middle Pliocene (13,706 – 3,727 Ma), and can identify into six calcareous nannoplankton zones that are more detailed than previous researchers, *Discoaster signus* zone (NN5), *Discoaster exilis* zone (NN6-NN7), *Discoaster berggrenii* zone (NN11), *Ceratolithus acustus* zone (NN12), *Helicosphaera sellii* zone (NN13-NN15), and the *Discoaster tamalis* zone (NN16). Biostratigraphic data also shows new information for the first time, the absence of three zones from zone NN8 to zone NN10. This result indicates an unconformity in the Late Miocene age (10.606–8.20 Ma).

Copyright: © 2024, J. Tropical Biodiversity Biotechnology (CC BY-SA 4.0)

INTRODUCTION

Calcareous nannoplankton are one of the major components of oceanic phytoplankton and are unicellular and autotrophic organisms. Nannoplankton is a group of microfossils with a size of 0.25 to 30 μm, including coccoliths, discoasters, and nannoconids that live in marine. Nannoplankton comes from Coccolithophore (Figure 1), which is generally round or oval in shape and this group is an important constituent of oceanic phytoplankton, providing a major food source for herbivorous plankton. Nannoplankton live by alternating motile and non-motile planktonic or benthic stages (Flores & Sierro 2013). The motile stage has a flexible skeleton with the coccolith embedded in a flexible cell membrane, but in the non-motile phase, the membrane calcifies and forms a rigid shell. Cenozoic calcareous nannoplanktons consistently have higher and more varied species, extinction, and evolution rates than the Mesozoic (Armstrong & Brasier 2005).

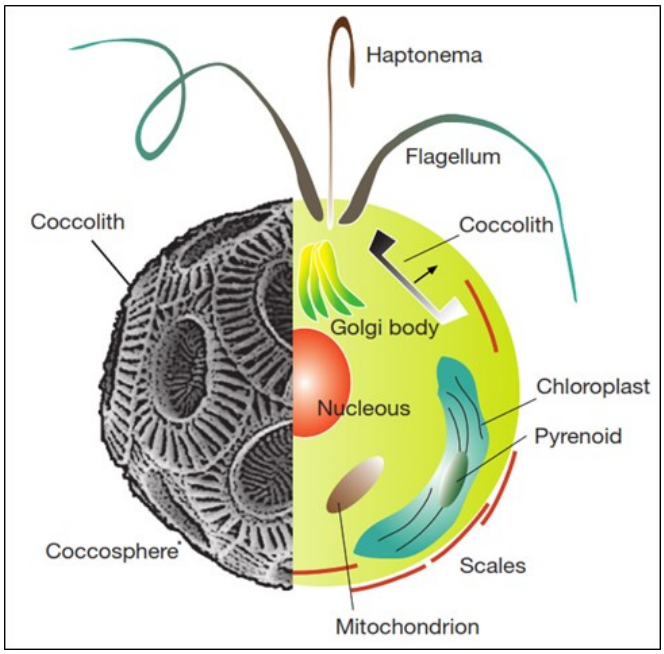

Figure 1. Schematic of a coccolithophore cell showing the coccolith non-motile (left) and motile (right) phases (Flores & Sierro 2013).

Thus, assemblages of nannoplankton fossils in rock strata will be useful for biostratigraphy. Biostratigraphy is defined as the branch of stratigraphy or stratigraphy by paleontological methods (McGowran 2005). Nannoplankton is also known as a high-resolution tool for determining biostratigraphic age because it is an abundant organism with a short age range and a wide geographical distribution throughout the world (Kapid 2003). Biostratigraphy is one of the stages of hydrocarbon exploration. Biostratigraphy plays a role as the main method because it provides a cost-effective, fast, and simple way to determine the age of sedimentary rock layers (strata) that are the constituents of a geological formation based on their fossil content (Simmons 2019; Ulfah et al. 2023). Furthermore, the results of the biostratigraphy will be used for stratigraphic correlation or rock layer correlation. This correlation is the process of determining the equivalence of age or stratigraphic position of layered rocks in different areas (Lucas et al. 2020).

The stratigraphy of the Banggai-Sula Basin results from two different depositional periods. First, the Salodik Group consists of the Tomori, Matindok, and Minahaki formations (as a division of formations for the subsurface), a series of continental margin rifts/drifts composed of limestone and clastic sedimentary rocks deposited before the collision. Second, it reflects the sequence deposited following the post-collision, consisting of flysch facies (Kintom Formation) and molasses sediments (Biak Formation) (Figure 2). Moreover, the Tomori, Matindok, and Minahaki Formations have been shown to generate hydrocarbons in the Banggai-Sula Basin. The Bangai-Sula Basin is one of the basins in Indonesia that has the "Giant" gas field on the island of Sulawesi in eastern Indonesia and has become a basin with the status of a production well (Hasanusi et al. 2004).

Kurniasih et al. (2021) used planktonic foraminifera to conduct a biostratigraphic study in the Banggai-Sula Basin. They identified the Minahaki Formations as Middle Miocene, while the Kintom Formation is Late Miocene to Holocene. However, the age of this formation differs from studies also conducted in Banggai-Sula Basin by Nugraha et al. (2022), who propose that the Minahaki Formation is Middle-Late Miocene, Kintom Formation is Early Pliocene, and Biak Formation (Mollase

sediments) is Pleistocene.

Therefore, it is interesting to study its biostratigraphy using nannoplanktons in more detail because of the difference in age between the Kintom and the Minahaki Formations from two previous studies, Kurniasih et al. (2021) and Nugraha et al. (2022). The research location is in the "SN" Field, a productive hydrocarbon-producing field that records the complete formations in the Banggai-Sula Basin (Figure 3). Stratigraphically, the MH-2 well was chosen because it is composed of the Minahaki, Kintom, and Biak Formations, which have not been reported previously for biostratigraphic results. Thus, based on these reasons, it is interesting to carry out biostratigraphic analysis and determine the age using nannoplankton for each formation in more detail.

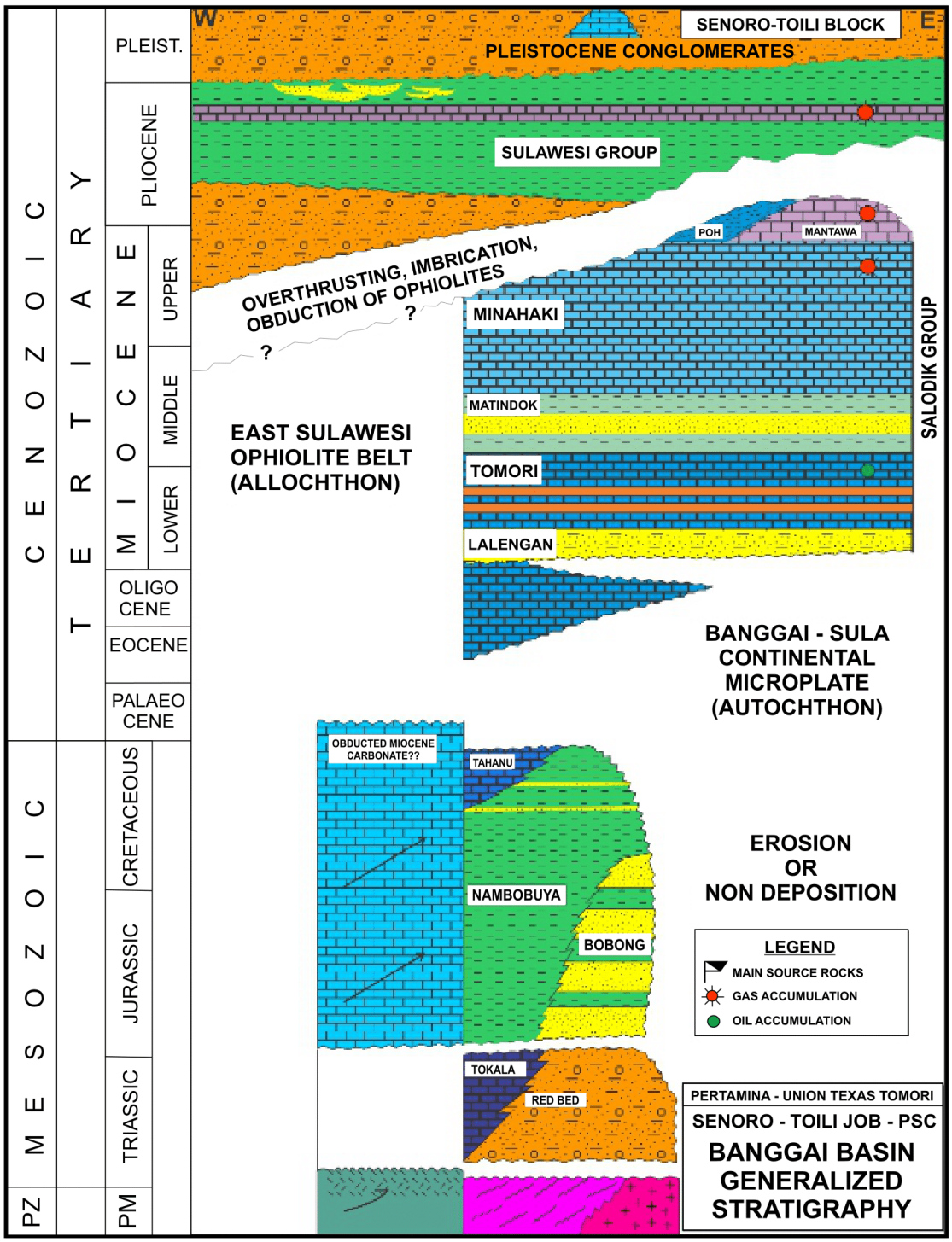

Figure 2. Regional Stratigraphy of the Banggai-Sula Basin (Pertamina-BPKA, 1996) in Hasanusi et al. (2004).

Figure 3. Locations of research well (red font), Central Sulawesi, Indonesia (image from Google Earth taken on July 20, 2023)

MATERIALS AND METHODS

Biostratigraphic analysis using nannoplankton was conducted using ditch-cutting samples from the MH-2 exploration well, which has a depth of 10 to 9100 feet (ft). Thirty-four cutting samples were used in this research, with sample intervals ranging from 30 to 230 ft (Figure 4).

Ditch-cutting sample preparation for nannoplankton was carried out using the gravity settling method according to the preparation rules based on Bown & Young (1998). A 1000x magnification Olympus polarizing microscope with XPL and PPL views was used to observe nannoplankton. Then, nannoplankton image capture was supported by the Olympus camera software. Data collection used a quantitative method by counting all specimens from 200 microslide sample fields of view (size 22mm x 22mm).

According to Bown & Young (1998), the semi-quantitative and qualitative species abundance notation is abundant (A) means >10 specimens/field of view, common (C) means 1–10 specimens/field of view, few (F) means 1 specimen/1–10 field of view, and rare (R) means 1 specimen/>10 field of view. It was determined that specimen preservation was G (good) for nannoplankton showing no or minor dissolution and overgrowth, M (moderate) for specimens showing some dissolution and overgrowth, and P (poor) for specimens showing significant dissolution and overgrowth, morphology was damaged, and many specimens were difficult to identify.

Identification of nannoplankton specimens based on morphological features using the Nannotax3 website (Young et al. 2023). The name of the biostratigraphic zone is given based on the biodatum or index fossils specimens found in the zone. The zone was determined using Martini (1971), Okada & Bukry (1980), and Backman et al. (2012) standard method based on the first (FO) and last (LO) occurrences of zone marker species. We used the absolute age of each identified marker species based on Backman et al. (2012), Bergen et al. (2017), Boesiger et al. (2017), and Bergen et al. (2019) (Table 1).

Table 1. Resume of the absolute age biodatum in the MH-2 well of Banggai-Sula Basin.

Biodatum	Bioevent	Martini (1971)	Absolute Age (Ma)	Source	Depth (feet)
Discoaster brouweri	FO	Base NN8	10.606	Backman et al. (2012)	8150
Discoaster berggrenii	FO	Base NN11	8.2	Backman et al. (2012)	8150
Amaurolithus primus	FO	Top NN11	7.374	Bergen et al. (2019)	6810
Discoaster quinqueramus	LO	Top NN11	5.53	Backman et al. (2012)	6540
Helicosphaera sellii	FO	Base NN13	4.978	Boesiger et al. (2017)	5220
Reticulofenestra pseudoumbilicus	LO	Top NN15	3.727	Bergen et al. (2019)	1620

RESULTS AND DISCUSSION

The results of nannoplankton observations for 34 samples showed moderate to good preservation, with frequencies ranging from rare to abundant. A total of 39 nannoplankton species from 14 genera were identified, resulting in seven nannoplankton biodatum species, *Sphenolithus abies*, *Discoaster brouweri*, *Discoaster berggrenii*, *Amaurolithus primus*, *Discoaster quinqueramus*, *Helicosphaera sellii*, and *Reticulofenestra pseudoumbilicus*. The six nannoplankton zonations have been successfully divided based on the six biodatum species including *Discoaster signus* zone (NN5), *Discoaster exilis* zone (NN6-NN7), *Discoaster berggrenii* zone (NN11), *Ceratolithus acustus* zone (NN12), *Helicosphaera sellii* zone (NN13- NN15), and the *Discoaster tamalis* Zone (NN16) (Table 2.). Based on the division of zones, it is known that there are three zones (zones NN8-NN10) absent in this study. The results of biostratigraphic analysis of each formation in the MH-2 well show that the Minahaki Formation is Middle Miocene - Late Miocene (NN5 – NN7 zone), the Kintom Formation is Late Miocene – Early Pliocene (Zone NN11 – NN15), and the Biak Formation is Early Pliocene - Middle Pliocene (Zone NN16) (Figure 4). The sections below briefly describe the six discovered nannoplankton zonations.

Discoaster signus/NN5 zone

The *Discoaster signus* zone is a partial range zone that is divided at the top by the first occurrence (FO) biodatum of *Sphenolithus abies* with an absolute age of 13.706 Ma (sample 8690), while the biodatum at the bottom is not found. *Discoaster signus* zone are equivalent to the *Sphenolithus heteromorphus*/NN5 zone (Martini 1971), and similar with CN4 zone (Okada & Bukry 1980), and the CNM7 zone (Backman et al. 2012). This zone is Middle Miocene age and is observed at a depth of 8690 ft to 9100 ft with a thickness of 410 ft. Another species that has the same age in this interval is *Sphenolithus neoabies*. Rework fossils from the Mesozoic age were also identified in this zone, *Cyclagelosphaera brezae* and *Watznaueria barnesiae*, which are Jurassic to Cretaceous in age, and *Cyclagelosphaera wiedmannii* and *Cyclagelosphaera lacuna*, which are Jurassic in age.

Discoaster exilis/ NN6 – NN7 zone

The *Discoaster exilis* zone is a concurrent range zone that is divided by the first occurrence (FO) FO *Sphenolithus abies* (13.706 Ma) at the bottom (sample 8150) and the first occurrence (FO) FO *Discoaster brouweri* (10.606 Ma) and at the top (sample 8690). *Discoaster exilis* zone is equiva-

Table 2. The distribution chart of nannoplankton in the MH-2 well shows the abundance of species from 34 samples and 7 biodatum species.

NUMBER	FOSSIL TYPE: SPECIES	DEPTH (FT)	FORMATION	PRESERVATION	CALCAREOUS NANNOFOSSILS: 1 *Arkhangelskiella cymbiformis*	2 *Amaurolithus primus*	3 *Calcidiscus premacintyrei*	4 *Catinaster calyculus*	5 *Coccolithus miopelagicus*	6 *Coccolithus pelagicus*	7 *Cyclagelosphaera brezae*	8 *Cyclagelosphaera jiangii*	9 *Cyclagelosphaera wiedmannii*	10 *Cyclagelosphaera lacuna*	11 *Cyclicargolithus abiectinus*	12 *Cyclicargolithus floridanus*	13 *Discoaster berggrenii*	14 *Discoaster brouweri*	15 *Discoaster deflandrei*	16 *Discoaster deflandrei*	17 *Discoaster exilis*	18 *Discoaster loeblichii*	19 *Discoaster patulus*	20 *Discoaster quinqueramus*	21 *Discoaster surculus*	22 *Discoaster variabilis*	23 *Helicosphaera carteri*	24 *Helicosphaera princei*	25 *Helicosphaera sellii*	26 *Pseudoemiliania lacunosa*	27 *Pontosphaera discopora*	28 *Pontosphaera multipora*	29 *Reticulofenestra bisecta*	30 *Reticulofenestra haqii*	31 *Reticulofenestra minuta*	32 *Reticulofenestra pseudoumbilicus*	33 *Reticulofenestra umbilicus*	34 *Small reticulofenestra*	35 *Sphenolithus abies*	36 *Sphenolithus apoxis*	37 *Sphenolithus dissimilis*	38 *Sphenolithus neoabies*	39 *Watznaueria barnesiae*	CALCAREOUS NANNOFOSSILS BIODATUM
1	900		Biak	M							*R					*R																										
2	1350			G							*F																F	F				*F		R								
3	1620			G													F										C		F	F	R			R	C	F					*R	
4	1920			G										*F			R										R		R							F		F	C				*F	
5	2130			G												*R											F			F					F		F						
6	2460			M						R	*F		*R																					F	F		F					*F	
7	2520		Kintom	G													R										F		F		R			F	C	F		C	C			*F	
8	2760			G							*R		*R	*F													F							F	F	F		C	F				
9	3240			M				*R				F				*F		F									R			R				F	C	F		F	F				
10	4080			G								`			*R		F	F									C		C					C	C	F		C	F		F	*F	
11	4650			G														F																			F	C				*F	
12	5220			G				*R		R	*F			*F			R	R	R			*F					C		R		R	R		F	C	F		A	A	*F		C	
13	5460			G								*F			*R	*F		F									C							R	C	F		C	A			F	*C
14	5760			G		F							*R				R	R	R								C							F	F			C	C			F	*F
15	6150			G									*F	*R			F	F									C				F			F	A	F		A	A			F	
16	6360			M								*R						R								R	F								C	F			A				
17	6450			M					*R				*C		*R	*F											F							R	F	F		C	F				
18	6540			G	*R	R	*R			R		*R	*F				R	R							F	F	C							F	C	F	*R	A	C			A	*F
19	6810			G		F			F					*C				F			R						F				F				F	F		A	A			A	
20	6990			G				*R					*F		*R		R							R	R		R								F				C	*R			C	
21	7200			G						R		*F	*F			*R	F	R						F			F				R				F	F		C	F			C	*F
22	7410			G							*F							R	F				R	F	R	R	F				R			F	C			C				A	*F
23	7620			G						R														F		R	F							F	C	F		A	F			A	
24	7740			G								*F	*A											C			C				R				F	F	*F	C	F			C	
25	7890			M													F				R			F			F								F	R		F	R			F	*F
26	8000			M													R	R						F											F	F	*R	C	F			F	
27	8070			G									*A	*C		*R											F							R	F	F			R			C	
28	8150		Minahaki	G						R			*F				F	F		*R	R						F							R	F			F	R			F	*F
29	8280			M							*F			*C	*F																			F	C			C	F	*R		F	
30	8500			G						R						*F				*R							C							F	A				R			F	*R
31	8690			G						R	*F			*A		*F											F								A					R	*F	*F	F	*F
32	8900			M									*F																					F						*R			
33	9000			M																														F									
34	9100			M									*F	*C													F								F								*F	

unconformity

A (abundant)	= >10 specimens per field of view	G = Good	FO = First Occurrence
C (common)	= 1–10 specimens per field of view	M = Moderate	LO = Last Occurrence
F (frequent)	= 1 specimen/1-10 per field of view	* = Rework fossil	
R (rare)	= 1 specimen/>10 per field of view		

lent to the *Discoaster exilis* and *Discoaster kugleri*/NN6-NN7 zone (Martini 1971), and similar with CN5a - CN45b zone (Okada & Bukry 1980), and the CNM8 - CNM11 (Backman et al. 2012). This zone is the Middle-Late Miocene age (13.706 – 10.606 Ma) and is observed at a depth of 8150 ft to 8690 ft with a thickness of 540 ft.

In this interval, other species of the same age are *Discoaster exilis* and *Discoaster bolli*. Rework fossils from the Mesozoic age were also identified in this zone, *Cyclagelosphaera brezae* and *Watznaueria barnesiae*, which are Jurassic to Cretaceous in age, and *Cyclagelosphaera wiedmannii* and *Cyclagelosphaera lacuna*, which are Jurassic in age.

Discoaster berggrenii/NN11 zone

The *Discoaster berggrenii* zone is a concurrent range zone that is divided by the first occurrence (FO) of *Discoaster berggrenii* (8.20 Ma) at the bottom (sample 8150) and the last occurrence (LO) of *Discoaster quinqueramus* (5.53 Ma) at the top (sample 6540). *Discoaster berggrenii* zone is equivalent to the *Discoaster quinqueramus* /NN11 zone (Martini 1971) and similar to the CN9 zone (Okada & Bukry 1980), and the CNM16 – CNM19 zones (Backman et al. 2012). This zone is the Late Miocene age (8.20 – 5.53 Ma) and is observed at a depth of 6540 ft to 8150 ft with a thickness of 1610 ft.

In this interval, other species with the same age are *Discoaster surculus*, *Discoaster variabilis*, and *Amaurolithus primus*. Rework fossils from the Mesozoic age were also identified in this zone, *Cyclagelosphaera brezae* and *Watznaueria barnesiae*, which are Jurassic to Cretaceous in age, *Cyclagelo-*

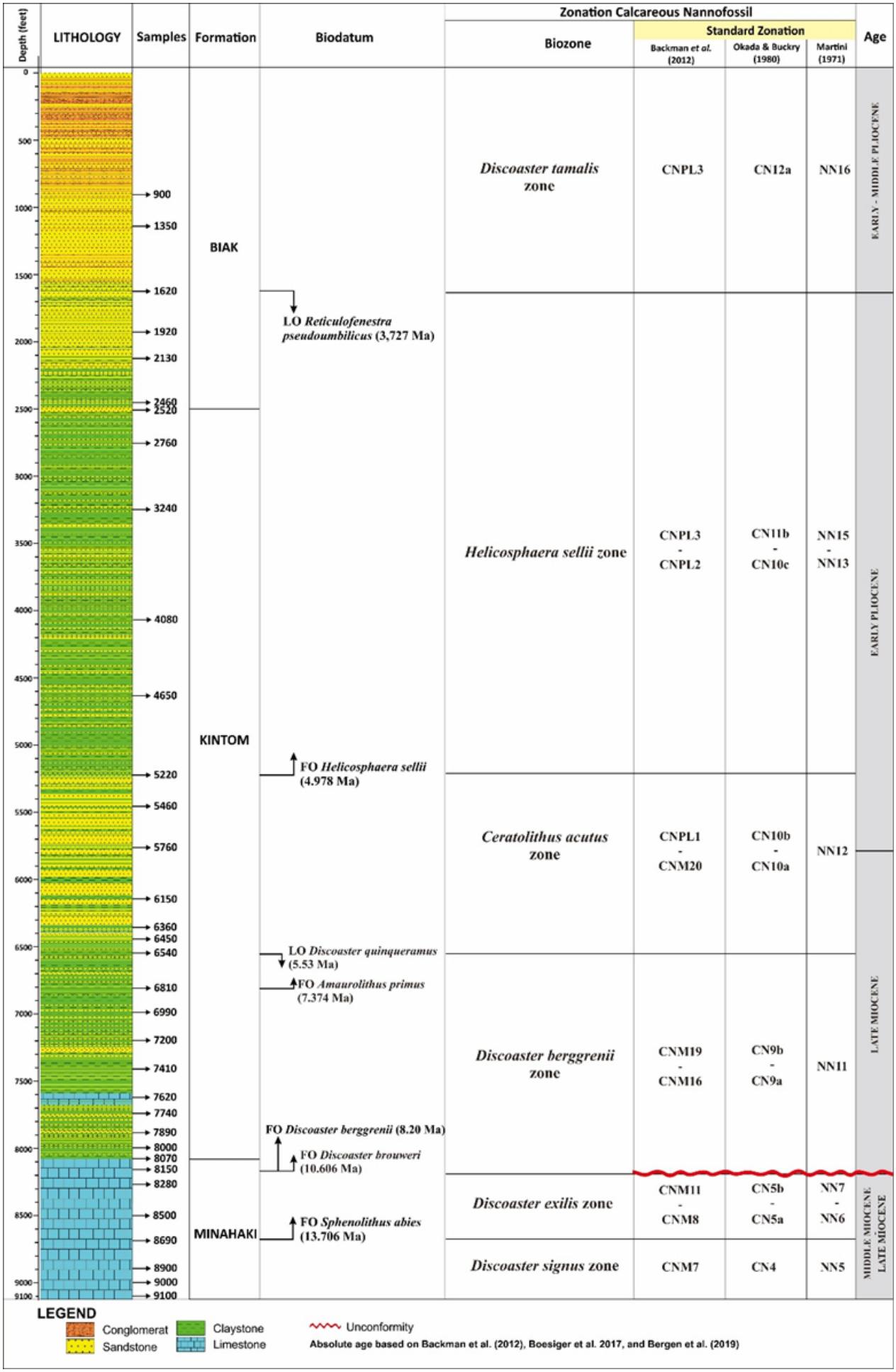

Figure 4. Calcareous nannoplankton biostratigraphic zone in the MH2 well of the Banggai-Sula Basin according to Backman et al. (2012), Okada & Bukry (1980), and Martini (1971). The biozonation calcareous nannoplankton of Minahaki, Kintom, and Biak formations can divided into 6 zones.

sphaera jiangii, which are Cretaceous age, *Cyclagelosphaera wiedmannii* and *Cyclagelosphaera lacuna* which are Jurrasic in age.

Ceratolithus acutus/NN12 zone

The *Ceratolithus acutus* zone is a concurrent range zone that is divided by the last occurrence (LO) of *Discoaster quinqueramus* (5.53 Ma) at the bottom (sample 6540) and the first occurrence (FO) of *Helicosphaera sellii* (4.978) at the top (sample 5220). *Ceratolithus acustus* zone is equivalent to the *Amaurolithus tricorniculatus*/NN12 zone (Martini 1971) and similar to the CN10a – CN10b zones (Okada & Bukry 1980), and the CNM20 – CNPL1 zones (Backman et al. 2012). The zone name from (Backman et al. 2012) was used to create the *Ceratolithus acutus* zone name. This zone is the Late Miocene – Early Pliocene age (5.53 Ma – 4.978 Ma) and is observed at a depth of 5220 ft to 6540 ft with a thickness of 1320 ft.

Another species that have the same age in this interval is *Amaurolithus primus*. Rework fossils from the Mesozoic age were also identified in this zone, *Cyclagelosphaera brezae* and *Watznaueria barnesiae*, which are Jurassic to Cretaceous in age, *Cyclagelosphaera jiangii*, which are Cretaceous age, *Cyclagelosphaera wiedmannii* and *Cyclagelosphaera lacuna* which are Jurrasic in age.

Helicosphaera sellii/NN13-NN15 zone

The *Helicosphaera sellii* zone is a concurrent range zone that is divided by the first occurrence (FO) of *Helicosphaera sellii* (4.978 Ma) at the bottom (sample 5220) and the last occurrence (LO) of *Reticulofenestra pseudoumbilicus* (3.727 Ma) at the top (sample 1620). *Helicosphaera sellii* zone are equivalent to the *Ceratholithus rugosus*, *Discoaster asymmetricus*, and *Reticulofenestra pseudoumbilicus*/NN13 – NN15 zones (Martini 1971) and similar with CN10c – CN11 zones (Okada & Bukry 1980), and the CNPL2 – CNPL3 zones (Backman et al. 2012). This zone is the Early Pliocene age (4.978 – 3.727 Ma) and is observed at a depth of 1620 ft to 5220 ft with a thickness of 330 ft.

Another species that has the same age in this interval is *Helicosphaera princei*. Rework fossils from the Mesozoic age were also identified in this zone, *Cyclagelosphaera brezae* and *Watznaueria barnesiae*, which are Jurassic to Cretaceous in age, *Cyclagelosphaera jiangii*, which is Cretaceous age, *Cyclagelosphaera wiedmannii* and *Cyclagelosphaera lacuna* which is Jurrasic in age.

Discoaster tamalis/NN16 zone

The *Discoaster tamalis* zone is a partial range zone that is divided by the last occurrence (LO) of *Reticulofenestra pseudoumbilicus* (3.727 Ma) at the bottom (sample 1620), and the biodatum at the top in this zone is not found. *Discoaster tamalis* zone are equivalent to the *Discoaster surculus*/NN16 zone (Martini 1971), and similar with CN12a zone (Okada & Bukry 1980), and the CNPL4 zone (3.82 – 2.76 Ma) (Backman et al. 2012). This zone is the Early Pliocene – Middle Pliocene age and is observed at a depth of 900 ft to 1620 ft with a thickness of 1020 ft.

In this interval, other species of the same age are *Pseudoemiliania lacunosa* and the absence of the genus *Sphenolithus*. Rework fossils from the Mesozoic age were also identified in this zone, *Cyclagelosphaera brezae* and *Watznaueria barnesiae*, which are Jurassic to Cretaceous in age.

The results of the biostratigraphic analysis of the MH-2 well show different results and can be compared with the age and stratigraphic data of the Banggai-Sula Basin by previous researchers Kurniasih et al. (2021) and Nugraha et al. (2022) (Figure 5). New age for Kintom Formation in

this study is Late Miocene – Early Pliocene (NN11-NN15) in age, while Kurniasih et al. (2021) are late Miocene - Holocene (N14-N23) and Nugraha et al. (2022) is Pliocene (Zanclean). Based on comparisons with previous researchers, it shows that the rocks from the Kintom Formation in this study are older than Kurniasih et al. (2021) and Nugraha et al. (2022). The results of the age analysis in this study prove that the Kintom Formation was formed before collision tectonic events occurred in Banggai-Sula basin. Hence, it is different from the previous regional stratigraphic age studies by Nugraha et al. (2022) and Hasanusi et al. (2004), which mention that the Kintom Formation was deposited in the Early Pliocene as post-collision deposits.

In addition, our biostratigraphic data show an indication of unconformity, which is identified by the presence of two biodatum with different relative ages in the same sample (sample 8150), FO *Discoaster berggrenii* (8.20 Ma) and FO *Discoaster brouweri* (10.606 Ma) (Table 2 and Figure 5). Based on the mud log data, the unconformity is at the boundary between the Minahaki Formation and the Kintom Formation. There is a difference in age and time gap with the disappearance of the NN8 zone to the NN10 zone with an age interval of 10.606 to 8.20 million years, equivalent to the Late Miocene age. The hiatus is presumably caused by subaerial erosion due to the Late Miocene sea-level drop based on the eustatic curve (Miller et al. 2020) (Figure 5). The position of the MH-2 well on the upper part of the Banggai continental shelf is easily subjected to sea level change. The tectonic uplift only occurred in Pliocene, as indicated by the deposition of Biak coarse clastics (Husein et al. 2014) and (Nugraha et al. 2022).

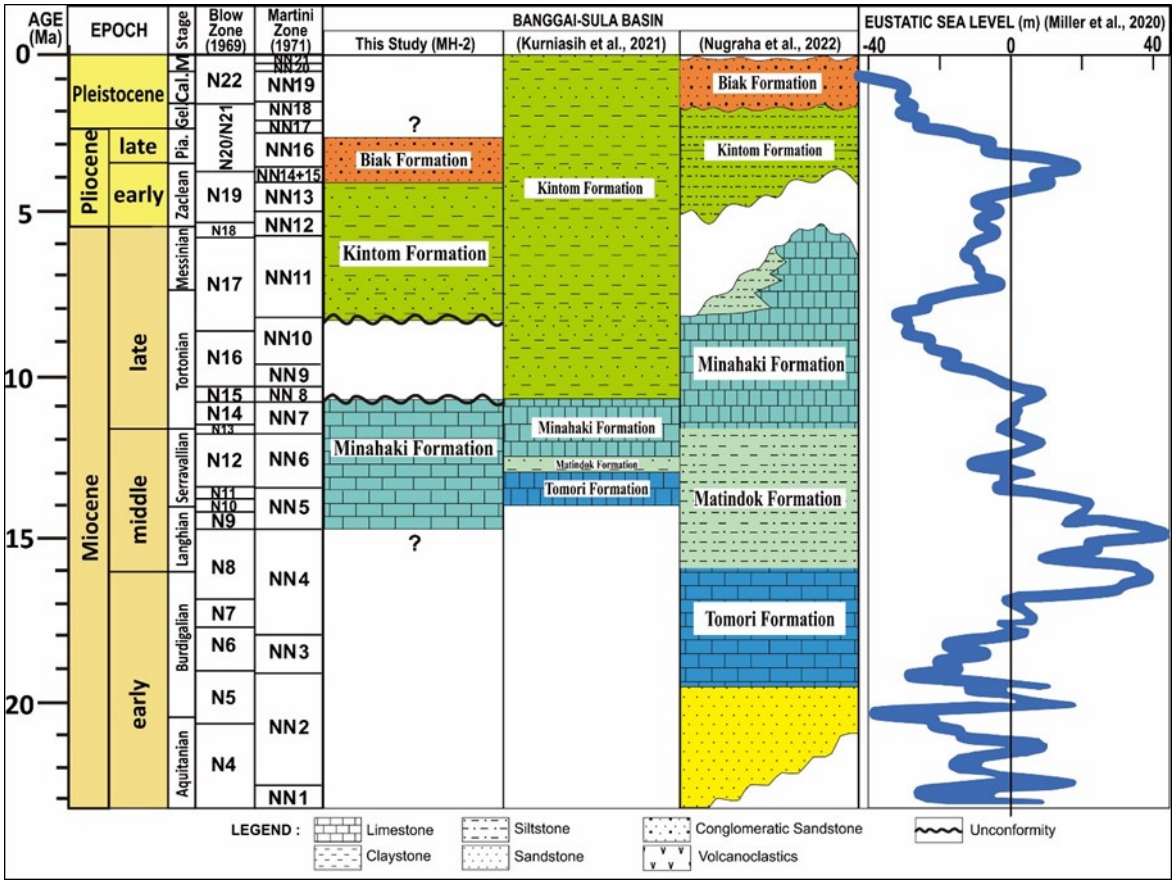

Figure 5. Comparison of the age stratigraphy of the Minahaki, Kintom, and Biak Formations from this study with the results of the ages of Kurniasih et al. (2021) using planktonic foraminifera and Nugraha et al. (2022) using planktonic foraminifera and U-Pb Zircon in the Banggai-Sula Basin. Unconformity in this study also correlates with a decrease in global sea levels (Miller et al. 2020).

Diversity and Systematic Taxonomy

Using combined data from coccolithophore biology and nannoplankton paleontology based on calcareous nannoplankton, Galović and Young (2012) and Nannotax website (https://www.mikrotax.org/Nannotax3/) (Young et al. 2023) to found more information on synonyms and species variants. Table 3 provides a summary of calcareous nannoplankton taxonomy. Selected sample species of calcareous nannoplankton in the MH-2 well can be seen in Figure 6-7.

Coccolithophores are categorized as follows by the ICBN (International Code of Botanical Nomenclature):
Protoctista Kingdom
Haptophyta Division
Prymnesiophyceae Class

Group Heterococcoliths Young and Bown 1997
Order Coccolithales Schwarz 1932 Jorand et al. 2004
Family Coccolithaceae Poche 1913 emend Young and Bown 1997
Genus Coccolithus Schwartz 1894

1. Species *Coccolithus miopelagicus* (Bukry 1971), (Figure 6, number 1)
Description: Placoliths of a large size and broad ellipse distinguished from *C. pelagicus*. Moreover, the central open is small, and the rim is relatively broad compared to the center area. This species is > 13µm, usually 15-17 µm. This species is present in samples 6450 and 6810.

2. Species *Coccolithus pelagicus* (Wallich 1877), (Figure 6, number 2)
Description: Most elliptical laccoliths have an open center and are of medium size. The average size of this species is 7 to 10 µm or about 13 µm. This species is present in samples 2460, 5220, 6540, 7200, 8150, 8500, dan 8690.

Order Coccolithales Schwarz, 1932
Family Calcidiscaceae Young and Bown 1997
Genus Calcidiscus Kamptner 1950

3. Species *Calcidiscus premacintyrei* (Theodoridis, 1984), (Figure 6, number 3)
Description: The elliptical and subcircular coccoliths are distinct, large, and have a closed center. Size ranges from 14 to 18 µm for this species. This species is present in sample 6540.

Order Prinsiales Young and Bown (1997)
Family Noelaerhabdaceae Jerkovic, 1970 Emend Young & Bown 1997
Genus Cyclicargolithus Bukry, 1971

4. Species *Cyclicargolithus abisectus* (Muller, 1970), (Figure 6, number 4)
Description: Large, sub-circular coccoliths typically have a narrow central area. The size of this species is >11 µm and is present in samples 8280, 6990, 6450, 5460, and 4080.

5. Species *Cyclicargolithus floridanus* (Roth and Hay in Hay et al., 1967), (Figure 6,number 5)
Description: The coccoliths are distinct, large, and have closed centers in the elliptical and subcircular varieties. The size of this species ranges

Table 3. Resume of the taxonomic ranks in MH-2 well.

Group	Order	Family	Genus	Species
Heterococcoliths	Coccolithales	Coccolithaceae	*Coccolithus*	*Coccolithus miopelagicus* (Bukry 1971)
				Coccolithus pelagicus (Wallich 1877)
		Calcidiscaceae	*Calcidiscus*	*Calcidiscus premacintyrei* (Theodoridis, 1984)
	Isochrysidales	Noelaerhabdaceae	*Cyclicargolithus*	*Cyclicargolithus abisectus* (Muller, 1970)
				Cyclicargolithus floridanus (Roth and Hay 1967)
			Reticulofenestra	*Reticulofenestra bisecta* (Hay, Mohler and Wade, 1966)
				Reticulofenestra haqii (Backman 1978)
				Reticulofenestra minuta (Roth 1970)
				Reticulofenestra pseudoumbilicus (Gartner 1967)
				Reticulofenestra umbilicus (Martini & Ritzkowski, 1968)
			Pseudoemiliania	*Pseudoemiliania lacunosa* Kamptner, 1963
	Arkhangelskiales	Arkhangelskiellaceae	*Arkhangelskiella*	*Arkhangelskiella cymbiformis* (Vekshina, 1959)
	Watznaueriales	Watznaueriales	*Watznaueria*	*Watznaueria barnesiae* (Black in Black & Barnes, 1959)
			Cyclagelosphaera	*Cyclagelosphaera brezae* (Applegate & Bergen, 1988)
				Cyclagelosphaera jiangii (Covington & Wise, 1987)
				Cyclagelosphaera wiedmannii (Reale & Monechi, 1994)
				Cyclagelosphaera lacuna (Varol & Girgis 1994)
	Zygodiscales	Helicosphaeraceae	*Helicosphaera*	*Helicosphaera carteri* (Wallich 1877)
				Helicosphaera princei (da Gama & Varol 2013)
				Helicosphaera sellii (Bukry and Bramlette, 1969)
		Pontosphaeraceae	*Pontosphaera*	*Pontosphaera discopora* (Schiller, 1925)
				Pontosphaera multipora (Kamptner 1948)

Table 3. Contd.

Group	Order	Family	Genus	Species
Nannoliths	Discoasterales	Ceratolithaceae	Amaurolithus	*Amaurolithus primus* (Bukry and Percival, 1971)
				Catinaster calyculus (Martini and Bramlette, 1963)
		Discoastersceae	*Discoaster*	*Discoaster berggrenii* (Bukry, 1971)
				Discoaster brouweri (Bramlette and Riedel, 1954)
				Discoaster druggii (Bramlette and Wilcoxon, 1967)
				Discoaster deflandrei (Bramlette & Riedel, 1954)
				Discoaster exilis (Martini and Bramlette 1963)
				Discoaster loeblichii (Bukry, 1971)
				Discoaster patulus (de Kaenel & Bergen)
				Discoaster quinqueramus (Gartner, 1969)
				Discoaster surculus (Martini and Bramlette, 1963)
				Discoaster variabilis (Martini and Bramlette 1963)
		Sphenolithaceae	*Sphenolithus*	*Sphenolithus abies* (Deflandre in Deflandre and Fert, 1954)
				Sphenolithus apoxis (Bergen & de Kaenel in Bergen et al. 2017)
				Sphenolithus disbelemnos (Fornaciari and Rio, 1996)
				Sphenolithus neoabies (Bukry & Bramlette 1969)

from 14 to 18 µm. This species is present in samples 900, 2130, 3240, 5460, 6450, 7200, 8070, 8500, and 8690.

Genus Reticulofenestra Hay, Mohler and Wade 1966

6. Species *Reticulofenestra bisecta* (Hay, Mohler and Wade, 1966), (Figure 6, number 6)
Description: Reticulofenestrids are large, with a central area covered by a solid and prominent distal 'plug' (birefringent). This species has a size of 5 - 10 µm. This species is present in sample 1350.

7. Species *Reticulofenestra haqii* (Backman 1978), (Figure 6, number 7)
Description: Similar to *Reticulofenestra pseudoumbilicus*, Reticulofenestra is small and has an open central area. This species has a size of 2 - 4 µm. This species is present in samples 8070, 8150, 8280, 8500, 7620, 7410, 6540, 6450, 6150, 5220, 5460, 5760, 2520, 2760, 3240, 4080, and 1620.

8. Species *Reticulofenestra minuta* (Roth 1970), (Figure 6, number 8)
Description: Reticulofenestrid has an open central area and is relatively compact. Sizes of this species range from 1 to 2 µm. This species is present in samples 1350, 1620, 2130, 2460, 2520, 2760, 3240, 4080, 5220, 5460, 5760, 6150, 6360, 6450, 6540, 6810, 6990, 7200, 7410, 7620, 7620, 8070, 8150, 8280, 8500, 8690, 8900, 9000, and 9100.

9. Species *Reticulofenestra pseudoumbilicus* (Gartner 1967), (Figure 6, number 9)
Description: Reticulofenestrid is medium size with a central open area of about 2 µm. This species has a size of 6 - 10 µm. This species was present in samples 1620, 1920, 2460, 2520, 2760, 3240, 4080, 5220, 5460, 6150, 6360, 6450, 6540, 6810, 7200, 7620, 7740, 7890, 8000, and 8070.

10. Species *Reticulofenestra umbilicus* (Martini & Ritzkowski, 1968), (Figure 6, number 10)
Description: The reticulofenestra is large with an open center and an elliptical form. Sizes for this species range from 14 to 18 µm. This species is present in samples 6540, 7740, 7890, and 8000.

Genus Pseudoemiliania Gartner, 1969

11. Species *Pseudoemiliania lacunosa* (Kamptner, 1963) (Figure 6, number 11)
Description: The coccolith is a square-shaped open area in a circular or subcircular structure. Reticulofenestrid is large, elliptical in shape, and has an open center. This species has a size of 5 µm and is present in samples 1620, 2130, and 3240.

Order Arkhangelskiales Bown & Hampton 1997 (in Bown & Young 1997)

Family Arkhangelskiellaceae Bukry, 1969 emend. Bown & Hampton
Genus *Arkhangelskiella* Vekshina, 1959

12. Species *Arkhangelskiella cymbiformis* (Vekshina, 1959), (Figure 6, number 12)
Description: This species varies in size, with narrow rims (<1.5 µm). This species has a size of 8 µm. This species is present in sample 6540.

Order Watznaueriales Bown, 1987

Family Watznaueriaceae Rood, Hay & Barnard, 1971
Genus Watznaueria Reinhardt 1964

13. Species *Watznaueria barnesiae* (Black in Black & Barnes, 1959) (Figure 6, number 13)
Description: This species has a narrow and closed central area with no structure in the middle area and a size of 6 - 8 µm. This species is present in samples 1620, 1920, 2460, 2520, 4080, 4650, 5460, 5760, 6540, 7200, 7410, 7890, 8150, 8500, 8690, and 9100.

Genus Cyclagelosphaera Noel, 1965

14. Species *Cyclagelosphaera brezae* (Applegate & Bergen, 1988), (Figure 6, number 14)
Description: Cyclagelosphaera moderate to large with a closed central area, a small proximal shield, large elements, and an indistinct cycle unit V. This species has a size of 6 - 8 µm. This species was present in samples 900, 1350, 2460, 2760, 5220, 7410, 8280, and 8690.

15. Species *Cyclagelosphaera jiangii* (Covington & Wise, 1987), (Figure 6, number 15)

Description: Cyclagelosphaera, which has a large central opening. This species has a size of 5 µm. This species is present in samples 3240, 5460, 6360, 6540, 7200, and 7740.

16. Species *Cyclagelosphaera wiedmannii* (Reale & Monechi, 1994), (Figure 6, number 15)
Description: The Cyclagelosphaera are large (8 - 9 µm) with small central openings and inconspicuous tube cycles. This species has a size of 8 – 10 µm. This species was present in samples 2460, 2760, 5760, 6150, 6450, 6540, 6990, 7200, 7740, 8070, 8150, 8900, and 9100.

17. Species *Cyclagelosphaera lacuna* (Varol & Girgis 1994), (Figure 6, number 16)
Description: Cyclagelosphaera has a small to medium size with a central opening. This species has a size of 4 µm. This species is present in samples 1920, 2760, 5220, 6150, 6810, 8070, 8280, 8690, and 9100.

Group Heterococcoliths Young and Bown 1997
Order Zygodiscales Young and Bown 1997
Family Helicosphaeraceae Black 1971
Genus Helicosphaera Kamptner 1954
{synonym: *Helicopontosphaera* Hay and Mohler 1967}

18. Species *Helicosphaera carteri* (Wallich 1877), (Figure 7, number 1)
Description: The wings of medium to large-sized *helicosphaera* are wide and thick to the edges, and they feature a closed core area with two pores in the center. This species has a size of 7 - 8 µm. This species is present in samples 1350, 1620, 1920, 2130, 2520, 2760, 3240, 4080, 5220, 5460, 5760, 6150, 6360, 6450, 6540, 6810, 6990, 7200, 7410, 740, 770, 7620, 8150, 8500, 8690, and 9100.

19. Species *Helicosphaera princei* (da Gama & Varol 2013), (Figure 7, number 2)
Description: A relatively large helicolith with a mantle of the *Helicosphaera carteri* type, broad wings, and a long longitudinal slit in the central area. This species has a size of 7 µm. This species was present in sample 1350.

20. Species *Helicosphaera sellii* (Bukry and Bramlette, 1969), (Figure 7, number 3)
Description: Like *H. carteri*, the central hole in the XPL view is larger. This species has a size of 7 - 8 µm. This species is present in samples 1620, 1920, 2520, 4080, and 5220.

Family Pontosphaeraceae Lemmermann, 1908
Genus Pontosphaera Lohmann, 1902

21. Species *Pontosphaera discopora* (Schiller, 1925), (Figure 7, number 4)
Description: A central area with few pores and a clear, high rim. This species has a size of 8 – 10 µm. This species is present in samples 1620, 2520, 5220, 6150, 810, 7200, 7410, and 7740.

22. Species *Pontosphaera multipora* (Kamptner 1948), (Figure 7, number 5)
Description: This species has pores on the outer cycle that are usually

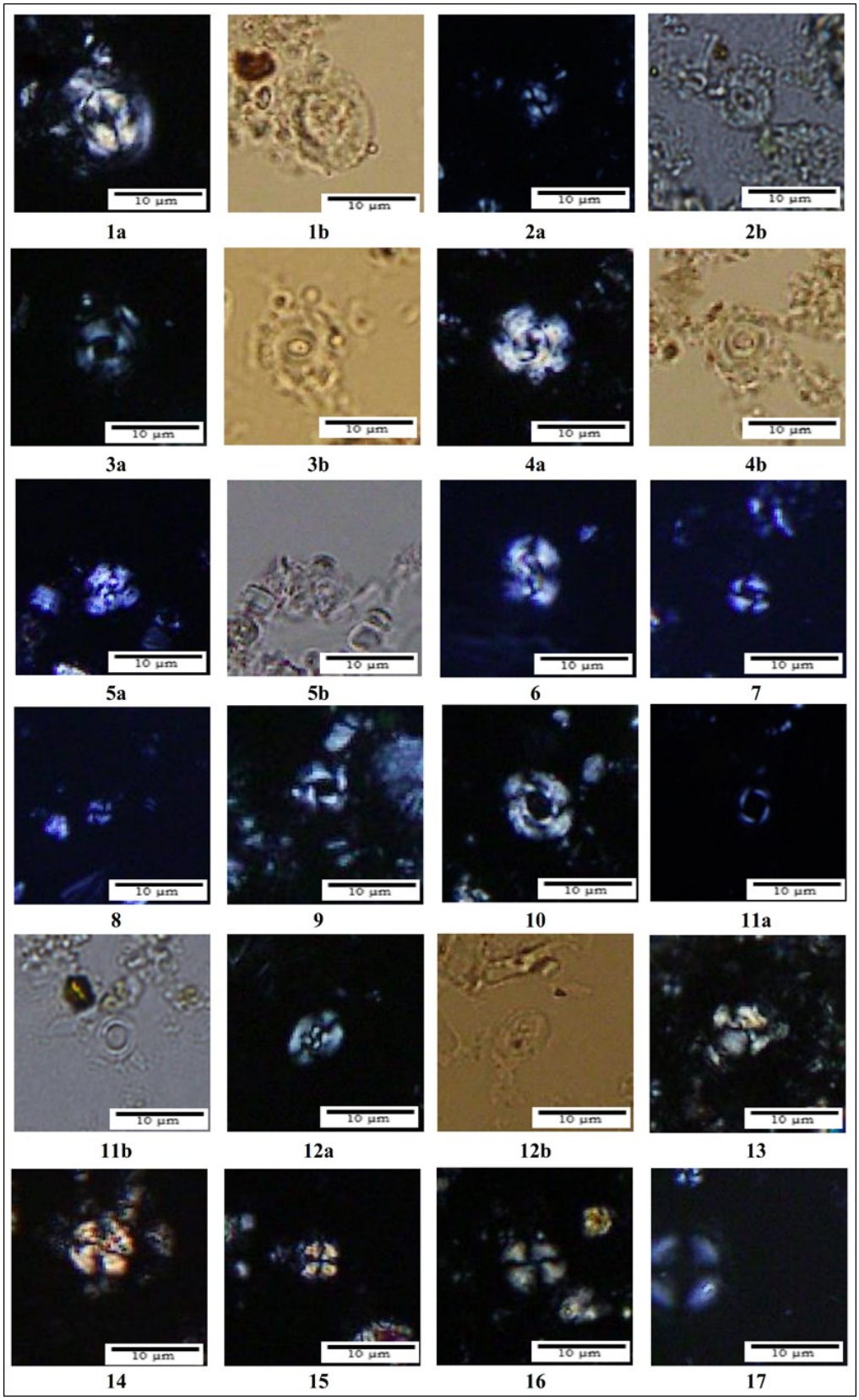

Figure 6. Selected image of nannoplanktons species in this research. XPL views (a) and PPL views (b). The Genus *Coccolithus* consists of (1) *Coccolithus miopelagicus* (sample 6810) and (2) *Coccolithus pelagicus* (sample 7620). The Genus *Calcidiscus* consists of (3) *Calcidiscus premacintyrei* (sample 6540). The Genus *Cyclicargolithus* consists of (4) *Cyclicargolithus abisectus* (sample 6450) and (5) *Cyclicargolithus floridanus* (sample 7200). The Genus *Reticulofenestra* consists of (6) *Reticulofenestra bisecta* (sample 1350), (7) *Reticulofenestra haqii* (sample 6540), (8) *Reticulofenestra minuta* (sample 6540), (9) *Reticulofenestra pseudoumbilicus* (sample 6150), (10) *Reticulofenestra umbilicus* (sample 6540). The Genus *Pseudoemiliania* consists of (11) *Pseudoemiliania lacunosa* (sample 1620). The Genus *Arkhangelskiella* consists of (12) *Arkhangelskiella cymbiformis* (sample 6540). The Genus *Watznaueria* consists of (13) *Watznaueria barnesiae* (sample 5220). The Genus *Cyclagelosphaera* consists of (14) *Cyclagelosphaera wiedmannii* (sample 6150), (15) *Cyclagelosphaera lacuna* (sample 3240), (16) *Cyclagelosphaera brezae* (sample 5220), and (17) *Cyclagelosphaera jiangii* (sample 5460).

elongated radially, the inner cycle is somewhat irregular, and the rim has a varying width. The size range for this species is 5 - 10 µm. Sample 5220 includes this species.

Group Nannoliths Young and Bown 1997
Order Discoasterales Hay 1977
Family Ceratolithaceae Norris, 1965
Genus Amaurolithus Gartner and Bukry, 1975

23. Species *Amaurolithus primus* (Bukry and Percival, 1971), (Figure 7, number 6)
Description: With curving arms, this species has a horseshoe-like form. This species is 7 µm in size. This species has samples 5760, 6540, and 6810.

Genus Catinaster Martini and Bramlette 1963

24. Species *Catinaster calyculus* (Martini and Bramlette, 1963), (Figure 7, number 7)
Description: Discoasterids have a basket-like structure with six arms extending beyond the basket. This species has a size of 7 - 9 µm. This species is present in samples 3240, 5220, and 6990.

Family Discoastersceae Tan 1927
Genus Discoaster Tan 1927

25. Species *Discoaster berggrenii* (Bukry, 1971), (Figure 7, number 8)
Description: Discoaster with five symmetrical arms and a prominent center. This species measures 8 - 11 µm. This species occurs in samples 4080, 5220, 5760, 6150, 6540, 6990, 7200, 7890, 8000, and 8150.

26. Species *Discoaster brouweri* (Bramlette and Riedel, 1954), (Figure 7, number 9)
Description: Discoaster with six symmetrical arms without branching and a proximal bulge; the central part has a protruding chip. This species has a size of 10 - 13 µm. This species is present in samples 1620, 1920, 2520, 3240, 4080, 4650, 5220, 5460, 5760, 6150, 6360, 6540, 6810, 7200, 7410, 8000, and 8150.

27. Species *Discoaster druggii* (Bramlette and Wilcoxon, 1967), (Figure 7, number 10)
Description: Similar to *D. deflandrei* but larger >15 µm. The asterolith is large and highly variable in its peripheral outline, with six arms that may be obtusely rounded or truncated with a broad and nearly flat central area. This species has a size of 15 µm. This species is present in samples 5220, 5760, and 7410.

28. Species *Discoaster deflandrei* (Bramlette & Riedel, 1954), (Figure 7, number 11)
Description: Has six arms, with the ends of the arms terminating in short, broad bifurcations that are strong and branched. This species has a size of 8 - 10 µm. This species is present in samples 8150 and 8500.

29. Species *Discoaster exilis* (Martini and Bramlette, 1963), (Figure 7, number 12)
Description: This discoaster has six arms with a small central area, usu-

ally with a bulge in the middle and slight ramifications at the ends of each arm. This species has a size of 8 µm. This species is present in samples 6810, 7890, and 8150.

30. Species *Discoaster loeblichii* (Bukry, 1971), (Figure 7, number 13)
Description: Has six arms, similar to *D.variabilis* like, but asymmetrical. The ends of the arms in the distal view are curved counter-clockwise. This species has a size of 10 - 12 µm. This species is present in sample 5220.

31. Species *Discoaster patulus* (de Kaenel & Bergen), (Figure 7, number 14)
Description: comparable to *D. exilis* in that it has six arms but differs in that it only has a central bulge larger than the distal bulge. This species has a size of 10 - 12 µm. This species is present in sample 7410.

32. Species *Discoaster quinqueramus* (Gartner, 1969), (Figure 7, number 15)
Description: Has five symmetrical arms, similar to *D. berggrenii*, with the central area having a large, prominent suture with a blunt tip. This species has a size of 6 - 8 µm. This species is present in samples 6540, 6990, 7200, 7410, 7620, 7890, and 8000.

33. Species *Discoaster surculus* (Martini and Bramlette, 1963), (Figure 7, number 16)
Description: This discoaster has six arms, similar to *D. variabilis*, but with a trifurcation appearance at the ends of the arms. This species has a size of 10 µm. This species is present in samples 6990 and 7410.

34. Species *Discoaster variabilis* (Martini and Bramlette, 1963), (Figure 7, number 17)
Description: This *discoaster* has six arms, the ends of which branch off at an approximately 90° angle. There is a bulge in the center of the central area. This species has a size of 8 µm and is present in samples 6360, 6540, 7410, and 7620.

Family Sphenolithaceae Deflandre 1952
Genus Sphenolithus Deflandre 1952

35. Species *Sphenolithus abies* (Deflandre in Deflandre and Fert, 1954), (Figure 7, number 18)
Description: Similar to *S. moriformis* but higher. The sphenolith is medium, with a sharp upper end and a downwardly elongated spine. This species has a size of 3-4 µm. This species is present in samples 1920, 2520, 2760, 3240, 4080, 4650, 5220, 5460, 5760, 6150, 6360, 6450, 6540, 6810, 6990, 7200, 7620, 7740, 7890, 8000, 8070, 8150, 8280, 8500, dan 8690.

36. Species *Sphenolithus apoxis* (Bergen & de Kaenel in Bergen et al. 2017), (Figure 7, number 19)
Description: Sphenolith is conical with multiple spines. This species has a size of 3 µm. This species is present in samples 5220, 6990, and 8690.

37. Species *Sphenolithus disbelemnos* (Fornaciari and Rio, 1996), (Figure 7, number 20)
Description: Similar to *S. belemnos*, but has a shorter spine. This species

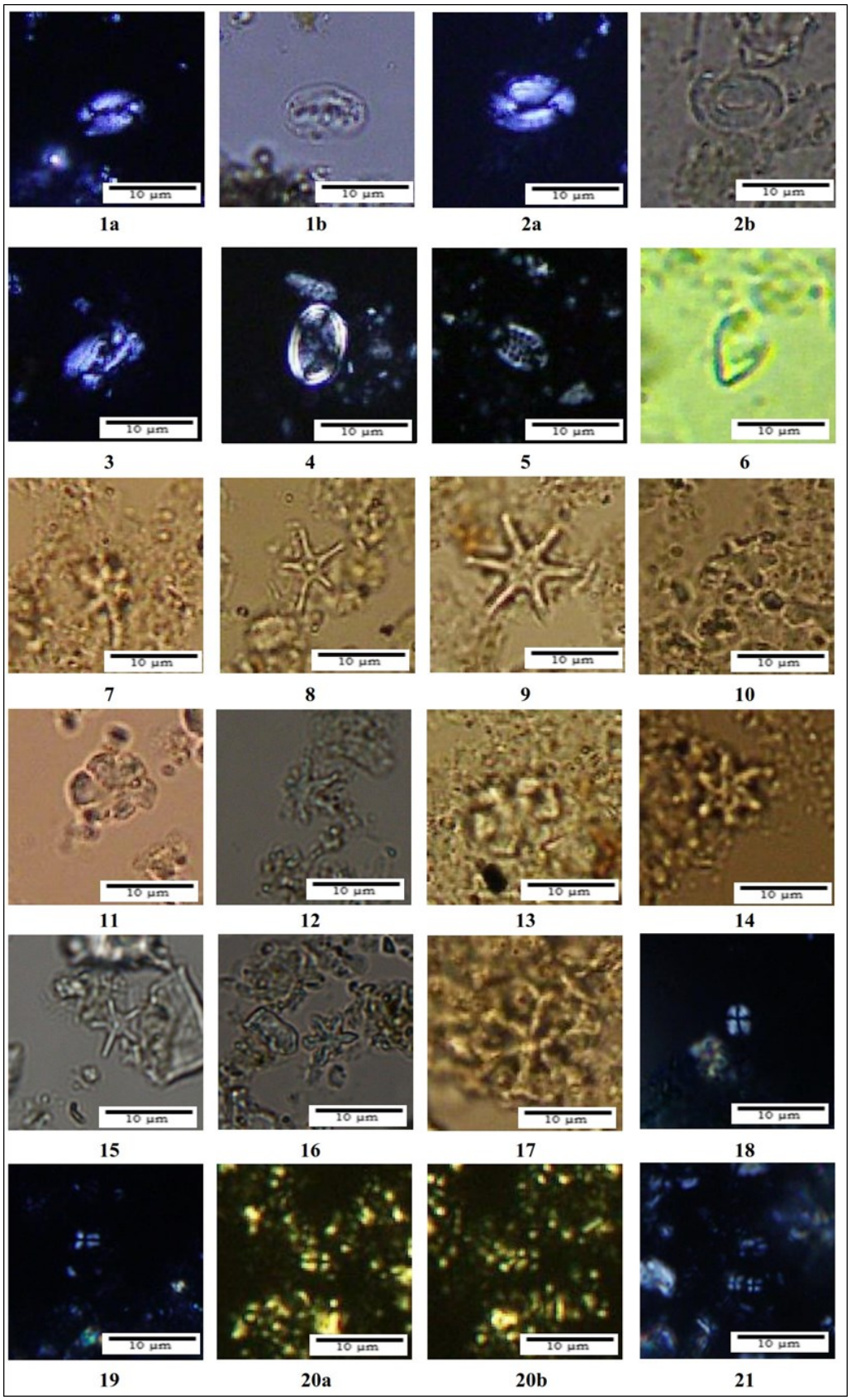

Figure 7. Selected image of nannoplanktons species in this research. XPL views (a) and PPL views (b). The Genus *Helicospahera* consists of (1) *Helicospahera carteri* (sample 4080), (2) *Helicosphaera princei* (sample 1350), (3) *Helicosphaera sellii* (sample 5220). The Genus *Pontosphaera* consists of (4) *Pontosphaera discopora* (sample 6150) and (5) *Pontosphaera multipora* (sample 5220). The Genus *Amaurolithus* consist of (6) *Amaurolithus primus* (sample 6810). The Genus *Catinaster* consist of (7) *Catinaster calyculus* (sample 5220). Genus *Discoaster* consists of (8) *Discoaster berggrenii* (sample 8150), (9) *Discoaster brouwreri* (sample 6150), (10) *Discoaster druggii* (sample 7410), (11) *Discoaster deflandrei* (sample 8150), (12) *Discoaster exilis* (sample 8150), (13) *Discoaster loeblichii* (sample 5220), (14) *Discoaster patulus* (sample 7410), (15) *Discoaster quinqueramus* (sample 6540), and (16) *Discoaster surculus* (sample 7410), and (17) *Discoaster variabilis* (sample 6540). Genus *Sphenolithus* consists of (18) *Sphenolithus abies* (sample 8690), (19) *Sphenolithus apoxis* (sample 8690), (20) *Sphenolithus disbelemnos* (Sample 8690), and (21) *Sphenolithus neoabies* (sample 6540).

has a size of 3 µm. This species was present in samples 8690 dan 8900.

38. Species *Sphenolithus neoabies* (Bukry & Bramlette 1969), (Figure 7, number 21)
Description: They are smaller, less conical, and less elongated on the apical spine. This species has a size of <4 µm. This species was present in samples 4080, 5220, 5460, 5760, 6150, 6540, 6810, 6990, 7200, 7410, 7620, 7740, 7890, 8000, 8070, 8150, 8280, and 8500.

CONCLUSION

The results of calcareous nannoplankton biostratigraphy obtained six zones using six biodatum, namely FO *Sphenolithus abies* as the top *Discoaster signus* zone (NN5), FO *Discoaster brouweri* as top *Discoaster exilis* zone (NN6-NN7), FO *Discoaster berggrenii* as base *Discoaster berggrenii* zone (NN11), LO *Discoaster quinqueramus* as base *Ceratolithus acutus* zone (NN12), FO *Helicosphaera sellii* as base *Helicosphaera sellii* zone (NN13-NN15), LO *Reticulofenestra pseudoumbilicus* as the base for the *Discoaster tamalis* zone (NN16). Formation ages were obtained in this study for the Middle Miocene–Late Miocene Minahaki Formation, the Late Miocene-Early Pliocene Kintom Formation, and the Early Pliocene-Middle Pliocene Biak Formation. The unconformity occurred in the Late Miocene age, equivalent to 10.606 Ma–8.20 Ma, with a duration of 2.406 million years.

AUTHORS CONTRIBUTION

E.M.N. collected data, analyzed data, and wrote scripts. A., D.H.B., S.H, and A.S. designed the research, supervised all the analysis processes, and corrected the manuscript's contents.

ACKNOWLEDGMENTS

The authors would like to thank SKK MIGAS and JOB Pertamina-Medco E&P Tomori Sulawesi for their permission to publish this data.

CONFLICT OF INTEREST

The authors declare no conflict of interest regarding the research or funding.

REFERENCES

Armstrong, H.A. & Brasier, M.D., 2005. *Microfossils* 2nd Editio., USA: Blackwell Publishing.

Backman, J. et al., 2012. Biozonation and biochronology of Paleogene calcareous nannofossils from low and middle latitudes. *Newsletters on Stratigraphy*, 47(2), pp.131–181. doi: 10.1127/0078-0421/2014/0042.

Bergen, J. et al., 2017. Oligocene-Pliocene taxonomy and stratigraphy of the genus Sphenolithus in the circum North Atlantic Basin: Gulf of Mexico and ODP Leg 154. *Journal of Nannoplankton Research*, 37(2–3), pp.77–112.

Bergen, J. et al., 2019. BP Gulf of Mexico Neogene Astronomically-tuned Time Scale (BP GNATTS). *Bulletin of the Geological Society of America*, 131(11–12), pp.1871–1888. doi: 10.1130/B35062.1.

Boesiger, T. et al., 2017. Oligocene to Pleistocene taxonomy and stratigraphy of the genus Helicosphaera and other placolith taxa in the circum North Atlantic Basin. *Journal of Nannoplankton Research*, 37(2–3), pp.145–175.

Bown, P. & Young, J.R., 1998. *Techniques*. In *Calcareous Nannofossil Biostratigraphy*, Kluwer, Dordrecht: British Micropalaeontological Society publication series.

Flores, J.A. & Sierro, F.J., 2013. Coccolithophores. *Encyclopedia of Quaternary Science: Second Edition*, pp.783–794. doi: 10.1016/B978-0-444-53643-3.00281-8.

Galović, I. & Young, J., 2012. Revised taxonomy and stratigraphy of Middle Miocene calcareous nannofossils of the Paratethys. *Micropaleontology*, 58(4), pp.305–334. doi: 10.47894/mpal.58.4.01.

Hasanusi, D. et al., 2004. Prominent Senoro Gas Field Discovery In Central Sulawesi. *Indonesian Petroleum Association Proceedings, Deepwater And Frontier Exploration In Asia & Australasia Symposium*, 101(3), p.55.

Husein, S., Novian, M.I. & Barianto, D.H., 2014. Geological Structures and Tectonic Reconstruction of Luwuk, East Sulawesi. *Proceedings, Indonesian Petroleum Association Thirty-Eighth Annual Convention & Exhibition, May 2014*, (October 2015). doi: 10.29118/ipa.0.14.g.137.

Kapid, R., 2003. *Nanofosil Gampingan: Pengenalan dan Aplikasi Biostratigrafi*, Bandung: ITB.

Kurniasih, A. et al., 2021. Biostratigraphy Analysis of Barbatos-1 Exploration Well in Tomori Block, Banggai Basin, East Arm of Sulawesi. *RISET Geologi dan Pertambangan*, 31(1), p.51. doi: 10.14203/risetgeotam2021.v31.1150.

Lucas, S.G., History, N. & States, U., 2020. Biostratigraphy. *Encyclopedia of Geology, 2nd edition*, pp.1–7. doi: 10.1016/B978-0-08-102908-4.00076-X.

Martini, E., 1971. *Standard Tertiary and Quaternary calcareous Nannoplankton biozonation*. In *Nannofossils Biostratigraphy Part III:12 Cenozoic Biostratigraphy*. Stroudsburg, Pensylvanian: Hutchinson Ross Publishing Company.

McGowran, B., 2005. *Biostratigraphy Microfossils and Geological Time*, U.S.A: Cambridge University Press.

Miller, K.G. et al., 2020. Cenozoic sea-level and cryospheric evolution from deep-sea geochemical and continental margin records. *Science Advances*, 6(20). doi: 10.1126/sciadv.aaz1346.

Nugraha, A.M.S., Hall, R. & BouDagher-Fadel, M., 2022. The Celebes Molasse: A revised Neogene stratigraphy for Sulawesi, Indonesia. *Journal of Asian Earth Sciences*, 228, 105140. doi: 10.1016/j.jseaes.2022.105140.

Okada, H. & Bukry, D., 1980. Supplementary Modification and Introuction of Code Number to the Low-Latitude Coccolith Biostratigraphic Zonation (Bukry, 1973; 1975). *Marine Micropaleontology*, 5(3), pp.321–325. Available at: doi:10.1016/0377-8398(80)90016-x.

Simmons, M., 2019. Biostratigraphy in Exploration – Exploration Handbook. In Halliburton Landmark, London.

Ulfah, A.A., Akmaluddin & Barianto, D.H., 2023. Biostratigraphy and Climate Change in the Late Miocene Age Based on Foraminifera in the Oyo Formation , Oyo River Section , Gunung Kidul , Yogyakarta. *Journal of Tropical Biodiversity and Biotechnology*, 8(2), jtbb81769. doi: 10.22146/jtbb.81769.

Young, J.R., Bown, P.R. & Lees, J.A., 2023, 'Nannotax3' in *Mikrotax*, viewed 8 March 2023, from https://www.mikrotax.org/Nannotax3/

Journal of Tropical Biodiversity and Biotechnology
Volume 09, Issue 01 (2024): jtbb76841
DOI: 10.22146/jtbb.76841

Research Article

Spatial Modelling Habitat Suitability of Javan Langur (*Trachypithecus auratus* É. Geoffroy Saint-Hilaire, 1812) in Bromo Tengger Semeru National Park (TNBTS), East Java

Ari Nadya Ningtyas[1], Nirmala Ayu Aryanti[2]*, Tander Scila Serata Dwi Susilo[3], Mahmuddin Rahmadana[4], Ika Yuni Agustin[5]

1)Department of Forest Resources Conservation, Faculty of Forestry, Gadjah Mada University 55281, Yogyakarta, Indonesia
2)Department of Forestry, Faculty of Agriculture-Animal Science, University of Muhammadiyah Malang 65144, Malang, Indonesia
3)Raden Soerjo Forest Park, Simpang Panji Suroso No. 144 Arjosari, Blimbing 65126, Malang, Indonesia
4)Bromo Tengger Semeru National Park, Raden Intan No.6 Polowijen, Blimbing, Malang City 65125, Malang, Indonesia
5)Island Ranger Community, Kabayam, Sumbawa Besar, West Nusa Tenggara, Indonesia
* Corresponding author, email: nirmalaaaryanti@gmail.com

Keywords:
Elevation
NDVI
Presence
Suitability
Temperature
Submitted:
03 August 2022
Accepted:
05 November 2023
Published:
15 March 2024
Editor:
Miftahul Ilmi

ABSTRACT

Javan Langur *(T. auratus)* is well-known as one of endemic primates from Java, Bali and Lombok Islands. The activities of land clearing, vegetation conversing, wild hunting and illegal wildlife trading are the main causes of the extinction of the Javan Langur. It can be used as an important issue for conservation action by making prediction maps of suitable habitat potential, especially for species facing a high risk of extinction in the wild. We were documenting an information about potential habitat for Javan langur using spatial suitability model in order to provide rigorous information as the basis for conservation activities of Javan langur in TNBTS. We used Landsat-8 TM image and geospatial data to support analysis as a representative of environmental parameters in order to develop the habitat model. We were using maximum entropy (MaxEnt) algorithm refers to Javan langur presence or absence. The results showed that the suitability of the Javan langur habitat in TNBTS has an excellent model accuracy level with an AUC (Area Under the Receiver Operating Characteristics) value of 0.964 and a standard deviation of 0.961. Parameters with the highest response values here are elevation, NDVI (Normalised Difference Vegetation Index) and temperatures.

Copyright: © 2024, J. Tropical Biodiversity Biotechnology (CC BY-SA 4.0)

INTRODUCTION

Human activities such as land clearing and vegetation conversing are the leading causes of habitat loss and fragmentation that threaten species into an extinction (Chapman & Onderdonk 1998). Illegal hunting regarding to consumption and illegal trading as pets pose a threats for wildlife populations (Ervina & Wasiq 2018). Those evidences are essential issues in relation to conservation activities by making prediction maps of suitable habitat potential (Gaston 1996) for species struggle from extinction in the wild, and Javan langur is one of species belong to those groups. They are endemic primate to the islands of Java, Bali and Lombok Indonesia (Nijman & Supriatna 2008) and protected by Minister of Environ-

ment and Forestry of the Republic of Indonesia No. P.20/MENLHK/SETJEN/KUM.1/6/2018. Javan langur found in various habitats: primary, secondary, coastal to mangrove forests (Nijman & Supriatna 2008).

Bromo Tengger Semeru National Park (TNBTS) is known as an essential habitat for Javan langur. This species characterised by wide home range and quadrupedal, which make this primate is very dependent on the presence of forest vegetation and canopies to support their movement behaviour. The potential density of tree stands is still high with conditions of various diameters, which are still commonly found in forest land cover in TNBTS (Noor'an et al. 2015). Javan Langur is closely related to the presence of trees for all of its activities (Subarkah et al. 2011). However, the essential habitat of the Javan langur is also an important area for the people who live and other villages around the TNBTS area (Sayektiningsih et al. 2008). TNBTS is also one of the leading star objects and natural tourist attractions for the East Java area (Sutiarso & Susanto 2018). Human activities around these wildlife habitats can indirectly affect movement (Doherty et al. 2021), health to population decline and quality of life (Fraser & MacRae 2011).

Species distribution modelling is widely used to predict habitat suitability and habitat used by a species (Peterson 2006). Javan langur are very dependent on forest vegetation (Fahmi & Bintarawati 2018), which predominantly consume leaves and the rest are flowers, fruits, insect and other plant parts (Zakki et al. 2017; Aryanti & Azizah 2019). Habitat suitability models can relate the presence of species and the biophysical environment (Elith et al. 2006; Kumar & Stohlgren 2009) at the study site. Moving animal objects such as Javan langurs can use spatial approaches and models such as the Species Distribution Model (SDM) or ecological niche modelling that can relate data on the presence of species with various impact components that affect them (Warren & Seifert 2011; Prasetyo 2017). Technically SDM can prepared using the Maximum Entropy Algorithm (MaxEnt) which can only use incident records along with environmental characterisation to identify the preferred environment of the organism under study (Morales et al. 2017; Widyastuti et al. 2020; Valencia-Rodríguez et al. 2021). We determined the potential habitat's spatial suitability model and expected that it will provide comprehensive information as recommendation related to planning for the conservation of Javan langur in TNBTS. Otherwise, we also identified the environmental factors that give significant influences to the suitability of the Javan langur habitat in TNBTS.

MATERIALS AND METHODS

Study Area

This research was conducted in October 2019 - January 2020 and carried out throughout the TNBTS area, an important habitat for Javan langur. TNBTS area covers Malang, Pasuruan, Probolinggo and Lumajang regencies in East Java with a total area of 50276.3 Ha (Figure 1).

Materials

The equipment used for data collection of Javan langur includes GPS (Global Positioning System), binoculars, rangefinder, hygrothermometer, camera, tally sheet and stationery. Analysing data using a PC/laptop, ArcGIS 10.3 software, Indonesian earth maps, DEMNAS (National Digital Elevation Model), Landsat 8 and MaxEnt 3.4.4 software. The material used in this study was the encounter point of the Javan langur as presence data for forming a habitat suitability model (Cahyana et al. 2016).

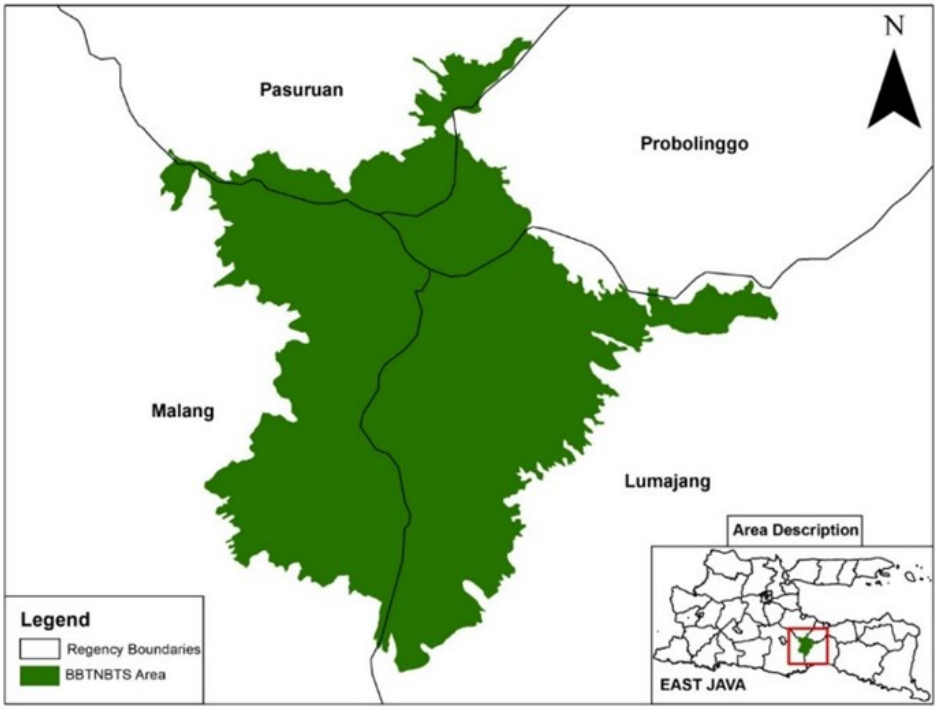

Figure 1. Map location for data collection on the habitat suitability of the Javan langur TNBTS.

Method

Occurrence data of Javan langurs with had survey and collected information from research that has been carried out and information from the community or TNBTS officers. We are collected GPS coordinates from the individual/population presence of Javan langur throughout the TNBTS area, using direct encounter and line transect sampling methods. GPS Coordinates of the Javan langur were recorded using the Garmin GPSMAP 60 CSx. The data presence coordinates were transferred into Microsoft Excel and saved in CSV.

Observations conducted during the active time of the Javan langur, starting from morning to evening (06.00-18.00 WIB) (Sulistyadi et al. 2013). Environmental data collected were elevation, slope, temperature, NDVI (Normalized Difference Vegetation Index) and distance from the road access. NDVI described the canopy condition from vegetation composition (El-Shikha et al. 2008; Sulistyo et al. 2010), where most of their daily activity utilizes the canopy plant (Subarkah et al. 2011). The elevation and slope map data were obtained from topographic data using 32-bit DEMNAS with a resolution of 5-8 m which downloaded from the BIG websites (Geospatial Information Agency) (Morales et al. 2017). NDVI and temperature data were obtained from Landsat-8 TM image data (Widyastuti et al. 2020). Distance of the Javan langur to roads were obtained from RBI (Rupa Bumi Indonesia) map.

Data analysis

GPS Coordinates of Javan langur presence were extracted using Arc.Gis 10.3 software. The objective was to determine variable's class and the relationships between each environmental variable based on the distribution of Javan langur (Elith et al. 2011). The results of the extracted data were used to perform multicollinearity tests on SPSS (Statistical Package for the Social Sciences) software. Multicollinearity test was conducted to determine the relationships between the used variables. When there is a linear relationships among variables, one of the variables should be removed (Hansen et al. 2020). Afterward, the coordinates point data was

extracted back to Ms Excel in CSV format, while the variable data was exported in ASCII format (Fitzgerald et al. 2018). The data presence coordinates and the environmental variable used to build the suitability habitat model by Maxent 3.4.1. (http://www.cs.princeton.edu/~schapire/maxent/) and effective even with the small number of occurrence records (Kumar & Stohlgren 2009).

MaxEnt generates logistic outputs with approximate relative probabilities of the type distribution with values from 0 (lowest probability) to 1 (highest probability) (Elith et al. 2011). To evaluate the performance of the habitat suitability model, we focused on how the five variables affect the model was measured by the AUC (Area Under the Receiver Operating Characteristics) value (Table 1). The AUC value was used to test the model's accuracy created by MaxEnt (Morales et al. 2017). The AUC value was higher than the standard deviation value, the model has a very high accuracy. However, if the standard deviation value was higher than the AUC value, then the accuracy of the model created by MaxEnt was very low (Fitzgerald et al. 2018). The standard deviation value was used to measure how the model values were distributed in the TNBTS area.

Table 1. Accuracy of model performance based on the AUC Value (Elith et al. 2011).

AUC Value	Model Performance
0,6 – ≤ 0,7	Not good
>0,7 - ≤ 0,8	Good
>0,8 – 0,9	Very Good

RESULTS

The results of spatial data from environmental parameters (NDVI, slope, distance from the road, temperature and elevation) are viewed in figure 2. The NDVI parameter has shown a value of -0.6 to 0.63, with the Javan langur are commonly found at the highest NDVI value. The condition of these area is a dry land forests with high density of forest vegetation. In this class, the dominant populations are Ficus spp, *Maesopsis eminii* (Engl.), *Erythirna variegate* (L.) Merr, *Trema orientalis* (L.) Blume and *Nauclea excelsa* (Bl.). It is obvious that the Javan langur very depending on the habitat conditions with dense canopies, since it will be related to movements of this population over branches, trees, and also the way to stay away from predator. Though, based on the slope parameter, it was known that the slope strongly influences the distribution of the Javan langur in TNBTS. The slope was related to the distribution of forage plants, safety from predators and human disturbances and the selection of sleeping trees for Javan langur (Abdillah 2014). The slope of the TNBTS area ranges from 0 - 70.30 %, but the Javan langur were mostly found on slopes of 10.76 % - 23.70 %. The categories of slope found of Javan langurs were 15-25% (wavy) and 25-40% (steep) (Sari et al. 2020).

The temperature parameter values in TNBTS range from 8-30°C. The presence of Javan langur was found in the morning with a temperature range of 8-24°C. When the weather warmer, the Javan langur prefers to take a rest by taking shelter under the dense canopy of trees (Santono et al. 2016), otherwise, these species will digests the food which has consumed previously (Sulistyadi et al. 2013). Thus, from the recorded elevation map of these presence, the Javan langur was mostly found at an 829 – 1,642 a.s.l. This elevation factor is closely related to the availability of foraging behaviour and safe from predators. Both become the dominant factors in determining the distribution and level of presence Javan langur in TNBTS. Additionally, the distance parameter is related to hu-

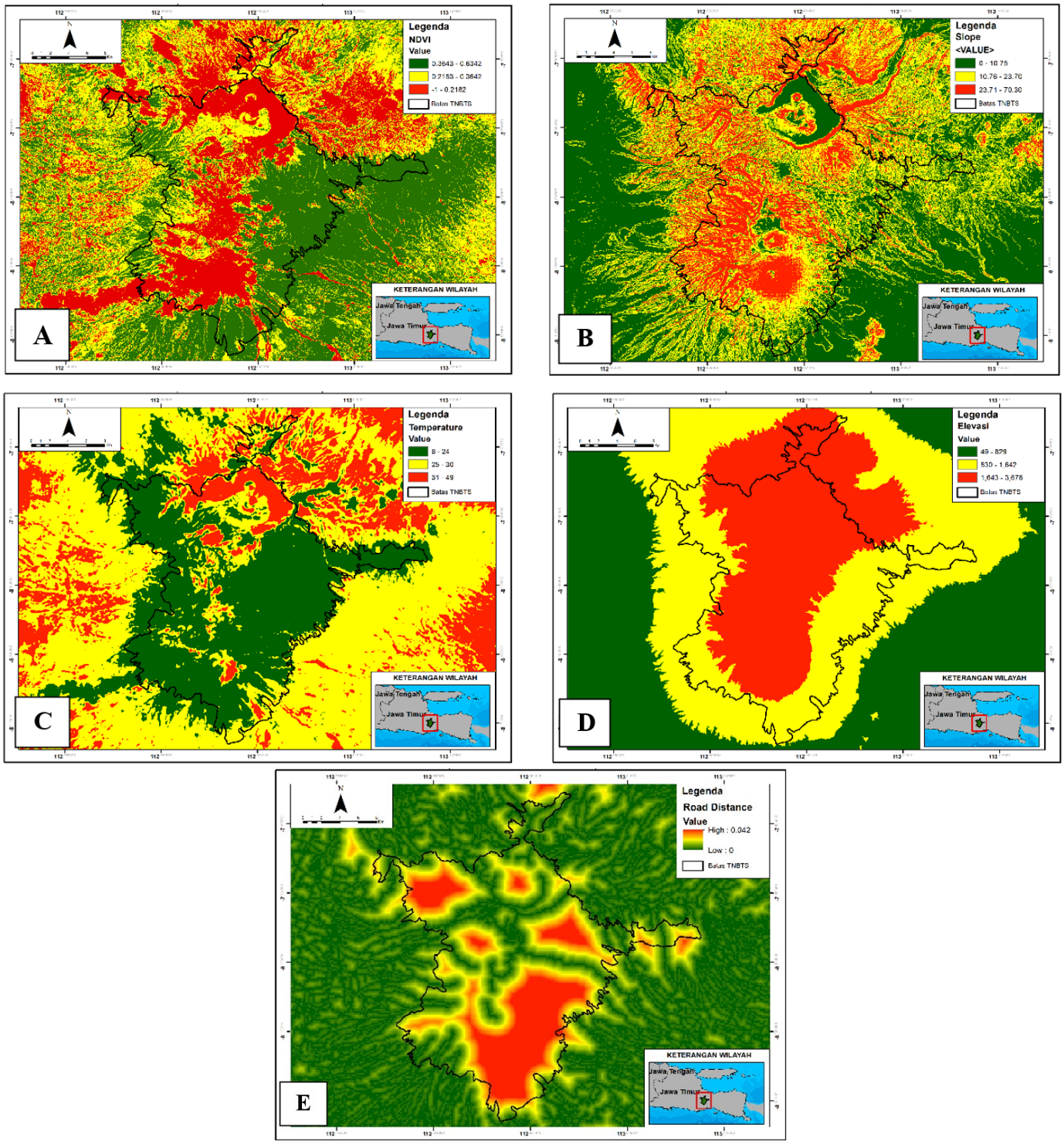

Figure 2. Map of environmental parameters to build the Javan langur habitat model : A. NDVI, B. Slope, C. Temperature, D. Elevation, E. Road Distance.

man disturbances through human activities and noises. Human pressure is also the suspected factor that could be a barrier to habitat conditions for the Javan langur family (Sulistyadi et al. 2013). Commonly, the Javan langur found at distance of 100 - 1000 meters from the activities of residents in the TNBTS area.

The presence of data collection Javan langur was needed to build models and validate map performance. We are detected 48 occurences of Javan langur in TNBTS. The amount was split 70% for model building and 30% for validation. Therefore, more data in the field will be accurate to the habitat suitability model for those animals (Onojeghuo et al. 2015). The value of each parameter was analysed by multicollinearity in order

to determine the correlation between the environmental variables. When the values increase, it will significantly influence the results of the modelling made (Nadler et al. 2007). The results of the multicollinearity test showed the Variance Inflating Factor (VIF) values are < 10 and the tolerance value > 0.10 for all environmental variables (Table 2). It means there was no multicollinearity in these parameters and no parameters that must be omitted in developing a habitat suitability for Javan langur.

Table 2. Multicollinearity test between parameters.

Parameter	Tolerance Value	VIF
Elevation	0.33	3.00
NDVI	0.18	5.38
Temperature	0.16	5.97
Slope	0.29	3.40
Road Distance	0.44	2.25

Habitat modeling was carried out using the MaxEnt 3.4.4 program. MaxEnt is considered capable of mapping the distribution of species where each pixel's value represents the possibility of species in suitable habitats (Rupprecht et al. 2011). The modelling used five parameters that were previously processed in the form of raster data types. Parameters and data presence of Javan langur were overlaid with MaxEnt. The habitat estimation model results in potential Javan langur habitat in Figure 3.

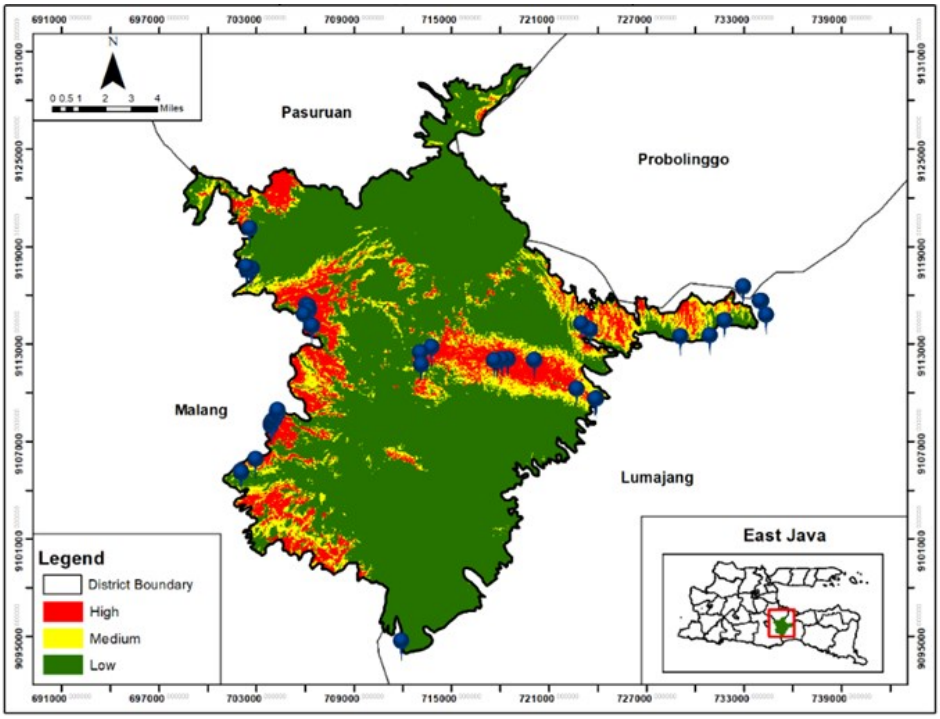

Figure 3. The map of suitability of habitat for Javan langur TNBTS.

It can be seen that there are three colors generated in establishing the model. Red color indicates very high habitat suitability, yellow color moderate habitat suitability and green color low habitat suitability (Prasetyo 2017). Each color has a proportion value which is the presentation value of Javan langur habitat suitability class in TNBTS. The habitat area with high suitability (4,783.4 Ha) for Javan langur in TNBTS was still a primary forest area with high vegetation with overlapping canopy conditions. The low (39,358 Ha) and medium (6,134.9 Ha) habitat suitability classes were volcanic areas with bush and savanna vegetation conditions. The Javan langur has chosen a location with good vegetation

cover such as primary forest, but its home range also includes secondary forest (Hansen et al. 2020). It was due to the availability of vegetation that supports the needs of diurnal primates, especially the availability of food from pole and tree growth form vegetation. In building a habitat model some parameters considered essential and contributed to the resulting model (Table 3). Essential parameters are considered capable of contributing if the value is > 10% (Abdillah 2014).

Table 3. Important parameter values in building a habitat suitability model Javan langur.

Parameter	Contribution Percentage (%)
Temperature	35.9
Elevation	34.7
NDVI	15.8
Road Distance	13.4
Slope	0.1

Based on the predicted percentage of environmental parameters that contribute to the presence of Javan langur in TNBTS to the model (Table 3), temperature (35.9%), elevation (34.7%), NDVI (15.8%) and distance from human roads (13.4%). In the TNBTS area at the highest elevation was the peak of a volcano in the form of savanna and bare ground so no Javan langur is found. Temperature also affected presence because high temperatures, the influence of volcanoes, were not found in Javan langur. The high activity of the Javan Langur is influenced by internal factors, namely the fulfillment of feed intake which will become energy, as well as external factors, namely temperature and humidity which tend to make the Javan Langur active between 10-30°C (Sulistyadi et al. 2013). The results of the important variable values were then further tested with the Area Under the Receiver Operating Characteristic (ROC) Curve AUC in order to determine the variables and their effects on the habitat suitability model of Javan langur in TNBTS (Figure 4) (Onojeghuo et al. 2015).

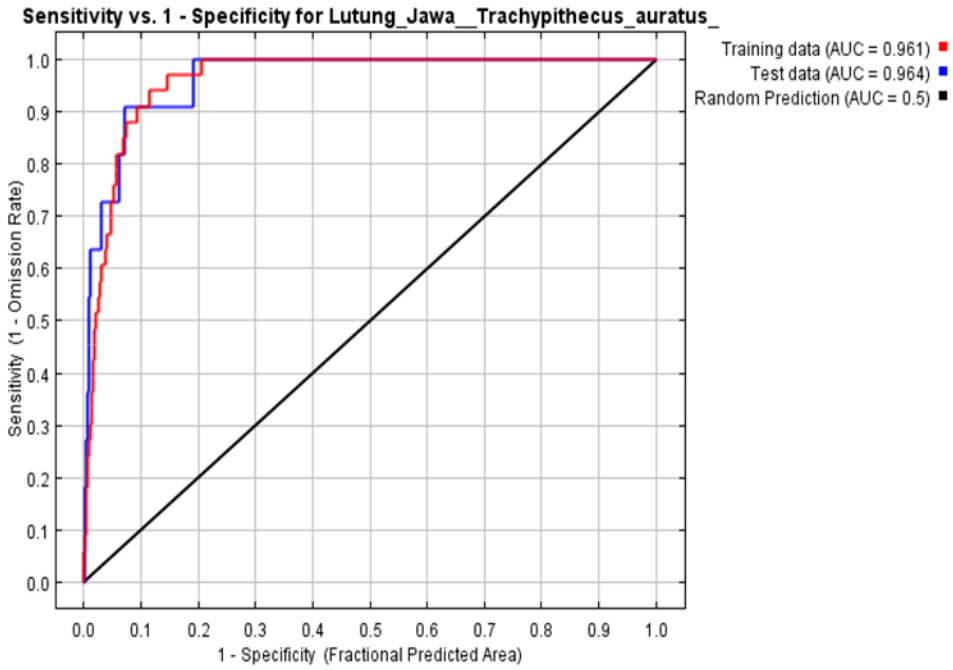

Figure 4. Graph of AUC test results for the suitability of Javan langur in TNBTS habitat.

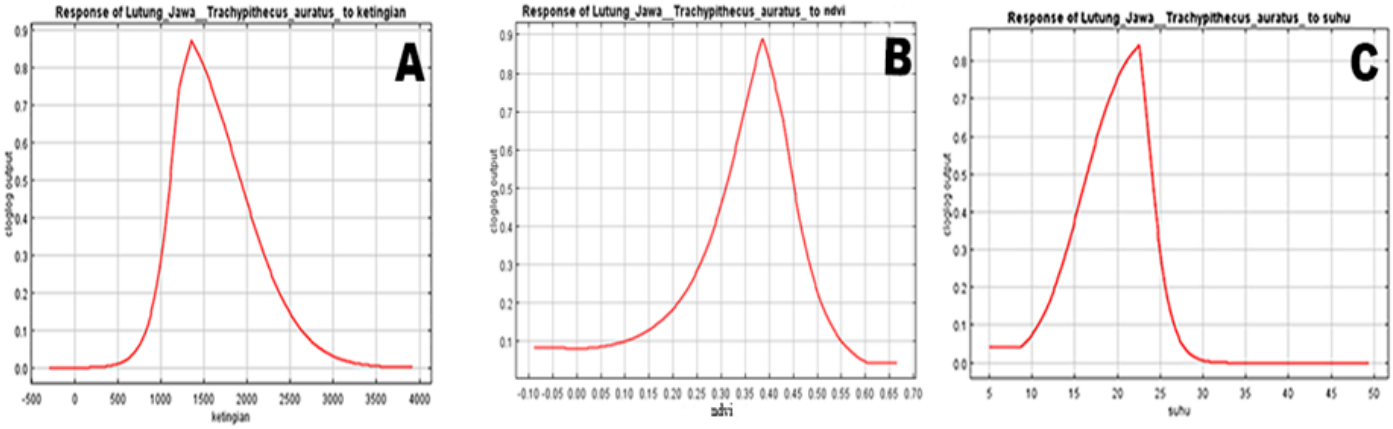

Figure 5. Graph of parameters response that contributes highly in building the habitat suitability model for the Javan langur TNBTS habitat A. Elevation, B. NDVI, C. Temperature.

The results of the AUC test were an evaluation of the model in estimating the suitability of Javan langur habitat in TNBTS. The results of this test showed an AUC value of 0.964 with a standard deviation of 0.961, which describes an excellent level of model accuracy. The value of the deviation was smaller than the AUC value, the AUC value was very good, which exceeds the value of 0.90 (Cahyana et al. 2016). The relationship between probability the presence of Javan langur with environmental parameters was shown by a graph of response each variable. In Figure 5, it can be seen that the variation of environmental parameters affect the prediction of of Javan langur's presence in TNBTS.

The results of the response parameters contribute highly to building the habitat suitability model of Javan langur TNBTS habitat and it was known that the area was at an altitude of 812 – 1,642 mdpl, NDVI class 0.37–0.63% and a temperature of 8–24°C. Therefore, it can be said that these parameters were associated in a complex manner and affected the habitat characteristics of Javan langur either directly or indirectly.

CONCLUSIONS

Based on the evaluation of the model using MaxEnt, the suitable habitat area for the Javan langur is in the high category (9.5%) and medium (12.2%) of the TNBTS area, with the model accuracy level of the AUC value of 0.964. In that area, the environmental conditions affecting Javan langurs' presence were elevation, NDVI and temperature. To increase Javan langur's area of suitable habitat because arboreal species, it is necessary to protect vegetated stands, especially with overlapping crowns at locations with an effective environmental variable approach.

AUTHOR CONTRIBUTION

The NAA, ANN and IYA analysed the data and wrote the manuscript. TSSDS and MR worked in the field and made research maps and habitat suitability maps.

ACKNOWLEDGMENTS

We would like to thank the Bromo Tengger Semeru Natíonal Park and all the local guides who have helped for collected data and also Rufford Small Grants Foundation for the financial support.

CONFLICT OF INTEREST

All authors declare that there was no personal or group conflict of interest. The author is fully responsible for the content and writing of the published article.

REFERENCES

Abdillah, R., 2014. Pemodelan Spasial Kesesuaian Habitat Lutung Jawa (*Trachypithecus auratus Geoffroy*, 1812) di Resort Rowobendo Taman Nasional Alas Purwo Reza Abdillah. Institut Pertanian Bogor.

Aryanti, N., & Azizah, L., 2019. Karakteristik Habitat Lutung Jawa (Trachypithecus auratus) di Kawasan Hutan Lindung RPH Sumbermanjing KPH Malang. *Indonesia, Jurnal Primatologi*, 16(1), pp.24–30.

Cahyana, A.N. et al., 2016. Pemodelan Spasial Kesesuaian Habitat Elang Jawa (*Nisaetus bartelsi* Stresemann, 1924) di Taman Nasional Gunung Halimun Salak. *Media Konservasi*, 20(3), pp.211–219. doi: 10.29243/medkon.20.3.

Chapman, C.A. & Onderdonk, D.A., 1998. Forests without primates: Primate/plant codependency. *American Journal of Primatology*, 45(1), pp.127–141. doi: 10.1002/(SICI)1098-2345(1998)45:1<127::AID-AJP9>3.0.CO;2-Y.

Doherty, T.S. et al., 2021. Human disturbance causes widespread disruption of animal movement. *Nature Ecology and Evolution*, 5(4), pp.513–519. doi: 10.1038/s41559-020-01380-1.

El-Shikha, D.M. et al., 2008. Remote Sensing of Cotton Nitrogen Status Using the Canopy Chlorophyll Content Index (CCCI). *Transactions of the ASABE*, 51(1), pp.73–82. doi: 10.13031/2013.24228.

Elith, J. et al., 2006. Novel methods improve prediction of species' distributions from occurrence data. *Ecography*, 29(2), pp.129–151. doi: 10.1111/j.2006.0906-7590.04596.x.

Elith, J. et al., 2011. A statistical explanation of MaxEnt for ecologists. *Diversity and Distributions*, 17(1), pp.43–57. doi: 10.1111/j.1472-4642.2010.00725.x.

Ervina, R. & Wasiq, H.J., 2018. Vegetation Structure of Ebony Leaf Monkey *(Trachypithecus auratus)* Habitat in Kecubung Ulolanang Nature Preservation Central Java-Indonesia. in *E3S Web of Conferences*. doi: 10.1051/e3sconf/20183108016.

Fahmi, R. & Bintarawati, V.S., 2018. Inventarisasi Jenis Pakan Lutung Jawa *(Trachypithecus auratus)* Pada Blok Cilame dan Blok Cimeudeum Taman Wisata Alam Gunung Tampomas Kabupaten Sumedang. *Wanamukti*, 21(1), pp.17–29.

Fitzgerald, M. et al., 2018. Modeling habitat suitability for chimpanzees *(Pan troglodytes* verus) in the Greater Nimba Landscape, Guinea, West Africa. *Primates*, 59(4), pp.361–375. doi: 10.1007/s10329-018-0657-8.

Fraser, D. & MacRae, A.M., 2011. Four types of activities that affect animals: Implications for animal welfare science and animal ethics philosophy. *Animal Welfare*, 20(4), pp.581–590.

Gaston, K.J., 1996. Biodiversity - Congruence. *Progress in Physical Geography*, 20(1), pp.105–112. doi: 10.1177/030913339602000108.

Hansen, M.F. et al., 2020. Habitat suitability analysis reveals high ecological flexibility in a "strict" forest primate. *Frontiers in Zoology*, 17, 6. doi: 10.1186/s12983-020-00352-2.

Kumar, S. & Stohlgren, T.J., 2009. Maxent modeling for predicting suitable habitat for threatened and endangered tree *Canacomyrica monticola* in New Caledonia. *Journal of Ecology and Natural Environment*, 1(14), pp.94–98.

Morales, N.S. et al., 2017. MaxEnt's parameter configuration and small samples: Are we paying attention to recommendations? A systematic review. *PeerJ*, 2017(3), e3093. doi: 10.7717/peerj.3093.

Nadler, T. et al., 2007. Conservation status of Vietnamese primates. *Vietnamese Journal of Primatology*, 1(1), pp.7–26.

Nijman, V. & Supriatna, J., 2008. Trachypithecus auratus ssp. auratus', *The IUCN Red List of Threatened Species 2008*, 8235 (e.T39848A10276744).

Noor'an, R.F., Jaya, I.N.S. & Puspaningsih, N., 2015. Estimating the Changes of Carbon Stocks in Bromo Tengger Semeru National Park. *Media Konservasi*, 20(2), pp.177–186.

Onojeghuo, A.O. et al., 2015. Habitat Suitability Modeling of Endangered Primates in Nigeria: Integrating Satellite Remote Sensing and Spatial Modeling Techniques. *Journal of Geoscience and Environment Protection*, 3(8), pp.23–38. doi: 10.4236/gep.2015.38003.

Peterson, A.T., 2006. Uses and Requirements of Ecological Niche Models and Related Distributional Models. *Biodiversity Informatics*, 3. doi: 10.17161/bi.v3i0.29.

Prasetyo, L.B., 2017. Pendekatan Ekologi Lanskap Untuk Konservasi Biodiversitas. *Institut Pertanian Bogor*.

Rupprecht, F., Oldeland, J., & Finckh, M., 2011. Modelling potential distribution of the threatened tree species Juniperusoxycedrus: how to evaluate the predictions of different modelling approaches? Journal *of Vegetation Science*, 22(4), pp.647–659. doi: 10.1111/j.1654-1103.2011.01269.x

Santono, D. et al., 2016. Aktivitas Harian Lutung Jawa (*Trachypithecus auratus* sondacius) di Kawasan Taman Buru Masigit Kareumbi Jawa Barat. *Jurnal Biodjati*, 1(1), p.39. doi: 10.15575/biodjati.v1i1.1031.

Sari, I. et al., 2020. Estimasi Populasi dan Vegetasi Habitat Lutung Jawa di Gunung Ungaran, Jawa Tengah. *Jurnal Biologi Tropika*, 3(2), pp.47–56.

Sayektiningsih, T. et al., 2008. Strategi Pengembangan Pendidikan Konservasi Pada Masyarakat Suku Tengger di Desa *Enclave* Taman Nasional Bromo Tengger Semeru. *Media Konservasi*, 13(1), pp.32–37.

Subarkah, M.H. et al., 2011. Javan Leaf Monkey *(Trachypithecus auratus)* Movement in a Fragmented Habitat, at Bromo Tengger Semeru National Park, East Java, Indonesia. *Jurnal Biologi Indonesia*, 7(2), pp.213–220.

Sulistyadi, E. et al., 2013. Pergerakan Lutung Jawa (*Trachypithecus auratus* E. Geoffroy 1812) Pada Fragmen Habitat Terisolasi Di Taman Wisata Alam Gunung Pancar Bogor. *Berita Biologi*, 12(3), pp.383–395.

Sulistyo, B. et al., 2010. Pemodelan Persentase Tajuk di DAS Merawu yang diturunkan dari Berbagai Indeks Vegetasi Data Penginderaan Jauh. *Forum Geografi*, 27(1), pp. 23–32.

Sutiarso, M.A. & Susanto, B., 2018. Pengembangan Pariwisata Berbasis Masyarakat di Taman Nasional Bromo Tengger Semeru Jawa Timur. *Ganaya: Jurnal Ilmu Sosial dan Humaniora*, 1(2), pp.144–154.

Valencia-Rodríguez, D. et al., 2021. Ecological niche modeling as an effective tool to predict the distribution of freshwater organisms: The case of the Sabaleta Brycon henni (Eigenmann, 1913). *PLoS ONE*, 16(3), e0247876. doi: 10.1371/journal.pone.0247876

Warren, D.L. & Seifert, S.N., 2011. Ecological niche modeling in Maxent: the importance of model complexity and the performance of model selection criteria. *Ecological Applications*, 21(2), pp.335–342.

Widyastuti, S. et al., 2020. Maxent modelling of habitat suitability for the endangered javan gibbon (*Hylobates moloch*) in less-protected Dieng Mountains, Central Java. *IOP Conference Series: Earth and Environmental Science.*, 457, 012014. doi: 10.1088/1755-1315/457/1/012014.

Zakki, A. et al., 2017. Preferensi Jenis - Jenis Pakan Lutung Jawa (*Trachypithecus auratus* É. Geoffroy Saint-Hilaire, 1812 .) di Hutan Lindung Coban Talun. *Konservasi Sumberdaya Hutan Jurnal Ilmu-Ilmu Kehutanan*, 1(4), pp.86–91.

Journal of Tropical Biodiversity and Biotechnology
Volume 09, Issue 01 (2024): jtbb82682
DOI: 10.22146/jtbb.82682

Review Article

A Mini Review on Analysis of Potential Antibacterial Activity of Symbiotic Bacteria from Indonesian Freshwater Sponge: An Unexplored and A Hidden Potency

Edwin Setiawan[1]*, Michael Einstein Hermanto[2], Nurlita Abdulgani[1], Endry Nugroho Prasetyo[1], Catur Riani[3], Dyah Wulandari[4], Anto Budiharjo[5,6]

1)Biology Department, Institut Teknologi Sepuluh Nopember, Jl. Teknik Kimia, Sukolilo, Surabaya, East Java 60111.
2)Post Graduate Student Biology Department, Institut Teknologi Sepuluh Nopember, Jl. Teknik Kimia, Sukolilo, Surabaya, East Java 60111.
3)School of Pharmacy, Institut Teknologi Bandung, Jl. Ganesa No.10 Bandung, 40132.
4)Food Technology Department, Faculty of Agricultural Technology - Soegijapranata Catholic University (SCU), Jl. Pawiyatan Luhur IV/1, Bendan Duwur, Semarang 50219
5)Biotechnology Study Program, Faculty of Science and Mathematics, Diponegoro University, Jl. Prof. Sudharto SH, Semarang 50275, Indonesia
6)Molecular and Applied Microbiology Laboratory, Center of Research and Service – Diponegoro University, Jl. Prof. Sudharto SH, Semarang 50275, Indonesia
* Corresponding author, email: edwin@bio.its.ac.id

Keywords:
Antibacterial substances
Indonesian Freshwater sponges
Mini literature analysis
Symbiotic microbes
Potency mapping
Submitted:
28 February 2023
Accepted:
12 August 2023
Published:
02 January 2024
Editor:
Ardaning Nuriliani

ABSTRACT

Marine sponges have been investigated as potential bioresources because of their symbiotic relationship with microbes such as Actinobacteria that produce antibacterial substances. In contrast, a group of sponges, that inhabits freshwater environments called freshwater sponges (Order Spongillida Manconi & Pronzato, 2002) and consists of only one percent among all of the sponges' species (Phylum Porifera Grant, 1836), has not yet intensively examined. For this reason, we screened, determined, evaluated, and reviewed by examining several databases in Scopus, Pub Med, and Google Scholar related to potential aspects of symbiotic bacteria and their antibacterial substances that can be further utilised and developed into synthesised antibacterial compounds, based on published metagenomic data of symbiotic bacteria in freshwater sponges. At the same time, we compared a composition of those freshwater symbionts to marine sponges' symbionts whether those possess a similar composition or not. Moreover, a current report and a revisit study of freshwater sponges in East Java, initiate further direction on mapping of those symbiotic bacteria from Indonesia that can be nominated as potential groups possessing antibacterial properties.

Copyright: © 2024, J. Tropical Biodiversity Biotechnology (CC BY-SA 4.0)

INTRODUCTION

Sponges (Phylum Porifera Grant, 1836) are multicellular animal that has been known for hosting various microbes e.g., bacteria, archaea, fungi, or microalgae organisms as symbionts and comprises 40 % of sponges' volume furthermore, symbionts might possess a unique and specific relationship with sponges' host (Hentschel et al. 2003; Fieseler et al. 2004; Webster & Taylor 2012). Besides providing energy for a certain host sponge, e.g., photosynthetic cyanobacteria, other microorganisms contribute to

sponges' defense mechanism through the production of a bioactive compound or secondary metabolites (Unson et al. 1994; Schmidt et al. 2000), which has been researched intensively for a decade as antibacterial potency of bacterial symbionts from sponges. In Indonesia, several bioprospecting studies have been conducted on screening these bacteria symbionts in sponges for antibacterial potency, particularly from marine sponges e.g., *Xestospongia testudinaria* from Papua (Cita et al. 2017), *Aaptos suberitoides*, *Agelas nakamurai* and other eight marine species from Sulawesi (Riyanti et al. 2020), *Spongia officinalis* from Nusa Tenggara (Prastiyanto et al. 2022) and *Jaspis* sp. from Enggano (Sipriyadi et al. 2022).

In contrast to marine sponges, freshwater sponges (Manconi & Pronzato 2002) are classified as a minor group of sponges (Phylum Porifera Grant 1836) that inhabit freshwater environments and ecosystems such as lakes and rivers. These sponges consist of only 1% of all sponge species, which contains around 8000 species according to the World Porifera Database (WPD), (de Voogd et al. 2023). A prominent feature of freshwater is the ability to survive in a fluctuating or extreme environmental condition like a shortage of water and the ability to individual dispersion over a long distance because of possessing an asexual reproduction organ called gemmules (Manconi & Pronzato 2002). Ecologically, freshwater sponges are linking energetic pathways between the pelagic and benthic community in the freshwater ecosystem by hosting zoochlorella and being eaten by spongivorous insects (Skelton & Strand 2013). Besides being recognised as a maritime country, Indonesia also possesses an abundance of freshwater streams (approximately 170 main rivers), with the longest river (Kapuas River) measuring up to 1143 km and a basin area of 98.740 km^2 (Suwarno et al. 2013). However, despite possessing a lot of freshwater streams, data on the diversity of freshwater sponges from Indonesia is overlooked.

As marine sponge symbiont often plays an important role in bioactive compounds production such as a member of Actinomycete, Proteobacteria, and firmicutes phyla, it is expected that sponge symbionts of freshwater sponges are members of these phyla (Bibi et al. 2017). Therefore, this mini review on comparing the composition of bacterial symbionts in a different environment can be used for exploring and mapping a potential sponge symbiont from a freshwater environment, especially Indonesian freshwater sponges, which can be utilised as an alternative source of antibacterial substances.

DISCOVERED "ANTIBACTERIAL-LIKE SUBSTANCES" FROM SPONGES

Joseph et al. (2017) reported the antibacterial activity of *Streptomyces pharmamarensis* isolated from the marine sponge *Clathria procera*. This symbiont exhibits antibacterial activity against *Acinetobacter baumanni*, *Enterococcus faecalis*, and even resistant strains such as methicillin-resistant *Staphylococcus aureus*. Based on TLC analysis, the antibacterial activity was due to two unknown substances recognised as PVI401 and PVI402. Furthermore, HR-LC-MS (High-Resolution Liquid Chromatography and Mass Spectroscopy) devices confirmed PVI401 and PVI402 are substances that structurally like phosmidosine and altermicidine, despite FTIR (Fourier-transform infrared spectroscopy analysis) device reported a functional group of substances did not match with the functional group of phosmidosine and altermicidine. Therefore, PVI401 and PVI402 possibly are novel compounds.

An antibacterial activity of Symbiotic bacteria isolated from a ma-

rine sponge *Haliclona* sp. was reported by Asagabaldan et al. (2017). This species is known as a source of antibacterial substances since the sponge extract contains Haliclonin A. However, symbionts of *Haliclona* sp. might also harbor and involve antibacterial properties. In this study, one of the isolates, PSP39.04 isolate, also exhibited antibacterial activity against *Pseudomonas aeruginosa*, *Enterobacter cloacae*, *A. baumannii*, and *S. aureus*. PSP39.04 was closely related to *Chromohalobacter salexigens* by 16S rRNA. For this reason, it is deduced antibacterial activity of PSP39.04 was due to its ability to produce cyclic peptides, which are effective against Multi-Drug Resistant (MDR) pathogens. Moreover, it is concluded while sponge extracts may exhibit bioactive properties, antibacterial compounds derived from symbionts are more effective since their activity against drug-resistant strains and pathogens commonly found causing diseases in humans (*Enterococcus faecium*, *Staphylococcus aureus*, *Klebsiella pneumoniae*, *Acinetobacter baumannii*, *Pseudomonas aeruginosa*, and *Enterobacter* spp. abbreviated as ESKAPE). In addition, because marine sponge symbionts possess potent antibacterial properties, symbionts of freshwater sponges might potentially exhibit a similar activity.

COMMUNITY STRUCTURE AND DIVERSITY OF BACTERIA SYMBIONT IN MARINE SPONGES RELATES TO ANTIBACTERIAL PRODUCTIONS

Altuğ et al. (2021) reported two different structures of bacterial communities from two different sponges collected from the Aegean and Marmara seas. Sponges collected from the Aegean seas were consisted of *Sarcotragus* sp., *Cocopongia scalaris*, *Acinella cannabina*, *Ircinia* sp. *Chondrosia reniformis*, *Agelas oroides*, *Sarcotragus spinosulus*, *Scalarispongia scalaris*, *Crambe crambe*, *Chondrosia reniformis*, *Aplysina aerophoba*, *Petrocia fisciformis*, while sponges collected from the sea of Marmara were consisted of *Ciocalypta penicillus*, *Ficulina ficus*, *Dictyonella plicatta*, *Haliclona mediterranea*, *Rapailia* sp., and *Hymeniacidon perlevis*. The study reported that phylum Proteobacteria (synonym: Pseudomonadota) was a notable microbe symbiont and frequently found among sponge samples from both Aegean and Marmara seas with percentages of 86% and 82% respectively. Furthermore, the percentage of phylum Proteobacteria in both seas consists of 30% of class Alphaproteobacteria, 8% of Betaproteobacteria, and 48% of Gammaproteobacteria from the Aegean Sea while the sample from the Marmara Sea only consists of two classes of Proteobacteria, which are 27% Alphaproteobacteria and 55 % of Gammaproteobacteria only. Furthermore, 8% and 18% of class Flavobacteria from phylum Bacteroidota were also recorded. Concurrent with that 6% of the Bacilli class from phylum Bacillota was solely recorded from The Aegean Sea. While the sponge samples show a high abundance of proteobacteria, the water samples show a moderate level of proteobacteria. In this study, Altug et al. (2021) also measured the antibacterial activity of crude sponges' extract. The result showed that the methanol extract of the sponges collected from the Aegean Sea showed stronger antibacterial activity than the samples collected from the sea of Marmara. Therefore, they suggest different environmental conditions obviously effects on antibacterial activity of the sponge and its bacterial symbiont.

A subsequent study by Pires et al. (2020) in Asian waters reported a community structure of bacterial symbionts isolated from several sponges identified as *Aaptos lobata*, *Xestospongia testudinaria*, *Stylissa carteri*, and *Stylissa massa* at Tioman Islands, Malaysia. Phylum Cyanobacteria was recorded as the most abundant symbiont in the *S. carteri*, while Phylum Chloroflexi (synonymized as Chloroflexeota) currently was

abundant in *X. testudinaria* (39%) followed by *A. lobata* (16%). This study also stated that Chloroflexi were commonly found in High Microbial Abundance (HMA) sponges, as it carries out an important role in sponges' diet in converting inorganic to organic carbon. Furthermore, Phylum Actinobacteria (synonymized as Actinomycetota currently) was found to be highly abundant in the *A. lobata* (27%) and *X. testudinaria* (17%). Actinobacteria are prolific antibacterial producers and play an important role in the host's defense mechanisms.

A following study by Retnowati et al. (2021) recorded the community structure of *Callyspongia* sp. from Kepulauan Seribu, Jakarta, Indonesia. *Callyspongia* sp. is a marine sponge species that belong to the order Haplosclerida Topsent, 1928 where a group of freshwater sponges (suborder Spongillina Manconi & Pronzato, 2002, currently invalid suborder rank) was used to be a member of the order Haplosclerida before elevated into order Spongillida Manconi & Pronzato, 2002 that is exclusively group for sponges inhabit the freshwater environment. The metagenomic data shows symbiont of *Callyspongia sp* is consisted of seven phyla with the highest abundance of 82 % Proteobacteria (currently synonymized as Pseudomonadota), followed by 12 % of Acidobacteriota, 2 % of Planctomycetota, 2% of Actinobacteria (currently synonymized as Actinomycetota), 1.08 % of Bacteroidetes (currently synonymized as Bacteroidota), 0.61 % of Firmicutes (currently synonymized as Bacillota), and 0.09% of Cyanobacteria.

Furthermore, the dominant abundance of Proteobacteria was noted and mentioned as a common occurrence in Low Microbial Abundance (LMA) Sponges (Giles et al. 2013). Moreover, among those studies on the Aegean Sea, Marmara Sea, Tioman Island Malaysia, and Kepulauan Seribu, Jakarta Indonesia shows that Proteobacteria are one of the most important phyla of marine sponges' symbionts, corroborate Proteobacteria as symbionts carry out and possess various crucial functions such as nitrogen fixation, host defense mechanism, and nitrification process (Mohamed et al. 2010). Likewise, the transcriptomic data from Moitinho-Silva et al. (2016) revealed that one genome bins namely "Cc Phy" from the family Phyllobacteriaceae from Proteobacteria involve metabolic production, synthesized between sponge *Cymbastela concentrica* –microbe symbiosis, besides other genome bins 'CcThau' and "CcNi" produced by the sponge and genus Nitrospira of bacterium and order Nitrosopumilales of thaumarchaeal respectively.

COMMUNITY STRUCTURE AND DIVERSITY OF BACTERIA SYMBIONT IN FRESHWATER SPONGES

In contrast to symbionts of marine sponges, the community structure of bacterial symbionts in the freshwater sponge is overlooked. For this reason, it results in a lack of information on "antibiotic-like substances" discovered from bacterial symbionts of freshwater sponges. An example of metagenomic data of *Ephydatia fluviatilis*, a cosmopolite freshwater sponge from the Netherlands (Costa et al. 2013), shows some bacterial phyla TM7 and BLUT were absent in the water. But it was found in the sponge with a substantial proportion of 22% and 9.1% respectively. It was reported that sequences from the Chlamydia phylum were present in a low abundance of 1.5% in the sponge but absent in the water. Furthermore, some noticeable differences in the abundance of certain phyla were also recorded that a higher abundance of Actinobacteria (40.9%) and Bacteroidetes (15.4%) than in the sponge sample (12.1% and 9.8% respectively). Together, despite the similar abundance of Proteobacteria phylum in the sponge and water, the domination of class Betaproteobacteria (71%)

and low abundance of Alpha- (24.4%) and Gamma- (2.25%) Proteobacteria were different. It happened because a proportion of Alpha-, Beta-, and Gamma- Proteobacteria were rather equal in a sponge (40%, 22.5%, and 37.5% respectively). Moreover, in the Bacteroidetes phylum, class Sphingobacteria accounts for 100% of the Bacteroidetes in the sponge whereas, Flavobacterium of Bacteroidetes dominated water (65%). The unusual existence of Phylum Chlamydia symbiont in freshwater sponges is comparable to marine sponges for antibacterial properties since Chlamydia mostly possesses a pathogenic character. Dharamshi et al. (2022) discovered two new Families: Candidatus Sororchlamydiaceae fam. Nov and *Candidatus* Parasimkaniaceae fam. Nov in three marine sponges' species *Haliclona* spp., which presumably possess novel natural products.

Graffius et al. (2023) discovered 380 isolates of symbiotic bacteria from freshwater sponges *Spongilla lacustris* that were sampled in Austria and consisted of 197 cultured vs 183 uncultured bacteria. Furthermore, among the 197 cultured symbionts,33 isolates that represented 31 bacteria genera e.g., *Micrococcus* sp., *Streptomyces* sp., *Ensifer* sp., *Roseateles* sp., *Rhizobium* sp., and *Masilia* sp., possess secondary metabolite biosynthesis gene clusters (BGCs). Moreover, the four highest number BGC per genome are two *Streptomyces* isolates SL203 and SL294, *Bacillus* sp. SL112 and *Gordonia* sp SL306 respectively, which reveals those bacteria possess a potential producer of metabolites, which have a wider range of biological effects, including antibacterial, antifungal, and cytotoxic activities.

Clark et al. (2022) isolated 522 symbionts from two specimens of freshwater sponges *Eunapius fragilis* that were sampled from St Lawrence River USA. They utilised another technology which is called Matrix-assisted laser desorption/ionization time-of-flight mass spectrometry (MALDI-TOF MS) and discovered at least four phyla commonly associated with sponges: Proteobacteria, Actinobacteria, Bacteroidetes, and Firmicutes. Among those four phyla, 11 genera e.g., *Paenibacillus*, *Streptomcyces*, *Bacillus*, *Micromonospora*, and *Pseudomonas*, are reported for having potential as bioactive producers, known as Specialized Metabolites (SMs) group.

Sugden et al. (2022) were investigating the microbiome composition of freshwater sponges *Ephydatia muelleri* from three different locations in Canada. They discovered that the composition of sponges' symbionts is Proteobacteria, Bacteriodetes Actinobacteria, Cyanobacteria, Planctomycetes, and Verruromicrobia. However, the most important finding is, the composition of symbionts among three specimens in all locations are significantly different, which is obviously influenced by geographical location and habitat.

Investigation on Actinobacteria reported that order Acidimicrobiales has become the most common symbionts in *E. fluviatilis* that might possess antibiotic and cytotoxic properties (Keller-Costa et al. 2014). This order also possesses the ability to oxidize or reduce iron and oxidize sulfur. The data also shows a common ribotype of *Pseudomonas* shared across four *E. fluviatilis* specimens. *Pseudomonas* has previously been reported for their ability to produce secondary metabolites, therefore further study regarding the ribotype may result in a better understanding of the ecological role of *Pseudomonas* in this symbiotic relationship.

Laport et al. (2019) showed the metagenomic data of other species of freshwater sponge *Tubella variabilis* from Pernambuco, Brazil. The study reported a higher OTU richness in sponges (3762 – 4709OTUs) than in surrounding waters (3419 – 3522). The majority of discovered phyla were Proteobacteria, Verrucomicrobia, and Cyanobacteria, whereas 39 phyla and candidate phyla were reported as a minor abundance. Fur-

thermore, Proteobacteria were discovered in great abundance in both sponges (60 – 82%) and water (85-89%). Despite a high abundance of Proteobacteria, dissimilarity among classes between sponge and water was recorded as Betaproteobacteria was dominant in the sponge, while water was dominated by Alphaproteobacteria. At the same time, a significant difference was also observed for phylum Bacteroidetes, in which abundance in sponges was significantly higher compared to water samples. Furthermore, class Cytophagia, which is a member of Bacteroidetes was reported to be a hundred times higher in sponge water samples.

Seo et al. (2016) recorded the community structure of three freshwater sponge species in Lake Baikal, Rusia, *Lubomirska baicalensis*, *Baikalospongia intermedia*, and *Swartschewskia papyracea*. Six bacterial phyla can be found among the samples, which were Cyanobacteria, Proteobacteria, Actinobacteria, Bacteroidetes, Planctomycetes, and Verrucomicrobia. Cyanobacteria were found to be the most abundant in all sponges with the highest value found in *B. intermedia* (78%), *L. baicalensis* (70%), and *S. papyracea* (43%). Furthermore, Cyanobacteria discovered in those three samples were dominated by the genus *Prochlorococcus*. However, it should be noted that *Prochlorococcus marinus* can only be found in *S. papyracea* while symbiont from phylum actinobacteria was also found in a higher abundance in *S. papyracea*.

Kumar et al. (2020) reported a diversity of microbe symbionts on freshwater sponge *Spongilla* sp. and marine sponges *Ciocalypta* sp. from a wetland ecosystem in Gujarat, India. They recorded bacterial symbionts from various phyla such as Actinobacteria, Firmicutes, Chloroflexi, Planctomycetes, Acidobacteria, and Gemmatimonodetes as well as a few candidates' phyla such as BRC1, GN02, GN04, H-178, KSB3, NKB19, OD1, OP8, SR1, TM6, TM7, WPS2, WS1, WS3, WS4, WWE1, and ZB31. Proteobacteria were recorded as the most abundant phyla in both sponges despite different compositions for marine sponges *Ciocalypta* sp. was dominated by Alpha-, Beta-, and Gammaproteobaceria class, while in freshwater sponges *Spongilla* sp. Delta-, and Epsilonproteobacteria were the dominant class.

In another study by Gaikwad et al. (2016) in India, metagenomic data of freshwater sponge *Eunapius carteri* and *Corvospongilla lapidosa* symbionts in lake Talegaon Dabhade and Pashan respectively were discovered. The study reported a difference in community structure in sponge and water, in which sponge samples possess the highest abundance in the Firmicutes phylum and are followed by proteobacteria. Furthermore, the highest abundance of OTU belonged to the genus *Clostridium* (50.3%) followed by *Synechococcus* (8.67%). At the same time, there are also OTUs that are exclusively found in sponges such as *Acinetobacter*, *Vogesella*, and *Rhizobiales*. Those reported data in contrast to the community structure of water because, the highest OTU symbiont in a sponge, genus *Clostridium* is absent in water, which the disparity of abundance infers heritability factor in symbiont's related to hosting specificity and community structure. The capability of *Clostridium* to utilize *a* sponge extracellular matrix that is rich in glycoproteins, proteoglycans, spongin, and other organic substances might also allow the sponge to achieve a high abundance of OTU. Moreover, some members of the *Clostridium* are known to be able to do fermentation and exhibit antibacterial activity when cultured with *Pseudomonas* and *E. coli*.

HOST SPECIFICITY AND SYMBIONT RELATIONSHIP ON SYNTHESISING ANTIBACTERIAL PROPERTIES

Once discussing sponge symbionts, host specificity plays a huge role in

the community structure of symbionts in Figure 1 (Carrier et al. 2022). It is important that symbionts are a genealogical factor in sponges. Therefore, the sponge may have a unique community structure of symbiont, i.e., lateral gene transfers of symbionts living in mesohyl occur through a pathway when the sponge embryo is brooded or developed externally. Furthermore, oocytes of sponges obtain symbionts by directly engulfing them or through the help of nurse cells. When the nurse cells acquire symbionts, they transfer symbionts via a cytoplasmic bridge or phagocytosed by the oocyte. Alternatively, the brooded embryos may obtain symbionts from two pathways, infiltration of the follicle or nurse cells containing symbionts through cleavage furrows, or direct infiltration of the symbiont through the space between follicles. Moreover, while recruiting symbiotic bacteria from ambient water, epithelial cells of the sponge assist free-living bacteria from surroundings water to adhere to its surface and enter sponge mesohyl forming a pocket-like structure.

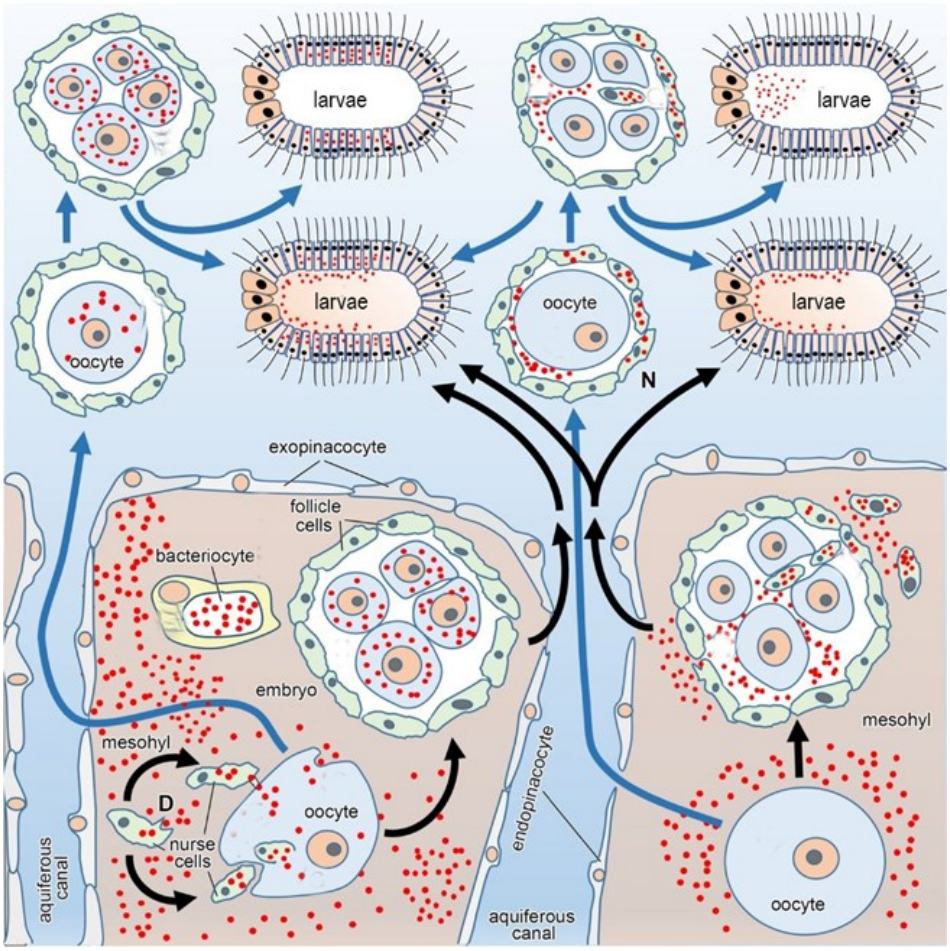

Figure 1. A modified schematic diagram from the study and permission of copyright from Carrier et al. (2022) explains two pathways of symbionts through vertical transfer, which make sponges possess a unique community structure of bacterial symbiont from the surrounding water. Sponge mesohyl's or bacteriocytes were inhabited freely by microbes (red dots) occur transmitted from mother to offspring (black arrows) or develop externally (blue arrows).

Host specificity of symbionts is a crucial factor in linking sponge symbiont–derived compounds productions. It specifically refers to which sponge should discover for obtaining a certain symbiont. Sponge symbiont has been previously explored for various properties as they have exhibited. A study by Sirpu Natesh et al. (2018) shows the anticancer properties of *Bacillus subtilis* isolated from the marine sponge *Clathria frondifera* through activation of the caspase-3 protein in the human breast can-

cer cell line. Another study by Schmidt et al. (2000) recorded the antifungal activity of the symbionts from the marine sponge *Theonela swinhoei*. These symbionts contain a novel peptide, recognised as "Theopalaumide" and have been proposed to be classified as *Entotheonella palauensis* as a subdivision of Gammaproteobacteria. Furthermore, Kaluzhnaya et al. (2012) recorded the activity of symbionts from the freshwater sponge *Lubomirskia baicalensis* in producing Non-Ribosomal Peptide Synthase (NRPS) and Polyketide Synthase (PKS). Moreover, it was recorded that symbionts from the phylum Cyanobacteria produce PKS I, while symbionts from the phyla Proteobacteria and Cyanobacteria produce NRPS/PKS hybrid. The abundance of bioactive compounds should be considered since sponge symbionts have exhibited antibacterial and antifungal properties i.e., productions of antibacterial compounds commonly utilize bacteria from Actinobacteria phylum, as well as bacteria from Genus Bacillus and Pseudomonas because those bacteria are exhibited antibacterial properties (Dita et al. 2017; Lee 2020)

POTENCY OF BACTERIAL SYMBIONTS FROM FRESHWATER SPONGES IN INDONESIA

While marine sponge has been studied extensively regarding the community structure of the symbionts and the antibacterial compounds produced by the symbionts, the study of freshwater sponge symbionts either regarding the community structure or the antibacterial compounds producing is overlooked. Therefore, only a minor data on the metagenomic study of freshwater sponge microbiome or symbiotic microbe and a lack of data from freshwater sponges in Indonesia. For this reason, the first step is performing metagenomic analysis or symbionts profiling of the identified freshwater sponges from Indonesia. Currently, The WPD listed 14 species of freshwater sponges that are recorded in Indonesia (Manconi et al. 2013; de Voogd et al. 2023). Two species from families Metaniidae Volkmer-Ribeiro, 1986; *Metania pottsi* (Weltner, 1895), *Metania vesparium* (Martens, 1868) recorded in Borneo, followed by 11 species of Family Spongillidae Gray, 1867. Those are *Stratospongilla sumatrana* (Weber, 1890) that are recorded from Sumatra Island, *Ephydatia fortis* Weltner, 1895, *Ephydatia ramsayi* (Haswell, 1883) *Radiospongilla cerebellata* (Bowerbank, 1863), *Radiospongilla crateriformis* (Potts, 1882), *Radiospongilla indica* (Annandale, 1907), *Trochospongilla latouchiana* Annandale, 1907 *Umborotula bogorensis* (Weber, 1890), *Eunapius carteri* (Bowerbank, 1863) recorded Java Province, *Nudospongilla vasta* (Weltner, 1901) from Sulawesi, and *Rosulaspongilla alba* (Carter, 1849) from Bali. Another two species from two different families were additionally added currently, which are *Pachydictyum globosum* (Weltner, 1901) recorded in Sulawesi (Meixner et al. 2007) and *Oncosclera asiatica* Manconi & Ruengsawang, 2012 recorded in Java, Figure 2 (Setiawan et al. 2023) from the family Malawispongiidae Manconi & Pronzato, 2002 and Potamolepidae Brien, 1967 respectively.

Furthermore, there is few culturable sponges' symbionts and can be processed by a culture-dependent test to screen the symbionts. Finally, we should identify the antibacterial compounds from the culture in which this step is applicable for sponge study in general. Many of the recorded symbionts that previously exhibited antibacterial activity were only reported as cell extract or culture extract. Simple productions by fermentation are the first cornerstone in the sponge–symbiont-derived technology. For the next step, it could be multiple routes that can be explored. The first route is the co-culture route, as some symbionts could have a

higher yield of antibacterial compounds. Kanagasabhapathy and Nagata S (2008) reported a higher antibacterial activity of epibiotic bacteria isolated from marine sponges *Pseudoceratina purpurea* when cross-cultured with pathogenic bacteria *Staphylococcus aureus* and *Bacillus licheniformis*. It was deduced that the higher antibacterial activity is induced by quorum sensing as chemical signals for competitive bacteria resulting in higher production of antibacterial substances.

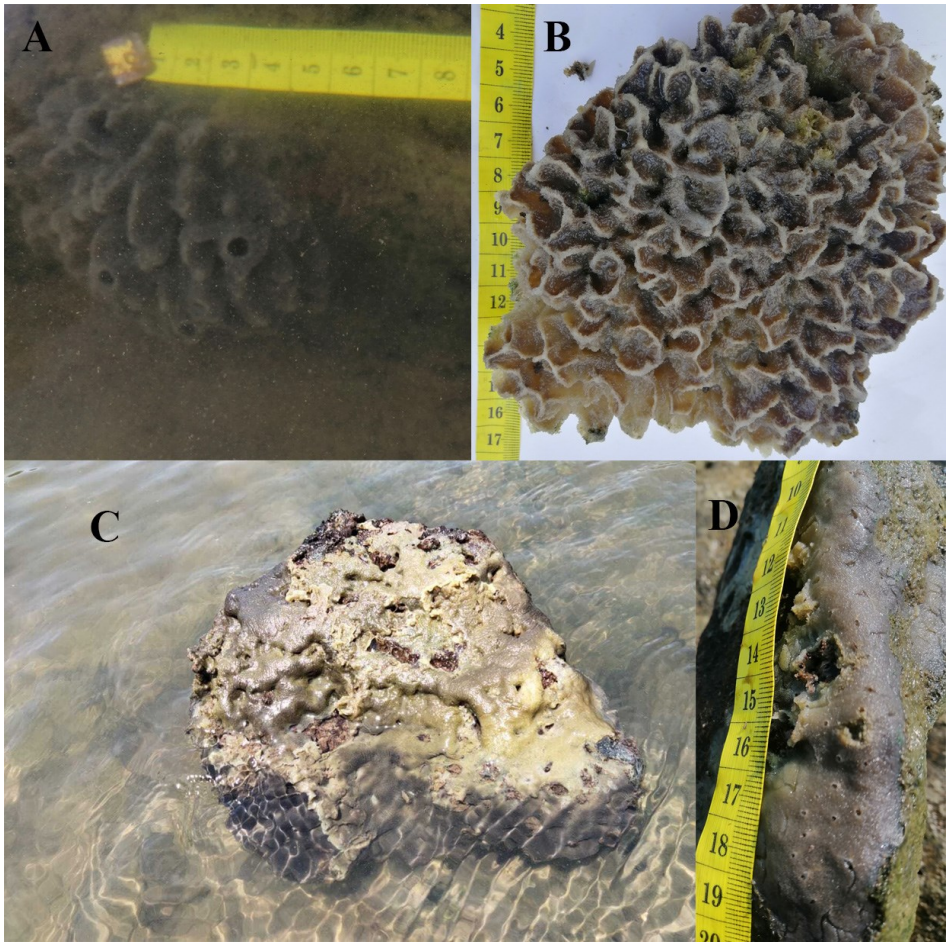

Figure 2. A & B., Specimen of *Eunapius carteri*, a cosmopolite freshwater sponges' species, and C & D, *Oncosclera asiatica*, which currently reported inhabiting part of Porong river, East Java, Indonesia (Setiawan et al. 2023)

An antagonistic assay is a further approach besides the cross-culture method where instead of a cooperative relationship between one symbiont and another, a competitive relationship between symbionts is detected. This process aims to screen symbionts with the highest antibacterial activity, which can be used as a donor for genetic modification. An example of this process can be observed in a study by Riyanti et al. (2020) (Figure 3). They reported symbionts from 10 species of marine sponges from Sangihe islands, North Sulawesi, Indonesia, for antibacterial activity screening. Symbionts of these samples are selected through a few screenings for antibacterial activity. In this step, isolated symbionts that consisted of 12 genera were present, which covers two third of the strains belonged to Bacillus (66.7%), followed by Pseudomonas (6.5%), Staphylococcus (5.6%), Lysinibacillus (4.6%), and Solwaraspora (3.7%), were cross cultured with two pathogen species of bacteria: the gram-negative *E. coli*, and the gram-positive *Micrococcus luteus*. After 48 hours of incubation, those identified and isolated symbionts show a clear zone, and furthermore determined as "active" produce antibacterial activity. Among 835 isolates, only 108 isolates (12%) exhibited antibacterial activity. Further-

Table 1. Sponge symbionts and their antibacterial compounds.

Bacterial Symbiont	Phylum	Host sponge	Habitat	Produced Antibacterial Compound	Note	References
Micrococcus luteus	Actinomycetota	*Xestospongia* sp.	Marine	Lutoside	Exhibits antibacterial activity to *Staphylococcus aureus*, *Vibrio anguilarum*, and *Candida albicans*	(Bultel-Poncé et al. 1998)
Brevibacterium sp.		*Callyspongia* sp.	Marine	Phenazine-carboxamide 1,6-phenazine-dimethanol	Exhibits activity against *Enterococcus hirae* and *Micrococcus luteus*	(Choi et al. 2009)
Streptomyces sp. Actinomycetota		*Baikalo-spongia bacilifera*	Fresh water	Variapeptin	Exhibits antibacterial activity against *Staphylococcus aureus*, *Escherichia coli, and Candida albicans*	(Axenov-Gribanov et al. 2016)
Pseudonocardia sp.				Culture extracts	Exhibits antibacterial activity against *Staphylococcus aureus*, *Escherichia coli*, and *Staphylococcus carnosus*	
Janibacter limnosus		*Lubomirska baicalensis*	Fresh water	Helquinoline	Exhibits activity against *Streptomyces viridochromogenes, Staphylococcus aureus, Mucor miehei, Chlorella vulgaris, Chlorella sorokiniana, and Scenedesmus subspicatus*	(Kaluzhnaya et al. 2021)
Rathayibacter sp.				Tunica-minyluracil	Exhibits potent activity against gram-positive bacteria, especially species of *Bacillus.*	
Janthinobacterium sp.	Pseudomonadota	*Lubomirska baicalensis*	Fresh water	Violacein	Exhibits activity against gram-positive bacteria increases cell permeability followed by rupture of cytoplasmic membrane	(Belikov et al. 2021)
Bacillus sp	Bacillota	*Metania reticulata*	Fresh water	Cyclosporin A	Exhibits activity against gram-positive bacteria *Staphylococcus aureus* and fungus *Aspergillus* sp.	(Rozas et al. 2015)

more, among 108 isolates, only 4.6% show activity against *E. coli*, 78.7% show activity against *M. luteus*, and 16.7% show activity against both *E. coli and M. luteus*. Despite combination competition assay revealed the highest antibacterial activity (*Bacillus* sp.), producing compounds like surfactin. However, this method is only applicable for culturable bacteria.

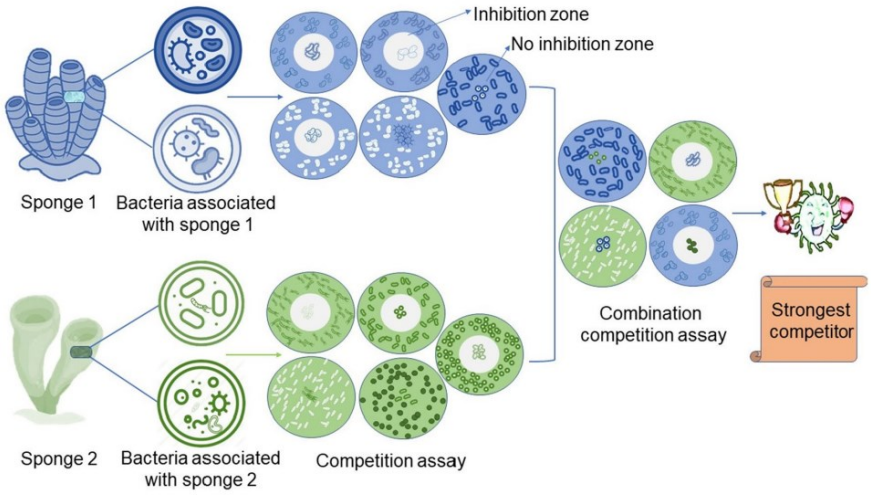

Figure 3. The diagram of the methodology from the permitted copyright of Riyanti et al. (2020) is to cross-culture symbionts and to determine the highest activity and most potent antibacterial property.

A further alternative is utilising genetic modification tools. After the identification of an antibacterial substance. We could observe which proteins have roles for producing the potential antibacterial compound. The gene of interest could select and insert into a vector. Furthermore, the inserted vector is transformed into host *E. coli*. Moreover, it would increase the production of antibacterial substances.

POTENTIAL SYMBIONTS OF BACTERIA

Actinobacteria: a diverse multipotential symbiont

Actinobacteria are one of the most known phyla for their ability to produce bioactive compounds. The compounds produced by bacteria have been recorded as possessing antibacterial, antifungal, antiparasitic, antimalarial, immunomodulatory, antioxidant, and even anticancer properties (Mayer & Hamann 2005; Bull & Stach 2007; Pimentel-Elardo et al. 2010; Blunt et al. 2018). Compounds produced by actinobacteria include polyketides, alkaloids, fatty acids, peptides, and terpenes. Several investigations on sponge-derived actinobacterial products i.e., the antibacterial activity of sponge actinobacterial symbiont from either marine or freshwater environments can be listed in the following Table 1. Two examples of marine sponges, *Xestospongia and Callyspongia* have been recorded to host actinobacteria with antibacterial properties. *Xestospongia* and *Callyspongia* were members of the order Haplosclerida, where freshwater sponges were previously assigned to a sub-order Sponggilina (disused and unaccepted rank currently, see World Porifera Database in Manconi & Pronzato 2002) as a member of order Haplosclerida. Currently, freshwater sponges have been established and elevated as ranked into order Spongillida (Morrow & Cárdenas 2015; de Voogd et al. 2023) despite the fact that Spongillida and Haplosclerida are phylogenetically shared a closely related Actinobacteria – derived antibacterial compounds, in which those compounds have been recorded to be highly effective against gram-positive bacteria (Cartwright et al. 2020). At the same

time, almost every compound presented in freshwater sponges in the Table 1 has exhibited a potential activity against *Staphylococcus* bacteria. The potential antibacterial activity against gram-positive pathogenic bacteria also exhibits the importance of biofilm prevention. Conjugation in gram-positive bacteria requires cell-to-cell contact. This conjugation commonly transfers resistant genes, therefore by preventing cell-to-cell contact, bacteria susceptibility to antibacterial compounds is conserved.

In freshwater sponges, two examples from endemic species of Baikal Lake Rusia, have been explored on having symbiotic microbe possessing antibacterial potency. First, isolates of *Streptomyces* sp. from *Baikalospongia bacilifera* is producing Variapeptin, which is like the antibacterial activity of Azinothricin family and shown to inhibit the growth of numerous gram-positive bacteria, but not gram-negative or fungus (Axenov-Gribanov et al. 2016). Second, three bacterial symbionts of another freshwater sponges from Baikal Lake Rusia, *Lubomirska baicalensis* are reported to have the ability to produce secondary metabolites that are important for antibacterial compounds (Kaluzhnaya et al. 2021). Those compounds are Helquinoline which exhibits high antibacterial and antifungal activity from the *Janibacter limosus*. Furthermore, *Rathayibacter* on producing Tunicaminyluracil antibiotics.

Pseudomonas: the most ubiquitous symbiont

Pseudomonas is a genus of the proteobacteria phylum (Gammaproteobacteria) that can be found in as symbionts in marine and freshwater sponges with a range of moderate to high abundance and possess a potential producer as a source of antibacterial compounds. A study by Keller-Costa et al. (2014) on freshwater sponge *Ephydatia fluviatilis* recorded the antibacterial activity of various *Pseudomonas* symbionts against common human pathogens such as *Bacillus subtilis*, which also reported showing anti-biofilm properties. Pseudomonas can produce compounds in the phenazine group. The metabolism of phenazine is regulated by the *Phz* gene cluster (*Phz A, B, C, D, E, F, G*). Depending on which gene takes part in the regulation, there are four main products of phenazine metabolism: Phenazine (PHZ), Pyocyanin (PYO), Phenazine-1-carboxamide (PCN), and Phenazine-1,6-dicarboxylic acid (PCD). The production of phenazine is affected by extracellular signals, as for symbiotic Pseudomonas, these extracellular signals are a means of communication with the sponge host. The signals are received by the GacA/ GacS protein complex which would start a cascade reaction with the Rsm protein group (Bilal et al. 2017). The method of action of the Phenazine compound group is to induce a cellular redox reaction. When Phenazine is introduced to the cell, it would penetrate the cell wall and infiltrate the mitochondria. In the mitochondria, Phenazine would act as an electron acceptor, forming the O^{2-} and $ONOO^{-}$ superoxide. These oxides are highly radical and may damage the cell's organelles (Briard et al. 2015). Moreover, another compound called Violacein isolated from symbiotic bacteria *Janthinobacterium sp* is reported to be an important antibacterial compound. This symbiont is also isolated from freshwater sponges of Baikal Lake Rusia, *Lubomirska baicalensis* (Kaluzhnaya et al. 2021).

Bacillus: biosurfactant and its broad applications

Bacillus is one of the most versatile bacteria in biosynthesis since it can produce a broad variety of bioactive compounds such as non-ribosomal peptide synthase (NRPS) and Polyketide synthase (PKS) (Prastiyanto et al. 2022). Furthermore, bacillus could also produce compounds with anti-

bacterial properties. According to Rozas et al. (2015) reported the antibacterial activity of *Bacillus* sp. isolated from the Amazonian freshwater sponge *Metania reticulata*. The culture extract exhibits antibacterial activity against *Staphylococcus aureus*, after mass spectroscopy and HPLC analysis, it is concluded that the compounds producing this bactericidal effect were similar in structure to Cyclosporin A. Cyclosporine is produced by Cyclosporin synthase (CySyn). It is made from D-alanine, (4R)-4-[(E)-2-butyl]-4-methyl-l-threonine (Bmt), and L-2-aminobutyric acid) (see detail Lawen 2015). First D-alanine is activated, then delineated from the sequence of the *sim A* gene. This delineation opens an open reading frame that would be translated into Cyclosporine A. Cyclosporine A antibacterial activity was due to its ability to inhibit cell wall synthesis. Cyclosporine would bind with cyclophilin creating a protein complex, this complex would then bind with Calcineurin which prevents dephosphorylation of the lipid carrier in the cell wall synthesis (Masaki & Shimada 2022).

CONCLUSIONS

The diversity study of freshwater sponges in Indonesia is overlooked, which made a lack of data on symbiotic bacteria from the region. Nevertheless, symbionts' potency that possesses antibacterial properties can be predicted and mapped by comparing the composition of the sponges that are recorded in Indonesia to similar species in another region e.g., *Eunapius carteri* and *Spongilla* sp., from India. Currently, studies on symbionts of freshwater sponges are mapping the diversity, and groups of Actinomycete, Proteobacteria, and Firmicutes, have been recognised as possessing potential antibacterial compounds. Moreover, identification, followed by synthesising antibacterial compounds produced by Indonesian freshwater sponges is needed, since most of described antibacterial compounds e.g., Helquinoline and Violacein are mostly described from Russian freshwater area at Baikal Lake. At the same time, differences in geographical habitat despite similar freshwater sponges' species influence the discrepancy of symbionts' composition, and obviously, a bioactive compound produced by the symbionts.

AUTHOR CONTRIBUTION

M.E, ES & A.B designed research on reviewing literature process, analysed data and wrote manuscripts. N.A, E.P, C.R, D.W, suggested on improvement on every important aspect related on manuscript.

ACKNOWLEDGMENTS

The authors gratefully acknowledged financial support from the Institut Teknologi Sepuluh Nopember for this work, under the project scheme of the Publication Writing and IPR Incentive Program (PPHKI) 2023. This work is also a part of Program Penelitian Kolaborasi Indonesia (PPKI) PTNBH 2020 that involves the Directorate of Research and Community Service (DPRM) at the Institut Teknologi Sepuluh Nopember Surabaya, Universitas Diponegoro Semarang, and Institut Teknologi Bandung for the consortium grant schemed as number 952/PKS/ITS/2020, 193.03/UN7.6.1/PP2020, and 069/I1. B04.1/SPP-LPPM/III/2020. Likewise, we also acknowledged authors whose copyright figures are allowed and permitted to be used in this manuscript and three anonymous reviewers who contribute to suggesting, criticizing, and improving the quality of this manuscript.

CONFLICT OF INTEREST

There is no conflict of interest among authors on this mini-review paper.

REFERENCES

Altuğ, G. et al., 2021. The distribution and antibacterial activity of marine sponge-associated bacteria in the aegean sea and the sea of Marmara, Turkey. *Current Microbiology*, 78(6), pp.2275-2290. doi: 10.1007/s00284-021-02489-7

Asagabaldan, M.A. et al., 2017. Identification and antibacterial activity of bacteria isolated from marine sponge *Haliclona* (*Reniera*) sp. against Multi-Drug Resistant Human Pathogen. *IOP Conference Series: Earth and Environmental Science*, 55, 012019. doi: 10.1088/1755-1315/55/1/012019

Axenov-Gribanov, D. et al., 2016. The isolation and characterization of actinobacteria from dominant benthic macroinvertebrates endemic to Lake Baikal. *Folia Microbiol (Praha)*, 61(2), pp.159-168. doi: 10.1007/s12223-015-0421-z

Belikov, S.I. et al., 2021. Genome analysis of the *Janthinobacterium* sp. Strain SLB01 from the diseased sponge of the *Lubomirskia baicalensis*. *Current Issues in Molecular Biology*, 43(3), pp.2220-2237. doi: 10.3390/cimb43030156

Bibi, F. et al., 2017. Bacteria from marine sponges: a source of new drugs. *Current Drug Metabolism*, 18(1), pp.11-15. doi: 10.2174/1389200217666161013090610

Bilal, M. et al., 2017. Engineering *Pseudomonas* for phenazine biosynthesis, regulation, and biotechnological applications: a review. *World Journal of Microbiology and Biotechnology*, 33(10), pp.191. doi: 10.1007/s11274-017-2356-9

Blunt, J.W. et al., 2018. Marine natural products. *Natural product reports*, 35(1), pp.8-53. doi: 10.1039/c7np00052a.

Briard, B. et al., 2015. *Pseudomonas aeruginosa* manipulates redox and iron homeostasis of its microbiota partner *Aspergillus fumigatus* via phenazines. *Sci Rep*, 5, 8220. doi: 10.1038/srep08220

Bull, A.T., Stach, J.E., 2007. Marine actinobacteria: new opportunities for natural product search and discovery. *Trends in Microbiology*, 15 (11), pp.491-499. doi: 10.1016/j.tim.2007.10.004

Bultel-Poncé, V.V. et al., 1998. Metabolites from the sponge-associated bacterium *Micrococcus luteus*. *J Mar Biotechnol*, 6, 233-236.

Carrier, T.J. et al., 2022. Symbiont transmission in marine sponges: reproduction, development, and metamorphosis. *BMC Biology*, 20(1), 100. doi: 10.1186/s12915-022-01291-6

Cartwright, A. et al., 2020. Effects of freshwater sponge *Ephydatia fluviatilis* on conjugative transfer of antimicrobial resistance in *Enterococcus faecalis* strains in aquatic environments. *Letters in Applied Microbiology*, 71(1), pp.39-45. doi: 10.1111/lam.13310

Choi, E.J. et al., 2009. 6-Hydroxymethyl-1-phenazine-carboxamide and 1,6-phenazinedimethanol from a marine bacterium, *Brevibacterium* sp. KMD 003, associated with marine purple vase sponge. *J Antibiot (Tokyo)*, 62(11), pp.621-624. doi: 10.1038/ja.2009.92

Cita, Y.P. et al., 2017. Antibacterial activity of marine bacteria isolated from sponge *Xestospongia testudinaria* from Sorong, Papua. *Asian Pacific Journal of Tropical Biomedicine*, 7(5), pp.450-454. doi: 10.1016/j.apjtb.2017.01.024

Clark, C.M. et al., 2022. Relationship between bacterial phylotype and specialized metabolite production in the culturable microbiome of two freshwater sponges. *ISME Communications*, 2, 22. doi: 10.1038/s43705-022-00105-8

Costa, R. et al., 2013. Evidence for selective bacterial community structuring in the freshwater sponge *Ephydatia fluviatilis*. *Microbial Ecology*, 65(1), pp.232-244. doi: 10.1007/s00248-012-0102-2

de Voogd, N.J. et al., 2023, 'The World Porifera Database', in *World Porifera Database* viewed 2 February 2023, from https://www.marinespecies.org/porifera/

Dharamshi, J.E., et al., 2022. Genomic diversity and biosynthetic capabilities of sponge-associated chlamydiae. *ISME Journal*, 16(12), pp.2725-2740. doi: 10.1038/s41396-022-01305-9

Dita, S.F., Budiarti, S. & Lestari, L., 2017. Sponge-associated actinobacteria: Morphological character and antibacterial activity against pathogenic bacteria. *Jurnal Sumberdaya Hayati*, 3(1), pp.21-26. doi: 10.29244/jsdh.3.1.21-26

Fieseler, L. et al., 2004. Discovery of the novel candidate phylum "Poribacteria" in marine sponges. *Appl Environ Microbiol*, 70(6), pp.3724-3732. doi: 10.1128/aem.70.6.3724-3732.2004

Gaikwad, S., Shouche, Y.S. & Gade, W.N., 2016. Microbial community structure of two freshwater sponges using illumina miseq sequencing revealed high microbial diversity. *AMB Express*, 6, 40. doi: 10.1186/s13568-016-0211-2

Giles, E.C. et al., 2013. Bacterial community profiles in low microbial abundance sponges. *FEMS Microbiol Ecol*, 83(1), pp.232-241. doi: 10.1111/j.1574-6941.2012.01467.x

Graffius, S. et al., 2023. Secondary metabolite production otential in a microbiome of the freshwater sponge *Spongilla lacustris*. *Microbiology Spectrum*, 11(2), e04353-22. doi:10.1128/spectrum.04353-22

Grant, R.E., 1836. Animal Kingdom. In *The cyclopaedia of anatomy and physiology*. London: Sherwood, Gilbert, and Piper. pp.107-118.

Hentschel, U. et al., 2003. Microbial diversity of marine sponges. *Prog Mol Subcell Biol*, 37, pp.59-88. doi: 10.1007/978-3-642-55519-0_3.

Joseph, F.R.S., Iniyan, A.M. & Vincent, S.G.P., 2017. HR-LC-MS based analysis of two antibacterial metabolites from a marine sponge symbiont *Streptomyces pharmamarensis* ICN40. *Microb Pathog*, 111, pp.450-457. doi: 10.1016/j.micpath.2017.09.033

Kaluzhnaya, O.V., Lipko, I. & Itskovich, V., 2021. PCR-screening of bacterial strains isolated from the microbiome of the *Lubomirskia baicalensis* sponge for the presence of secondary metabolite synthesis genes. *Limnology and Freshwater Biology*, 4(2), pp.1137-1142. doi: 10.31951/2658-3518-2021-A-2-1137

Kaluzhnaya, O.V., Kulakova, N.V., Itskovich, V.B., 2012. Diversity of Polyketide Synthase (PKS) genes in metagenomic community of freshwater sponge *Lubomirskia baicalensis*. *Molecular Biology*, 46(6), pp.790-795. doi: 10.1134/S002689331206009X

Kanagasabhapathy, M., Nagata, S., 2008. Cross-species induction of antibacterial activity produced by epibiotic bacteria isolated from Indian marine sponge *Pseudoceratina purpurea*. *World Journal of Microbiology and Biotechnology*, 24(5), pp.687-691. doi: 10.1007/s11274-007-9525-1

Keller-Costa, T. et al., 2014. The freshwater sponge *Ephydatia fluviatilis* harbours diverse *Pseudomonas* species (Gammaproteobacteria, Pseudomonadales) with broad-spectrum antimicrobial activity. *PLOS ONE*, 9(2), e88429. doi: 10.1371/journal.pone.0088429

Kumar, G. et al., 2020. Bacterial communities of sponges from the wetland ecosystem of Little Rann of Kutch, India with particular reference to Planctomycetes. *3 Biotech*, 10(11), pp.1-10. doi: 10.1007/s13205-020-02449-1

Laport, M.S., Pinheiro, U., Rachid, C.T.C.d.C., 2019. Freshwater sponge *Tubella variabilis* presents richer microbiota than marine sponge species. *Frontiers in Microbiology*, 10, 2799. doi: 10.3389/fmicb.2019.02799

Lawen, A., 2015 Biosynthesis of cyclosporins and other natural peptidyl prolyl cis/trans isomerase inhibitors. *Biochim Biophys Acta*, 1850 (10), pp.2111-2120. doi: 10.1016/j.bbagen.2014.12.009

Lee, N.M., 2020. *Biotechnological Applications of Extremophilic Microorganisms*, Germany: Walter de Gruyter GmbH & Co KG.

Manconi, R. & Pronzato, R., 2002. Suborder Spongillina subord. nov.: Freshwater sponges. In *Systema Porifera: A guide to the classification of sponges*. Kluwer Academic/ Plenum Publishers, New York, Boston, Dordrecht, London, Moscow, pp.921-1020.

Manconi, R. et al., 2013. Biodiversity in South East Asia: an overview of freshwater sponges (Porifera: Demospongiae: Spongillina). *Journal of Limnology*, 72(s2), pp.15. doi: 10.4081/jlimnol.2013.s2.e15

Masaki, T. & Shimada, M., 2022. Decoding the Phosphatase Code: Regulation of Cell Proliferation by Calcineurin. *International Journal of Molecular Sciences*, 23(3), 1122. doi: 10.3390/ijms23031122

Mayer, A.M. & Hamann, M.T., 2005.Marine pharmacology in 2001–2002: marine compounds with anthelmintic, antibacterial, anticoagulant, antidiabetic, antifungal, anti-inflammatory, antimalarial, antiplatelet, antiprotozoal, antituberculosis, and antiviral activities; affecting the cardiovascular, immune and nervous systems and other miscellaneous mechanisms of action. *Comp Biochem Physiol C Toxicol Pharmacol*, 140(3-4), pp.265-286. doi: 10.1016/j.cca.2005.04.004.

Meixner, M.J. et al., 2007. Phylogenetic analysis of freshwater sponges provide evidence for endemism and radiation in ancient lakes. *Molecular Phylogenetics and Evolution*, 45(3), pp.875-886. doi: 10.1016/j.ympev.2007.09.007

Mohamed, N.M. et al., 2010. Diversity of aerobic and anaerobic ammonia -oxidizing bacteria in marine sponges. *The ISME Journal*, 4(1), pp.38-48. doi: 10.1038/ismej.2009.84

Moitinho-Silva, L. et al., 2017. Integrated metabolism in sponge–microbe symbiosis revealed by genome-centered metatranscriptomics. *ISME Journal*, 11, pp.1651–1666. doi: 10.1038/ismej.2017.25

Morrow, C. & Cárdenas, P., 2015. Proposal for a revised classification of the Demospongiae (Porifera). *Frontiers in Zoology*, 12, 7. doi: 10.1186/s12983-015-0099-8

Pimentel-Elardo, S.M. et al., 2010. Anti-Parasitic Compounds from *Streptomyces* sp. strains isolated from Mediterranean sponges. *Marine Drugs*, 8(2), pp.373-380. doi: 10.3390/md8020373

Pires, A.C.d.C. et al., 2020. Bacterial composition and putative functions associated with sponges, sediment and seawater from the Tioman coral reef system, Peninsular Malaysia. *Marine Biology Research*, 16 (10), pp.729-743. doi: 10.1080/17451000.2021.1891250

Prastiyanto, M.E. et al., 2022, Bioprospecting of bacterial symbionts of sponge *Spongia officinalis* from Savu Sea, Indonesia for antibacterial potential against multidrug-resistant bacteria. *Biodiversitas Journal of Biological Diversity*, 23(2), pp.1118-1124 doi: 10.13057/biodiv/d230256

Retnowati, D. et al., 2021. Next-generation sequencing-based Actinobacteria community associated with *Callyspongia* sp. from Kepulauan Seribu Marine National Park, Jakarta, Indonesia. *Biodiversitas Journal of Biological Diversity*, 22(9), pp.3702-3708 doi: 10.13057/biodiv/d220913

Riyanti et al., 2020. Selection of sponge-associated bacteria with high potential for the production of antibacterial compounds. *Scientific Reports*, 10, 19614. doi: 10.1038/s41598-020-76256-2

Rozas, E.E. et al., 2015. Reduction of RBL–2H3 cells degranulation by nitroaromatic compounds from a *Bacillus* strain associated to the Amazonian sponge *Metania reticulata*. *Journal of the Marine Biological Association of the United Kingdom*, 96(2), pp.567-572. doi: 10.1017/S002531541500106X

Schmidt, E.W. et al., 2000. Identification of the antifungal peptide-containing symbiont of the marine sponge *Theonella swinhoei* as a novel δ-proteobacterium, "Candidatus *Entotheonella palauensis*". *Marine Biology*, 136(6), pp.969-977. doi: 10.1007/s002270000273

Seo, E.-Y. et al. 2016., Comparison of bacterial diversity and species composition in three endemic Baikalian sponges. In *Annales de Limnologie-International Journal of Limnology*. EDP Sciences, pp. 27-32

Setiawan, E. et al., 2023. Revisit Study of Freshwater Sponges *Eunapius carteri* (Bowerbank, 1863) and a New Record of *Oncosclera asiatica* Manconi and Ruengsawang, 2012 (Porifera: Spongillida) in Porong River, East Java, Indonesia. *HAYATI Journal of Biosciences*, 30(2), pp.232-245. doi: 10.4308/hjb.30.2.232-245

Sipriyadi, S. et al., 2022. Potential of marine sponge *Jaspis* sp.-associated bacteria as an antimicrobial producer in Enggano Island. *Indonesian Journal of Biotechnology*, 27(3), pp.163-170. doi: 10.22146/ijbiotech.65943

Sirpu, N.N., Arumugam, M. & Karanam, G., 2018. Apoptotic role of marine sponge symbiont *Bacillus subtilis* NMK17 through the activation of caspase-3 in human breast cancer cell line. *Molecular biology reports*, 45(6), pp.2641-2651. doi: 10.1007/s11033-018-4434-y

Skelton, J. & Strand, M., 2013. Trophic ecology of a freshwater sponge (*Spongilla lacustris*) revealed by stable isotope analysis. *Hydrobiologia*, 709(1), pp.227-235. doi: 10.1007/s10750-013-1452-6

Sugden, S. et al., 2022. Microbiome of the freshwater sponge *Ephydatia muelleri* shares compositional and functional similarities with those of marine sponges. *ISME Journal*, 16, pp.2503–2512. doi: 10.1038/s41396-022-01296-7

Suwarno, D. et al., 2013. Past and future trends in nutrient export by 19 rivers to the coastal waters of Indonesia. *Journal of Integrative Environmental Sciences*, 10(1), pp.55-71. doi: 10.1080/1943815X.2013.772902

Unson, M.D., Holland, N.D. & Faulkner, D.J.,1994. A brominated secondary metabolite synthesized by the cyanobacterial symbiont of a marine sponge and accumulation of the crystalline metabolite in the sponge tissue. *Marine Biology*, 119, pp.1-11. doi: 10.1007/BF00350100

Webster, N.S. & Taylor, M.W., 2012. Marine sponges and their microbial symbionts: love and other relationships. *Environ Microbiol*, 14(2), pp.335-346. doi: 10.1111/j.1462-2920.2011.02460.x.

Journal of Tropical Biodiversity and Biotechnology
Volume 09, Issue 01 (2024): jtbb84753
DOI: 10.22146/jtbb.84753

Review Article

Lessons from the Mass Production of Wolbachia-infected *Aedes aegypti* for Egg Release in the Sleman and Bantul Districts of Yogyakarta

Iva Fitriana[1#], Indah Nurhayati[1#], Budi Arianto[1], Defriana Lutfi Chusnaifah[1], Indira Diah Utami[1], Nabhela Ayu Purwaningrum[1], Utari Saraswati[1], Endah Supriyati[1], Adi Utarini[1,2], Riris Andono Ahmad[1,3], Citra Indriani[1,3], Eggi Arguni[1,4*], Warsito Tantowijoyo[1*]

1)World Mosquito Program Yogyakarta, Centre for Tropical Medicine, Faculty of Medicine, Public Health and Nursing, Universitas Gadjah Mada, Yogyakarta, Indonesia, 55281
2)Department of Health Policy and Management, Faculty of Medicine Public Health and Nursing, Universitas Gadjah Mada, Yogyakarta, Indonesia, 55281
3)Department of Biostatistics, Epidemiology and Population Health, Faculty of Medicine, Public Health and Nursing, Universitas Gadjah Mada, Yogyakarta, Indonesia, 55281
4)Department of Child Health, Faculty of Medicine, Public Health and Nursing, Universitas Gadjah Mada, Yogyakarta, Indonesia, 55281
* Corresponding author, email: eggiarguni@ugm.ac.id, warsito.tantowijoyo@gmail.com
# Co-first Author

Keywords:
mass production
production protocol *Aedes aegypti*
*w*Mel Wolbachia
Submitted:
24 May 2023
Accepted:
17 October 2023
Published:
09 February 2024
Editor:
Ardaning Nuriliani

ABSTRACT

An efficacy study on *w*Mel Wolbachia-infected *Aedes aegypti* technology conducted by the World Mosquito Program (WMP) Yogyakarta showed the reducing of dengue incidence in Yogyakarta City. Following this successful result, the intervention was scaled up into two neighbouring districts: Sleman and Bantul. This paper describes our experience in mass production for providing release material for a larger area to reach the deployment target, which includes insectary requirements, mass production protocols, and diagnostic screening. This review may serve as a reference guidance for national mass production for *w*Mel Wolbachia-infected *Ae. aegypti*.

Copyright: © 2024, J. Tropical Biodiversity Biotechnology (CC BY-SA 4.0)

INTRODUCTION

Dengue is still a major public health problem in Indonesia. In the absence of an effective dengue vaccination program, strategies for dengue elimination have relied on vector controls, such as eradication of preadult and adult vectors, chemical control by larvicide and insecticide, and biological control by predators (World Health Organization 2009) The Wolbachia-infected *Aedes aegypti* technology introduced by the World Mosquito Program (WMP) is a novel dengue vector control method that complements the existing vector control methods by blocking effects on DENV replication in the vector to decrease the ability to transmit dengue. In addition, Wolbachia is maternally inherited through the insect egg cytoplasm and therefore will be sustained once after it is established in the natural habitat of *Ae. aegypti*. The WMP project started with a field site in Townsville, Australia, and to date this project has successfully expanded to more than ten countries (Segoli et al. 2014; O'Neill 2018).

The World Mosquito Program (WMP) Yogyakarta started the

project in 2011. Small-scale releases at the subvillage level, which were conducted in 2014 in Sleman and Bantul Districts, showed the successful establishment of the Wolbachia *w*Mel strain in the natural *Ae. aegypti* population (Tantowijoyo et al. 2020). Further efficacy studies in a larger area in Yogyakarta City also showed a decline in dengue incidence by 76-77% and the decline in the rate of hospitalization due to dengue infection by 86% (Indriani et al. 2020; Utarini et al. 2021). Following these promising results, WMP Yogyakarta scaled up the technology to district-wide level in neighbouring districts with the highest reported dengue cases. The strategy of mosquito production shifted from small scale to mass production for increasing the release material supply.

This review describes *w*Mel Wolbachia-infected *Aedes aegypti* mass production based on our experience to supply the requirement for egg release materials for wider areas in Sleman and Bantul Districts. This protocol can serve as a reference guide for other institutions involved in nationwide Wolbachia implementation.

PROTOCOL

Target production based on release area requirement

The size of the target areas for implementation defines the plan for mosquito production. Sleman and Bantul District are the part of Yogyakarta Special Region (Daerah Istimewa Yogyakarta, DI Yogyakarta; Figure 1A). Sleman District is located at 110° 33' 00" east longitude and 7° 34' 51" and 7° 47' 30" south latitude. It has a total area of 574.8 km² and is divided into 17 subdistricts (Figure 1B). There were 13 subdistricts out of the existing 17 subdistricts targeted for release (Figure 1C) due to the high burden of dengue transmission that contributed to 80% of dengue cases in 2017-2019 (official communication with Sleman Health District Office). This area was divided into two release areas: 254.3 km² as the administrative area and 122.94 km² as the residential area. By releasing

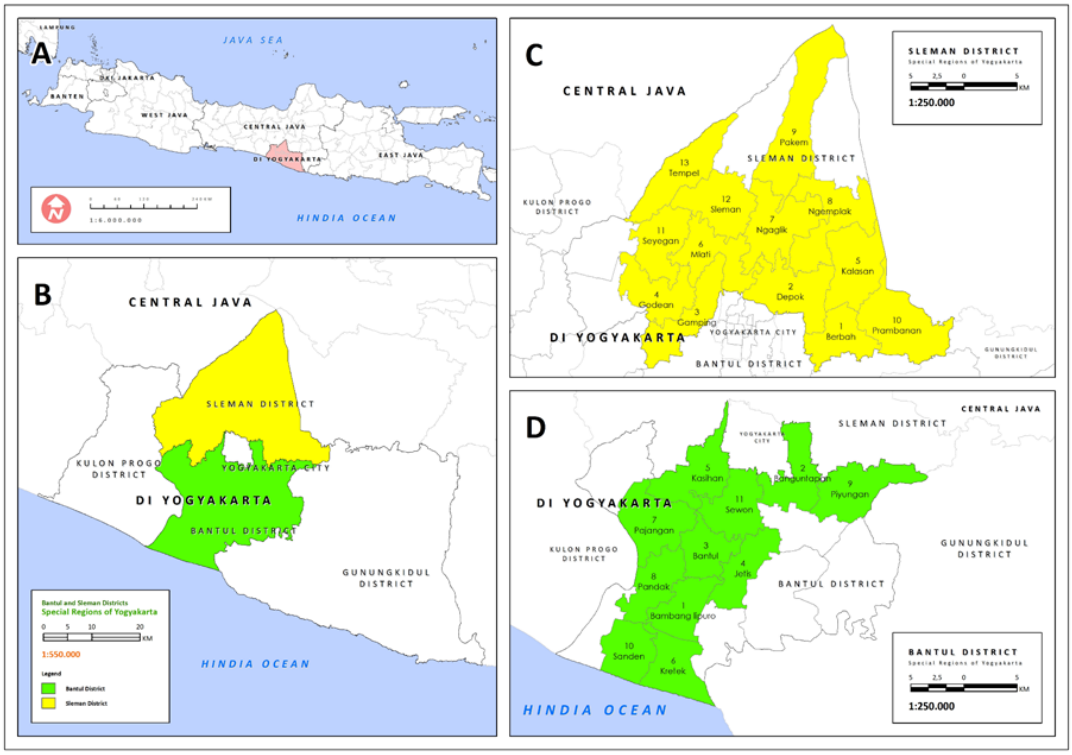

Figure 1. Release sites. A. Map of Yogyakarta Special Region (pink), B. Sleman and Bantul District, C and D. The subdistricts of Sleman District and Bantul District those were chosen for release sites (yellow and green, respectively).

Wolbachia-infected *Ae. aegypti* eggs in egg release containers (ERCs) in residential and public spaces, these areas were provided with 22.322 buckets of ERC within 75x75 m grid squares. A total production of 3 million eggs/per week was required for release, and the release was conducted in approximately 12 biweekly rounds over a six-month period with a target of Wolbachia frequency of over 60% by the end of release period.

Bantul District is located between 110° 12' 34" and 110° 31' 08" east longitude and 7° 44' 04" - 8° 00' 27" south latitude. It has a total area of 506.85 km² (Figure 1B) and is divided into 17 subdistricts. There were 11 subdistricts out of the existing 17 subdistricts targeted for release (Figure 1D) due to the high burden of dengue transmission that contributed to 75% of dengue cases in 2017-2019 (official communication with Bantul Health District Office). The release area has 254.37 km² of administrative area and 75.64 km² of residential area with a total human population of 985.770 people. Using the 75x75 m grid area as the basis, a total of 19.117 ERCs were needed, however the number was increased to a total of 24.462 ERCs to address challenges in the field. A total of 4 million eggs/week was produced to accomplish the requirement for the Bantul release area.

The rearing process for Sleman started in January 2021 but due to the COVID-19 situation, the release was delayed until May 2021. In November 2021, we began to prepare the colony for the Bantul area, and the release commenced in May 2022. We gradually set up approximately 130 -140 cages to supply the target for the Sleman area and approximately 160-170 cages for Bantul. There was an overlapping time when we maintained two colonies in the last Sleman release and the beginning of Bantul release (Figure 2).

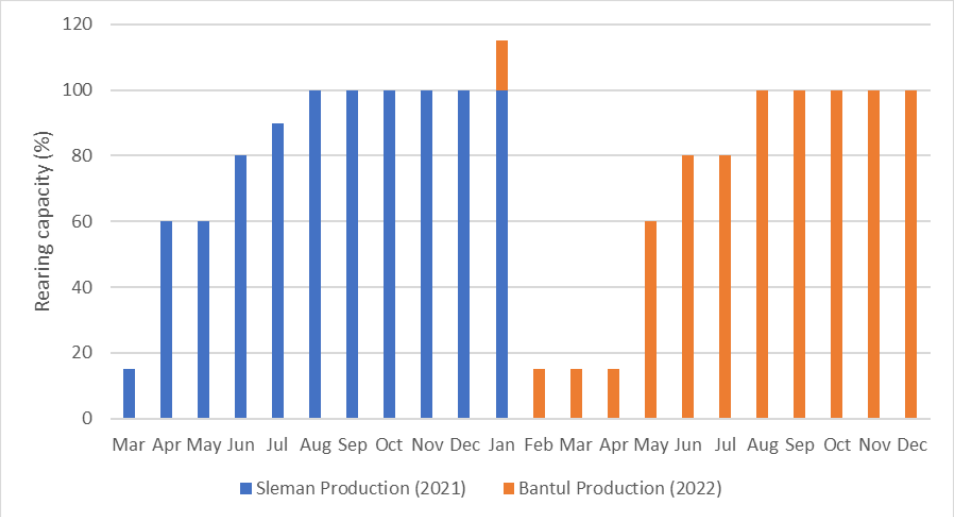

Figure 2. Mass production was maintained gradually to reach the maximum capacity of 100%, depending on the release target. There was an overlapping time for maintaining targets in both areas in January 2022.

Insectary requirement

Temperature and humidity

The insectary is located in Sleman District, Yogyakarta, which has a suitable temperature range for *Ae. aegypti*. Sleman District recorded average temperature of 27.7 and 27.8 °C, relative humidity of 74.1 and 77.9%, and rainfall of 106.2 and 275.1 mm during the dry season and wet season, respectively. In the insectary, mosquitoes were maintained at 25.5-26.5 °C and 50-70% relative humidity, which are the optimal conditions for *Ae. aegypti* development (Ross et al. 2017). Temperature can influence

the speed of larval development, hatch rate, and even pupal sex ratio (Mohammed & Chadee 2011; Imam et al. 2014). In the temperature range of 28°-34 °C, *Ae. aegypti* can have a better hatching rate rather than above this range. At 40 °C, no eggs will hatch, and there is high larval-pupal mortality (Sukiato et al. 2019). Wolbachia infections from mosquito colonies may be lost due to high temperatures, hence this should be prevented (Ross et al. 2017).

Room Facility

The insectary consisted of at least five rooms prepared for the preadult rearing room, adult colony room, wild-type colony and extra room, a storage room for equipment and consumables, and a storage room for egg and egg strip release preparation. The preadult rearing room was designed in a humid condition with a relatively natural photoperiod made by a half shade of the roof, including blower air flow for 24 hours. The egg storage room was maintained at an air-conditioned laboratory temperature of 25 °C. The insectary design is shown in Figure 3.

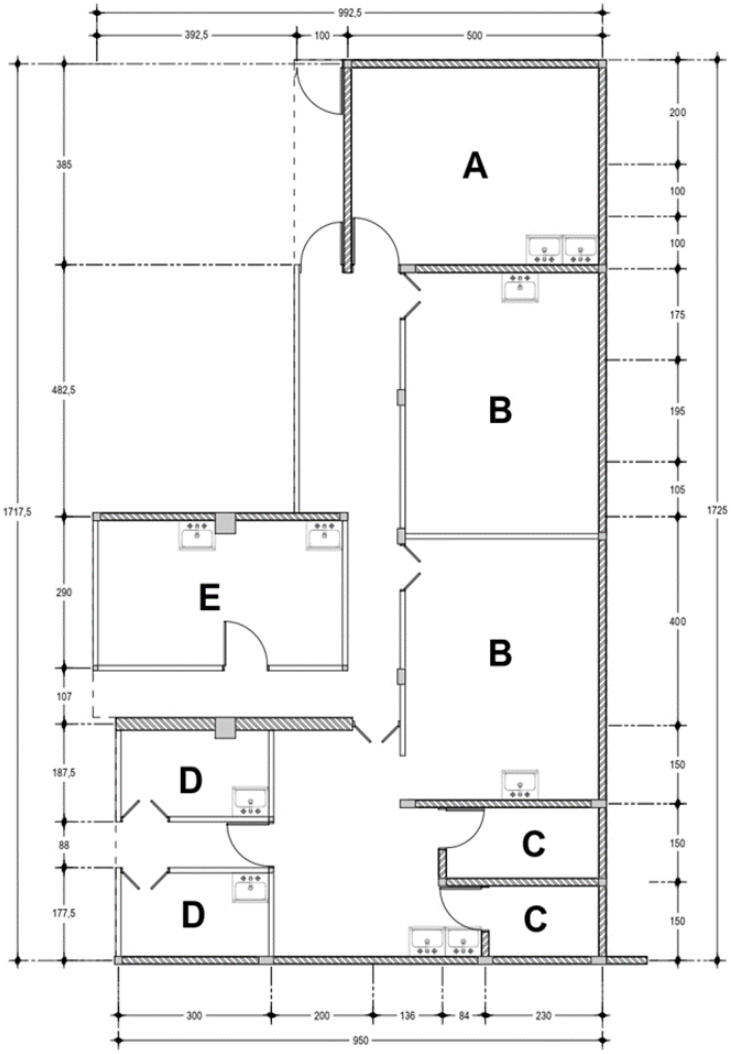

Figure 3. The insectary consists of five main rooms (1:100 cm); A. Egg storage room, B. Preadult rearing room, C. Storage room for equipment and rearing consumables, D. Wild-type colony and extra room, and E. Adult colony room.

Tools and Consumables

The tools for preadult rearing consisted of pipettes, small spoons, buckets of 18,5 cm in diameter and 16 cm in height and cups for pupal emergence containers. During mass production, a total of approximately 450

buckets were used. Tools for adult maintenance were customized cages of 30 x 30 x 30 cm in size muslin cloth and stainless steel frame and that had a, modified sugar cups, and modified oviposition cup (ovicup) for harvesting eggs. The 2 ml tubes and modified cups for screening diagnostic sample collection were used. The list of consumables consisted of Tetramin Tropical Flakes, Tetra Holding (U.S.) Inc., Germany for larvae food, tap water, 10% sugar solution, and 80% ethanol solution for the samples. Detailed pictures of the tools and consumables are shown in Figure 4.

Figure 4. A. Tools and consumables for rearing preadult stage, B. Tray to slow -dry eggs with a cloth, C. Emergence cup for the pupae, D. Container ovicup with the strips, E. Modified sugar cup, F. Customized cage, and G. Bucket for larval rearing.

Production Methods

Colony preparation (backcrossing-outcrossing)

WMELYOG was the colony of *w*Mel-infected *Ae. aegypti* previously used during the Applying Wolbachia to Eliminate Dengue (AWED) trial in the Yogyakarta City (Utarini et al. 2021). The *w*Mel Wolbachia-infected *Ae. aegypti* colony mass reared in Yogyakarta was maintained as an open (outcrossing) and closed population at different times. We started the production with backcrossing by mating female *w*Mel Wolbachia-infected *Ae. aegypti* with local wild-male *Ae. aegypti* and then continued it with outcrossing. Backcrossing was conducted once with the wild-type males from the Sleman and Bantul populations, and outcrossing was continued once every two cohorts generation colony maintenance to refresh the ge-

netic pool. We performed outcrossing (open colony) by adding 10-20% wild-type males to each successive generation (O'Neill et al. 2019; Garcia et al. 2019). Colony preparation activity was started by placing ovitraps to obtain wild-type *Ae. aegypti* eggs. Ovitrapping was perfomred periodically for one month in Bantul and Sleman in each of the 10 locations. After one week, eggs were collected from the flannel strips in ovitraps, then air-dried slowly for one or two days and pooled until sufficient eggs were acquired. Eggs were hatched and then reared up to the stage of 3rd or 4th stage of instar larvae to identify *Ae. aegypti* individuals, and these were separated from *Aedes albopictus* individuals, which were sometimes trapped in the same ovitraps. The eggs were further reared to obtain wild-type colonies, which were pooled into three cages for each target area (Dieng et al. 2012; Tantowijoyo et al. 2016) Adult *Ae. aegypti* was set up as a wild-type colony from the release target area. The harvested eggs (F1) were pooled for backcross and outcross material until eight gonotrophic cycles. Eggs were then transferred to a sealed container with a salt solution (2:1) and stored at air-conditioned laboratory temperature (25 ^{0}C±2 ^{0}C). Wild-type colonies were maintained up to the F2 generation. A simplified version of the flow of the rearing plan is shown in Figure 5.

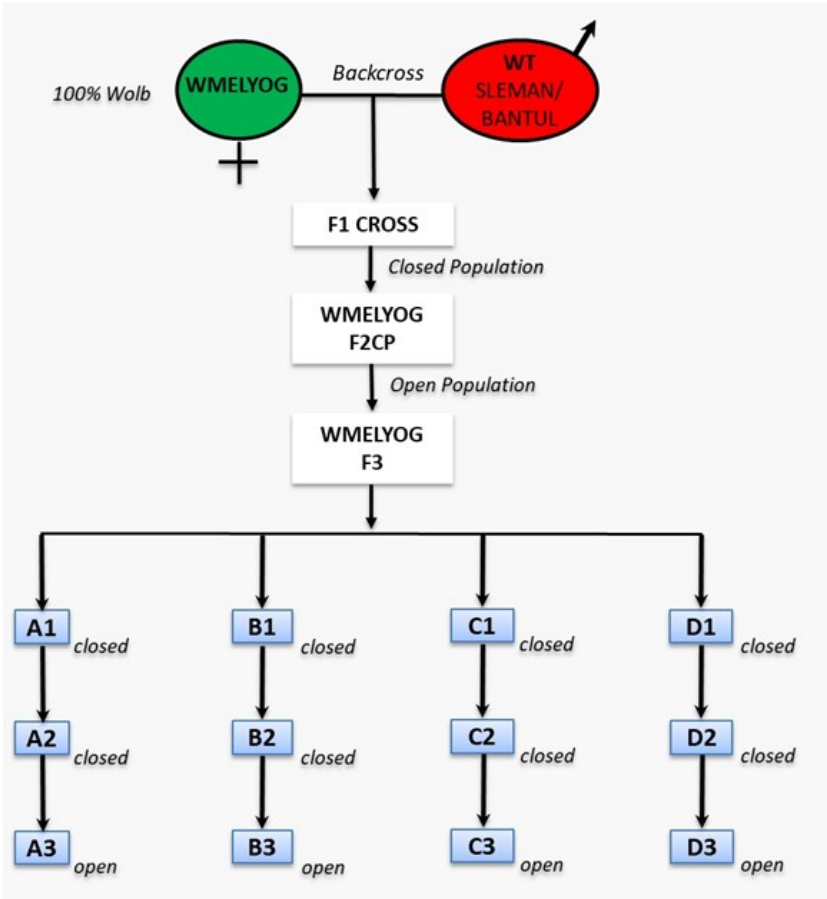

Figure 5. Backcrossing and outcrossing of WMELYOG. Female *w*Mel Wolbachia-infected *Ae. aegypti* (WMELYOG) were backcrossed to male wild-type mosquitoes derived from the field (Sleman or Bantul). After obtaining the F1 generation (F1 cross), a closed population was generated (WMELYOG F2CP). To obtain a similar genetic background to that of a natural population, outcrosses were performed by adding uninfected males from the field. The colonies (WMELYOG F3) were then divided into four cohorts of 'anakan' (brood stock) colonies (A, B, C, and D), and outcrossing was repeated for three consecutive generations. The screening for Wolbachia frequency was conducted in every outcrossing colony, with a threshold of 100% positivity. CP = closed population; WT = wild-type.

Production Methods for Mass Rearing

Production methods for mass rearing were divided into preadult and adult rearing. Every time hatching was performed, the step continued with three gonotrophic cycles (GC). The whole rearing phase can take one month in length of time. This method is shown in Figure 6.

Every broodstock had approximately 100 flannel strips, each containing around 3000 eggs per strip of *w*Mel Wolbachia-infected *Ae. aegypti* and continued to be reared in the preadult step. Preadult rearing room was conditioned with humid temperatures although temperature was not measured regularly. The larvae were reared in the rack trolley system for efficiency. Temperature, density, and nutrition are key factors in larval growth (Imam et al. 2014). The eggs were hatched (Day 0) using yeast solution that was made by adding 0.20 g baker's yeast into 1 L water for early nutrition for the larvae, the larvae were separated on Day 1 to a density of approximately 500-600 individuals per rearing bucket. The best practice, which is also convenient, was hatching the eggs on Thursday, separating the larvae on Friday, and continuing with preadult rearing can be continued on Monday. The larvae were fed immediately after being separated with ¼ teaspoon (tsp) of grounded Tetramin Tropical Flakes to ensure that food was always available during the weekend (Day 2-Day 3). Larval development and rearing water conditions were then monitored every day. The larvae were fed with ¼ teaspoon (tsp) of ground larvae food on Day 4 and ½ teaspoon on Day 5. The feeding time was scheduled and stirred with a zig-zag pattern; this allowed the food to sink as *Aedes aegypti* was the bottom feeder (Kinney et al. 2014).

On Day 7, larval density will reach approximately 500-600 larvae in 1.2 liters tap water per bucket (approximately 80% pupation occurred). All pupae and remaining larvae of each 2-2.5 rearing buckets were sieved and placed in the emergence cups that were filled with clean water. A pinch of food was added to the cups to feed the remaining larvae. Each emergence cup was then transferred into a cage that was clearly labelled with colony type, generation, and the date when the pupae were placed in the cage.

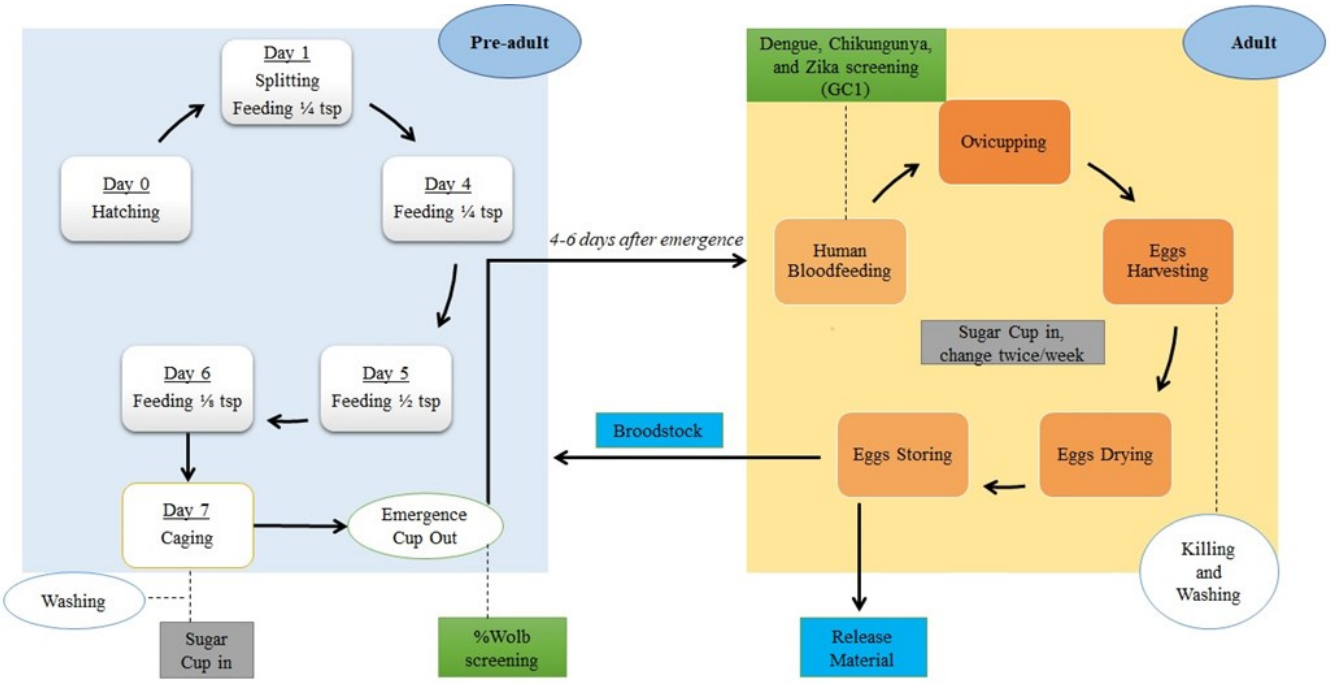

Figure 6. Activity flows in colony rearing. The steps are the preadult rearing stage, continuing with the adult stage with the human blood feeding method, and egg harvesting until the 3rd gonotrophic cycle (GC3). Tsp = teaspoon.

After reaching the pupal stage, the rearing adult stage began. According to the requirement of material release for Sleman and Bantul, for adult rearing need in a total of 130-170 cages were needed with a capacity of ± 1000 - 1250 adult mosquitoes in each cage. The adult colony was maintained at an average room temperature. Each colony cage was provided with 10% sugar solution *ad libitum* prepared by soaking cotton balls in a small plastic bowl filled with 1 tablespoon of sugar solution that was changed twice a week. On Days 4-6 after pupae emerged into adults, the females had access to a blood source using a human blood feeding method. Blood feeding was conducted once a week for three gonotrophic cycles by allowing the females to feed for 15-20 minutes on the limb or leg of a healthy volunteer. Exclusionary criteria for the volunteers was not having signs and symptoms of arboviral infection (fever, myalgia, headache, etc.) and not being acutely proven to be infected by arboviral infection (as diagnosed by registered clinicians or by laboratory results). Other exclusionary criteria were (1) taking any antibiotic, (2) a history of allergic reactions to insect bites, and (3) not providing consent before giving blood-meal. Approval for human blood-feeding of mosquito colonies, including field release of mosquitoes, was provided by the Medical-Health Research Ethical Committee, Faculty of Medicine, Public Health and Nursing, Universitas Gadjah Mada, with the reference number of KEI0611112011, KE/FK/818/EC, and KE/FK/1274/EC/2021.

In general, there are many techniques to give blood meals for maintaining female *Ae. aegypti*, including membrane feeding devices (Carvalho et al. 2014) and confined animals (Day & Edman 1984). However, according to several studies, mosquitoes with experimental Wolbachia infections frequently demonstrate poor performance on nonhuman blood, may have lower hatch rates, and may only partially transmit Wolbachia to their progeny (McMeniman et al. 2011; Caragata et al. 2014; Suh et al. 2016).

Ratio of Female and Male

The ratio of females and males per cage was taken into account when calculating the insectary necessity and evaluation. We determined that there were always fewer females than males in each rearing bucket. The number of female was substantial due to their fecundity in egg harvesting. In Sleman and Bantul, the female ratio reached 40-50% (Figure 7). The ratio may predict the production expectation. Egg production from each female may vary. In the field, each female can lay between 20-60 eggs, but in the insectary, it can reach up to 100-150 eggs (Clemons et al. 2010; Arévalo-Cortés et al. 2022). Based on our data, each female can produce approximately 70 eggs in the first gonotrophic cycle (GC1), and it will drop in the 3rd gonotrophic cycle (GC3) to up to 50 eggs (unpublished result).

Egg Harvesting and Production Capacity

Ae. aegypti has a strong interest in human blood. Due to this reason and the quality of the eggs, we allowed one-week-old adult colony to be blood-fed by human volunteers once a week (Gunathilaka et al. 2017; Al-Rashidi et al. 2022; Arévalo-Cortés et al. 2022). One cage was only blood fed by one person. After allowing 2-3 days for females to develop their eggs prior to oviposition, the modified ovicup (Figure 4D) was put into the cage. Each modified ovicup had five compartments. By adding wet flannel strips (ovistrips) and pouring water approximately 0.5 cm deep in each compartment, females were allowed to lay the eggs on the flannel. After two days of leaving the ovicup in the cage, harvesting was per-

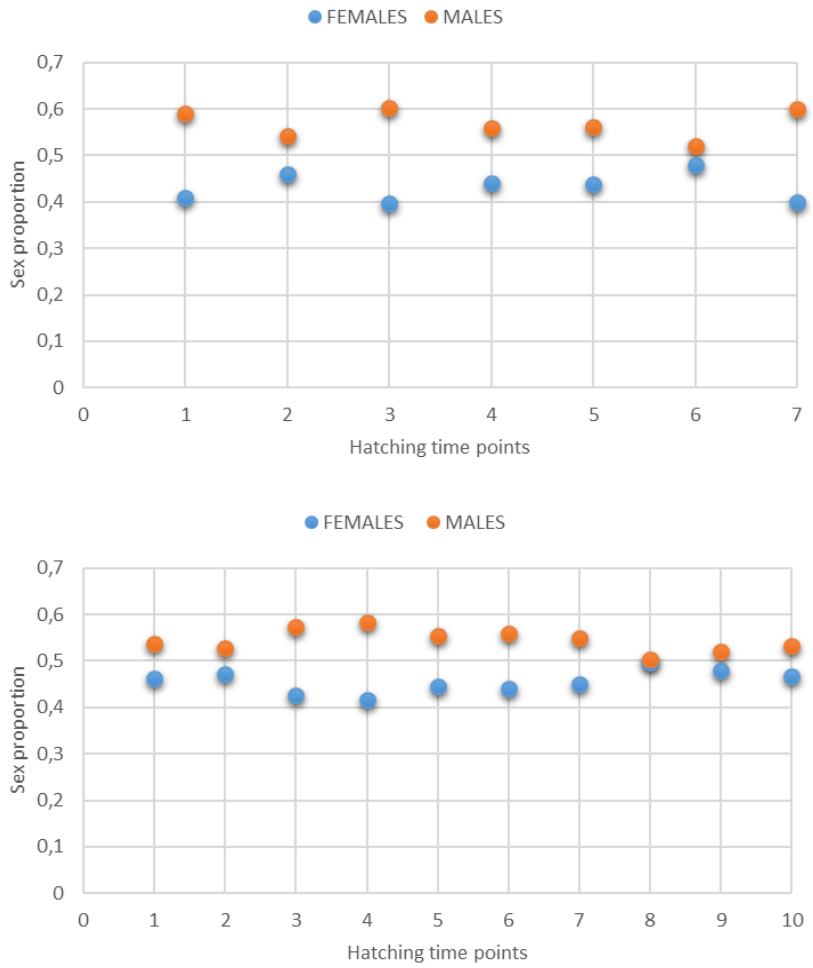

Figure 7. The ratio of female and male *Aedes aegypti* per cage in the insectary to supply release implementation in Sleman (upper) and Bantul (lower).

formed by removing the ovicup from the cage to collect the eggs. The ovistrips were then put into a tray with a dry cloth underneath to remove excess water. Any dead mosquitoes that may be stuck on the ovistrip were removed to minimize fungal growth. The eggs were dried slowly overnight. On the following day, the eggs were transferred to a sealed plastic container with saturated solutions of NaCl (2:1) to maintain humidity at ~75% and stored at an air-conditioned laboratory temperature of approximately 25^{0}C. From all three gonotrophic cycles in each cohort, usually in the 2nd and 3rd GC, egg production was less than that in the first cycle, so the ovistrip could be reduced from ten pieces of flannels (GC1) to only eight pieces for the 2nd GC and six pieces for the 3rd GC. This would make the egg clutch easy to observe and cut for the release strips.

We attempted to give a good quality egg to fulfil the release material needed. The newest harvested eggs were prepared to meet the need for release. After selecting the harvested eggs from 10-13 cages for the next parent colony of mass production (broodstock), the remaining eggs were used as egg release material. By using a visual reference that was obtained by counting the egg strips precisely under microscope, the ovistrips were cut into a small piece of between 150-200 eggs/strip for Sleman needs and 250-300 eggs/strip and 300-400 eggs/strip for Bantul. This step needed good practice among the staff. The egg strips were pooled in a large container and transferred to the field staff to be packed for release the following week. By our calculation, the capacity of our

Table 1. Production capacity to supply release material in Sleman and Bantul Areas.

Area	Sleman	Bantul
Target release area	126.8 km²	76 km²
Total cage	130-140	160-170
Density per cage	±1000	±1250
Female ratio	40%-50%	40%-50%
Egg production	GC 1= 3,166,000 – 3,410,000	GC1= 4,677,000 – 4,969,000
	GC2= 2,620,000 – 2,822,000	GC2= 3,870,000 – 4,112,000
	GC3= 2,080,000 – 2,240,000	GC3= 3,072,000 – 3,264,000

production in this implementation can be explained in the table below. It may become important to implement this technology in other areas.

Diagnostics

During release material preparation, two diagnostic tests were performed, i.e., the Wolbachia frequency screening and arbovirus screening (for dengue, chikungunya, and zika infection). The wolbachia frequency test was performed by screening the samples with a PCR Taqman assay that included the WD0513 gene on a Roche LightCycler 480 while the screening for arboviruses was performed by qRT-PCR as previously described (Yeap et al. 2014; Quyen et al. 2017; Tantowijoyo et al. 2020).

The first Wolbachia rate screening had to be done after backcrossing offspring. This time, the colony had to reach 100% Wolbachia to start mass production. Routine Wolbachia frequency screening was conducted by collecting 100 female and 100 male mosquitoes with a threshold of 96%; if the result was <96%, close colony maintenance had to be performed (just by crossing the offspring against each other) and the screening had to be repeated. Routine arbovirus screening was conducted by sampling ten blood-fed female mosquitoes from each blood feeder of the 1st gonotrophic cycle (GC1). If the result corresponded to a positive result in the screening, all the blood-fed cages and their offspring were discontinued or destroyed. Even though one volunteer can feed more than one cage, it is recommended that four cages is the maximum per volunteer due to the drop in egg production when this number is exceeded. In our study, screening for arboviruses never gave positive results.

CONCLUSION

Wolbachia-infected *Ae. aegypti* mass production plays important role to the success of Wolbachia technology implementation in wider areas. The standardized protocol and sufficiently wide and functional insectary ensure the quality of the entire process. It should be possible to maintain *Ae. aegypti* high fitness for open field releases by maintaining large population sizes, avoiding strong selective pressures through rearing methods, and regularly outcrossing to wild mosquitoes. The techniques do not need any specific tools, and they may be scaled up to produce more mosquito eggs for outdoor releases. For other advancements, particularly for the blood meal feeding system, the approaches are still adaptable. This protocol had successfully been adapted to support the two district-wide Wolbachia implementation programs in Sleman and Bantul, and might serve as a reference for other implementations in Indonesia.

AUTHORS CONTRIBUTION

All authors reviewed and agreed upon the final manuscript. IF and IN contributed equally to study conceptualization, data collection, writing of the original draft and revision of the final manuscript. BA, DLC, IDU, and NAP contributed to the investigation, data collection, writing the original draft and revision of the final manuscript. US and ES contributed to the investigation and writing of the original draft. AU, RAA, and CI contributed to revision of the final manuscript. EA contributed to study conceptualization, investigation, and revision of the final manuscript. WT designed the research and supervised all the processes, writing of the original draft and revision the final manuscript.

ACKNOWLEDGMENTS

We thank Yayasan Tahija for providing funding for this program. We are also appreciative to our program partner, the Yogyakarta District Health Office. We also thank our blood feeder volunteers for donating their blood and contributing to our egg production. Finally, we would like to express our gratitude to every employee who contributed make this initiative a success.

CONFLICT OF INTEREST

The authors declare there is no conflicts of interest.

REFERENCES

Al-Rashidi, H.S. et al., 2022. Effects of blood meal sources on the biological characteristics of Aedes aegypti and Culex pipiens (Diptera: Culicidae). *Saudi Journal of Biological Sciences*, 29(12), 103448. doi: 10.1016/j.sjbs.2022.103448.

Arévalo-Cortés, A. et al., 2022. Differential Hatching, Development, Oviposition, and Longevity Patterns among Colombian Aedes aegypti Populations. *Insects*, 13(6), 536. doi: 10.3390/insects13060536.

Carvalho, D.O. et al., 2014. Mass production of genetically modified Aedes aegypti for field releases in Brazil. *Journal of Visualized Experimental*, 4(83), e3579. doi: 10.3791/3579.

Caragata, E.P. et al., 2014. Competition for amino acids between Wolbachia and the mosquito host, Aedes aegypti. *Microbial Ecology*, 67(1), pp.205-218. doi: 10.1007/s00248-013-0339-4.

Clemons, A. et al., 2010. Aedes aegypti Culturing and Egg Collection. *Cold Spring Harbor protocols*, 2010(10), pdb.prot5507. doi: 10.1101/pdb.prot5507

Day, J.F. & Edman, J.D., 1984. Mosquito engorgement on normally defensive hosts depends on host activity patterns. *Journal of Medical Entomology*, 21(6), pp.732-740. doi: 10.1093/jmedent/21.6.732

Dieng, H. et al., 2012. Unusual developing sites of dengue vectors and potential epidemiological implications. *Asian Pacific Journal of Tropical Biomedicine*, 2(3), pp.228–232. doi: 10.1016/S2221-1691(12)60047-1.

Garcia, G. de A. et al., 2019. Matching the genetics of released and local Aedes aegypti populations is critical to assure Wolbachia invasion P. Kittayapong, ed. *PLOS Neglected Tropical Diseases*, 13(1), e0007023. doi: 10.1371/journal.pntd.0007023.

Gunathilaka, N. et al., 2017. Efficacy of Blood Sources and Artificial Blood Feeding Methods in Rearing of Aedes aegypti (Diptera: Culicidae) for Sterile Insect Technique and Incompatible Insect Technique Approaches in Sri Lanka. *BioMed Research International*, 2017, 3196924. doi: 10.1155/2017/3196924.

Imam, H. et al., 2014. The basic rules and methods of mosquito rearing (Aedes aegypti). *Tropical Parasitology*, 4(1), pp.53–55. doi: 10.4103/2229-5070.129167.

Indriani, C. et al., 2020. Reduced dengue incidence following deployments of *Wolbachia*-infected *Aedes aegypti* in Yogyakarta, Indonesia: a quasi-experimental trial using controlled interrupted time series analysis. *Gates open research*, 4, 50. doi: 10.12688/gatesopenres.13122.1.

Kinney, M.P., Panting, N.D. & Clark, T.M., 2014. Modulation of appetite and feeding behavior of the larval mosquito Aedes aegypti by the serotonin-selective reuptake inhibitor paroxetine: shifts between distinct feeding modes and the influence of feeding status. *Journal of Experimental Biology*, 217(6), pp.935–943. doi: 10.1242/jeb.094904.

McMeniman, C.J. et al., 2011. A Wolbachia symbiont in Aedes aegypti disrupts mosquito egg development to a greater extent when mosquitoes feed on nonhuman versus human blood. *Journal of Medical Entomology*, 48(1), pp.76-84. doi: 10.1603/me09188.

Mohammed, A. & Chadee, D.D., 2011. Effects of different temperature regimens on the development of Aedes aegypti (L.) (Diptera: Culicidae) mosquitoes. *Acta Tropica*, 119(1), pp.38–43. doi: 10.1016/j.actatropica.2011.04.004.

O'Neill, S.L., 2018. The Use of Wolbachia by the World Mosquito Program to Interrupt Transmission of Aedes aegypti Transmitted Viruses. In *Dengue and Zika: Control and Antiviral Treatment Strategies*. Advances in Experimental Medicine and Biology, vol 1062. Singapore: Springer Singapore, pp.355–360. doi: 10.1007/978-981-10-8727-1_24.

O'Neill, S.L. et al., 2019. Scaled deployment of Wolbachia to protect the community from dengue and other Aedes transmitted arboviruses. *Gates Open Research*, 2, 36. doi: 10.12688/gatesopenres.12844.3.

Ross, P.A. et al., 2017. Maintaining Aedes aegypti Mosquitoes Infected with Wolbachia. *Journal of Visualized Experiment*, 14(126), 56124. doi: 10.3791/56124.

Quyen, N.T.H. et al., 2017. Chikungunya and Zika Virus Cases Detected against a Backdrop of Endemic Dengue Transmission in Vietnam. *The American Journal of Tropical Medicine and Hygiene*, 97(1), pp.146–150. doi: 10.4269/ajtmh.16-0979.

Segoli, M. et al., 2014. The Effect of Virus-Blocking Wolbachia on Male Competitiveness of the Dengue Vector Mosquito, Aedes aegypti. *PLOS Neglected Tropical Diseases*, 8(12), e3294. doi: 10.1371/journal.pntd.0003294.

Suh, E. et al., 2016. Interaction of Wolbachia and bloodmeal type in artificially infected Aedes albopictus (Diptera: Culicidae). *Journal of Medical Entomology*, 53(5), pp.1156-1162. doi: 10.1093/jme/tjw084.

Sukiato, F. et al., 2019. The effects of temperature and shading on mortality and development rates of Aedes aegypti (Diptera: Culicidae). *Journal of Vector Ecology*, 44(2), pp.264–270. doi: 10.1111/jvec.12358.

Tantowijoyo, W. et al., 2016. Spatial and Temporal Variation in Aedes aegypti and Aedes albopictus (Diptera: Culicidae) Numbers in the Yogyakarta Area of Java, Indonesia, With Implications for Wolbachia Releases. *Journal of Medical Entomology*, 53(1), pp.188–198. doi: 10.1093/jme/tjv180.

Tantowijoyo, W. et al., 2020. Stable establishment of wMel Wolbachia in Aedes aegypti populations in Yogyakarta, Indonesia. *PLOS Neglected Tropical Diseases*, 14(4), e0008157. doi: 10.1371/journal.pntd.0008157.

Utarini, A. et al., 2021. Efficacy of Wolbachia-Infected Mosquito Deployments for the Control of Dengue. *New England Journal of Medicine*, 384(23), pp.2177–2186. doi: 10.1056/NEJMoa2030243.

World Health Organization, 2009. Dengue guidelines for diagnosis, treatment, prevention and control : new edition World Health Organization. https://iris.who.int/handle/10665/44188

Yeap, H.L. et al., 2014. Assessing quality of life-shortening Wolbachia-infected Aedes aegypti mosquitoes in the field based on capture rates and morphometric assessments. *Parasites & Vectors*, 7(1), 58. doi: 10.1186/1756-3305-7-58.

Journal of Tropical Biodiversity and Biotechnology
Volume 09, Issue 01 (2024): jtbb74403
DOI: 10.22146/jtbb.74403

Review Article

Plant Growth Promoting Endophytic Microorganisms from Orchids for A Sustainable Agriculture

Lucky Poh Wah Goh[1], Benardette Lyovine Jaisi[1], Roslina Jawan[1], Jualang Azlan Gansau[1]*
1)Faculty of Science and Natural Resources, Universiti Malaysia Sabah, Jalan UMS, 88400 Kota Kinabalu, Sabah, Malaysia
* Corresponding author, email: azlanajg@ums.edu.my

Keywords:
chemical fertilizer
endophytes
microorganisms
plant growth promoting
Submitted:
27 April 2022
Accepted:
16 March 2023
Published:
16 February 2024
Editor:
Furzani Binti Pa'ee

ABSTRACT
Conventional agriculture practice has heavily relied on chemical fertilizers to increase crop yield. However, long-term application of chemical fertilizers carries tremendous negative impact on the environment and is unsustainable. Hence, the search for an alternative source of fertilizers is required. Orchids are flowers and can be found in tropical countries. The growth and development of orchids are closely tied to the presence of plant growth promoting endophytic microorganisms (PGPM). PGPM harbours various beneficial traits such as potassium and phosphorus solubilization and indole acetic acid and siderophore production which enhance and support plant growth and development. This review article showed that PGPM isolated from orchids could be utilized in conventional agriculture to reduce dependency on chemical fertilizer.

Copyright: © 2024, J. Tropical Biodiversity Biotechnology (CC BY-SA 4.0)

INTRODUCTION
Orchidaceae, commonly known as the orchid family is one of the most diversified monocotyledonous, flowering plant family with over 20,000 species found around the world and approximately 75% are distributed in the tropical region (Cetzal-Ix et al. 2014) . The orchid species, with its significant ornamental value and a diverse range of vegetative and floral features, has piqued the interest of numerous horticulturists and scientists due to its uniqueness (Cetzal-Ix et al. 2014). One of the numerous reasons for the ecological significance of orchid species is their diverse biodiversity and habitat which spans from tree bark to wet areas such as sand dunes (Ma et al. 2016). Biodiversity is described as the variety of flora and fauna found worldwide or in a specific ecosystem. High levels of biodiversity in a region are considered significant and valuable. The presence of diverse orchid species demonstrates that the specific ecosystem provides optimum environment, resulting in a healthy and functional ecosystem. There are approximately 25,000 orchid species that have evolved to become a prominent feature of the world's vegetation (De & Singh 2015). Over 1350 species were classified into 186 genera accounting for 5.98% of the total orchid flora and 6.8% of flowering plants (De & Singh 2015).

ENDEMIC ORCHID
Overhunting of plant biodiversity and pollution due to human activities

contribute to the endangerment of previously dominant life forms because of deterioration of ecosystem. The increase-land use intensity such as logging resulted in a clear a significant negative impact on fish communities. Logging up to two cycles are sufficient to have negative impact on freshwater ecosystems (Wilkinson et al. 2018). Orchids also faced similar threats from human activities (De & Singh 2015). Overharvesting and rainforest deforestation led to the endemic of several species of orchids (Rubluo et al. 1993). Therefore, orchid conservation measures are necessary across all countries to avoid the extinction of orchid biodiversity in the wild.

The tropical and alpine zones such as woody plants, secondary vegetations, floodplains, bamboo and palm thickets, woodland, grassy slopes, and rugged regions are highly prevalent orchid sites (Chowdhery 2004). Two regions, Sikkim and Arunachal Pradesh Himalayas are examples of other home states harboring distribution endemic orchid species (Nayar 1996). Sabah is the key location for orchid diversity, with around 1300 species representing 250 orchid taxa classified as endemic species (Juiling et al. 2020). An evaluation of the International Union for Conservation of Nature's (IUCN) Red List revealed that 136 endemic orchid species are in the areas near the Kinabalu and Crocker Range parks located in North Borneo, Sabah (Juiling et al. 2020). Maximum entropy (MaxEnt) algorithm generated species distribution models for 47 endemic orchid species and gained insights into their adaptive behavior and development through natural selection (Dewar 2010). The findings suggested that approximately 83% of the researched species were imperiled, and urgent conservation efforts are required in areas with significant species diversity to avert orchid species extinction. In Crocker Range National Park located in Sabah, 100 of the park's 341 orchid species are endemic to Borneo, whilst 53 are indigenous to Sabah (Majit et al. 2014). Bulbophyllum is the most recently found genus, followed by Dendrobium and Dendrochilum. *Bulbophyllum neilgherrense* is an epiphytic orchid that has been actively used by the communities of Karnataka to treat a variety of ailments, such as skin allergies and rheumatism (Nair et al. 2018). A study also reported that *Bulbophyllum neilgherrense* possesses analgesic and anti-inflammatory effects in response to radiant heat-induced pain and carrageenan-induced acute inflammation (Nair et al. 2018).

Phalaenopsis amabilis is commonly called as moth orchid, is amongst the most economically significant orchid species in the Orchidaceae family. It is mostly recognized in international trade and the global ornamental market (Ko 2018). *Phalaenopsis* orchids are notable for their unique biological metabolism as they participate in crassulacean acid metabolism (CAM) photosynthesis. They are also recognized for their large, thick leaves and robust flowers (Košir et al. 2004). *Phalaenopsis* is an Indonesian native orchid, giving it the country's national flower due to its dazzling white colour (Semiarti 2018). Stomatal identification of *Phalaenopsis amabilis* demonstrated that it is a type of monopodial orchid with anomocyctic stomata (Zahara & Win 2019).

ORCHIDACEAE FUNGAL AND BACTERIAL ENDOPHYTES

The terminology "Endophyte" relates to microorganisms that reside either partially or their entire life within the plant cells without inflicting any obvious harm of having a symbiotic relationship (Hardoim et al. 2015; Wilson 1995). Endophytes have been thoroughly researched due to their propensity to create biochemicals and exert beneficial effects towards plant growth and development (Chutulo & Chalannavar 2018). Numerous research have been conducted on the biodiversity of endo-

phytes, notably mycorrhizal and bacterial endophytes in orchids. *Penicillium*, *Fusarium*, and *Daldinia* are examples of endophytic fungi derived from traditional medicines (Kuo et al. 2021). Endophytic bacteria such as *Dyella marensis*, *Collimonas pratensis*, and *Luteibacter rhizovicinus* have been associated with terrestrial orchids (Herrera et al. 2020). The colonization and penetration mechanisms of Orchidaceae fungal endophytes (OFEs) differ compared to other fungal pathogens as the OFEs penetrated through the stomata laterally in the cells of the anticlinal epidermal. In comparison, pathogenic endophytes gain entry directly through the cell wall (Sarsaiya et al. 2019). The localization of OFEs are confined along with the intercellular in the shoots, in contrast to pathogens where they grow extracellularly (Sarsaiya et al. 2019).

Mycorrhizal and non-mycorrhizal endophytic microbes have been isolated and characterized from orchid species in order to determine their direct or indirect impact on orchid growth and secondary metabolite synthesis (Pant et al. 2017). The symbiotic relationship between the seeds in orchids with species-specific Basidiomycetes fungus symbionts were reported where germination initiated once the seed receives nourishment from the colonizing fungal symbiont after penetrating the seed that lacks endosperm (Pant et al. 2017). Orchid plants could influence the extent of fungal interaction to fungus colonization which create a symbiotic relationship (Arditti & Pridgeon 1997). Plant growth-promoting endophytes are bacterial endophytes that enhance plant growth via the synthesis of phytohormones such as Indole-3-Acetic Acid (IAA) primarily using the indole acetamide pathway (Arditti & Pridgeon 1997). IAA is naturally abundant phytohormone in plants; the latest mutagenesis and molecular research discovered that IAA is engaged in mediating plant growth (Teale et al. 2006) DNA barcode pyrosequencing observed that Proteobacteria is the prominent genus of endophytic diazotrophic bacteria capable of producing IAA in *Dendrobium catenatum* (Li et al. 2017).

Nitrogen (N) is a key element of plants, particularly chlorophyll, which enables photosynthesis and ensures the healthy growth of plants (Leghari et al. 2016). Numerous endophytic bacteria are capable of fixing nitrogen which provides plants with crucial nitrogen sources and they offer an alternative solution to chemical fertilizers (Puri et al. 2017). Li et al. (2017) discovered that the orchid-associated cyanobacteria in *Dendrobium catenatum* perform nitrogen fixation, ensuring the host plant's ecological stability.

Relationship between Endophytes with Orchidaceae Plants

Orchidaceae is the finest plant family attributed to their nutrition strategy being associated with endophytes (Sarsaiya et al. 2019). *Streptomyces* sp., *Bacillus* sp., and *Erwinia* sp. are examples of bacteria having a symbiotic relationship with orchid which contributed to their resiliency against external harm (Tsavkelova et al. 2007; Yang et al. 2008). However, majority of evidence on orchid-endophytes interactions has centered on terrestrial and temperate orchid mycorrhizal. This is because the majority of orchid species are epiphytic and tropical, hence increasing their relationship with endophytes, particularly endophytic fungi (Salazar et al. 2020). Despite that, the critical role of bacteria in mycorrhizal development was examining the influence of *Laccaria laccata* mycorrhizas and sporocarps on *Douglas-fir* ectomycorrhizal development (Duponnois & Garbaye 1991). The study reported the term "mycorrhiza helper bacterium" (MHB), which has demonstrated that *Pseudomonas fluorescens* BBC6 aids the formation of ectomycorrhiza. Endophytic bacteria are capable of secreting secondary metabolites in response to environmental

stress. An endangered orchid species, *Anoectochilus formosanus* (*A. formosanus*) also known as "Jewel Orchid", is well-known for its therapeutic properties due to secondary metabolites produced via mycorrhizal interaction with endophytes (Zhang et al. 2013). The endophytic fungal growth promotes shoot elevation and leaf density in *A. formosanus* by secreting ginsenosides and flavonoids which carries therapeutic effects (Zhang et al. 2013) . Plants and endophytes have a symbiotic relationship through the exchange of nutrients.

A study has reported that mycorrhizal-associated plants acquire phosphate from fungi in exchange for sugar (Al-Karaki & Al-Raddad 1997). Plant growth-promoting endophytic bacterial have been isolated from the leaf of *Vanda cristata* (Shah et al. 2021). The endophyte is capable of producing phytohormones during root colonization and antimicrobial substances that aid in repairing the orchid plant's immunological capacities.

Gastrodia elata (*G. elata*) is an orchid species that are dependent on mycorrhizal fungi for growth in its lifespan it was reported to transition from Mycena, a single-fungus relationship, to Armillaria, another single-fungus relationship (Chen et al. 2019). This transition of different growth phases of *G. elata* also alters the fungal community (Chen et al. 2019). Epiphytic and terrestrial orchid seeds exhibit distinct responses to fungus isolated from roots (Liu et al. 2010). This suggested that epiphytic orchids have a more extensive mycorrhizal association with fungi during the seed germination stage compared to terrestrial orchid species.

Endophytes from Orchidaceae Shoots

Orchidaceae-fungal endophytes (OFEs) occurring on the shoots of orchids have the potential to significantly advance the symbiotic relationships of diverse fungal endophytes with distinct mycota via horizontal transmission into the Orchidaceae (Sarsaiya et al. 2019). Numerous articles have demonstrated the recovery of OFEs from various Orchidaceae species. A study described the association of a broad base of filamentous fungi, *Fusarium* with orchids, as it can reside as pathogens or non-pathogens which could be isolated from the orchid's shoot segments (Srivastava et al. 2018). The non-pathogenic *Fusarium* sp. may behave as a decomposer or a mutualist in orchid plants, such as stimulating seedling growth (Booth 1971; Vujanovic et al. 2000). Orchid seed germination using *Fusarium* isolates from *Cypripedium reginae* revealed the formation of protocorm and induction of seed germination (Vujanovic et al. 2000). Meanwhile a pathogenic *Fusarium* caused progressive increase in orchid infections, impeding the production of high-quality orchids by causing symptoms such as leaf withering (Wedge & Elmer 2008).

Colletotrichum is a fungal endophyte that was isolated from the shoots of *Dendrobium aqueum*. A study has recovered endophytes which exhibit organ specialization, with a greater ensemble in stem sections and only a single endophyte was found in the leaf segments (Parthibhan et al. 2017). Pathogenic endophytes did not cause any significant negative impact on orchids despite their presence (Parthibhan et al. 2017). *Colletotrichum* species are considered a pathogenic fungus which can be found on a diverse variety of ornamental plants, including orchids (Guarnaccia et al. 2021). To ensure that *Colletotrichum* does cause negative infection in host plants, the plants must first be capable of detecting the presence of potential pathogens and afterwards establish a strong defense against the pathogenic invasion (Scherr et al. 2014). Therefore, plant defense mechanism is important for mediating fungal-host plant interactions.

Orchidaceae Roots Endophytes

Several terrestrial genera have their roots structured in the way of a three-layered epidermis when examining a cross-section of velamentous roots (Einzmann et al. 2019). Despite several studies indicating that the operational impacts of a velamen are not significant in terrestrial plants, one study attempted to prove its role by focusing on the roots of epiphytic orchids (Benzing 1996). Bacteria and fungi have been shown to aid plant growth by solubilizing vital phosphorus, phosphate, and nitrogen, as well as being a significant nutrient supplier for orchid seeds germination rate and during the cotyledonary development (Shakeel et al. 2015; Herrera et al. 2020). S. Chen et al. (2019) investigated the role of root associated bacteria (RAB) in wheat maturation and discovered that various bacterial genera were associated with plant ripening in roots when exposed to nitrogen fertilization. Among RAB that were isolated were *Streptomyces*, *Pseudomonas*, and *Bacillus* colonizing the roots of terrestrial orchids that have the ability of producing indole-3-acetic acid (IAA) which is an important plant growth hormone (Tsavkelova et al. 2007).

The terminology "Orchidaceae root-associated fungal endophytes" (ORAFEs) refers to endophytes that dwell within the cortical or velamen tissues of Orchidaceae roots. Numerous studies had established the existence of these endophytes in the roots of a wide variety of orchid species. A total of 13 species of endophytic fungi have been identified including, *Aspergillus flavus* (*A. flavus*) and *Trichoderma harzianum*, from the roots of *Dendrobium moniliforme* and *Dendrobium transparens*, and their discoveries indicated the presence of bioactive substances, corroborating the claim that these endophytic fungi possess antimicrobial properties that inhibits the bacterial growth (Shrestha et al. 2018). *A. flavus* is well-known for being used in the fermentation market, specifically in the production of Asian fermented foods (Chang & Ehrlich 2010). Similarly, *A. flavus* can be brought into the crop environment to help prevent preharvest contamination of crops, such as aflatoxin contamination which is linked to human sickness. The roots of epiphytic and lithophytic orchids in the genus Lepanthes were reported to harbour fungal endophytes, which were later identified as the *Xylaria* species and *Rhizoctonia*-like fungal species (Bayman et al. 1997). The habitat of orchid mycorrhizal fungi such as *Rhizoctonia* is restricted to the roots of orchids only, whereas orchid shoots are believed to contain defensive substances which deter fungal endophytes (Hadley 1982). This has suggested that endophytic microorganisms could only be found at a specific site of a plant due to different metabolic functions of different plant parts. Hence, the research could consider investigating the mechanism of action of plants which resulted in the distribution of endophytes.

ENDOPHYTES AS PLANT GROWTH PROMOTERS

Potassium Solubilization

Potassium (K) is an essential element in nutrient uptake in plants. It is also an element commonly used as fertilizer in agricultural production, as seen by the widespread use of potassium chloride fertilizer mixes (Tajer 2021). When an adequate concentration of K is supplied to plants, it improves the photo-assimilate transfer from leaves to roots and boost nitrogen use efficiency by regulating photosynthesis, carbon and nitrogen metabolizing enzyme activities, nitrate assimilation gene activities, and nitrate transport (Xu et al. 2020). Typically, soil contains higher concentrations of K compared to any nutrient. K is the seventh most prevalent element in the Earth's crust, after oxygen and silicon. In soil, the total potassium level ranges between 0.04 and 3 percent. Even though K is an

abundant element in soil, only 1 to 2 percent of this element is available for plant uptake (Sparks & Huang 1985). Nevertheless, fixed potassium and structural potassium are not accessible for plant uptake, and these two forms of potassium are referred to as exchangeable and non-exchangeable forms of potassium, respectively (Mouhamad et al. 2016).

The use of chemical fertilizers has a significant negative impact on the long-term sustainability of the environment. Hence, alternative measures to chemical fertilizers are needed. Several bacteria and fungi have been shown to be able to solubilize potassium-bearing minerals and converting the insoluble K into soluble forms of K which are readily available for plant uptake, however, the exact biochemical pathways remain unexplored (Rashid et al. 2016). The manufacture and management of biological fertilizers including potassium solubilizing bacteria and fungi are alternative to chemical fertilizers which can reduce reliance on chemical fertilizers. Because of the growing interest in using endophytes to solubilize inaccessible forms of potassium, isolation and screening must be evaluated. A study developed a modified and enhanced agar plate for the process by adding an indicator dye to an Aleksandrov medium to allow better visualization of the formation of halo zones around colonies that had successfully shown a positive result (Rashid et al. 2016). The better visibility of potential K solubilizers also helped in the discovery of weak producers based on organic acid secretion in the medium and accelerated the isolation and screening process.

Phosphate Solubilization

Phosphorus (P) is a macronutrient essential for a sustainable agricultural output since it promotes optimal plant growth and productivity (Zapata & Zaharah 2002). Additionally, P is necessary for plant growth as it is involved in a number of critical plant functions such as transfer of energy in the form of ATP, enabling the process of photosynthesis, converting sugars and starches, and also the passing of biological characteristics to the next population (Sultenfuss & Doyle 1999). The majority of P in soil is present in trace amounts, and it is in the inactive state of a phosphate, which is bonded to a number of soil minerals elements that inhibited the absorption by plant (Hinsinger 2001). P has also been utilized as a fertilizer to encourage high agricultural yields, but due to the emergence of edaphic processes, P has become immobilized in soil, preventing sufficient availability for plant absorption.

P is assimilated and distributed by the root hairs, root tips, or the exterior coats of root cells, which can be aided by mycorrhizal fungi that occur in conjunction with the roots of several plants (Sultenfuss & Doyle 1999). The discovery of a phosphate-solubilizing endophyte is among the breakthroughs that have the potential to deliver an environmentally benign yet economically viable solution to phosphate deficiency. These beneficial microbes could convert insoluble P compounds to soluble P for greater uptake by plants through the hydrolysis of organic and inorganic insoluble phosphorus molecules (Kalayu 2019). Endophytes such as *Pseudomonas* are extremely effective at phosphate solubilization for plants due to their involvement in synthesizing organic acids and acid phosphatases (Rodríguez & Fraga 1999). Hence, numerous research studies have focused on assessing the ability of the endophyte in phosphate solubilization. The isolates of *Enterobacter* sp. and *Serratia* sp. have been reported to be able to solubilize P and the increased solubilization process is associated with the decrease in pH value of the media (Sánchez-Cruz et al. 2019). The results also indicated that the pH value declines during the early phases of bacterial growth, which coincides with phosphate solubilization.

Indole Acetic Acid Synthesis

Endophytes that are able to generate indole-3-acetic acid (IAA) are amongst the well-known significant plant growth-promoting traits because of their relevance in regulating key facets of plant growth and development (Fu et al. 2015). Thus, studies on exploiting the potential of endophytic microorganisms that are able to synthesize IAA has been conducted globally in hopes of finding alternatives to chemical fertilizers for sustainable agriculture. IAA is predominantly synthesized in the young shoot organs to aid its growth and stimulating vascular differentiation (Aloni et al. 2006). Li et al. (2017) compared several studies regarding the mechanism of auxin regulation in plant growth by controlling the gene expression via auxin response factors (ARFs). ARFs bind to auxin response DNA elements (AuxRE) in the promoters of auxin-regulated genes and either activate or repress transcription of these genes depending on a specific domain in the middle of the protein. The lateral root of Arabidopsis was used as a model to study the roles of hormonal signals that are responsible for regulating lateral root development (Casimiro et al. 2001). A study has reported that modification of root structure by AUX1 mutations disrupted the transportation of IAA and exogenous application of 1-napthylacetic acid recovered the *aux1* lateral root phenotype (Marchant et al. 2002). *Enterobacter cloacae* MSR1 is a plant growth-promoting endophytic bacteria isolated from the roots of Medicago sativa by culturing them in a Lauria Bertani broth supplemented with tryptophan (Khalifa et al. 2016). The tryptophan served as the precursor for IAA synthesis as plant roots tend to produce an amount of nutrients when consumed by the endophytic bacteria. Evidence have shown that IAA could act as a signaling molecule due to its mode of action that enabling efficient switching among transcriptional repression and activation of genes via auxin-dependent degradation of transcriptional repressors (Lavy & Estelle 2016). IAA has multiple functional roles which are crucial to plant growth and development. The close interaction of plant growth promoting microorganisms and its ability to produce IAA have a significant impact on the environment as well.

Siderophore Synthesis

Plants or microorganisms that grow in a low concentration of iron produce an organic substance, namely siderophores (Schwyn & Neilands 1987). Siderophores play a vital role in chelating ferric iron [FE(III)] from varied terrestrial and aquatic habitats, making it accessible to plant cells (Ahmed & Holmström 2014). In order for the siderophores to be available for the endophytic cells, they must have the ability to form complexes with essential components such as molybdenum, manganese, and carbon monoxide (Bellenger et al. 2008). However, reports on the link between endophytes that produce siderophores and plants are uncommon. However, the most frequently encountered siderophores is in crops that resulted in the induction of systemic resistance mediated by endophytic rhizobacteria (Aznar & Dellagi 2015). Endophytes may uptake Fe from the apoplast of the root when there is a high concentration of Fe in the root, as Fe(III) can be supplied to the apoplast of the root. (Abadía 1995; Kosegarten et al. 1999). The ability of endophytic bacteria *Methylobacterium* sp. in producing siderophores were observed through several bioassays including chrome-azurol agar assay test (CAS), Csáky test and Arnow test (Lacava et al. 2008). Another study reported that the siderophore producing endophytes aided the plant growth by supplying iron to the plants (Maheshwari et al. 2019). Endophytic microorganisms can produce numerous types of siderophore in nature, including Hy-

Table 1. A summary of endophytes and their known abilities.

Endophytes	Activities	References
Dyella marensis, Collimonas pratensis, Luteibacter rhizovicinus	Associated with terrestrial orchids	(Herrera et al. 2020)
Laccaria laccata	Douglas-fir ectomycorrhizal development	(Duponnois & Garbaye 1991)
Pseudomonas fluorescens BBC6	Aids the formation of ectomycorrhiza	(Deveau et al. 2007)
Fusarium sp.	Protocorm induction and seed germination	(Vujanovic et al. 2000)
Colletotrichum	Enhance plant defence mechanisms	(Scherr et al. 2014)
Strepyomyces sp., *Pseudomonas* sp., *Bacillus* sp.	Produce indole-3-acetic acid (IAA) plant growth hormone	(Tsavkelova et al. 2007)
Aspergillus flavus, Trichoderma harzianum	Possesses antimicrobial which inhibits bacterial growth.	(Shrestha et al. 2018)
Xylaria sp., *Rhizoctonia* sp.	Contain defensive substances	(Hadley 1982)
Pseudomonas sp, *Enterobacter* sp., *Serratia* sp.	Phosphate solubilization activity	(Kalayu 2019; Sánchez-Cruz et al. 2019)
Enterobacter cloacae MSR1	Plant growth promoting properties	(Marchant et al. 2002)
Methylobacterium sp.	Siderophores production	(Lacava et al. 2008)

droxymate and Catecholates which are required in small amounts by plants to enrich the yield of crops (Pahari et al. 2017). Siderophores are often overlooked in conventional farming which utilized chemical fertilizers that focus on supplying the NPK nutrients, further studies that investigate the role and mechanism of action by different siderophores can create a deeper understanding.

CONCLUSIONS

The agriculture sector has long heavily relied on chemical fertilizer. The negative impact of such practice is huge towards the environment as well as to human well-being in future. This review article has provided insights towards the potential of plant growth promoting microorganisms isolated from Orchid. The microorganisms carry potassium, phosphorus as well as other bioactivities towards plant growth and development. These plant growths promoting microorganisms can be utilized to enhance the crop yield and reduce dependency on chemical fertilizers. The mode of interactions and mechanism between plant growth promoting microorganisms and plant can be further explored in future studies to increase the understanding in this aspect.

AUTHOR CONTRIBUTION

Conceptualization, J.A.G. and L.P.W.G.; formal analysis and investigation, B.L.J. and R.J.; resources, X.X.; data curation, R.J.; writing—original draft preparation, L.P.W.G. and B.L.J.; writing—review and editing, J.A.G., L.P.W.G., B.L.J., R.J.; supervision, J.A.G.; project administration, J.A.G. All authors have read and agreed to the published version of the manuscript.

ACKNOWLEDGMENTS

This study was supported by Malaysian Ministry of Higher Education (MoHE Code: FRGS/1/2023MAB11/UM3/01/1; UMS Code: FRG0609-1/2023). This study was supported by UMS External Grant (TLS2112).

CONFLICT OF INTEREST

The authors declare no conflict of interest.

REFERENCES

Abadía, J. 1995. *Iron Nutrition in Soils and Plants*, Springer Netherlands. doi: 10.1007/978-94-011-0503-3

Ahmed, E., Holmström, S.J.M., 2014. Siderophores in environmental research: roles and applications. *Microb Biotechnol.*, 7, pp.196–208. doi: 10.1111/1751-7915.12117.

Al-Karaki, G.N. & Al-Raddad, A., 1997. Effects of arbuscular mycorrhizal fungi and drought stress on growth and nutrient uptake of two wheat genotypes differing in drought resistance. *Mycorrhiza*,7, pp.83–88. doi: 10.1007/S005720050166.

Aloni, R. et al., 2006. Role of Cytokinin and Auxin in Shaping Root Architecture: Regulating Vascular Differentiation, Lateral Root Initiation, Root Apical Dominance and Root Gravitropism. *Ann Bot.*, 97, 883. doi: 10.1093/AOB/MCL027.

Arditti, J. & Pridgeon, A.M., 1997. Orchid Biology: Reviews and Perspectives, VII. Springer-Science+Business Media, B.V.

Aznar, A. & Dellagi, A., 2015. New insights into the role of siderophores as triggers of plant immunity: what can we learn from animals? *J Exp Bot.*, 66, pp.3001–3010. doi: 10.1093/JXB/ERV155.

Bayman, P. et al., 1997. Variation in endophytic fungi from roots and leaves of Lepanthes (Orchidaceae) | Treesearch. *New Phytologist.*, 135(1), pp.143–149. doi: 10.1046/j.1469-8137.1997.00618.x.

Bellenger, J.P. et al., 2008. Uptake of molybdenum and vanadium by a nitrogen-fixing soil bacterium using siderophores. *Nature Geoscience*, 1, pp.243–246. doi: 10.1038/ngeo161.

Benzing, D.H., 1996. Aerial Roots and Their Environments. In *Plant Roots The Hidden Half, Marcel Dekker, New York*. Scientific Research Publishing.

Booth, C., 1971. The genus Fusarium.

Casimiro, I. et al., 2001. Auxin transport promotes Arabidopsis lateral root initiation. *Plant Cell.*, 13(4), pp.843–852. doi: 10.1105/TPC.13.4.843.

Cetzal-Ix, W., Basu, S. & Noguera-Savelli, E., 2014, 'Orchidaceae: The Largest Family of Flowering Plants', in *The Encyclopedia of Earth*, from https://editors.eol.org/eoearth/wiki/Orchidaceae:_The_Largest_Family_of_Flowering_Plants

Chang, P.K. & Ehrlich, K.C., 2010. What does genetic diversity of Aspergillus flavus tell us about Aspergillus oryzae? *Int J Food Microbiol.*, 138, pp.189–199. doi: 10.1016/J.IJFOODMICRO.2010.01.033.

Chen, L. et al., 2019. Dynamics of fungal communities during Gastrodia elata growth. *BMC Microbiol.*, 19, 158. doi:10.1186/S12866-019-1501-Z/FIGURES/5.

Chen, S. et al., 2019. Root-associated microbiomes of wheat under the combined effect of plant development and nitrogen fertilization. *Microbiome.*, 7, 136. doi:10.1186/S40168-019-0750-2/FIGURES/5.

Chowdhery, H.J., 2004. *Orchid Flora of Arunachal Pradesh: New Hardcover*. Bishen Singh Mahendra Pal Sing.

Chutulo, E.C. & Chalannavar, R.K., Endophytic Mycoflora and Their Bioactive Compounds from Azadirachta Indica: A Comprehensive Review. *J Fungi* (Basel)., 4, pp.42. doi:10.3390/JOF4020042.

De, L.C. & Singh, D.R., 2015. Biodiversity, conservation and bio-piracy in orchids-an overview. *Journal of Global Bioscience.*, 4, pp.2030–2043.

Deveau, A. et al., 2007. The mycorrhiza helper Pseudomonas fluorescens BBc6R8 has a specific priming effect on the growth, morphology and gene expression of the ectomycorrhizal fungus Laccaria bicolor S238N. *New Phytologist*., 175(4), pp.743–755. doi: 10.1111/J.1469-8137.2007.02148.X.

Dewar, R.C., 2010. Maximum entropy production and plant optimization theories. *Philosophical Transactions of the Royal Society B: Biological Sciences*., 365, pp.1429–1435. doi: 10.1098/RSTB.2009.0293.

Duponnois, R. & Garbaye, J., 1991. Mycorrhization helper bacteria associated with the Douglas fir-Laccaria laccata symbiosis: effects in aseptic and in glasshouse conditions. *Annales des Sciences Forestières*., 48, pp.239–251. doi: 10.1051/FOREST:19910301.

Einzmann, H.J.R., Schickenberg, N. & Zotz, G., 2019. Variation in root morphology of epiphytic orchids along small-scale and large-scale moisture gradients. *Acta Bot Brasilica*., 34, pp.66–73. doi: 10.1590/0102-33062019ABB0198.

Fu, S.F. et al., 2015. Indole-3-acetic acid: A widespread physiological code in interactions of fungi with other organisms. *Plant Signal Behav*., 10(8), e1048052. doi: 10.1080/15592324.2015.1048052.

Guarnaccia, V. et al., 2021. Colletotrichum spp. causing anthracnose on ornamental plants in northern Italy. *Journal of Plant Pathology*., 103, pp.127–137. doi: 10.1007/S42161-020-00684-2/FIGURES/2.

Hadley, G., 1982. *Orchid Biology VIII: Reviews and Perspectives*, Google Books.

Hardoim, P.R. et al., 2015. The Hidden World within Plants: Ecological and Evolutionary Considerations for Defining Functioning of Microbial Endophytes. *Microbiol Mol Biol Rev*., 79(3), pp.293–320. doi: 10.1128/MMBR.00050-14.

Herrera, H. et al., 2020. Isolation and Identification of Endophytic Bacteria from Mycorrhizal Tissues of Terrestrial Orchids from Southern Chile. *Diversity*., 12(2), 55. doi: 10.3390/D12020055.

Hinsinger, P., 2001. Bioavailability of soil inorganic P in the rhizosphere as affected by root-induced chemical changes: a review. *Plant and Soil*., 237(2), pp.173–195. doi: 10.1023/A:1013351617532.

Juiling, S. et al., 2020. Conservation assessment and spatial distribution of endemic orchids in Sabah, Borneo. *Nature Conservation Research*., 5, pp.136–144. doi: 10.24189/NCR.2020.053.

Kalayu, G., 2019. Phosphate solubilizing microorganisms: Promising approach as biofertilizers. *International Journal of Agronomy*., 2019. 4917256. doi: 10.1155/2019/4917256.

Khalifa, A.Y.Z. et al., 2016. Characterization of the plant growth promoting bacterium, Enterobacter cloacae MSR1, isolated from roots of non-nodulating Medicago sativa. *Saudi J Biol Sci*., 23(1), pp.79–86. doi: 10.1016/J.SJBS.2015.06.008.

Ko, R.S.-S., 2018. Phalaenopsis aphrodite (moth orchid): Functional genomics and biotechnology. *J Plant Pathol Microbiol*., 09. doi: 10.4172/2157-7471-C2-010.

Kosegarten , H. et al., 1999. Effects of NH(4)(+), NO(3)(-) and HCO(3)(-) on apoplast pH in the outer cortex of root zones of maize, as measured by the fluorescence ratio of fluorescein boronic acid. *Planta*., 209, pp.444–452. doi: 10.1007/S004250050747.

Košir, P., Škof, S. & Luthar, Z., 2004. Direct shoot regeneration from nodes of Phalaenopsis orchids. *Acta Agriculturae Slovenica*, 83, pp.233-242.

Kuo, J., Chang, C.F. & Chi, W.C., 2021. Isolation of endophytic fungi with antimicrobial activity from medicinal plant Zanthoxylum simulans Hance. *Folia Microbiol (Praha)*., 66, pp.385–397. doi:10.1007/S12223-021-00854-4.

Lacava, P.T. et al., 2008. Detection of siderophores in endophytic bacteria Methylobacterium spp. associated with Xylella fastidiosa subsp. pauca. *Pesqui Agropecu Bras*., 43, pp.521–528. doi: 10.1590/S0100-204X2008000400011.

Lavy, M. & Estelle, M., 2016. Mechanisms of auxin signaling. *Development*., 143, pp.3226–3229. doi:10.1242/DEV.131870.

Leghari, 2016. Role of Nitrogen for Plant Growth and Development: A review. *Advances in Environmental Biology*., 10,pp.209–218.

Li, O. et al., 2017. Bacterial and diazotrophic diversities of endophytes in Dendrobium catenatum determined through barcoded pyrosequencing. *PLoS One*., 12, e0184717. doi: 10.1371/JOURNAL.PONE.0184717.

Liu, H., Luo, Y. & Liu, H., 2010. Studies of Mycorrhizal Fungi of Chinese Orchids and Their Role in Orchid Conservation in China—A Review on JSTOR. *The Botanical Review*., 76, pp.241–262.

Maheshwari, R., Bhutani, N. & Suneja, P., 2019. Screening and characterization of siderophore producing endophytic bacteria from Cicer arietinum and Pisum sativum plants. *J Appl Biol Biotechnol*., 7, pp.7–4. doi:10.7324/JABB.2019.70502.

Majit, H.F. et al., 2014. The wild orchids of Crocker range national park, Sabah, Malaysia. *Malayan Nature Journal*., 66(4), pp.440–462.

Marchant, A. 2002. AUX1 Promotes Lateral Root Formation by Facilitating Indole-3-Acetic Acid Distribution between Sink and Source Tissues in the Arabidopsis Seedling. *Plant Cell*., 14(3), pp.589-597. doi:10.1105/TPC.010354

Ma, X. et al., 2016. Non-mychorrizal endophytic fungi from orchids. *Curr Sci*., 109, pp.72-87.

Mouhamad, R., Atiyah, A. & Iqbal, M., 2016. Behavior of potassium in soil: a mini review. *Chemistry International*., 2, pp.58–69.

Nair, V.G. et al., 2018. Analgesic and anti-inflammatory activities of Bulbophyllum neilgherrense Wight. pseudobulb: A folklore plant. *AYU*., 39, pp.76–80. doi: 10.4103/AYU.AYU_134_16.

Nayar, M.P., 1996. *Hot spots of endemic plants of India, Nepal and Bhutan*, Tropical Botanic Garden and Research Institute.

Pahari, A. et al., 2017. Bacterial Siderophore as a Plant Growth Promoter. In *Microb Biotechnol*. Singapore: Springer. doi:10.1007/978-981-10-6847-8_7.

Pant, B. et al., 2017. An overview on orchid endophytes. In *Mycorrhiza - Nutrient Uptake, Biocontrol, Ecorestoration*. Springer International Publishing. doi:10.1007/978-3-319-68867-1_26.

Parthibhan, S., Rao, M.V. & Senthil Kumar, T., 2017. Culturable fungal endophytes in shoots of Dendrobium aqueum Lindley – An imperiled orchid. *Ecol Genet Genom*., 3–5, pp.18–24. doi: 10.1016/J.EGG.2017.06.004.

Puri, A., Padda, K.P. & Chanway, C.P., 2017. Nitrogen-Fixation by Endophytic Bacteria in Agricultural Crops: Recent Advances. Nitrogen in Agriculture - Updates. doi: 10.5772/INTECHOPEN.71988.

Rashid, M.I. et al., 2016. Bacteria and fungi can contribute to nutrients bioavailability and aggregate formation in degraded soils. *Microbiol Res*., 183, pp.26–41. doi: 10.1016/J.MICRES.2015.11.007.

Rodríguez, H. & Fraga, R., 1999. Phosphate solubilizing bacteria and their role in plant growth promotion. *Biotechnol Adv.*, 17, pp.319–339. doi:10.1016/S0734-9750(99)00014-2.

Rubluo, A. et al., 1993. Strategies for the recovery of endangered orchids and cacti through in-vitro culture. *Biol Conserv.*, 63(2), pp.163–169. doi: 10.1016/0006-3207(93)90505-U.

Salazar, J.M. et al., 2020. Endophytic fungi associated with roots of epiphytic orchids in two Andean forests in southern Ecuador and their role in germination. *Lankesteriana*, 20(1), pp.37–47. doi: 10.15517/LANK.V20I1.41157.

Sánchez-Cruz, R. et al., 2019. Isolation and characterization of endophytes from nodules of Mimosa pudica with biotechnological potential. *Microbiol Res.*, 218, pp.76–86. doi: 10.1016/J.MICRES.2018.09.008.

Sarsaiya, S., Shi, J. & Chen, J., 2019. A comprehensive review on fungal endophytes and its dynamics on Orchidaceae plants: current research, challenges, and future possibilities. *Bioengineered.*, 10, pp.316–334. doi: 10.1080/21655979.2019.1644854.

Scherr, S.J. et al., 2014. Ecoagriculture: Integrated Landscape Management for People, Food, and Nature. In *Encyclopedia of Agriculture and Food Systems.* Elsevier.

Schwyn, B. & Neilands, J.B., 1987. Universal chemical assay for the detection and determination of siderophores. *Anal Biochem.*, 160, pp.47–56. doi: 10.1016/0003-2697(87)90612-9.

Semiarti, E., 2018. Orchid biotechnology for Indonesian orchids conservation and industry. *AIP Conf Proc.*, 2002, 020022. doi: 10.1063/1.5050118.

Shah, S. et al., 2021. A prospectus of plant growth promoting endophytic bacterium from orchid (Vanda cristata). *BMC Biotechnol.*, 21, 16. doi: 10.1186/S12896-021-00676-9/FIGURES/4.

Shakeel, M. et al., 2015. Root associated Bacillus sp. improves growth, yield and zinc translocation for basmati rice (Oryza sativa) varieties. *Front Microbiol.*, 6, 1286. doi: 10.3389/FMICB.2015.01286/BIBTEX.

Shrestha, R., Shah, S. & Pant, B., 2018. Identification of endophytic fungi from roots of two Dendrobium species and evaluation of their antibacterial property. *Afr J Microbiol Res.*, 12, pp.697–704. doi: 10.5897/AJMR2018.8924.

Sparks, D.L. & Huang, P.M., 1985. *Physical Chemistry of Soil Potassium*, Scientific Research Publishing.

Srivastava, S., Kadooka, C. & Uchida, J.Y., 2018. Fusarium species as pathogen on orchids. *Microbiol Res.*, 207, pp.188–195. doi: 10.1016/J.MICRES.2017.12.002.

Sultenfuss, J.H. & Doyle, W.J., 1999. Functions of phosphorus in plants. *Better Crops with Plant Food.*, 83, pp.6–7.

Tajer, A., 2021, 'What is the Best Potassium Fertilizer?' in *Greenway Biotech, Inc.*, viewed 4 March 2022, from https://www.greenwaybiotech.com/blogs/gardening-articles/what-is-the-best-potassium-fertilizer

Teale, W.D., Paponov, I.A. & Palme, K., 2006. Auxin in action: signalling, transport and the control of plant growth and development. *Nature Reviews Molecular Cell Biology.*, 7, pp.847–859. doi: 10.1038/nrm2020.

Tsavkelova, E.A. et al., 2007. Bacteria associated with orchid roots and microbial production of auxin. *Microbiol Res*, 162, pp.69–76. doi: 10.1016/J.MICRES.2006.07.014.

Vujanovic, V. et al., 2000. Viability Testing of Orchid Seed and the Promotion of Colouration and Germination. *Ann Bot.*, 86(1), pp.79–86. doi: 10.1006/ANBO.2000.1162.

Wedge, D. & Elmer, W., 2008. Fusarium Wilt of Orchids. *Trade Journal.*, 2, pp.9–11.

Wilkinson, C.L. et al., 2018. Land-use change is associated with a significant loss of freshwater fish species and functional richness in Sabah, Malaysia. *Biol Conserv.*, 222, pp.164–171. doi: 10.1016/J.BIOCON.2018.04.004.

Wilson, D., 1995. Endophyte: The Evolution of a Term, and Clarification of Its Use and Definition. *Oikos.*, 73, pp.274. doi: 10.2307/3545919.

Xu, X. et al., 2020. Effects of Potassium Levels on Plant Growth, Accumulation and Distribution of Carbon, and Nitrate Metabolism in Apple Dwarf Rootstock Seedlings. *Front Plant Sci.*, 11, 904. doi: 10.3389/FPLS.2020.00904/BIBTEX.

Yang, Y.L., Liu, Z.-Y. & Zhu, G.-S., 2008. Study on Symbiotic Seed Germination of Pleione bulbocodioides(Franch) Rolfe. *Microbiology.*, 35, pp.909–912.

Zahara, M. & Win, C.C., 2019. Morphological and Stomatal Characteristics of Two Indonesian Local Orchids. *Journal of Tropical Horticulture.*, 2, pp.65–69. doi: 10.33089/JTHORT.V2I2.26.

Zapata, F. & Zaharah, A.R., 2002. Phosphorus availability from phosphate rock and sewage sludge as influenced by the addition of water soluble phosphate fertilizer. *Nutr Cycl Agroecosyst.*, 63, pp.43–48. doi: 10.1023/A:1020518830129.

Zhang, F.S et al., 2013. Promoting role of an endophyte on the growth and contents of kinsenosides and flavonoids of Anoectochilus formosanus Hayata, a rare and threatened medicinal Orchidaceae plant. *J Zhejiang Univ Sci B.*, 14(9), pp.785-792. doi: 10.1631/JZUS.B1300056.